2018 IPL SYMPOSIUM ON LANDSLIDES

03 December 2018
Kyoto University, Uji campus, Kyoto, Japan

Organized by
International Consortium on Landslides (ICL)

Picture on the cover page
Kure landslide in Hiroshima after the heavy rainfall in July 2018
Taken from UAV by Kyoji Sassa, Khang Dang, and Nguyen Duc Ha

2018 IPL SYMPOSIUM ON LANDSLIDES

03 December 2018
Kyoto University, Uji campus, Kyoto, Japan

Kyoji Sassa・Khang Dang *Editors*

Organized by
International Consortium on Landslides (ICL)

Supported by
Disaster Prevention Research Institute of Kyoto University

Editors
Kyoji Sassa, Khang Dang
International Consortium on Landslides
Kyoto, Japan

This proceedings is registered in the Online Public Access Catalog of the National Diet Library of Japan

ISBN 978-4-9903382-0-6

Published by: The International Consortium on Landslides

Contents

SRSG Statement for the International Landslide Consortium Conference 1
Mami Mizutori

Risk Conditions for possible failure of HidroItuango Dam in Colombia 3
Guillermo Ávila

Review of remedial measures adopted for rainfall-induced landslides in Nilgiris, India 9
V Santhosh Kumar, S S Chandrasekaran

Improvement of Landslide EWS at Banjarnegara, Central Java, Indonesia 15
Dwikorita Karnawati, Munawar, Agus Safril, Rista Hernandi Virgianto, Amir Mustofa Irawan, Suharni, Hapsoro Agung Nugroho, Puji Ariyanto

Development of landslide detection system based on rainfall prediction and seismic aspect in Banjarnegara, Central Java, Indonesia 25
Dwikorita Karnawati, Munawar, Agus Safril, Rista Hernandi Virgianto, Suharni, Puji Ariyanto

Selection of Optimal Parameters Characterizing Mobility of Rock Avalanches 31
Alexander Strom

Landslide processes as a risk factor for Russian cultural heritage objects 36
Igor Fomenko, Denis Gorobtsov, Daria Shubina, Fedor Bufeev

IPL Project 181 – Study of slow moving landslide Umka near Belgrade, Serbia – progress report for 2017 & 2018 41
Uroš Đurić, Biljana Abolmasov, Miloš Marjanović, Mileva Samardžić-Petrović, Marko Pejić, Nenad Brodić, Jovan Popović

IPL Project 210 – Massive landsliding in Serbia following Cyclone Tamara in May 2014 - progress report 47
Biljana Abolmasov, Miloš Marjanović, Uroš Đurić, Mileva Samardžić-Petrović, Jelka Krušić

Ecosystem Observation of Upland Soil Erosion Reduction in Mountain Slopes in Sri Lanka 52
N Nimesha Katuwala, P V I P Perera, H M J M K Herath, K Pavani C Perera & A A Virajh Dias

Historical Monuments Located Within Landslide Hazardous Site 57
Oleksandr Trofymchuk, Iurii Kaliukh, Oleksij Lebid

Impact of Vegetation Loss Due to Wildfire on Debris Flow Volume 63
Binod Tiwari, Beena Ajmera

Update on the Ripley Landslide (IPL #202) and the activities of the University of Alberta / GSC WCoE 68
Michael T. Hendry, David Huntley, Renato Macciotta, Peter Bobrowsky

Temporal-spatial distribution characteristics and prevention of landslides developing in Jurassic stratum in Three Gorges Reservoir region, China 77
Changdong Li

Strengthening the resilience by reducing risk from sediment-related disasters 101
Teuku Faisal Fathani, Wahyu Wilopo

Initial Development of the Digital Crowd Mapping for Landslide Monitoring and Early Warning System 108
Wahyu Wilopo, Teuku Faisal Fathani, Hendy Setiawan, Budi Andayani, Dwikorita Karnawati

Advanced Technologies for LandSlides (ATLaS) 114
Nicola Casagli, Filippo Catani, Riccardo Fanti, Giovanni Gigli, Sandro Moretti, Veronica Tofani, Paolo Canuti

IPL project 198: Multi-scale rainfall triggering models for Early Warning of Landslides (MUSE) 155
Veronica Tofani, Filippo Catani, Nicola Casagli, Guglielmo Rossi

Landslide risk analysis and mitigation for the Monastery of Vardzia - 2018 166
Daniele Spizzichino

EO4GEO - Towards an innovative strategy for skills development and capacity building in the space geo-information sector supporting Copernicus User Uptake 179
Daniele Spizzichino, Luca Guerrieri, Gabriele Leoni, Valerio Comerci

Challenges for Operational Forecasting and Early Warning of Rainfall Induced Landslides 185
Fausto Guzzetti

Landslides and Climate and Environmental Changes Advances & Perspectives 196
Stefano Luigi Gariano & Fausto Guzzetti

A multi-parametric field laboratory for the investigation on the relationship between material behavior and morphodynamic of landslides 209
Andrea Segalini, Emma Petrella, Fulvio Celico, Alessandro Chelli, Roberto Francese, Andrea Carri, Alessandro Valletta

A new methodology for assessing earthquake-induced landslide scenarios 215
Carlo Esposito, Salvatore Martino,Francesca Bozzano, Gabriele Scarascia Mugnozza

Characteristics of recent landslides triggered by two moderate-strong earthquakes in Japan 225

Fawu Wang, Shuai Zhang, Ran Li, Akinori Iio

The Landslides triggered by the Hokkaido Iburi-Tobu Earthquake on September 6th 2018 247
Hiromitsu Yamagishi, Fumiaki Yamazaki

Recognition of potentially hazardous torrential fans using geomorphometric methods and simulating fan formation (IPL-225 Project) 257
Matjaž Mikoš, Nejc Bezak, Matej Maček, Tomaž Podobnikar, Jošt Sodnik, Sandi Kaltak

IPL-216 Project Annual Report for 2018: Diversity and hydrogeology of mass movements in the Vipava Valley, SW Slovenia 269
T. Verbovšek, T. Popit, J. Jež, A. Petkovšek, M. Maček

Contribution of Landslide group in National Central University to IPL 279
Ray-Shyan Wu, Chih-Chung Chung

UNISDR
United Nations Office for Disaster Risk Reduction

SRSG STATEMENT
FOR
THE INTERNATIONAL LANDSLIDE CONSORTIUM CONFERENCE
KYOTO, JAPAN

2018 will go down as one of the hottest years on record and another remarkable year for extreme weather events. This confirms the long term trend of the last forty years which has seen a doubling in the number of recorded extreme weather events which now regularly account for 90% of disasters caused by natural hazards notably floods, storms, landslides and wildfires.

Landslides in particular have become a growing cause for concern. A recent study published by the University of Sheffield indicates that so far this century over 50,000 people have lost their lives in landslides. It is deeply worrying that human-induced landslides are on the increase from construction works, legal and illegal mining, as well as unregulated cutting of hillsides.

A nightmare scenario for any community is to be taken by surprise in the middle of the night by a landslide which sweeps away hundreds of lives without warning following heavy precipitation which often combines with the risk already created by deforestation and unstable soils.

A landslide such as this was responsible for the single greatest loss of life in the world last year when over 1,100 people died in the middle of the night as heavy rains brought mudslides and landslides down on flimsy homes built on the outskirts of the Sierra Leone capital, Freetown. This trend has continued into 2018. Landslides with high death tolls are often a result of failures in risk governance, poverty reduction, environmental protection, land use and the implementation of building codes.

Climate change is adding immeasurably to the risk of landslides, starting with the growing unpredictability of rainfall patterns. Latest analysis from weather stations across the world indicates that 50% of the world's measured precipitation over a year falls in just 12 days. Distribution of snow and rain could become even more skewed in the future, according to the US National Center for Atmospheric Research.

This underlines why the UN Office for Disaster Risk Reduction places so much value on its partnership with the International Consortium on Landslides (ICL) and the International Programme on Landslides (IPL). The work of the ICL and the scientific community is vital in the effort to achieve the 2030 Agenda for Sustainable Development through coherent implementation of the Sendai Framework for Disaster Risk Reduction 2015-2030, the Paris Agreement and the SDGs.

Floods, storms, earthquakes and heavy precipitation all contribute to landslide risk and the work of the ICL is vital to reducing that risk.

I would like to thank the ICL for its leadership and commitment as reflected in the Kyoto 2020 Commitment for Global Promotion of Understanding and Reducing Landslide Risk and I am confident that the outcomes of the 2018 ICL-IPL Conference will not only ensure a successful 5th World Landslide Forum but also make an excellent contribution to the Global Platform for Disaster Risk Reduction when it convenes in Geneva in May 2019.

I wish you every success in your deliberations.

Mami Mizutori
United Nations Special Representative
of the Secretary-General for Disaster Risk Reduction.

Risk Conditions for possible failure of HidroItuango Dam in Colombia

Guillermo Ávila[(1)]

1) National University of Colombia, Department of Civil and Agricultural Engineering, Bogotá, Carrera 30 Calle 45, geavilaa@unal.edu.co.

Abstract In the month of May of 2018, occurred the collapse of the water evacuation tunnel in the Hidro-Ituango dam, located in the central-western zone of Colombia (Fig. 1). The dam is projected to 225 m height to reservoir of about 20 millions of cubic meters of water. It is one of the greatest hydro-electric projects in the country and at the moment of the tunnel collapse, the final stage of the construction was in process but other two relief tunnels had been plugged to accelerate the filling, so the reservoir was left with not possibilities of relief. This situation generated a very serious risk condition for many municipalities located downstream, due to possible water overflow causing an enormous debris flow, so the powerhouses had to be flooded to allow the evacuation of water and to have some extra time to reach the design height of the dam and to finish the construction of the dump. This non controlled water flow inside the dam and the presence of water at very high pressure in rock mass may cause landslides or rock failures. Slopes around the reservoir have also shown instability problems and they may produce waves that can affect the dam. The article discusses this complex risk situation analyses probable risk scenarios and highlights the technical, economical and social problems associated to the design and construction of the dam.

Keywords Risk management, vulnerability, dam failure, landslide, debris flow.

General description of the Hidro-Ituango project.

Hidroituango dam project is located in the Cauca Canyon, about 100 km north west from Medellín city (Colombia), near Ituango town (Fig. 1). Construction started in 2010 with the purpose of generating, from December 2018, electric power of 2.400 MW, that represent about 17% of the electric power demand in the Country for the next 10 years (EPM, 2018), becoming in the largest-ever hydroelectric project in Colombia.

The Cauca River is 1.350 km length, has a basin of about 37.800 km^2 and middle annual flow of 1184 m^3/s (IDEAM, 2014) with pick flows up to 4.500 to 5.000 m^3/s. As shown in Fig. 1, there are many towns downstream that may be severely affected in case of a dam failure, as Puerto Valdivia, Cáceres, Caucasia and Nechí, but, as indicated by Vargas (2018), who published maps of possible affected areas, based on geomorphological analysis, near 500 km downstream many towns may suffer the consequences of an eventual debris flow produced by the dam break.

The dam is located in an area of metamorphic rocks affected by some faults that have caused fractures in the rock masses. Probably this was one of the main factors that produced the collapse of the auxiliary tunnel.

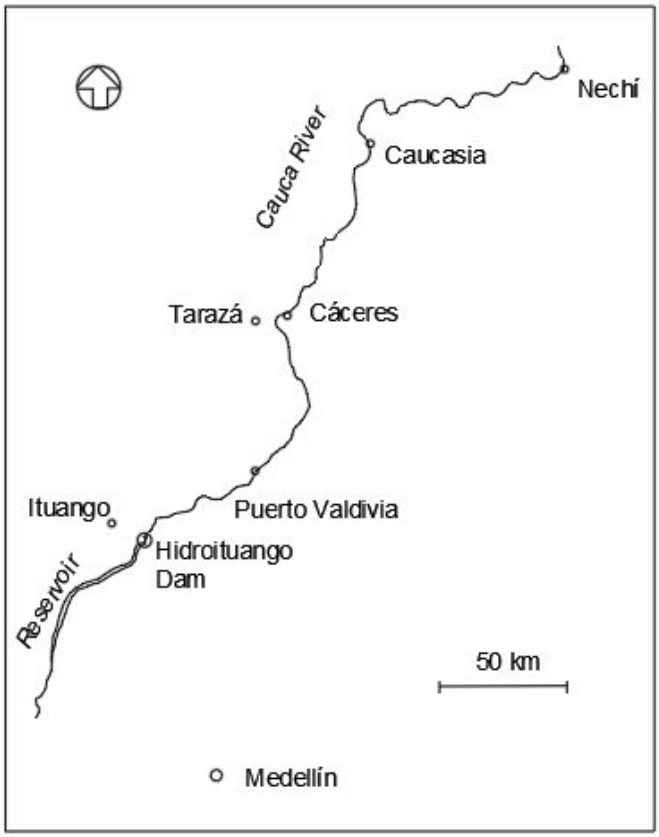

Figure 1. General location of the Hidroituango Project and main influence area in case of an eventual dam failure.

The main structure of the project is the dam, technically described as a rock fill dam with impervious clay core. Figure 2 shows a simple schematic representation of the dam geometry and the tree main complementary structures: the cofferdam (cd) and the pre-cofferdam (p-cd) in the upstream side and the counter-cofferdam (c-cd) in the downstream side. The dimensions of the dam are: 225 m height, 550 m crest

length (not shown in Fig.2), 750 m base, and 18 m crest width.

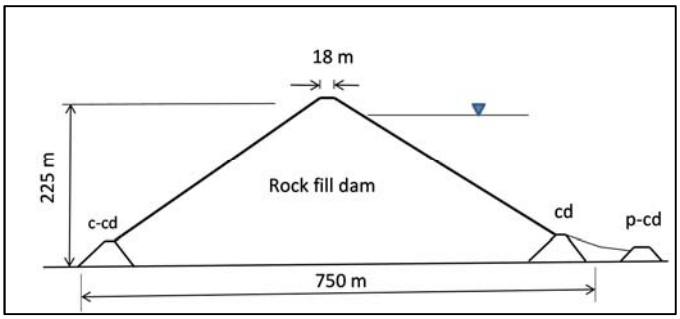

Figure 2. Schematic dam characteristics. (cd) cofferdam, (c-cd) counter-cofferdam and (p-cd) pre-cofferdam (Adapted from EPM, 2015).

Fig. 3 shows a simplified sketch in plain view of the dam, the diverse tunnels (tunnel 1 and tunnel 2), the auxiliary tunnel, not planned in the original design, the powerhouse, with capacity for 8 turbines to generate electric energy, and the spillway. This sketch is useful for the description of the evolution of the emergency in the next paragraphs.

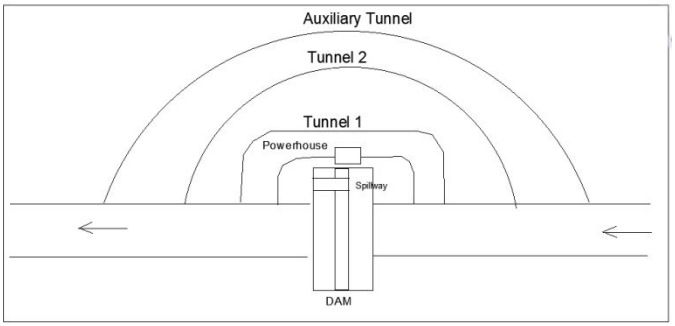

Figure 3. Simplified sketch drainage structures of Hidroituango dam.

The significant magnitude of the project may be observed in the photograph of Fig. 4 that shows the dam during the construction process. Here the dump trucks serve as reference scale.

Time evolution of the emergency situation

Based on the official press releases of the Project Managers (EPM, 2018), and newspaper documents (Rubiano, 2018, Ortiz, 2018, El País, 2018a), a time evolution of the main emergency is described here. This description is important to see the problems faced by the Project Managers, the emergency offices and the affected community:

April 29, 2018: A partial obstruction of the auxiliary tunnel (Fig. 3) of 2000 m^3/s flow capacity occurred, causing upstream damming and flow reduction downstream. It is indicated by the Project staff that they have made a blast to unblock the tunnel and during the night the tunnel was unblocked.

Figure 4. Photo of the dam construction process (Cortesy of R. Moreno).

April 30: A new obstruction of the auxiliary tunnel occurred. In this moment the emergency condition was evident: one of the vehicular bridges located upstream the dam (Pescadero Bridge) had to be closed because water level was very high. For this reason it was necessary to establish a mobility plan for the people upstream. The main concern in that moment was that tunnel obstruction produced a rapid increase of water level in the reservoir because the other two diverse tunnels (tunnels 1 and 2 in Fig. 3) have been previously clogged with concrete in order to accelerate the dam fill, despite that the design height of the dam had not been reached and the spillway was not finished yet (Dam construction was in about 85% advance).

May 1: The Project General Manager indicated that an emergency dam fill (locally called "priority" fill) will be constructed in a very short time, to increase the dam level, to avoid uncontrolled water flow over the unfinished dam (overtopping), that could generate a catastrophic debris flow.

May 5: Works were focused on four fronts: a) unblock the two initial diverse tunnels, b) increase the dam height, c) inform the emergency situation to the community and d) develop an environmental management to protect wildlife (affected for the rapid water rising upstream).

May 7: A new and big collapse of fractured rock material occurred during the early morning, blocking the auxiliary tunnel, and leaving on the mountain surface, an enormous collapse hole. This was, undoubtedly, the most critical situation from the technical point of view, because it was impossible to evacuate the collapsed material to permit water flow.

May 9: One of the diverse tunnels initially constructed and clogged with concrete was partially unblocked. The evacuation of water partially relived the critical situation, but the inflow was still too much higher than the outflow because the rainy season in the basin was in its maximum level.

May 10: It was decided to evacuate water through the power station (that already had installed two of the

turbines) to avoid the imminent overtopping. This decision implied that energy generation will be postponed for undefined time, but it was absolutely necessary to avoid tragic consequences downstream, caused by an enormous debris flow and also upstream, due to rapid lowering of water level, that could induce new landslides near the dam area.

May 12: The auxiliary tunnel was naturally unblocked, and the water outflow increased significantly, causing unexpected floods in many villages downstream, but 4 hours later, the tunnel was blocked again in natural way. After the flood, 600 people were evacuated in Puerto Valdivia town, the nearest to the dam and most vulnerable (see Fig. 1), 22 houses were destroyed and 30 were affected. Also two class rooms and one health center resulted affected by the flood. By fortune it was Saturday and no students were at the school that day.

May 13. At midday a temporal obstruction of the powerhouse produced unexpected and explosive water flow trough the access galleries, affecting, although not severely, four persons that were working near that area. Many television news showed that day the impacting images and how workers had the fortune to escape from the high velocity flow. Those images produced additional worries to the project workers and to the general public in the whole country.

May 14: As a consequence of the critical situation, "Public Calamity" was declared by the National Government, at the request of the Department Emergency Committee (El Tiempo, 2018).

May 20: An obstruction in the powerhouse, probably caused for a rock mass failure, reduced to about one half the water outflows, this situation, together with the heavy rains in the area, caused increase rate of the water level in the reservoir, of 0.20 m per hour. It was a race against time, because dam level should be increased to 410 m (above sea level) and at that moment it was at the level 407 m.

May 23: The goal of reaching level 410 m for the dam was finally met. The new goal was to finish the construction of the spillway and reach the level 415 m.

May 26: A landslide occurred near the dam and as a prevention measure the traffic trough a tunnel near the unstable area was temporally suspended.

May 28. New landslides of small volumes were generated in the same area of the previous one with not significant consequences.

June 1. Attending to the precautionary principle, the national authority that issues environmental licences for the construction projects (ANLA), imposed to the Project´s owner (EPM) the obligation of monitoring and report many hydrological and geotechnical variables to control the hazard evolution, to adopt the necessary measurements to reduce the risk condition and to attend the necessities of the affected population.

June 4. The Project´s owner (EPM) informs about national and international technical assistance and about monitoring systems installed in the project. Moderate landslides continued to occur near the dam. Monitoring system indicate that movements were less than 10 mm/h. Traffic trough the road tunnel was open again. Infiltration in the emergency fill is registered and cracks are closed with clayed material. Also bentonite was applied in 30 boreholes to reduce water infiltration.

June 6: Risk is high considering the possibility of significant water flows, landslides and stability and infiltrations in the dam. Priorities are continue the emergency fill to the level 415 m., close the diversion tunnel and close the auxiliary tunnel (probably to avoid unexpected and excessive flows in case of unblocking).

June 11: The spillway was finally concluded. This structure will permit to evacuate up to 6000 m^3/s, corresponding a return period 500 years, however, maximum flows registered in the Cauca River are around 5.000 m^3/s. EPM informs that this structure reduces the risk of overtopping

June 14. The National Disaster Risk Management Unit, keeps the evacuation alert for possible increase in water flow, despite the water level shows a tendency to decrease. It also informs that the probability of a big landslide in the dam is low because accelerations from 0.6 to 0.68 g would be required to generate instability. The probability of occurrence of landslides in residual soils with maximum volumes of about 250.000 m^3 is 1% and is such as case if a water wave (seiche) is generated, this would not overpass the dam crest.

June 17. Level 415 m in the "priority fill" was reached.

June 25. EPM puts on service a big temporary shelter with capacity for 2000 people from Puerto Valdivia.

From July to end of September 2018, water level has lower and the project managers inform that the emergency situation is under control, the next rainy period, starting on October may bring another emergency situation.

The emergency from the affected community point of view

According to the social movement Rios Vivos (Alive Rivers), more than 6000 families have been displaced from their homes and they suffer from psychological insecurity because they think that the dam project will cause a tragedy (Martinez, 2018). This social movement complains that local communities have not been taken into account, and from the beginning of the project, many people have been against the construction of the dam because of the significant environmental damage due to extensive flooding areas and changes in natural water flow, which have caused reduction in crops and fishing and, in general, losses of daily income and deterioration of working conditions, as expressed in many meetings and in its web page (Movimiento Rios Vivos Antioquia, 2018).

Due to the emergency situation many families from towns that are close to the dam had to leave their houses and, contrary to the official version, they live in very

difficult conditions in the temporary shelters (Fig. 4), children may not go to schools and most of the business are closed. Monetary support from the government is not enough to cover minimal conditions because they have to pay for a house rent (which amount increased due to the emergency) and for food. Moreover, their houses and small industries have loose worth because they are now in a risk area with no possibilities to change that condition.

Perhaps the most difficult situation for the people is that they do not have a defined time to return to their normal conditions and many of them have no choice to go anywhere else. In front of this situation, some social groups claim for dismantle the hole project.

Figure 5. Temporary shelters for people from Puerto Valdivia (Elpais.com, 2018b)

Design and construction problems

Dam failures and dam incidents are not scarce in the world. For example the Association of State Dam Safety Officials of the USA (2018) reports for this country 173 dam failures and 578 incidents from January 2005 and June 2017. On March 12 1928 (this year was the 90th anniversary) occurred the St Francis Dam failure in California, considered the worst American civil engineering failure of the 20th Century, killing 450 people and causing economical losses for the State of California of more than 7 million US dollars in restitution to the victim´s families and affected landowners (Rogers, 2006). The investigation post failure revealed many human factors that contributed to the dam´s failure as: a) signs of distressed conditions were dismissed by inspectors, b) overconfidence on the designer and c) shortcomings in Californias´s laws that resulted in lack of outside review of design and construction.

Other significant dam failures in the world are the 1963 failure of Vajont dam in Italy caused 2600 deaths, the 1976 failure of Teton dam in USA caused hundred deaths and economic loss about 1 billion dollars, and the 1993 failure of Gouhou dam in China caused 300 death (You et al 2012). Most common causes of dam failure are overtopping, foundation defects, cracking, inadequate maintenance and upkeep and Piping (Association of State Dam Safety Officials of the USA, 2018). According to a statistical analysis of 534 dam failures before 1974, reported by ICOLD bulletin in 1998 and cited by You et al (2012), most of the dam failures have occurred on rock-earth dams. The main cause of failure is overtopping (49%), followed by seepage foundation (29%) and seepage in the dam body (28%).

Yen and Tang (1979), cited by Marengo (1996) state that factors causing dam failures may be grouped in a) hydrological factors: controls the reservoir level, produce pick flows, and affect the sediment transport and accumulation near the dam, b) hydraulic factors: capacity of the spillway, gates, pipelines and valves., c)geotechnical factors: unfavourable soil conditions as weak strata, cracks, unfavourable joints, infiltration, soil piping, excess of pore pressures, settlements, slope failures during dam releasing or in any area around the dam d) seismic factors: seismic stability of the dam, liquefaction, cracks induced by seismic actions, seismic surge and hydrodynamic pressure, e) structural and construction problems: incorrect structural design, poor quality of construction materials and poor quality control and f) operational factors.

The unexpected risk situation in Hidroituango, dismantled some abnormal conditions during the design and construction that may have influenced the actual condition: according to the Department Governor, based on the reports of an expert group of the Colombian National University at Medellín (cited by RCN Radio, 2018) eight important mistakes were identified: 1) delay and over cost in the construction of diversion tunnels, 2)Inconvenience of constructing auxiliary tunnel because the risk conditions were already warned, 3) The auxiliary tunnel did not have the require environmental licence. 4) The auxiliary tunnel did not have the required lining for high flow velocities, 5) closing, before time tunnels 1 and 2 because dam height was lower the 390 m over sea level and the intermediate discharge was not finished, 6)failure to unplug tunnels 1 and 2 due to misuse of the blasting techniques, 7) blasting affected the surrounding slopes, causing instability and some landslides and 8) delay in the communication of the emergency situation to take timely actions.

Risk management in the critical situation

The very complicated risk condition for a probable dam break, that emerged after the auxiliary tunnel collapse, added to the situation of intense raining and the rapid increase of water level, made necessary to evacuate water through the power station. That was the first difficult decision during the emergency, because it would seriously affect the project but it was absolutely necessary in order to avoid that the rapid increase of the water level

in the reservoir overpassed the dam height, still under construction.

The second main decision during the emergency was to increase in very short time the dam height and finish the construction of the spillway. To raise the dam, people worked 24 hours per day during one month, making the so called priority filling, in a record time. Although necessary, the disadvantage of this fill is that it was constructed during severe rainy period, probably compacted with water content well above the optimum and with poor compaction control, for what it may present stability and infiltration problems when subject to important hydraulic pressures or hydrodynamic waves. The spillway was finally constructed and it is supposed that it will work properly; nerveless it depends on the good functioning of the filling.

Related to vulnerability reduction, people from Puerto Valdivia, Tarazá and Cáceres were evacuated but considering a moderate flooding scenario, however, in front of a possible dam break, evacuation needs to be too much extensive and require specific emergency plans. It is important to say that maps of possible affectation area for dam break scenario were not available in that moment and now (October 2018) the only susceptibility maps for dam break that may be publically consulted are those elaborated independently by Vargas (2018). This kind of maps is the necessary tools to identify safe temporary shelters.

An important and effective action taken by the project's owners was to increase the monitoring system and to have real time information of many variables related to dam and slopes stability but it is necessary to have specific action plans in case of variation of certain variables that indicate eventual instability problems.

According to EPM monitoring consists of: Radar Interferometry and LIDAR Radar, hydrometry measurements, drones to inspect the dam area and surrounding slopes, geotechnical instrumentation (piezometers, inclinometers), TV cameras and meteorological instruments. A unified command post was stablished and this is the entity in charge of stablishing alert conditions in the area of influence of the dam project. Monitoring information and risk alerts are available by internet in real time panel post as shown in Fig. 6.

Despite the installed monitoring system, It is important to review the required evacuation time in the different towns downstream, because experience from previous events show that is not easy to evacuate people without opportune advice and previous and frequent exercises. The case of the recent dam failure in Laos (23 July 2018) that killed 40 people with more than 90 missing (wykipedia, 2018) highlights these types of problems. Ives (2018) in a report for The New York Times writes: "The day before this week's catastrophic dam failure in Laos, the companies building the dam knew that it was deteriorating, and one of them saw a potential trouble sign three days in advance. Yet many people living downstream received no warning of the deadly flood that was about to sweep away villages, farms, livestock and people".

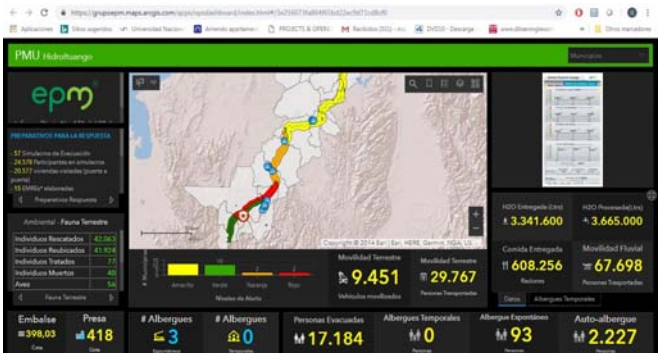

Figure 6. Real time panel post. Technical and logistic variables are indicated in the panel (EPM, 2018b).

Conclusions

The Hidroituango dam project is the most important hydroelectric project in Colombia. It was expected to start working on December 2018, however, due to the collapse of a diverse tunnel in May 2018, and the previous clogging of other two diversion tunnels, water had to be evacuated trough the powerhouse and the whole project entered into a critical risk condition for possible dam failure.

The construction problems and the risk management during the emergency have left some important lessons: large projects that may significantly affect people and induce risk conditions, require rigorous supervision by technical authorities and by external technical and social observers, to identify, in advance, potential problems that may put people and the project itself at risk. This supervision has to be carried in the different project stages: pre-feasibility, feasibility, design and construction and confidentiality clauses should not reduce the possibility of that external control.

Redundancy of critical elements that may affect the project safety is required and the excess of confidence to reduce construction time and costs, may derive in critical risk situations as those described here.

Very high risk conditions in Hidroituango project has not cessed and affected people is still suffering and they require a definite and fear solution.

Monitoring, emergency plans and evacuation exercises are recommended, particularly to check if evacuation time for dam break scenario is enough, because probably is not.

Acknowledgments

The Author thanks the professors Jaime Ordoñez, Felix Hernández, Carlos Cubillos and Modesto Portilla from the National University of Colombia in Bogotá, for their valuable contributions to understand the project problems and to put into the public opinion the delicate risk situation in Hidroituango project.

References

Association of State Dam Safety Officials. (2018). Dam failures and incidents. URL:https://damsafety.org/dam-failures). [Last accessed: 26 October 2018]

Dam Safety Officials of the USA. (2018). Dam failures and incidents. URL: https://damsafety.org/dam-failures. [Last accessed: 29 October 2018].

El Pais.com (2018a). Cronología: esta es la historia de la crisis de Hidroituango que tiene en alerta al país. URL:ttps://www.elpais.com.co/colombia/cronologia-esta-es-la-historia-de-la-crisis-de-hidroituango-que-tiene-en-alerta-al-pais.html. [last accessef: 25 October, 2018]

El País.com (2018b). Más de 8000 personas continúan en zonas de albergues en Hidroituango. URL: https://www.elpais.com.co/colombia/mas-de-8-200-personas-continuan-en-albergues-en-zona-de-hidroituango.html. [last accessed: 27 October, 2018].

El Tiempo (2018). Decretan calamidad pública por alto riesgo en Hidroituango.. URL: https://www.eltiempo.com/colombia/medellin/decretan-calamidad-publica-por-alto-riesgo-en-hidroituango-217386. [Last accessed: 22 October 2018]

EPM (2015). Las principales obras físicas de Hidroituango. In: el Colombiano.com. Hace un año se cambió el curso del río Cauca. URL: http://www.elcolombiano.com/antioquia/hace-un-ano-se-cambio-el-curso-del-cauca-en-ituango-FY1302456. [last accessed: 23 October 2018].

EPM (2018a). epm.com.co. URL: https://www.epm.com.co/site/home/sala-de-prensa/noticias-y-novedades/comunicado-proyecto-hidroelectrico-ituango/preguntas-y-repuestas-ituango. [Last accessed: 19 October 2018].

EPM (2018 b). epm.com.co URL: https://grupoepm.maps.arcgis.com/apps/opsdashboard/index.html#/3e256073fa864f65bd22ec9d71cd8cf0. [Last accessed: 25 October 2018].

IDEAM, (2015). Estudio Nacional del Agua 2014. IDEAM (Eds). Bogotá D.C. (ISBN_978-985-8067-70-4).

IGAC, (2018). Geoportal. Mapas Nacionales. URL: http://geoportal.igac.gov.co/es/contenido/mapas-nacionales. [Last accessed: 18 October 2018).

Ives, M. (2018). A Day Before Laos Dam Failed, Builders Saw Trouble. The New York Times. July 26, 2018. URL: https://www.nytimes.com/2018/07/26/world/asia/laos-dam-collapse.html. [Last accessed: 20 October 2018].

Martinez, N. (2019). Publimetro.co. URL: https://rm.metrolatam.com/pdf/2018/05/16/20180516_bogota.pdf. [Last accessed: 19 October 2018].

Movimiento Rios Vivos Antioquia. (2018). Riosvivosantioquia.org. URL: https://riosvivosantioquia.org/. [Last accessed: 25 October 2018].

RCN RADIO (2018). Gobernador de Antioquia reveló los ocho errores de EPM en Hidroituango. URL: https://www.rcnradio.com/colombia/antioquia/gobernador-de-antioquia-revelo-los-ocho-errores-de-epm-en-hidroituango. Last accessed: 29 October 2018].

Rogers, J.D. (2006). Lessons learned from the St. Francis Dam Failure. Geo-Strata 6(2):14-17.

Ureña, A, Cardona, M, (2018). Eltiempo.com. URL: https://www.eltiempo.com/colombia/medellin/explicacion-de-la-emergencia-de-hidroituango-mapas-videos-y-fotos-219014. [Last accessed: 25 October 2018].

Vargas, G. (2018). Diez zonas de amenaza del río Cauca frente al escenario de desastre del río Cauca. UN Periodico Digital. URL: http://unperiodico.unal.edu.co/pages/detail/diez-zonas-de-amenaza-del-rio-cauca-frente-al-escenario-de-desastre-en-hidroituango/. June 6, 2018. [Last accessed: 22 October 2018]

Wykipedia (2018). 2018 Laos Dam Collapse. URL: https://en.wikipedia.org/wiki/2018_Laos_dam_collapse. [Last accessed: 29 October 2018]

You, L, Li, Chen, Min, Xu and Xiaolei,T. (2012). Review of Dam-break Research of Earth-rock Dam Combining with Dam Safety Management. 2012 International Conference on Modern Hydraulic Engineering. Procedia Engineering 28 (2012) 382 – 388

Review of remedial measures adopted for rainfall-induced landslides in Nilgiris, India

V Santhosh Kumar (1), S S Chandrasekaran (2)

1) Research Scholar, School of Civil Engineering, Vellore Institute of Technology (VIT), Vellore, Tamil Nadu (632014), India,

2) Professor, School of Civil Engineering, Vellore Institute of Technology (VIT), Vellore, Tamil Nadu (632014), India,

e-mail: chandrasekaran.ss@vit.ac.in.

Abstract: High intense rainfalls trigger frequent and massive landslides in mountain ranges of Nilgiris district of the state of Tamil Nadu in India. Government of India categorised this area as severe to high landslide prone area. The present study reviews the landslide remedial measures adopted in the Nilgiris region. So far in Nilgiris, conventional type remedial measures such as masonry retaining walls, cantilever reinforced concrete retaining walls, drainage culverts and gabion walls are constructed. The performance of these remedial measures during rainfalls in successive monsoons needs much to be desired with repeated failures of retaining walls in Chinnabikatty and many other locations along Mettupalayam–Ooty road network. Hence, it is necessary to adopt advanced, effective and sustainable remedial systems such as stabilising piles with vertical drainage shafts connected to surface drains, subsurface horizontal drains with surface shotcreting, check dams attached with high tensile steel nets/mesh to reduce debris flow, rockfall protective systems, retaining walls incorporated with horizontal drains, soil nailing, ground anchors and Reinforced Earth walls in the Nilgiris region. The paper deals with a case study of retaining wall failure at Coonoor location in Nilgiris. Numerical analysis was performed and causes of slope and retaining wall failure were reported.

Keywords landslides, rainfall, remedial measures,

Introduction

Rainfall induced landslide is a major natural hazard in India as fifteen percent of Indian landmass is prone to low to severe landslides. Rainfall induced landslides have been reported in Nilgiris district of Tamil Nadu state, Uttarkand state, Kozhikode and Idukki districts of Kerala state in the recent past. Nilgiris district is a part of western Ghats located in north western side of Tamil Nadu state of India (Fig.1). The Nilgiris district is well-known tourism place in India as hill station and also famous for tea and coffee plantation. The Nilgiris lies between latitude and longitude ranges 11°12'N to 11°37'N and 76°30' E to 76°55'E. Nilgiris mountain ranges receives an average rainfall of 1500 to 3000 mm (Senthilkumar et al. 2016) and average temperature of 15 °C (59 °F). The Nilgiris district is located in seismic zone III (IS 1893: 2016). The district has an elevation from 1000 to 2630 m above mean sea level (MSL) (Jaiswal 2011). As per Landslide Hazard Zonation Atlas of India, the Nilgiris district is designated as high to severe landslide hazard zone (Thennavan et al. 2016). Rainfall is considered as a one of the major factors for triggering of landslides in Nilgiris mountain ranges which receive high annual and seasonal rainfall with high intensity.

Many rainfall-induced landslides have been reported in the Nilgiris district. Some of the major landslides are, 1824 Sispara Ghat road landslide at Kundah hills, 1865 Ooty landslide, 1881 Kotagiri-Mettupalayam road slide, 1990 Kundah hills landslide, 1902 Coonoor, Kotagiri Landslides, 1993 Marappalam landslide, 1998 Mettupalayam to Coonoor road landslide, 2006 Burliyar, Silver bridge, Kallar landslides, 2009 Marappalam, Achanakkal, Madithorai, Kattabettu, Chinnabikatty, Aravankadu, Coonoor Ghat roads, Hillgroove and Kurumbadi landslides (Ganapathy et al. 2010, Senthilkumar et al. 2016, 2017a and 2018). Cut slopes along transportation corridors (national highways, state highways and Nilgiris Mountain Railway (NMR)) are most vulnerable to landslides. In the year 2009, landslides occurred in more than 300 locations in Nilgiris, and resulted in severe damages to infrastructural facilities (Chandrasekaran et al. 2013a).

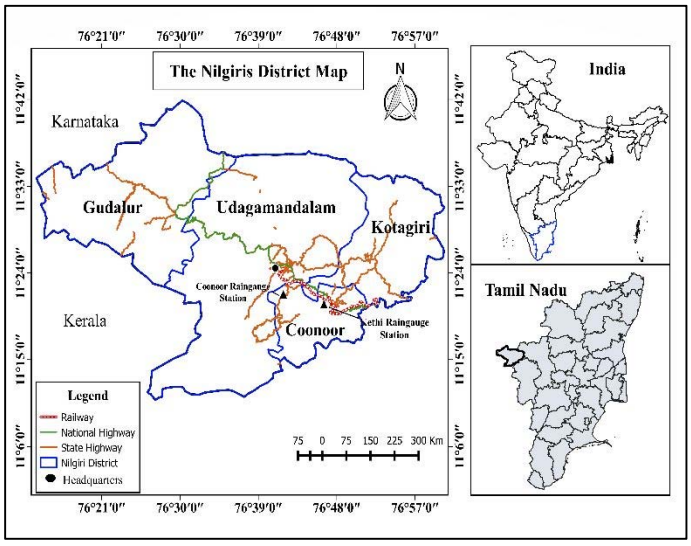

Figure 1 Location map of the Nilgiris district.

Remedial measures practiced in Nilgiris:

So far in Nilgiris, only conventional remideal measures such as gravity retaining walls, cantilever retaining walls and drinage culverts are used as protective systems. Various remedial measures adopted in Nilgiris are depicted in figs. (2 to 9). Fig. 2 shows the gravity retaining wall constructed along Mettupalayam-Ooty highway for widening of road. Marappalam 2009 landslide damaged the Mettupalayam-Coonoor road for about 100 m width. A gravity retaining wall with drainage culvert and weep holes were constructed in Marappalam landslide location as shown in fig. 3. Fig.4 shows the gravity retaining wall in Madithorai village located along Ooty-Kotagiri highway. The retaining wall was constructed after the shear failure of slope occurred during 2009 rainfall that damaged half of the road. The retaining wall constructed with weep holes to dissipate the porewater pressure in backfill soil to protect the slope from future rainfall. Fig. 5 shows the gravity retaining wall constructed at Chinnabikatty location where landslide occurred in the 2009. A gravity retaining wall constructed to support a school building in Lovedale town near Ooty is shown in fig. 6. The major landslide occurred at Aravankadu made damages to Nilgiris mountain railway line. The subgrade soil and railway track ballast were swept away due to mudflow (fig. 7a). The reinforced concrete cantilever retaining wall and bridge constructed at Aravangadu 2009 landslide location is shown in fig. 7b. A cantilever retaining wall constructed to support a vertical cut at Ooty is shown in fig. 8. Gabion walls with steel mesh are constructed at many locations in Nilgiris. A gabion wall constructed at Mettupalayam – Ooty highway is shown in fig. 9.

Figure 2 Gravity retaining wall constructed along Mettupalayam - Ooty Highway

Figure 3 Retaining wall at Marappalam 2009 landslide location

Figure 4 Retaining wall at Madithorai village, Ooty – Kotagiri highway

Figure 5 Retaining wall at Chinnabikatty
(a) Top view from road (b) Over all view from toe

Figure 6 Retaining wall supporting school building at Lovedale, Ooty,

Figure 7 Aravankadu 2009 landslide (a) View of landslide (b) Retaining wall near new railway bridge

Figure 8 Cantilever retaining wall at Ooty

Figure 9 Gabion walls constructed along Mettupalayam – Coonoor highway

Case study- Coonoor retaining wall failure

The site considered for this study is located at Coonoor in the Nilgiris district. Series of buildings were constructed at steep slope supported by reinforced concrete retaining walls as shown in fig. 10a. Retaining walls were constructed in three steps. No weep holes or drainage provisions were provided. During heavy rainfall in November 2009, the retaining walls failed along with sliding of soil which led to exposure of foundation of buildings (Fig. 10b and c). The retaining walls at top was damaged totally, with middle and bottom retaining walls tilted substantially (Fig. 10).

(a)

(b)

(c)

Figure 10 Coonoor retaining wall failure (a) View of buildings and retaining wall, (b) and (c) failure of retaining wall

Laboratory experiments were carried out on soil samples collected from sliding surface. Index properties such as grain size analysis, specific gravity, consistency limits and engineering properties such as shear strength, permeability were evaluated according to ASTM standards and as well as Indian standards (Chandrasekaran et al. 2013). The soil sample has high percentage of fines. The fines have liquid limit of 45% and plastic limit of 25%. Soil has very low value of coefficient of permeability. The soil is classified as lean clay with sand (CL) as per Unified Soil Classification System (Chandrasekaran et al. 2013).

Numerical analysis of the slope is carried out by finite difference method using FLAC2D programme (Itasca. 2016). The sectional profile of slope, retaining wall and buildings are depicted in fig. 11. The stability analysis is carried out by strength reduction method. The soil is represented by orthogonal grid elements (fig.12). The partial difference equations and stress strain displacement evaluations are used to determine the maximum displacement in soil model. The factor of safety (FOS) was calculated by strength reduction method which can reduce the shear strength of soil mass until soil slope fails (Cala et al. 2004).

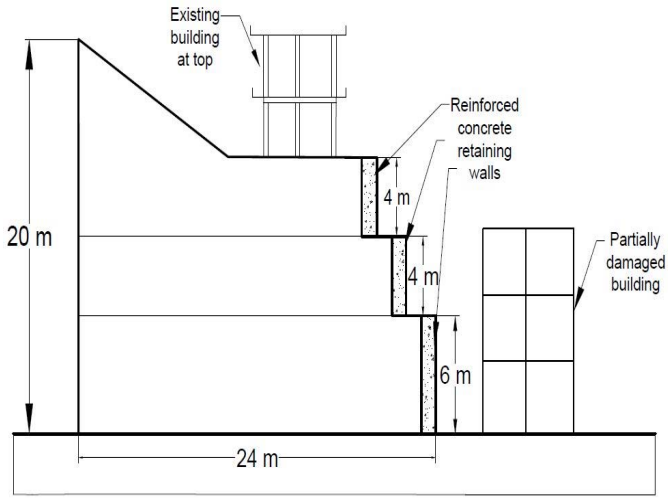

Figure 11 Sectional profile of slope, retaining wall and buildings

Properties of soil and reinforced concrete retaining wall are considered for the analysis as per authors earlier reported study (Chandrasekaran et al. 2013a). The geometry of the structure and boundary conditions adopted for the analysis are shown in fig. 12. The displacement of retaining wall is depicted in fig. 13. The displacement contours (fig. 14a) and shear strain increments (fig .14b) show the slip surface which agrees with field observations.

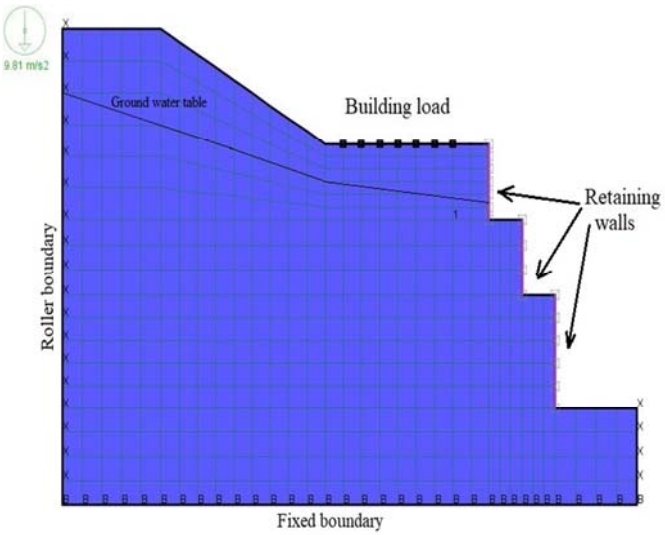

Figure 12 Geometry of slope showing grid elements and boundary conditions

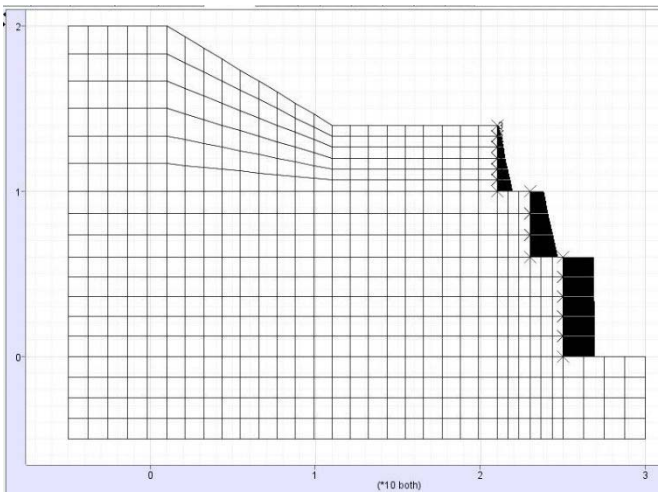

Figure 13 Linear displacement of retaining walls

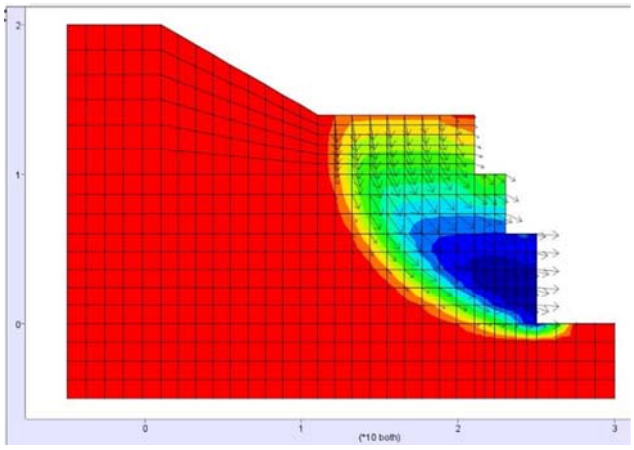

(a)

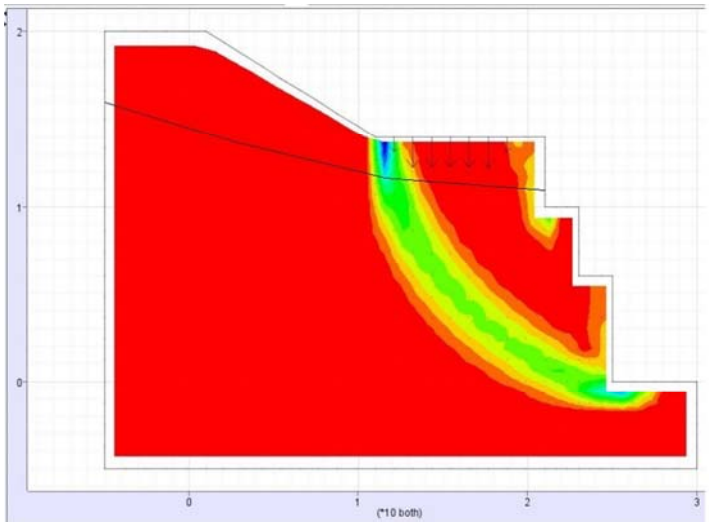

(b)

Figure 14 Numerical analysis (a) Displacement contours (b) Shear strain increment

Summary

The present study provides an overview of remedial measures practiced in Nilgiris for rainfall induced landslides. Based on the review, it can be stated that the remedial measures practiced in Nilgiris comprising of gravity retaining walls, cantilever retaining walls, gabion walls and drainage culverts. As the preventive measures adopted for rainfall induced landslides are not site specific and due to improper maintenance of drainage systems, the retaining walls and gabion walls experiencing frequent failures which emphasis the importance of site specific remedial measures. The numerical analysis of Coonoor retaining wall revealed that, the saturation of soil mass due to rainfall infiltration along with surcharge load on the slope crest led to increase in pore water pressure which intern reduces the shear strength of the soil along the critical slip surface caused failure of retaining walls. As can be observed from the shear strain increment contour, the soil behind top two retaining walls were experienced higher strain value which completely displaced the top two retaining walls as noticed from the field observation. From the study it can be suggested that, the use of advanced, effective and sustainable site specific remedial systems will enhance the stability of slopes and efficiency of remedial measures in Nilgiris district.

References

ASTM D3080-04 (2004) Standard test method for direct shear test of soils under consolidated drained conditions. ASTM International, USA.

Cala, M., Flisiak, J. and Tajdus, A. (2004) Slope stability analysis with modified shear strength reduction technique. Proc. Landslides'04, Rio de Janeiro.

Chandrasekaran SS (2010) Assessment of damages induced by recent landslides in Ooty, Tamil Nadu. In: Proceedings of the Indian geotechnical conference (IGC-2010) GEOtrendz, IIT Bombay, Mumbai, India, Dec 16–18, pp 687–688.

Chandrasekaran SS, Sayed Owaise R, Ashwin S, Jain Rayansh M, Prasanth S, Venugopalan RB (2013a) Investigations on infrastructural damages by rainfall-induced landslides during November 2009 in Nilgiris, India. Nat Hazards 65(3):1535–1557.

Chandrasekaran, S. S., S. Elayaraja, and S. Renugadevi. 2013b. "Damages to transport facilities by rainfall-induced landslides during November 2009 in Nilgiris, India." In Vol. 6 of Landslide Science and Practice: Risk Assessment, Management and Mitigation, 2nd World Landslide Forum, edited by C. Margottini, P. Canuti, and K. Sassa, 171–176. Berlin: Springer.

Cruden DM, Varnes DJ (1996) Landslide types and processes. In:Turner AK, Schuster RL (eds) Landslides investigation and mitigation. Transportation research board, US National Research Council. Special Report 247, Washington, DC, Chapter 3, pp. 36–75.

Duncan, J. M. (1996). State of the Art: Limit Equilibrium and Finite-Element Analysis of Slopes. Journal of Geotechnical Engineering, 122, 577-596.

Duncan, J.M. and Wright, S.G. (2005) Soil Strength and Slope Stability, John Wiley & Sons, Inc., Hoboken, NJ.

Ganapathy, G. P., and C. L. Hada. 2012. “Landslide hazard mitigation in the Nilgiris district, India—Environmental and societal issues.” Int. J.Environ. Sci. Dev.3 (5): 497–500. https://doi.org/10.7763/IJESD.2012 .V3.274.

Ganapathy, G.P., Mahendran, K. and Sekar, S.K. (2010). Need and Urgency of Landslide Risk Planning for Nilgiri District, Tamil Nadu State, India, International Journal of Geomatics and Geosciences, 1(1). 30-40.

IS 1893 (2016) Criteria for earthquake resistant design of structures, part 1: general provisions and buildings, B.I.S

Itasca. 2016. FLAC—Fast Lagrangian analysis of continua version 8.0 user’s manual. Minneapolis: Itasca.

Jaiswal P (2011) Landslide risk quantification along transportation corridors based on historical information. ITC doctoral dissertation, The Netherlands.

NDMG (2009) National disaster management guidelines—management of landslides and snow avalanches, a publication of the National Disaster Management Authority. Government of India, New Delhi.

Senthilkumar, V., S. S. Chandrasekaran, and V. B. Maji. 2017a. “Geotechnical characterization and analysis of rainfall-induced 2009 landslide at Marappalam area of Nilgiris district, Tamil Nadu state,India.”Landslides14(5):1803–1814.

Senthilkumar, V., S. S. Chandrasekaran, and V. B. Maji. 2017b. “Overview of rainfall-induced landslide events and importance of geotechnical investigations in Nilgiris District of Tamil Nadu, India.” In Vol. 4 of Proc. of 4th World Landslide Forum, edited by M. Mikos, N. Casagli, and K. Sassa, 281–287. Cham, Switzerland: Springer.

Senthilkumar, V., S. S. Chandrasekaran, and V. B. Maji. 2018. Rainfall-Induced Landslides: Case Study of the Marappalam Landslide, Nilgiris District, Tamil Nadu, India. Int. J. Geomech., vol. 18, no. 9, Sep. 2018.

Improvement of Landslide EWS at Banjarnegara, Central Java, Indonesia

Dwikorita Karnawati[(1)], Munawar[(1,2)], Agus Safril[(1,2)], Rista Hernandi Virgianto[(1,2)], Amir Mustofa Irawan[(1,2)], Suharni [(1,2)], Hapsoro Agung Nugroho[(1,2)] ,Puji Ariyanto[(1,2)]

1) Agency for Meteorology, Climatology, and Geophysics of the Republik of Indonesia (BMKG Indonesia)

2) School of Meteorology, Climatology, and Geophysics (STMKG-BMKG)

Abstract

Sijeruk Village, Banjarnegara is an area prone to landslides. Because it has a high annual rainfall (> 3,000 mm / year), steep topography, and a unique lithological conditions which consist of clay stone above the local fault as known as Kalibening-Wanayasa fault. Landslide early warning which was piloted in Sijeruk Village, Banjarnegara uses the parameters of rainfall, soil moisture, and seismicity. Measurement of rainfall threshold triggers landslides using equation I = 50.256D-0.98 with rain duration between 24 <D <260 hours. Rainfall prediction uses ANFIS method with a correlation value of 0.78. Rainfall prediction using ANFIS is better able to capture irregularities compared to predictions with the ARIMA method. Sijeruk Village has 2 layers of soil which are alluvium soil and mixed gravel with a high resistivity value of 0.37-2.99. Relatively high seismic (kg) susceptibility index values of 5.97761 and 6.64729. The clay layer at a depth of 2-3 m can be a slip surface of soil movement so we need to be aware of the dangers of landslides in this area.

Keywords:landslide, ANFIS, rainfall, EWS

Introduction

Banjarnegara is a region with a high potential for landslides in Central Java, Indonesia. Geographical conditions and high rainfall make this area prone to landslide hazards(Fathani, Karnawati, & Wilopo, 2016). Banjarnegara has a high average rainfall of 3,000 mm / year. The highest rainfall is in the northern Banjarnegara, while the peak of the rainy season is in December-January. In addition to the topographic rainfall factors and soil types in Banjarnegara are also influential on landslides in Banjarnegara. About 75.39% of the area of Banjarnegara has a steep slopes. Approximately 45.04% of the area has a slope of 15-40% covering Madukara, Banjarmangu, Wanadadi, Punggelan, Karang Kobar, Pagentan, Wanayasa, and Kalibening areas. While approximately 30.35% of the area has a slope of over 40% covering the Susukan, Banjarnegara, Sigaluh, Banjarmangu, Pejawaran, and Batur.

Other causes of landslides in Banjarnegara in general are seismic factors and human activities. Local faults such as the Kalibening-Wanayasa Fault in Banjarnegara is alleged to be a trigger of the Earthquakes which also result in landslides as shown in Fig,1. Landslide disaster on 4 January 2006 in Gunungraja Hamlet, Sijeruk Village, Banjarmangu has claimed more than 100 lives with 4 hectares of agricultural damage and more than 100 houses severely damaged (Priyono & Priyana, 2006). Again the same incident happened on the same place on 11 December 2014, resulting in 16 houses being damaged by landslides (Naryanto, 2017).

Based on these conditions, the early detection system for landslide hazards in Banjarnegara, especially in Sijeruk Village and its surroundings is very necessary to reduce the risk and the impact of the landslide.

Establishment of the rainfall threshold as an indicator of landslides in Sijeruk Village, Banjarnegara

Rainfall-induced landslides are occurred as response to hydrological processes that come from the accumulation of precipitation for a specific period of time (Iverson, 2000). Establishment rainfall threshold is necessary to help in analyse the rainfall-induced landslides.

Figure 1 A plain that was once an ancient lake, Kalibening-Wanayasa fault (left and centre) and Ancient Lake of Kalibening (right)

Rainfall can be categorized based on regional coverage, they are global, regional and local. Global rainfall is determined using data available in all parts of the world. The easiest way to define global rain is to find out the value of the lower limit on all the rainfall data recorded that coincide with landslide event. Regional rainfall is defined as a collection of rainfall data in areas that have similar characteristics in terms of meteorology, geology and physiography. Local rainfall is explicit and implicit considering the local climate conditions and geomorphology of a region(von Ruette, Papritz, Lehmann, Rickli, & Or, 2011).

Establishment of the rainfall threshold that causes landslides can be determined through three approaches, they are empirical based model, physical process model and statistical model based on Guzzetti, Reichenbach, Cardinali, Galli, and Ardizzone (2005). Empirical based models are determined by learning the rain conditions that occur at alandslide point. Most empirical modeling shows relatively good results at the location where the model was developed, but it is not appropriate to use it in other places even the characteristic is quite similar (Guzzetti, Peruccacci, Rossi, & Stark, 2007, 2008). The rainfall threshold in the empirical model uses rain observation data near to the landslide location.

In this study, we plot the average rainfall (mm per hour) and rainfall duration using the logarithmic (Intensity - duration / ID) function, and determine the formula for cumulative rainfall (CT Treshold / CT) as the calculated landslide threshold from rainfall (mm) for 3 days and 15 days prior to the 3-day period (Guzzetti et al., 2008), it was reconstructed from the historical landslide data of Banjarmangu for the period 2011 - 2017. Rainfall data when landslides were obtained from Banjarmangu Geophysics Station, and historical data on landslide events were obtained from the Agency for National Disaster Management (BNPB) Banjarnegara, Central Java, Indonesia.

ID curves can be written in a general form, as:

$$I = c + \alpha . D^{\beta} \qquad [1]$$

with,

I = rain intensity (mm/hour),

D = rain duration (hour)

c, α, β = empirical parameters

Fig.2 shows a plot of the Intensity and Rainfall Duration (ID) thresholds for Banjarmangu, reconstructed from the daily rainfall data of Banjarmangu Geophysics Station (converted to mm / hour) during landslides in Banjarmangu. On determining the ID threshold for Banjarmangu area, wet days are determined if rainfall is above 2 mm / day. From Fig.2, it can be seen that the rainfall threshold (ID) in Banjarmangu is determined by $I = 43.2D^{-0.87}$

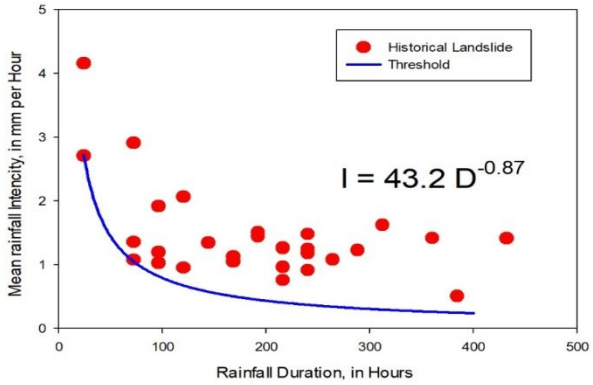

Figure2 Intensity threshold and Rainfall Duration (ID) for Banjarmangu

Because the rain threshold is defined empirically, the equations vary from location to location. Thus, the accuracy of the relationship can be categorized in global, regional and local scope. Table 1 shows 18 models of local scale empirical equations proposed by several researchers,

compared with the empirical equation model of Banjarmangu case.Each of the empirical equations in Table 1 is displayed in a logarithmic curve as in Fig. 2, in order to find out the comparison between the Banjarmangu rainfall ID threshold and the local regions in various other parts of the world.

Table 1 Empirical equations of rainfall intensity threshold - length of time triggering landslides (Guzzetti et al., 2007)

	Authors	Threshold Type	Location	Landslide Type	Equation	Range
1	Cancelli & Nova (1985)	L	Northern Italy	S	$I=44.67D^{-0.78}$	1<D<1000
2	Rodolfo & Agurden (1991)	L	Mayon, Philipine	L	$I=27.3D^{-0.38}$	0.167<D<3
3	Tungol & Regalado (1996)	L	Philipine	L	$I=5.94D^{-1.50}$	0.167<D<3
4	Barbero, et al. (2004)	L	Piedmont, Italy	A	$I=44.668D^{-0.78}$	1<D<1000
5	Zezere et al. (2005)	L	Lisbon, Portugal	A	$I=84.3D^{-0.57}$	0.1<D<2000
6	Dwikorita, et al. (2018)	L	Banjarmangu, Indonesia	Sh	$I=43.2D^{-0.87}$	24<D<260

Notes:

Threshold types: G = global, R = regional, L = local; Landslide type: D = debris, S = soil slips, Sh = shallow landslides, L = lava, A = all; Equation: I = rain intensity (mm / hour), D = duration of rain (hours)

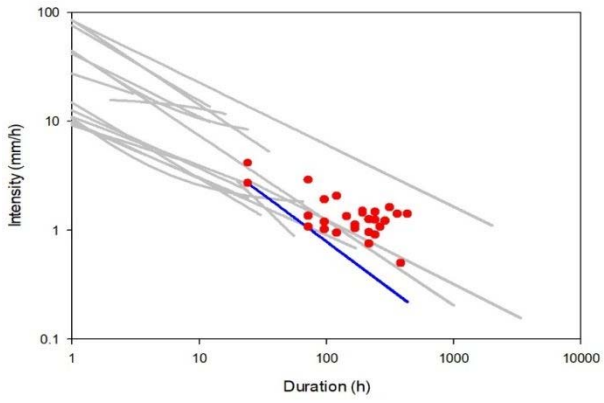

Figure 3 Logarithmic plot function between the Intensity threshold -Duration duration (ID) of the Banjarmangu (blue line) with the Intensity threshold function - Rainfall duration (ID) of other locations (gray line). The red dot is a historical occurrence of landslides in the Banjarmangu

Analysis of Fig. 3 shows that the local threshold of Banjarmangu is slightly smaller than the other locations thresholds. This indicates that at a certain length of time, the prediction of rain that triggers landslides from the local threshold of Banjarmangu is smaller than the average rainfall intensity of the local threshold at other locations.

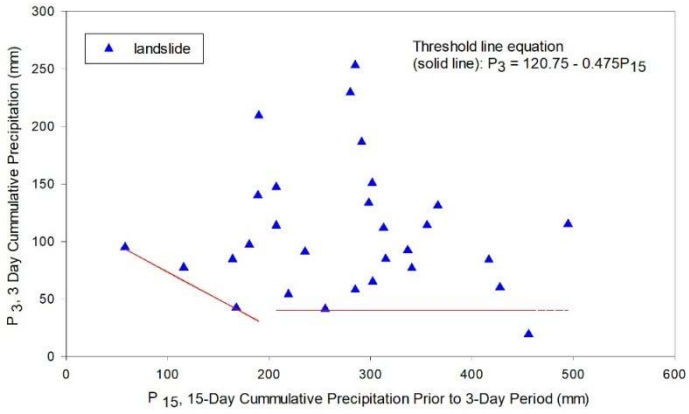

Figure 4 Cumulative rainfall threshold 3 days and 15 days prior the landslide event. P3 is cumulative rainfall 3 days prior the landslide event, while P15 is cumulative rainfall 15 days priorto 3 days of landslide events.

Fig. 4 is an empirical function of the cumulative rainfall threshold 3 days and 15 days prior the landslide event. The cumulative rainfall (CT) threshold equation was introduced by Chleborad (2000) by comparing rainfall 3 days to 15 days prior landslides in a region. For

the Banjarmangu region, the function of the empiric CT equation is P3 = 120.75-0.475P15 for rainfall 15 days prior the landslide event is less than 200 mm, and P3 <40 mm for rainfall 15 days prior the landslide is more than 200 mm.

Rainfall prediction for landslide detection in Sijeruk Village, Banjarnegara

The Banjarnegara region in Central Javais a disaster-prone area, including landslides and earthquakes. Landslides not only cause losses in material but also in human life. High rainfall can increase the potential of landslides in a specific area. The variables of landslide such as slopes, rainfalls, and land uses have been used in several research(Dahal et al., 2008; Sipayung, Cholianawati, Susanti, & Maryadi, 2014). Banjarnegara has a Monsoonal type of rainfall that has one peak of rainy season (Aldrian & Dwi Susanto, 2003). High variability of rainfalls in Banjarnegara as an area in tropical climate region, mainly caused by irregularities in rain patterns due to the La Nina and El Niño phenomena (Ashok, Guan, Saji, & Yamagata, 2004; Chang, Wang, Ju, & Li, 2004). One of strategies to reduce the impact of landslides is to provide early warning information based on the amount of rainfall that will fall. Rain-gauge stations located at Banjarnegara Geophysics Station, Banjarmangu at -7.36 LU and 109.69 BT as shown in Fig. 5.

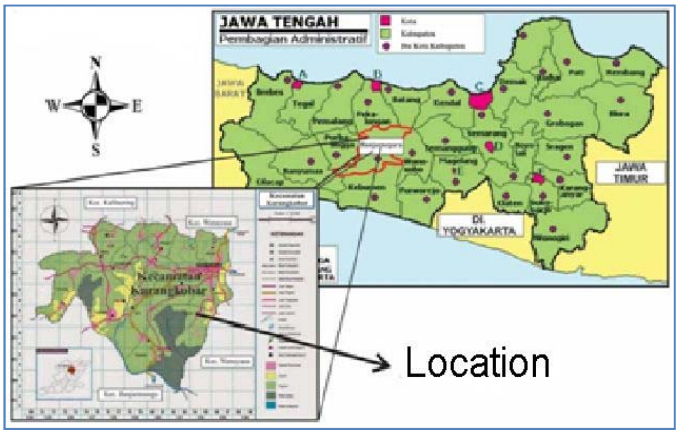

Figure 5 Location of Sijeruk Village, Banjarmangu, Banjarnegara

Rainfall prediction model with model output can be divided into three stages. The first stage is the determination of independent and dependent variables as predictors and predictors. In this stage, the power relations analysis between independent variables (TCW) and dependent (rainfall) in the prediction area is carried out. The next stage, the prediction model is developed using ANFIS and ARIMA. The third stage is to obtain the ability of the model to do reliability analysis.

Rainfall pattern in the Banjarnegara hasa monsoon type rainfall with one peak. The amount of rainfall less than 150 millimeters occurred in June, July, August, September. Rainfall was generally ranged from 350 millimeters to 550 millimeters. Rainfall above 500 millimeters in March and November as shown in Fig. 6

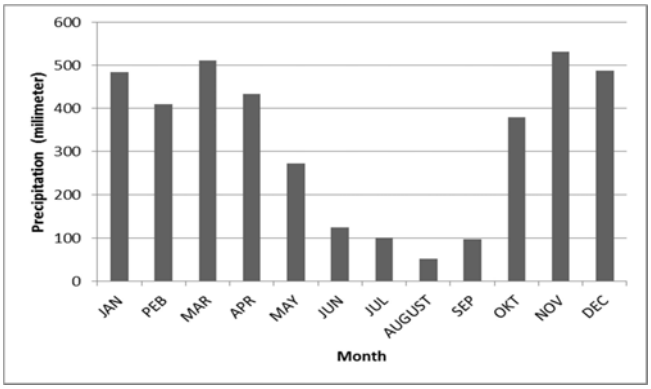

Figure 6Banjarmangu monthly rain pattern in 1997-2011

The prediction with ARIMA (1,1) indicate the monsoon rain pattern. Rainfall can reach above 500 millimeters but the minimum pattern generally has not produced optimal results. Prediction results with independent data were carried out for 3 years in 2012-2015 as in Fig.7.

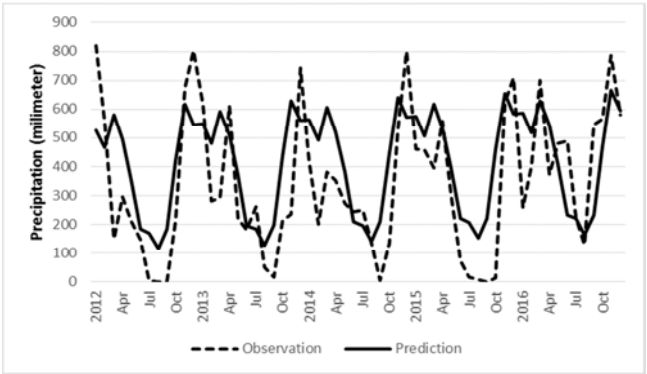

Figure 7. Seasonal rainfall prediction based on ARIMA (thick line) compared to the observations (dashed lines) for 2003-2005 period.

Prediction based on ANFIS using TCW predictors can capture 500 millimeters and extreme minimum rainfall. The pattern of dry season rain can be captured better than based on the ARIMA model, but has not been able to reach the extreme maximum. However, rainfall prediction during the dry season provides information on

the landslides potential due to rain after several dry months that can cause the soil to break and potentially landslide during the rainy season. In general, the prediction and observation of rainfall shows the same pattern and seems to be more accurate in determining the onset of the rainy season as in Fig.8.

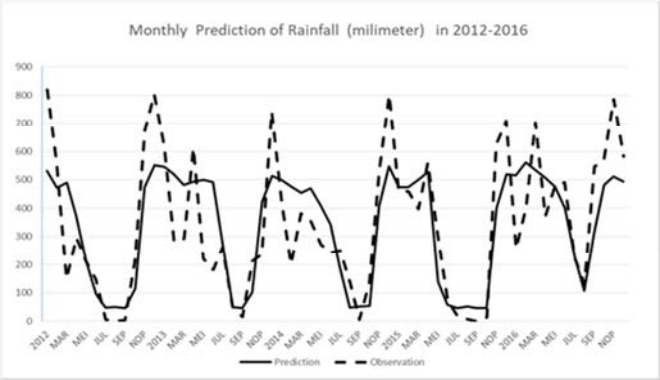

Figure 8. Seasonal rainfall prediction based on (thick line) compared to the observations (dashed lines) for 2012-2016 period.

Quantitatively, the predicted results are analyzed based on the correlation, RMSE and values between predictions and observations. Prediction based on ARIMA method has correlation of 0.69 and RMSE of 157 mm compared with ANFIS method that has correlation of 0.78 and RMSE of 119 mm. We can see there is an increase in RMSE accuracy by 25%. From these results, prediction based on ANFIS are better able to capture irregularities in rain pattern than prediction with ARIMA method.

Verify rainfall predictions as a result of applying the model

Quantitatively, the predicted results are analyzed based on the correlation values and values between predictions and observations and RMSE values. The prediction results with the ARIMA method with a correlation value of 0.69 (157 millimeters) compared to the ANFIS method with a correlation value of 0.78 (119 millimeters) there is an increase in RMSE accuracy by 25%. From these results predictions using ANFIS are better able to capture irregularities compared to predictions with the ARIMA method.

Lithological structure conditions triggering landslides in Sijeruk Village, Banjarnegara

The results of the interpretation of 4 geoelectric trajectories with wenner configuration showed subsurface lithology in Sijeruk Village, Banjarmangu, Banjarnegara composed of clay rocks at the bottom with resistivity values of 0 to 3 ohm meters indicated in dark blue to light blue, then soil cover is alluvium with resistivity values from 8.47 to 542 ohm meters which is shown in green to brownish red.

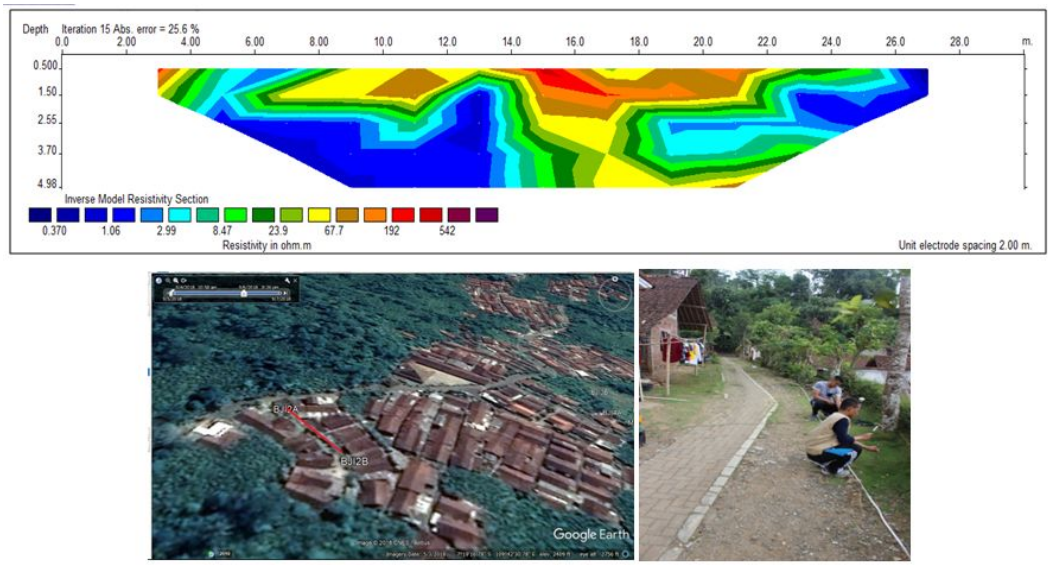

Figure 9 2D cross-sectional model on the first track in Sijeruk Village (above) and measurement location (bottom)

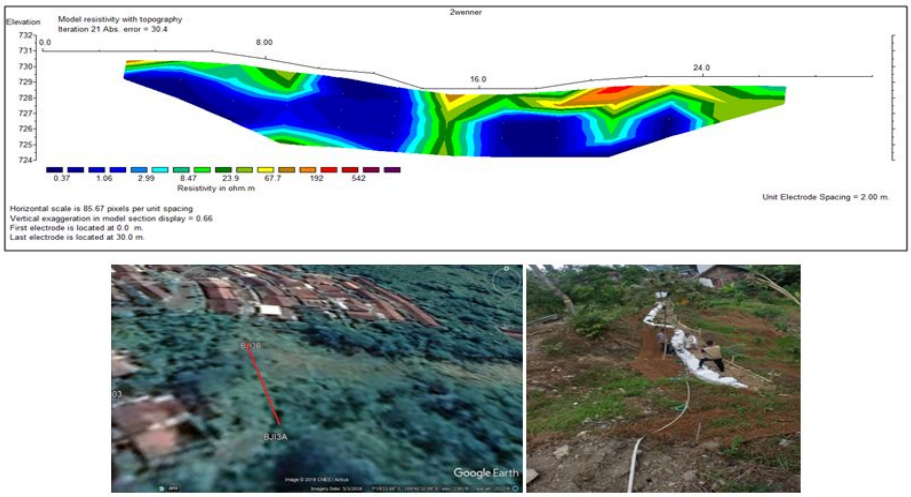

Figure 10 Model cross section of 2D resistivity on the second track in Sijeruk Village (above) and measurement location (bottom)

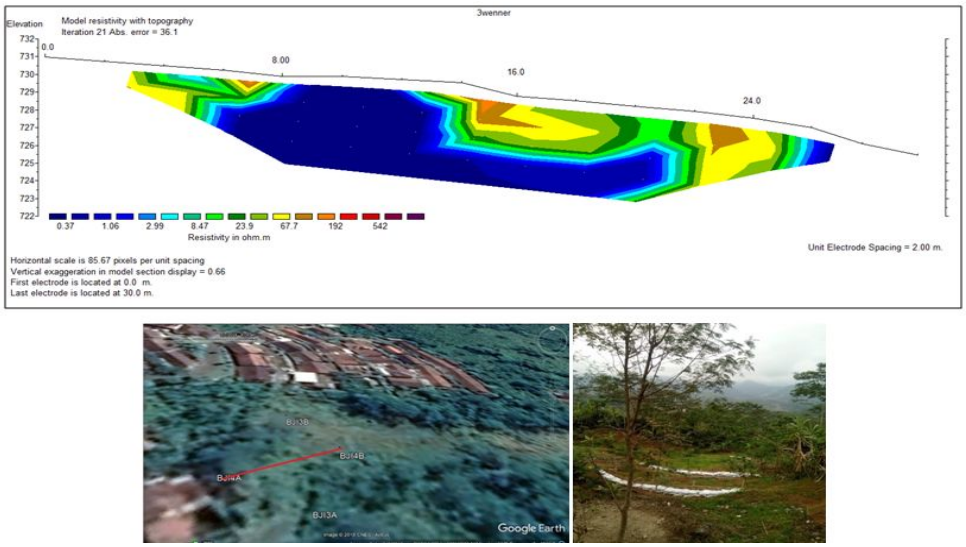

Figure 11 Model of 2D resistivity section on the third trajectory in Sijeruk Village (above) and measurement location (bottom)

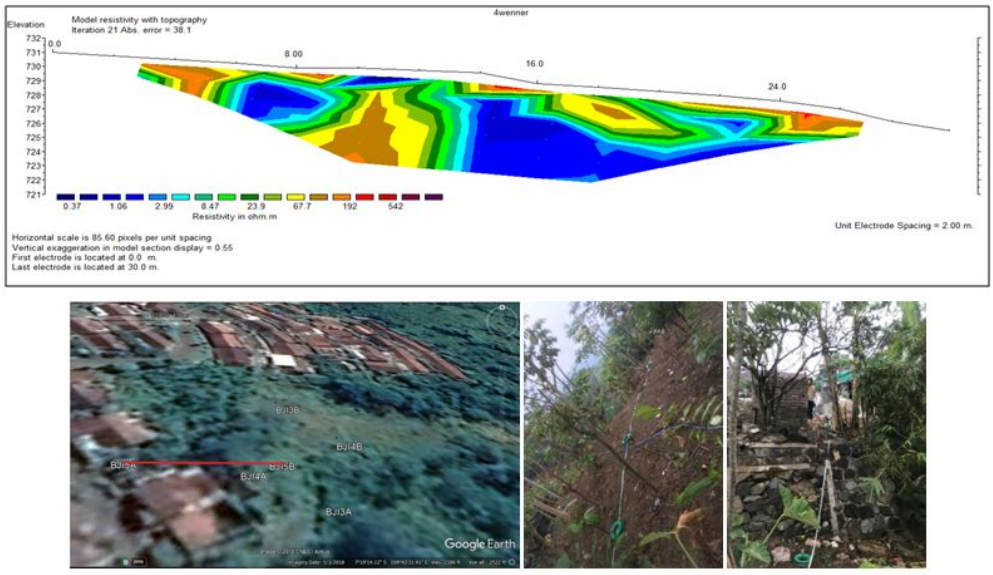

Figure 11 2D cross-sectional model on the fourth track in Sijeruk Village (above) and measurement location (bottom)

From the results of inversion, it shows generally in the study area there are 2 layers of soil which are composed of alluvium soil and mixed with gravel with a high enough resistivity value between 2.39 to 542 ohmmeter as a cover layer, then underneath there is clay soil material with a range of rock resistivity values are quite low between 0.37 to 2.99 ohmmeter. The clay layer which is at a depth of ~ 2-3m is thought to be a slip field of ground motion in this area. The slope and slope area is quite steep up to more than 30 ° and the type of landslide in the research location is rotational landslide.

Seismic vulnerability index for landslide detection in Sijeruk Village, Banjarnegara

Microtremor is vibration on the ground surface with low amplitude caused by natural causes such as wind, human activity, vehicle noise and others(Mirzaoglu & Dýkmen, 2003). Microtremor studies are often used in local site analysis. One method is HVSR (Horizontal to Vertical Spectral Ratio). HVSR analysis can be used to obtain local dynamic characteristics (Nakamura, 1989). Mathematically formulated by:

$$HVSR = \frac{\sqrt{(A_{east}(f))^2+(A_{north}(f))^2}}{(A_{vertical}(f))} \quad [2]$$

A_{east}= Spectral Amplitude EWComponents

A_{north}= Spectral Amplitude NSComponents

$A_{vertical}$= Spectral Amplitude Components

Data obtained from microtremor measurements in trace format. Then it is converted using DataPro software into a miniseed format so that it can be processed using Geopsy to generate the HVSR curve. To get the previous H / V curve, windowing must be done to eliminate interference from other activities other than ambient noise. From this curve, the dominant frequency value and amplification factor are obtained. Then the calculation of the value of seismic vulnerability (Kg). Seismic vulnerability index is calculated based on the following equation (Nakamura, 2000):

$$K = \frac{{A_0}^2}{f_0} \quad [3]$$

K_g = Vulnerability Index

A_0 = Amplitude H/V

f_0 = Dominant frequency (Hz)

$A_0$and$f_0$obtained from microtremor measurements with HVSR method.

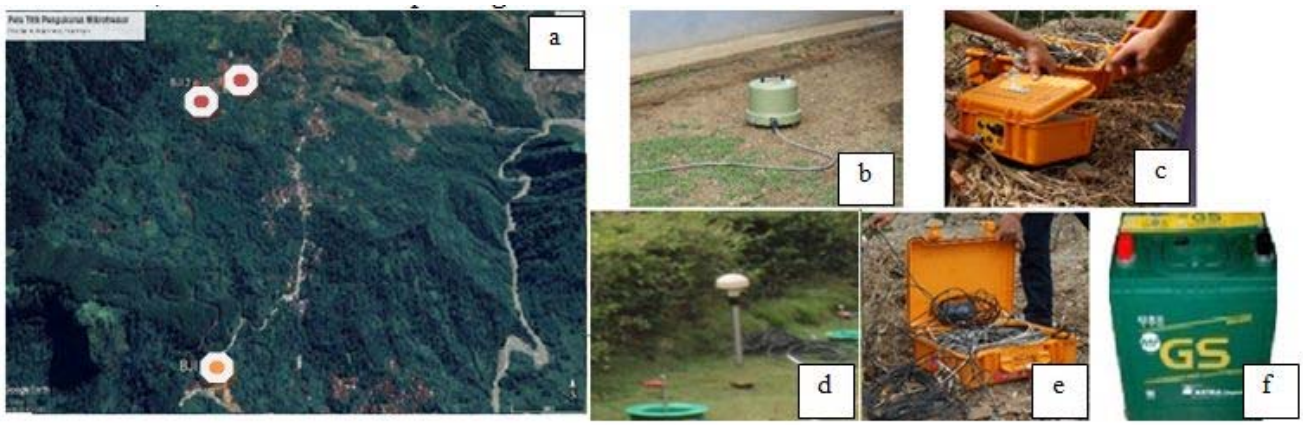

Figure 11. Location of measurements (a), Seismometer (b), Data logger (c), GPS (d), Connector (e), Accu 12 Volt (f)

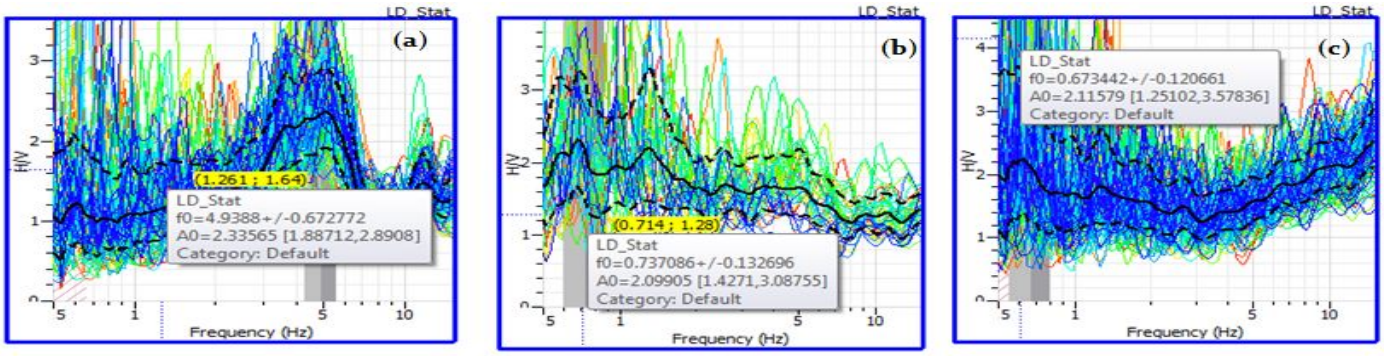

Figure 12 Results of the H / V curve at point (a) BJI1 (b) BJI2 and (c) BJI3

From the curve above, the values of Ao and fo are obtained which are used as inputs in calculating the value of seismic vulnerabilities. Seismic vulnerability index (Kg) shows the physical magnitude of vulnerability of an area affected by earthquake shaking or rock layers. The greater the value of the seismic vulnerability index, the more vulnerable the area is affected by shocks(Mala, Susilo, & Sunaryo, 2015).

Table 1. Results of Calculation of Seismic Vulnerability Index (K_g)

Location	A_0	f_0	K_g
BJI1	2,33565	4,9338	1,10457
BJI2	2,09905	0,737086	5,97761
BJI3	2,11579	0,673442	6,64729

From the table above shows that the locations of BJI2 and BJI3 have relatively high seismic vulnerability indexes. This indicates that the local site location of BJI2 and BJI3 is in the soft category. So that the movement of the soil is relatively high. Whereas the location of BJI1 has a relatively low seismic vulnerability index value. So that the impact will not be too severe as in the BJI2 and BJI3 locations.

BJI2 and BJI3 locations are locations that are likely to be affected more severely in the event of shocks or other ground movements. This is because the value of the seismic vulnerability index (kg) is relatively high at these locations, which are respectively valued at 5,97761 and 6,64729.

Early Warning System (EWS) landslide in Sijeruk Village, Banjarnegara.

Measurement of rainfall parameters, soil moisture, and soil movements can be monitored by accessing the website https://thingspeak.com/channels/539055.

If the user accessing via smartphone can download the Thing View application on the Play Store then input the 539055 channel to view the graph in realtime. The following is the system view on websites and smartphones as in Fig. 13.

Figure 13 (a) Trial of EWS instruments in Sijeruk Village, Banjarnegara, (b) display of measured parameters on the website and (c) Smartphone

Conclusions

We define the threshold formula based on the lower-bound threshold line as a power function of I=43.2D-0.87 represent that with increased rainfall duration the minimum intensity likely to trigger slope failures decreases linearly against time. Cumulative rainfall threshold also identified in this study as P3=120.75–0.475P15 in addition to the empirical intensity-duration threshold to assess the impact of accumulated rainfall 3-day to 15-day prior to the landslide occurrence.Prediction based on ANFIS using total column water as predictors can capture rain pattern with 500 millimeters and minimum extreme rainfall. The rainpattern of dry season can be captured better than based onARIMA model, but has not been able to reach the maximum extreme rainfall. In general, the rainfall predictionand observation show a same pattern and more accurate in determining the onset of the rainy season. Banjarnegara has relatively high seismic vulnerability indexes and movement of the soil is relatively high. Several points at Banjarnegara are likely to be affected more severely in the event of shocks or other ground movements.

Acknowledgments

We wish to thank our colleagues at the Agency for Meteorology, Climatology and Geophysics of Indonesia (BMKG) and the other members of Landslides Research Group at School of Meteorology Climatology and Geophysics (STMKG) for their contributions in this work.

We also would like to thank Agency for National Disaster Management (BNPB) for providing the landslide data.

References

Aldrian, E., & Dwi Susanto, R. (2003). Identification of three dominant rainfall regions within Indonesia and their relationship to sea surface temperature. *International Journal of Climatology, 23*(12), 1435-1452.

Ashok, K., Guan, Z., Saji, N., & Yamagata, T. (2004). Individual and combined influences of ENSO and the Indian Ocean dipole on the Indian summer monsoon. *Journal of Climate, 17*(16), 3141-3155.

Chang, C., Wang, Z., Ju, J., & Li, T. (2004). On the relationship between western maritime continent monsoon rainfall and ENSO during northern winter. *Journal of Climate, 17*(3), 665-672.

Chleborad, A. F. (2000). *Preliminary method for anticipating the occurrence of precipitation-induced landslides in Seattle, Washington*: Citeseer.

Dahal, R. K., Hasegawa, S., Nonomura, A., Yamanaka, M., Masuda, T., & Nishino, K. (2008). GIS-based weights-of-evidence modelling of rainfall-induced landslides in small catchments for landslide susceptibility mapping. *Environmental Geology, 54*(2), 311-324.

Fathani, T. F., Karnawati, D., & Wilopo, W. (2016). An integrated methodology to develop a standard for landslide early warning systems. *Natural Hazards Earth System Sciences, 16*(9), 2123-2135.

Guzzetti, F., Peruccacci, S., Rossi, M., & Stark, C. P. (2007). Rainfall thresholds for the initiation of landslides in central

and southern Europe. *Meteorology atmospheric physics, 98*(3-4), 239-267.

Guzzetti, F., Peruccacci, S., Rossi, M., & Stark, C. P. (2008). The rainfall intensity–duration control of shallow landslides and debris flows: an update. *Landslides, 5*(1), 3-17.

Guzzetti, F., Reichenbach, P., Cardinali, M., Galli, M., & Ardizzone, F. (2005). Probabilistic landslide hazard assessment at the basin scale. *Geomorphology, 72*(1-4), 272-299.

Iverson, R. M. (2000). Landslide triggering by rain infiltration. *Water resources research, 36*(7), 1897-1910.

Mala, H. U., Susilo, A., & Sunaryo, S. J. N. B. (2015). Microtremor and Geolistrik Resistivity Study Around the Trans Timor Primary Arterial Road for Disaster Mitigation. *3*(1), 024-034.

Mirzaoglu, M., & Dýkmen, Ü. J. J. o. t. B. G. S. (2003). Application of microtremors to seismic microzoning procedure. *6*(3), 143-156.

Nakamura, Y. (2000). *Clear identification of fundamental idea of Nakamura's technique and its applications.* Paper presented at the Proceedings of the 12th world conference on earthquake engineering.

Naryanto, H. S. (2017). Analisis Kejadian Bencana Tanah Longsor Tanggal 12 Desember 2014 Di Dusun Jemblung, Desa Sampang, Kecamatan Karangkobar, Kabupaten Banjarnegara, Provinsi Jawa Tengah. *Jurnal ALAMI: Jurnal Teknologi Reduksi Risiko Bencana, 1*(1), 1-10.

Priyono, K. D., & Priyana, Y. (2006). Analisis Tingkat Bahaya Longsor Tanah di Kecamatan Banjarmangu Kabupaten Banjarnegara.

Sipayung, S. B., Cholianawati, N., Susanti, I., & Maryadi, E. (2014). Development of empirical equation model in predicting the occurrence of landslide at watershed of Citarum (West Java) based on the TRMM satellite data. *Jurnal Sains Dirgantara, 12*(1).

von Ruette, J., Papritz, A., Lehmann, P., Rickli, C., & Or, D. (2011). Spatial statistical modeling of shallow landslides—Validating predictions for different landslide inventories and rainfall events. *Geomorphology, 133*(1-2), 11-22.

Development of landslide detection system based on rainfall prediction and seismic aspect in Banjarnegara, Central Java, Indonesia

Dwikorita Karnawati[(1)], Munawar[(1,2)], Agus Safril[(1,2)] , Rista Hernandi Virgianto[(1,2)], Suharni [(1,2)], Puji Ariyanto [(1,2)]

1) Agency for Meteorology, Climatology, and Geophysics of the Republic of Indonesia (BMKG Indonesia)

2) School of Meteorology, Climatology, and Geophysics (STMKG-BMKG Indonesia)

Abstract The objective of the research are (1) to apply the rainfall prediction models using downscaling and clustering models based on seismic characteristics to recognize landslide hazard in Banjarnegara , Central Java Indonesia, and (2) to develop a reliable landslide detection system in Banjarnegara Central Java Indonesia. The prediction method uses ANFIS (adaptive neuro-fuzzyinference system) to capture high rainfall patternson a 12.5 kilometers scale. To obtain information on the daily landslide early warning, we use the WRF (Weather research forecasting) prediction model at the local scale (1 km). The model is run for several times with the difference in initial condition as an ensemble model to producethe probabilistic predictionon a 12.5 kilometers scale. The threshold for rainfall probabilistic is based on historical rainfall data when the landslides occurred. Furthermore, for a real time information, we use a fuzzy-based system model to determine whether the warning level is low, medium, or high. This real time warningusesthe rainfall thresholds based on the automatic rain data observation system.Other inputs for the construction of models are seismic aspects obtained from analyzes of local earthquakes that have potential to cause landslides from historical earthquake data. Both rainfalls and earthquakes data are inputted into the equations of landslide model. The landslide model equation is built based on landslide events with two inputs for real time, daily and monthly time scales. Prototype of landslide detection instrument includes a digital rain detector, a digital extensometer to measure soil shift, tiltmeter to measure slope in a structure at ground level and soil moisture sensor to measure groundwater fluctuations).

Keywords : landslide, Banjarnegara, WRF, ANFIS

Introduction

Banjanegara has a high rainfall intensity during the wet period with geographical characteristics that are prone to landslides(Fathani, Karnawati, & Wilopo, 2016). In the development of the landslide model, it is necessary to input rainfall data on a local scale thatdescribe the rain probability that will occur in an area(Crozier, 1999). The information on rain predictionitself, requires in a long-. medium-, and short-term timescale. Landslide early warning information on a monthly time scale supports a longer preparation to take an action to mitigate the landslides(Intrieri, Gigli, Mugnai, Fanti, & Casagli, 2012).

Objective

(1) To apply the rainfall prediction models using downscaling and clustering models based on seismic characteristics to recognize landslide hazards in Banjarnegara , Central Java Indonesia

(2) To develop a reliable landslide detection system in Banjarnegara , Central Java Indonesia.

General overview of Banjarnegara

Banjarnegara is located between $7^0$12 ’- $7^0$31’ S and $109^0$29’- $109^0$45’50” E. Located on the mountain path in the central part of the western Central Java Province that stretches from west to east. Banjarnegara has a tropical

climate with more wet months than dry months. Temperatures range from 20-26°C, air humidity ranges from 80% -85% with the highest rainfall on average 3,000 mm/year. Geographically, Banjarnegara is classified into three regions.The northern part consists of Kendeng Mountains with wavy and steep slope (Fathani & Karnawati, 2009). The middle part consists of areas with flat slope which are Serayu River valleys, and the southern part is a region with steep slope from the Serayu mountains. Landslide area is located mostly in the northern part of Banjarnegara (Warnadi, 2014)with an altitude of more than 1,000 MASL with an area of24.4% of the total area ofBanjarnegara with a slope of above 15-40%. Soil characteristics in landslide-prone areas are soil with latosol and grumosol types which are widely distributed in the Karangkobar , Wanayasa, Kalibening, Pejawaran, and Batur(Priyono & Priyana, 2006).

Landslide potential in Banjarnegara Central Java

In most landslide events (rainfall-induced landslides), slope collapse always occurs during the rainy season or when rainstorm bring very high rainfall up to more than 100 mm. In Fig. 1 shows the occurrence of landslides which are settlements as a result of rainfall in Banjarnegara, Central Java.

Figure 1Landslides due to high rainfall in Banjarnegara , Central Java

Research Group of School of Meteorology, Climatology, and Geophysics (STMKG) has conducted a site-survey and installation of an early warning system for landslides located in Sijeruk Village, Banjarmangu , Banjarnegara , Central Java Province. Banjarnegara was chosen as the location of research and community service because the region was one of the landslide-prone areas in Indonesia(Karnawati, Fathani, Wilopo, & Maarif, 2018; Karnawati, Ma'arif, Fathani, & Wilopo, 2013).

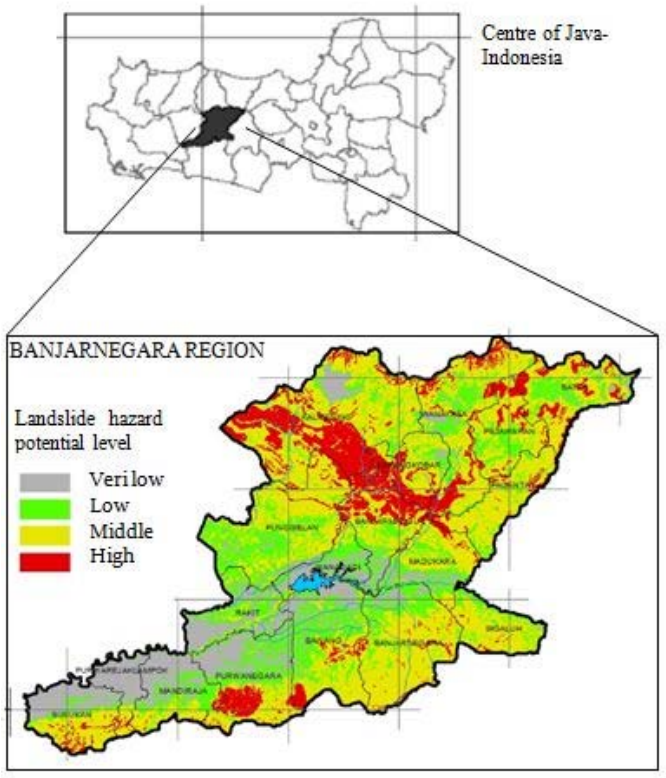

Figure 2 Distribution of potential land movement in Banjarnegara

Development landslide detection system

This early warning using a statistical downscaling method from the global numerical model (Global Circulation Model) to provide an information on rain probabilistic from approximately 30 members of ensemble model. The prediction method uses ANFIS (adaptive neuro-fuzzy inference system) to capture high rainfall patternson a 12.5 kilometers scale. To obtain information on the daily landslide early warning, we use the WRF (Weather research forecasting) prediction model at the local scale (1 km). The model is run for several times with the difference in initial condition as an ensemble model to producethe probabilistic predictionon a 12.5 kilometers scale. The threshold for rainfall probabilistic is based on historical rainfall data when the landslides occurred. Furthermore, for a real time information, we use a Fuzzy-based model on system and instruments to determine whether the warning level is low, medium, or high. This

real time warningusesthe rainfall thresholds based on the automatic rain data observation system.Other inputs for the construction of models are seismic aspects obtained from analyzes of local earthquakes that have potential to cause landslides from historical earthquake data. Both rainfalls and earthquakes data are inputted into the equations of landslide model. The landslide model equation is built based on landslide events with two inputs for real time, daily and monthly time scales. Prototype of landslide detection instrument includes a digital rain detector, a digital extensometer to measure soil shift, tiltmeter to measure slope in a structure at ground level and soil moisture sensor to measure groundwater fluctuations. Step by step for working on this activity are as follows:

(1) Development and analysis of ensemble of monthly rainfall prediction using statistical methods

Empirical based rainfall model is developed by learning the rain conditions that occur in landslide slope (Caine, 1980). Most empirical modeling shows relatively good results at the location where the model was developed, but it is not appropriate to use it in other places even the characteristic is quite similar (Guzzetti, Peruccacci, Rossi, & Stark, 2007, 2008)). The rain threshold in the empirical model uses rainfall observation data. In this study, we plot the average rainfall (mm per hour) and rainfall duration using the logarithmic (Intensity - duration / ID) function, and determine the formula for cumulative rainfall (CT Treshold / CT) as the calculated landslide threshold from rainfall (mm) for 3 days and 15 days before the 3-day period (Guzzetti et al., 2008), it was reconstructed from the historical landslide data of Banjarmangu for the period 2011 - 2017. Rainfall data when landslides were obtained from Banjarmangu Geophysics Station, and historical data on landslide events were obtained from the Agency for National Disaster Management (BNPB) Banjarnegara, Central Java, Indonesia.

ID curves can be written in a general form, as:

$$I = c + \alpha . D^{\beta} \quad [1]$$

with,

I = rain intensity (mm/hour),

D = rain duration (hour)

c, α, β = empirical parameters

(2) Prediction of ensemble daily rainfall using atmospheric dynamics method

To obtain information on the daily landslide early warning, we use the WRF (Weather Research Forecasting) prediction model at the local scale (1 km). The model is run for several times with the difference in initial condition as an ensemble model to producethe probabilistic predictionon a 12.5 kilometers scale. The threshold for rainfall probabilistic is based on historical rainfall data when the landslides occurred. Furthermore, for a real time information, we use a fuzzy-based model on system and instrument to determine whether the warning level is low, medium, or high. This real time warningusesthe rainfall thresholds based on the automatic rain data observation system.

(3) Earthquake data analysis that potential to cause landslides

Other inputs for the construction of models are seismic aspects obtained from analyzes of local earthquakes that have potential to cause landslides from historical earthquake data. In order to determine the type of soil and the depth of landslide slip surface that cause soil movement in the location, geoelectrical resistivity survey were carried out in Gunungraja, Sijeruk Village, Banjarmangu , Banjarnegara . In this study, the resistivity data were acquired using a resistivitymeter 32 channel along four lines each 30 m long (Fig. 4). The method is based on measuring the electrical potential between a pair of electrodes caused by direct current injection between another pair of electrodes. Afterwards, the apparent resistivity is calculated using the geometric factor. For field practice different electrode configurations have been designed. In this study, we used Wenner array (Fig. 3). The geometric factor (K) of Wenner array can be obtained using,

$$K = \frac{2}{\frac{1}{a} - \frac{1}{2a} - \frac{1}{2a} + \frac{1}{a}} = 2pa \quad [2]$$

The apparent resisivity (r) becomes,

$$r = 2pa\frac{\Delta V}{I} \quad [3]$$

Where a is the distance between the electrodes, ΔV is the potential difference between the electrodes, and I is the applied current(Telford, Telford, Geldart, Sheriff, & Sheriff, 1990).

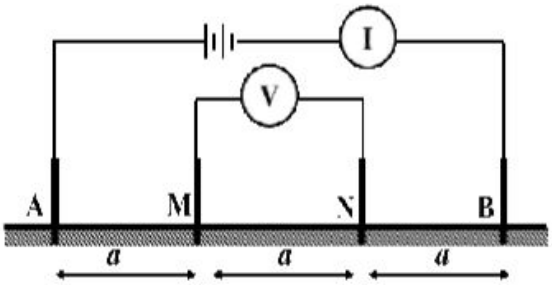

Figure 3 Wenner arrray, four space point electrodes are place at the surface of the ground with equal distance. Where a is the distance between adjacent electrodes, A & B is the current electrodes and M & N is the potential electrodes.

The distribution of resistivity beneath the area is obtained from the 2D inversion of apparent resistivity data using Res2Dinv software. The 2D electrical resistivity image has been used to identify the discontinuity between the landslide material and its slip surface. 2D data are generally presented in the form of a pseudo section, which is a representation of the apparent resistivity variations in the subsurface. The electrical resistivity values of rocks vary in a wide range and its depend on a grain size, porosity, contents of water and mineralization of the rocks.

(4) Prototype design of the landslide detector

Prototype of landslide detection instrument includes a digital rain detector, a digital extensometer to measure soil shift, tiltmeter to measure slope in a structure at ground level and soil moisture sensor to measure groundwater fluctuations. The communication system for landslide detection devices will provide early warning via short messages, internet of thing and radio frequency. The system that will be designed consists of three main parts, which are Input, Process, and Output as shown in Fig. 5. In the Input section, consists of three sensors which are part of the physical measurements of the trigger of a landslide disaster. Physical measurements are adjusted based on meteorological, climatological and geophysical parameters. The sensors used are:

1. Accelerometer sensor is used to measure the soil movement and acceleration.
2. Tipping bucketsensor is used to measure the rainfall.
3. Soil moisture sensor.

In processingpart we use the ATMega2560 micro-controller device functions as the main processor. The process includes processing data received from the sensor,data storage in the micro-SD module, synchronizing time using Real Time Clock (RTC), and forwarding data to the internet network using the ESP8266 WiFi module.

In the output section of the system, the data will be stored in the micro-SD module and the data will be sent to the database via Internet of Things (IoT) communication and also displayed on an LCD.

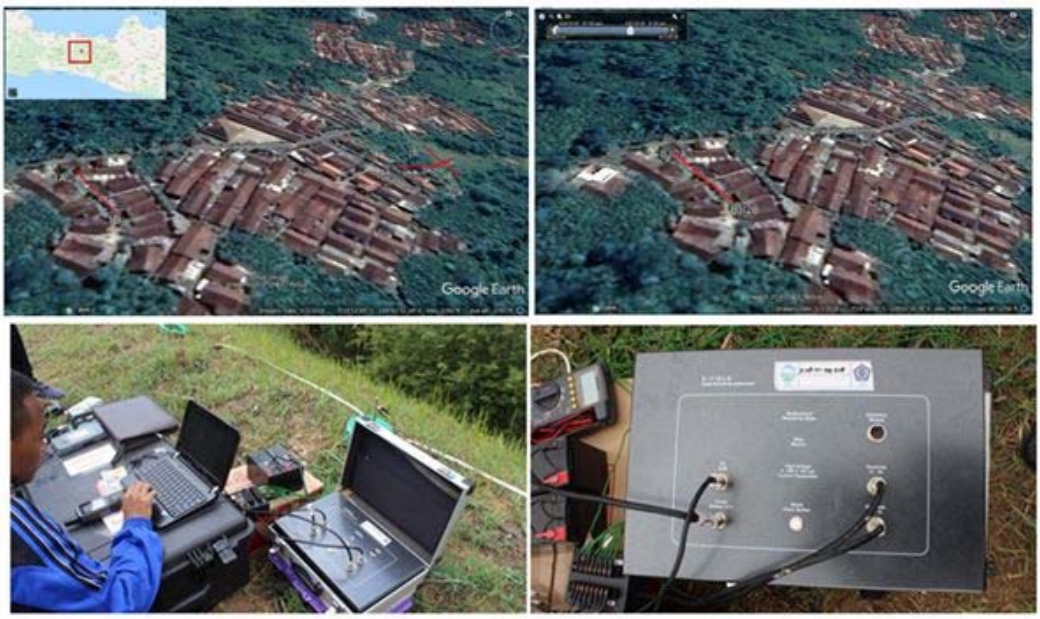

Figure4 Resistivity measurement location and process

The concept of early warning is built using the threshold parameters of meteorology, climatology and geophysics that have been analyzed based on the characteristics of the study area. Furthermore, the system will provide warnings consisting of several levels (low, medium, andhigh). The alarm will sound if the warning level has reached high status.

Figure 5 Block landslide detection system diagram

(5) development of the equation in the landslide model

Both rainfalls and earthquakes data are inputted into the equations of landslide model. The landslide model equation is built based on landslide events with two inputs for real time, daily and monthly time scales.

(6) development of the interface for landslides mapping with geographic information system

In the communication section,we that will buildit using Internet of Things (IoT) technology in monitoring and disseminating early warning information.The microcontroller sends data through a Wifi modem that acts as a publisher.

The ThingsPeak application becomes a broker to collect data from sensors that are then sent to the user. Users will receive data on rainfall parameters, soil humidity, and ground movement. In addition, early warning information in the form of vulnerability will also displayed in graphical form. The following communication design will be constructed as shown in Fig. 6.

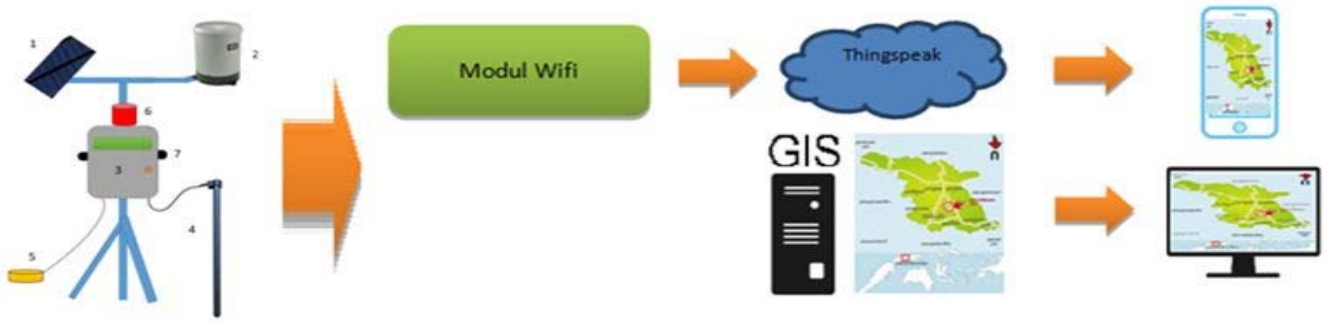

Figure 6 Interface design for landslide detection

Conclusions

Landslide early warning system is important to reduce losses caused by landslide in Banjarnegara . The system utilizethe threshold for rainfall that determined based on historical rainfall data when the landslides occurred. Afuzzy-based system will generate the warning levels which are low, medium or high. Other inputs for the construction of models are seismic aspects obtained from analyzes of local earthquakes that have potential to cause landslides from historical earthquake data. Both rainfalls and earthquakes data are inputted into the equations of landslide model. The warning system will cover daily and monthly time scales. Sensors used in the Prototype of landslide detection instrument includes a digital rain detector, a digital extensometer to measure soil shift, tiltmeter to measure slope in a structure at ground level and soil moisture sensor

Acknowledgments

We wish to thank our colleagues at the Agency for Meteorology, Climatology and Geophysics of Indonesia (BMKG) and the other members of Landslides Research Group at School of Meteorology Climatology and Geophysics (STMKG) for their contributions in this work. We also would like to thank Agency for National Disaster Management (BNPB) for providing the landslide data.

References (in the alphabetical order)

Caine, N. (1980). The rainfall intensity-duration control of shallow landslides and debris flows. *Geografiska annaler: series A, physical geography, 62*(1-2), 23-27.

Crozier, M. (1999). Prediction of rainfall□triggered landslides: A test of the antecedent water status model. *Earth Surface Processes Landforms, 24*(9), 825-833.

Fathani, T. F., & Karnawati, D. (2009). *Mitigasi Bencana Berbasis Masyarakat Pada Daerah Rawan Longsor Di Desa Kalitlaga Kecamatan Pagetan Kabupaten Banjarnegara Jawa Tengah.* Paper presented at the Civil Engineering Forum Teknik Sipil.

Fathani, T. F., Karnawati, D., & Wilopo, W. (2016). An integrated methodology to develop a standard for landslide early warning systems. *Natural Hazards Earth System Sciences, 16*(9), 2123-2135.

Guzzetti, F., Peruccacci, S., Rossi, M., & Stark, C. P. (2007). Rainfall thresholds for the initiation of landslides in central and southern Europe. *Meteorology atmospheric physics, 98*(3-4), 239-267.

Guzzetti, F., Peruccacci, S., Rossi, M., & Stark, C. P. (2008). The rainfall intensity–duration control of shallow landslides and debris flows: an update. *Landslides, 5*(1), 3-17.

Intrieri, E., Gigli, G., Mugnai, F., Fanti, R., & Casagli, N. (2012). Design and implementation of a landslide early warning system. *Engineering Geology, 147*, 124-136.

Karnawati, D., Fathani, T. F., Wilopo, W., & Maarif, S. (2018). TXT-tool 4.062-1.1: A Socio-technical Approach for Landslide Mitigation and Risk Reduction. In *Landslide Dynamics: ISDR-ICL Landslide Interactive Teaching Tools* (pp. 621-630): Springer.

Karnawati, D., Maʾarif, S., Fathani, T. F., & Wilopo, W. (2013). Development of socio-technical approach for landslide mitigation and risk reduction program in Indonesia. *ASEAN Engineering Journal Part C, 2*(1), 22-47.

Priyono, K. D., & Priyana, Y. (2006). Analisis Tingkat Bahaya Longsor Tanah di Kecamatan Banjarmangu Kabupaten Banjarnegara.

Telford, W. M., Telford, W., Geldart, L., Sheriff, R. E., & Sheriff, R. E. (1990). *Applied geophysics* (Vol. 1): Cambridge university press.

Warnadi. (2014). Inventarisasi Daerah Rawan Longsor Kabupaten Banjarnegara Jawa Tengah. *Jurnal SPATIAL Wahana Komunikasi dan Informasi Geografi, 12*(2), 35-45.

Selection of Optimal Parameters Characterizing Mobility of Rock Avalanches

Alexander Strom[1, 2]

1) Geodynamics Research Centre – branch of JSC "Hydroproject Institute", Moscow, strom.alexandr@yandex.ru;

2) School of Geological Engineering and Geomatics, Chang'an University, Xi'an

Abstract Analysis of the Central Asian rockslides' database that includes more than 550 features for which quantitative parameters such as volume, area, runout, height drop, etc. are available, and comparison of the correlation coefficients of the relationships between them allows selection of parameters characterizing mobility of rockslides and rock avalanches in optimal way. Such parameters are the runout (L) and the total affected area (A_{total}) that have most tight relationships with landslide volume (V) and with the product of volume with maximal height drop ($V \times H_{max}$) – parameter somehow proportional to the potential energy released during slope failure.

Keywords rockslide, rock avalanche, mobility, runout, affected area, volume, exposure

Introduction

Rock avalanches are classified (Hungr, et al, 2014) as flow slides (dry granular flows) that are formed by large-scale bedrock landslides with volumes, usually exceeding 1 million cubic meters. The extremely high mobility of such features is governed by the internal processes evolving during their emplacement and by the specific interaction of granular flow with its substrate. Various mechanisms explaining these phenomena have been proposed (see, e.g. Hsü, 1975; Grigorian, 1979; Davies, 1982; Melosh, 1986; Sassa et al., 1994; Kobayashi, 1997), among which the dynamic fragmentation model seems to be most realistic and universal (Davies, 1982; Davies et al., 2017).

Study of numerous rock avalanches that originated on slopes composed of various types of rocks allows comparison of the mutual position of these lithologies in the source zone and in the deposits. Debris that originated from different types of rocks in the source zone do not mix and form "belts" or "layers" in the deposits composed of the specific types of rocks (see, e.g., Abdrakhmatov, Strom, 2006; Strom, 2006; Strom, Abdrakhmatov, 2018). It is typical of most of rock avalanches and demonstrates that they move as laminar granular flows, without evidence of turbulence. Such internal structure is typical of rock avalanches that moved over unconfined surfaces, along and across narrow valleys. The latter form relatively compact blockages. Thus, despite final morphology of large-scale rockslide bodies most of them can be classified as flow-like granular flows – rock avalanches.

Considering extreme danger provided by such phenomena for settlements, infrastructure and population in mountainous regions, quantitative assessment of rock avalanche mobility is of high importance both from scientific and practical points of view. This paper presents results of the analysis of the Central Asian rockslides' database (Strom, Abdrakhmatov, 2018) that includes more than 550 features with their quantitative parameters such as volume (V), total affected area (A_{total}), runout (L), height drop (H), and maximal height drop (H_{max}) measured up to now. This analysis allowed selecting of parameters characterizing rock avalanch mobility in the optimal way.

Unidimensional and dimensionless parameters – runout and fahrborshung

Traditionally the mobility of long-runout landslides is characterized by the unidimensional parameter – runout (L) defined as horizontal projection of the distance between headscarp crown and the most distant point of rock avalanche body (Kilburn, Sørensen, 1998; Legros, 2002). Another, even more commonly used parameter is the dimensionless efficient coefficient of friction H/L (Sheidegger, 1973; Hsü, 1975; Davies, 1982; Li, 1983; Shaller, 1991; Corominas, 1996) or "fahrborshung" (term introduced by A. Heim in 1932). Here H is the vertical distance between headscarp crown and deposits tip (Fig. 1). H may be equal to maximal height drop H_{max} (H_1 for case 1 on Fig. 1) or $H < H_{max}$ (H_2 for case 2 on Fig. 1).

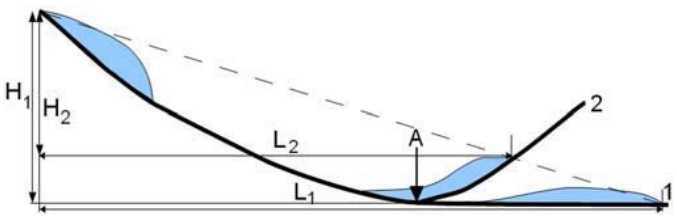

Figure 1 Relationships between H and H_{max}. Case 1 is typical of unconfined and laterally confined rock avalanches; case 2 – of frontally confined rock avalanches. Despite significant difference between H_1 and H_2 and L_1 and L_2, H/L ratio here is the same. Point "A" marks the limit beyond which forces governing rock avalanche motion differ. Modified from (Strom, Abdrakhmatov, 2018) with permission of Elsevier.

It was found that both parameters strongly depend on rock avalanche volume – slope failures with larger volumes produce rock avalanches with longer runout and smaller H/L ratio. Analysis of such relationships for the Central Asian case studies revealed much more close correlation between V and L, with higher correlation coefficients than between V and H/L, regardless of the confinement type (Strom, Abdrakhmatov, 2018) (Tab. 1). Thus, runout seems to be preferable to characterize rock avalanche mobility if we are interested in assessment of the distance from the slope foot that might be affected.

Two-dimensional parameter – affected area

The abovementioned parameters, however, seem to be optimal to characterize mobility of large-scale bedrock landslides neither for better understanding of the so high mobility, nor for risk assessment. The latter requires knowledge of the exposure of elements at risk (Corominas et al., 2015). Rock avalanche debris can move not only straight forward as the Chaartash-3 rock avalanche (Fig. 2), but can form fan-shape or pancake-shape bodies (Fig. 3) with significant sidewise spreading.

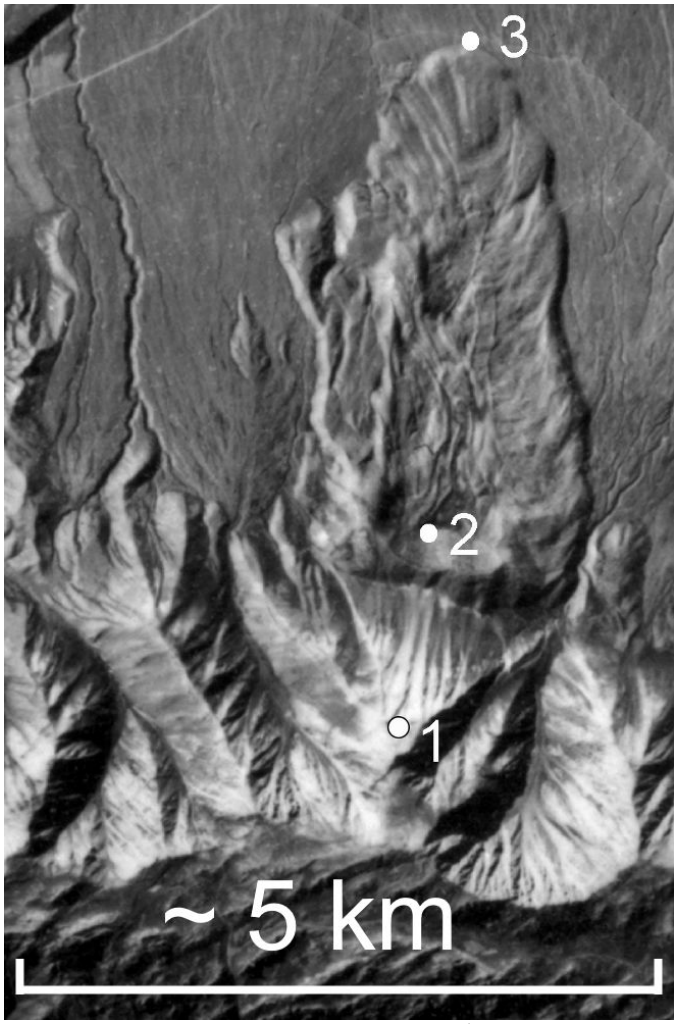

Figure 2 The Chaartash-3 rock avalanche (Central Tien Shan, Kyrgyzstan) that moved forward without sidewise spreading. 1 – crown of the triangular headscarp, 2 – approximate position of the headscarp base, 3 – the deposits' tip. KFA-1000 space image.

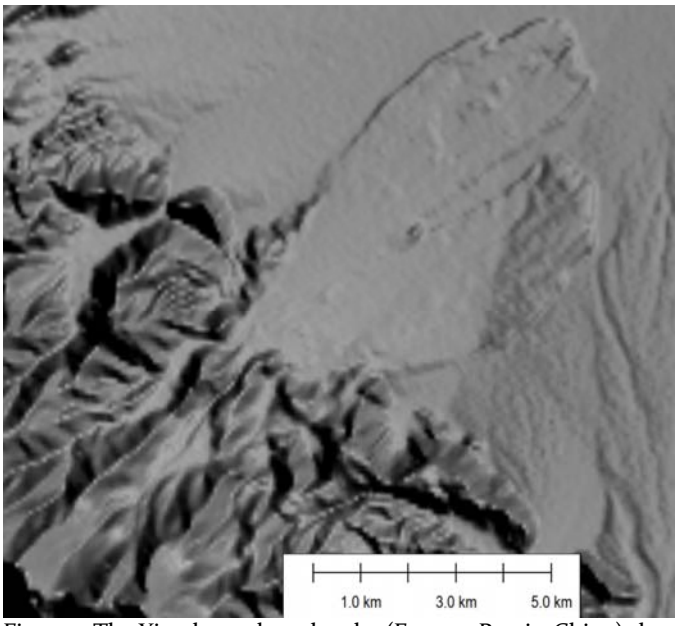

Figure 3 The Yimake rock avalanche (Eastern Pamir, China) that formed fan-shape body about 5 km wide. 3" SRTM DEM visualized by Global Mapper software.

In the latter cases, the affected area might exceed that of rock avalanche that moves forward even if the latter's runout would be larger. I want to notice that area as a parameter characterizing rock avalanche mobility was analyzed by Li (1983), though based on much smaller database than used in this study.

It is not so critical from the practical point of view if an element at risk (building, lifeline, etc.) would be located within the rockslide source zone, in the transition or deposition zone. It would be affected severely in any case, though in different way. That is why, following the approach proposed in (Strom, Abdrakhmatov, 2018), the total affected area (A_{total}) – two-dimensional parameter characterizing rock avalanche mobility, and its relationships with volume, considering confinement conditions were analyzed. Relationships between its inverse ratio with H (H/A_{total}) and rockslide volume were analyzed as well. A_{total} is defined as the plan area of the polygon embracing the source zone, the transition zone (often marked by trimlines) and the deposition zone. Additional argument to use just this parameter is that total affected area can be measured more precisely than areas of the source, transition and deposition zones separately that often overlap each other masking their limits.

It was found that correlation coefficients of the A_{total}÷V and the H/A_{total}÷V relationships are higher than such coefficients of the L÷V and H/L÷V relationships. Similarly to the unidimensional parameters described above, correlation coefficients of the A_{total}÷V relationships are higher than such coefficients of the H/A_{total}÷V relationships, though difference is not as high as between L÷V and H/L÷V (see Tab. 1).

Table 1 Correlation coefficients of the relationships between parameters characterizing rock avalanches.

Confinement	$L \div V$	$H/L \div V$	$L \div V \times H_{max}$	$A_{total} \div V$	$H/A_{total} \div V$	$A_{total} \div V \times H_{max}$
Frontal	0.7335	0.3008	0.8160	0.9008	0.8006	0.9258
Lateral	0.7301	0.4497	0.051	0.8833	0.8686	0.9267
unconfined	0.8066	0.3962	0.8824	0.9151	0.8330	0.9361

Mobility vs. potential energy

It was found that highest correlation coefficients characterize relationships between total affected area (A_{tota}) and the product of rockslide volume and maximal height drop ($V \times H_{max}$) (see Tab. 1). Here just maximal height drop (H_{max}) is used that corresponds to H_1 on Fig. 1 for both cases – 1 and 2 shown on this Figure.

Such conclusion is not surprising, considering that such product is proportional, at a first approximation, to the potential energy of the collapsing rock mass that is released during its emplacement. For case 1 on Fig. 1 this energy is used to overcome basal friction and to enable different internal processes in the moving debris (crushing, heating, etc.); for case 2 – besides all abovementioned – to overcome gravity force while raising material on the opposite slope.

Strictly speaking, more precise estimate of the potential energy requires determination of the position of the center of gravity before and after emplacement and data on the rock mass bulk density. However, accuracy of the position (altitude) estimate of the center of gravity is rather poor, in most of cases, due to very complex and irregular geometry of the source zone and of the deposits and due to lack of data about the pre-slide topography. Densities of the most common types of rocks, on the other hand, vary within ±20%, while accuracy of volume estimate in most of cases seem to be about±30%, if not worst. Besides, position of the center of gravity after the emplacement says almost nothing about real runout. That is why use of the proposed value ($V \times H_{max}$) seems to be optimal, at least for the analysis of large, statistically representative databases.

High correlation coefficients were found also for the relationship between this product ($V \times H_{max}$) and runout (L) (see Tab. 1). They are much higher than correlation coefficients of other unidimensional relationships for frontally confined and unconfined rock avalanches, but are surprisingly low for laterally confined sampling (Fig. 4). Same regularity was found for the relationships between height drop and runout (Fig. 5), while the $A_{tota} \div V \times H_{max}$ relationship for laterally confined rock avalanches is, practically, the same as for samplings with other confinement conditions (see Tab. 1). I must notice that volume and height drop are not totally independent parameters. Generally, higher slope is, large (more voluminous) slope failure might occur on it (Fig. 6). In this figure slope height, corresponding to elevation difference from the headscarp crown up to point A on Fig. 1 is used instead of maximal height drop. It corresponds to H_{max} for frontally confined rock avalanches, while for most of laterally confined and unconfined rock avalanches debris stops at lower altitude than the foot of the source slope.

It can be hypothesized that an abnormal behavior of laterally confined rock avalanches might be caused either by quite variable sidewise friction, or by the complexity of their geometries. Indeed, some rock avalanches that moved down-valley finally either collide with valley slope band as the Seit rock avalanche (Fig. 7), or enter wider valley where they spread sidewise forming fan-shape bodies, as the 1949 Khait rock avalanche (Fig. 8).

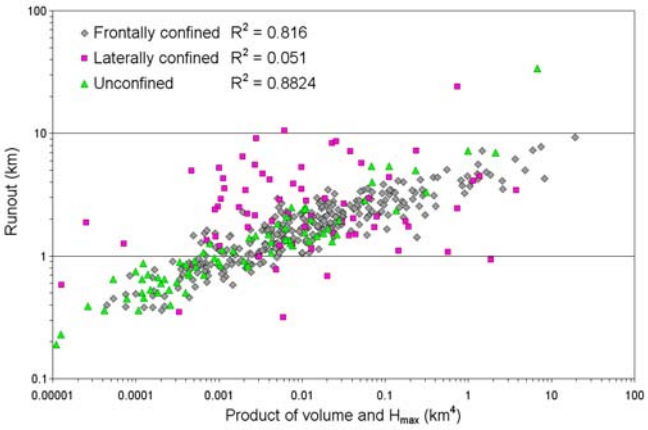

Figure 4 Relationships between runout and product of rockslide volume and maximal height drop for rockslides with different confinement. Corresponding R^2 values are added to the legend and shown in Tab. 1. After (Strom, Abdrakhmatov, 2018) with permission of Elsevier.

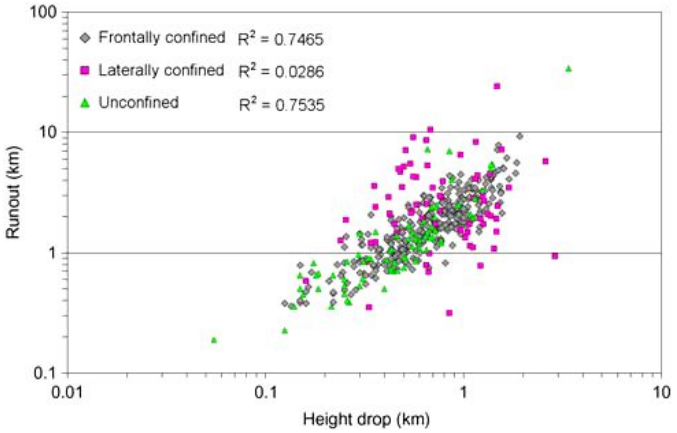

Figure 5 Relationships between runout and maximal height drop for rockslides with different confinement. Corresponding R^2 values are added to the legend. After (Strom, Abdrakhmatov, 2018) with permission of Elsevier.

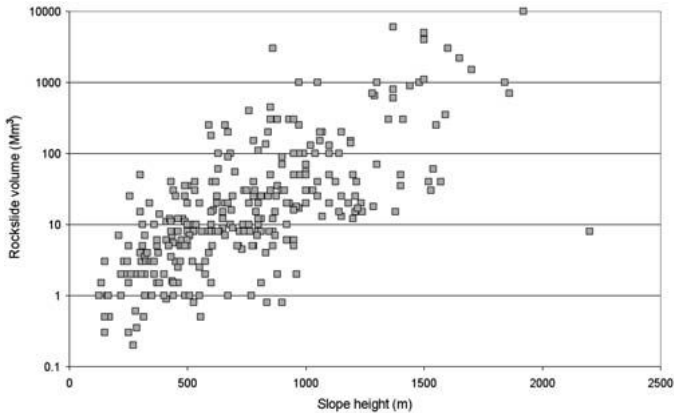

Figure 6 Relationship between slope height and rockslide volume for Central Asian rockslides that occurred in frontally confined conditions (298 case studies) for which effect of the down valley debris spreading should be minimal and can be neglected. Modified from (Strom, Abdrakhmatov, 2018) with permission of Elsevier.

Figure 7 The 3.2 km long Seit rock avalanche, Central Tien Shan, Kyrgyzstan, with most of the way lateral and final frontal confinement. Modified from (Strom, Abdrakhmatov, 2018) with permission of Elsevier.

Figure 8 The 7.41 km long 1949 Khait rock avalanche, Southern Tien Shan, Tajikistan, with most of the way lateral confinement and final unconfined fan-shape deposition. Modified from (Strom, Abdrakhmatov, 2018) with permission of Elsevier.

Conclusions and perspectives of further studies

The analysis of the Central Asia database clearly demonstrates that the total area affected by rock avalanches is the parameter characterizing mobility of such features in the best way and most tightly related to rockslide volume and to its product with height drop (the latter is almost equal to slope height for frontally confined features).

Further analysis should include use of triple regressions allowing comparison of the influence of two parameters, e.g. failure volume and height drop, on rock avalanches' mobility.

It will be interesting to perform same analysis of the complete Central Asian database (about 1000 case studies) that would be nearly two times larger than the sampling available at present, and, further, of the global database (Central Asia, European Alps, Southern Alps of New Zealand, North and South America, Himalaya, etc.). Compilation of such database that should include thousands case studies will allow statistically representative analysis considering not only confinement conditions, but also types of rocks (igneous, carbonate, terrigenous, etc.), types of the initial failure (translational, rotational, wedge, compound), climate conditions and other factors that, hypothetically, can affect rockslide mobility.

Acknowledgments

I want to thank Dr. Langping Li from State Key Laboratory of Resources and Environmental Information System, Institute of Geographic Sciences and Natural Resources Research, Chinese Academy of Sciences, with whom we discussed further steps of the statistical analysis of the Central Asia rockslides' database.

References

Abdrakhmatov K, Strom A. (2006) Dissected rockslide and rock avalanche deposits: Tien Shan Kyrgyzstan. Evans S G, Scarascia Mugnozza G, Strom A, Hermanns R L (eds). Landslides from Massive Rock Slope Failure. NATO Science Series: IV: Earth and Environmental Sciences. 49. Springer, New York. pp. 551-572.

Corominas J (1996) The angle of reach as a mobility index for small and large landslides. Canadian Geotechnical Journal. 33: 260-271.

Corominas J, Einstein H, Davis T, Strom A, Zuccaro G, Nadim F, Verdel T (2015) Glossary of terms on landslide hazard and risk. Lollino G, et al. (eds). Engineering Geology for Society and Territory, 2. Springer International Publishing, Switzerland. pp. 1775-1779.

Davies T R (1982) Spreading of rock avalanche debris by mechanical flu-idization. Rock Mechanics. 15: 9-24.

Davies T R, McSaveney M J, Reznichenko N (2017) The fate of elastic strain energy in brittle fracture. Leith, K., Ziegler, M., Perras, M., Loew, S. (eds). Progressive rock failure. An ISRM Specialized Conference, Monte Verità, 5-9 June 2017. ETH, Extended abstracts. pp. 107-108.

Grigorian S S (1979) New friction law and mechanism of large-scale rockfalls and landslides, Proceedings of Academy of Sciences of USSR. 244: 846-849 (in Russian).

Heim A (1932) Bergsturz und Menschenleben. Fretz and Wasmuth, Zurich. 218 p.

Hsü K J (1975) Catastrophic debris streams (sturzstroms) generated by rock falls. Geological Society of America Bulletin. 86: 129-140.

Hungr O, Leroueil S, Picarelli, L (2014) Varnes classification of landslide types, an update. Landslides. 11: 167-194.

Kilburn C R J, Sørensen S-A (1998) Runout length of sturzstroms: the control of initial conditions and of fragment dynamics, J. Geophys. Res. 103(B8): 17877-17884.

Kobayashi Y (1997) Long runout landslides riding on basal guided wave. Marinos K, Tsiambaos, Stoumaras (eds). Engineering Geology and the environment. 1997. Balkema, Rotterdam. pp 761-766.

Legros F (2002) The mobility of long-runout landslides. Engineering Geology. 63: 301-331.

Li T (1983) A mathematical model for predicting the extent of a major rockfall. Z. für Geomorphologie N.F. 2: 473-482.

Melosh H J (1986) The physics of very large landslides. Acta Mechanica, 64: 89-99.

Sassa K, Fukuoka H, Lee J-H, Shoaei Z, Zhang D, Xie Z, et al. (1994) Prediction of landslide motion based on the measurement of geotechnical parameters. In: Development of a new Cyclic Loading Ring Shear Apparatus to study earthquake-induced landslides. Report for Grant-in-Aid for Developmental Scientific Research by the Ministry of Education, Science and Culture, Japan (Project No 03556021), DPRI, Kyoto. pp. 72-106.

Shaller P J (1991) Analysis and Implications of Large Martian and Terrestrial Landslides, Ph.D. Thesis. California Institute of Technology.

Sheidegger A E (1973) On the prediction of the reach and velocity of catastrophic landslides. Rock Mechanics. 1973. 5: 231-236.

Strom A L (2006) Morphology and internal structure of rockslides and rock avalanches: grounds and constraints for their modeling. Evans S G, Scarascia Mugnozza G, Strom A, Hermanns R L (eds). Landslides from Massive Rock Slope Failure. NATO Science Series: IV: Earth and Environmental Sciences. 49. Springer, New York. pp. 305-328.

Strom A, Abdrakhmatov K (2018) Rockslides and Rock Avalanches of Central Asia: Distribution, Morphology, and Internal Structure. Elsevier. 459 p.

Landslide processes as a risk factor for Russian cultural heritage objects

Igor Fomenko[(1)], Denis Gorobtsov[(1)], Daria Shubina[(1)], Fedor Bufeev[(1,2)]

1) The Engineering Geological Department of Russian State Geological Prospecting University, Moscow, Mikluho-Maclaya st. 23, 117997, e-mail: inzh-geo-kaf@mgri-rggru.ru ;

2) «IGIT» LLC, Russia, Moscow Luzhnetskaya nab., 10

Abstract This article is concerned with problems of stability assessment of slopes that are part of the interaction scope of historical natural-technical systems (HNTS). The need of using the new methods is caused by increasing development of landslide processes near the architecture monuments. Examples include landslides in the Nizhny Novgorod, Smolensk, Mozhaisk Kremlins, on the northern slope of the Resurrection New Jerusalem Monastery, the western slope of the Savvino-Storozhevsky Monastery, the southern slope of the Bogolyubsky Monastery, on the slopes of the Spaso-Evfimiyev and Vasiliyevsky Monasteries in the Suzdal region, Pechorsky Monastery in Nizhny Novgorod. The temples and monasteries of Russia are unique monuments of history and architecture, treasures of the cultural heritage of the state and a place of pilgrimage and reverence for many people. Many of them are protected by UNESCO.

Keywords pre-setting of engineering geological conditions, historical natural-technical systems, landslide, modelling of slope stability.

Introduction

The state of the Russian cultural heritage at the present time can be considered as critical. There is a steady decline in the cultural wealth of the country. According to various estimates, the state from 50 to 70% of the historical and cultural monuments that are under state protection is characterized as unsatisfactory, for most of them it is necessary to take urgent measures to save them from breakdown, damage or destruction. Over the past 10 years, more than 2.5 thousand monuments have been destroyed in the Russian Federation, including 2 thousand - under the influence of adverse natural and man-made processes and landslides have played one of the leading roles.

In engineering geology there is a separate scientific direction of study the historical territories. It is impossible to consider historical buildings and structures separately from their ground base and the preservation and trouble-free operation of the monument depend on their interaction.

Ancient architects built temples and monasteries in Russia using the principle “How the measure and beauty will say”. This often led to the selection of a construction site on elevated places near the slopes. Many slopes under the influence of changes in natural conditions in in time became landslide dangerous. Therefore at present engineering geologist are often faced with the need to study landslide processes developing within the boundaries of historical natural-technical systems. And this is very difficult. Each architectural monument is unique as the natural conditions of each of them. The evolutionary transformations of the historical territories relief began with the construction of the first buildings. This was expressed in the leveling of the territory and its adaptation to the requirements of economic needs. Over the centuries-long history of the HNTS functioning the surface topography as a rule has been changed very significantly. A change in the terrain entails a change in quantitative and qualitative indicators of engineering geological processes.

Professor of RGGRU E.M. Pashkin introduced the term “pre-set” that means a set of conditions that serve as a sign of processes realization which is determined by the conditions of previous events. With new construction there is an opportunity to avoid areas with landslide process active development. Dealing with HNTS there is no such possibility and the significance of the landslide danger forecast reliability increases. The disclosure of the “pre-set” concept for landslide processes within the historical areas can be given through the definition and evolution of landslide formation factors. These factors primarily include topography, geological structure, hydrogeological conditions and physical and mechanical soil properties. The relief and geological structure of HNTS slopes upper part are determined by the latest history of the territory development and are associated with human activity, which lead to the formation of various technogenic soil layers that overlap the original natural relief. Artificial changes in hydrogeological conditions and surface runoff can cause waterlogging of the contact zone between technogenic accumulations and natural soils. Thus, the pre-determined sliding surface of landslides developed within the HNTS is most often located on the border of natural and technogenic soils.

The distribution of properties in technogenic soils is very heterogeneous due to the peculiarities of their formation conditions, which are not always possible to establish. This makes the task of separating layers of different physical and mechanical properties within a series of technogenic soils extremely difficult. And the slopes that are included in the HNTS interaction sphere are often composed of multimeter strata of technogenic soils, so the quantitative assessment of such slopes stability is rather difficult. All mentioned above requires the development of a special approach to the study of such landslide slopes.

General statements of the methodology for HNTS slope stability calculation.

One of the main stages of work concerned with quantitative assessment of the slope stability is schematization in the mathematical model construction. This kind of schematization can be generalized and special. Under generalized schematization in this context we should understand the process of simplifying a real natural object, which has an infinite degree of complexity to a conceptual model. On the one hand it is limited by scientific knowledge and on the other hand – by the information security degree achieved in the engineering geological survey (Zerkal OV, Fomenko I.K., 2013). Special schematization implies simplification of the conceptual model to a specialized (geomechanical) scheme which within the framework of the task preserves the adequacy of the obtained scheme and the initial conceptual model. Ultimately the special schematization provides the required detail of the real natural object description. The purpose of a special schematization can be expressed in the following thesis: maximum simplification with minimal loss of adequacy (Pendin VV, Fomenko IK, 2015).

One of the special schematization main stages is the assignment of soil properties distribution model in a landslide massif (Bufeev F.K., Fomenko I.K., Sirotkina O.N., 2016)

When calculating the stability of HNTS slopes composed of technogenic soils, the most interesting is the possibility of using models with the construction of soil strength properties distribution fields (Cho, 2007), (Allan, F.C. Yacoub, T.E. Curran, J.H., 2012).

The technique of field specification of properties is as follows: the field of cohesion and the internal friction angle distribution (Bufeev, 2016) is constructed using known actually determined values of soil properties at points with determined coordinates (during the sampling process). Interpolation methods are used to construct the field, such as: the Chaga method (Chugh, AK, 1981), the Delaunay method (Delone BN, 1934), the inverse distance method (IAD) (Shepard, D., 1968), the thin spline method (Franke, Richard, 1985). Next, using traditional methods of calculation based on limiting equilibrium, the position of the sliding surface is determined and the slope stability coefficient is calculated.

Landslide danger assessment on the cultural heritage objects

The Holy Bogolyubsky monastery

The largest of the monasteries of Vladimir and its environs, the Holy Bogolyubsky monastery (Fig. 1) is a witness of more than 8 centuries of Russian history, in whose events he repeatedly played an important role. It is known that on May 20, 1851 during the procession a bridge collapsed as a result of a landslide. Then about 160 people died. In the beginning of the 2010s, the suffusion process intensity increased on the territory of the monastery. The main indicator was the volume of silty-clay material removal the water from a spring at the base of the slope. Two dips with a diameter of up to 1.5 m and a depth of up to 3 m were formed on the slope. Slope movements also began (Fig. 2). The UNESCO World Heritage Site of the Virgin Mary, the Ladder Tower and the passages of Andrei Bogolyubsky's chambers are under the impact of the landslide process.

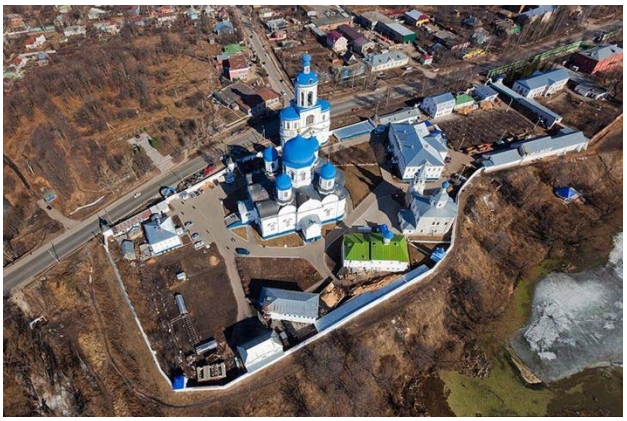

Fig.1 General view of The Holy Bogolyubsky monastery. You can see landslide signs on the modelling slope.

Fig.2 The landslide shape of a slope.

To estimate the landslide hazard various models of interpolation methods were used to build models of soil strength properties distribution of the near-slope array (an example of the model is shown in Figure 3 and 4) and a series of calculations were performed (Figure 5) using the Morgenstern-Price method. This method was chosen because it satisfies the equilibrium conditions of moments and forces.

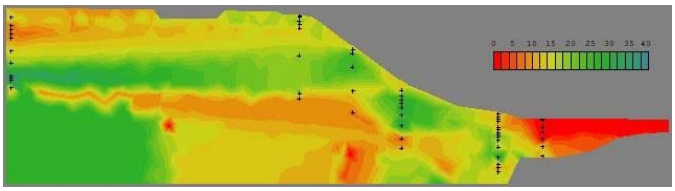

Figure 4 The distribution of internal friction angle in soil massif

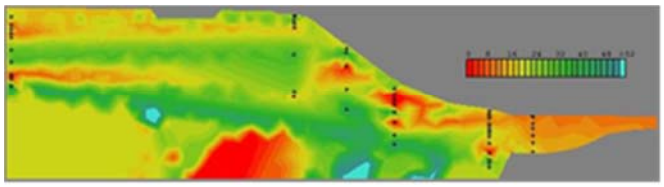

Figure 3 The distribution of cohesion in soil massif

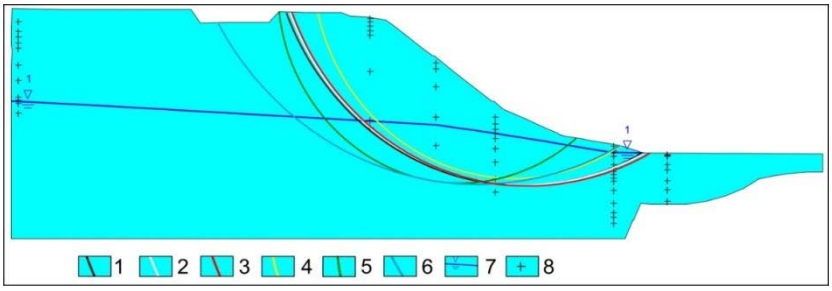

Fig.5 Geomechanical model of calculation by the limiting equilibrium methods. The results of the slip surface calculations: 1-according to the designed characteristics, 2-according to the standard characteristics, 3-using the interpolation method of inverse weighted distances, 4-using the Delaunay method, 5-using the Chag method; 6- using the method of thin spline; 7-level groundwater; 8- ground sampling sites.

Table. 1 The results of slope stability calculation

Parameter/Calculation scheme	Designed soil values	Standard soil values	Interpolation by IWD method	Interpolation by the Delaunay method	Interpolation by the Chag method	Interpolation by the thin spline method of
Safety Factor (Ky)	1,03	1,17	1,20	1,06	0,80	0,92
Landslide body volume	335	327	330	270	354	447

Analyzing the results we can draw the following conclusions. The most comparable with the traditional approach (based on standard values) results were obtained using the interpolation method of inverse weighted distances. This follows from the fact that the values of equivalent volumes differ from the normative soil properties calculations by less than 2%. That is the position of the potential critical sliding surface coincided almost perfectly. The safety factor value differs from calculated by standard values by less than 5%.

Novo-Nikolsky Cathedral of Mozhaisk Kremlin.

The complex of Mozhaisk Kremlin is located in the Moscow region, in the city of Mozhaisk. The Kremlin was founded in the XIII century. The cathedral was built in the 17th century, and since then it has been repeatedly rebuilt. The cathedral acquired this view at the beginning of the XIX century. In April 2013 a landslide (Fig. 6) descended a few meters from the south-western corner of the Novo-Nikolsky Cathedral. It was formed in technogenic soils. Their thickness on this slope reached 12 m. (Bufeev, 2016).

..

Fig.6 The landslide near the south-western corner of the Novo-Nikolsky Cathedral.

Table. 2 The results of slope stability calculation – Ky (landslide body volume)

Soil properties distribution models / Calculation method	Designed soil values Model 1	Standard soil values Model 2	Soil strength properties distribution with different types of interpolation			
			Delaunay Model 3	Chag Model 4	The thin spline Model 5	IWD Model 6
Bishop	1,23 (99)	1,16 (185)	1,11 (94)	1,08 (101)	1,14 (103)	1,13 (98)
Yanbu	1,18 (104)	1,14 (202)	1,09 (97)	1,05 (98)	1,10 (109)	1,10 (99)
Morgerstern-Price	1,27 (90)	1,19 (199)	1,13 (89)	1,10 (99)	1,17 (92)	1,16 (94)

From the calculation results analysis it follows that when quantifying the slope stability using the designed characteristics, the values of the safety factor (Ky) not always will be lower than when using standard values. Thus, taking into account the actual unstable state of the slope (see Fig. 6) the values of Ky obtained from the first model should be considered overestimated.

Comparison of the simulation results also shows that the maximum value of the equivalent volume was obtained using the second model, which is explained by the displacement of the sliding surface from the boundary of indigenous and technogenic soils to the underlying sediments with lower strength properties. That is, the position of the sliding surface and the value of the safety factor are influenced not only by the strength properties absolute values, but also by the ratio of the lower strata technogenic soils strength properties.

According to the actual engineering geological survey results, it was established that a landslide that had come down was formed at the boundary of primary and technogenic soils. In the field description of bore holes the line between technogenic and indigenous soils was clearly distinguished. The contact zone was represented by soils with high humidity; within the landslide circus, bedrock rocks outcropped, and technogenic accumulations were deposited in the bottom of the descended landslide.

Thus, the calculation according to the second model with the moving of the sliding surface into the bedrock, does not correspond to the actual data of the engineering-geological survey.

The minimum Ky of the studied slope were obtained using the third model (when the field of strength properties distribution was set). At the same time it is worth noting that the potential equivalent volume of a landslide body is almost the same as that obtained in the calculation using the first model.

Thus, we can conclude that the method of inversely weighted distances allows us to obtain the best results using the interpolation of the technogenic soils properties.

Conclusion

Historical territories as a rule are characterized by an increased thickness of technogenic accumulations. Their presence requires a special approach to the study of engineering geological conditions. The current state of Russian architecture monuments depends on unfavourable engineering geological processes developing within them. The main danger for the historical natural-technical systems located near the slopes is the landslide process. Slip-landslides often occur on such slopes, when technogenic accumulations slide along the bedrock. It happens due to relief changes in the process of human activity, which entails a change in the gradients of surface runoff and to the stress field's reformation in the soil massifs. As a result the hydrogeological conditions of the territory and the

physical and mechanical properties of upper part of the section soils change.

Distribution of properties in technogenic soils is unpredictable due to their heterogeneity, and also it is not always possible to establish the conditions for their formation. So the selection of various physical and mechanical properties of the layers and the assignment within them the averaged values represents a certain complexity. Therefore, it is proposed to calculate such slopes based on the fact that the variability of technogenic soils should be taken into account by interpolating the strength properties values between the points in which it is known. When using this technique, it is necessary to substantiate the method of interpolation.

Acknowledgments

The authors of the article would like to thank Victor M. Kuvshinnikov, PhD, state expert of the ministry of culture, the engineer-restorer of the highest category for the materials provided. Authors also express deep gratitude to Dr. Viktor V. Dmitriev, professor, member of the Scientific Council of the Russian Academy of Sciences certified expert of the Ministry of Culture for materials provided and invaluable contribution to the project creation.

References

Allan, F.C. Yacoub, T.E. Curran, J.H., 2012. 46th US Rock Mechanics / Geomechanics Symposium. Chicago, ARMA.

Bufeev FK, Kuvshinnikov VM, Fomenko IK, 2015. Dependence of the results of slope stability quantitative s on the choice of soil properties distribution model. GeoRisk, Issue 4.

Bufeev, F., 2016. Modeling of sliding landslides on the historical natural-technical systems slopes composed of technogenic soils: dissertation for Ph.D. of Geological and Mineralogical Sciences: 25.00.08. Moscow: MGRI-RGGRU.

Cho, S., 2007. Effects of spatial variability of soil properties on slope stability. Engineering Geology, 92((3–4)), pp. 97-109.

Chugh, A.K., 1981. Pore Water Pressure in Natural Slopes. p. 449 – 454.

Franke, Richard, 1985. Thin plate splines with tension. Computer Aided Geometric Design, Issue 2, p. 87 – 95.

Krahn J., 2004. Stability modeling with SLOPE/W. An Engineering Methodology: First Edition, Revision 1. Calgary, Alberta: GEO-SLOPE International Ltd..

Shepard, D., 1968. A two dimensional interpolation function for irregularly spaced data. Proc. 23rd Nat. Conf., pp. 517-524.

Pendin V.V., Fomenko I.K., 2015. Methodology for the assessment and prediction of landslide hazard. Moscow: LENAND

Zerkal O.V., Fomenko I.K., 2013. Evaluation of soil anisotropy influence on the slope stability. Engineering Survey, Issue 9.

IPL Project 181 – Study of slow moving landslide Umka near Belgrade, Serbia – progress report for 2017 & 2018

Uroš Đurić [(1)], Biljana Abolmasov [(2)], Miloš Marjanović [(2)], Mileva Samardžić-Petrović [(1)], Marko Pejić [(1)], Nenad Brodić [(1)], Jovan Popović [(1)]

1) University of Belgrade, Faculty of Civil Engineering, Belgrade, Bulevar Kralja Aleksandra 73/I, Serbia, +381113218587, e-mail: udjuric@grf.bg.ac.rs

2) University of Belgrade, Faculty of Mining and Geology, Đušina 7, Serbia

Abstract This paper presents a brief working progress report on realization of the IPL project 181 "Study of slow moving landslide Umka near Belgrade, Serbia". In this paper we will present results of the project targets performed by Project participants during 2017 and 2018, with plans for future project realization.

Keywords questionnaire, historical aerial images, elements at risk, PSInSAR

Introduction

The IPL project No 181 titled "Study of slow moving landslide Umka near Belgrade" started in November 2012. The study area is located on the right bank of the Sava River, 25 km south-west of Belgrade (Figure 1), the capital of Serbia. Basic objective of the Project is to enable the analysis, correlation and synthesis of data obtained from various phases of investigation of Umka landslide after a few decades of research. More details about the project mission, objectives can be found at Abolmasov et. al (2017).

Umka landslide is one of the most investigated and the only landslide that is systematically and continuously monitored using geotechnical and geodetic methods in Serbia for more than 87 years. Some parts of right bank of the Sava River near Umka are known as unstable slopes for a long time. Luković (1951) noticed that both Umka and Duboko landslides are examples of a typical Tertiary and Quaternary landslides in former Yugoslavia. The presence of landslide was evident even before, so the part of the Belgrade-Obrenovac railroad (opened in 1928. and abandoned in 1968.) was redesigned and moved away from the unstable right riverbank of the Sava River. Public debate between professional designing and construction enterprises and authorities about the location of the new modern highway started during the middle of the XX century and lasted until the 2016, when the authorities finally decided that the new road should avoid territory Umka, and pass through the left side of the Sava River. However, Umka landslide is still urbanized and populated with more than 490 inhabitants who are actually still living on the body of an active landslide (cca. 10% of all population of the Umka settlement). The traffic on the state road IB 26 (from Belgrade to the border with BiH), that is affected by Umka landslide, is showing increasing number of average vehicles per day in the last three years. More details about the slopes of the right banks of the Sava and Danube rivers, which are already well-known for instability occurrences, can be found at Vujanić et al. (1981; 1984), Lokin et al. (1988), Rokić et al. (1998; 2002), Abolmasov et. al (2015).

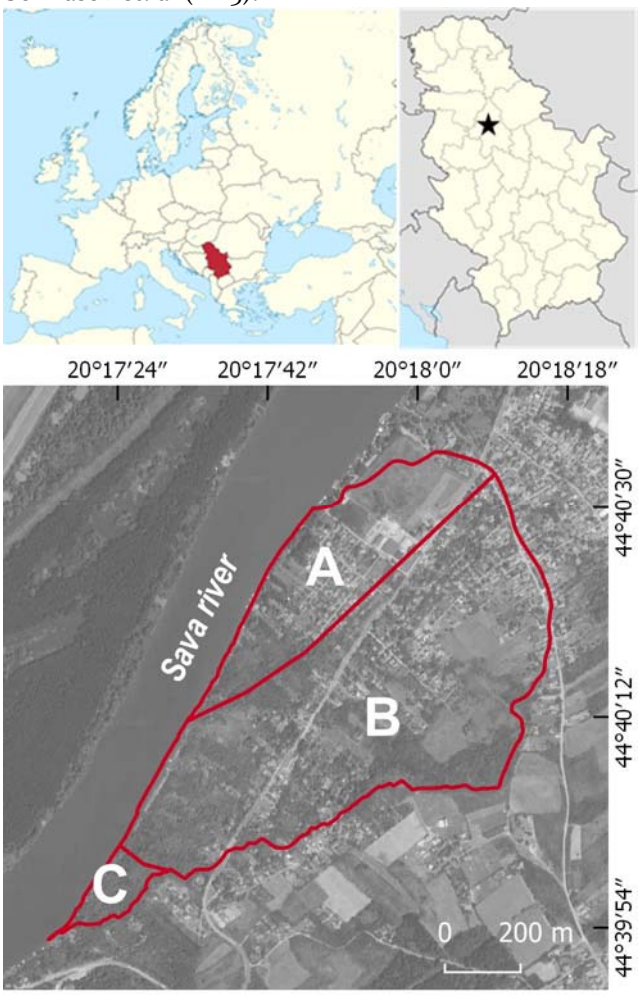

Figure 1 Geographical position of the Republic of Serbia in Europe (upper left) and Belgrade area within Serbia (upper right). Umka landslide border is outlined in red, with relative positions of blocks A, B & C.

Previous research

Most of the Umka landslide investigation and research during the 1970-1990 period, were performed for the Main Design for the Belgrade-Obrenovac highway and for the Umka urban plans and regulations (Mitrović & Jelisavac, 2006). During the 1990-2005, on the Umka landslide there were more than 70 boreholes (wherein, many of these had inclinometer construction installed), 19 standard penetration tests, 10 geological wells, 6 geological pits, 4 deep shafts, and more than 30 surveying benchmarks that were monitored. During the 1990 investigation campaign more than 430 objects were surveyed for deformations and damage. This number includes dozens of objects in the stable part near the landslide boundaries.

Geometry, geological setting, mechanism and dynamics of the Umka landslide were well defined by previous research. A summary of the geotechnical investigations results until 1995 can be found in Vujanić et al. (1996), while the summary of investigations until 2005 can be found in Jelisavac et al. (2006) and Mitrović & Jelisavac (2006).

Since the monitoring of the landslide was interrupted and discontinued after 1990 and 2005 geotechnical investigation campaigns, there was a need for setting up permanent geotechnical and geodetic monitoring. Automated continuous real-time GNSS monitoring was established in March 2010 (Abolmasov et al. 2012b; 2013). Simultaneously, the levels of the Sava river are observed in near-real time, i.e. on daily basis, as well as the average daily temperature and type and amount of precipitation. More detailed report with results of monitoring and conclusions about landslide recent dynamics can be found in Abolmasov et al. (2014, 2015). Photogelogical analysis was performed by Marković (1980) and later for a new landslide inventory of Belgrade by Lokin et al. (2010). Basic photogrammetric analyses of the Umka landslide have been revealed from aerial images from 1970–2007 period and orthophotos that were taken in 2001, 2005 and 2010 (Abolmasov et al., 2012).

Previous research has shown that Umka landslide can be described as complex landslide within the stiff fissured clayey marls (Abolmasov et. al., 2015). Landslide is active, with various phases of deceleration and acceleration, which are mostly in correlation with the Sava River level drop, while landslide velocity is characterized as slow to very slow. More details and brief report of investigations conducted by IPL 181 project until 2017 can be found at Abolmasov et al. (2017).

Research and investigation performed during 2017.

Control borehole and inclinometer

One borehole was drilled in cooperation with the Highway Institute from Belgrade within the B block of the Umka landslide in April 2017. Borehole was 21 m deep, with coring and standard geotechnical logging and sampling of the core for laboratory tests and mineralogical analysis (Figure 2, left). Inclinometer construction was subsequently installed in the borehole to the depth of 19 m. Reading was performed continuously every second week until mid of the June, when inclinometer cap was destroyed, and construction was buried with illegal construction waste dump (Figure 2, right). Borehole logs has shown high correlation with the previous research and established terrain models. Slip surface was detected at the depth of 16.9 m. Eight core samples were taken and packed for ring shear apparatus ICL-1 testing at Faculty of Civil Engineering of University of Rijeka (Croatia). Position of inclinometer is displayed on Figure 5.

Detailed mapping of elements on risk

Since the last survey of damaged objects on the Umka landslide was finished 25 years ago, it was necessary to be performed again for quantitative risk assessment. Detailed survey of all accessible objects was done from September 2017 until April 2018 with more than 360 evidenced objects together with brief population census. This approach was necessary because orthophoto analysis and field survey has shown that there are more than 40 new objects were built from last investigation campaign (2005). Plenty of old objects were upgraded or renovated by residents or even destroyed by landslide activity, so new conditions of elements at risk were established. Survey was designed to be complementary with previous research, so the basic layout was taken from previous study. Survey that was carried out during 90's didn't considered data about population and their working habits or evidence of highly exposed and vulnerable population at risk - like children, elders or disabled.

Figure 2 Borehole logging on the Umka landslide (left), destroyed inclinometer construction after 4 months from installation (right).

New questionnaire was designed, and divided into several categories:

- ***Basic data about object;***

This category included basic info about exposed object like: location, position, coordinates info about cadaster parcel number, type of object (resident, cottage, ancillary...), number of floors, roofs, ground floor area and number of vehicles in household.

- ***Data about construction;***

This category included questions about type of dominant building material (concrete, reinforced concrete, brick, and block) and construction type (supporting walls, armored concrete beams, wooden beams etc.).

- ***Damage classification;***

Herein two descriptive scales were used for typology of damage on objects, first scale was adopted from previous questionnaire (Highway institute) and all objects were categorized in 5 classes (without damage - destroyed). Second scale divided objects in 6 classes by damage and this scale is still the only official one, defined by *"Unique methodology for damage assessment from natural hazards in SFR Yugoslavia"*, adopted and published in Official Gazette in 1987.

- ***Data about foundation;***

This category included questions about type of foundations and material.

- ***Data about household;***

This category includes questions of number of inhabitants within the object and their employment, number of children and number of disabled if any.

- ***Data about damage estimation, emergency measures and possible remediation measures;***

Those three categories, include field about relative damage estimation (expressed in total value of the housing or object and % of damage), estimation of a possible emergency geotechnical measures (drainage, construction works) and possibility of remediation measures (descriptive: possible, not possible, not needed).

- ***Information about surface and groundwater;***

This category includes fields about ground and underground waters, presence of water system, drainage system, position of water wells and their conditions, water level in wells, and presence of sewage system with current condition.

- ***Object and surface deformation***

This category contains blank sketch of all four sides of an object. Walls are always oriented in such manner, that A side is looking toward general slide direction. Other sides are named B, C & D and they are always oriented clockwise from A. During surveying, all cracks are drawn on these sketches, with their relative position, width, and intensity. This category also includes information about house or object tilt toward predefined directions, as well as sinking and deformation of surrounding terrain.

- ***Other remarks***

This field represent blank text field for general remarks and description of all other relevant information that are not covered by previous field investigations, but could be significant for other conclusions.

Preliminary results of detailed mapping of housing and objects on the Umka landslide are shown on Figure 3, where all objects are categorized by level of damage.

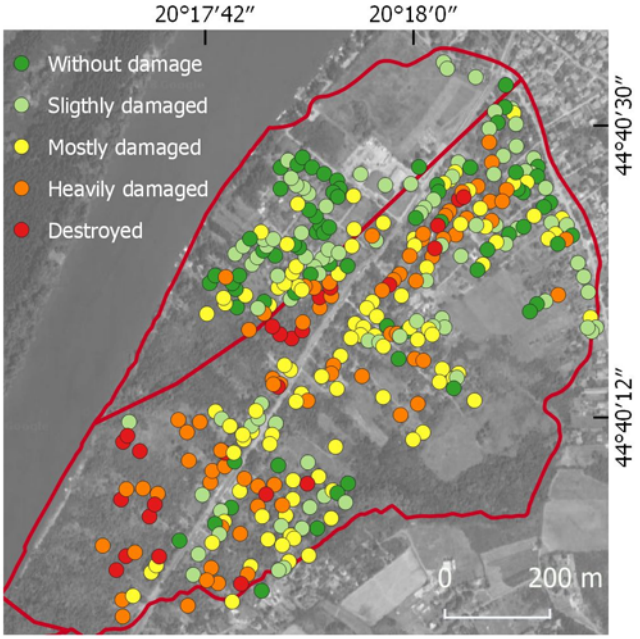

Figure 3 Results of detailed mapping of housing and objects on the Umka Landslide (2017-2018). Objects are classified by damage. Red line outlines the landslide border

Research and investigation performed during 2018.

UAV imaging and mapping

More than 2000 images were taken by UAV during March 2018, but after manually removing blurred and oblique imagery, 1982 images were left for further processing. Forward image overlap was at least 90% and overlap kept between rows of images was around 60%. UAV was flying at height of 80 m above take-off station achieving average pixel size of 2.2 cm. Seven flights were performed in order to cover the area of block A and B (Figure 4). Block C was not imaged for several reasons. Firstly, there are no objects present, and secondly, terrain is heavily vegetated and extremely inaccessible.

Only 45 Ground Control Points were used in bundle adjustment, achieving Root Mean Squared Error of 2.5 cm and optimal measurements coverage. Photos alignment produced 894 923 tie points. Dense cloud was generated by using medium quality option resulting in 188 103 597 points in total. Processing lasted 48 hours by using conventional desktop machine with 16 GB of RAM, 4-core processor at 2GHz each. After ground point filtering, there was 4 896 664 points left classified as ground. Aircraft was DJI MATRICE 600 PRO, industrial hexacopter with mounted DSLR camera Canon EOS 6D with resolution of 20.2 megapixels and focal length of 24 mm.

High resolution orthophoto and DEM were created, and used for object precise spatial location, and for

mapping damage on the road and local street infrastructure.

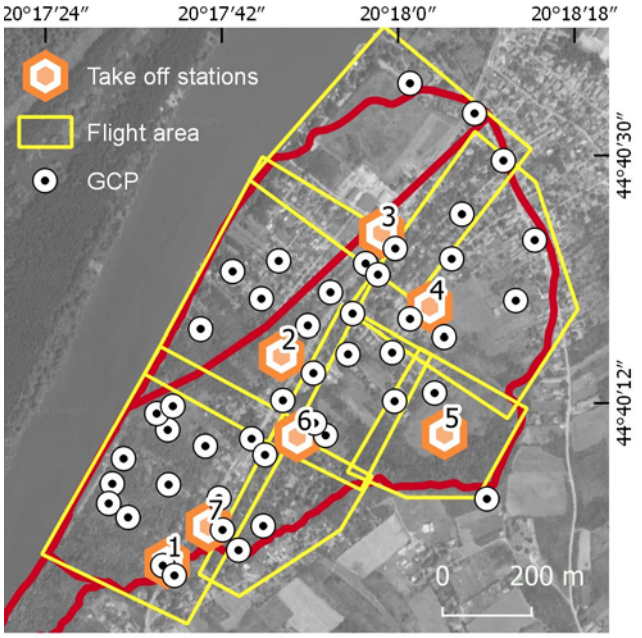

Figure 4 Positions of the drone take-off stations, GCP's and image footprint coverage. Red line outlines the landslide border.

Road damage assessment

Field campaign and UAV mapping, included all streets and roads, mapped for accessing landslide damage during 2018. Streets were treated as linear objects that were segmented and categorized by level of damage and accessibility. Beside visual field inspection, high resolution ortophoto was used for damage assessment.

Beside the state road IB 26, there is a network of local streets across the Umka landslide affected by the landslide. Most of the streets in lower part of block B are totally damaged and inaccessible, while situation is slightly better in the upper parts of block B, where some areas and parts are accessible by standard passenger vehicles. The best situation is in block A, where most of the streets are accessible with slight damage or cracks in the upper part.

Collecting and analyzing the traffic data

Annual average daily traffic (AADT) data were collected for landslide risk assessment from the Public Enterprise Roads of Serbia for the period 2005–2016. These data include information about daily traffic on section of road Barič – Umka, with details about vehicle category, velocity and traffic direction per hour.

Information about car accidents was collected from OpenData portal of the Republic of Serbia (https://data.gov.rs). This data contains information about traffic accidents on the territory of Belgrade. All data are tabular with most important parameters such as: accident ID, date and time, location, type of accident, number of vehicle and people affected, as well as a brief description.

Establishing geodetic network for landslide monitoring

During March 2018, 61 geodetic benchmarks were stabilized inside the landslide area and measured by RTK GNSS rover (Figure 5), as well as the four baseline points outside the landslide body. After processing, 59 valid solutions were obtained from initial measurement.

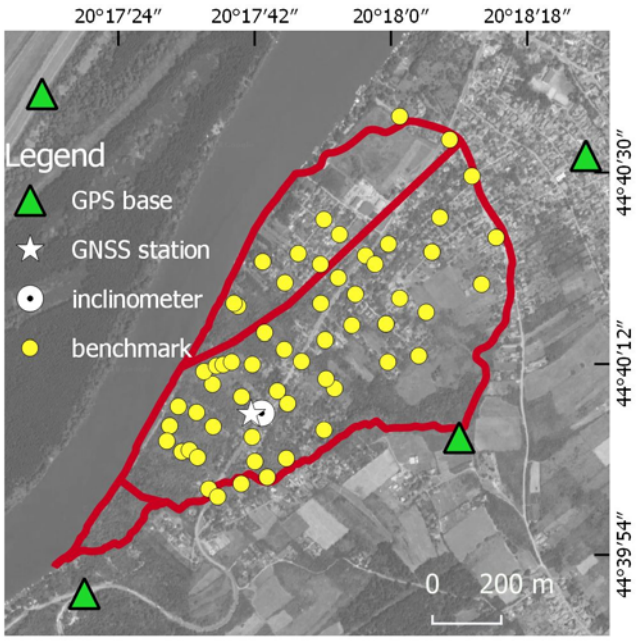

Figure 5 Position of geodetic benchmarks, permanent GNSS station, stable base stations and inclinometer.

Historical aerial images

Historical aerial images of the Umka landslide were obtained from Military Geographic Institute of the Serbian Army for 1959, 1962, 1967, 1970, 1981 & 1988, during 2017 & 2018. The analysis showed that only several images from 1959, 1967 & 1970 could be used for photogrammetric analysis and processing due to optimal scale, tone and brightness of images. For the testing purposes, only images from 1970 were used for processing, while GCP were simulated using DEM that was crated from UAV images. In such circumstances, final model precision was cca. 2 m so further calibration and processing is needed for obtaining desired precision which is less than 1 m. Images were processed by Agisoft software (Figure 6). High resolution DEM and orthophoto images were produced for 1970, since the scales of images were around 1:5000, and due the fact that images were correctly scanned with 1600 dpi.

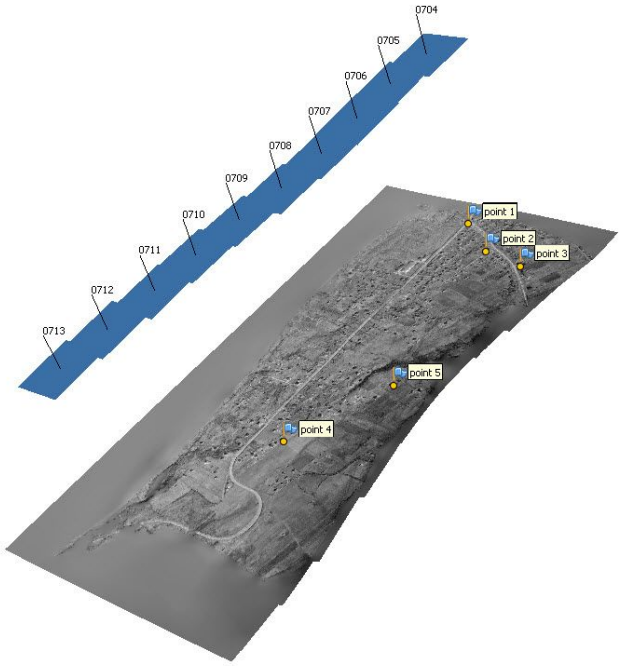

Figure 6 position of historical aerial images, orthophoto created with synthetic GCP's

Future work planned for 2019 and 2020

Remote sensing

According to the Project 181 objectives, it was planned to obtain aerial LIDAR images in cooperation with Military Geographic Institute of the Serbian Army.

Stereo images after 2000 should be collected from Republic Geodetic Survey for further photogrammetric analysis.

During 2019 Umka landslide will be mapped by UAV once more, while radar images from Sentinel 1a mission will be used for PSInSAR analysis and correlation with results that are obtained from other monitoring techniques.

Geotechnical and other geological analysis

Core samples that were taken will be sent for ring shear apparatus ICL-1 testing at Faculty of Civil Engineering of University of Rijeka.

Fifteen selected samples obtained from borehole drilling in 2017, will be investigated by X-ray powder diffraction methods. The main goal is to determine their mineralogical composition with an emphasis on clay mineralogical analysis. The results will give better insight in content variation of specific clay minerals by depth.

Surface geodetic monitoring

At least two new measurement of established geodetic network will be performed during 2019, while one more measurement will be finished during November 2018.

All available and collected data will be used for Performing Quantitative risk assessment of the Umka landslide.

Acknowledgments

The research was supported by the Ministry of Education, Science and Technological Development of the Republic of Serbia Project No TR 36009. UAV with camera was acquired with the funding of Erasmus+ Programme of the European Union-561902-EPP-1-2015-1-SE-EPPKA2-CBHE-JP Modernizing geodesy education in Western Balkan with focus on competences and learning outcomes (GEOWEB).

References

Abolmasov B, Đurić U, Pavlović R, Trivić B, (2012a). Tracking of slow moving landslides by photogrammetric data-a case study. Proceedings of the 11th International and 2nd American Symposium on Landslides and Engineered Slopes, Banff, Canada, 3-8 June, 2012. Eds. Eberhardt E, Froese C, Turner K, Leroueil S, Taylor&Francis Group, London, Vol 2, pp. 1359-1363.

Abolmasov B, Marjanović M, Milenković S, Đurić U, Jelisavac B, Pejić M, (2017). Study of Slow Moving Landslide Umka Near Belgrade, Serbia (IPL-181) In: Sassa K, Mikoš M, Yin Y (eds) Advancing Culture of Living with Landslides. WLF 2017. Springer, Cham, https://doi.org/10.1007/978-3-319-59469-9_37: 419-427

Abolmasov B, Marjanović M, Milenković S, Đurić U, Jelisavac B, Pejić M, (2017). Study of Slow Moving Landslide Umka Near Belgrade, Serbia (IPL-181). Springer International Publishing, pp.419-427. DOI: 10.1007/978-3-319-59469-9_37. pp 419-427

Abolmasov B, Milenković S, Jelisavac B, Vujanić V, (2013). Landslide Umka: The First Automated Monitoring Project in Serbia. Landslide Science and Practice, Volume 2: Early Warning, Instrumentation and Monitoring, Eds. Margottini C, Canuti P, Sassa K, Springer Verlag, pp. 339-346.

Abolmasov B, Milenković S, Jelisavac B, Vujanić V, Pejić M, Pejović M, (2012b). Using GNSS sensors in real time monitoring of slow moving landslides-a case study. Proceedings of the 11th International and 2nd American Symposium on Landslides and Engineered Slopes, Banff, Canada, 3-8 June, 2012. Eds. Eberhardt E, Froese C, Turner K, Leroueil S, Taylor&Francis Group, London, Vol 2, pp. 1381-1385.

Abolmasov B, Milenković, S, Marjanović M, Đurić U, Jelisavac B (2015). A geotechnical model of the Umka landslide with reference to landslides in weathered Neogene marls in Serbia. Landslides, Vol 12 (4): 689-702. DOI 10.1007/s10346-014-0499-4

Abolmasov B, Pejić M, Šušić V, (2014). The analysis of landslide dynamics based on automated GNSS monitoring. Proceeding of the 1st Regional Symposium on Landslides in the Adriatic-Balkan Region - 1st ReSyLAB 2013, Zagreb 6-9 March 2013. Eds. Sassa K., Mihalić Arbanas S., Arbanas Ž. Univesrity of Zagreb, Faculty of Mining, Geology and Petroleum Engineering and University of Rijeka, Faculty for Civil Engineering, Zagreb, Croatia. pp. 187-191

Jelisavac B, Milenković S, Vujanić V, Mitrović P (2006). Geotechnical investigations and repair of the landslide Umka - Duboko on the route of motorway E-763 Belgrade–South Adriatic. International Workshop-Prague-Geotechnical days, Prague, 2006.

Lokin P, Pavlović R, Trivić B (2010). Projekat istraživanja terena za izradu katastra klizišta područja Generalnog urbanističkog plana

područja Beograda. J.P. Direkcija za građevinsko zemljište grada Beograda (in Serbian). Unpublished material. (in Serbian)

Lokin P, Sunarić D, Cvetković T (1988). Landslides in Neogene sediments on the right Danube bank, Yugoslavia. Proceedings of the 5th International Symposium on Landslides, 10-15 July 1988, Lausanne, Ed Ch Bonnard, Vol 1, Balkema Rotterdam, pp. 213-217

Luković M, (1952). Važniji tipovi naših klizišta i mogućnosti njihovog saniranja. Geološki vesnik. Vol IX.275-310 (in Serbian)

Marković M, (1980) Fotogeološka ispitivanja stabilnosti na području Umka-Barič, Fond stručnih dokumenata Instituta za puteve - Beograd (in Serbian)

Mitrović P, Jelisavac B, (2006). Sanacija klizišta "Duboka". Materijali i konstrukcije 49(1-2): 46-59 (in Serbian)

Rokić Lj, Vujanić V (2002). A contribution on the study of landslide origins in Neogene sediments of Danube river coastal area. Proceedings of the 1st European Conference on Landslides, Prague, Czech Republic, June 24-26 2002, Eds, Rybar J, Stemberk J, Wagner P, Balkema Publishers, pp. 291-298.

Rokić Lj, Vujanić V, Jotić M (1998). Forecast of the landslide development processes based on the study of erosion processes of rivers in the plains. Proceedings of 8th International IAEG Congress, 21-25 September 1998, Vancouver, Canada, Eds, Moore D, Hungr O, Vol 3, Balkema Rotterdam: 1485-1491.

Vujanić V, Livada N, Božinović D (1984). On an Old Landslide in Neogene Clays on the Right Bank of the Sava near Belgrade. Proceedings of 4th International Symposium on Landslides, Toronto, Canada, 1984, Vol 2: 227-233.

Vujanić V, Livada N, Jotić M, Gojković S, Ivković J, Božinović D, Sunarić D, Šutić J (1981). Klizište "Duboko" na Savi kod Beograda. Zbornik radova Simpozijuma istraživanje I sanacija klizišta, Bled 1981, Knjiga 1, pp. 119-134 (in Serbian).

IPL Project 210 – Massive landsliding in Serbia following Cyclone Tamara in May 2014 - progress report

Biljana Abolmasov [(1)], Miloš Marjanović [(1)], Uroš Đurić [(2)], Mileva Samardžić-Petrović [(2)], Jelka Krušić [(1)]

1) University of Belgrade, Faculty of Mining and Geology, Đušina 7, Serbia, +381113219225, e-mail: biljana.abolmasov@rgf.bg.ac.rs

2) University of Belgrade, Faculty of Civil Engineering, Belgrade

Abstract The IPL project No 210 titled "Massive landsliding in Serbia following Cyclone Tamara in May 2014" started at March 2016. The study area is located in the Western and Central part of the Republic of Serbia territory affected by Cyclone Tamara in May 2014. The project aims to summarize and analyse all relevant collected data, including historic/current rainfall, landslide records, aftermath reports, and environmental features datasets from the May 2014 sequence. Objectives of the proposed project include: collecting all available and acquiring new landslides data, analysing the trigger/landslide relation in affordable time span and May 2014 event, relating the landslide mechanisms and magnitudes versus the trigger, locating spatial patterns and relationships between landslides and geological and environmental controls, proposing an overview susceptibility map of the event and numerical modelling on the site specific location/landslide mechanism. The Project is organized by University of Belgrade, Faculty of Mining and Geology and Faculty of Civil Engineering. Project beneficiaries are local community and local and regional authorities. In this paper we will present progress report of the proposed project targets performed by project participants.

Keywords Landslides, floods, extreme precipitation

Introduction

Republic of Serbia is located on the Balkan Peninsula in south-east Europe and covers the area of 88,361km² and has a population of 7,181,505 (http://stat.gov.rs) (Fig 1).

Serbia's climate varies between continental climate in the North, with cold winters, and hot, humid summers with well distributed rainfall patterns, more Adriatic climate in the South with hot, dry summers and autumns and relatively cold winters with heavy inland snowfall. Differences in elevation and large river basins, as well as exposure to the winds account for climate differences, especially for annual precipitation sums, whichrise with altitude. In lower regions annual precipitation levels range in the interval from 540 to 820 mm. Areas with altitude over 1,000 m have on average 700-1000 mm of precipitation, and some of the mountainous summits in South Western part of Serbia have heavier precipitation up to 1,500 mm. June is the rainiest month with the average of 12-13% of total annual rainfall. Complex geological history and terrain composition, morphological and climate characteristics have caused that 15.08% of the territory of Serbia is affected by landslides (Dragićević et al, 2011).

Figure 1 Geographical position of the Republic of Serbia in Europe

In the third week of May 2014, Serbia and Bosnia and Herzegovina experienced its severest floods in the last 120 years caused by Cyclone Tamara. Huge amounts of rainfall of 250 to 400 mm for three days caused sudden and extreme flooding of several rivers – in particular the Sava River, but also the Drina, Bosna, Una, Sana, Vrbas, Kolubara, Morava - and their tributaries. In the Western and Central Serbia for instance, daily precipitation on May 15th exceeded the expected average of the entire month. Urban, industrial and rural areas were completely submerged under water, cut off without electricity or communications, while roads and other transport facilities were damaged.

As a result, 1.6 million persons (one fifth of the population) were directly or indirectly affected in Serbia. The floods and landslides caused 51 casualties and around 32000 people were evacuated. The Serbian Recovery Needs Assessment (RNA) revealed that the total effects of the disaster in the 24 affected municipalities amounts to

EUR 1.525 billion (equal to 3% of the Serbian Gross Domestic Product).

In March 2016, the Faculty of Mining and Geology applied for the IPL project and during the 11th Session of the IPL-GPC in Kyoto in 2016, a joint project number 210 was approved. It was entitled "Massive landsliding in Serbia following Cyclone Tamara in May 2014" (Abolmasov et al 2017a).

This paper will show progress report obtained during two years of project conduct, as described in project plan and program.

Project description

Objectives

Landslides are amongst the most dangerous natural threats to human lives and property, especially in times of dramatic climate change effects on one hand, and urban sprawl and land consumption on the other.

The project attempts to prove that the May 2014 extreme landsliding event was preconditioned by soil saturation, caused by a high precipitation yield, within several weeks to the event. All relevant data, including historic/current rainfall, landslide records, aftermath reports, and environmental features datasets, have to be analyzed for characterizing the extreme nature of the event and identifying key environmental controls of landslide occurrences.

In this respect, it was essential to produce unified large-scale inventories of May 2014 event and use them for the state-of-the-art hazard analysis. Thus, the project aims to summarize and analyze collected landslide information from the May 2014 sequence. Following these ideas, objectives of the proposed project include: (1) collecting all available (existing) and acquiring new landslides data, (2) analyzing the trigger/landslide relation in affordable time span (past 15 years) and May 2014 event, (3) relating the landslide mechanisms and magnitudes versus the trigger and its aftermath, (4) locating spatial patterns and relationships between landslides and geological and environmental controls, (5) proposing an overview susceptibility map of the event and (6) numerical modeling on the site specific location/landslide mechanism.

Work plan-expected results

The following activities are planned during the project conduct:

- Collecting, review and harmonization of landslides data (Phase 1)
- Analysis of trigger/landslide data (Phase 2)
- Analysis of landslides vs. geological/environmental controls (Phase 3)
- Proposing landslide susceptibility map (Phase 4)
- Numerical modeling on site specific locations/landslide mechanism (Phase 5)
- Compilation and analysis of all results (Phase 6)

After certain activities, it was planned to prepare partial reports, and to prepare a comprehensive report at the end. Preparation of papers for the Landslide journal was also foreseen. Deliverables and time frames are as follow:

- Report 1. Compilation of results of Phase 1 and Phase 2 (end of the 1st year)
- Report 2. Compilation of results Phase 3 (end of the month 18th)
- Report 3. Proposing landslide susceptibility map Phase 4 (end of the month 24th)
- Report 4. Numerical modeling on site specific locations/landslide mechanism Phase 5 (end of the month 30th)
- Report 5. Final report-Phase 6 (end of the 3rd year)

Personel - Beneficiaries

The Project is organized by the University of Belgrade, Faculty of Mining and Geology and Faculty of Civil Engineering. University and staff will provide all necessary documentation for Project finalization. Project Leader is Full Professor Biljana Abolmasov from University of Belgrade, Faculty of Mining and Geology. Core members of the Project are: Assistant Professor Miloš Marjanović from University of Belgrade Faculty of Mining and Geology, Uroš Djurić, PhD student from University of Belgrade Faculty for Civil Engineering, Jelka Krušić, PhD student from University of Belgrade Faculty of Mining and Geology and Katarina Andrejev, PhD student from University of Belgrade Faculty of Mining and Geology.

Direct beneficiaries will be local community – municipalities affected by landslide occurrences during May 2014 event. Local and regional authorities – housing sector, infrastructure authorities, Civil protection units and land/use sectors within affected area.

Progress report

Rainfall event

In the third week of May 2014, a massive low-pressure cyclone Tamara swept through Western Balkan resulting in extensive flood in the Sava River system and partly in the Morava river catchment. The Cyclone moved from Adriatic Sea to Balkan Peninsula very slowly, and from 14 to 16 May was deepened at all altitudes at territory of Serbia and Bosnia and Herzegovina. The result of that unusual cyclone activity was extreme precipitation for short period that caused floods, torrential floods and massive landsliding in the Republic of Serbia, and in the Bosnia and Herzegovina (BiH) (Fig 2).

Fig. 2 MODIS satellite image of Extratropical Storm Yvette (Tamara) taken on May 15, 2014. (Credit: LANCE Rapid Response/MODIS/NASA)

The analysis of precipitation data included available monthly and daily precipitation from Hydro-meteorological Service of the Republic of Serbia, Hydro-meteorological Service of the Republic of Srpska (BiH) and Hydrometeorological Service of the Federation of Bosnia and Herzegovina (BiH) from the Main Meteorological Stations for April and May 2014 (Fig 3).

The highest statistical significance of 48-h duration in Serbia was registered at the Loznica Main Meteorological Station (MMS), where precipitation of 160 mm corresponded to a 1000-y return period, while MMS in Valjevo and Belgrade recorded precipitation of a 400-y return period for the same duration (Prohaska et al, 2014). The highest precipitation for 72-h duration recorded at Loznica (213 mm), Valjevo (190 mm) and Belgrade (174 mm) MMS. The flood event (14-15 May 2014) and landslides occurrences (15-18 May 2014) were caused simultaneously by extreme Cyclone Tamara activity, but massive landsliding was additionally initiated by antecedently introduced rainfall from April 15 to May 14 (Alleoti, 2004). The main triggering factor for all landslides activities was extreme cumulative precipitation from April 15 up to May 18, where precipitation amount exceeded one half of a yearly average precipitation for just one month in Western and Central part of Serbia (Marjanović and Abolmasov, 2015). The analysis of monthly precipitation for April and May 2014 was shown on Fig 3.

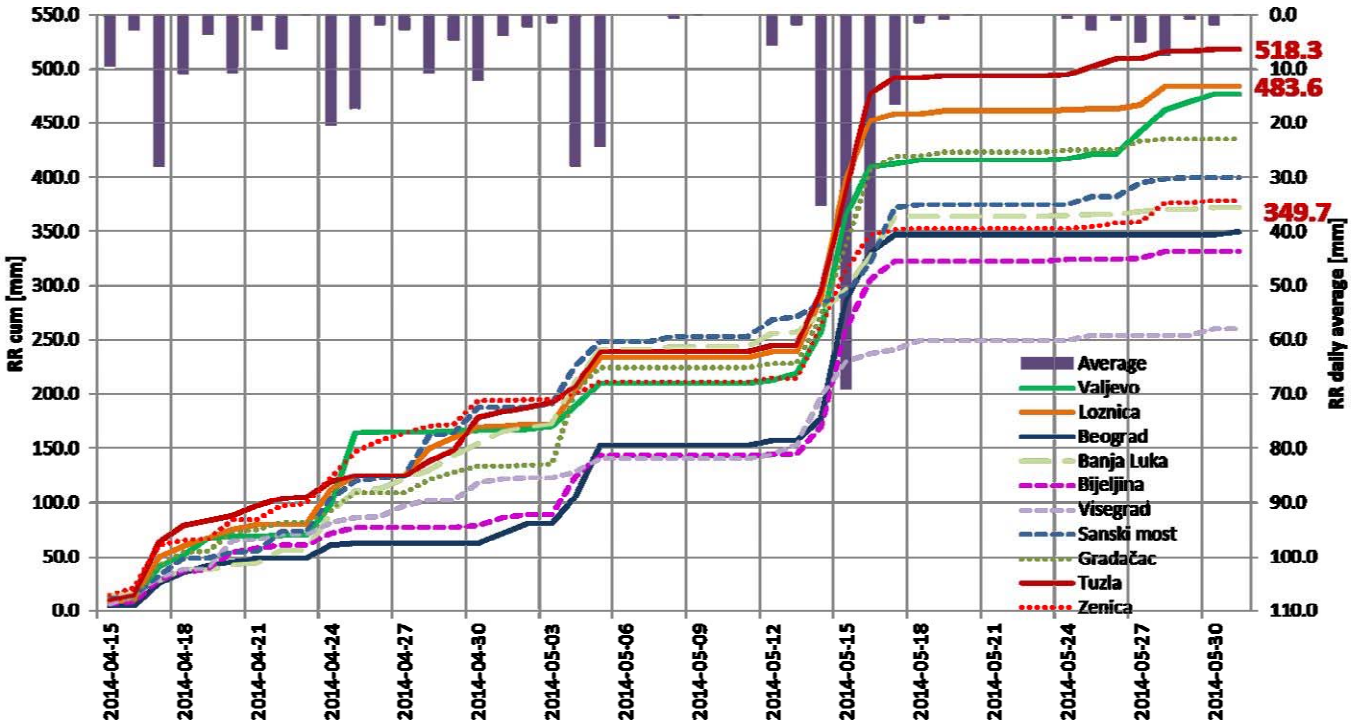

Figure 3. Precipitation data from Main Meteorological Stations in Serbia and Bosnia and Herzegovina for April and May 2014

Study area

Study area covered 11.840 km^2, i.e. 23 of 27 municipalities affected by different type of landslides in Western and Central part of the Republic of Serbia. These municipalities were recognized as most vulnerable to floods, torrential floods and landslides by UNDP Office in Serbia during the post-disaster phase after May 2014 event. Four municipalities were excluded from the IPL 210 Project activities because no landslides occurrences linked to May 2014 rainfall episode were found, and there were only flood damages. Geological and geomorphological settings are very complex as well as other environmental conditions in such a wide area. The type of movement and the type of material involved (Cruden and VanDine, 2013) were depending on lithological type, local geomorphological characteristics, engineering geological properties, degree and depth of

weathering substratum etc. as well as precipitation amount received during May 2014 event.

Landslide data

Usual landslide triggers are floods and high-yield rainfall, which was the case in the catastrophic cyclone Tamara episode that stroke Serbia and surrounding countries in May 2014. At the time, disastrous effects were closely followed by media and public and handled by responsible state services, such as Civil Protection offices, and volunteers, but little has been done after the waters retreated and landslides settled, especially regarding landslide analysis and mitigation. Landslide reports (in analogue form) greatly understated the realistic number of landslides (concentrating more on urgent/acute cases), while report quality standard and consistency was uneven (because they were collected by different institutions, depending on the acute needs), so resulting inventories remain incomplete and far from standardized. In this respect, it was essential to produce unified large-scale inventories of May 2014 event and beyond, and use them for the further analysis.

According to the classification (Cruden and VanDine 2013) a harmonized landslide data report was created. The total number of 2203 landslides are mapped as an open data file reports, according to the BEWARE Project deliverables (Abolmasov et al 2017b). Different type of movement and type of involved material were registered during extensive field campaign and analysis of remote sensing data (Đurić et al 2017). A total number of 1888 different type of movement were certified by supervisor (1539 slides, 78 flows, 48 falls, 1 topple, 23 complex, 138 flows and slides, 55 falls and slides and 6 falls and flows). According to the material involved 925 type of movement were formed from debris, 894 from earth, 20 from rock, 33 from mixed and 16 from artificial material. The simple analysis performed based on landslide distribution by municiaplities shows that the highest number of landslide occurrences were recorded in the Western part of Serbia (Fig 4).

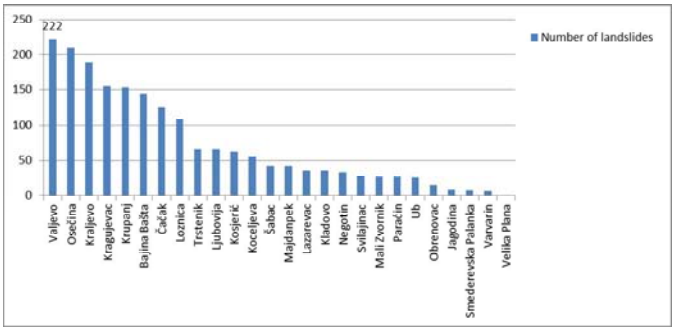

Figure 4. Number of landslides per municipality included in BEWARE project http://geoliss.mre.gov.rs/beware/

Analysis rainfall data vs. landslides

The analysis rainfall data vs. landslides attempted to examine the hypothesis that massive landsliding is preconditioned by soil saturation, caused by high cumulative precipitation yield within several days to several weeks prior to the activation (mid/ long-term conditioning). It was first reasonable to identify the areas where rainfall conditions for massive landsliding are met (Marjanović et al, 2018). Therein, Loznica (Western Serbia) area was both, anomalous in terms of long-term spatial rainfall patterns (Fig 5) and sufficiently covered with landslide reports in a desired period (2001-14). The idea was to predict the pattern of rainfall-induced landsliding in respect to antecedent rainfall data, and thereby, predict/extrapolate additional landslide-triggering rainfall events that have not been reported in 2001-14. Predictions were implemented via Machine Learning (ML) classification task, using Decision Tree (DT) algorithms in particular. Extrapolated events were then used to establish approximate thresholds, by benchmark procedures. In addition, the DT model itself was used as a criterion for defining the upper/lower threshold (Fig 6).

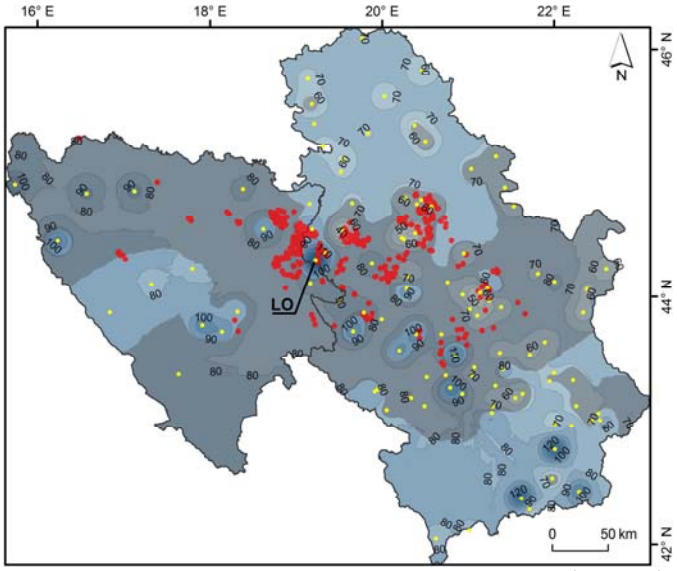

Figure 5. Average monthly rainfall for 2001-14 (in mm), transected with the baseline monthly average (1961-90). Zones higher than this baseline values are non-shaded. Landslide events are depicted as red dots. Yellow dots are weather stations used for the interpolation (station Loznica is labeled - LO)

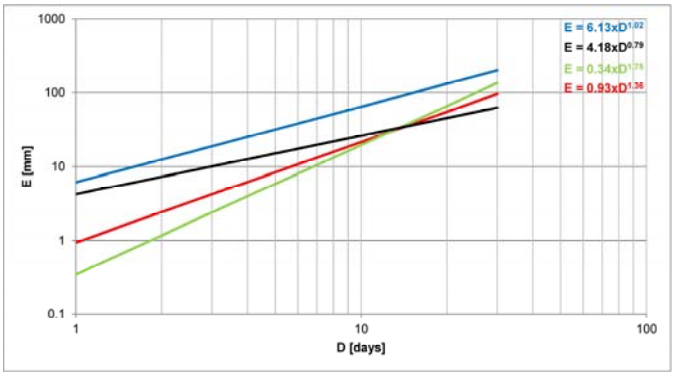

Figure 6. Threshold for LO extracted from Random Tree model minimal – black curve, and maximal thresholds – blue curve, with corresponding curve formulas

Conclusion

Further research within IPL210 will be focused on analyzing: (1) the trigger/landslide relation in affordable time span (past 15 years) for other areas and May 2014 event; and (2) relating the landslide mechanisms and magnitudes versus the trigger and its aftermath.

Raised landslide awareness in Serbia offers better information resources for 2014 onward, through: municipal legislative (activities and reports of recently established emergency response teams in each municipality), media, and social media.

Acknowledgments

IPL Project 210 will be not possible without Project BEWARE (BEyond landslide aWAREness) funded by People of Japan and UNDP Office in Serbia (grant No 00094641). The project was implemented by the State Geological Survey of Serbia, and the University of Belgrade Faculty of Mining and Geology. All activities are supported by Ministry for Energy and Mining and Ministry for Education, Science and Technological Development of the Republic of Serbia Project No TR36009, too.

References

Abolmasov B, Damjanović D, Marjanović M, Stanković R, Nikolić V, Nedeljković S, Petrović Ž (2017a) Project BEWARE—Landslide Post-disaster Relief Activities for Local Communities in Serbia. In: M. Mikoš et al. (eds.), Advancing Culture of Living with Landslides, Proceedings of 4th World Landslide Forum, Ljubljana 29 May-02 June 2017. Vol 3. pp. 413-422. Springer International Publishing. DOI 10.1007/978-3-319-53487-9_48

Abolmasov B, Marjanović M, Đurić U, Krušić J, Andrejev K (2017b) Massive Landsliding in Serbia Following Cyclone Tamara in May 2014 (IPL-210) In: K. Sassa et al. (eds.), Advancing Culture of Living with Landslides, Proceedings of 4th World Landslide Forum, Ljubljana 29 May-02 June 2017, Vol. 1. pp. 473-484. Springer International Publishing. DOI 10.1007/978-3-319-59469-9_4

Aleotti P (2004) A warning system for rainfall-induced shallow failures. Engineering Geology 73 (3-4): 247-265. doi:10.1016/j.enggeo.2004.01.007

Cruden D, VanDine DF, (2013) Classification, Description, Causes and Indirect Effects-Canadian Technical Guidelines and Best Practices related to Landslides: a national initiative for loss reduction, Geological Survey of Canada Open File 7359, 2013.

Dragićević S, Filipović D, Kostadinov S, Ristić R, Novković I, Živković N, Anđelković G, Abolmasov B, Šećerov V, Đurđić S (2011) Natural Hazard Assessment for Land-Use Planning in Serbia.Int J of Env Research. 5(2): 371-380.

Đurić D, Mladenović A, Pešić-Georgiadis M, Marjanović M, Abolmasov B (2017) Using multiresolution and multitemporal satellite data for post disaster landslide inventory in the Republic of Serbia. Landslides 14 (4): 1467-1482. DOI 10.1007/s10346-017-0847-2, ISSN 1612-510X. IF (2016) 3.657, Engineering geological (1/35) https://doi.org/10.1007/s10346-017-0847-2

http://geoliss.mre.gov.rs/beware/ (acessed October 28, 2018)

http://stat.gov.rs/ (acessed October 27, 2018)

Marjanović M, Abolmasov B, (2015) Evidencija i prostorna analiza klizišta zabeleženih u maju 2014. Časopis Izgradnja 69 (5-6). pp 129-134. (on Serbian).

Marjanović M, Krautblatter M, Abolmasov B, Đurić U, Sandić C, Nikolić V (2018) The rainfall-induced landsliding in Western Serbia: A temporal prediction approach using Decision Tree technique. Engineering Geology 232: 147–159. https://doi.org/10.1016/j.enggeo.2017.11.021

Prohaska S, Đukić D, Bartoš Divac V, Božović N (2014) Statistical Significance of the Rainfall Intensity That Caused the May 2014 Flood in Serbia. Water Research and Management, Vol. 4, No. 3 (2014) 3-10

Ecosystem Observation of Upland Soil Erosion Reduction in Mountain Slopes in Sri Lanka

N Nimesha Katuwala, P V I P Perera, H M J M K Herath, K Pavani C Perera & A A Virajh Dias

Centre for Research & Development, Natural Resources Management & Laboratory Services,

Central Engineering Consultancy Bureau, Sri Lanka

Abstract: High endemism plants were recorded in the wet zone including Central Highlands and South Western Wet Zone. The core endemic forest areas such as Sinharaja, Adams Peak, Knuckles, Horton Plains and Kandy are usually subjected to high rainfall conditions and also have relatively less records of upland major soil erosions. Moderate slopes consist of a composite nature of deep-rooted trees, shrubs and grass that can reduce the occurrence of shallow rapidly moving landslides by strengthening and reinforcing soils through their tensile strength and improving drainage. Famers and communities in hill country are used to select some native species and planted on contours along slopes, allow reservation areas and used to grow their agricultural plantation without much issues from the erosional potential of slopes and found to be performing well.

Keywords soil erosion, deep rooted trees, native spices

Introduction

The use of natural systems already in place if reciprocated in these disturbed areas could be a solution or a major contributing factor to such a remedy and in that light this study would bridge the existing knowledge gap of natural solutions. Sri Lanka's hill country too encounters many earth slips during heavy rainfall events, especially in and around tea estates where the natural cover has been disturbed.

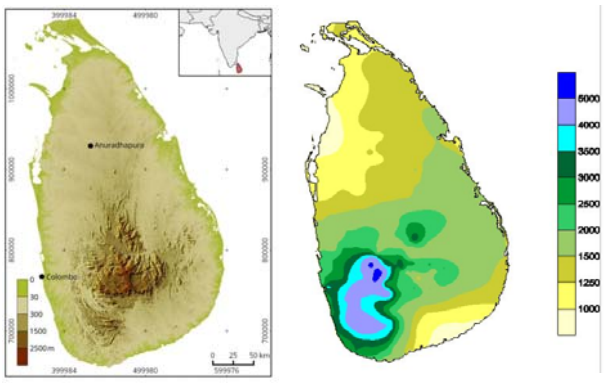

Figure 1: Topography and average annual rainfall (in millimetres) in Sri Lanka

Figure 2: Typical use of ecosystem addoptation staregy in tea plantations in Sri Lanka. Obsrvations clearly indicate stability of the toe of the slope adjoing to the stream.

Geography of the Country

Sri Lanka is an Island in the Indian Ocean having an area of 65,610 km^2. Topographically the country shows well defined three plains of erosion cut named as the lowest peneplain, the middle peneplain and the highest peneplain. The lowest peneplain stretches from coastal line and altitude varies from 0.00 to 100m, while the middle peneplain between 30.0 to 300m. The highest peneplain, central core of the country is a complex of plateaus, mountain chains, massifs and basins having altitude greater than 300m.

Rainfall

The Climate of Sri Lanka is dominated by the above mentioned topographical features of the country and the Southwest and Northeast monsoons regional scale wind regimes. The rainfall pattern is influenced by the monsoon winds of the Indian Ocean and Bay of Bengal and is marked by four seasons as follows.

First Intermonsoon Season - March - April
Southwest Monsoon Season - May - September
Second Intermonsoon Season - October - November
Northeast Monsoon Season - December - February

The mean annual rainfall varies from under 900mm in the southeastern and northwestern to over 5000mm in the wettest parts or the western slopes of the central highlands, Figure 1. Sometimes tropical cyclones bring overcast skies and rains to the southwest, northeast, and eastern parts of the island. The average yearly temperature for the country, as a whole, ranges from 26° C to 28° C.

Mountain Rainforest Ecosystem in Sri Lanka

The mountain rainforest (upland rainforest) ecosystem ranges between 900m – 1525m of elevation in the wet zone. Based on the pattern of distribution of the dominant trees and their endimicity different regions have been identified.

a. Lower Montane Notophyllous Dipterocarp Rain Forests
This forest type is restricted to the elevation of 900m–1500 m of the Peak Wilderness, Knuckles, Namunukula and the Rakwana-Deniyaya ranges. The canopy is dominated by Dipterocarpaceae, Clusiaceae, Myrtaceae, Shorea, Calophyllum, Cryptocarya, Myristica and Syzygium species. From this vegetation, aound 50% of plants are endemic. The Knuckles (Dumbara Hills) range exhibits high heterogeneity in its vegetation distribution with respect to the monsoonal climatic regimes to which it is exposed. According to the Forest Department of Sri Lanka, the southwest-facing slopes are moist throughout the year. Ambagamuwa around Kitulgala in the south and eastwards to Maratenna above Balangoda- encompasses a centre of exceptionally high endemism22 .

b. Lower Montane Notophyllous Evergreen Mixed Rain Forests
This forest type is found in the elevation ranging between 900m to 1370m. The main species found in this forest type are *Eleaeocarpus glandulifer, Myristica dactyloides, Semecarpus nigro-viridis, Cryptocarya wightiana, Palaquium hinmolpedde, Aglaia congylos, Calophyllum acidus, Fahrenheltia spp, Pygeum zeylanicum, Bhesa montana, Gordonia ceylanica, Nothopegia beddomei, Hortonia floribunda 15 Elaeagnus latifolia, Asparagus falcatus, Freycinetia walkeri, Fagraea ceilanica, Pothos remotiflorus Rauvolfia densiflora, Agrostichachys coriacea, Strobilanthes spp. Hedyotis spp. Scutellaria, Pogostemon, Impatiens spp.*

c. Upper Montane Microphyllous Evergreen Dipterocarp Rain Forests Such forests are widespread in the southern escampment above 1525 m. The forest cover is dominated by Stemonoporus, Garcinia, Alphonsea, Gordonia, Palaquium, Syzygium, Mastixia, Cinnamomum, Semecarpus, Agrostistachys, Strobilanthes species.

d. Upper Montane Microphyllous Evergreen Mixed Rain Forests These forests are common at elevations above 1370 m.
This forest type is dominated by the species of Clusiaceae, Myrtaceae, Lauraceae, Symplocaceae and Rubiaceae families. Some of the common tree species in them are *Calophyllum walkeri, C. trapezifolium, Syzygium revolutum, S. rotundifolium, S. umbrosum, Symplocos cochinsinensis, Neolitsea fuscata, Cinnamomum ovalifolium* whereas with the increase in elevation and windy conditions the canopy species become quite stunted giving way to pygmy forests.

The hepatophyta and bryophyte flora and of island is the rich in these montane ecosystems .

Figure 3: Native grass / tree combination of structure adjoin to a perennial stream

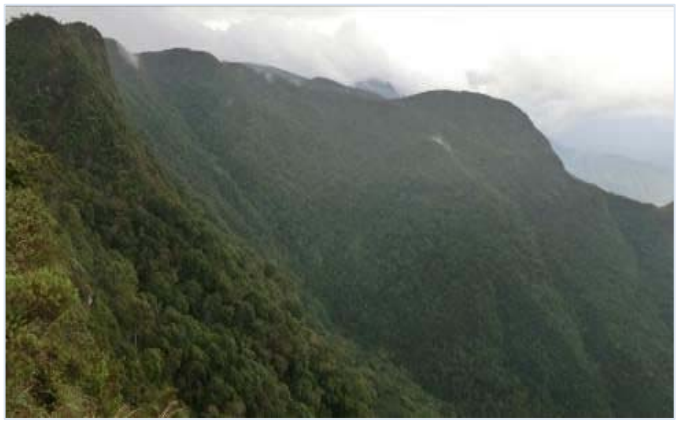

Figure 4: Observation of native species; Typical forest reserves in steep slopes with no record of landslides

Method of Approach

Vegetation cover also plays an important role in soil erosion reduction. Therefore, in recent years, the extent to which mountain slope stability and studies on stabilize slopes with native speices has become of interest. However, present stage, there were not many studies related to the plant root study data on slope stability with native species.

This study reports the observed details and patterns of vegetation which support slope protection and the roles played by different species in such scenarios. Plant functional traits have been well recognized as important predictors for soil erosion. In theory, both plant morphological traits, such as root diameter, and biomechanical traits, such as root tensile strength, have all been shown to significantly affect soil erosion (Gyssels et al. 2005; De Baets et al. 2006, 2008; Pohl et al. 2009; Burylo et al. 2012a,b).

Technicality of Root Growth in Upland Slope Systems

The upland slope means slope well above the human settlements or the area at which defines agriculture in slopes. In general, steep terrain couple with more geological instabilities under heavy rainfall make large parts of area highly susceptible to landslides. In addition, population growth, expansion of infrastructure, and increased forestry and agricultural activity in sloping areas, the significance of landslides is set to increases nowadays. In most cases, high rainfall saturation was the key triggering factor of the landsides including weak management practices of the upper watersheds.

Considering, all above it is interesting to understand the upland forestry related to the plant and root growth in Sri Lanka. To understand the stability of upland slope segments, effects of each of the biodiversity was recorded and infer the best model, rather than one single approach, and therefore can provide more stable and reliable inference results under observational method of assessment. The differences among the observations did not consider any human interventions on slopes.

Understanding the original stability and sequence of the development of natural instability potential and regaining stability due to plant root growth structure is somewhat interesting and understandable only after scientifically disintegrated in slope segments as in Figure 5. Most of the upper slopes consist of rock outcrops and native spices are reinforcing with flexible canopies and root systems and thereby reinforcing the protective effect of plants against soil erosion. Immediate below the outcrop structure usually shows steep slope until reaching the upper segment of the talus slope. High moist soil environment always support to the growth of the canopy and thick and deep rooted tree canopy standing as a passive wedge for the stability.

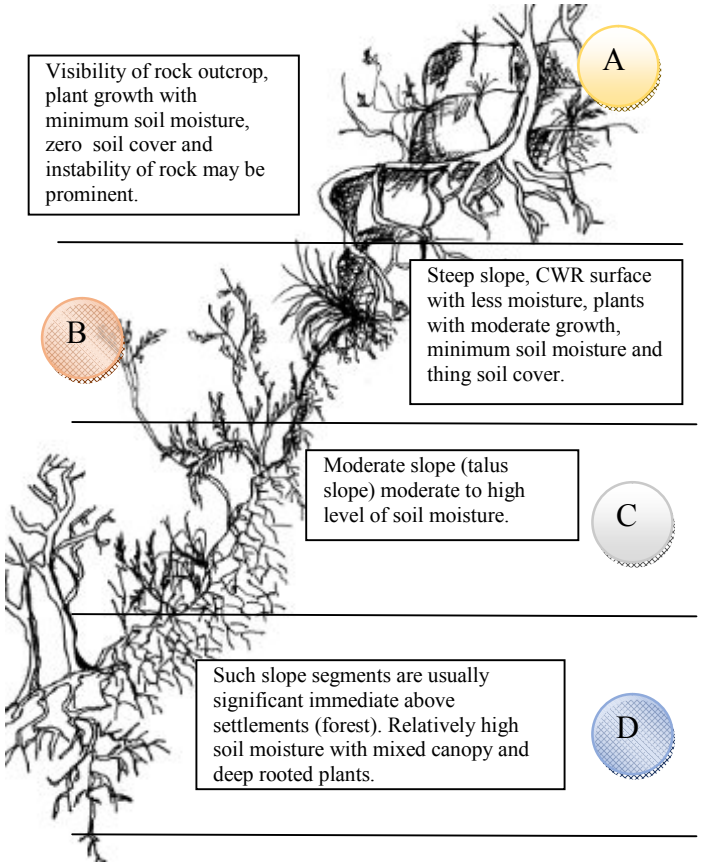

Figure 5: Understanding the slope segment categorisation according to the root grown and type of roots growth.

Zone A: Area usually belongs to the top or the upper mountain slope. The rain-fed soil saturation is the only opportunity to grow plants. Moderately depth rooted plants with grass cover is visible in such slopes.

Zone B: Completely to moderately weathered rocks faces with steep sloping angles of 70 to 90 degrees. Such slopes are usually covered with grass with less vegetation. Some selective indigenous spices are also visible.

Zone C: Contains talus (colluvium) material and showing high soil and water mixture. Such slopes are approximately 26 to 29 degrees and more vulnerable to landslide. Growth of mix vegetation which includes deep and laterally speeded root structure. Area usually stable due to the strength of the laterally speeded structure of the roots.

Zone D: Area immediately above the human settlements. Usually highly stable due to deep rooted plants mixed with composite rooted plant growth. No significant observation on activation of landslides such slopes. However, such areas are more vulnerable if the upper slopes are geologically unstable.

Figure 6: Plant roots providing a cover of a laterally strong fine root systems close to the surface

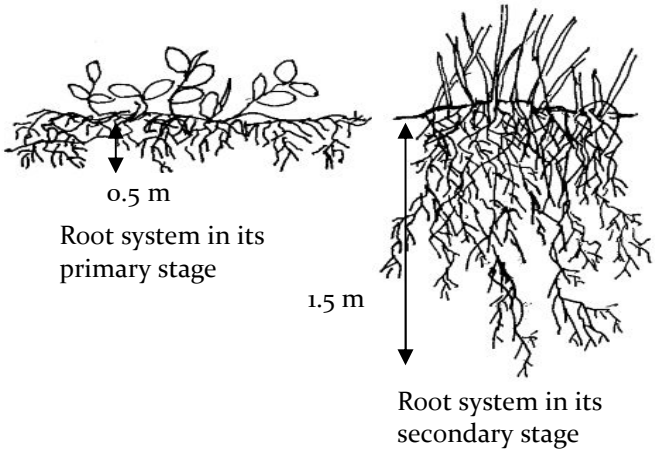

Plant roots act in several ways to increase slope stability:
(1) they bond unstable soil mantles to stable subsoils or substrata,
(2) they provide a cover of a laterally strong fine root systems close to the surface, and
(3) they provide localized centers of reinforcement in the vicinity of individual trees where embedded stems act like a buttress pile or arch-abutment on a slope.

Figure 7: The large single root (taproot) usually which grows straight down anchors the plant in the ground and the lateral roots connected to anchor the soil preventing soil erosion

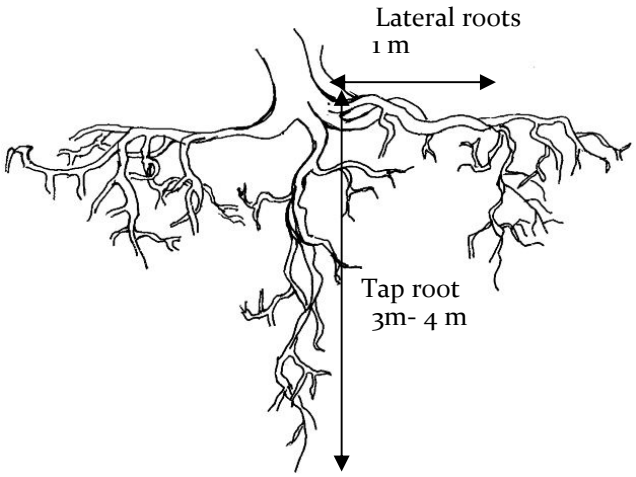

Conclusions

The loss of soil from land surfaces by erosion is widespread globally and adversely impacts the productivity of all natural, agricultural, forest, and ecosystems. Understanding the behaviour patterns of roots growth and impact of root architecture on the soil erosion reducing potential is an essential tool in geo-engineering design and applications. For an example, the large single root usually which grows straight down, anchors the plant in the ground and the lateral roots connected to anchor the soil preventing soil erosion and buttress root system which distributes on all sides of a shallowly rooted tree, does not penetrate to deeper surface layers. It prevents the tree from falling over while also gathering more nutrients.

Our study suggests that functional divergence of restored native forest lands is an important predictor for long term stability and soil erosion of the mountains slope.

Thus results of the study can be directly used for practical application in critical slopes which lie above small villages or the restored communities. Plant cover always protects soil against erosion by reducing water runoff and roots structure. In the long term, vegetation influences the fluxes of water and sediments by increasing the soil-aggregate stability and cohesion as well as by improving water infiltration

However, practitioners can formulate specific plant species (which species) and their abundance (how many individuals), rather than the selection based with the technicality of the roots performances. Therefore, a trait-based restoration framework is recommended to bridge the gap between what we know and how to utilise such knowledge ground.

Acknowledgments

This paper forms an integral part of the IPL-199 registered research on "The Effect of Root Systems in Natural Slope Erosion Protection in the Hill Country of Sri Lanka" being implemented by the Centre for Research & Development, Central Engineering Consultancy Bureau (CECB) of the Ministry of Irrigation and Water Resources Management. It is published with their permissions. The views expressed in the paper are however those of the authors only. Our grateful thanks are due to Eng. N Rupasinghe Chairman Central Engineering Consultancy Bureau and Eng. K L S sahabandu, General Manager for the permission and encouragements.

References .

Burylo, M., Rey, F., Bochet, E. & Dutoit, T. (2012a) Plant functional traits and species ability for sediment retention during concentrated flow erosion. Plant and Soil, 353, 135–144. Burylo, M., Rey, F., Mathys, N. & Dutoit, T. (2012b) Plant root traits affecting the resistance of soils to concentrated flow erosion. Earth Surface Processes and Landforms, 37, 1463–1470.

De Baets, S., Poesen, J., Gyssels, G. & Knapen, A. (2006) Effects of grass roots on the erodibility of topsoils during concentrated flow. Geomorphology, 76, 54

De Baets, S., Poesen, J., Reubens, B., Wemans, K., De Baerdemaeker, J. & Muys, B. (2008) Root tensile strength and root distribution of typical Mediterranean plant species and their contribution to soil shear strength. Plant and Soil, 305, 207–226.

Forests and landslides The role of trees and forests in the prevention of landslides and rehabilitation of landslide-affected areas in Asia; by Keith Forbes and Jeremy Broadhead; Food and Agriculture Organization of the United Nations Regional Office for Asia and the Pacific Bangkok 2011 .

Gyssels, G., Poesen, J., Bochet, E. & Li, Y. (2005) Impact of plant roots on the resistance of soils to erosion by water: a review. Progress in Physical Geography, 29, 189–217.

Leiser, A.T., 1998, 'Biotechnology for Slope Protection and Erosion Control' paper presented to Peaks to Prairies: A Conference on Watershed Stewardship, Rapid City, South

Pohl, M., Alig, D., Korner, C. & Rixen, C. (2009) Higher plant diversity enhances soil stability in disturbed alpine ecosystems. Plant and Soil, 324, 91 –102

Soil Bioengineering for Upland Slope Protection and Erosion Reduction; Part 650 Engineering Field Handbook; U.S. Department of Agriculture, Washington, DC 20250.

N N Katuwala

Environmental Chemist, Centre for Research & Development, NRM&LS, Central Engineering Consultancy Bureau, No. 415, Bauddhaloka MW, Colombo 7, Sri Lanka

E-mail: nkatuwala@gmail.com

H M Janaki M K Herath

Engineering Geologist, Centre for Research & Development, NRM&LS, Central Engineering Consultancy Bureau, No. 415, Bauddhaloka MW, Colombo 7, Sri Lanka;

E-mail:jmkherath@yahoo.com

P V I P Perera,

Environmental Scientist, Centre for Research & Development, NRM&LS, Central Engineering Consultancy Bureau, No. 415, Bauddhaloka MW, Colombo 7, Sri Lanka ; E-mail: ishastha@gmail.com

K Pavani C Perera

Research Assitant, Centre for Research & Development, NRM&LS, Central Engineering Consultancy Bureau, No. 415, Bauddhaloka MW, Colombo 7, Sri Lanka ; E-mail: pavanichanika@gmail.com

Eng. A A Virajh Dias

Addl. General Manager, NRM&LS, Central Engineering Consultancy Bureau, No. 415, Bauddhaloka MW, Colombo 7, Sri Lanka ;

E-mail: aavirajhd@yahoo.com

Historical Monuments Located Within Landslide Hazardous Site

Oleksandr Trofymchuk [(1)], Iurii Kaliukh [(1,2)], Oleksij Lebid [(1)]

1) Institute of Telecommunications and Global Information Space, NASU, 13, Chokolivsky Blvd., Kyiv, 03186, Ukraine, e-mail: itelua@kv.ukrtel.net

2) State Enterprise "Research Institute of Building Constructions", 5/2, Preobrajenskaya St., Kyiv, 03680, Ukraine, e-mail: kalyukh2002@gmail.com

Abstract Ukraine (Institute of Telecommunications and Global Information Space of National Academy of Sciences of Ukraine) has been a member of the "Landslides and Cultural & Natural Heritage" (LACUNHEN) thematic Network of the ICL since 2012 (head of the LACUNHEN is - Margottini C. The purpose of the LACUNHEN - International Consortium on Landslides is to create a platform for scientists and experts who are ready to contribute to safeguarding relevant endangered Natural and Cultural Heritage sites Margottini, Vilimek, (2014). LACUNHEN will share and disseminate their respective experience Margottini, Vilimek (2014), demonstrating how these special "objects" require approaches, techniques and solutions that go far beyond traditional civil engineering perspectives. Within this view, landslides and more generally slope instabilities are an important factor endangering cultural heritage sites and its degradation and require additional protection measures, creation of the monitoring and early warning systems, etc. More than 90% of the territory of Ukraine has complex ground conditions and about 120 000 sq. km of the Ukrainian territory are located in the zone with seismicity of natural origin with a magnitude varying from 6 to 9. Therefore, unpredictable changes of natural geological and man-made factors governing ground conditions may lead to dangerous deformation processes in the Ukraine heritage sites.

Keywords IPL-153, heritage sites, slope instabilities, deformation

Introduction

During the 2012 - 2018 period LACUNHEN Ukrainian Department has studied three Ukrainian Heritage Sites located in complicated geological and geotechnical conditions within the framework of the "Landslide protection structures and their development in the Autonomous Republic of the Crimea, Ukraine" IPL Project № 153 (headed by Trofymchuk O., 2012) and a part of the research activities within the LACUNHEN. Two of the above sites are: Livadia Palace and St. Andrew's Church located within active landslide systems. The third is the Swallow's Nest castle situated on the top of the 40-meters high Aurora Cliff of Cape Ai-Todor in the Black Sea, Autonomous Republic of Crimea, Ukraine (temporary occupied in 2014 by Russian Federation), and is a subject of intensive destruction during the recent years.

Livadia Palace

Monitoring and early warning system (EWS) of Livadia Palace building constructions located within active Central Livadia Landslide system has been described in details in the articles by Trofymchuk, Kaliukh, Klimenkov (2018) as an example of **s**ystem approach for monitoring of World Heritage Sites placed on active landslides. There are also results of EWS performance.

The Swallow's Nest castle

The site has been investigated within IPL Project № 153 and a part of the research activities within the LACUNHEN. The Swallow's Nest castle is a landmark of the whole Crimean coast (fig.1). In 1927, the Swallow's Nest survived a serious earthquake. There were two shocks at night. The first one was weak but made people to leave their houses. The second one rated at 9 on the Richter scale. The castle was not damaged. However, the cliff itself developed a huge crack from its top to the middle so that the castle could break at any time (fig.2). Part of support cliff was thrown into the sea and observation platform was hanging over the precipice. The building itself was not damaged apart from some small decorative items along with a small portion of the cliff under the bottom balcony. However, the cracks appeared on the walls and the castle was closed for uncertain term. At the end of 1950s the cracks indicating the threat of the castle collapse were detected. The castle was recognized as dangerous and was not used for a long time. It was an idea to take the castle to pieces, to number the stones and slabs and assemble on a new safe place. In 1960-1970s the castle was renovated and successfully used up to the present moment. However, the Aurora Cliff – the Swallow's Nest foundation has been intensively destroyed during recent years (fig.1-2). Therefore, Ukrainian ICL Department and State Research Institute of Building Constructions (RIBC) undertook scientific and research

works on the above issue and developed recommendations as for the Aurora Cliff suspension as well as reconstruction and preservation of the castle structures.

Figure 1 Swallow's Nest castle. South-west view. The crack in the cliff is obvious (the crack width is up to 0,5 ~ 0,7 м).

Figure 2 – The northern view. The huge crack separating some part of the rock from the main cliff part and a range of smaller cracks covering the whole Swallow's Nest castle base could be seen on the figure 2.

Visual and instrumental survey of the cliff Swallow's Nest castle foundation and castle itself performed by the group of RIBC specialists under the supervision of Prof. Iurii Kaliukh has revealed that whole chalkstone rock mass has been affected by different types of destruction with perspective of cracks and cavernous porosity consolidation and extension.

The above creates an immediate threat to the preservation of the unique monument of architecture, history and culture - the Swallow's Nest castle. On the photographs (fig. 3), there are underwater damages that penetrate the rock massif-base of the castle from all sides are seen.

a) b)

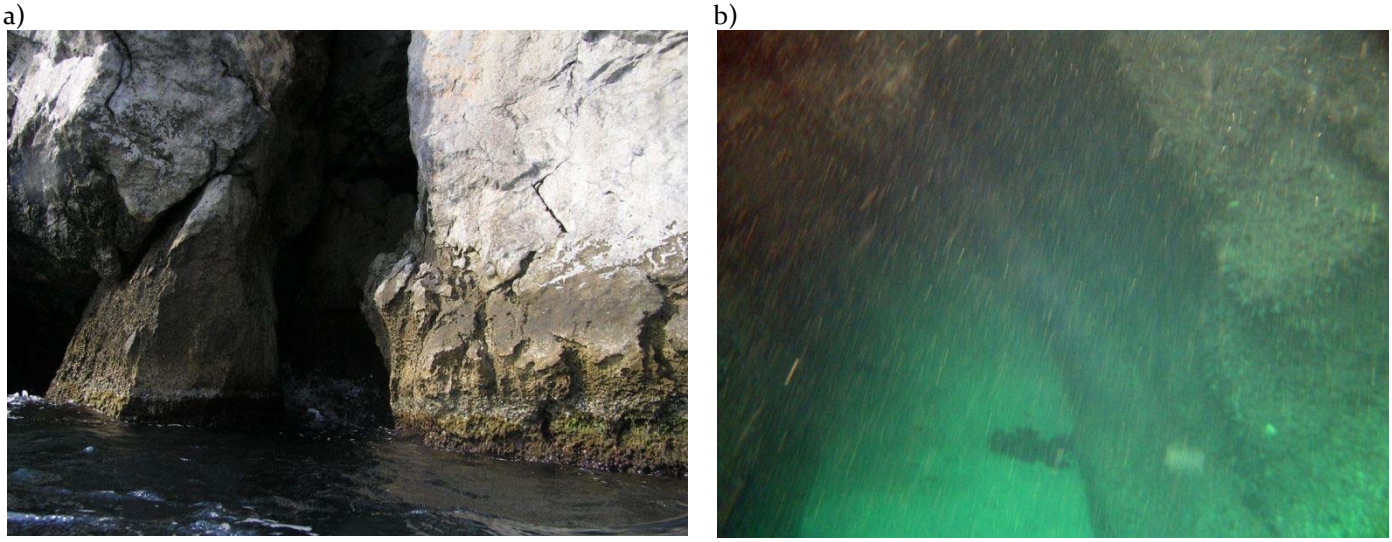

Figure 3(a,b) Surface and underwater parts of the Swallow's Nest castle rock-base perforated with deep cracks, surface and underwater caves from all the sides.

More detailed results of the stressed-deformed state (SDS) of the rock survey, rock base and castle itself are about to be reported on the WLF5 as part of the research activities of Ukraine within the LACUNHEN thematic Network of the ICL and results of the "Landslide protection structures and their development in the Autonomous Republic of the Crimea, Ukraine" IPL Project № 153 (headed by Trofymchuk O., 2012).

St. Andrew's Church

St. Andrew's Church is a unique historical and architectural monument of the eighteenth century built in 1747-1762 by I.Michurin according to B.Rastrelli's design. Since 1968 St. Andrew's Church is a museum, branch of the "Sofiya Kyivska" National reserve, Nationally significant site, number 14 (fig.4).

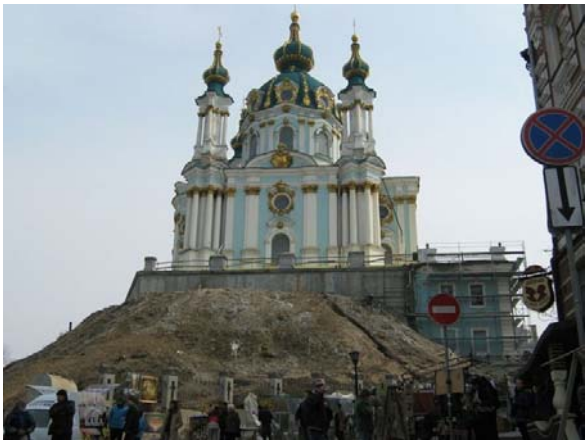

Figure 4. St. Andrew's Church general view.

St. Andrew's Church was built in Baroque style. This style is characterized by pageantry, dynamic architectural forms, riches of design, play of light and shadow. The church was built on the remains of the earth's fortress of the seventeenth century. The church building is completed with a central dome and four corner decorative towers. Building fronts are decorated with columns, pilasters, cornices of complex profile, cast iron and copper gilded details. The size of the church: length - 32 m, width - 20 m, height from the terrace to the top of the cross of the central dome - 50 m. The size of the superstructure is 33,5 x9,5 m. The church is located on a hill situated on the top of the Andriivskyi Descent (one of the most ancient streets in the Ukrainian capital) in the central historical district of Kyiv. The ground level varies from 181.7 m (area around the church) to 118.5 m (foot of the hill (fig. 5)).

Figure 5 Foot of the hill where the Church is situated.

The slopes of the hill are dissected by a thick girder-netting network where landslide processes were actively developing and are developing with active movements and erosion processes (fig.6). Around the development site there is a complex of unfavorable physical and geological phenomena such as landslides, considerable thickness of fill-up ground, significant ground heterogeneity, mechanical suffixation of clay particles into an existing inactive gallery, and external erosion of the hill massif. The base of the foundations of the southern, western and northern Church facades is eolian-deluvial loess-like loamy sands, which have sagging properties. The base of the foundations of the eastern part is morainic loam. Hydrogeological conditions are characterized by the presence of two groundwater levels.

Figure 6 An example of the active development of landslide processes with active developments and erosion processes on the slope of the Church.

The visible superstructure of the church is based on a slightly wider in terms of underground two-story foundation part of the church. The superstructure is joined to the underground foundation and is connected by a common entrance - a two-storey building, the covering of which is part of the church porch (see fig. 7).

Figure 7 General view of the church superstructure and the runway construction.

The foundation of the superstructure is brick masonry in the section from 3 to 5 meters. The church foundation

base lays on different marks: in the western part (on the side of the Andriivsky Descent) - on the marks from 166.6 m to 165.8 m; in the eastern part that hangs over the hill - from 165.7 m to 167.8 m.

Analysis of the slopes stability around St. Andrew's Church site and adjacent territory

Study and analysis of slopes stability around St. Andrew's Church site and on the adjacent territory, as well as the study of current erosion processes on the surrounding slopes was carried out. According to Ukrainian State Construction Standards requirements, for normal operation of a structure built on a landslide slope, the value of the normative slope stability factor should not be less than 1.25. For the calculation of St. Andrew's Church slope stability, a software complex that has a wide range of opportunities for calculating and interpreting the results by 9 methods (Bishop, Yanbu, Spencer, Fellenius, etc.) was used. To improve results reliability, the calculations of slope stability were also carried out using software, developed based on the Terzaghi-Chugaev method. Comparison of the obtained results showed that they are mostly similar. Thus, the coefficients of soil stability in the lower and upper sections of the church landslide hazard slope due to the first variant were 1.015 and 1.229, and to the second one - 1.083 and 1.219. Based on historical materials study and visual survey of the slopes adjacent to the church building and the calculations performed, it was determined that a considerable part of the slopes of St. Andrew's Church hill is in a state close to the limit equilibrium. To increase slopes stability a new drainage system was designed in the form of concrete trays, which intercepts the atmospheric water from the church porch and conveys it into the drain pipe near the retaining wall. The main purpose of the new drainage system is to prevent ground saturation on the slopes of St. Andrew's Church hill that reduces the local stability of its slopes and leads to water and wind erosion of the hill ground.

The SDS analysis of the building was carried out taking into account the deformations of the ground base. As a result, the stresses and deformations of the bearing constructions of the building are obtained and compared with the strength values of the materials. The following groups of calculations of the "building-foundation" system were carried out:

Group 1 - calculation to determine the causes of cracking in the walls of the building and its substructure: with the values of soil properties in the natural state; with the water saturation of the foundation under the whole church building and its substructure; with water saturation of the base under the north-eastern part of the building; with the water saturation of the base under the superstructure and the southwestern part of the building; with water saturation of the base under the central part of the building (under the dome).

Group 2 - calculation to determine the actual structures SDS, taking into account the damages recorded during visual and instrumental survey.

Group 3 - analysis of prospecting SDS of building structure with possible changes in its foundation state. Various versions of water saturation of the base under the whole church building and its substructure were considered.

Modeling of water saturation of the ground in calculations was carried out by giving ground, lying at the base, values of properties corresponding to water saturation. It also took into account the appearance of zones of weakening and emptiness in the ground as a result of suffusion in the drainage system, which is located near the foundations.

In order to avoid subsequent uneven deformations of the foundations and ground fixing at the baseline of the bearing walls, a jet grouting (the "jet"-columns device) was performed. Proportioning of the building with reinforcement elements was carried out on the basis of a mathematical and geometric model, in which existing cracks in the walls and overstressed sections of the foundations were taken into account. The results of the calculations gave a picture of actual SDS constructions after reinforcement. In the calculation model, the device "jet" -columns under the part of the foundations was taken into account by replacing the soil deformation module in the natural state by the average module of deformation of the natural ground "jet" columns.

The calculation for determining the SDS of the ground mass and loads on the piles was carried out in an iterative way due to hardening ground model. This model is of elastic-plastic type, which is formed in the framework of plasticity with hardening during ground sliding, as well as compression during hardening for modeling of soil consolidation during the first compression loading. The model includes the following parameters: rigidity parameters (1), Poisson's coefficient (2), clutch (3), internal friction angle (4), and dilatation angle (5). The program also takes into account the volumetric weight of the soil in the dry (6) and saturated water (7) states, the filtration coefficients K1 (8) and K2 (9). Thus the model is nine-parameter. The calculation scheme is presented in fig. 8. Calculation in PLAXIS PC Trofymchuk, Kaliukh, at all (2014) was divided into three phases: phase 1 - assessment of stresses and displacements in the previous period of operation of the building; phase 2 - assessment of stresses and displacements during the period of operation of the building during stabilization of the ground of the base; phase 3 - estimation of stresses and displacements during the period of operation of the building during stabilization of the foundation's grounds and arrangement of the superstructure runway. Some results of calculations of the stresses of the building are shown in fig. 9.

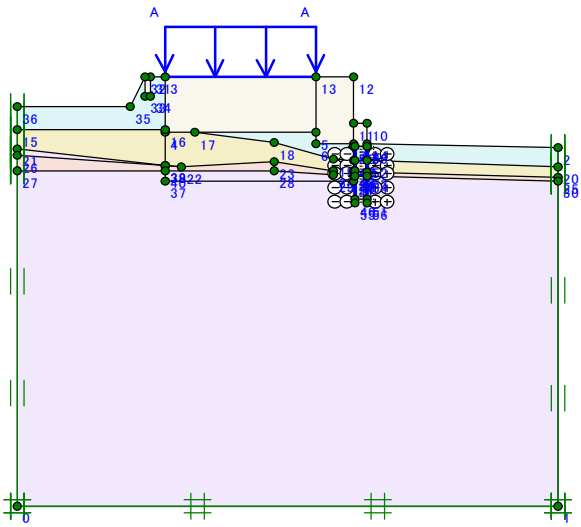

Figure 8 Calculation scheme.

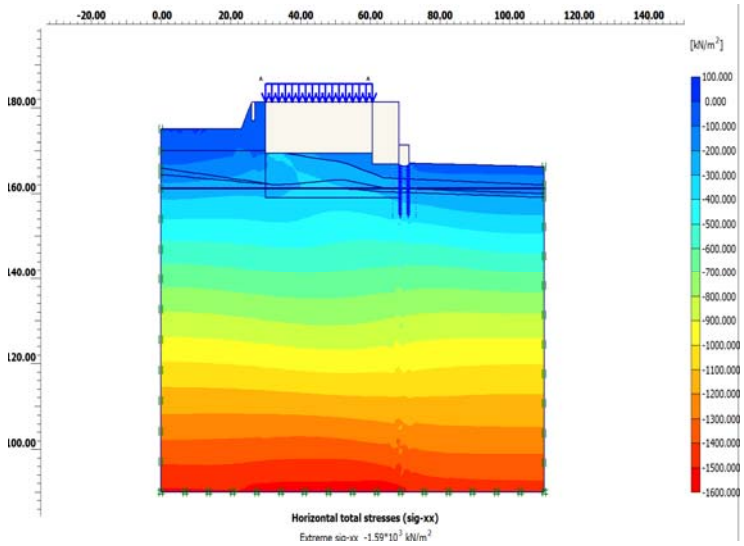

Figure 9 Isofields of general horizontal stresses in soil massif during the period of operation and base soil stabilization and arrangement of the superstructure platform, PC PLAXIS.

According to the results of geotechnical studies, design solutions and general concept of renovation works were developed.

CONCLUSIONS

1. In recent decades, the concept of cultural heritage Migon (2013) has evolved into one that encompasses an understanding of the history of humanity, together with scientific knowledge and intellectual attitudes. This changing concept has prompted a subsequent reevaluation of what constitutes the outstanding universal values of World Heritage sites and the operational methods for implementing the UNESCO World Heritage Convention (1972). The scope has broadened from studying a single monument in isolation to one that values a multidimensional, multiregional, and inter-disciplinary approach and encapsulates vast spans of human history, as demonstrated by the above: Livadia Palace and St. Andrew's Church, located within active landslide systems; the Swallow's Nest castle situated on the top of the 40-meters high Aurora Cliff of Cape Ai-Todor in the Black Sea, Autonomous Republic of Crimea, Ukraine.
2. Up-to-date methods of geotechnical protection for historical monuments of architecture can provide them with reliable protection against adverse geological processes and ensure long-term reliable operation, as shown by the example of Livadia Palace, St. Andrew's Church and Swallow's Nest castle situated on the top of the 40-meters high Aurora Cliff of Cape Ai-Todor in the Black Sea, Autonomous Republic of Crimea, Ukraine (temporary occupied in 2014 by Russian Federation).
3. Renovation of St. Andrew's Church was carried out in the following areas: geotechnical actions; renovation and reinforcement of damaged building structures; restoration of facades and interiors; improvement of technical condition of the surrounding landslide area. In addition to geotechnical work, the restoration of church building structures unity was carried out by means of reinforcement of the damaged sections of the stone masonry walls by cracks injection and reinforcement methods.
4. Based on the working design developed by "OSNOVA-SOLSIF" joint venture, the reinforcement of the church foundation by "jet" -columns was performed. Jet grouting of the grounds has been made by the method of installation of "jet" –columns of 10,81-14,25 m long with an angle of 100-130 vertically, with a diameter of 0,6 m (with an 0,8 m extension under the foundation), the spacing is 1,0- 2.7 m. The installation of "jet"-columns is performed outside and inside the church.
5. The introduction of a new drainage system and a new water discharge system facilitated dewatering of the slopes grounds of St. Andrew's Church hill and stabilization of landslide processes on it.
6. Monitoring of SDS status of St. Andrew's Church building surrounding landslide hazardous area after the restoration work has approved that the deformation of the ground basis almost has stopped and new damages in the building do not arise.

Acknowledgments

Results presented herein have been obtained with the financial and scientific support from the RIBC, the private consulting firm "OSNOVA-SOLSIF", Kyiv, Ukraine. We would like to express our very great appreciation to the Ukrainian RIBC scientist, who have been directly involved in visual and instrumental survey and mathematic simulation of SDS building structures of St. Andrew's Church and adjacent area.
We would like to express our very great appreciation to the Ukrainian experts from "OSNOVA-SOLSIF" private Consultancy, who have performed not just working

design for St. Andrew's Church foundations reinforcement, but also all the work on foundations reinforcement by "jet"-columns.
Our special thanks are extended to our colleagues Ph.D, now retiree, Iakov Chervinskii, Ph.D, Valerii Shuminskii from the RIBC and Sergej Dvornik from the private Consultncy "OSNOVA-SOLSIF" for their support in the site and office work.

References

Margottini C, Vilimek V (2014) The ICL Network on "Landslides and Cultural & Natural Heritage (LACUNHEN)". Landslides 11, ISSN:1612-510X: 934-938.

Migon P (2013) Cultural heritage and natural hazards. In: Bobrovsky (ed) Encyclopedia of natural hazards. Springer Science + Business media, Dordrecht

The World Heritage Convention (1972) URL:http://whc.unesco.org/en/convention/

Trofymchuk O. (2012) IPL-153 Project "Landslide protection structures and their development in the Autonomous Republic of the Crimea, Ukraine".

Trofymchuk O., Kaliukh I., Silchenko K., Polevetskiy V., Berchun V., Kalyukh T. (2015) Use Accelerogram of Real Earthquakes in the Evaluation of the Stress-Strain State of Landslide Slopes in Seismically Active Regions of Ukraine. In: Lollino G. et al. (eds) Engineering Geology for Society and Territory - Volume 2. Springer, Cham. pp 1343-1346.

Trofymchuk O, Kaliukh I, Klymenkov O, (2018) TXT-tool 2.380-1.1. Monitoring and Early Warning System of the Building Constructions of the Livadia Palace, Ukraine. Landslide Dynamnics: ISDR-ICL Landslide Interactive Teaching Tools. Volume 1. Springer, Cham. pp 491-508.

Impact of Vegetation Loss Due to Wildfire on Debris Flow Volume

Binod Tiwari[(1)], Beena Ajmera[(2)]

1) California State University, Fullerton, Civil and Environmental Engineering Department, 800 N State College Blvd., E-419, Fullerton, CA 92831, USA, e-mail: btiwari@fullerton.edu

2) North Dakota State University, Department of Civil and Environmental Engineering, CIE Building Room 201Q, NDSU Dept. 2470, P.O. Box 6050, Fargo, ND 58108-6050, USA, email: beena.ajmera@ndsu.edu

Abstract Wildfires are one among the natural disasters that cause a significant loss of lives and properties every year. The loss is dramatically high in dry regions such as southern California. Occasionally, post-wildfire areas, due to loss of vegetation cover and change in permeability of surface soil, experience slope disasters such as mudslides and debris flows. The recent Thomas Fire in southern California followed by an unprecedented rainfall caused a significant property damage and death which triggered the incident to be federally declared emergency. We collected first hand disaster information and geotechnical as well as hydrological investigation of the area and postulated the cause of debris flow. This paper includes details of those investigations and analyses performed based on the study results.

Keywords wildfire, debris flow, shear strength, seepage, rainfall, runoff

Background information

Wildfires are strong blaze that are spread by strong wind and supported by dry and hot weather. They are known with different terms such as wildland fire, forest fire, vegetation fire, grass fire, peat fire, bushfire, hill fire, etc. Such wildfires, if not contained in time, can also consume houses or agricultural resources. Wildfires often begin unnoticed, but are later fuelled by various sources such as woods and are spread quickly by wind. Such fires can ignite brushes, trees, homes, or anything that comes in contact with them, expanding to hundreds of acres of land within a few hours. It has been estimated that in the past 45 years, there are, in average, over 300,000 wildfire cases in a year throughout USA. Those wildfires are reported to destroying almost 8M acres of land.

Although Southern California has regularly suffered from large scale wildfires that cause a significant loss in properties (Keaton et al., 2014), the largest in the history was the Thomas Fire, which burned approximately 300,000 acres of vegetation covers in the hills of Santa Barbara and Ventura Counties of California. It started on December 4, 2017 and was officially declared to be contained on January 12, 2018. Over 1000 buildings were damaged by this fire causing a total damage exceeding over US $2.2B. Even before the fire was contained, the area received a series of rainfall events that caused a devastating debris flow events in the city of Montecito, Santa Barbara County, CA, USA, on January 9, 2018, that killed 21 people and injured over 150 people, in addition to causing over US $200 of property damage. Among the damaged structures include complete damage of over 60 residential buildings, partial damage of over 450 residential buildings, complete damage of 8 commercial buildings and partial damage of 20 commercial buildings. The major highways and local streets were completely buried under 10-12 ft of debris. People in the area were evacuated. The area did not have utilities such as power, gas, etc. due to the mudflow. Most of the water-ways for bridges and culverts were blocked by the mudslides and debris that carried a huge amount of tree branches with the debris mass. As a result, several bridges and culverts were washed away. Shown in Figs. 1 through 8 are few close-up view pictures of the debris as well as damaged bridges and structures.

With the help of the officials of the county of Santa Barbara, the first author visited the debris flow site and collected first-hand information pertinent to the debris flow event as well as a few soil samples that were later analysed in the geotechnical engineering laboratory of California State University, Fullerton to evaluate the soil types involved in the flow process. Moreover, the authors performed extensive analyses for the meteorological information to calculate the intensity and rainfall as well as the cumulative rainfall for the past few decades so that the causative factor of the debris flow could be identified.

Figure 1 A bridge washed away due to waterway blockade.

Figure 2 Damage to buildings due to the debris flow and damage of culverts/bridges.

Figure 3 Damage to buildings due to diversion of debris mass towards residential area.

Figure 4 Tree roots and branches that travelled down with debris mass to block the waterways.

Figure 5 Size of boulders that slid down with debris mass.

Figure 6 Culvert structure, right bank of which had debris flow diversion that caused a massive loss of properties.

Figure 7 Gas pipeline that were damaged during the debris flow event and caught fire.

Figure 8 Depth of debris mass that came down and blocked the culvert as well as the elevated roads.

Field Investigation

The authors investigated the field situation after the Montecito debris flow disaster. As a response to the federally declared emergency, Google released high resolution images for public use right after the debris flow disaster. Shown in Figs. 9 and 10 are the aerial views of the debris flow area at Montecito, CA before and after the wildfire and debris flow disasters, respectively. As can be observed, the vegetation cover was completely removed after the wildfire, leaving thick ash deposits on the ground surface, which not only reduced permeability of the soil to cause a significant increase in the run-off, but also changed the properties of top soil due to high heat to cause brittle and cracked surface for localized seepage of rainwater. The 2-3 m wide creek expanded to 20-40 m wide channel after the debris flow incidence. More importantly, loose debris mass, as can be observed in Fig. 10 were abundantly available along the channel bed, which are prone to flow in next rainy season if proper mitigation measures are not applied.

The debis flow carried a large amount of debris, with tree branches and roots that completely filled the two debris basins and the overflow mass flowed down to the community, local roads, highways, and even over 100 m distance into the Pacific Ocean, as can be seen in Figs. 11 and 12. Due to the blockage of waterways for bridges and culverts with large size boulders and tree branches, and overflow of the debris basins, the debris mass was diverted to the community. As can be seen in Fig. 10, there are still significant amount of loose debris that had not slid down by the January 9 event. With the loss of vegetation cover, those loose boulders throughout the slope and even along the creek channel have a strong potential to slide down if the area receives intense rainfall in future.

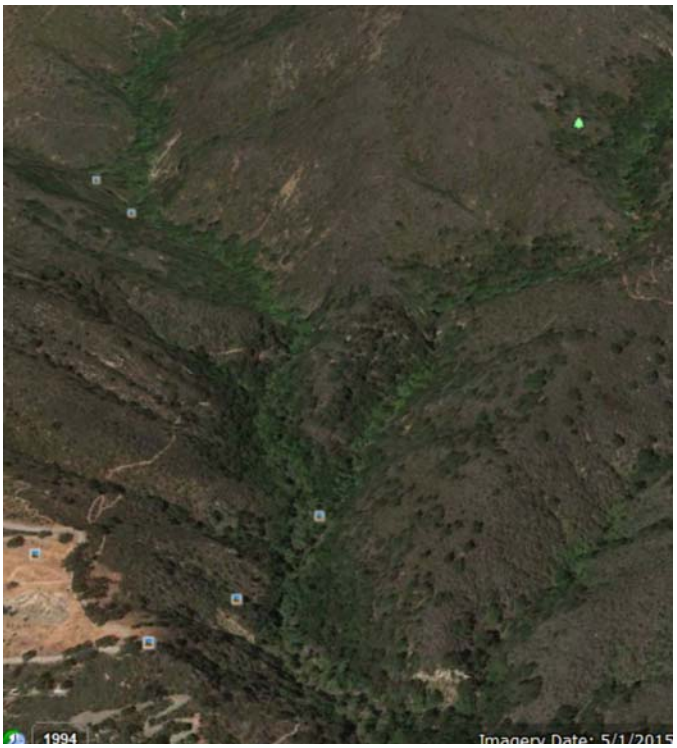

Figure 9 Creek and watershed prior to wildfire (source: Google Earth).

Figure 10 Creek and watershed after the Thomas wildfire and the debris flow incident (source: Google Earth).

Figure 11 Highway 101 covered with the debris flow deposits (source: Google Earth).

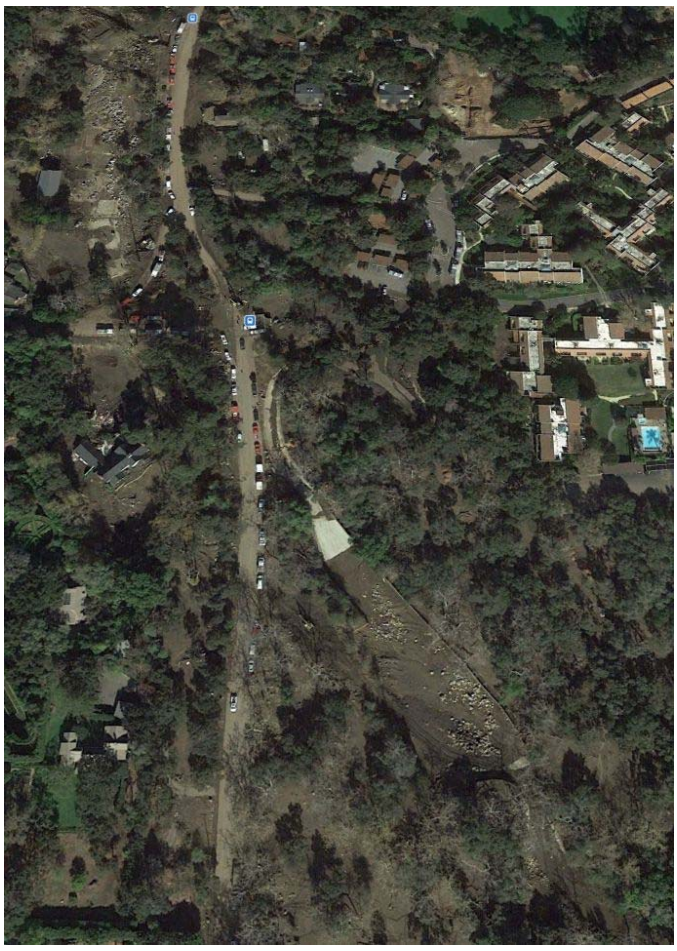

Figure 12 Debris basin overflown after the debris flow disaster (source: Google Earth).

Laboratory investigations

Based on the sieve analysis and Atterberg's test results, the soils collected from the bank of the creek (excluding large boulders and coarse gravels) are classified as SP-SM (poorly graded sand with silt and gravel) and SW-SM (well graded sand with silt and gravel) according to the USCS classification system.

Rainfall pattern in the area

The authors collected daily rainfall information for 8 different stations throughout the Thomas fire from the Desert Research Institute (DRI) stations (Fig. 13). As the hourly intensity of rainfall was not available at those stations, data available from NEXRAD Doppler stations were analysed to calculate the rainfall intensity of each Doppler station to the intensity of rainfall as explained in Keaton et al. (2014). Shown in Fig. 14 is the monthly rainfall comparisons for December and January (wet season) for Montecito Station 2 (near the debris flow site). As can be seen in Fig. 14, 2018 January rainfall was much less than 2016 and 2017 January rainfalls.

In order to evaluate the effect of rainfall intensity and duration on triggering the debris flow event, rainfall intensity obtained from the NEXRAD data for the Montecito Station 2 was plotted with time period as shown in Fig. 15. As observed in Fig. 15, there was a concentrated rainfall with an intensity of over 50 mm/hr for a short period of a few minutes with a cumulative rainfall of approximately 20 mm in 6 hours and relatively intense rainfall of 38 mm within a period of 30 hours. This concentrated rainfall event was responsible for the huge debris flow event that was mentioned earlier.

Figure 13 Eight DRI stations used to collect the data for rainfall study pertinent to the debris flow event.

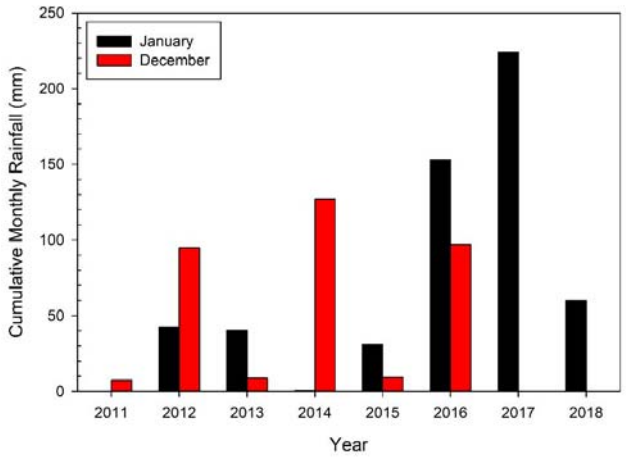

Figure 14 Comparison between daily rainfalls obtained in December and January at Montecito 2 DRI station for the past 7 years.

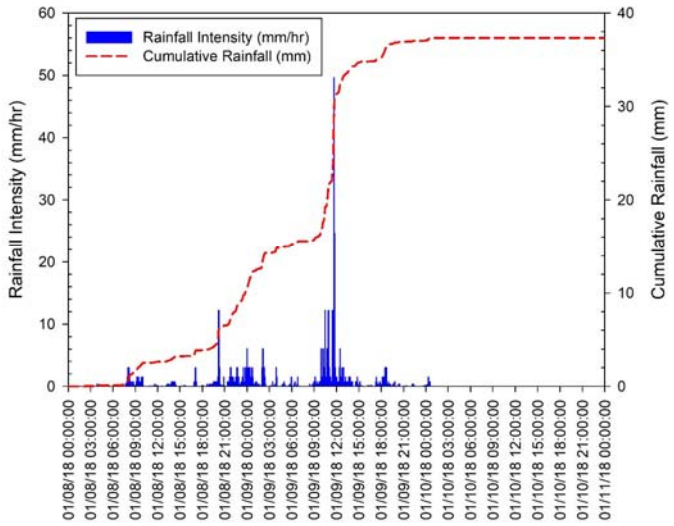

Figure 15 Intensity and duration of rainfall at Montecito Station 2 for the 2 days prior to the debris flow event, obtained from the NEXRAD data. Cumulative rainfall is also presented on the right-side y-axis. Time is expressed in GMT.

Summary and conclusion

The recent Thomas Fire that occurred in Southern California not only caused a significant loss of lives and properties, but also caused a devastating debris flow event at the city of Montecito, Santa Barbara County of California. The loss of vegetation cover and alteration of geotechnical properties of soil on slope coupled with high intensity of rainfall for a duration long enough to trigger the debris flow is attributed to the cause of the debris flow event. The Montecito debris flow event occurred in a year that had less than half the monthly rainfall compared to the previous two years. This shows that the debris flow event triggered by post-wildfire precipitation is a complex phenomenon and an extensive research is required to evaluate the potential post-wildfire debris flow sites so that a realistic model can be developed in future to alleviate community resiliency against possible debris flow hazards.

Acknowledgments

The authors thank Mr. Chris Doolittle of the Santa Barbara County for providing access to the first author to the disaster area and providing some pertinent information related to the debris flow event. Likewise, the authors would like to thank Mr. Basil Habhab, an undergraduate student at California State University (CSU), Fullerton for obtaining and analysing the rainfall data. Moreover, the authors express their appreciation to, Rupert Barnett, a graduate student at CSU Fullerton for running soil tests to classify the debris mass. Last but not the least, the authors acknowledge the RCA grant of CSU Fullerton that provided financial support to conduct this study.

References (in the alphabetical order)

Keaton, J. R., Ajmera, B., Upadhyaya, S., Tiwari, B., Turner, B. Kwak, D. Y., and Brandenberg, S. J. 2015. DECEMBER 2014 STORM DAMAGEBELOW RECENTLY BURNED SLOPES, LOS ANGELES, ORANGE, AND VENTURA COUNTIES, CALIFORNIA, Geotechnical Extreme Event Reconnaissance GEER Association Report No. GEER- 042. Version 1 July 31, 2015. DOI: 10.18118/g66k56

Update on the Ripley Landslide (IPL #202) and the activities of the University of Alberta / GSC WCoE

Michael T. Hendry [1], David Huntley[2], Renato Macciotta[1], Peter Bobrowsky[2]

1) University of Alberta, Edmonton, Canada
e-mail: hendry@ualberta.ca
2) Geological Survey of Canada

Abstract

The ground hazards research groups at the University of Alberta and the Geological Survey of Canada continue to monitor and study the Ripley Landslide (IPL #202). The Ripley Landslide has been extensively characterized with drilling, geophysical surveys, local meteorological monitoring and monitoring of pore pressures and river elevation. Displacements and kinematics of the landslide have been monitored with ShapeAccelArrays and a survey quality dGPS system, and is being used to trial developing technologies such a low cost dGPS systems, acoustic monitoring, InSAR, and LiDAR change detection. A recent addition to this program has been the monitoring of the moisture content within the backscarp of the landslide with a near-real time ERT system, soil suction sensors and TDR probes. This study has expanded to other active landslides within the same valley as the Ripley Landslide with similar geology, kinematics and seasonal changes in velocity; the most notable of these is the 'South Slide'. This presentation will also note the five additional field sites monitored, or being developed, by the University of Alberta's Geohazards group.

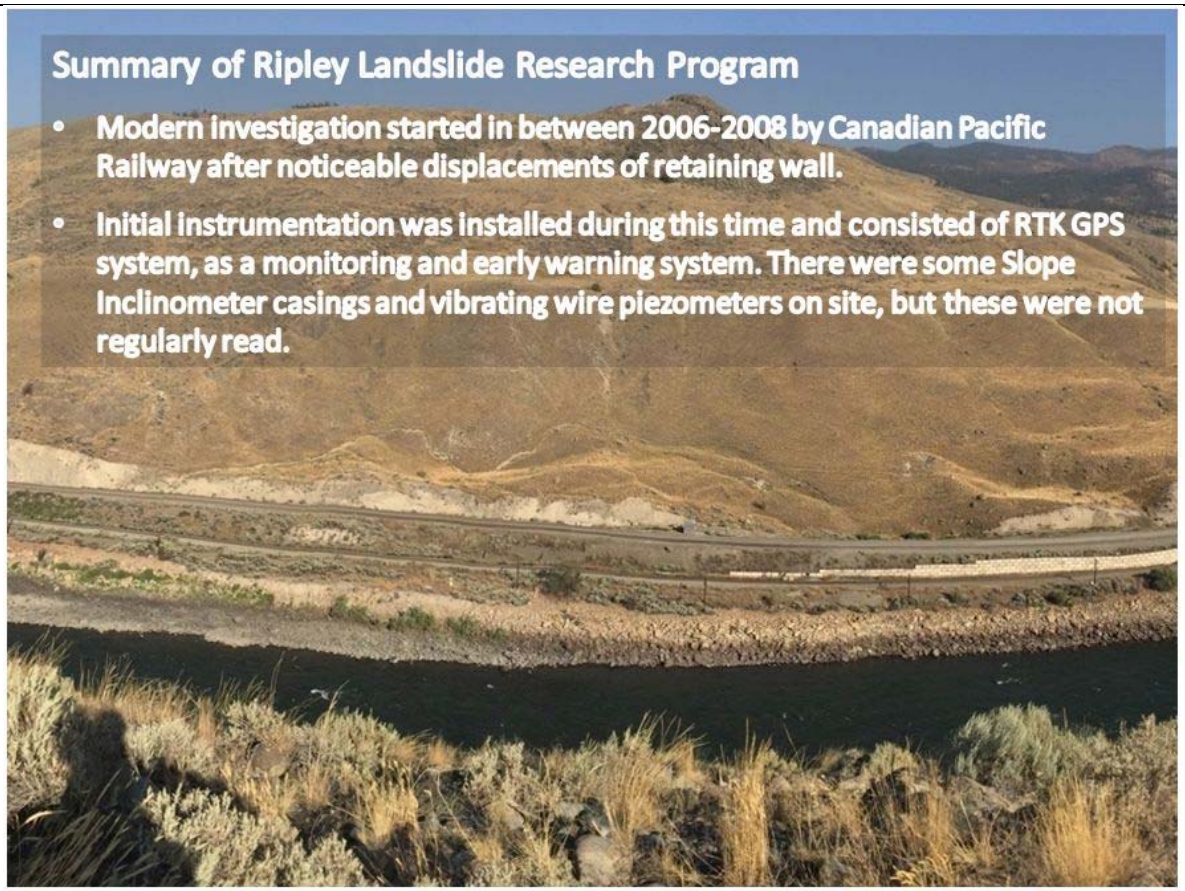
Summary of Ripley Landslide Research Program
• Modern investigation started in between 2006-2008 by Canadian Pacific Railway after noticeable displacements of retaining wall.
• Initial instrumentation was installed during this time and consisted of RTK GPS system, as a monitoring and early warning system. There were some Slope Inclinometer casings and vibrating wire piezometers on site, but these were not regularly read.

Summary of Ripley Landslide Research Program
• 2013 Installation of 1st ShapeAccelArrays and continuously monitored vibrating wire piezometers.
• 2014 – *ongoing* Ground Based LiDAR imaging.
• 2015 extensive drilling, retrieval of continuous core samples, installation of multiple SI casings, 2nd SAA, piezometers installed directly on the shear plane.
• 2015 installation of ALARMS acoustic monitoring system (UK).

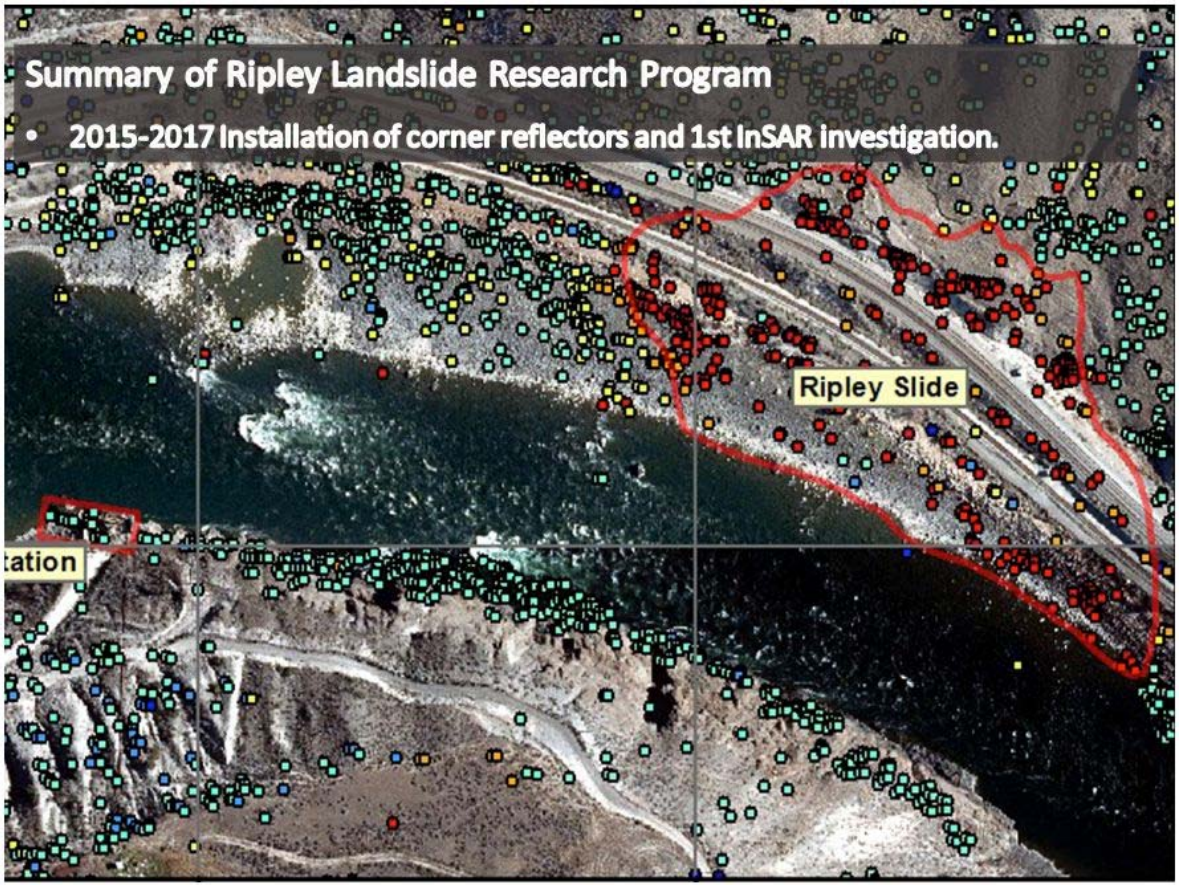
Summary of Ripley Landslide Research Program
• 2015-2017 Installation of corner reflectors and 1st InSAR investigation.
Ripley Slide

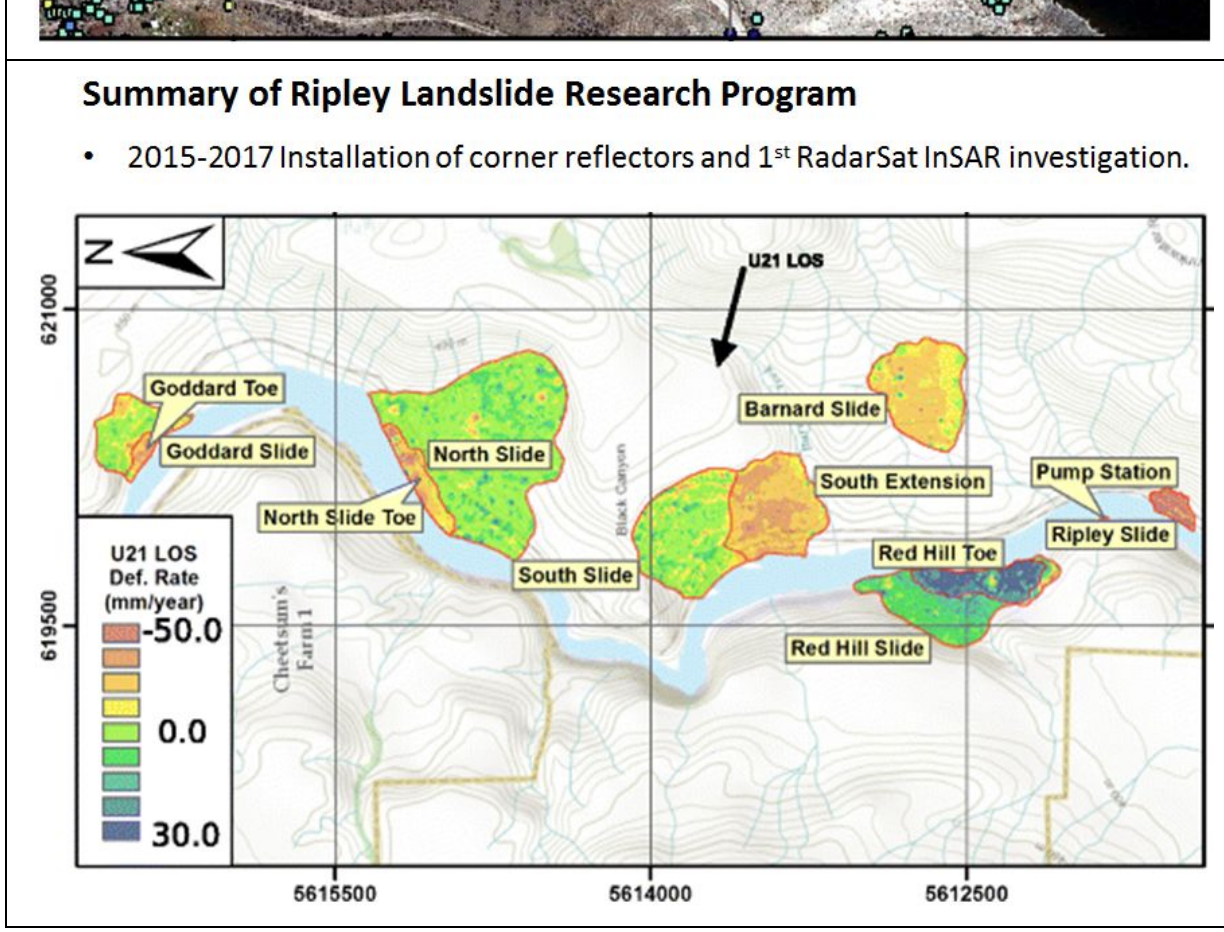
Summary of Ripley Landslide Research Program
• 2015-2017 Installation of corner reflectors and 1st RadarSat InSAR investigation.
N
U21 LOS
Goddard Toe
Goddard Slide
North Slide
North Slide Toe
South Slide
Barnard Slide
South Extension
Pump Station
Ripley Slide
Red Hill Toe
Red Hill Slide
Black Canyon
Cheetsum's Farm 1
U21 LOS Def. Rate (mm/year)
-50.0
0.0
30.0
621000
619500
5615500
5614000
5612500

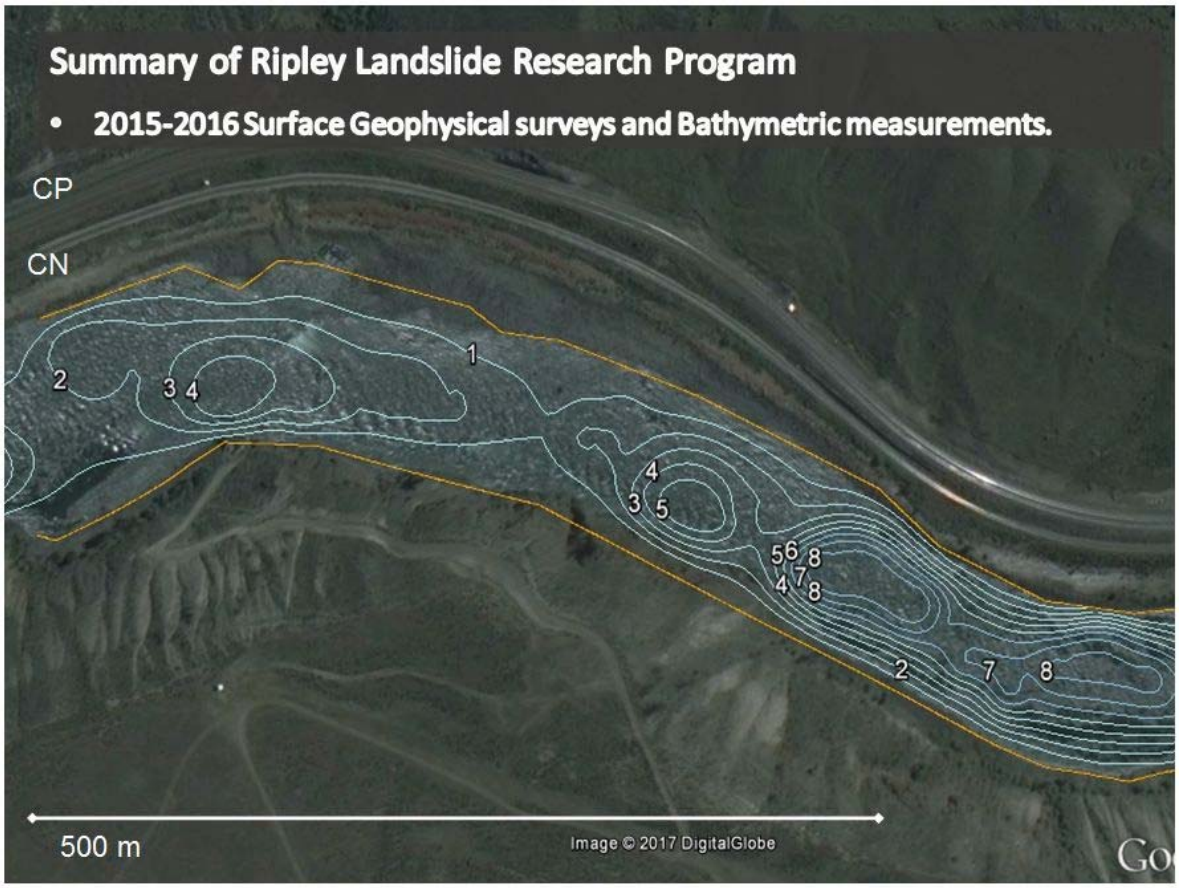
Summary of Ripley Landslide Research Program
• 2015-2016 Surface Geophysical surveys and Bathymetric measurements.
CP
CN
1
2
3 4
4
3 5
5 6 8
4 7 8
2
7
8
500 m
Image © 2017 DigitalGlobe

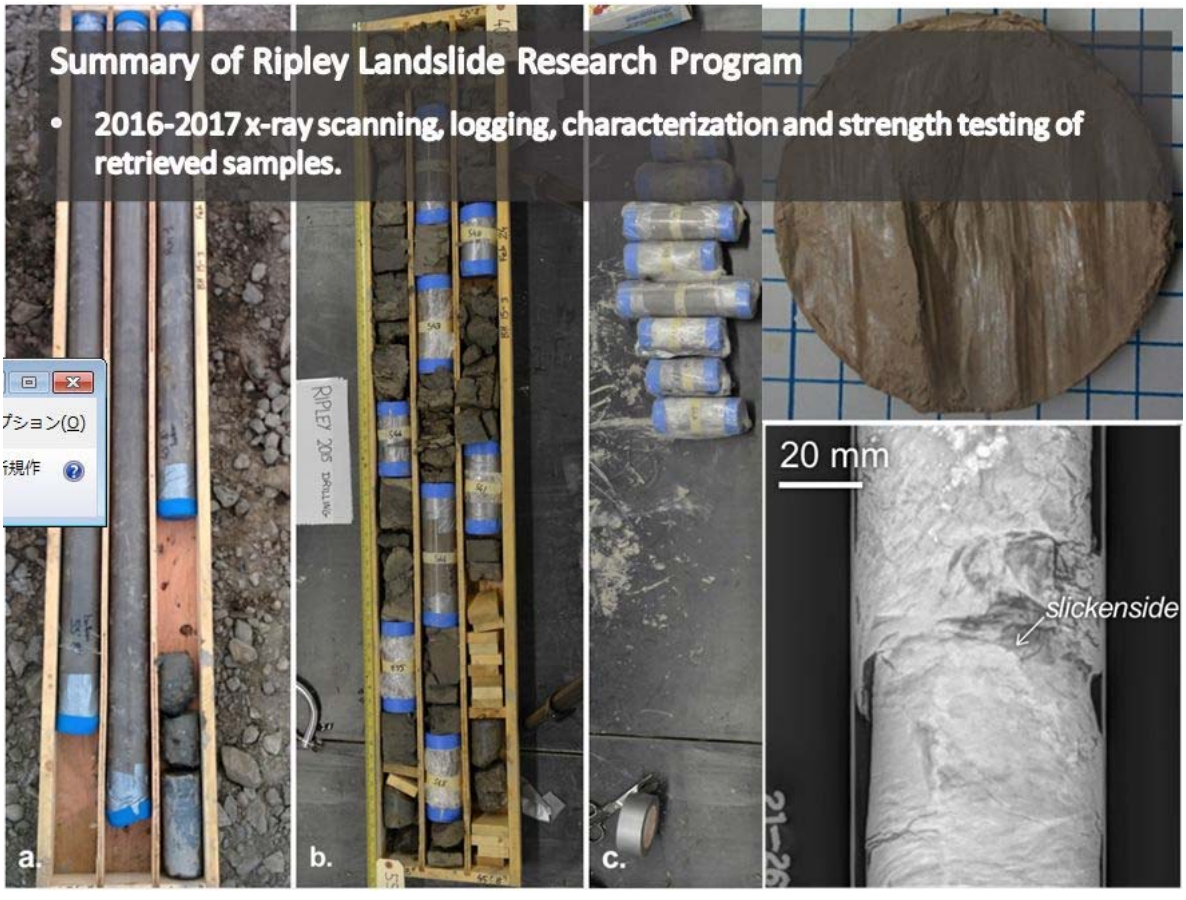
Summary of Ripley Landslide Research Program
• 2016-2017 x-ray scanning, logging, characterization and strength testing of retrieved samples.
a.
b.
c.
20 mm
slickenside

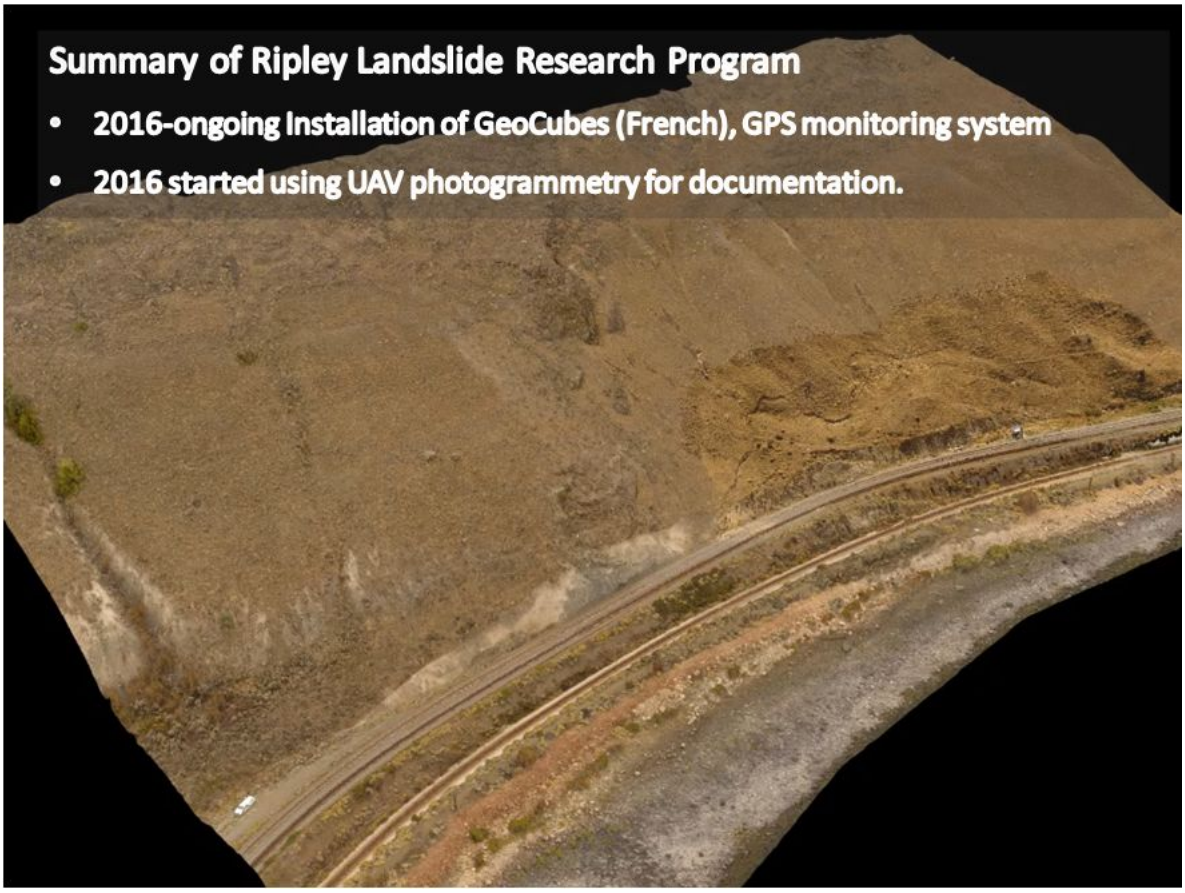
Summary of Ripley Landslide Research Program
• 2016-ongoing Installation of GeoCubes (French), GPS monitoring system
• 2016 started using UAV photogrammetry for documentation.

Recent work on the Ripley Landslide Research Program
• 2017 Installation of British Geological Survey PRIME system.
• 2017 Installation of soil suction probes in back scarp.
• 2018 Installation of water content probes and more soil suction probes.

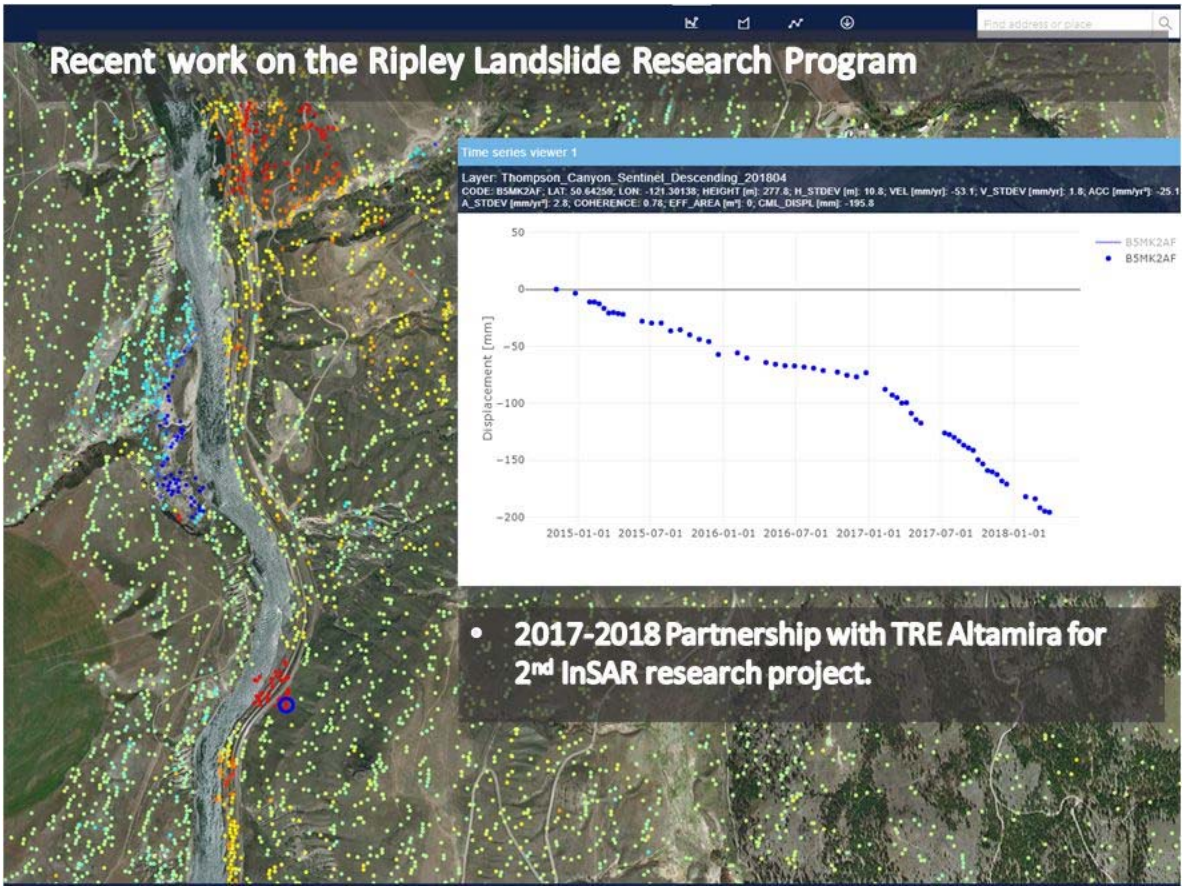
Recent work on the Ripley Landslide Research Program
Time series viewer 1
Layer: Thompson_Canyon_Sentinel_Descending_201804
B5MK2AF
Displacement [mm]
2015-01-01 2015-07-01 2016-01-01 2016-07-01 2017-01-01 2017-07-01 2018-01-01
• 2017-2018 Partnership with TRE Altamira for 2nd InSAR research project.

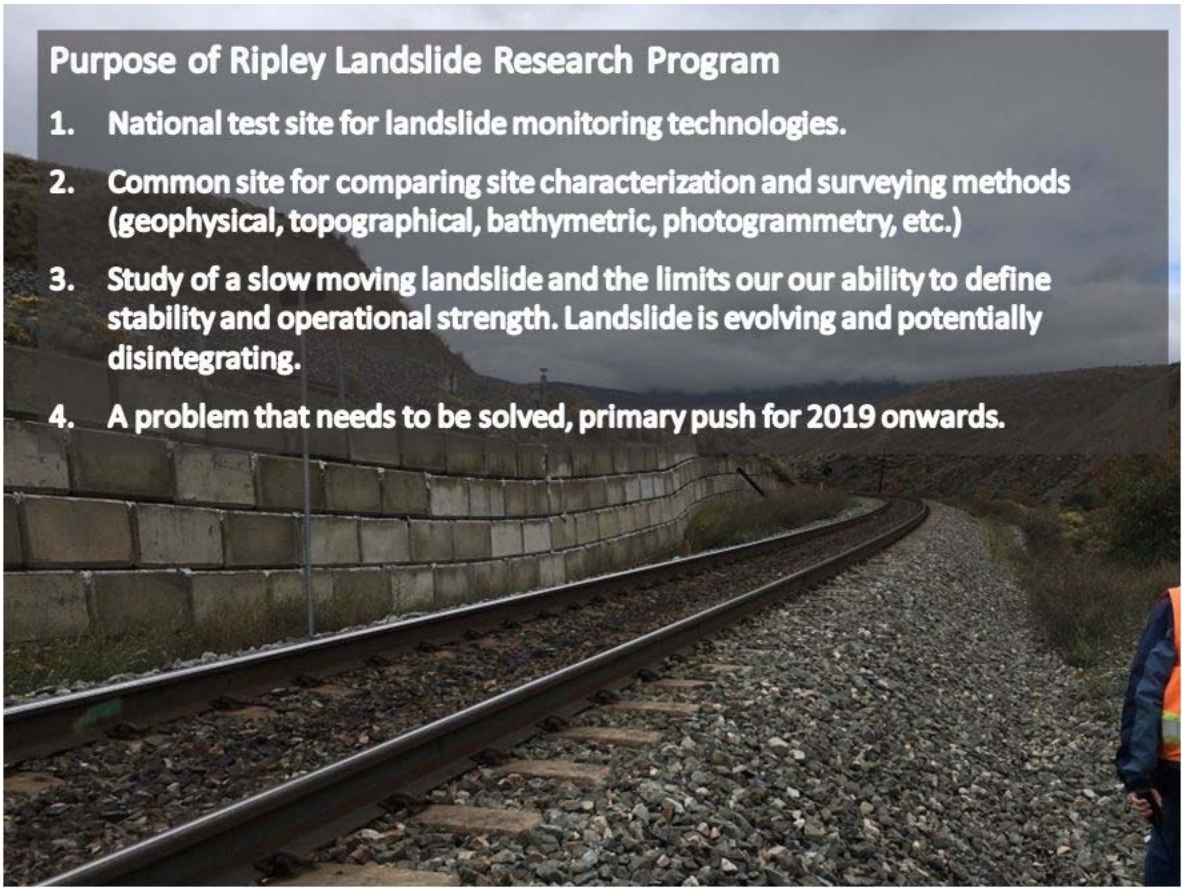
Purpose of Ripley Landslide Research Program
1. National test site for landslide monitoring technologies.
2. Common site for comparing site characterization and surveying methods (geophysical, topographical, bathymetric, photogrammetry, etc.)
3. Study of a slow moving landslide and the limits our our ability to define stability and operational strength. Landslide is evolving and potentially disintegrating.
4. A problem that needs to be solved, primary push for 2019 onwards.

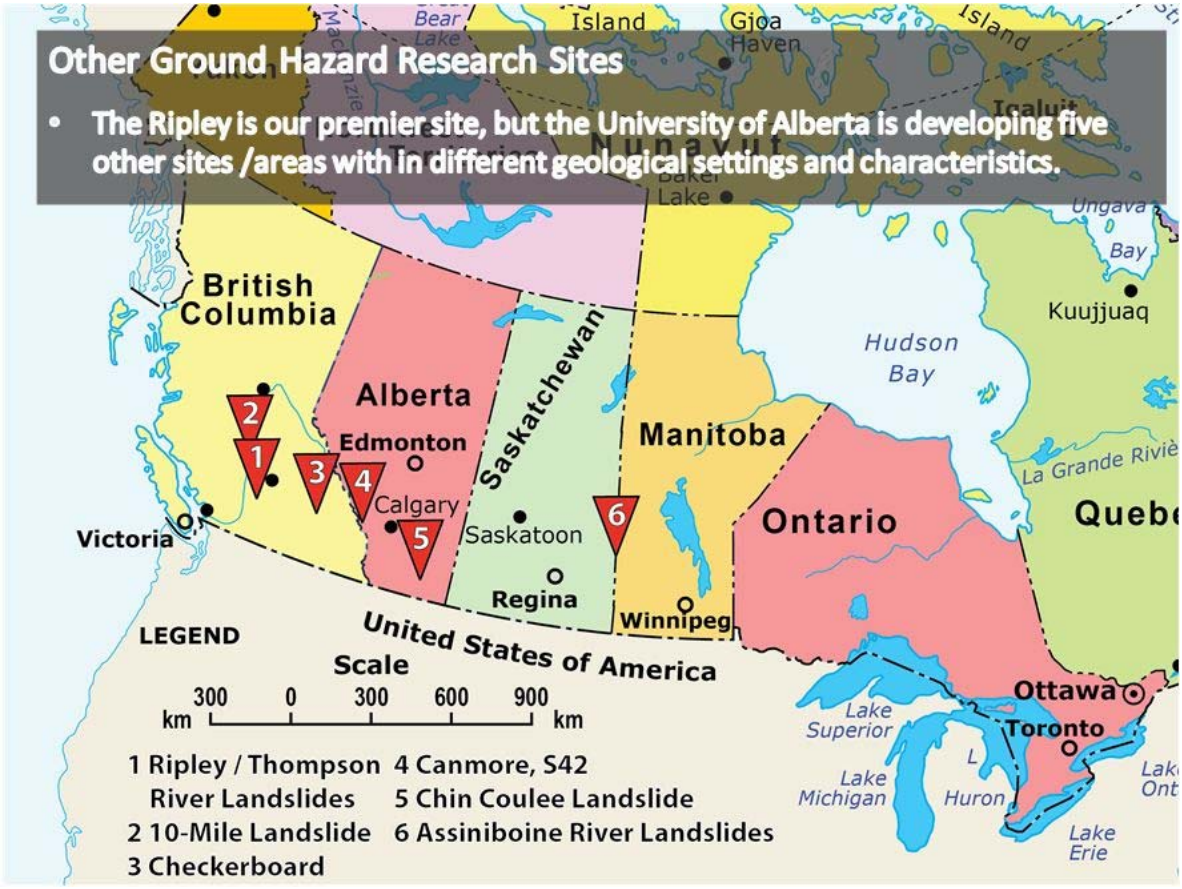
Other Ground Hazard Research Sites
• The Ripley is our premier site, but the University of Alberta is developing five other sites /areas with in different geological settings and characteristics.
British Columbia
Alberta
Saskatchewan
Manitoba
Ontario
Edmonton
Calgary
Saskatoon
Regina
Winnipeg
Victoria
Kuujjuaq
Hudson Bay
Ottawa
Toronto
Lake Superior
Lake Michigan
Lake Huron
Lake Erie
United States of America
LEGEND
Scale
300 0 300 600 900
km km
1 Ripley / Thompson River Landslides
2 10-Mile Landslide
3 Checkerboard
4 Canmore, S42
5 Chin Coulee Landslide
6 Assiniboine River Landslides

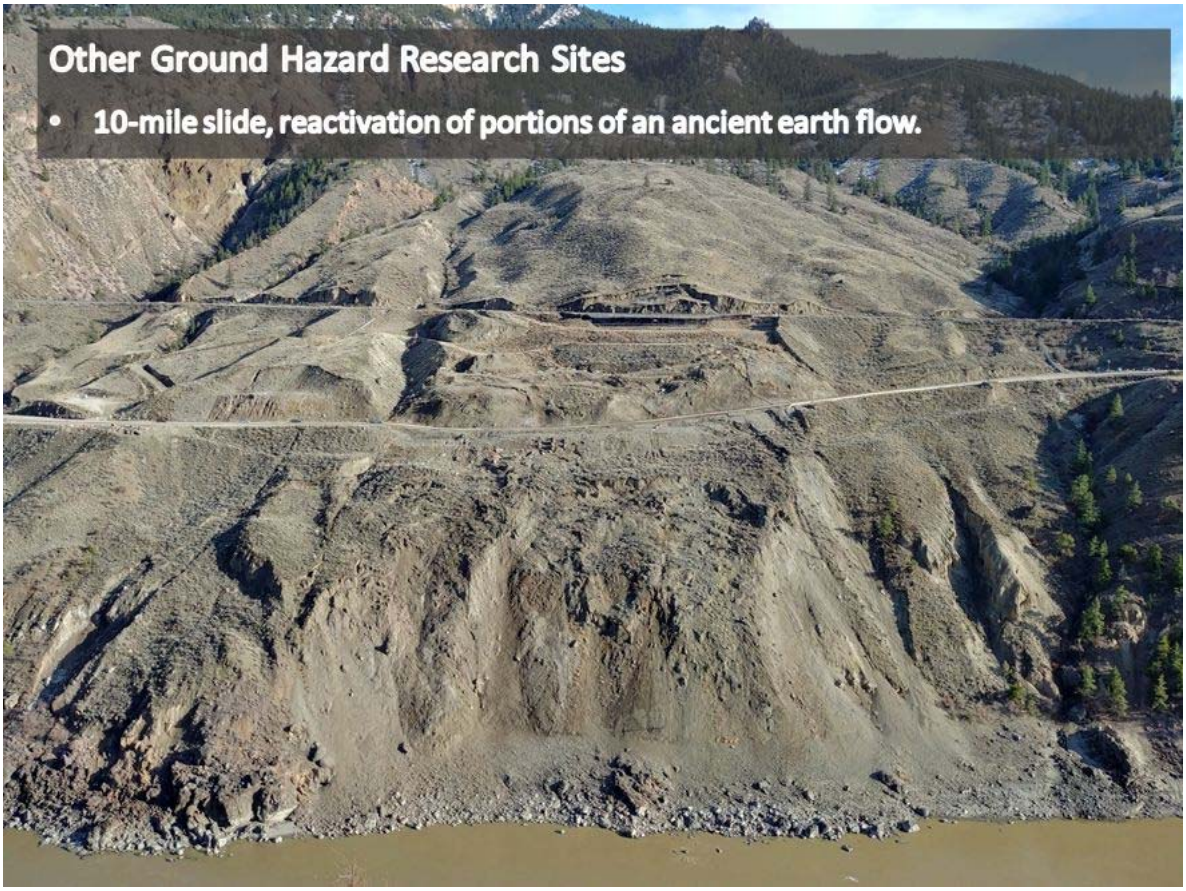
Other Ground Hazard Research Sites
• 10-mile slide, reactivation of portions of an ancient earth flow.

Other Ground Hazard Research Sites
DANGER
• Translational Prairie River Valley Landslides, Chin Coulee, AB.

Other Ground Hazard Research Sites
• Monitoring of moving rock faces with GB InSAR.
• Checkerboard creek Revelstoke Dam Reservoir, B.C.

Other Ground Hazard Research Sites
• Change detection and monitoring of rock faces that are hazardous to highway traffic and the public near Canmore, AB.
HONDA

Temporal-spatial distribution characteristics and prevention of landslides developing in Jurassic stratum in Three Gorges Reservoir region, China

Prof./Dr. Changdong Li

China University of Geosciences, Wuhan, No. 388 Lumo Road, P.R. China
e-mail: lichangdong@cug.edu.cn

Abstract

Zigui Basin is a typical region with Jurassic stratum widely distributed. Jurassic stratum in this area are sliding-prone stratum and show significant interbedding structure, i.e., flysch contains alternate sandstone and silty mudstone. Coupled with the effect of fluctuation of reservoir level, rainfall and other influence factors, the landslides in this region are dense and active. The impoundment patterns of Three Gorges Reservoir (TGR) changed several times, which influence the evolution mechanism and evolution stages of these landslides. The susceptibility varies in different areas of Zigui Basin because of the stratum, topography and human activities. Thereafter, the reinforcement mechanism of different countermeasures especially stabilizing piles was studied using model test, analytical approaches and numerical simulation, and the countermeasure strategies of landslides with different evolution mechanism were also discussed. Finally, based upon the interaction between stabilizing piles and landslides, which mainly includes soil arch effect and embedded mechanism, different methodologies for optimization of stabilizing piles were proposed accordingly.

Distribution of landslides

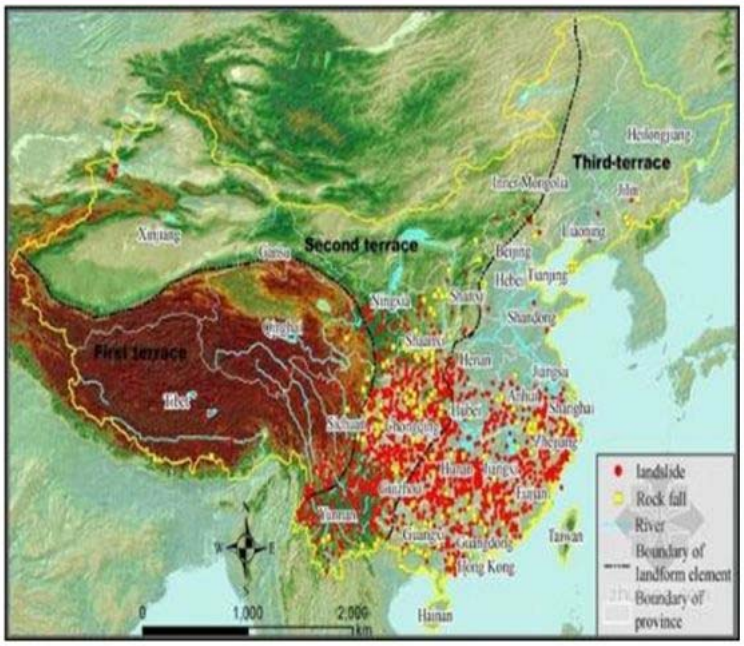

Distribution of landslides

Damage caused by landslides

Hazards to Residents

Hazards to Transportation

Main structure — stabilizing pile

1.Theoretical study lag behind the engineering practice

2.How to obtain safety + economy

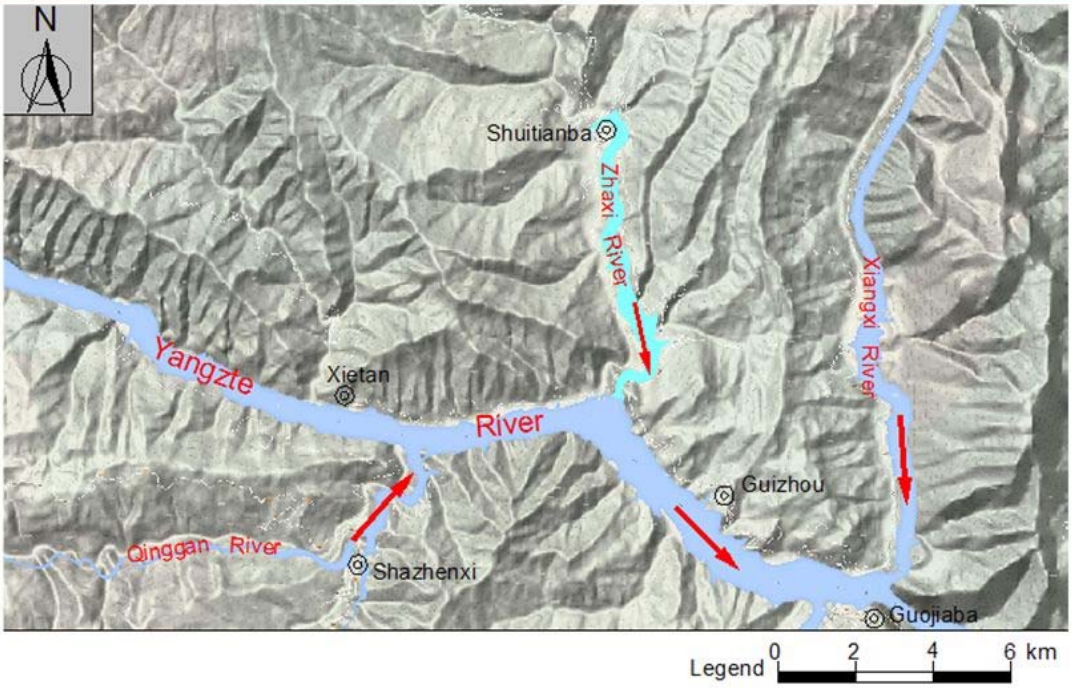

3D model by UAV images

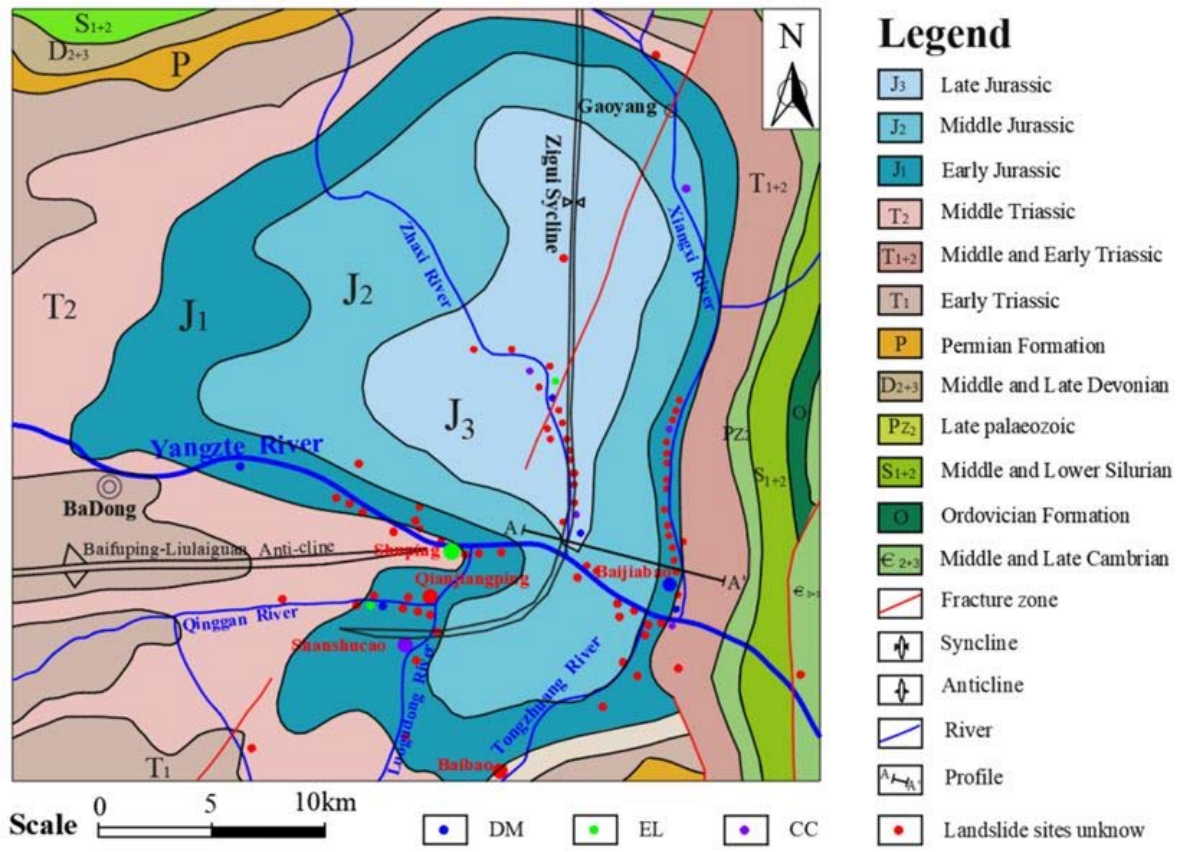

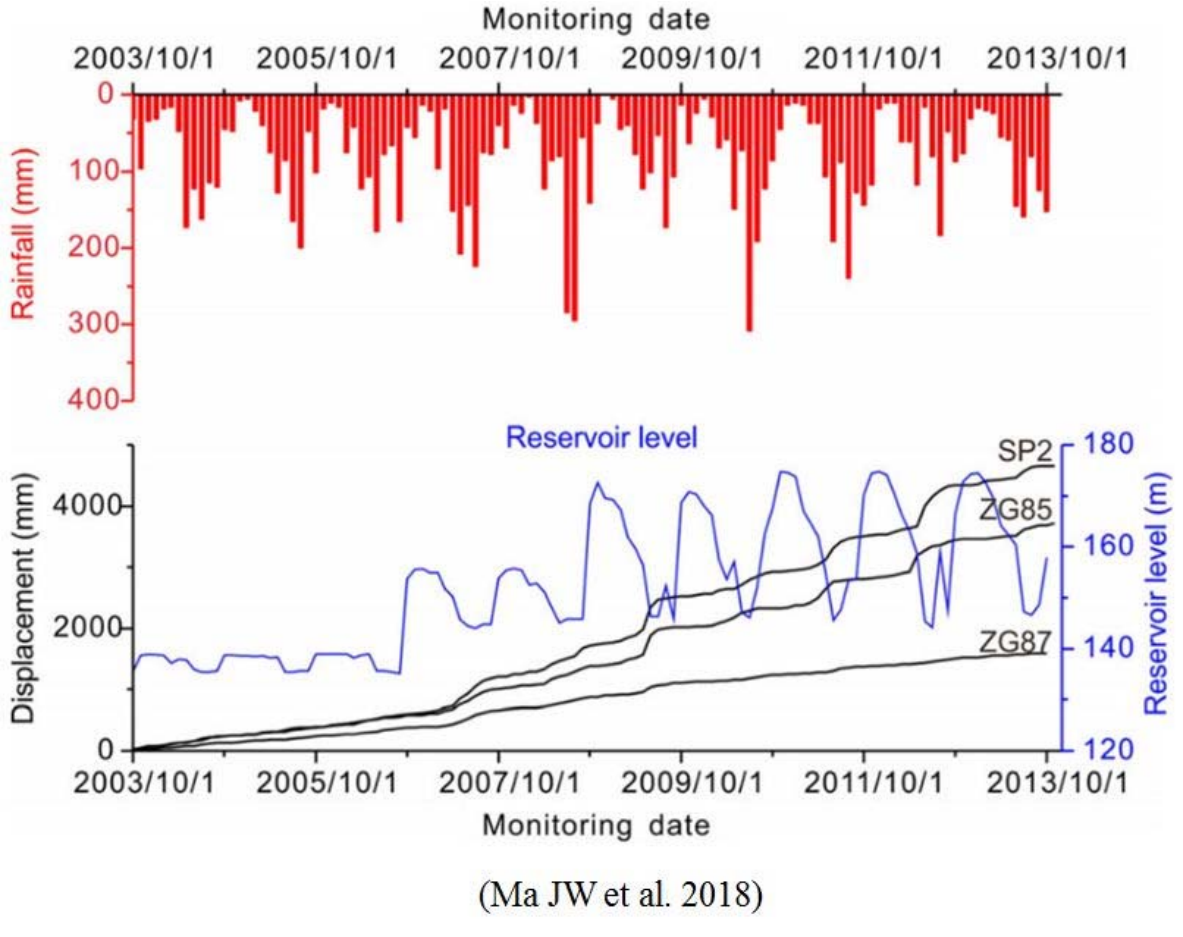

(Ma JW et al. 2018)

Representative landslides

Baishuihe landslide

Qianjiangping landslide

Baijiabao landslide

Majiagou landslide

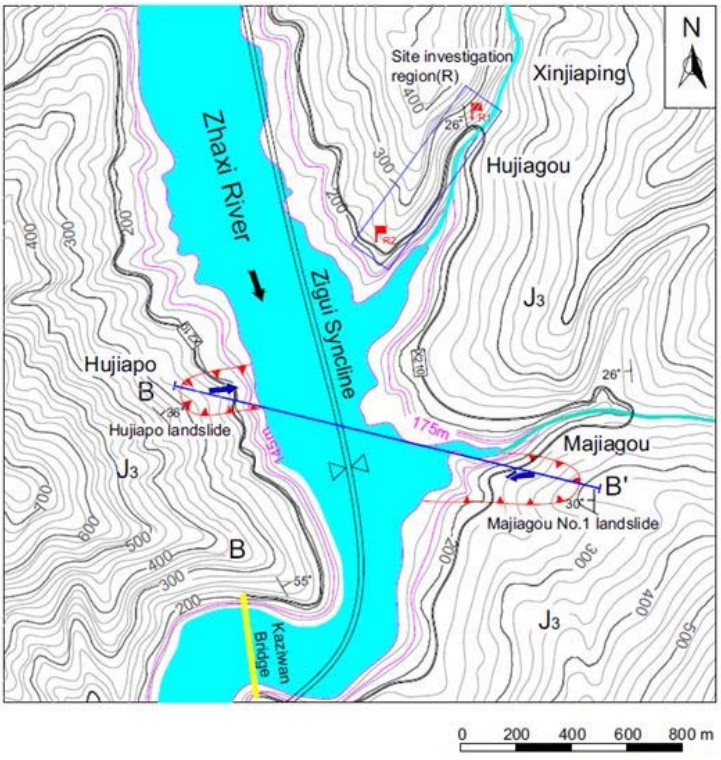

Legend

- Late Jurassic Formation
- Syncline
- Boundary of landslide
- Section line
- Sliding direction
- Attitude
- In-situ rock test sites
- Site investigation region(R)
- County road
- River
- Water level line

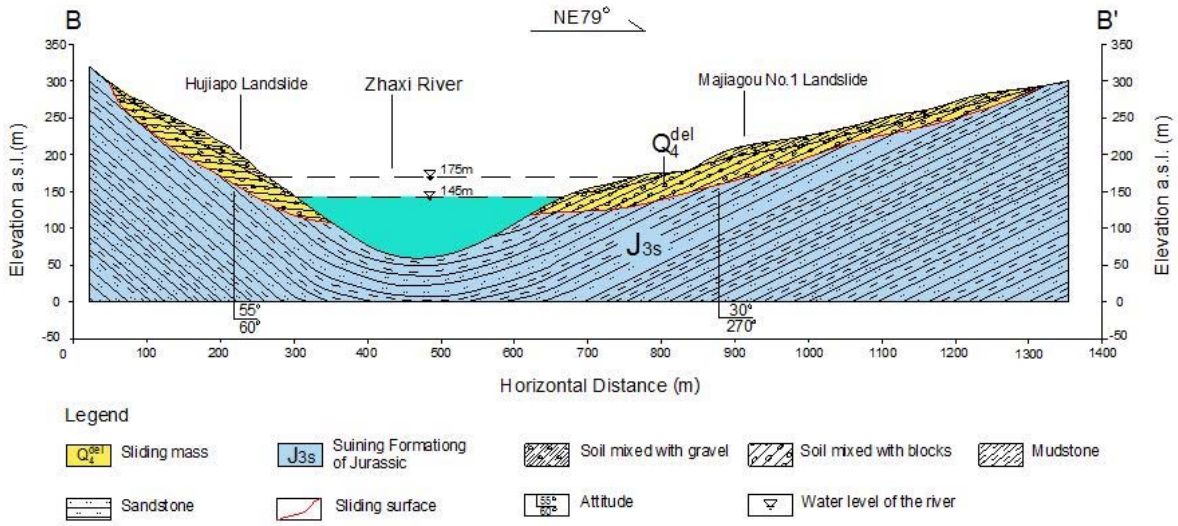
B
NE79°
B'
Hujiapo Landslide
Zhaxi River
Majiagou No.1 Landslide
Q4del
175m
145m
J3s
55°
60°
30°
270°
Elevation a.s.l.(m)
Horizontal Distance (m)
Legend
Sliding mass
Suining Formationg of Jurassic
Soil mixed with gravel
Soil mixed with blocks
Mudstone
Sandstone
Sliding surface
Attitude
Water level of the river

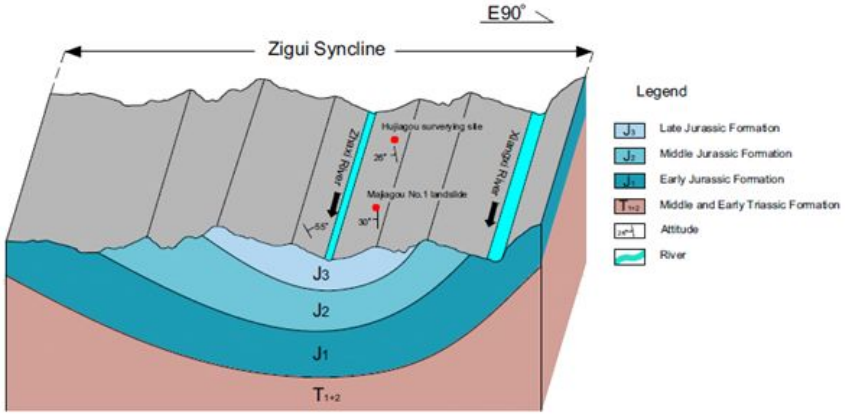
E90°
Zigui Syncline
Legend
Late Jurassic Formation
Middle Jurassic Formation
Early Jurassic Formation
Middle and Early Triassic Formation
Attitude
River
Hujiagou surveying site
Majiagou No.1 landslide
Zhaxi River
Xiangxi River
J3
J2
J1
T1+2

Generator
PC
Stabilizing pile Hole
1
1-Digital encoder
2-Stepper motor
3-Motor reducer
4-Screw jack
5-Force sensor
6-Bearing plate
Controller
Motor driver
Rock
2. Test in mudstone
3. Test in sandstone

In-situ test by self-developed apparatus

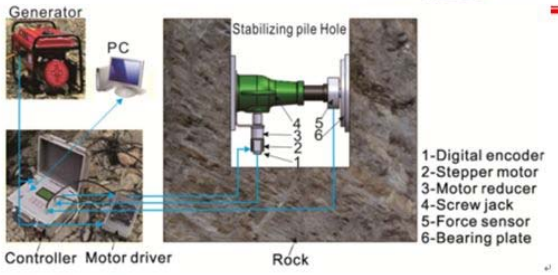

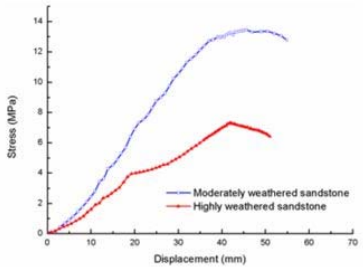

➢Huiming Tang, Yongquan Zhang, **Changdong Li***, Xinwang Liu, Junjie Wu, Feng Chen, Xiaoyi Wang, Junfeng Yan. Development and Application of in situ Plate-Loading Test Apparatus for Landslide-Stabilizing Pile Holes. ASTM Geotechnical Testing Journal, 2016, Vol. 39, No. 5, pp. 757–768.

Trigger factors

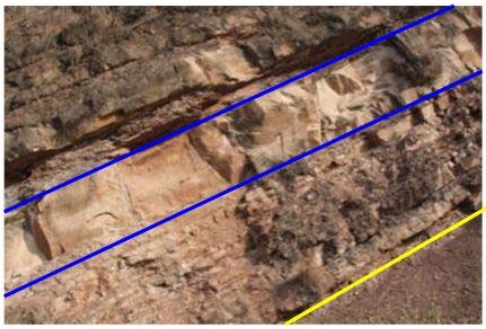

- **Slide-prone strata**
- **Zigui Syncline**
- **Fluctuation of reservoir water**
- **Rainfall**
- **Human activities (eg. road excavation, building, agriculture)**

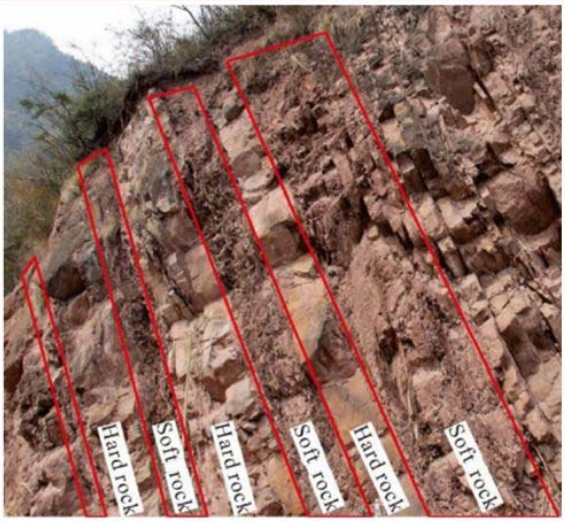

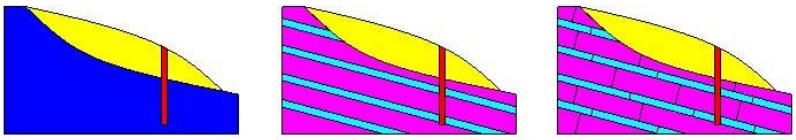

Effects of rainfall

Horizontal thrust －Lateral water pressure

Uplift pressure－Reduce the effective stress on the slip surface

Softening effect－Reduce the shear strength of rock and soil

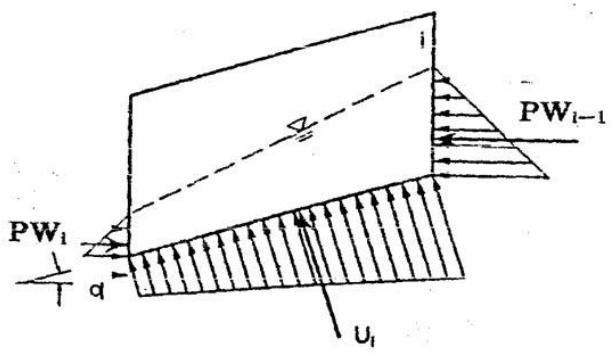

Improved Green-Ampt model

Conventional GA model assumes that the object of study for infinite slope, without taking into account the above the saturation of the wetting front with parallel to slope surface seepage caused by water loss.

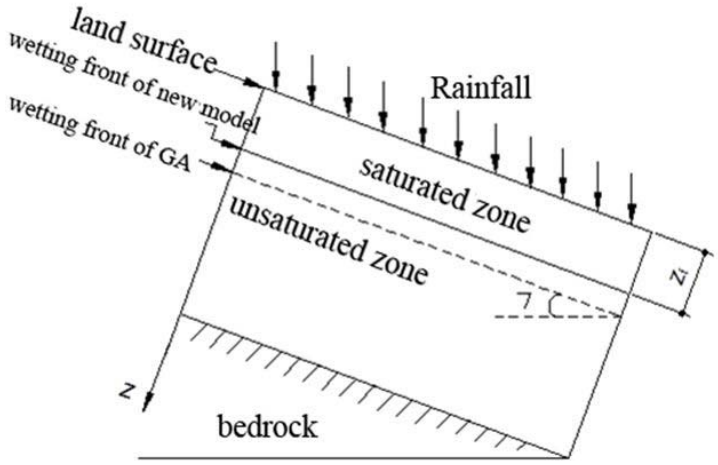

Stability analysis of landslide

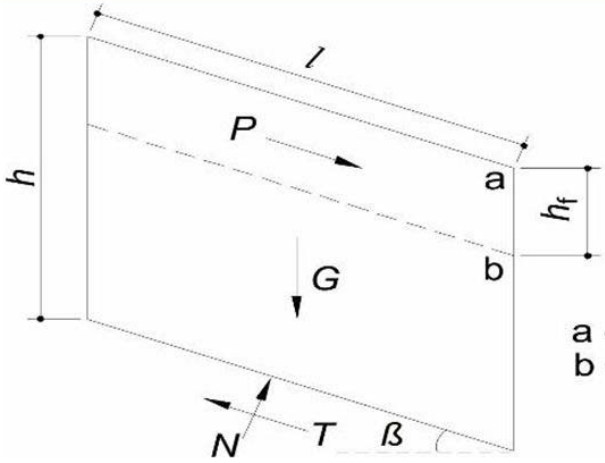

a -saturated zone
b - unsaturated zone

P-seepage force

$$P = \gamma_w h_f l \sin\beta \cos\beta$$

$$F_s = \frac{G\cos\beta \tan\phi' + c_\psi l}{G\sin\beta + P}$$

Comparison of stability evaluation methods

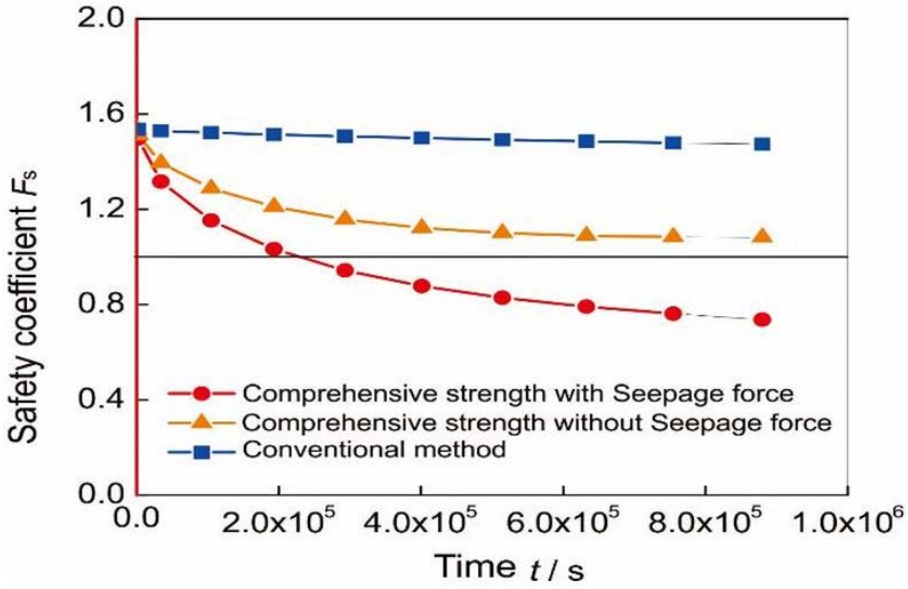

The variation of safety factor with the change of rainfall time is calculated by different methods

4.1 Rational choice of pile location

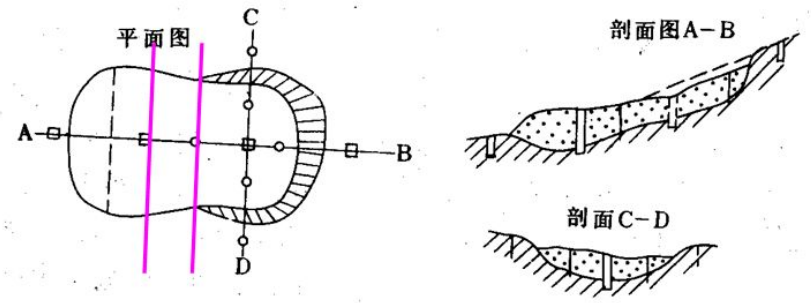

Case study

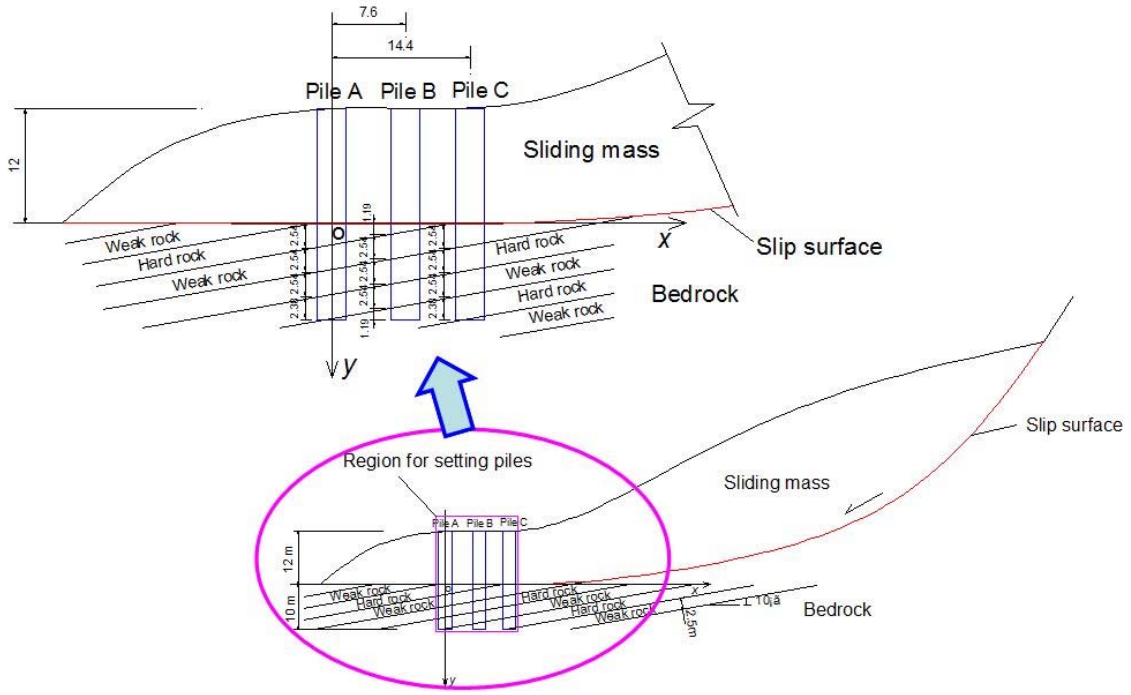

Comparison of force and displacement

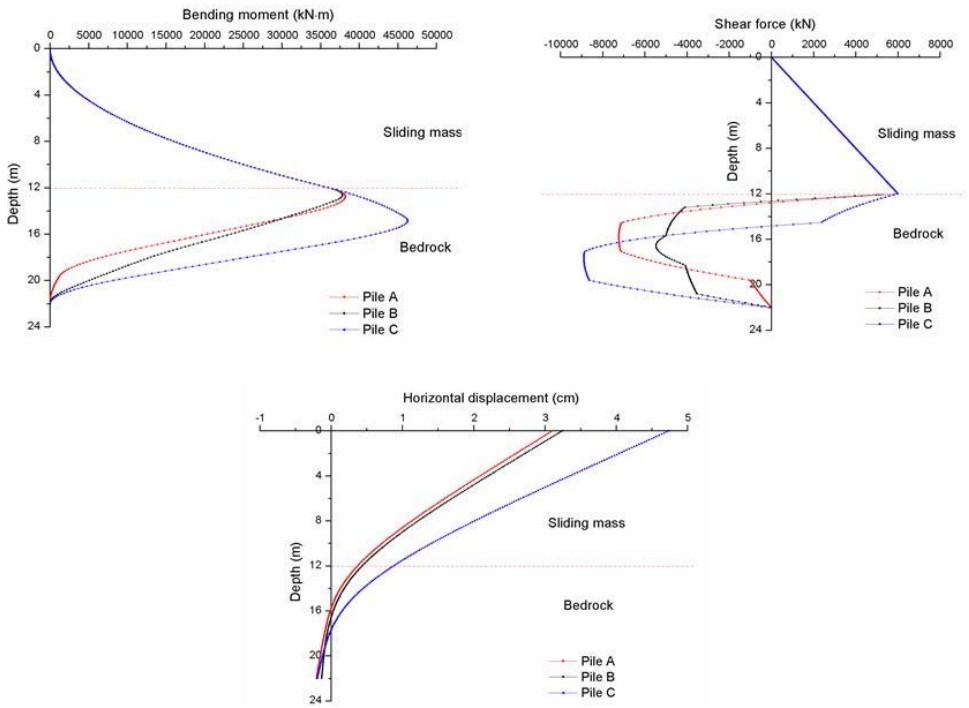

Result of Comparison

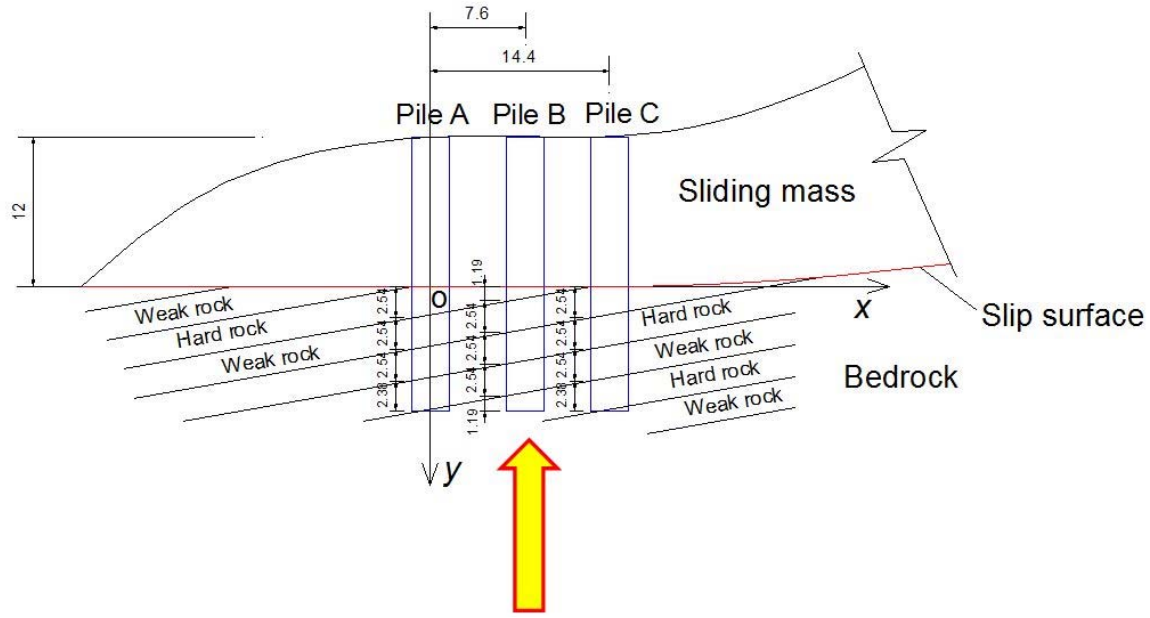

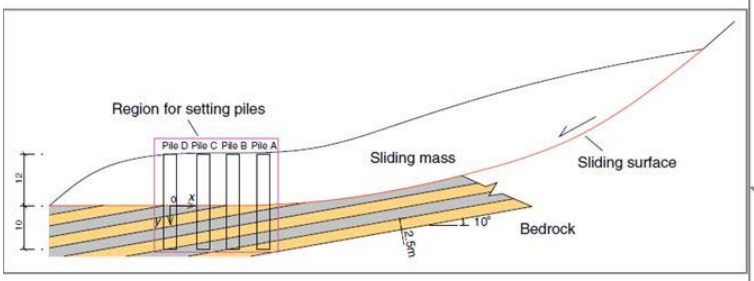

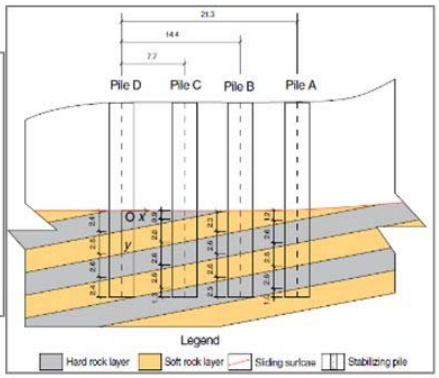

➢**Changdong Li**, Xiaoyi Wang, Huiming Tang, et al.. A preliminary study on the location of the stabilizing piles for colluvial landslides with interbedding hard and soft bedrocks. Engineering Geology, 2017, 224, 15–28.

4.2 Basic models for pile-slope

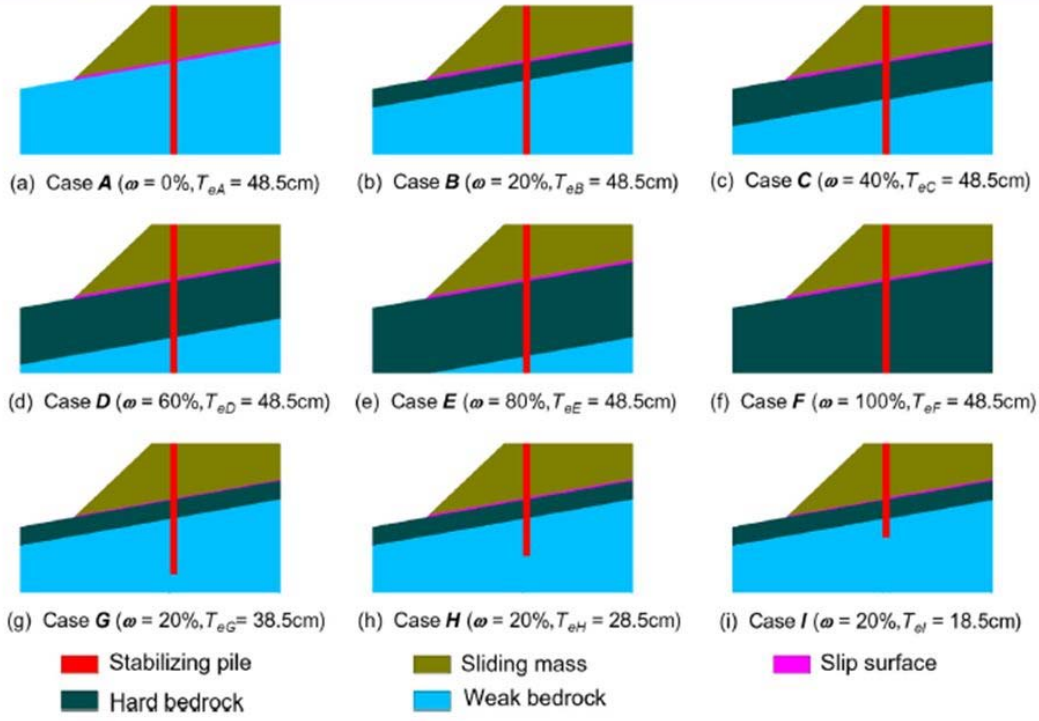

4.3 Solution for Multi-layer bedrock

Pile in homogenous bedrock:

$$EI\frac{d^4x}{dy^4}+xKB_p=0$$

$$\frac{d^4x}{dy^4}+4\beta^4x=0$$

$$\begin{cases} x_y = x_A\varphi_1+\dfrac{\varphi_A}{\beta}\varphi_2+\dfrac{M_A}{\beta^2EI}\varphi_3+\dfrac{Q_A}{\beta^3EI}\varphi_4 \\ \varphi_y = \beta\left(-4x_A\varphi_4+\dfrac{\varphi_A}{\beta}\varphi_1+\dfrac{M_A}{\beta^2EI}\varphi_2+\dfrac{Q_A}{\beta^3EI}\varphi_3\right) \\ M_y = -4x_A\beta^2EI\varphi_3-4\varphi_A\beta EI\varphi_4+M_A\varphi_1+\dfrac{Q_A}{\beta}\varphi_2 \\ Q_y = -4x_A\beta^3EI\varphi_2-4\varphi_A\beta^2EI\varphi_3-4M_A\beta\varphi_4+Q_A\varphi_1 \\ \sigma_y = Kx_y \end{cases}$$

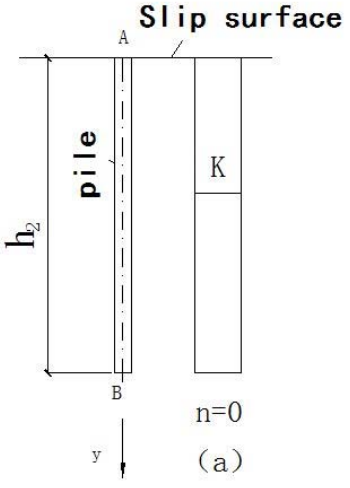

Model for pile in multi-layer bedrock

Slip surface

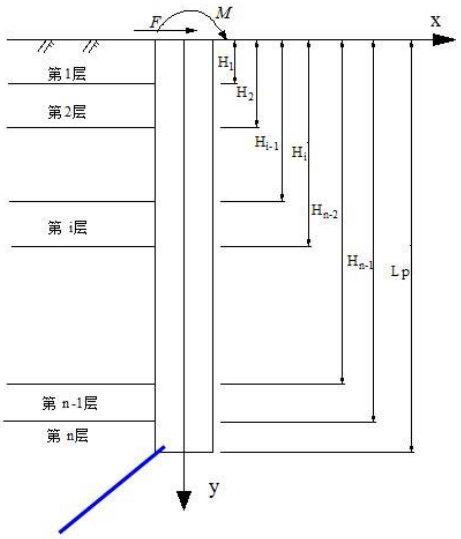

Stabilizing pile

Solution for pile in multi-layer bedrock

Bedrock, from single layer to （i）layer:

$$EI\frac{\mathrm{d}^4x}{\mathrm{d}y^4}+xK_iB_p=0$$

$$\begin{pmatrix} x_i \\ \dfrac{\theta_i}{\beta_i} \\ \dfrac{M_i}{\beta_i^2EI} \\ \dfrac{Q_i}{\beta_i^3EI} \end{pmatrix}=\begin{pmatrix} \varphi_1 & \varphi_2 & \varphi_3 & \varphi_4 \\ -4\varphi_4 & \varphi_1 & \varphi_2 & \varphi_3 \\ -4\varphi_3 & -4\varphi_4 & \varphi_1 & \varphi_2 \\ -4\varphi_2 & -4\varphi_3 & -4\varphi_4 & \varphi_1 \end{pmatrix}\cdot\begin{pmatrix} x_{i-1} \\ \dfrac{\theta_{i-1}}{\beta_i} \\ \dfrac{M_{i-1}}{\beta_i^2EI} \\ \dfrac{Q_{i-1}}{\beta_i^3EI} \end{pmatrix}$$

$$\varphi_1=\cos\beta\Delta y\cdot\mathrm{ch}\beta\Delta y$$

$$\varphi_2=\frac{1}{2}(\sin\beta\Delta y\cdot\mathrm{ch}\beta\Delta y+\cos\beta\Delta y\cdot\mathrm{sh}\beta\Delta y)$$

$$\varphi_3=\frac{1}{2}\sin\beta\Delta y\cdot\mathrm{sh}\beta\Delta y$$

$$\varphi_4=\frac{1}{4}(\sin\beta\Delta y\cdot\mathrm{ch}\beta\Delta y-\cos\beta\Delta y\cdot\mathrm{sh}\beta\Delta y)$$

$$\beta_i=\sqrt[4]{\frac{K_iB_p}{4EI}}$$

$$\Delta y=y_i-y_{i-1}$$

$$\begin{pmatrix} x_i \\ \theta_i \\ M_i \\ Q_i \end{pmatrix} = \begin{pmatrix} \varphi_1 & \frac{\varphi_2}{\beta_i} & \frac{\varphi_3}{\beta_i^2 EI} & \frac{\varphi_4}{\beta_i^3 EI} \\ -4\varphi_4\beta_i & \varphi_1 & \frac{\varphi_2}{\beta_i EI} & \frac{\varphi_3}{\beta_i^2 EI} \\ -4\varphi_3\beta_i^2 EI & -4\varphi_4\beta_i EI & \varphi_1 & \frac{\varphi_2}{\beta_i} \\ -4\varphi_2\beta_i^3 EI & -4\varphi_3\beta_i^2 EI & -4\varphi_4\beta_i & \varphi_1 \end{pmatrix} \cdot \begin{pmatrix} x_{i-1} \\ \theta_{i-1} \\ M_{i-1} \\ Q_{i-1} \end{pmatrix}$$

$$\{x_i\} = [\varphi_i] \cdot \{x_{i-1}\}$$

Where,$[x_{i-1}][x_i]$are the deformation of the top and bottom of the ith layer.

4.4 Model test of pile in multi-layers

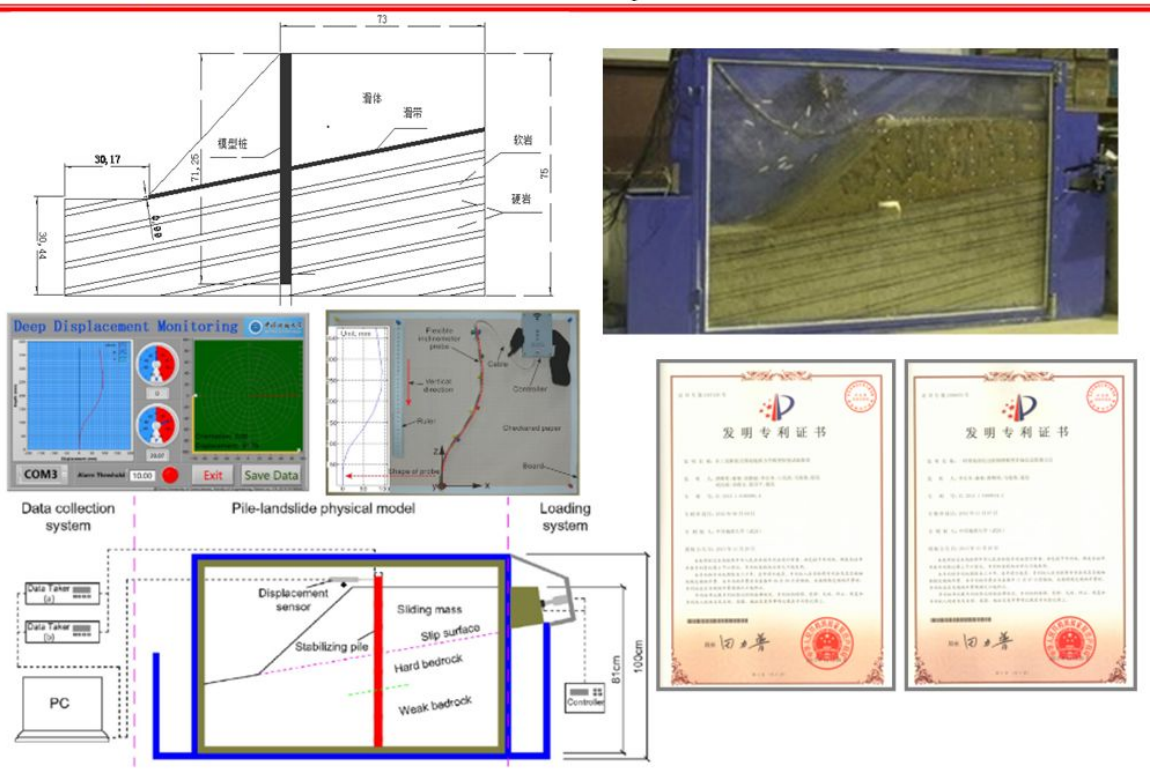

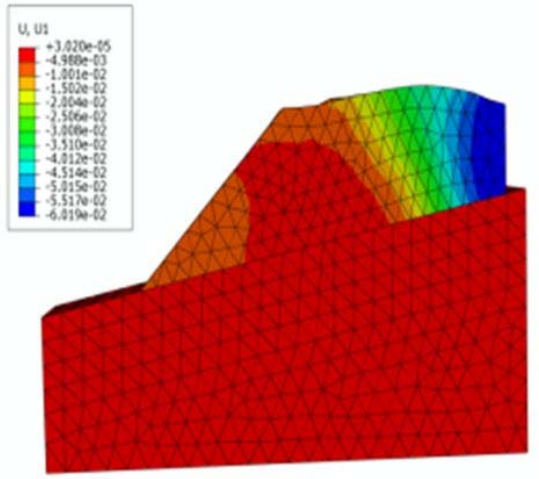

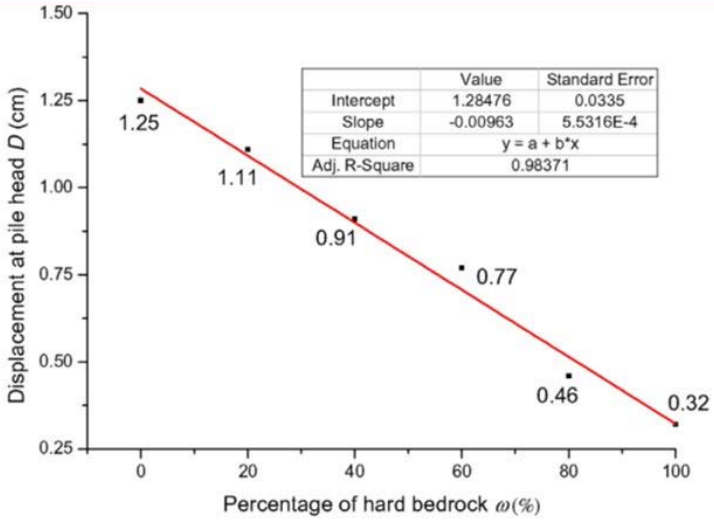

➢**Changdong Li**, Junjie Wu, Huiming Tang, Xinli Hu, Xinwang Liu, Chenqi Wang, Tao Liu, Yongquan Zhang. Model testing of the response of stabilizing piles in landslides with upper hard and lower weak bedrock. Engineering Geology, 2016, 204, 65–76.

Modified arrangement scheme for piles

- Considering the change of thickness of sliding mass:

$$S_i = \frac{c \cdot a \cdot (2H_i + 1)}{q_i \cdot (1 - \tan\varphi) - \gamma \cdot H_i \cdot (\cos\theta \cdot \tan\varphi - \sin\theta)}$$

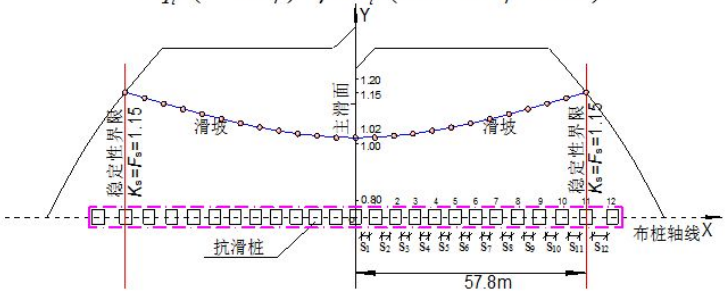

- The conventional scheme 31 piles, the optimization scheme 25 piles, with a saving of 19.4%.

➢**Changdong Li**, Junjie Wu, Huiming Tang, Jiao Wang, Feng Chen, Deming Liang. A novel optimal plane arrangement of stabilizing piles based on soil arching effect and stability limit for 3D colluvial landslides. Engineering Geology, 2015, 195, 236–247.

Improved plane layout for piles

- **Considering the irregular driving force of sliding mass:**

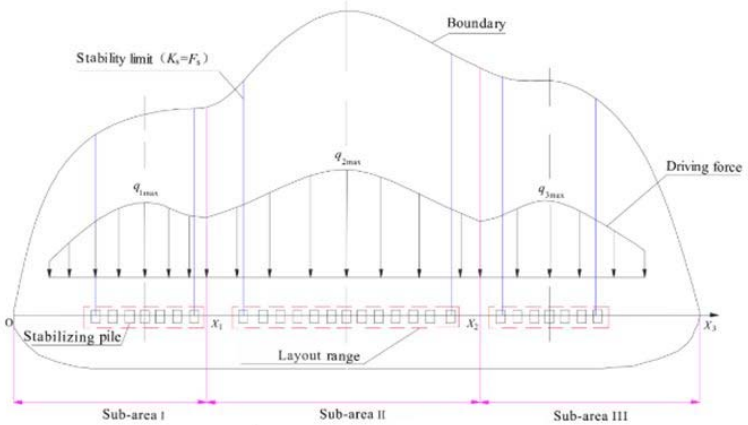

$$q(x) = \begin{cases} q_{1\max}\left(1 - \dfrac{4x^2}{d_1^2}\right), & 0 \le X < X_1 \\ q_{2\max}\left(1 - \dfrac{4x^2}{d_2^2}\right), & X_1 \le X \le X_2 \\ q_{3\max}\left(1 - \dfrac{4x^2}{d_3^2}\right), & X_2 < X \le X_3 \end{cases}$$

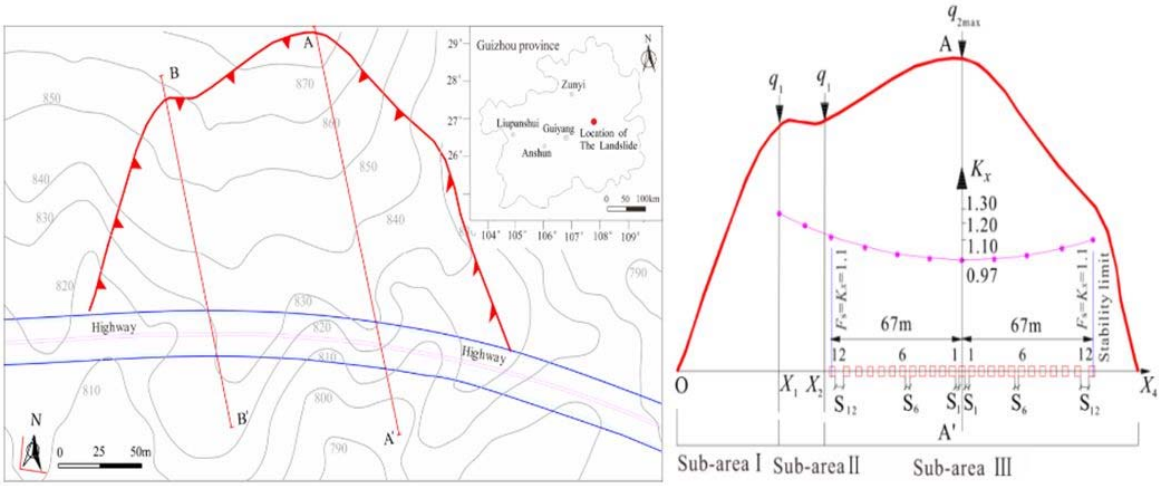

- **The conventional scheme 35 piles, the improved plane layout scheme 25 piles, with a saving of 28.6%.**

➢Wenqiang Liu, Qun Li, Jian Lu, **Changdong Li***, et al.. Improved plane layout of stabilizing piles based on the piecewise function expression of the irregular driving force. Journal of Mountain Science. 2018, 15(4):871-881.

Summary of piles' optimization

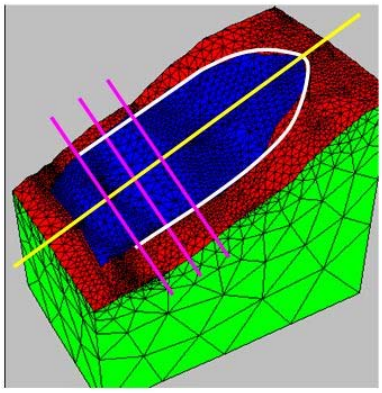

Step1

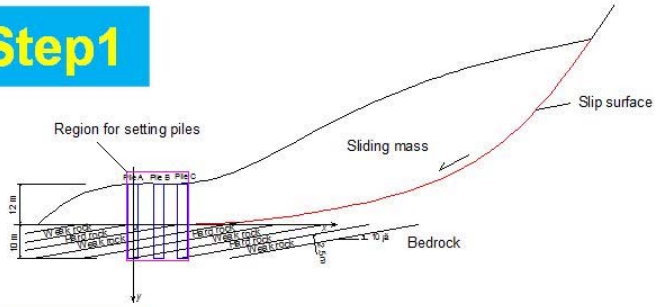

Step2

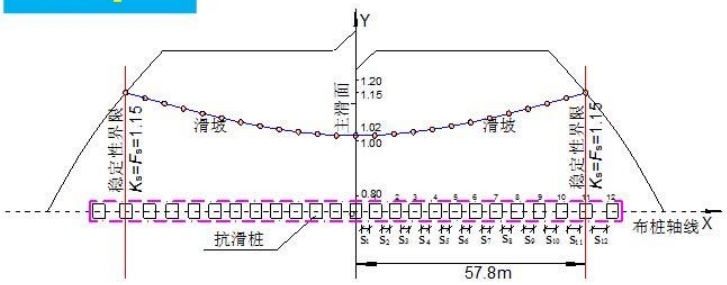

4.5 Rational pile spacing

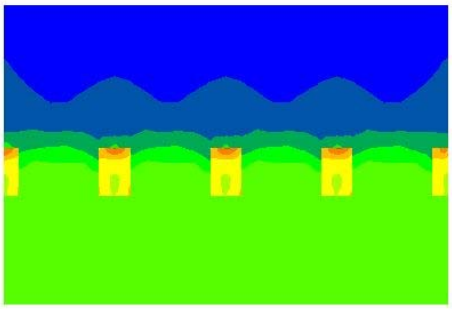

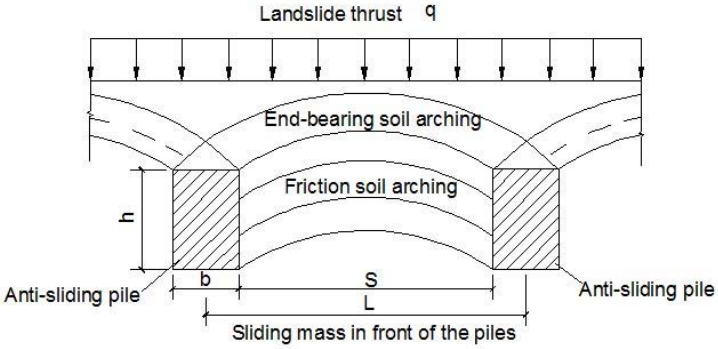

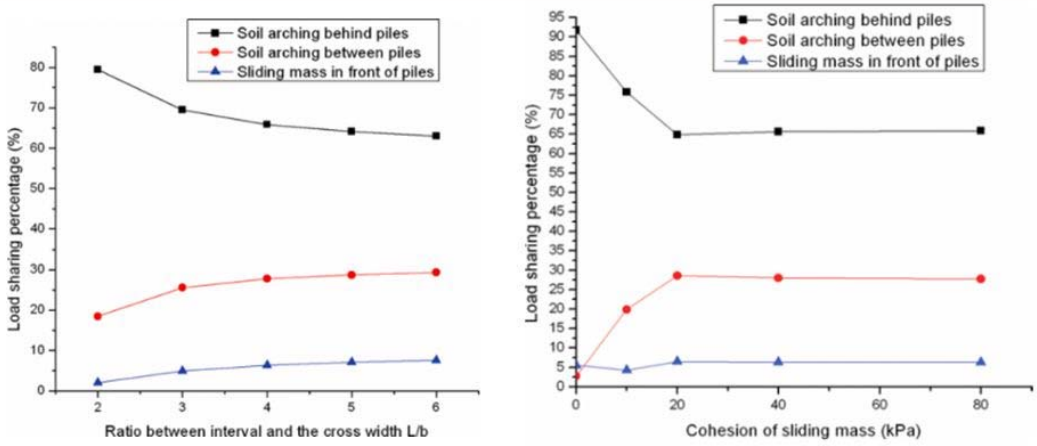

➢**Changdong Li**, Huiming Tang, Xinli Hu, Liangqing Wang. Numerical modelling study of the load sharing law of anti-sliding piles based on the soil arching effect for Erliban landslide, China. KSCE Journal of Civil Engineering, 2013, 17(6):1251-1262.

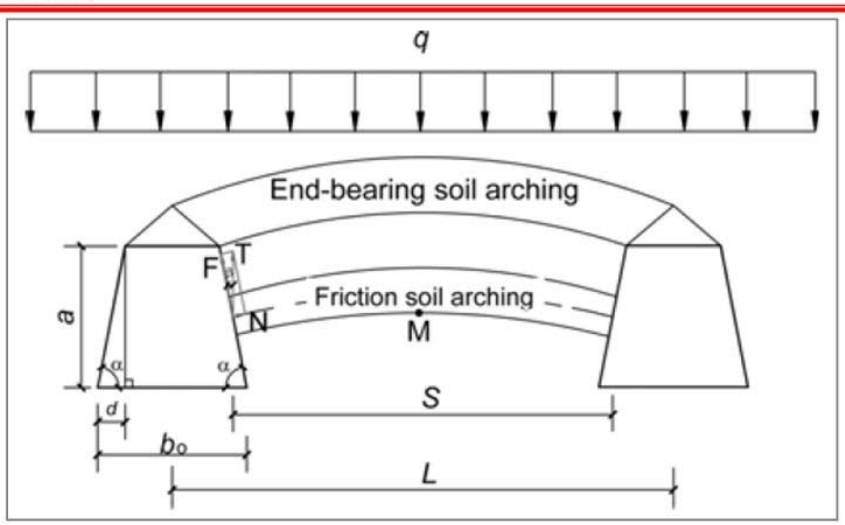

$$\omega = \frac{d}{a} = \cot\alpha = \tan\beta \quad \Rightarrow \quad S = \frac{2c \cdot a \cdot H \cdot (1+\omega^2)}{q \cdot (1 - \tan\varphi \cdot \omega)}$$

$$\omega < \cot\varphi$$

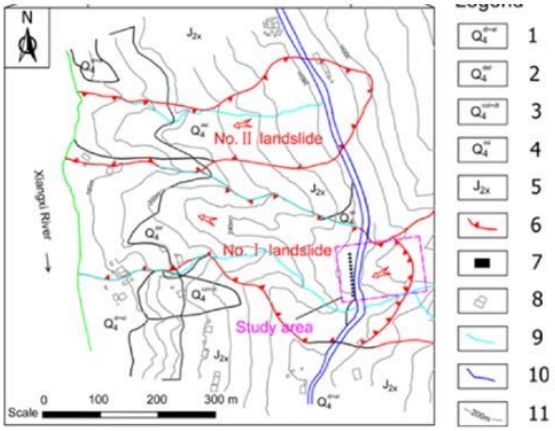

Table 1. Calculation Results of Gradient of Pile Sidewall and Reasonable Net Pile Spacing

Design scheme	Natural state		Saturated state	
	Gradient of pile sidewall ω	Reasonable net pile spacing S (m)	Gradient of pile sidewall ω	Reasonable net pile spacing S (m)
Conventional design scheme	0	4.20	0	4.20
Optimal design scheme	0.164	5.20	0.159	4.57

➢Junjie Wu, **Changdong Li***, Qingtao Liu, et al.. Optimal Isosceles Trapezoid Cross Section of Laterally Loaded Piles Based on Friction Soil Arching. KSCE Journal of Civil Engineering, 2017, 21(7):2655-2664.

4.6 Rational embedded depth of piles

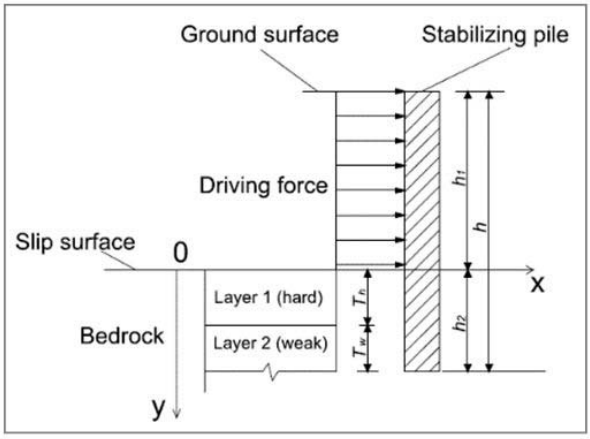

$$\begin{cases} \dfrac{d^4x}{dy^4} + 4\cdot\beta_i^4\cdot x = 0 \quad (i=1,2) \\ \beta_1 = \sqrt[4]{\dfrac{K_h B_p}{4EI}} \quad (0<y\le T_h) \\ \beta_2 = \sqrt[4]{\dfrac{K_w B_p}{4EI}} \quad (T_h<y\le h_2) \end{cases} \cdot \begin{pmatrix} x_2 \\ \theta_2 \\ M_2 \\ Q_2 \end{pmatrix} = \begin{pmatrix} \psi_{12} & \dfrac{\psi_{22}}{\beta_2} & \dfrac{\psi_{32}}{\beta_2^2 EI} & \dfrac{\psi_{42}}{\beta_2^3 EI} \\ -4\psi_{42}\beta_2 & \psi_{12} & \dfrac{\psi_{22}}{\beta_2 EI} & \dfrac{\psi_{32}}{\beta_2^2 EI} \\ -4\psi_{32}\beta_2^2 EI & -4\psi_{42}\beta_2 EI & \psi_{12} & \dfrac{\psi_{22}}{\beta_2} \\ -4\psi_{22}\beta_2^3 EI & -4\psi_{32}\beta_2^2 EI & -4\psi_{42}\beta_2 & \psi_{12} \end{pmatrix} \cdot \begin{pmatrix} x_1 \\ \theta_1 \\ M_1 \\ Q_1 \end{pmatrix}$$

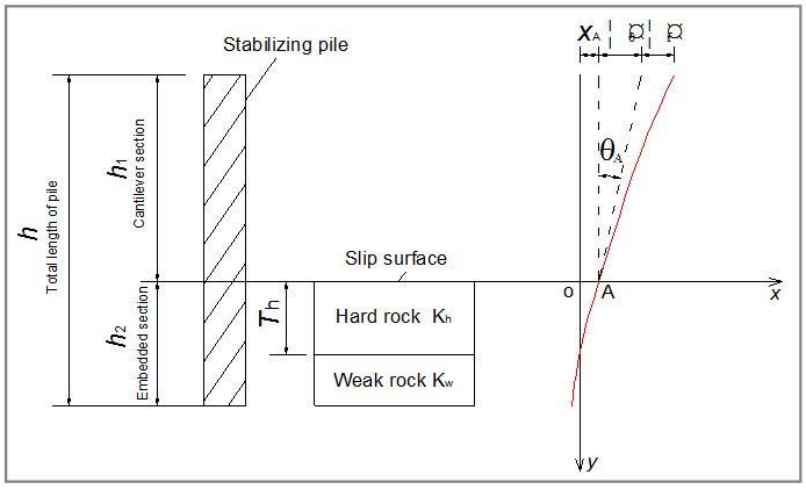

$$x(y) = x_A + \Delta_\theta(y) + \Delta_f(y) \quad (y<0),$$

$$M_y = \frac{T\cdot L}{2h_1}\cdot(h_1-|y|)^2 \quad (y<0)$$

$$\Delta_\theta(y) = |y| * \theta_A \quad (y<0).$$

$$Q_y = \frac{T\cdot L}{h_1}\cdot(h_1-|y|)\,(y<0),$$

$$\Delta_f(y) = \frac{T\cdot L}{EIh_1}\left(\frac{1}{24}(h_1-|y|)^4 - \frac{h_1^3}{6}(h_1-|y|) + \frac{h_1^4}{8}\right) \quad (y<0),$$

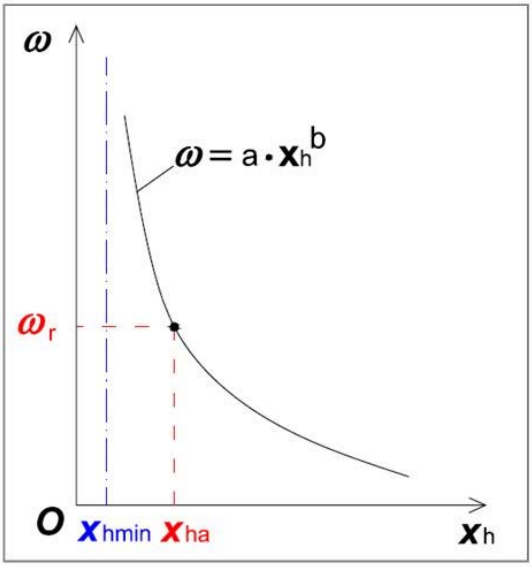

$$\begin{cases} x_{\mathrm{h}} = f(\omega, T_{\mathrm{h}}, K_{\mathrm{h}}, K_{\mathrm{w}}, P) \\ x_{\mathrm{ha}} \le 0.01 h_1 \\ x_{\mathrm{ha}} \le 10\ \mathrm{cm} \end{cases}$$

$$\begin{cases} \omega_{\mathrm{r}} = a x_{\mathrm{ha}}^{b} \\ x_{\mathrm{ha}} \le 0.01 h_1 \\ x_{\mathrm{ha}} \le 10\ \mathrm{cm} \end{cases}$$

$$x_{\mathrm{hmin}} = x_{\mathrm{h}}(y = -h_1) = \frac{PL}{EIh_1}\left[\frac{h_1^4}{8}\right] = \frac{PLh_1^3}{8EI_1}$$

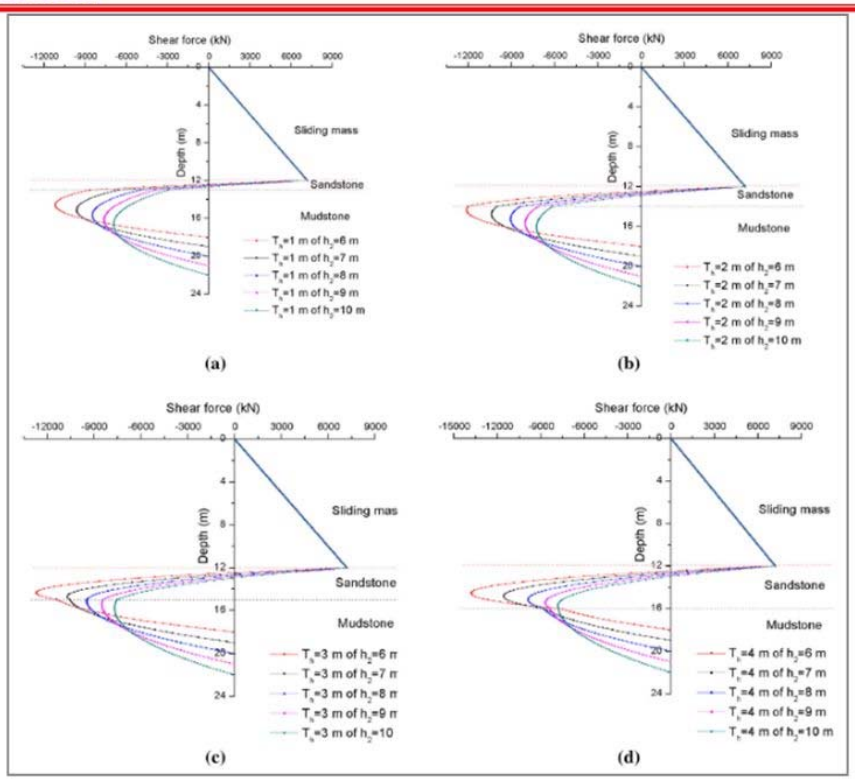

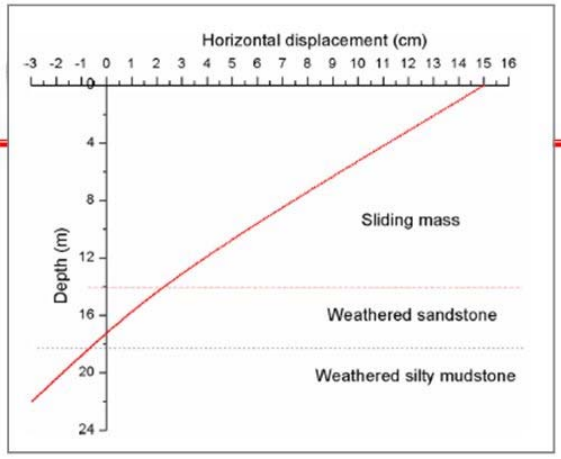

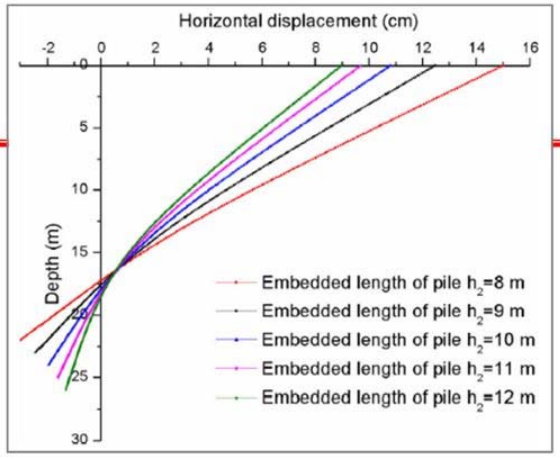

Since the length of the section above the slip surface (h_1) is 14 m and the length of the embedded section (h_2) is 8 m, the current embedded ratio of the stabilizing pile in the Majiagou No. 1 landslide is 0.364.

$$\omega = \frac{h_2}{h_1 + h_2}$$

Upon inserting x_{hmin} = 10 cm into Eq. 15, we find that the reasonable embedded ratio (ω_r) of the piles is 0.435. Therefore, the corresponding reasonable embedded length (h_{2r}) of the piles is 10.8 m according to Eq. 13, i.e., the embedded length must be at least 10.8 m to keep the pile head deformation within 10 cm, in line with industrial standards. The embedded ratio (ω) should also be increased from its current value of 0.364 to 0.435 to ensure that it meets the industrial standards. Therefore, the embedded ratio of the

➢**Changdong Li**, Junfeng Yan, Junjie Wu, et al.. Determination of the embedded length of stabilizing piles in colluvial landslides with upper hard and lower weak bedrock based on the deformation control principle. Bulletin of Engineering Geology and the Environment , 2017, 20 July, 1-20. (DOI 10.1007/s10064-017-1123-3)

Summary

- **Formation mechanism of landslides: slide-prone strata, Zigui Syncline, fluctuation of reservoir water, rainfall and human activities.**
- **Main effects of water: 1) Horizontal thrust —Lateral water pressure; 2)Uplift pressure—Reduce the effective stress on the sliding surface; 3)Softening effect.**
- **Interaction between piles and landslide: Theoretical analysis; numerical modeling; physical model test; in-situ test.**
- **Optimization of piles : 1) pile location; 2) pile arrangement; 3) length of pile; 4)cross-section of pile etc.**

Strengthening the resilience by reducing risk from sediment-related disasters

Teuku Faisal Fathani[1,3], Wahyu Wilopo [2,3]

1) Department of Civil and Environmental Engineering, Universitas Gadjah Mada Yogyakarta 55281, Indonesia
e-mail: tfathani@ugm.ac.id
2) Department of Geological Engineering, Universitas Gadjah Mada Yogyakarta, Indonesia
3) Center for Disaster Mitigation and Technological Innovation (GAMA-InaTEK) Universitas Gadjah Mada, Yogyakarta, Indonesia

Abstract

The sediment-related disasters occur in different topographic and geologic setting and causes great socio-economies losses. It may increase apparently due to the human development expands into unstable hill-slope areas under the pressures of increasing populations. The implementation of mitigation measure for sediment-related disaster usually focuses on avoiding the mass movement, diverting the moving mass away from vulnerable elements or building reinforcement to protect the threatened elements. However, the importance of monitoring and early warning system can rise when the mass movement mitigation works is considered expensive. This research describes the current progress of mitigation effort in term of the implementation of monitoring and warning system against sediment-related disasters in Indonesia. In order to guarantee the effectiveness of the sediment-related disaster early warning system, the developed system should be simple to operate and appropriately installed in the most suitable sites. It should include the incorporating technical and social approaches. The understanding on the cause and sediment disaster triggering mechanism is very crucial to establish an appropriate concept and method for risk reduction effort at the region.

Shift in paradigm

Risk Reduction is complex, difficult and it takes much longer to see results

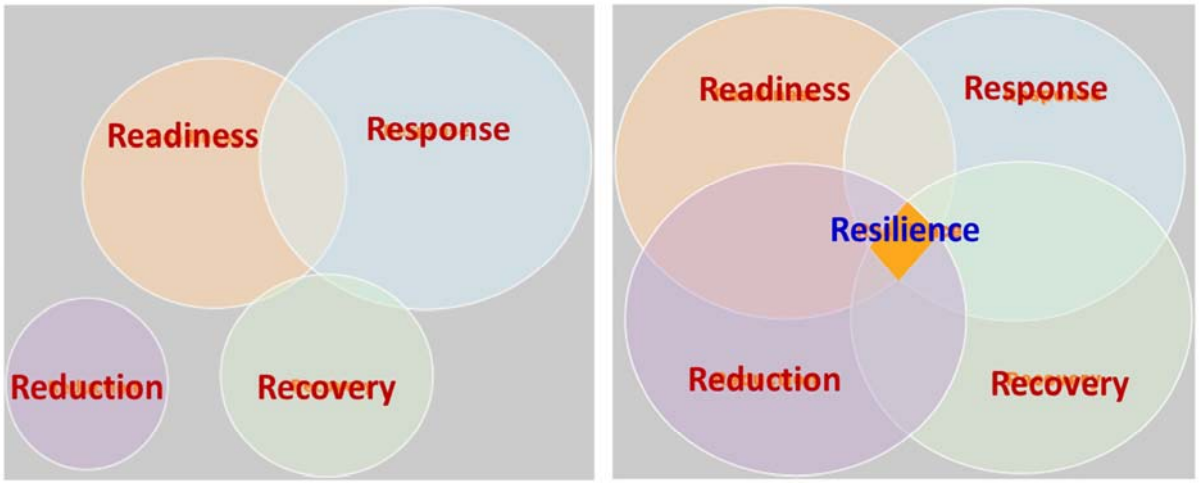

Focus on Disaster Risk Reduction (DRR)

"Disaster Risk Reduction (DRR) aims to reduce the damage caused by natural hazards like earthquakes, floods, droughts and cyclones, through an ethic of prevention." (UNISDR)

Shift in paradigm

Response Penanganan	→	Reduction Pengurangan
Hazards Kerawanan	→	Risk Resiko
Single mandates Mandat tunggal	→	Integrated Planning Perencanaan terintegrasi
Centralised Sistem terpusat	→	Increased local government and community responsibility Meningkatkan tanggung jawab pemerintah daerah dan masyarakat

Hybrid socio-preuner & technology approach for disaster mitigation

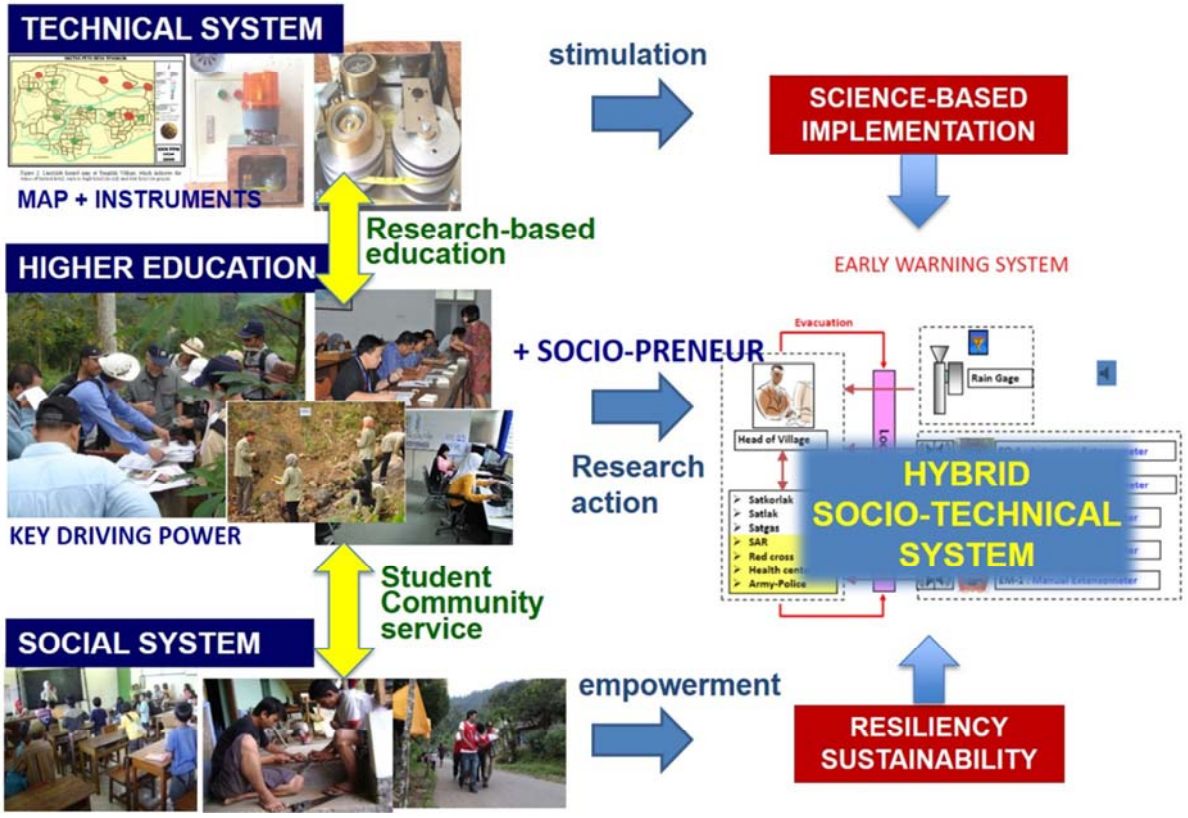

National Masterplan for Landslide DRR

Prepared by Universitas Gadjah Mada and approved by BNPB and 37 related Ministries/Institutions/Agencies

Outline of the masterplan

1. Introduction
2. Landslide disaster priority for each province
3. Issues, challenges and opportunities
4. Program:
   - National
   - Province
   - District/City
   - Community
5. Action plan
6. Budgeting
7. Monitoring, evaluation, reporting

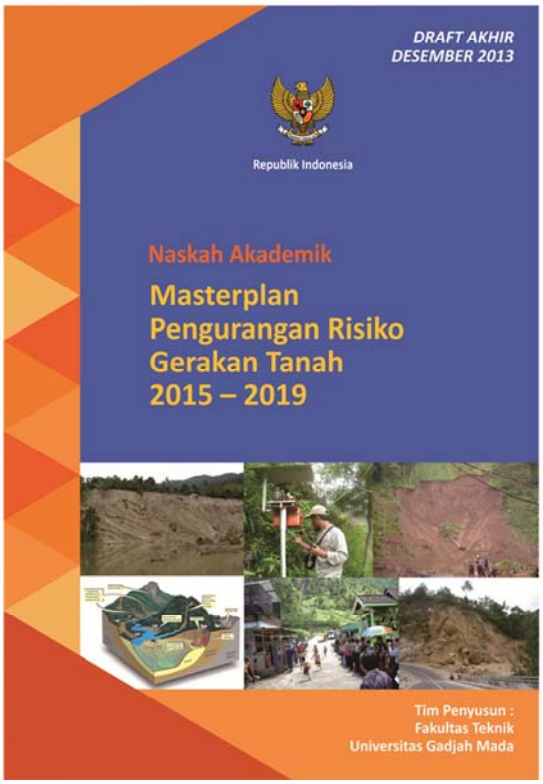

The Sendai Framework for Disaster Risk Reduction (2015-2030)

Sendai Framework is the first major agreement of the post-2015 development agenda, with seven targets and four priorities for action.

- Priority 1: Understanding disaster risk.
- Priority 2: Strengthening disaster risk governance to manage disaster risk.
- Priority 3: Investing in disaster risk reduction for resilience.
- Priority 4: Enhancing disaster preparedness for effective response and to "Build Back Better" in recovery, rehabilitation and reconstruction.

ISO/TC 292 Security and Resilience
ISO 22327: Guideline for the implementation of Landslide Early Warning System

Background

- It is difficult to relocate community living in vulnerable area
- The most effective DRR effort is to improve the community's preparedness by implementing EWS.

Objectives

- Integrating technical and social networks to establish an International Standard of landslide EWS.
- Increasing the community awareness and preparedness
- Community empowerment in landslide vulnerable area

Users

- International organization
- Central and local government
- Private sectors, NGOs
- Local community

4 Key Element for Community-based EWS (UNISDR, 2006)

RISK KNOWLEDGE

Systematically collect data and undertake risk assessments

Are the hazards and the vulnerabilities well known?

What are the patterns and trends in these factors?

Are risk maps and data widely available?

MONITORING & WARNING DEVICE

Develop hazard monitoring and early warning services

Are the right parameters being monitored?

Is there a sound scientific basis for making forecasts?

Can accurate and timely warnings be generated?

DISSEMINATION & COMMUNICATION

Communicate risk information and early warnings

Do warnings reach all of those at risk?

Are the risks and warnings understood?

Is the warning information clear and useable?

RESPONSE CAPABILITY

Build national and community response capabilites

Are response plans up to date and tested?

Are local capacities and knowledge made use of?

Are people prepared and ready react to warnings?

7 Sub-systems of Landslide Early Warning System

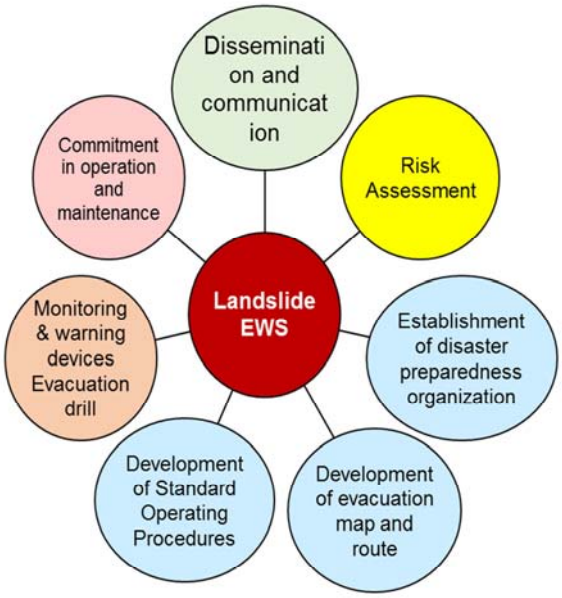

How the system works

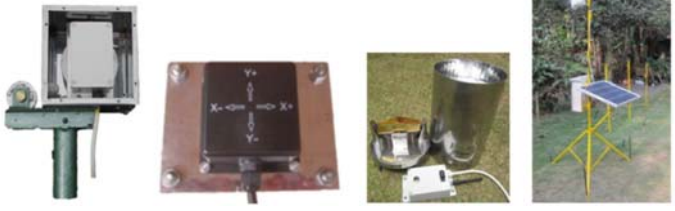

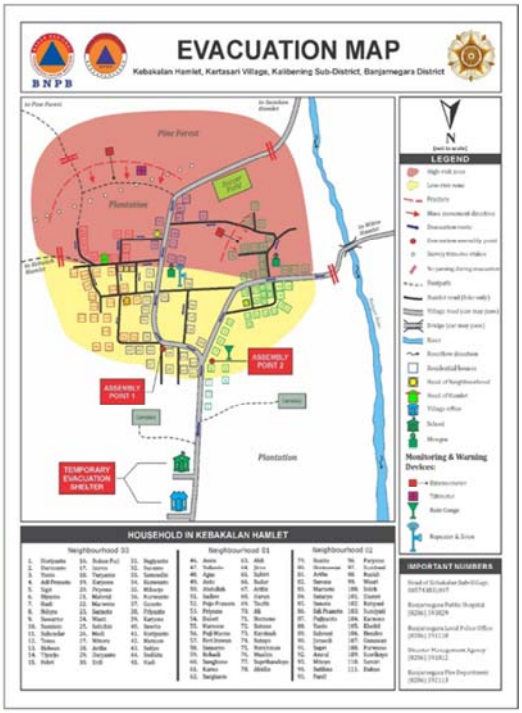

Implementation of Landslide EWS

- UGM in cooperation with National Authority for Disaster Management (BNPB) and Regional Authority for Disaster Management (BPBD)
- UGM in cooperation with Pertamina Geothermal Energy (PGE)
- UGM in cooperation with Ministry for the Development of Village, Disadvantage Region and Transmigration (KPDTT)
- UGM in cooperation with International Consortium on Landslides (ICL-UNESCO)
- UGM in cooperation with Private Mining Company

Net TV:
https://www.youtube.com/watch?v=aGDilO12cyg&t=158s
R3ADY:
https://www.youtube.com/watch?v=V2_L5aGf0EY

7 EWS Banjarnegara:
https://www.youtube.com/watch?v=frlqBsKJG24&t=48s
7 EWS UGM-BNPB:
https://www.youtube.com/watch?v=dc79xowmK0c

Kompas TV:
https://www.youtube.com/watch?v=GpB1I8llG80

Outcome

- The standard strengthens the community resilience and proved to be able to save lives
- Indonesian government includes this standard as a reference for National Medium-term Development Plan (2015-2019)

Challenges and Lessons Learned

- The application of ISO 22327 requires consistent commitment and support from all related stakeholders.
- The level of local community awareness and preparedness is not always constant → sustainability

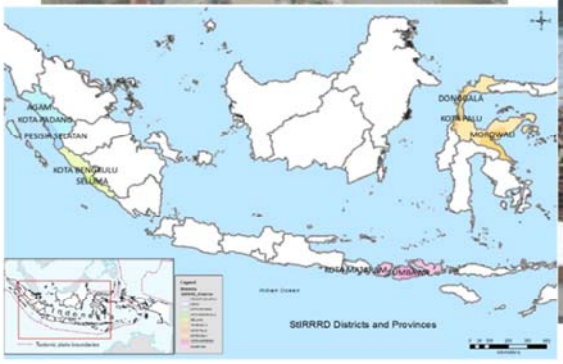

https://stirrrd.org/

Socio-Entrepreneurial university

District Profile

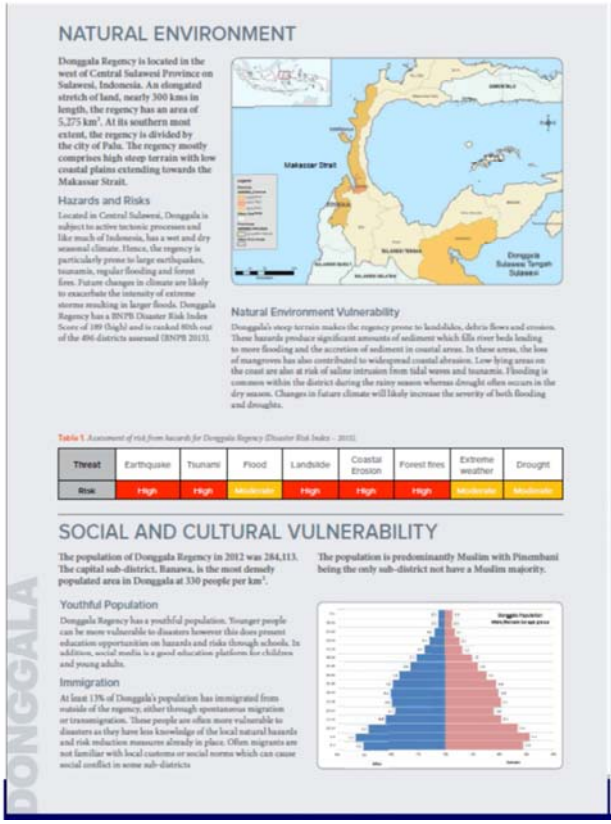

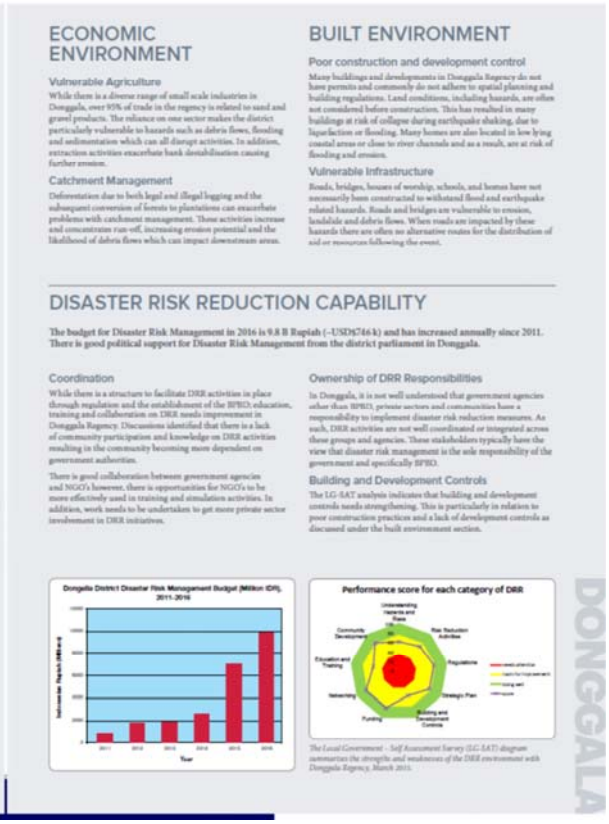

Initial Development of the Digital Crowd Mapping for Landslide Monitoring and Early Warning System

Wahyu Wilopo [1,2], Teuku Faisal Fathani [1,3], Hendy Setiawan [1,2], Budi Andayani [2], Dwikorita Karnawati [3]

1) Center for Disaster Mitigation and Technological Innovation (GAMA-InaTEK), Gadjah Mada University, Yogyakarta 55281, Indonesia. E-mail: wilopo_w@ugm.ac.id
2) Department of Geological Engineering, Fac. of Engineering, Universitas Gadjah Mada, Indonesia
3) Dep. of Civil and Environmental Engineering, Fac. of Engineering, Universitas Gadjah Mada, Indonesia
4) Faculty of Psychology, Universitas Gadjah Mada,, Indonesia
5) The Indonesia Agency for Meteorology, Climatology and Geophysics (BMKG), Jakarta 10720, Indonesia

Abstract

The innovation of the digital crowd mapping for landslide risk reduction is on the high and dynamic accuracy of the prediction on the risk and early warning based on the change in rainfall and the development of soil movement combined with "crowd information" from the community. In order to promote this system, a mapping and analysis on the community's social condition, the geological condition, landslide susceptibility level, landslide potential, and hazard level should be carried out to determine a hazard level for a dynamic and accurate early warning. The result of the landslide susceptibility mapping is analyzed by "smart system" which is integrated with rainfall data obtained from the monitoring sensors installed in the sites and also with "crowd information" from the community. Social mapping is highly necessary to carry out to support the right education and communication strategy for the community to guarantee the accuracy and reliability the crowd mapping system.

Introduction

- Landslide disaster risk reduction in vulnerable area with a dense population, need the strong integration between appropriate technologies and community participation (Karnawati et al. 2013).
- The active public or community-based participation here aims to achieve the sustainability of disaster management and risk reduction (Pearce, 2003).
- The application of low-cost landslide early warning technologies through proper training, education, simulation drill and guidance is very important to strengthening people awareness and preparedness when landslide took place (Fathani et al. 2014).

Roadmap of Research and Development for Community-based Landslide Disaster Risk Reduction in Indonesia 2003-2020

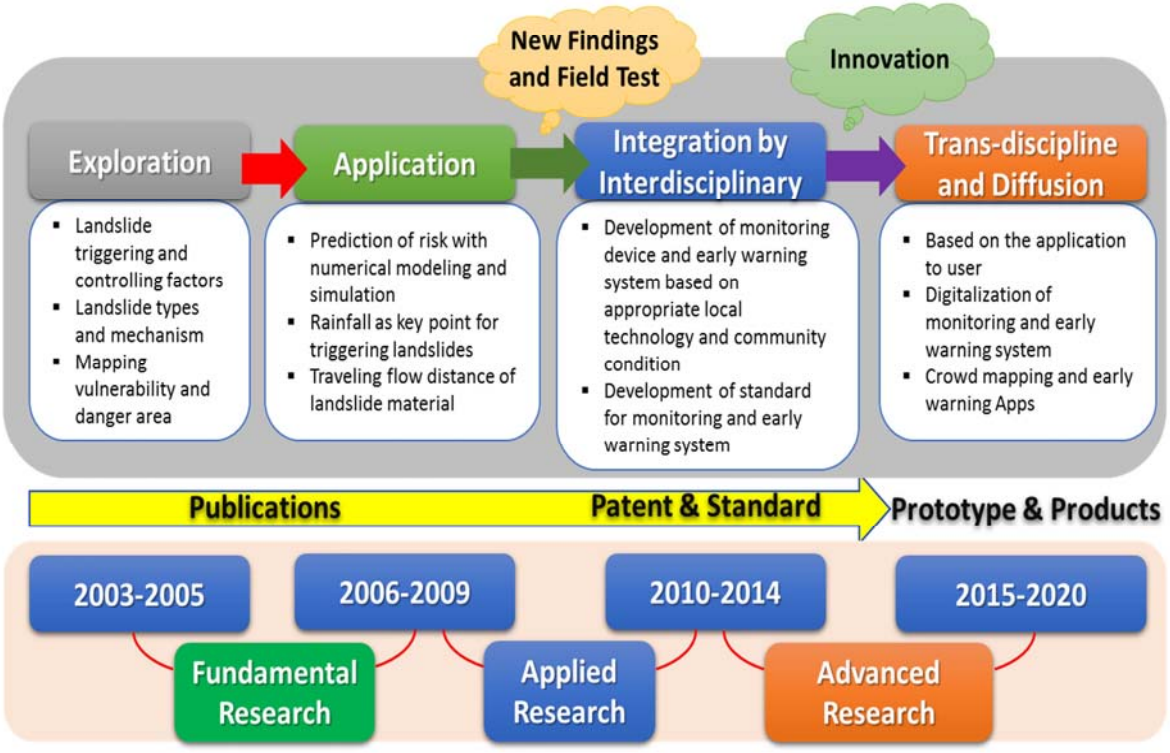

Objectives

- This paper presents our progress of the initial development framework of interdisciplinary product through digital crowd mapping for landslide and early warning in mobile apps.
- Not all of the landslide vulnerable area in Indonesia is covered by the monitoring and early warning technical instruments.
- The crowd information from local people or community in the real time as a 'human sensor' is necessary and main point in developing the crowd mapping.

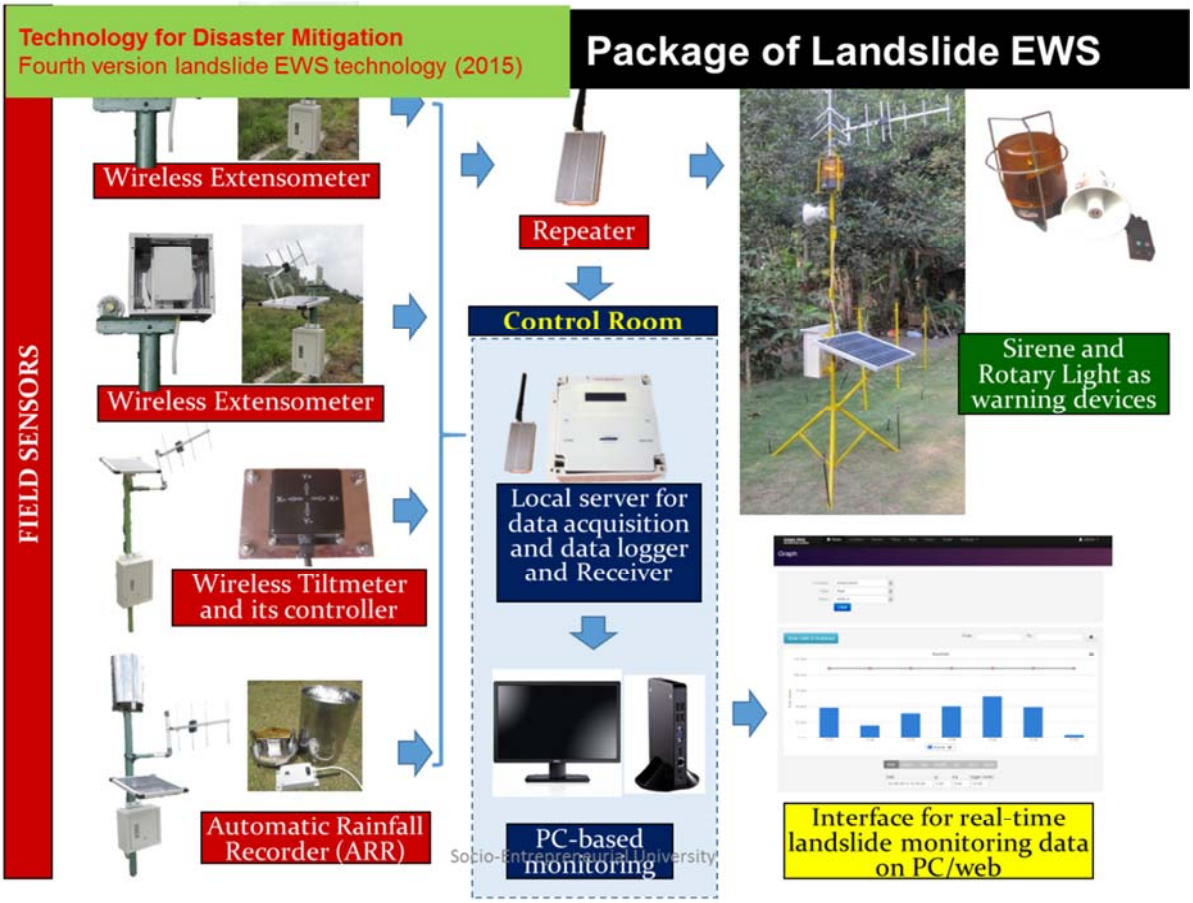

Implementation of Landslide Early Warning System 2007-2018

UGM in cooperation with National Authority for Disaster Management (BNPB) and Regional Authority for Disaster Management (BPBD)

UGM in cooperation with Pertamina Geothermal Energy (PGE)

UGM in cooperation with Ministry for the Development of Village, Disadvantage Region and Transmigration (KPDTT)

UGM in cooperation with International Consortium on Landslides (ICL-UNESCO)

UGM in cooperation with Private Mining Company

The Digital Crowd Mapping Framework

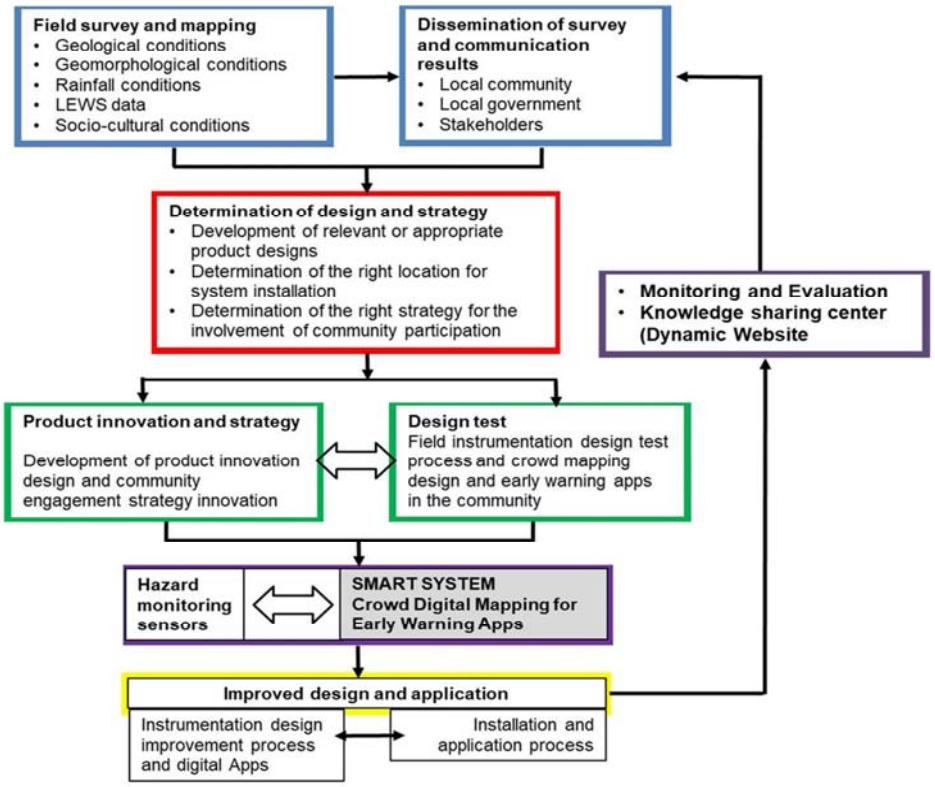

The Digital Crowd Mapping Framework

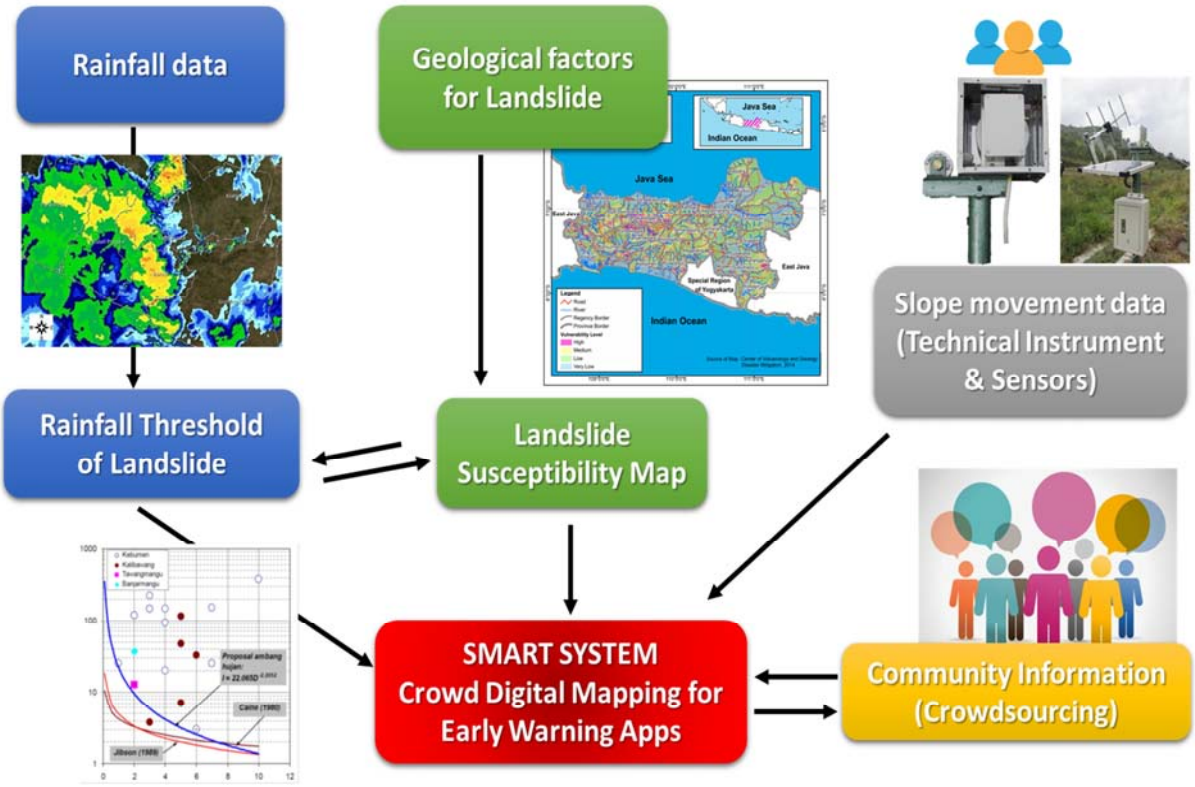

Recent Progress and Conclusion

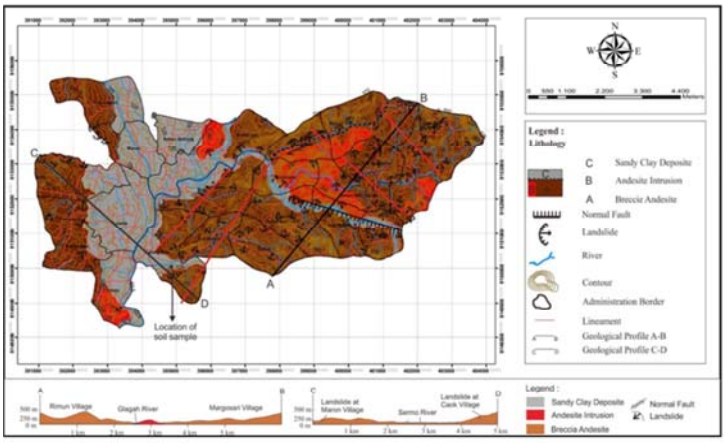

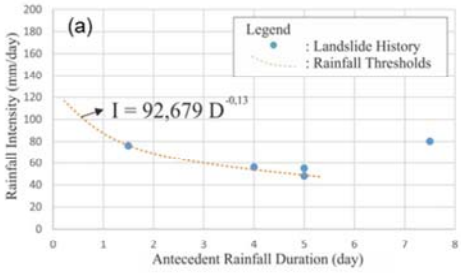

Sandy clay

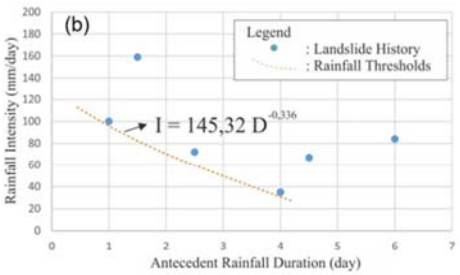

Andesite intrusion

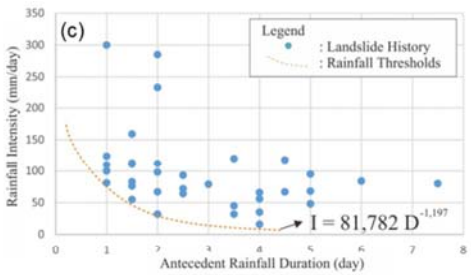

Andesite breccia

Recent Progress and Conclusion

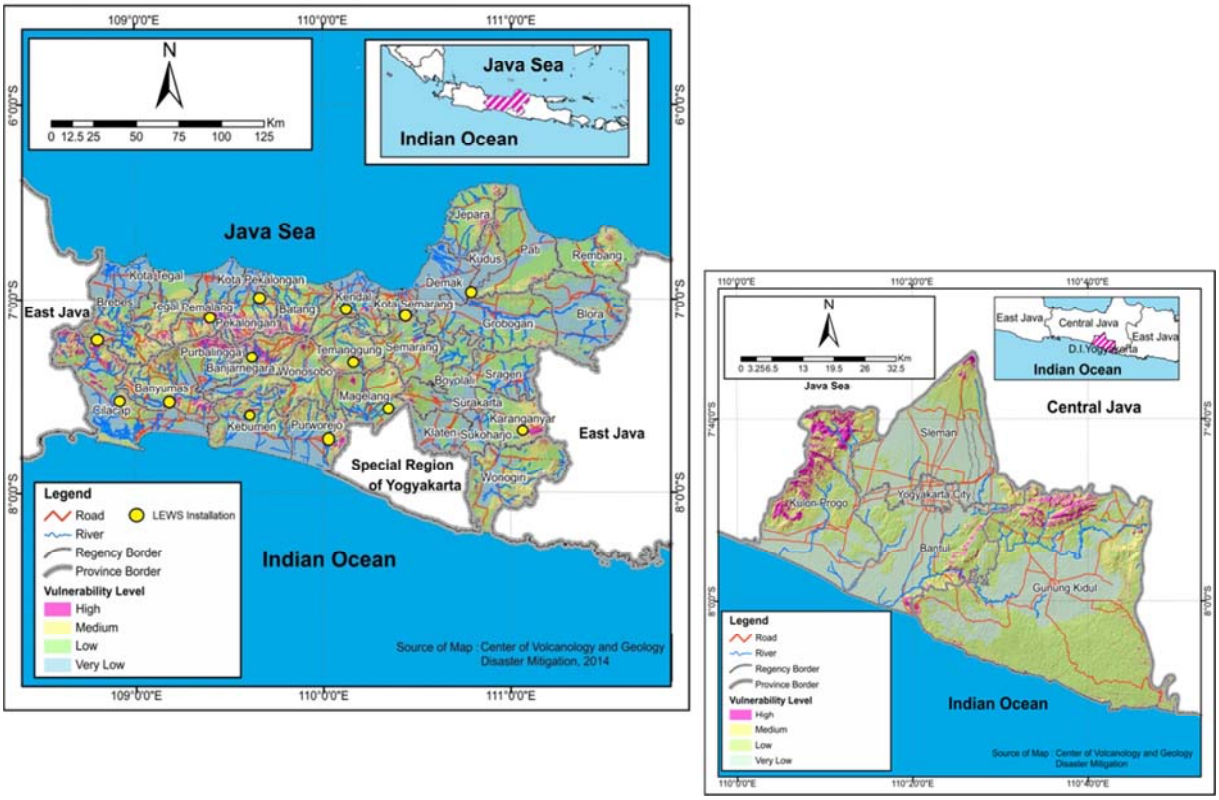

Recent Progress and Conclusion

Advanced Technologies for LandSlides (ATLaS)

Nicola Casagli, Filippo Catani, Riccardo Fanti, Giovanni Gigli, Sandro Moretti, Veronica Tofani, Paolo Canuti

UNESCO Chair on Prevention and Sustainable Management of Geo-hydrological Hazards
University of Florence, Italy

Abstract

In this presentation we report the activities carried out by the WCoE through the project Atlas, with particular reference to i) Ground-based SAR interferometry, for landslide monitoring and development of reliable procedures and technologies for early warming, ii) EO (Earth Observation) data and technology to detect, map, monitor and forecast ground deformations and iii) coupling of short-term weather forecasting with geotechnical modeling for shallow landslide prediction.

Research group

8 professors and associate professors
7 researchers, 12 technicians
10 post-doc fellows, 12 PhD students
11 collaborators and visiting

Total = 60 persons

Paolo Canuti
The Founder
UNESCO Chairholder

United Nations Educational, Scientific and Cultural Organization

UNESCO Chair on Prevention and sustainable management of geo-hydrological hazards (since 2015)

IPL World Centre of Excellence on Landslide Risk Reduction (2008-2020)

A Programme of the ICL for ISDR

PROTEZIONE CIVILE
Presidenza del Consiglio dei Ministri
Dipartimento della Protezione Civile

Center of Competence of the Civil Protection Department Presidency of the Council of Ministers (since 2005)

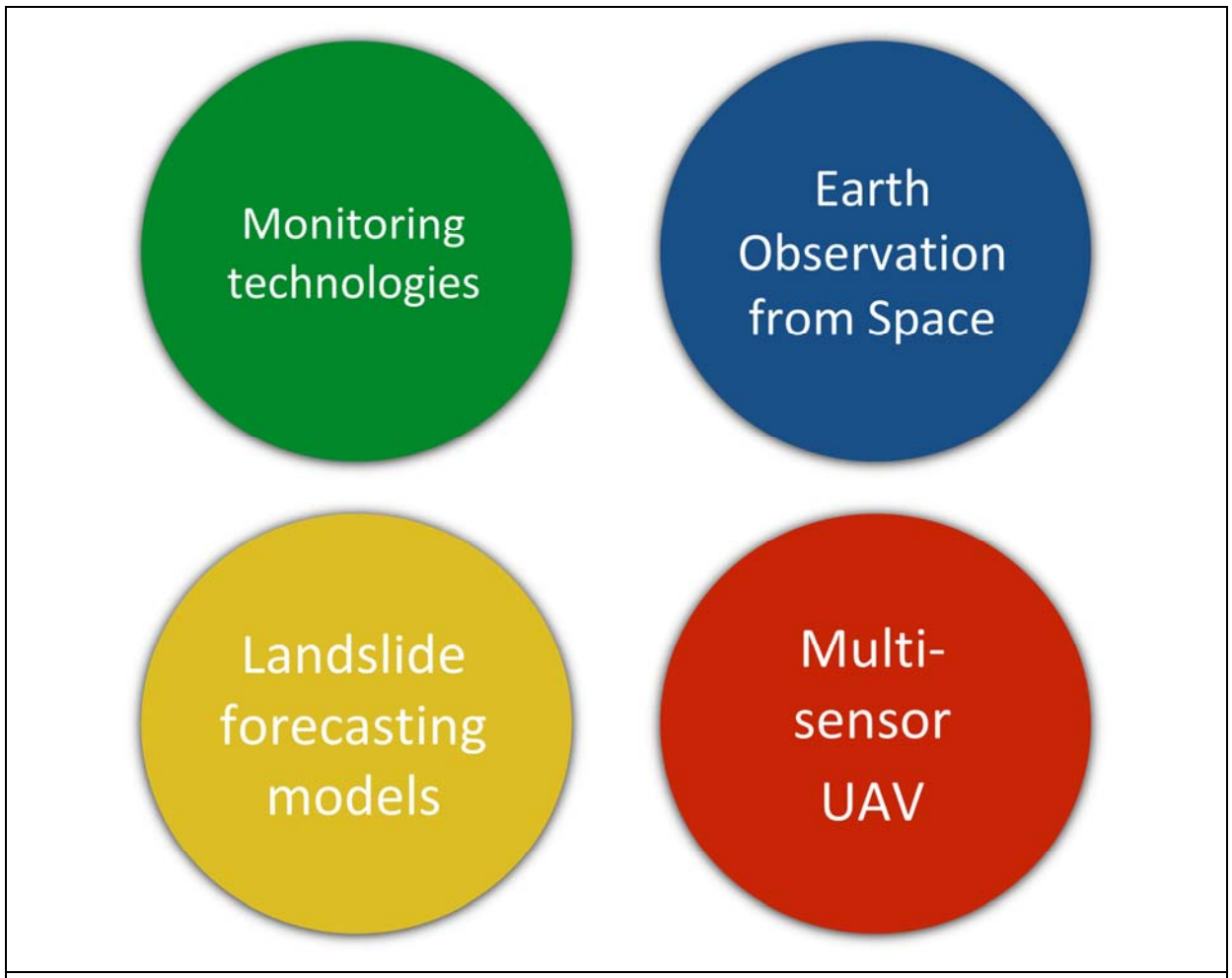
Monitoring technologies
Earth Observation from Space
Landslide forecasting models
Multi-sensor UAV

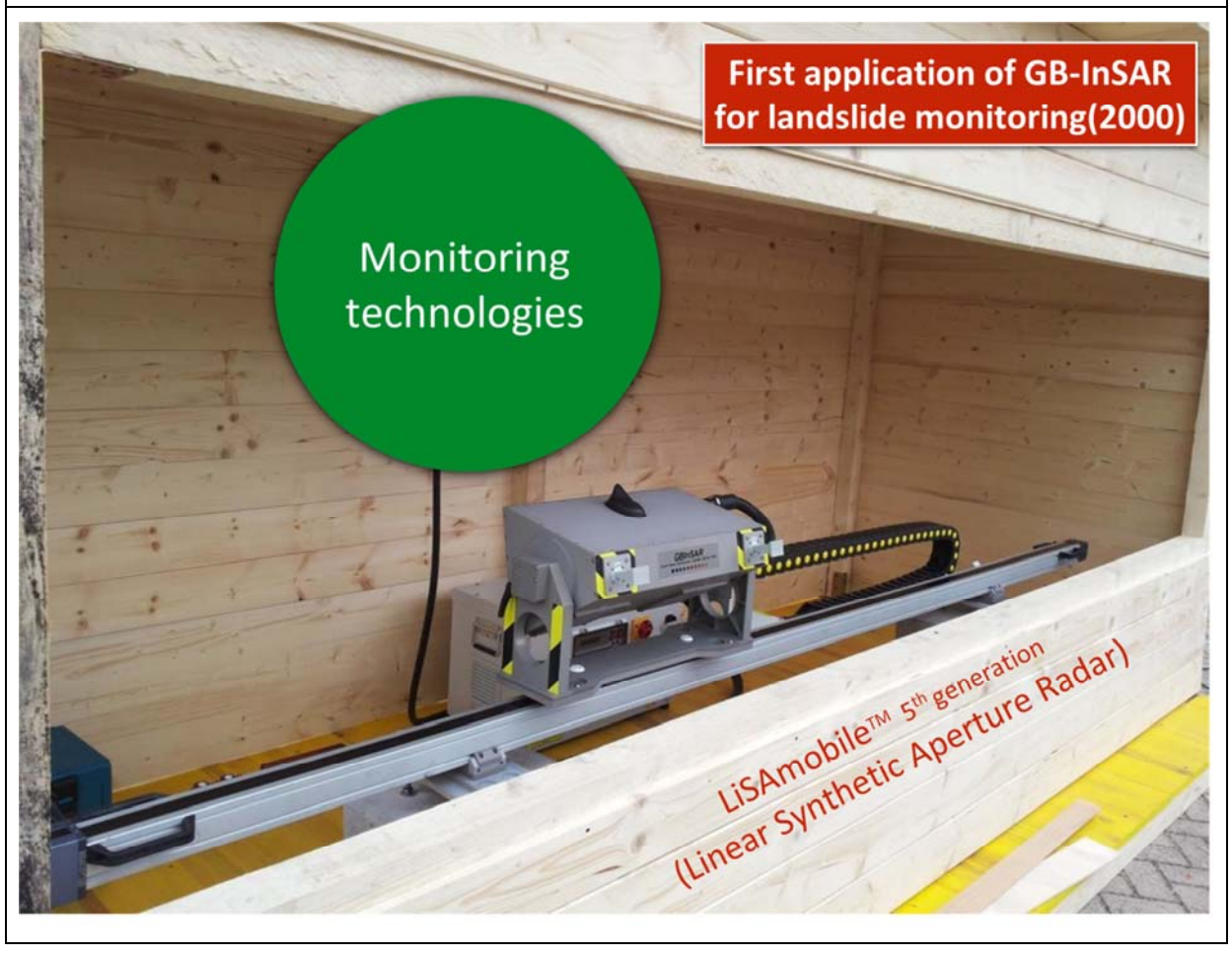
First application of GB-InSAR for landslide monitoring(2000)
Monitoring technologies
LiSAmobile™ 5th generation
(Linear Synthetic Aperture Radar)

Gallivaggio, 10 October 1492

Our Lady Sanctuary
13 April 2018

Radar monitoring

Radar monitoring

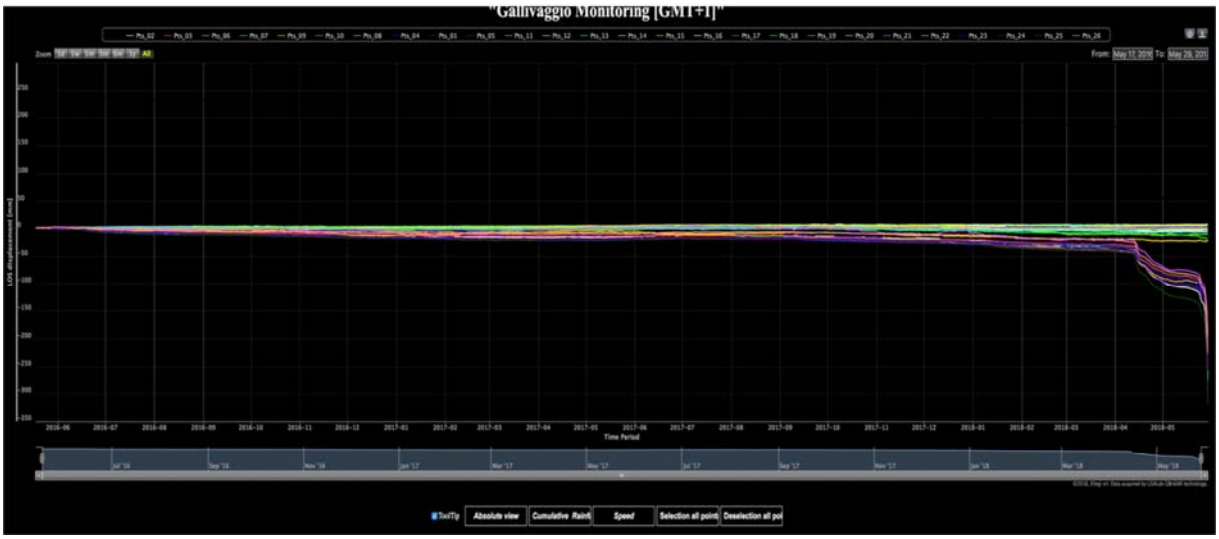

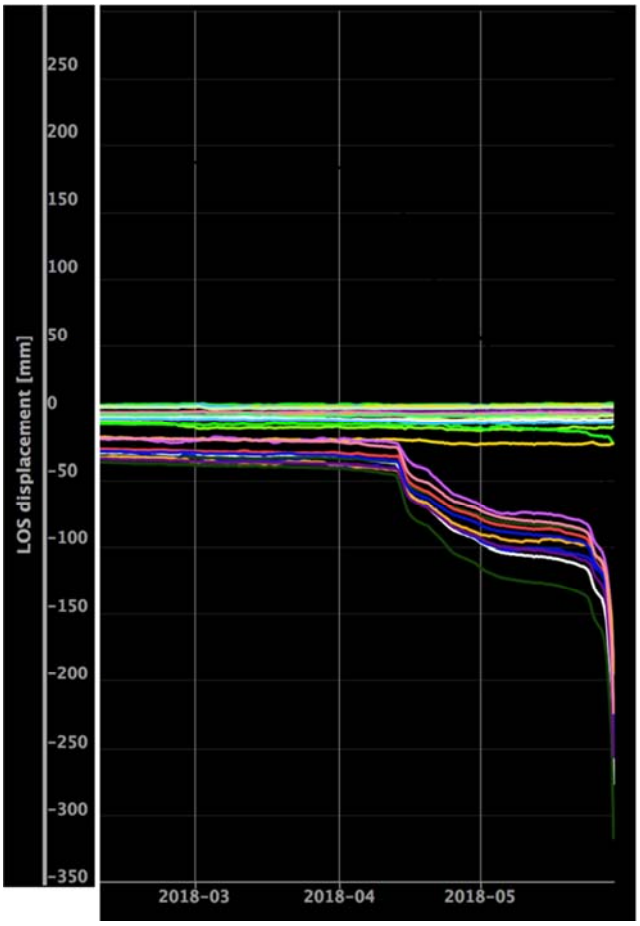

Collapse 29
May 2018
16:36

Collapse forecasting

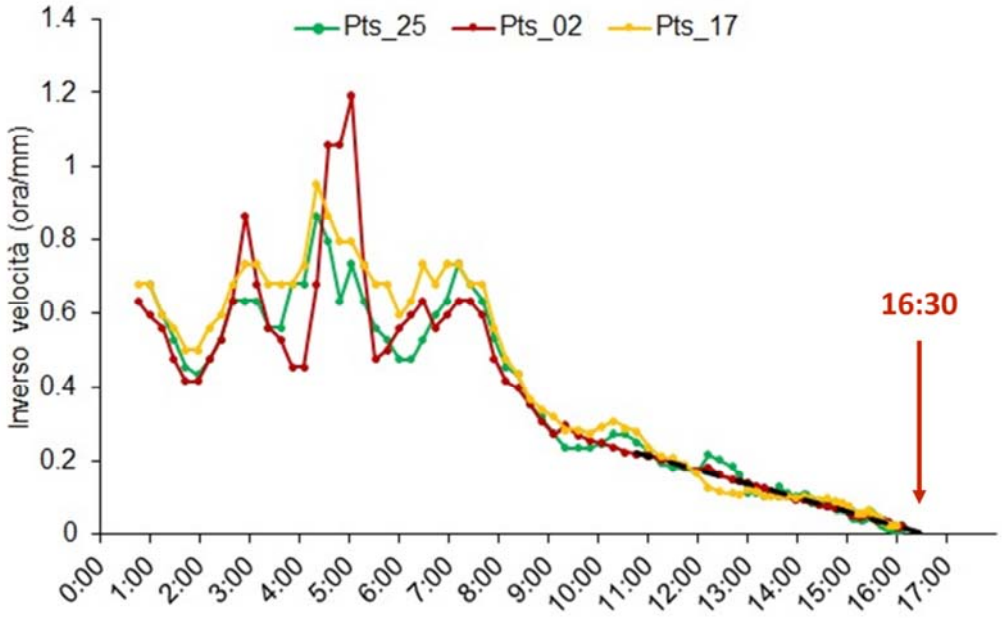

Gallivaggio 29 May 2018 16:36

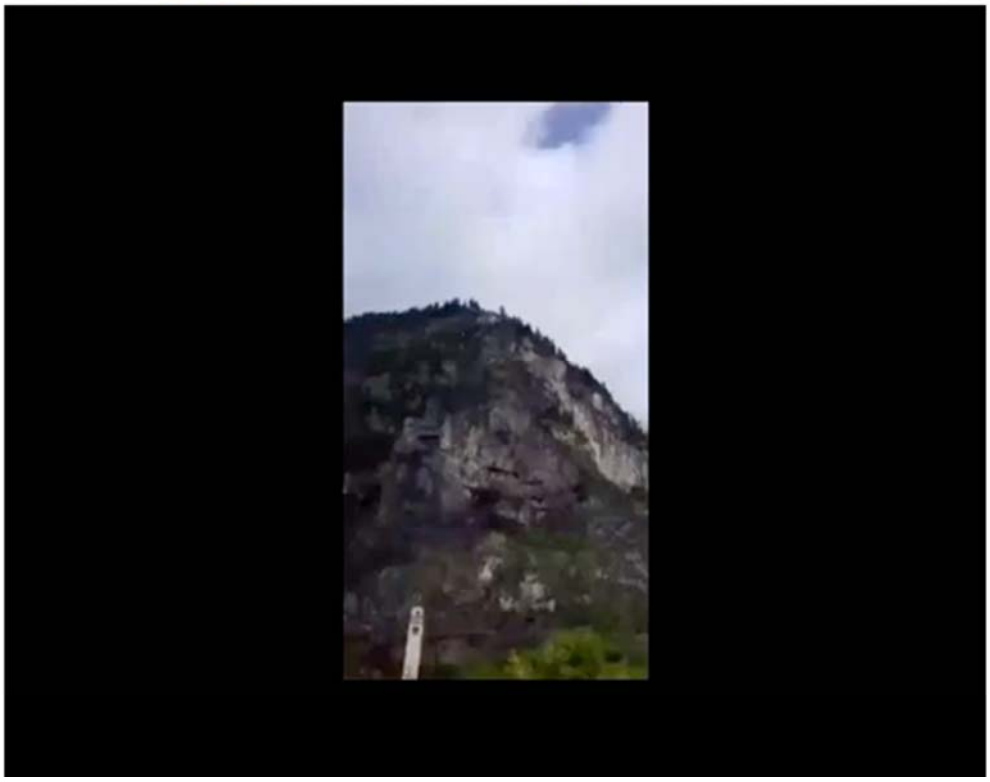

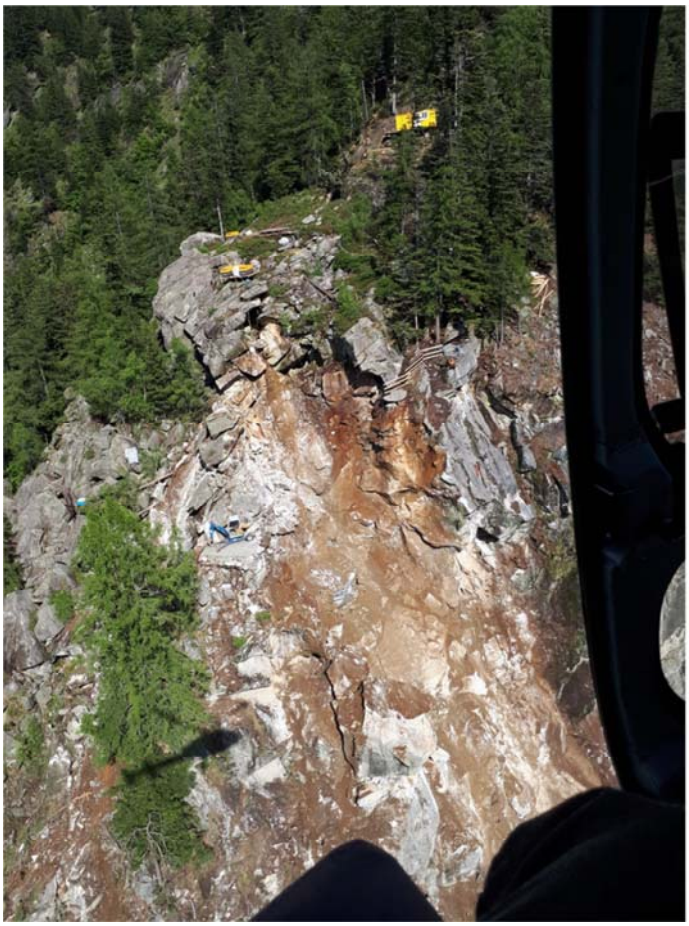

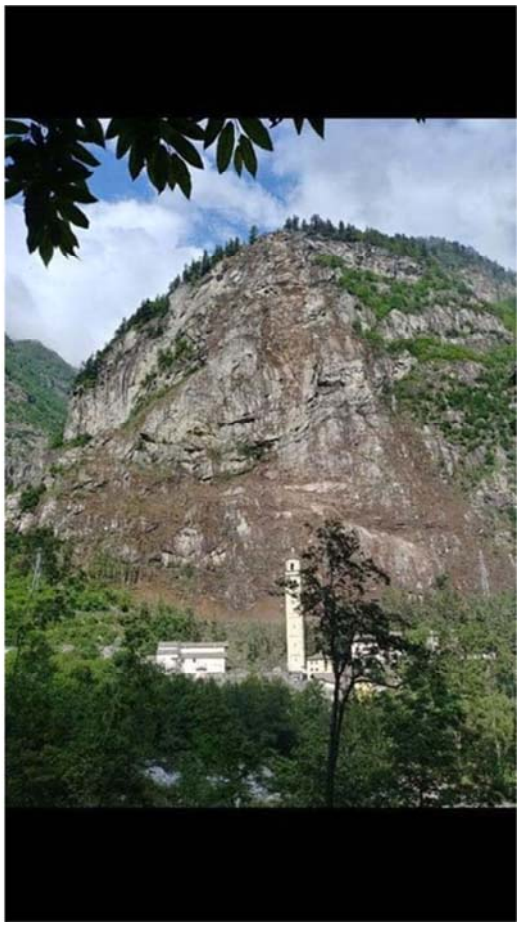

Zoom

Landslides and finances

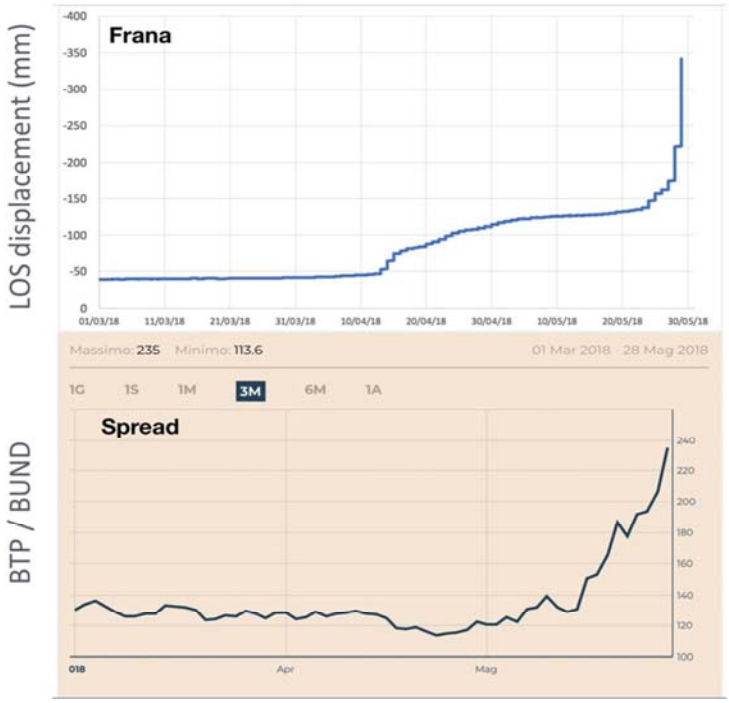

Creep law

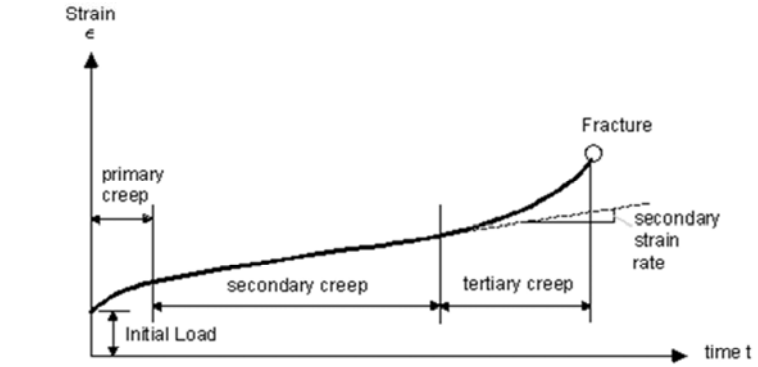

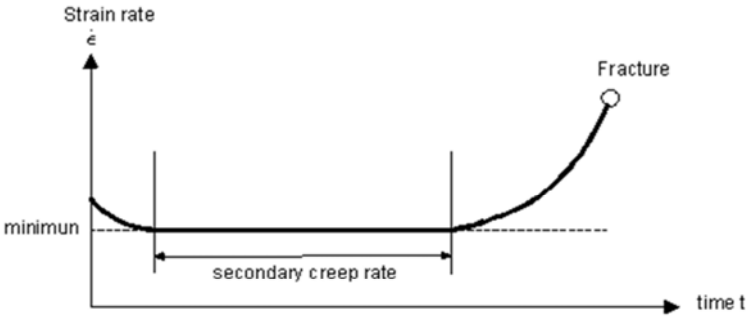

sentinel-1

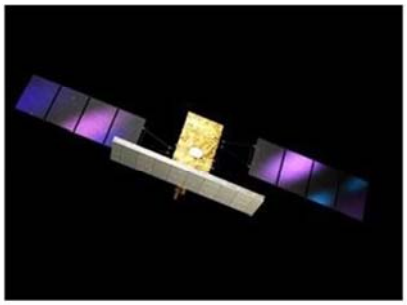

esa

Earth Observation from Space

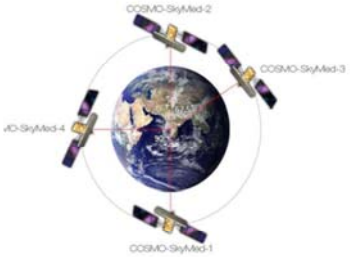

TERRASAR X

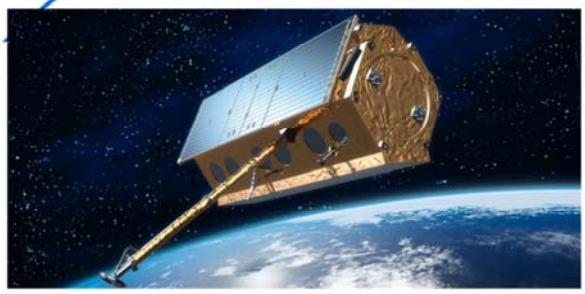

COSMO SkyMed
KEEPING AN EYE ON THE WORLD

Multi-interferometric approach

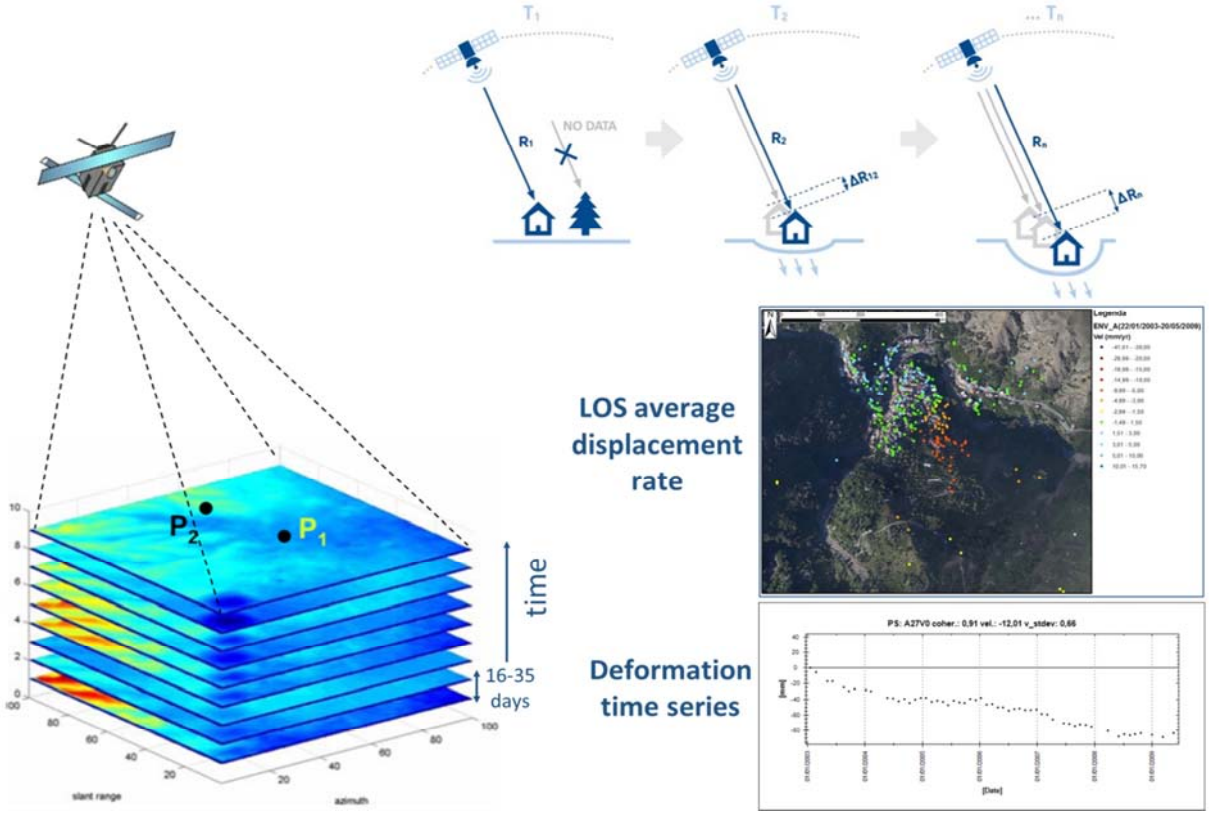

PS Continous Streaming

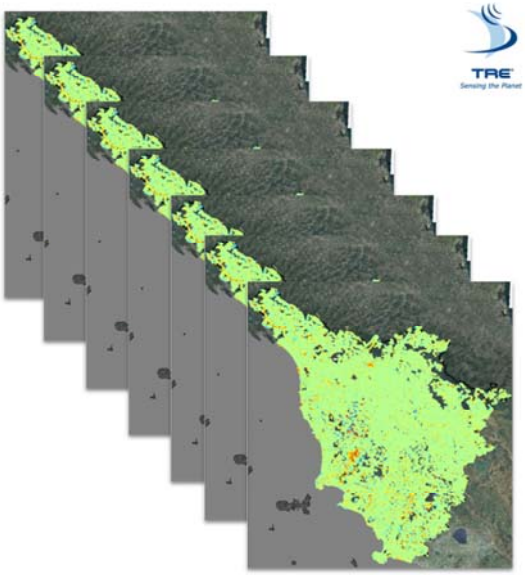

Revisiting time: 6 days

First application of PS-InSAR Continuous Streaming at regional scale (2016)

The Tuscany region

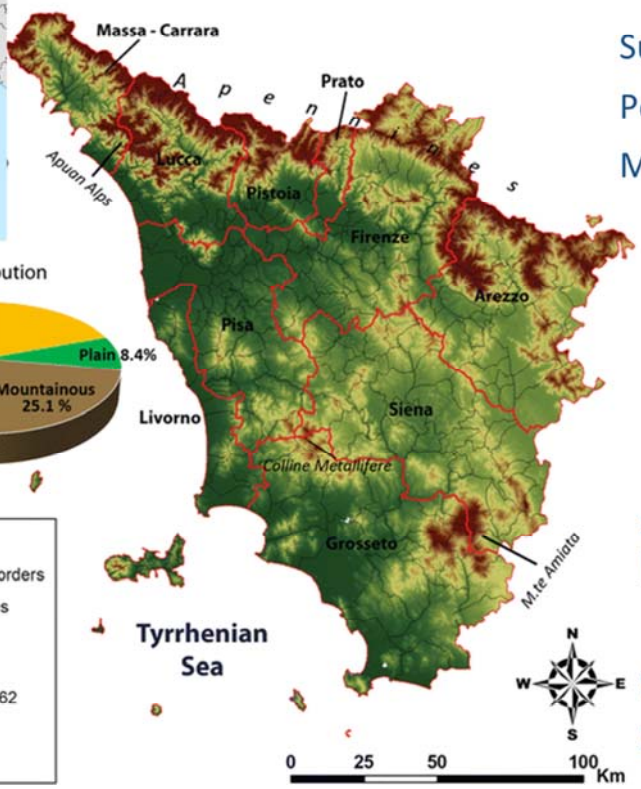

Surface = 22,987 km^2

Population = 3.7 million

Municipalities = 276

Relief Distribution

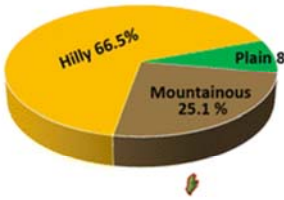

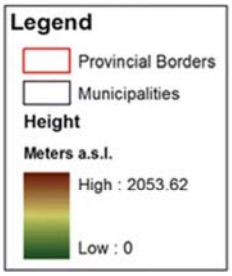

>90% of the territory is hilly of mountainous

90k landslides

390 landslides/100 km^2

From mapping to monitoring

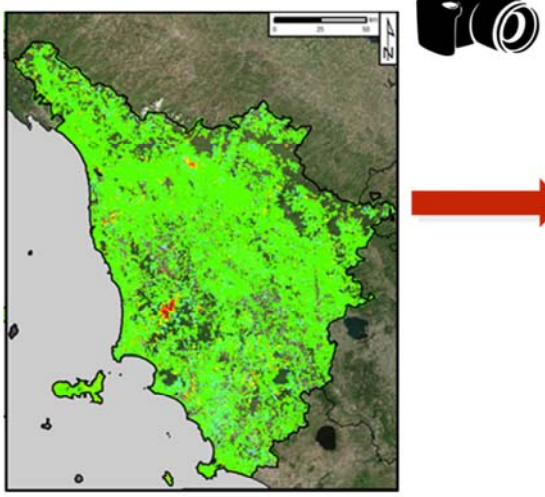

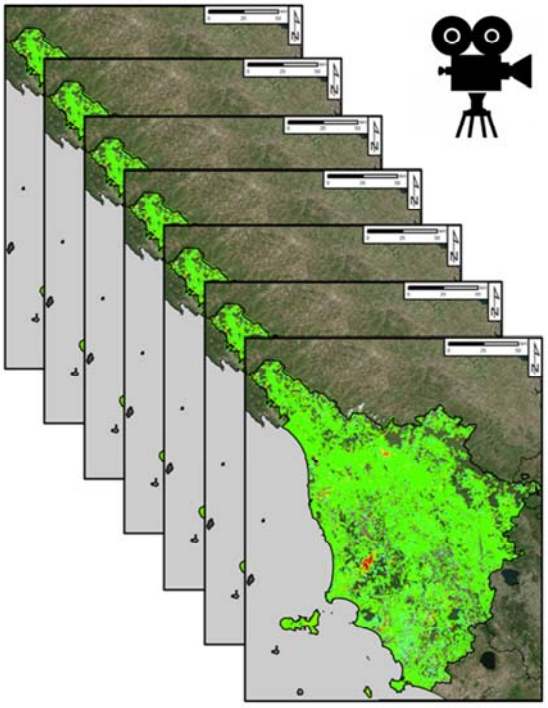

First application of PS-InSAR Continuous Streaming at regional scale (2016)

Sentinel-1 archive 2014-2016

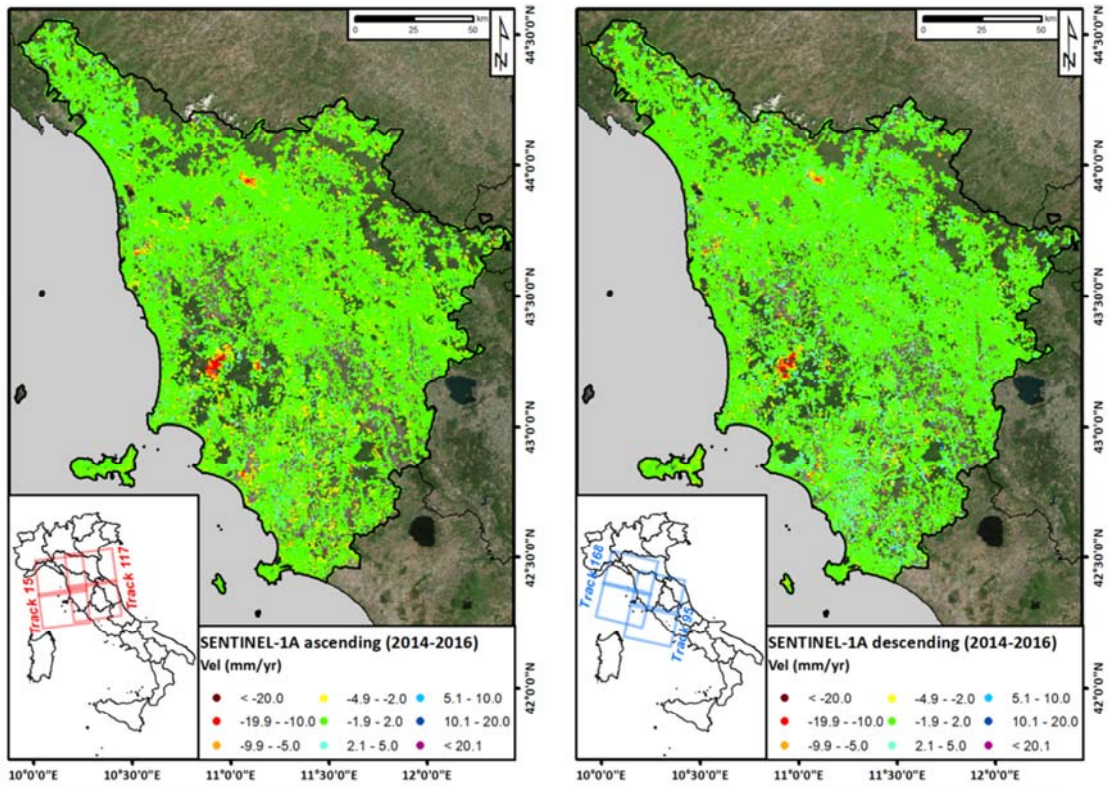

Structure	PS Mapping	PS Monitoring
Type	Single product	Continuous service
Time	deferred	real
Update	1 year	6 days
Aim	Update of landslides inventory maps	Update of scenarios for geohazard risks

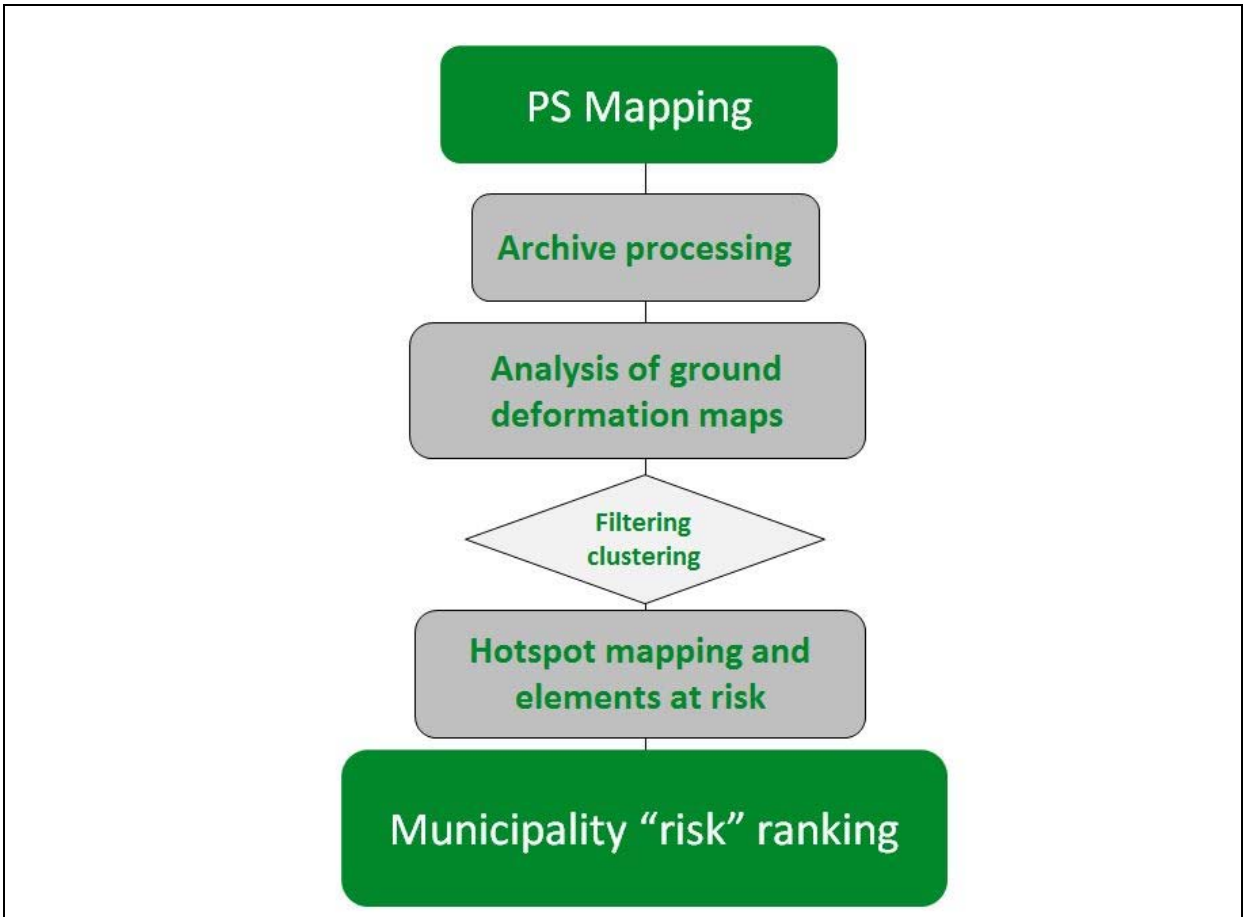
PS Mapping
Archive processing
Analysis of ground deformation maps
Filtering clustering
Hotspot mapping and elements at risk
Municipality “risk” ranking

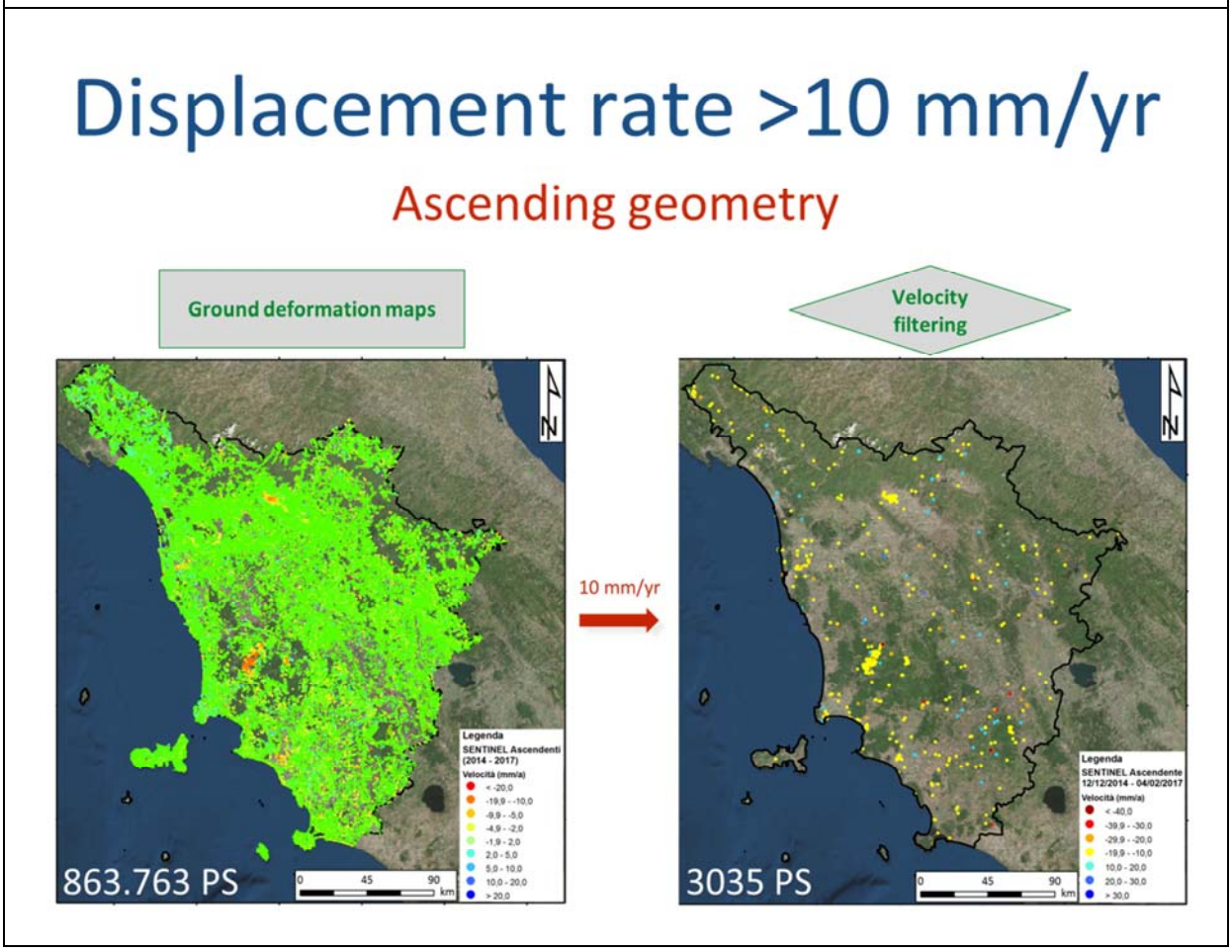
Displacement rate >10 mm/yr
Ascending geometry
Ground deformation maps
Velocity filtering
10 mm/yr
863.763 PS
3035 PS
Legenda
SENTINEL Ascendenti
(2014 - 2017)
Velocità (mm/a)
Legenda
SENTINEL Ascendente
12/12/2014 - 04/02/2017
Velocità (mm/a)
0 45 90 km

Displacement rate >10 mm/yr

Descending geometry

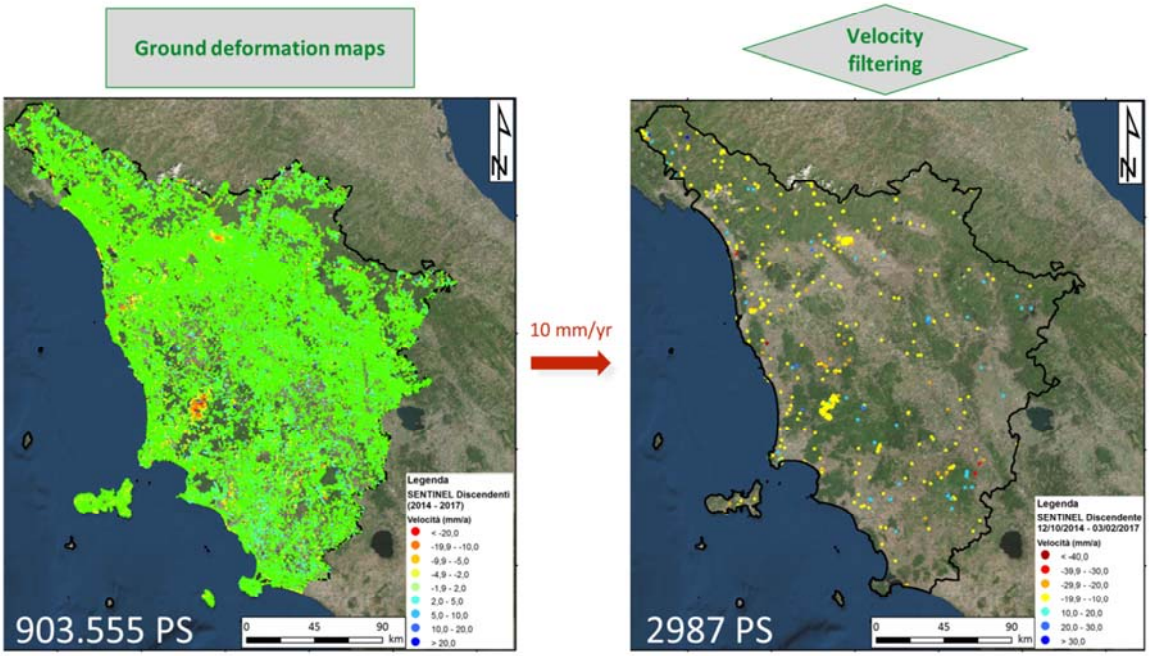

Risk ranking

Cluster of deformation and elements at risk

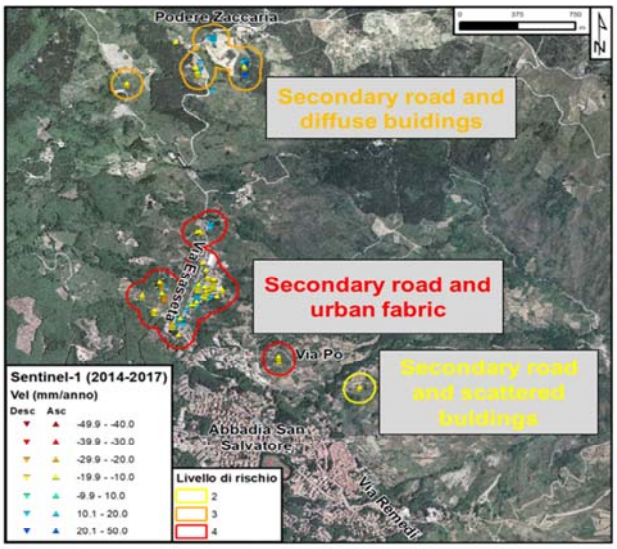

Abbadia San Salvatore (SI)

Class	Description
1	No clusters of deformation
2	Scattered elements at risk within the cluster of deformation
3	Diffused elements at risk within the cluster of deformation
4	Urban areas within the cluster of deformation

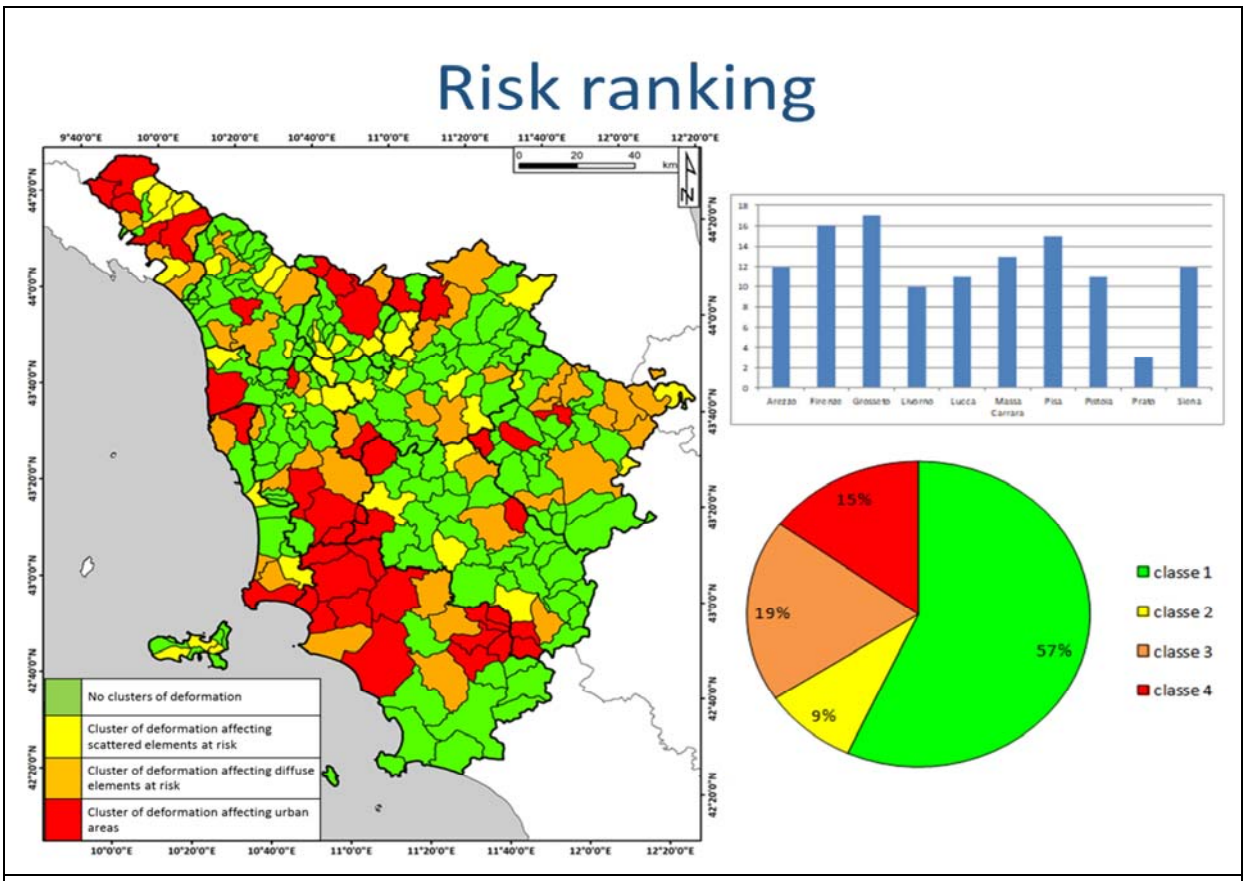
Risk ranking
No clusters of deformation
Cluster of deformation affecting scattered elements at risk
Cluster of deformation affecting diffuse elements at risk
Cluster of deformation affecting urban areas
Arezzo
Firenze
Grosseto
Livorno
Lucca
Massa Carrara
Pisa
Pistoia
Prato
Siena
15%
19%
9%
57%
classe 1
classe 2
classe 3
classe 4

Validation field surveys: Abbadia (Siena)

Validation field surveys: Abbadia (Siena)

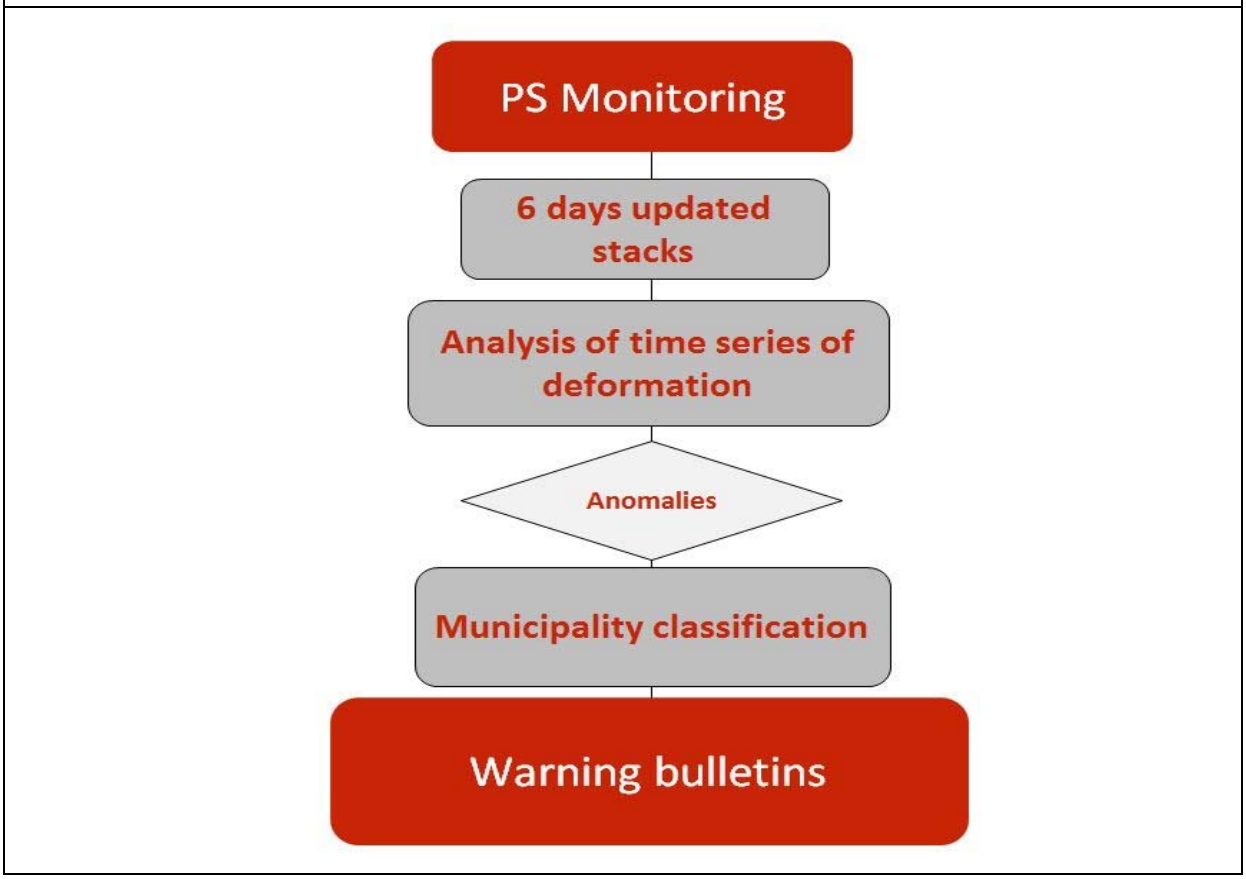
PS Monitoring
6 days updated stacks
Analysis of time series of deformation
Anomalies
Municipality classification
Warning bulletins

PS Monitoring

Capturing changes in the deformation pattern through time

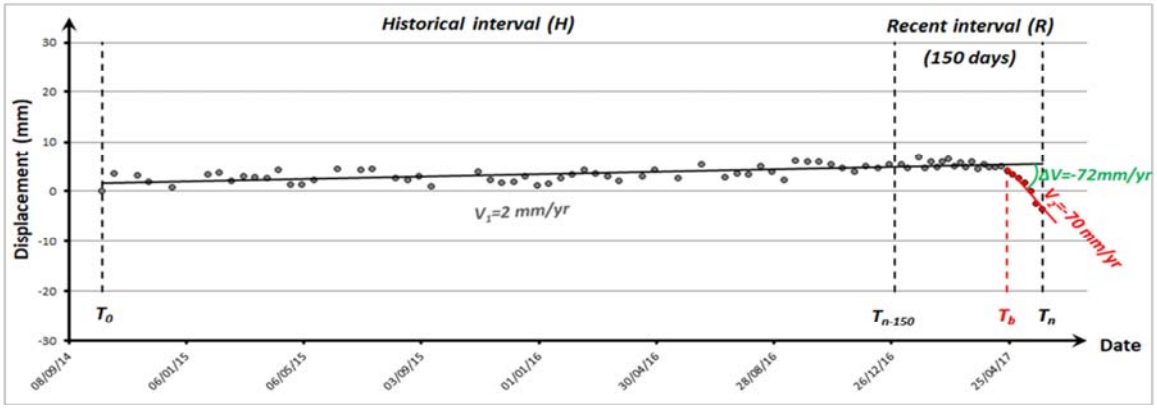

Identification of trend changes within the last 150 days in the displacement time series. An anomalous point is automatically highlighted as the difference between the deformation velocities (|ΔV|) recorded in the two-time intervals (T_0-T_b and T_b-T_n) is > 10 mm/yr.

Types of anomaly

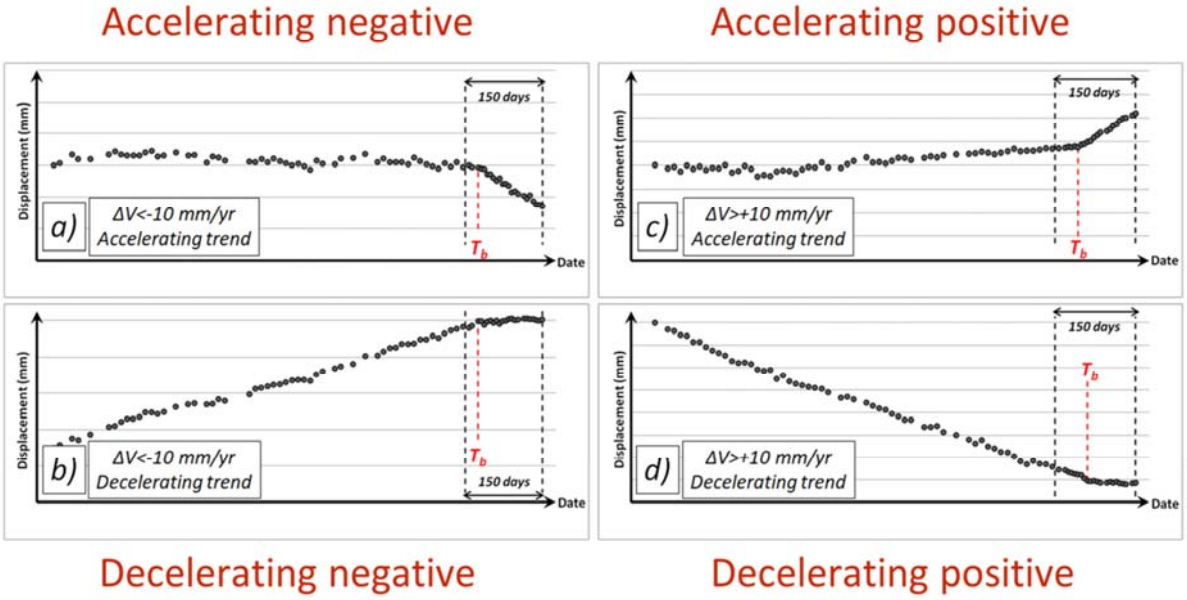

Linear trend = no anomaly

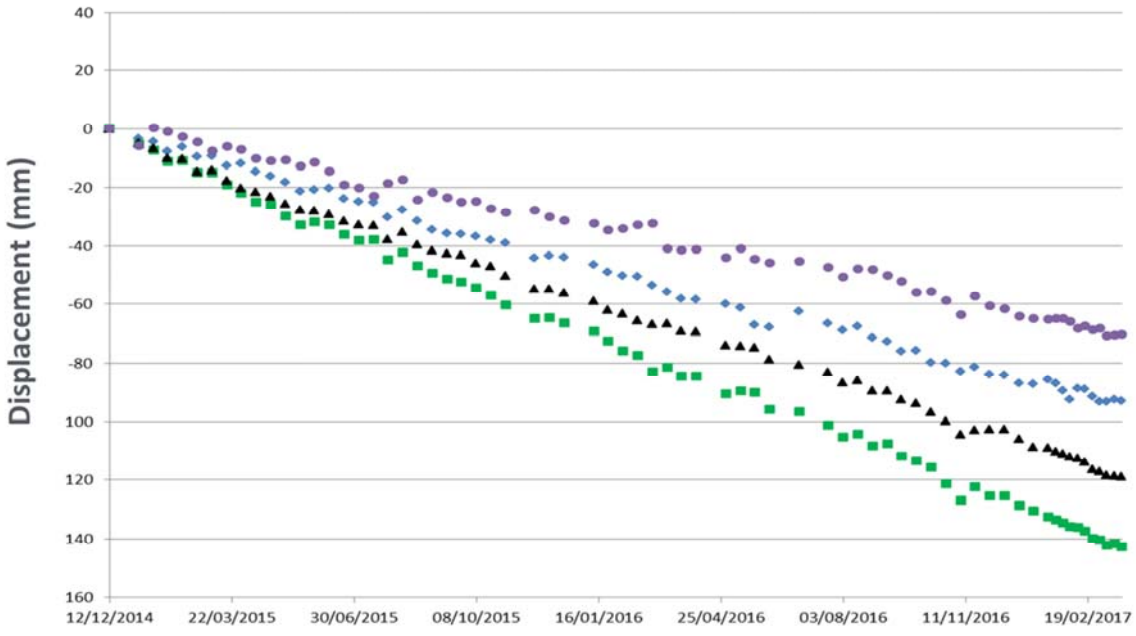

Field check

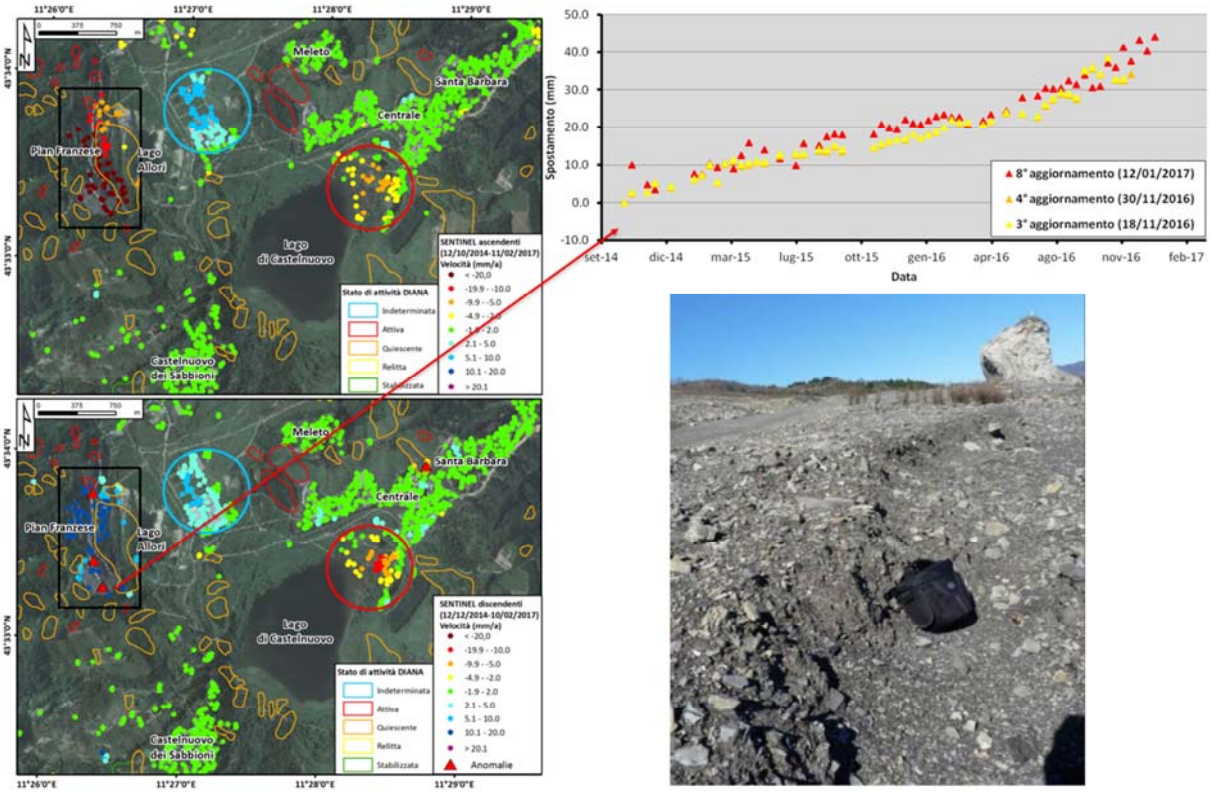

Validation field surveys

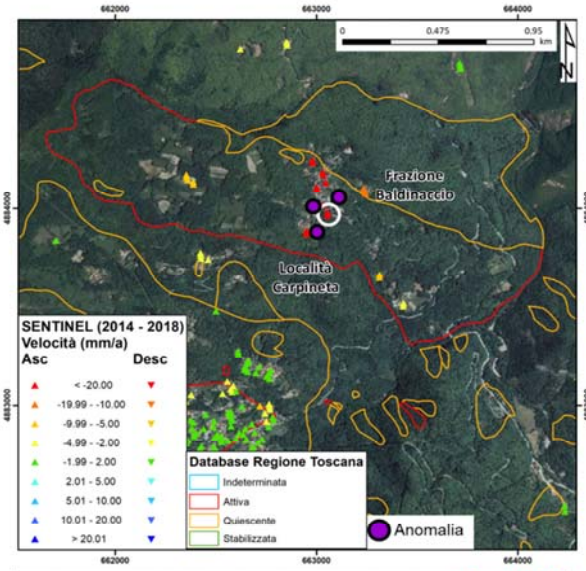

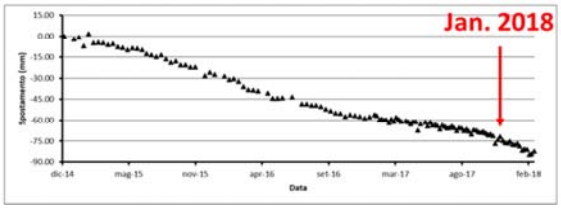

Sambuca Pistoiese (Pistoia)

Landslides

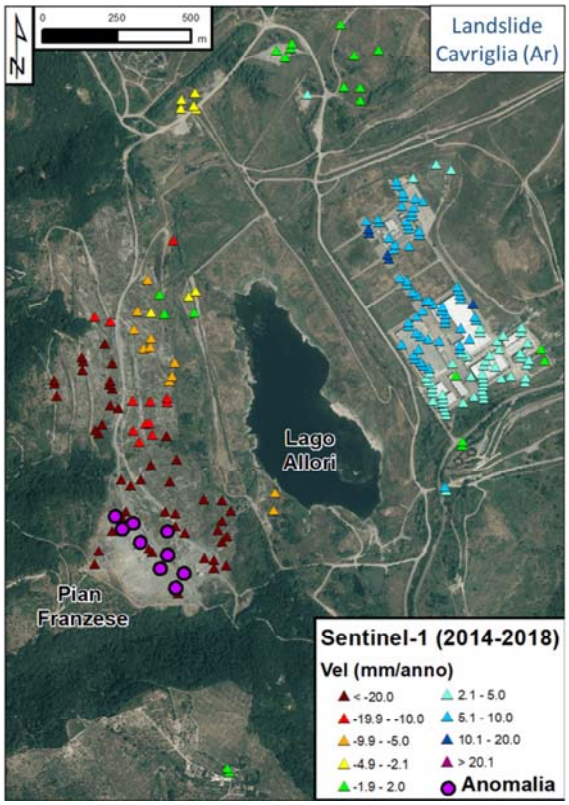

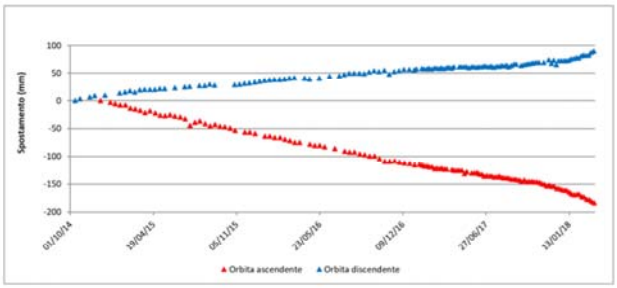

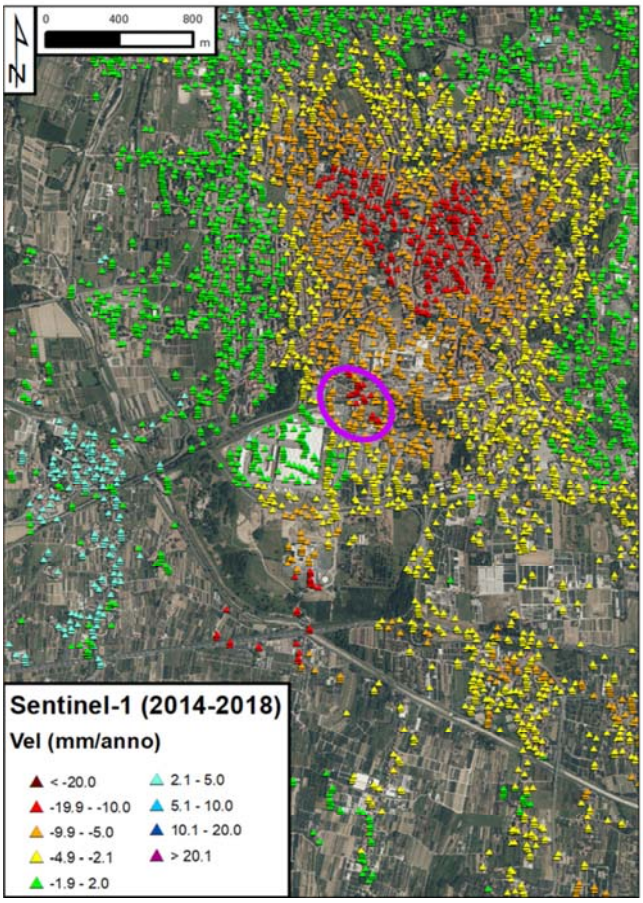

Subsidence

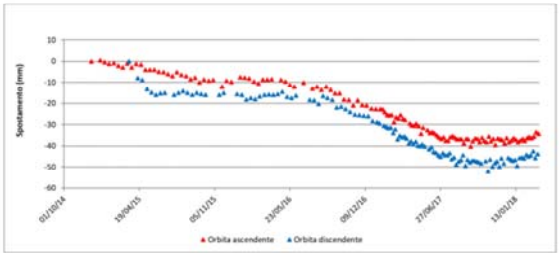

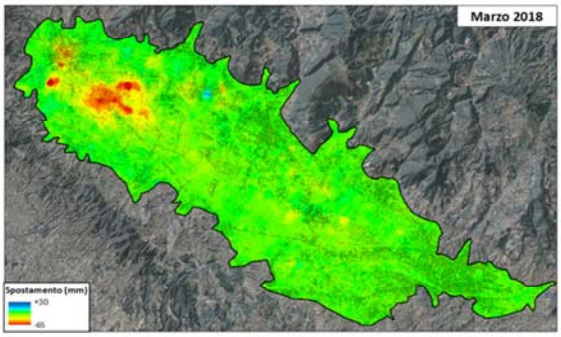

Mining activity

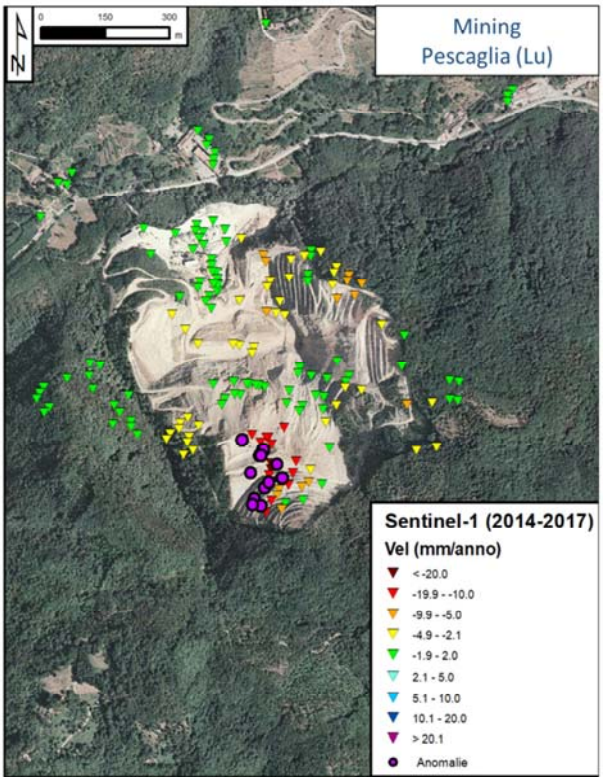

Levee instability

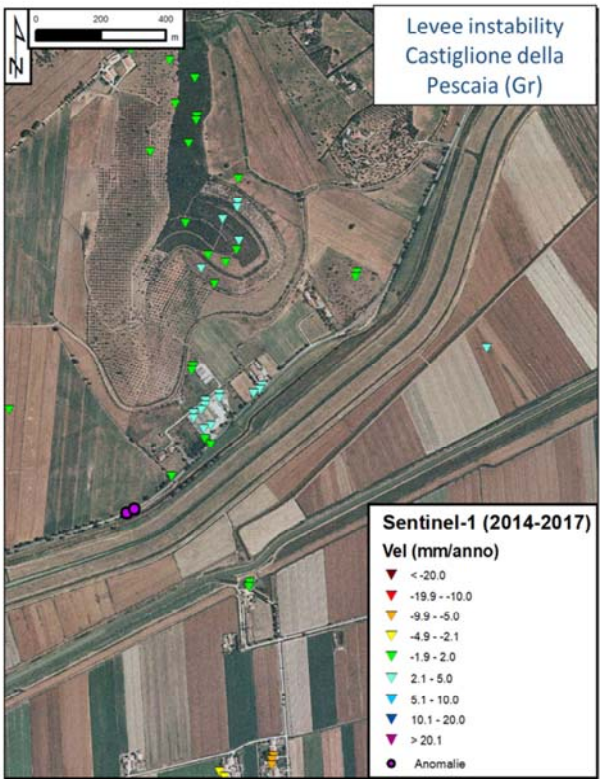

Uplift

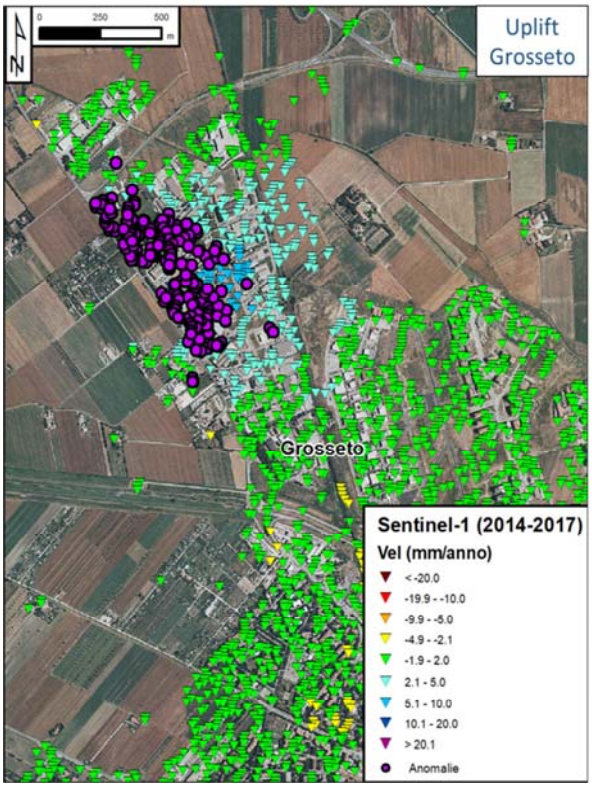

Geothermal activity

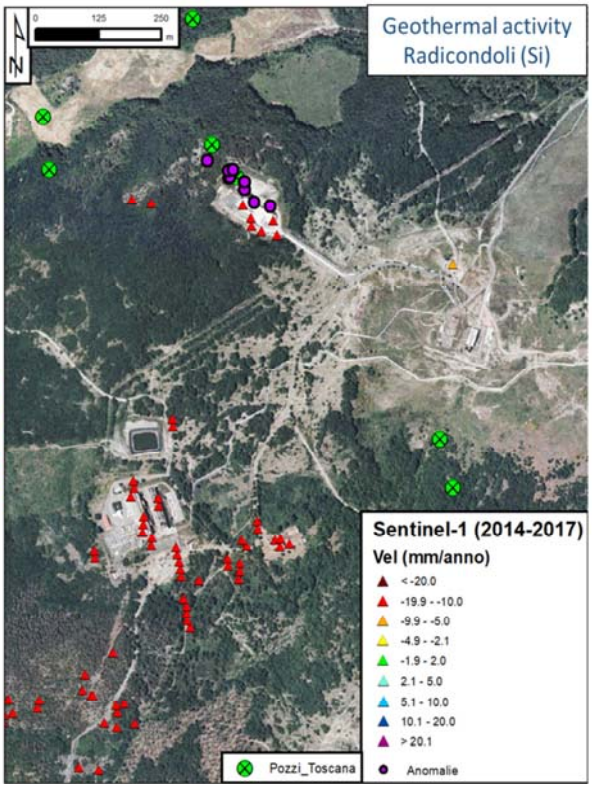

Causes of the anomalies

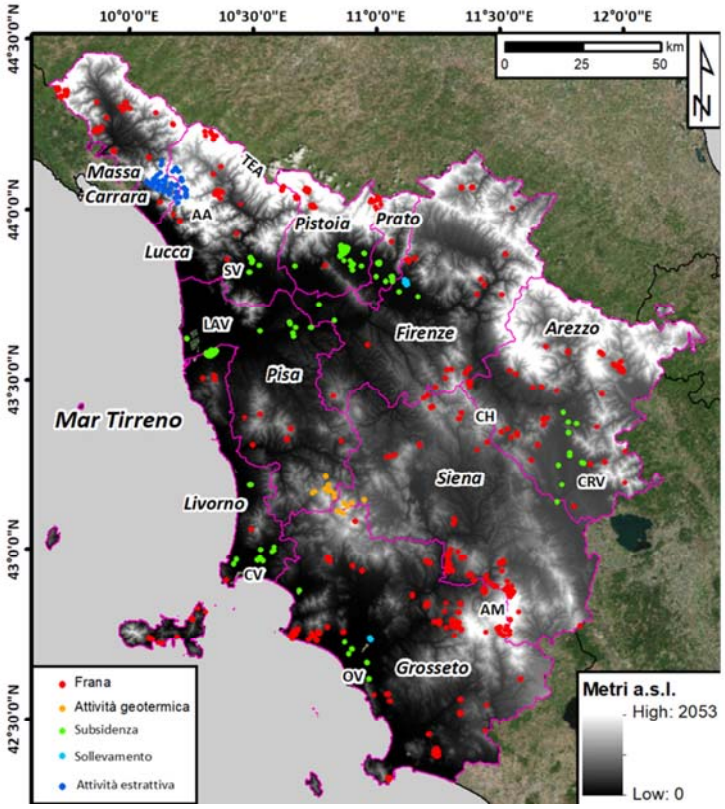

Cause	%
Subsidence (Local and areal)	64.74
Slope instability	29.58
Uplift (Local and areal)	3.5
Mining activity	1.63
Geothermal activity	0.48
Levee instability	0.05
Landfills	0.02

Anomalies 2016-2018

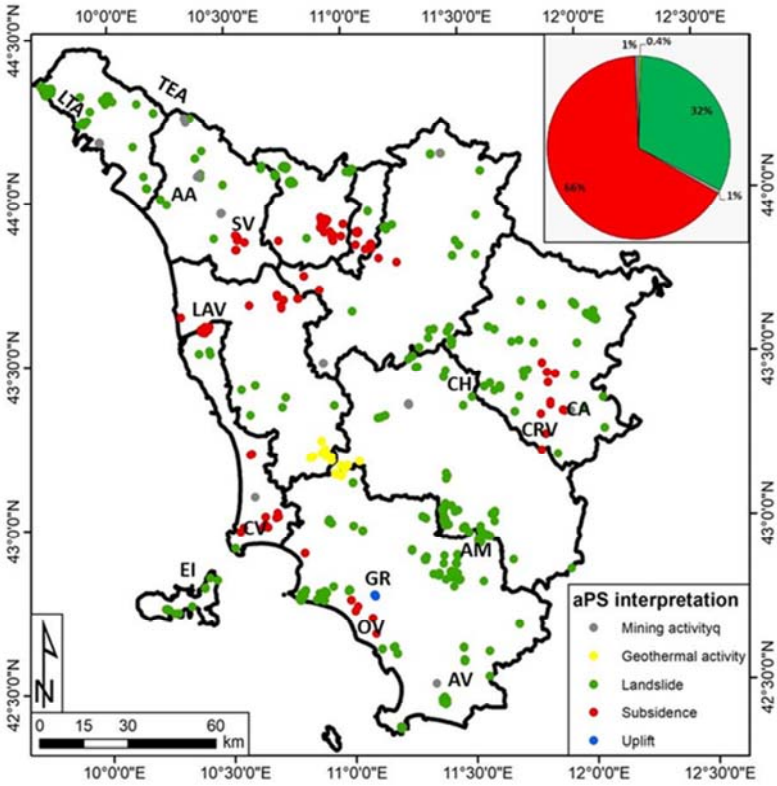

Update	Reference date	aPS number	Persistent aPS
2	06/11/2016 - 07/11/2016	67	25
3	18/11/2016 - 19/11/2016	78	21
4	30/11/2016 - 01/12/2016	42	14
5	12/12/2016 - 13/12/2016	77	34
6	24/12/2016 - 25/12/2016	130	54
7	05/01/2017 - 06/01/2017	110	72
8	17/01/2017 - 18/01/2017	78	46
9	29/01/2017 - 30/01/2017	83	39
10	10/02/2017 - 11/02/2017	110	85
11	22/02/2017 - 23/02/2017	175	94
12	06/03/2017 - 07/03/2017	255	126
13	18/03/2017 - 19/03/2017	308	257
14	30/03/2017 - 31/03/2017	650	412
15	11/04/2017 - 12/04/207	854	587
16	23/04/2017 - 24/04/2017	894	498
17	05/05/2017 - 06/05/2017	915	458
18	17/05/2017 - 18/05/2017	884	580
19	29/05/2017 - 30/05/2017	958	638

Monitoring bulletins

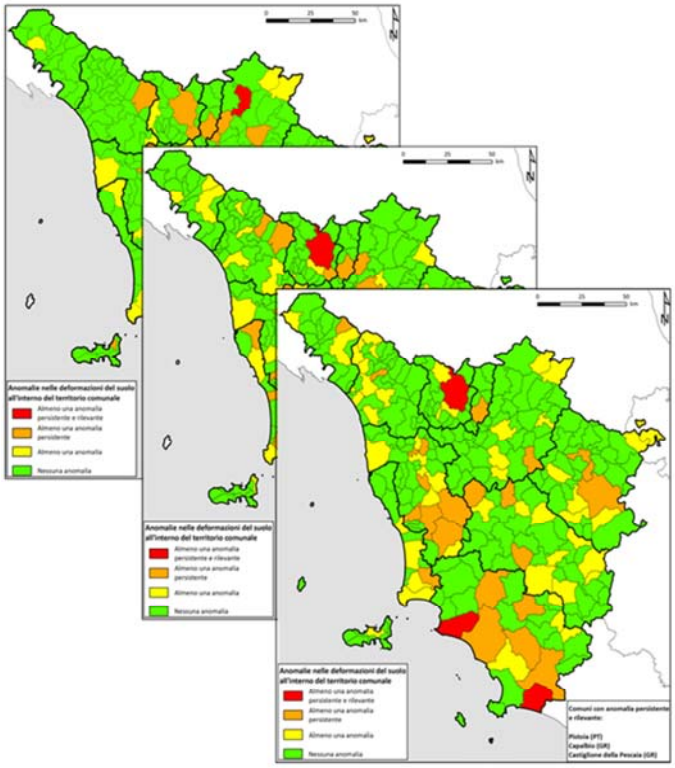

Class	Description
1	No anomaly within the municipality
2	At least one anomaly within the municipality
3	At least one persistent anomaly within the municipality
4	At least one persistent and relevant anomaly within the municipality

WebGIS

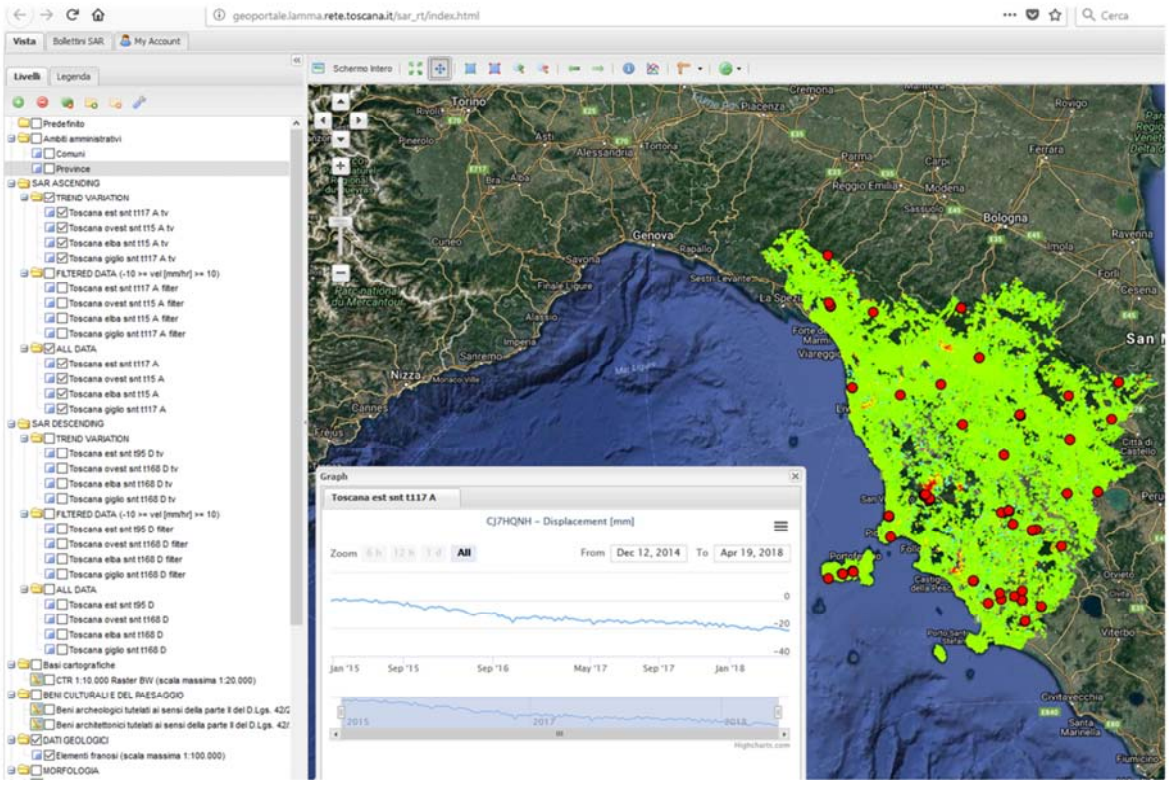

nature

www.nature.com/scientificreports

SCIENTIFIC REPORTS

OPEN

Continuous, semi-automatic monitoring of ground deformation using Sentinel-1 satellites

Received: 24 November 2017
Accepted: 17 April 2018
Published online: 08 May 2018

Federico Raspini[1], Silvia Bianchini[1], Andrea Ciampalini[1,3], Matteo Del Soldato[1], Lorenzo Solari[1], Fabrizio Novali[2], Sara Del Conte[2], Alessio Rucci[2], Alessandro Ferretti[2] & Nicola Casagli[1]

We present the continuous monitoring of ground deformation at regional scale using ESA (European Space Agency) Sentinel-1constellation of satellites. We discuss this operational monitoring service through the case study of the Tuscany Region (Central Italy), selected due to its peculiar geological setting prone to ground instability phenomena. We set up a systematic processing chain of Sentinel-1 acquisitions to create continuously updated ground deformation data to mark the transition from static satellite analysis, based on the analysis of archive images, to dynamic monitoring of ground displacement. Displacement time series, systematically updated with the most recent available Sentinel-1 acquisition, are analysed to identify anomalous points (*i.e.*, points where a change in the dynamic of motion is occurring). The presence of a cluster of persistent anomalies affecting elements at risk determines a significant level of risk, with the necessity of further analysis. Here, we show that the Sentinel-1 constellation can be used for continuous and systematic tracking of ground deformation phenomena at the regional scale. Our results demonstrate how satellite data, acquired with short revisiting times and promptly processed, can contribute to the detection of changes in ground deformation patterns and can act as a key information layer for risk mitigation.

Landslide forecasting models

Rainfall nowcasting

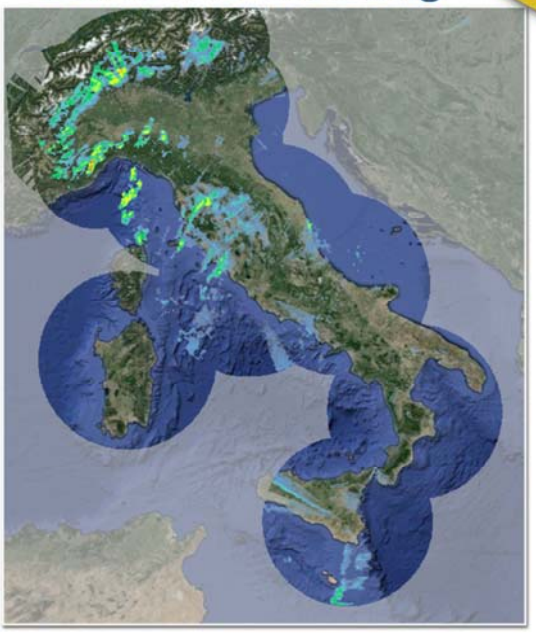

Landslide occurrence

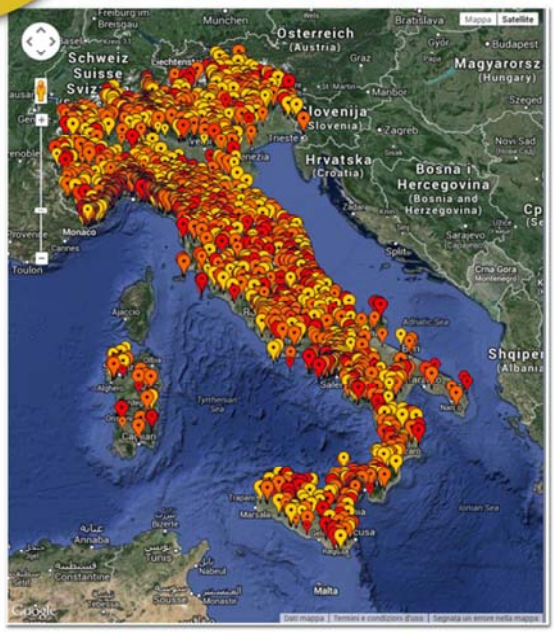

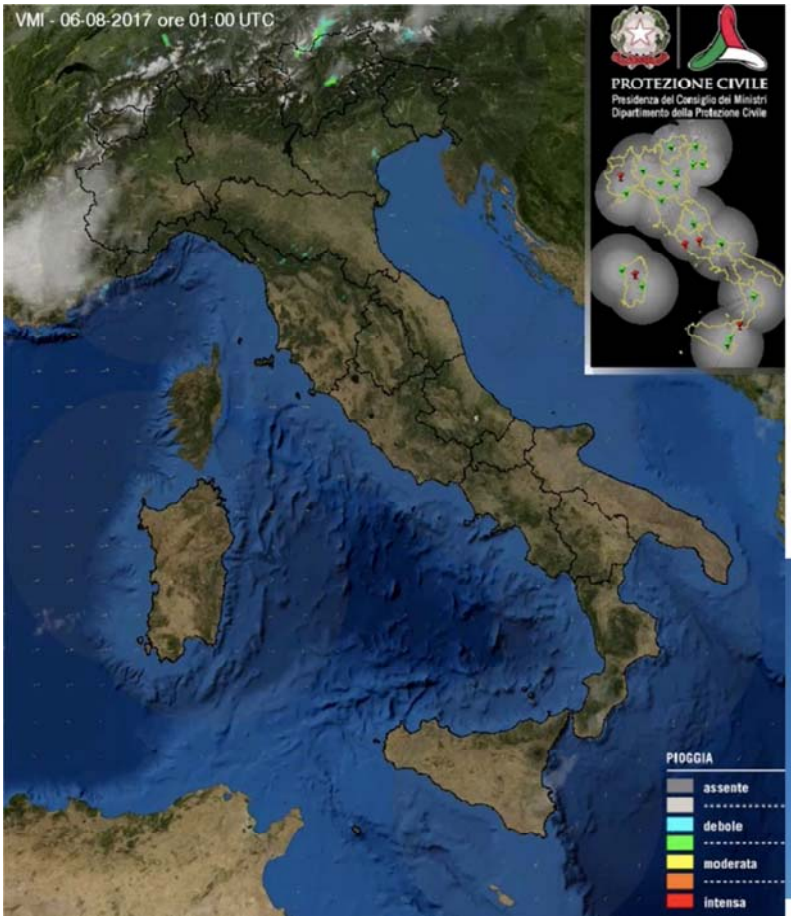

PROTEZIONE CIVILE
Presidenza del Consiglio dei Ministri
Dipartimento della Protezione Civile

Towards a multiscale system

Local thtreshold

Second level:
physically based probabilistic model

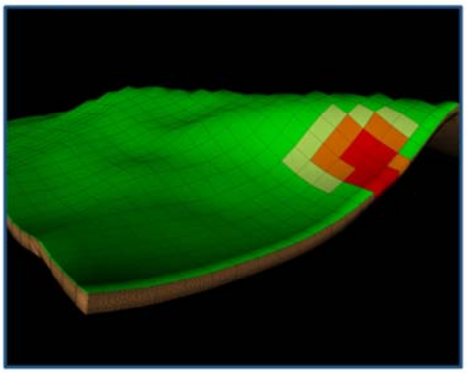

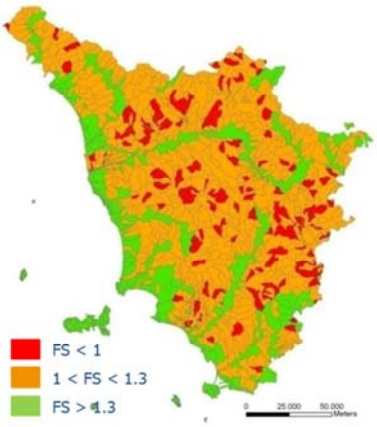

Output:
Sub-basin-scale aggregated alert levels based on multiple rainfall thresholds

Output: detailed FoS probability maps for the first-level warning areas

1st Level Statistical Model

Statistical analysis of Intensity-Duration Data

Massive CUMulate Brisk Analyzer

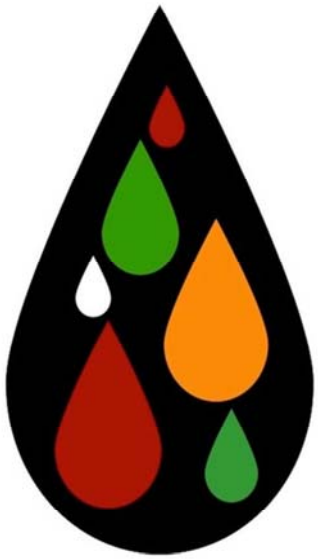

First level of alert

- Intensity-duration
- Automated analysis
- Standardized approach
- Definition of local thresholds
- Balancing between false and missed alarms

2nd Level Deterministic Model

HIgh REsolution Slope Stability Simulator

On areas with Level-1 Alert

HIRESSS

- Physically based, high resolution model
- Large scale operativity
- Coded for real-time applications
- Fast parallel computational scheme

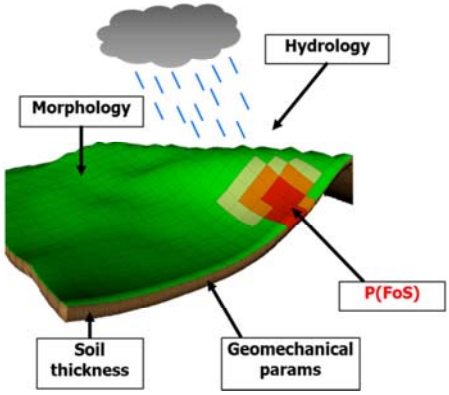

HIRESSS model (Rossi et al., 2013)

Model Structure and Governing Equations

Rainfall Intensity

Factor of Safety

Hydrological Model

$$\frac{\partial h}{\partial t}\frac{d\theta}{dh} = \frac{\partial}{\partial x}\left[K_x(h)\left(\frac{\partial h}{\partial x} - \sin\alpha\right)\right] + \frac{\partial}{\partial y}\left[K_y(h)\left(\frac{\partial h}{\partial y}\right)\right] + \frac{\partial}{\partial z}\left[K_z(h)\left(\frac{\partial h}{\partial z} - \cos\alpha\right)\right]$$

During rainfall

$$h(Z) = Z\beta\left(1 - \frac{d}{Z}\right) + Z\frac{I}{K_z}\left[R\left(\frac{t}{Z^2/4D_0\cos^2\alpha}\right)\right]$$

After rainfall

$$h(Z) = Z\beta\left(1 - \frac{d}{Z}\right) + Z\frac{I}{K_z}\left[R\left(\frac{t}{Z^2/4D_0\cos^2\alpha}\right) - R\left(\frac{t-T}{Z^2/4D_0\cos^2\alpha}\right)\right]$$

Pore Pressure

Slope Stability Model

Unsaturated conditions

$$FS = \frac{\tan\varphi}{\tan\alpha} + \frac{c'}{\gamma_{NS} z\sin\alpha} + \frac{(u_a - u_w)\tan\varphi^b}{\gamma_{NS} z\sin\alpha}$$

Saturated conditions

$$FS = \frac{\tan\varphi}{\tan\alpha} + \frac{c'}{(\gamma_{NS}(z-h) + \gamma_{SI} h)\sin\alpha} - \frac{h(z,t)\gamma_w\tan\varphi}{(\gamma_{NS}(z-h) + \gamma_{SI} h)\sin\alpha}$$

Hydrological mode

- Parallel code solution of Richards equations
- Inclusion of hydraulic diffusivity in the model
- Real-time computational steps (during rainfall event)

Slope Stability Model

- Infinite slope with distributed cell
- Suction effects
- Variable soil density with saturation
- Variable depth analysis

System Integration

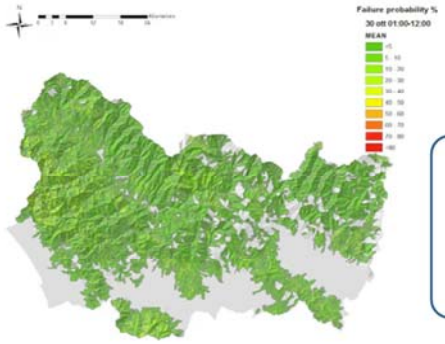

Level 1 – Criticality definition

None | Ordinary | Moderate | High

Level 2

Relative triggering probability

Input data

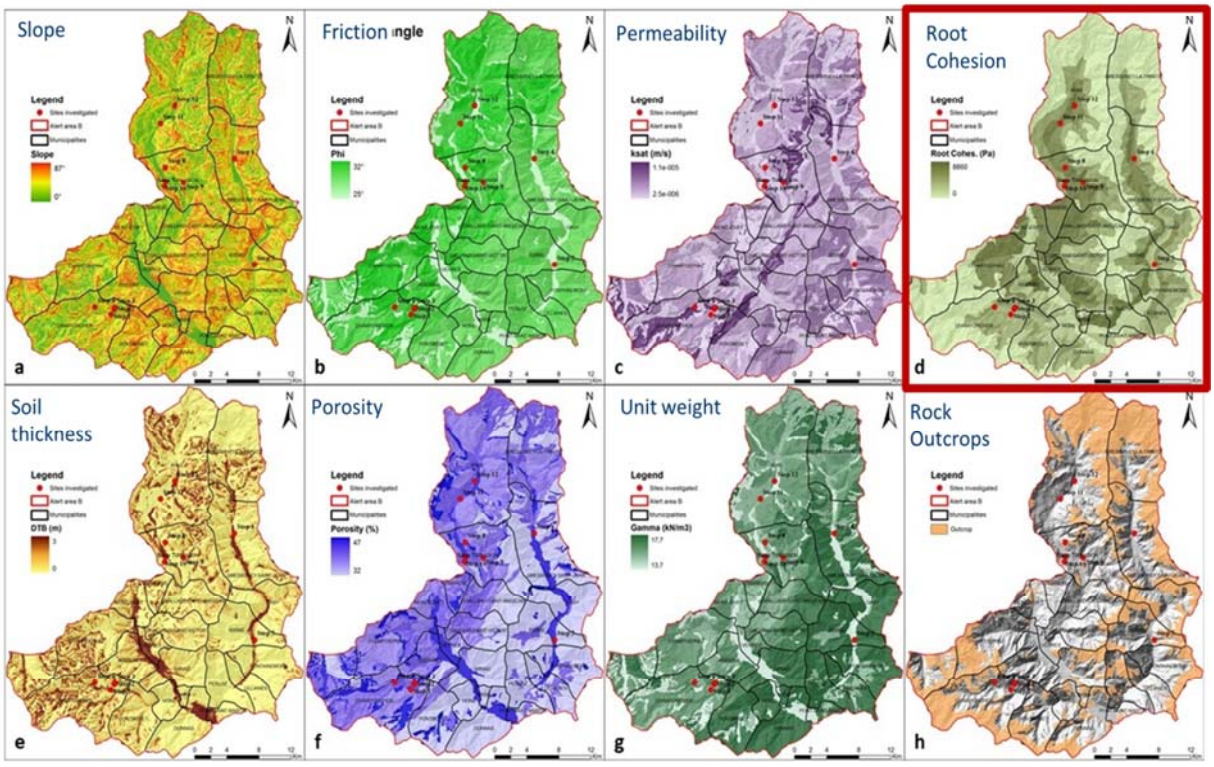

Simulation results

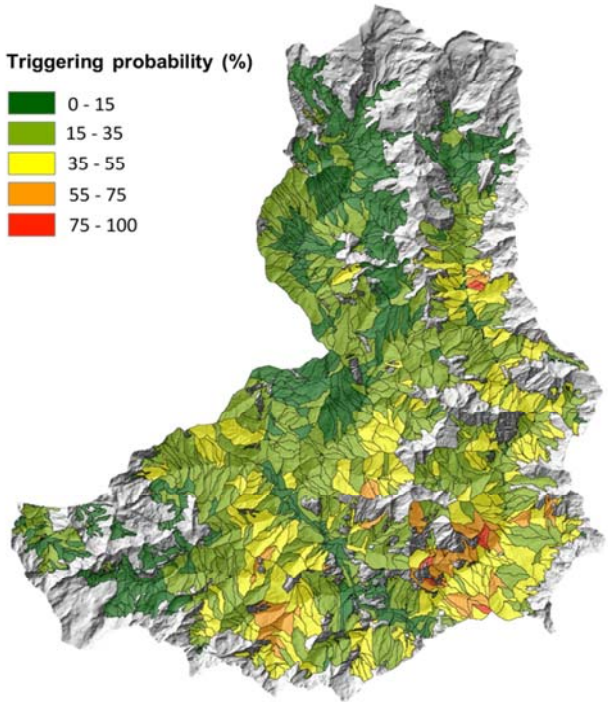

- Without root cohesion

- With root cohesion

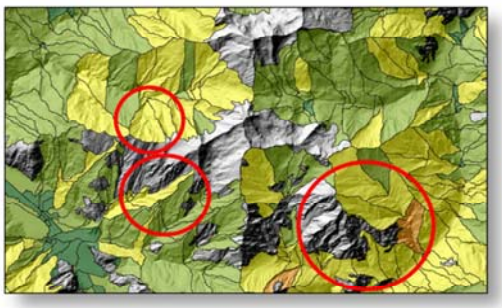

High Resolution Slope Stability Simulator

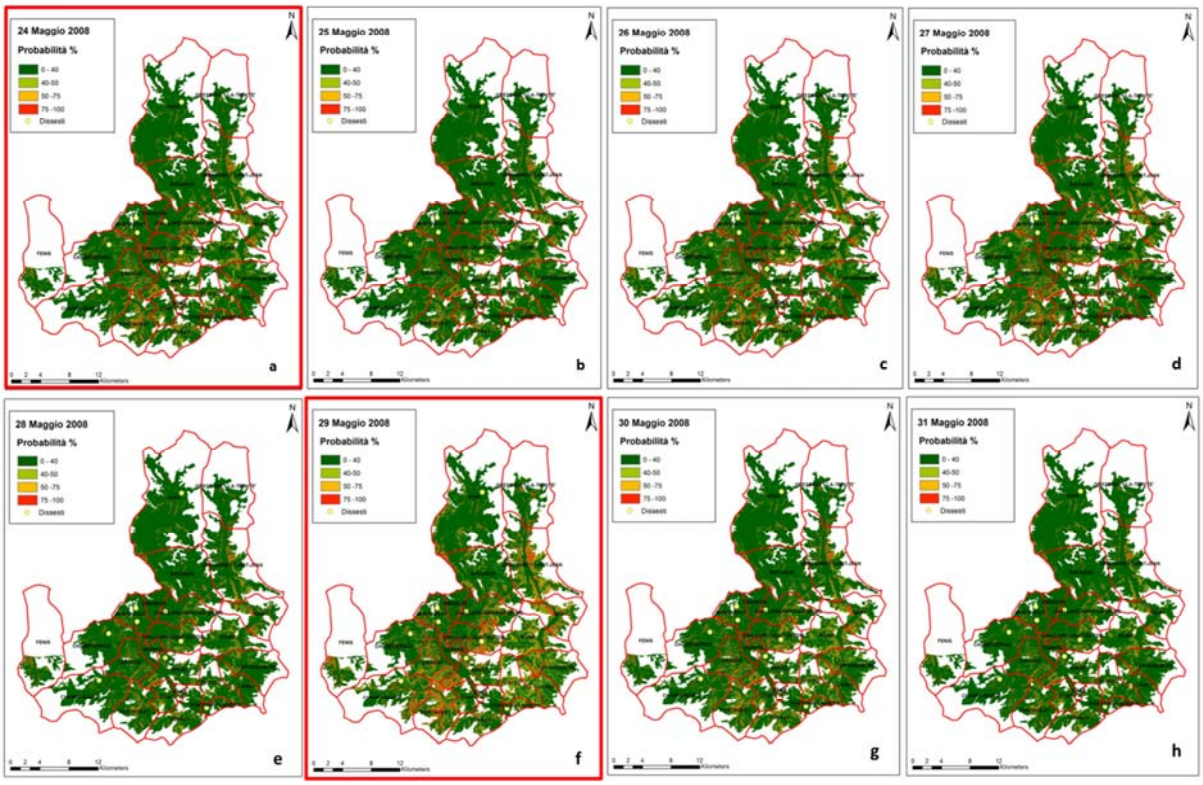

Web news data mining

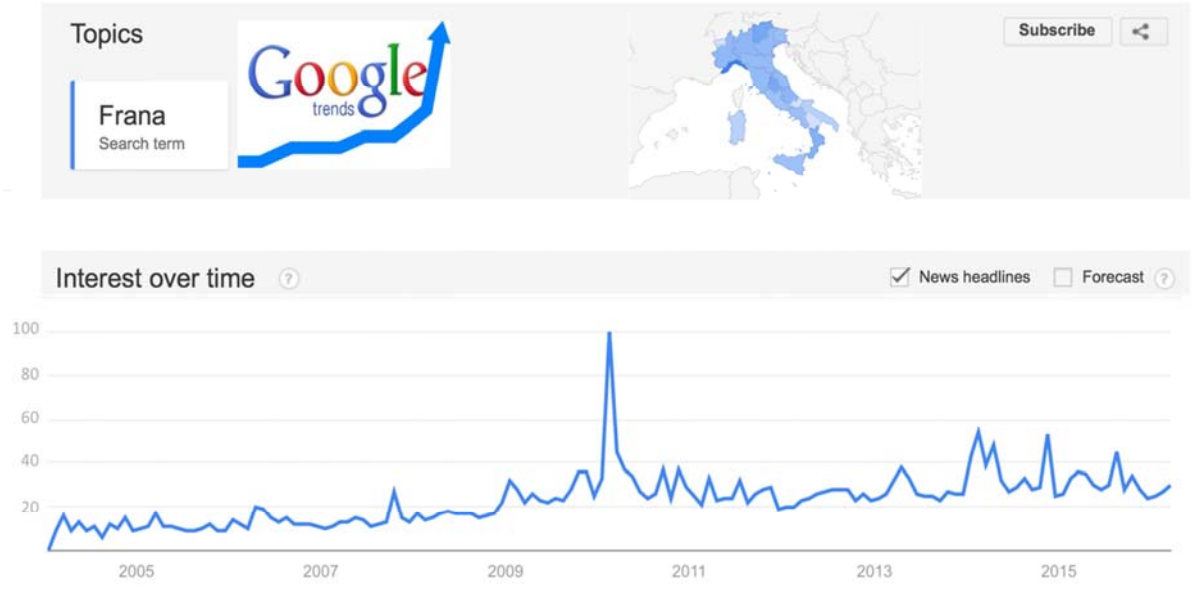

Web news data mining

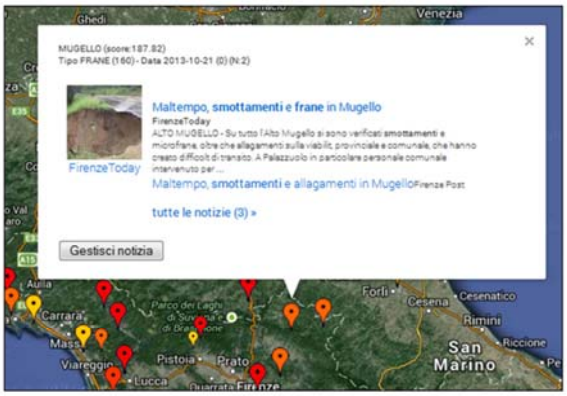

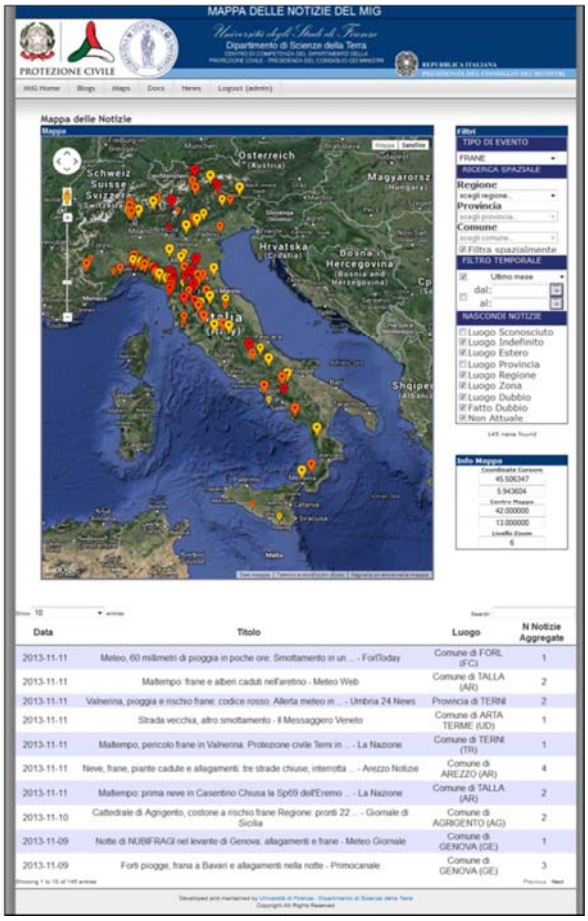

15.084+
landslides
2011-2018

1885 per year
5 per day

Legenda

	Score < 40	40 ≤ Score < 60	60 ≤ Score < 90	Score ≥ 90
news = 1				
news = 2				
3 ≤ news ≤ 20				
news > 20				

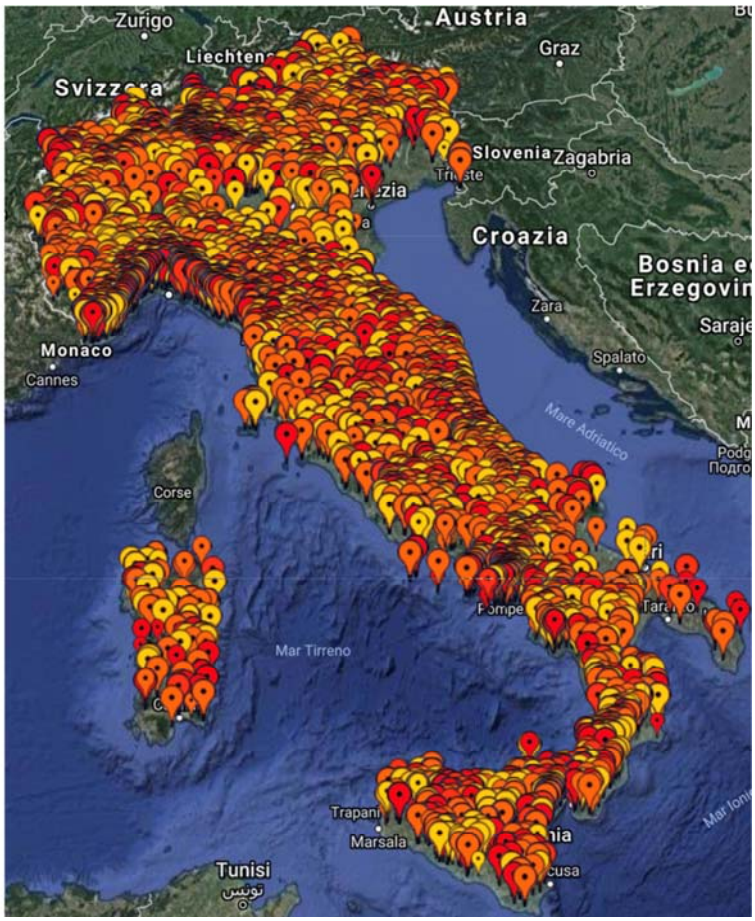

SATURN Drone

- Mission flexibility
- Light solution
- No constraint for cargo area
- Optimal placement of any sensor
- Improved and flexible flight time
- High payload mass
- Powerful computation and acquisition unit

Multi-sensors drone

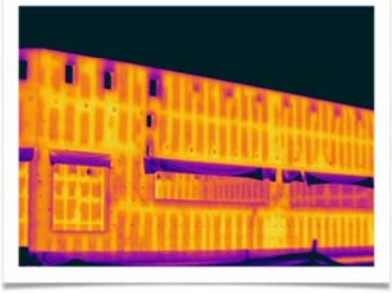

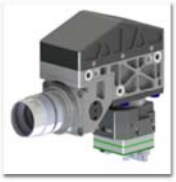

- hi-res camera
- multispectral camera
- hyperspectral sensor
- thermal camera
- radar
- up to 15 kg of payload

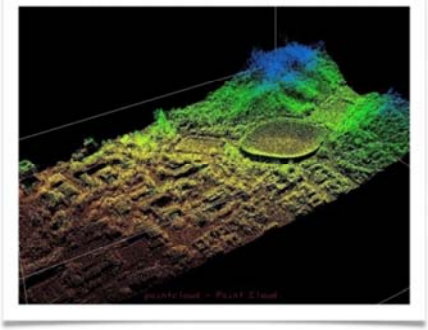

Earth flow

Slow long runout

D-INSAR
GB-InSAR

Marano, february 1996

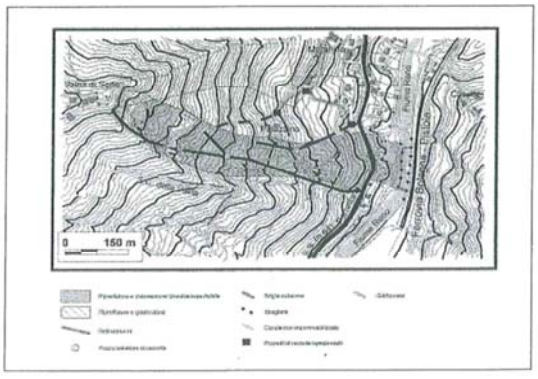

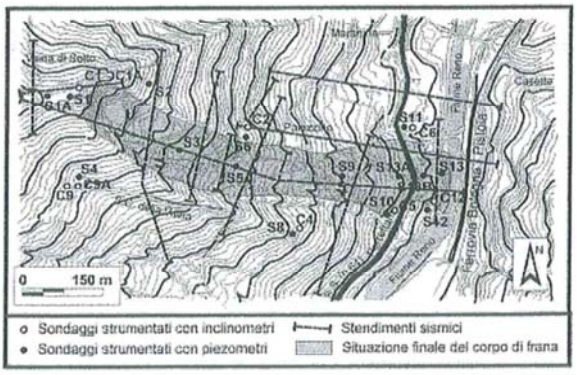

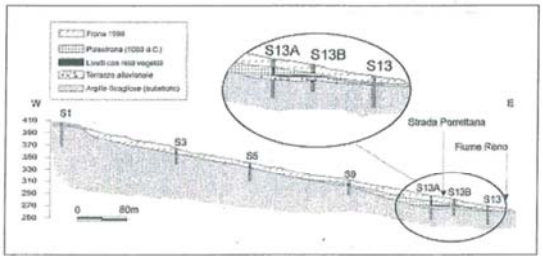

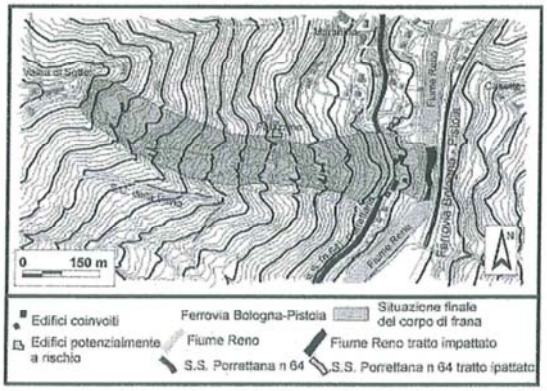

© Aldo Fantini
6/3/2018

2 March 2018

D-InSAR analysis

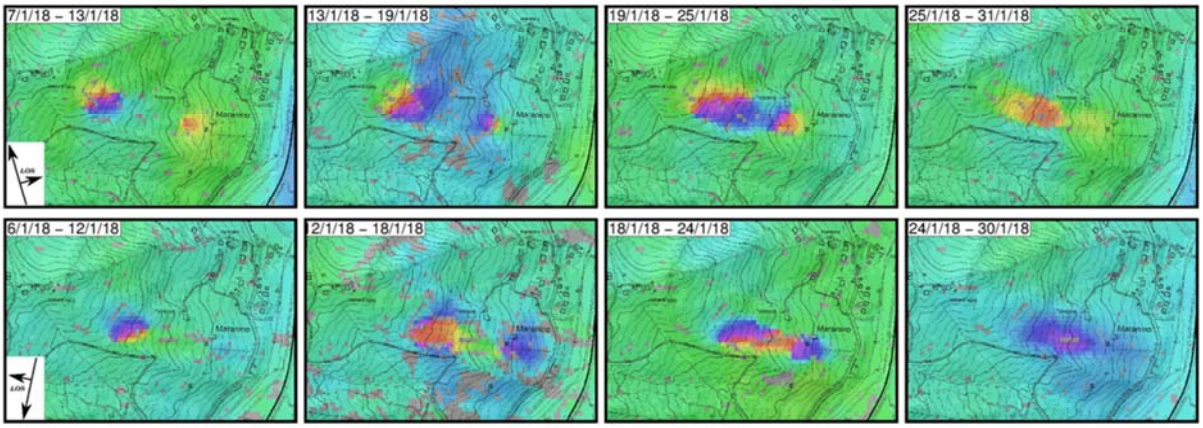

Matteo Berti

Dipartimento BIGEA

Università di Bologna

GB-InSAR

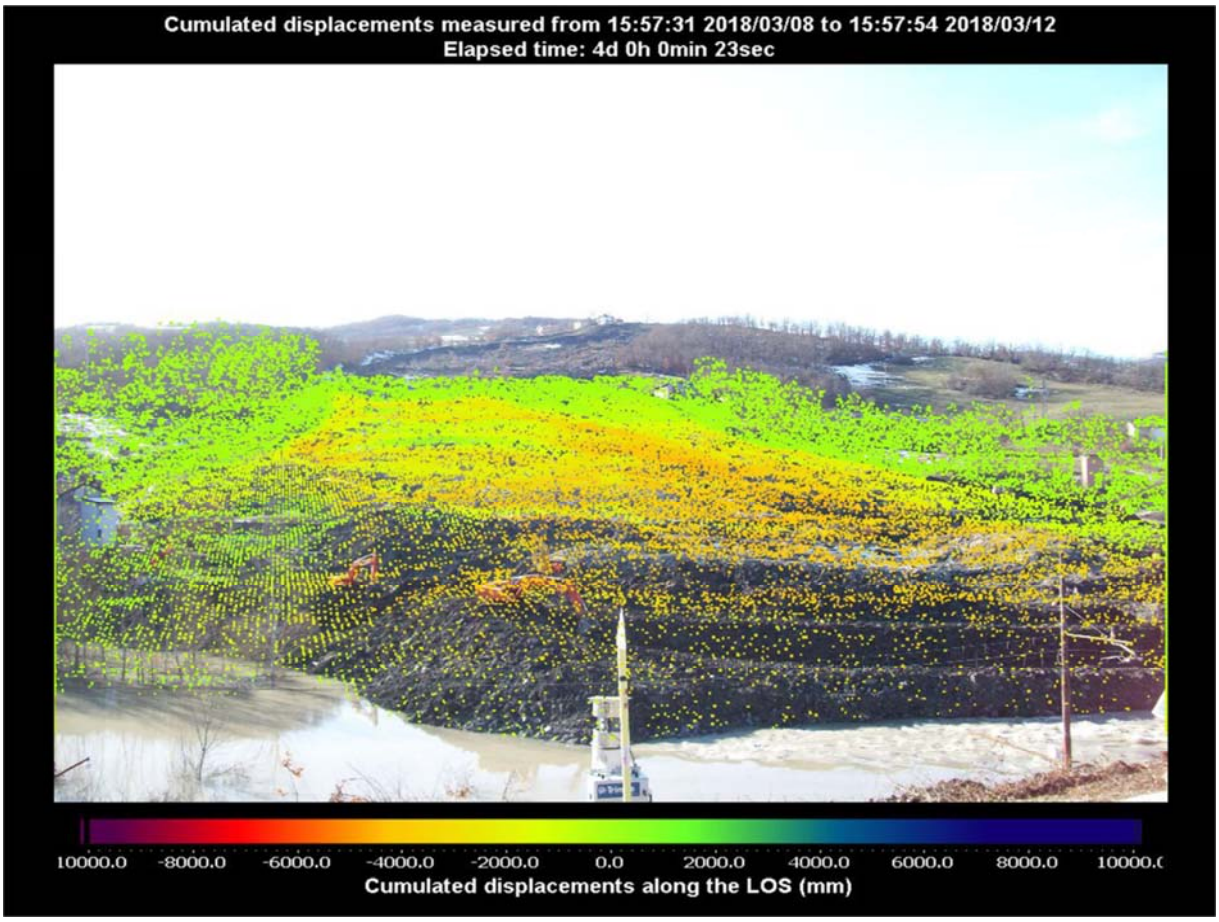
Cumulated displacements measured from 15:57:31 2018/03/08 to 15:57:54 2018/03/12
Elapsed time: 4d 0h 0min 23sec
10000.0 -8000.0 -6000.0 -4000.0 -2000.0 0.0 2000.0 4000.0 6000.0 8000.0 10000.0
Cumulated displacements along the LOS (mm)

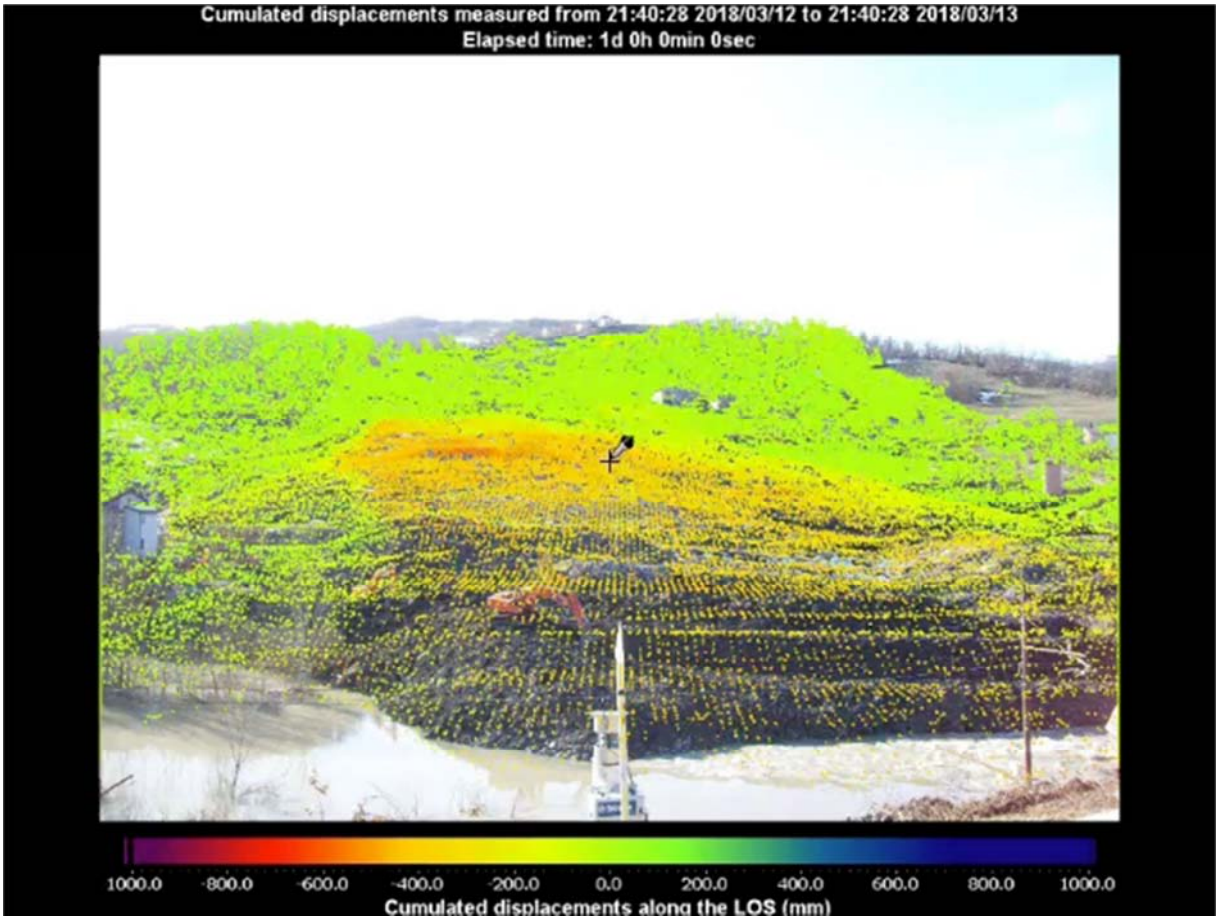
Cumulated displacements measured from 21:40:28 2018/03/12 to 21:40:28 2018/03/13
Elapsed time: 1d 0h 0min 0sec
1000.0 -800.0 -600.0 -400.0 -200.0 0.0 200.0 400.0 600.0 800.0 1000.0
Cumulated displacements along the LOS (mm)

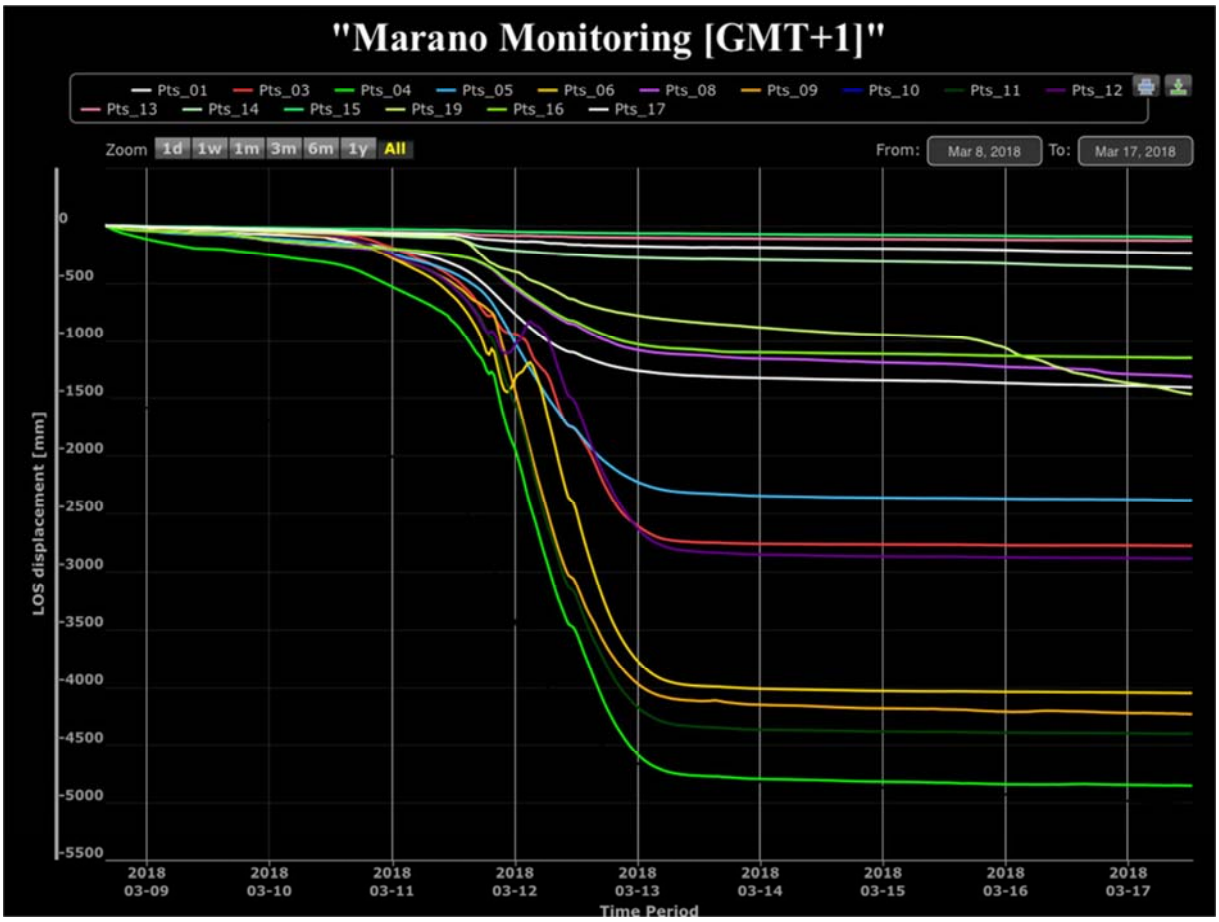

Rainfall correlation

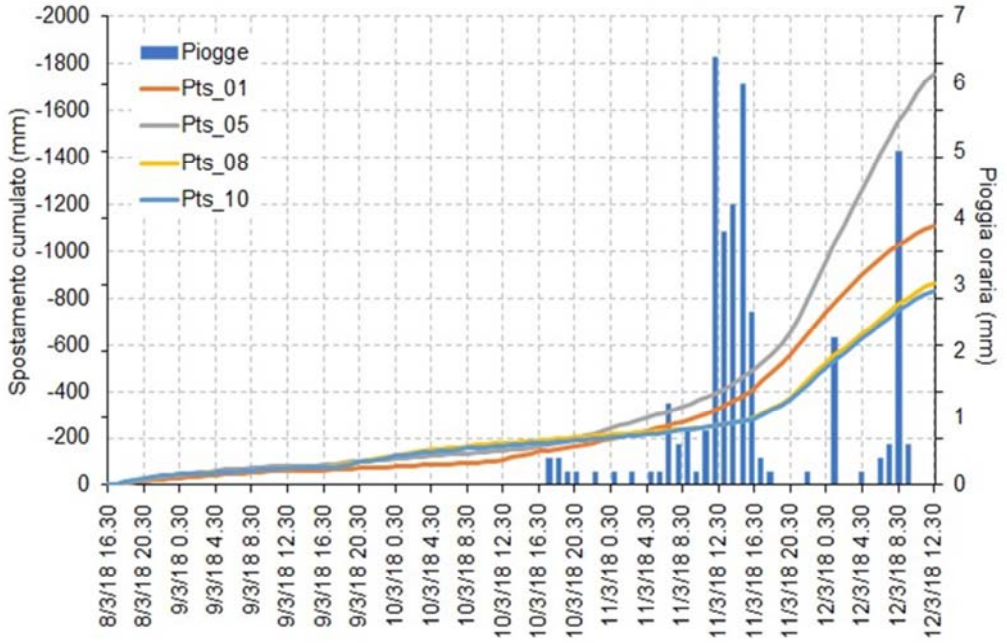

Failure prediction

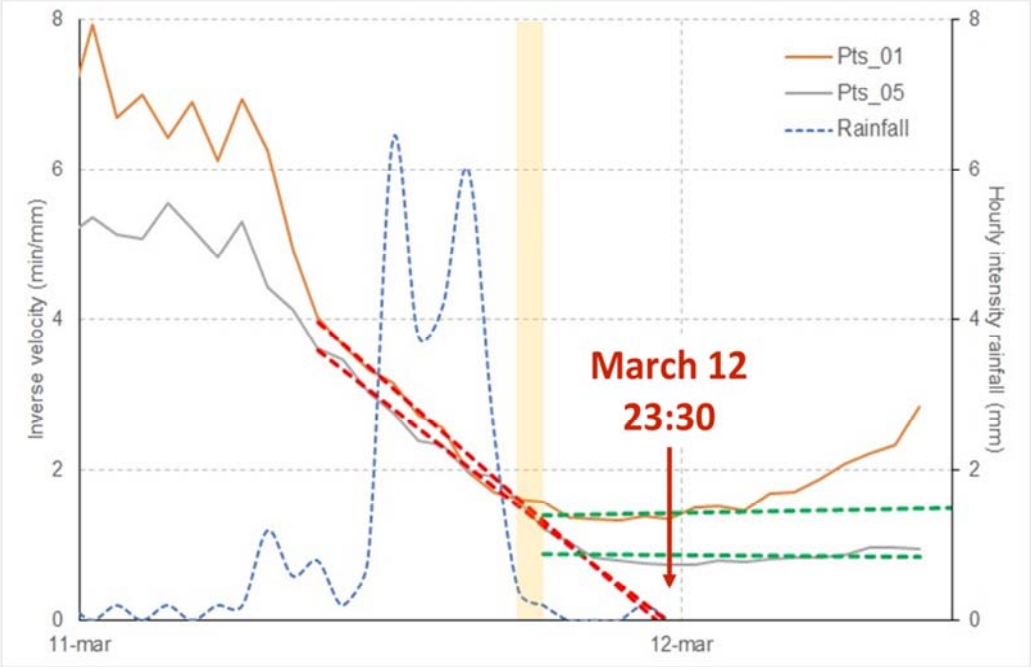

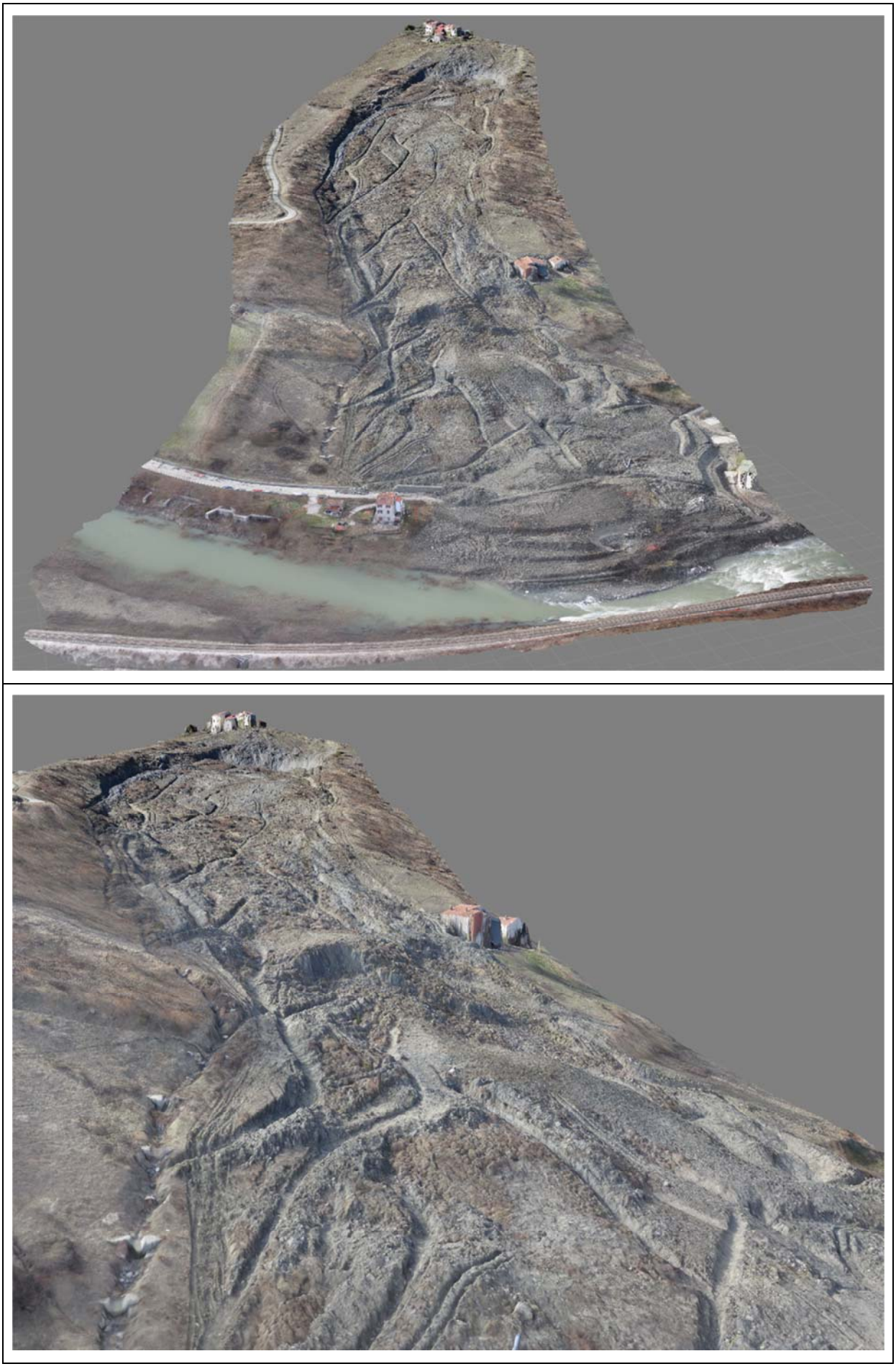

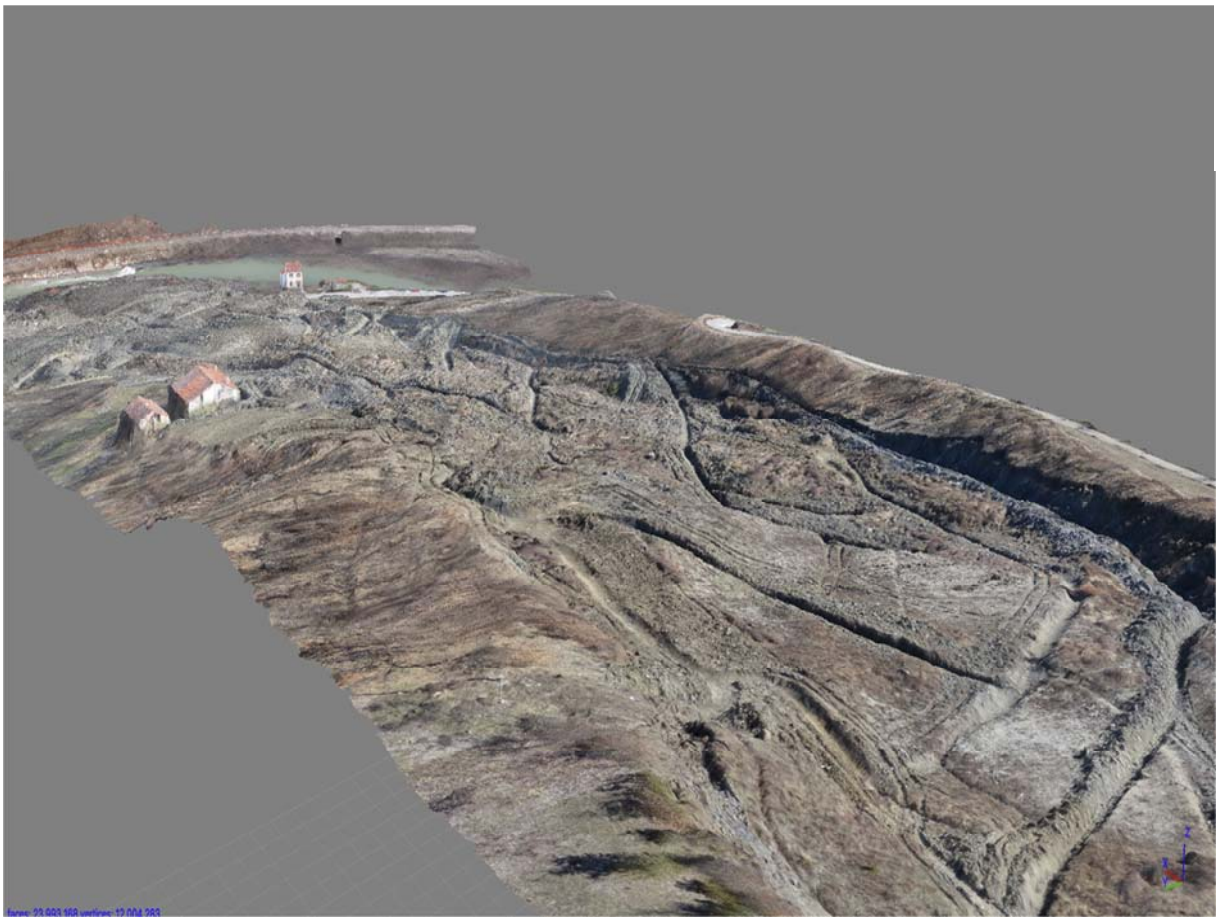

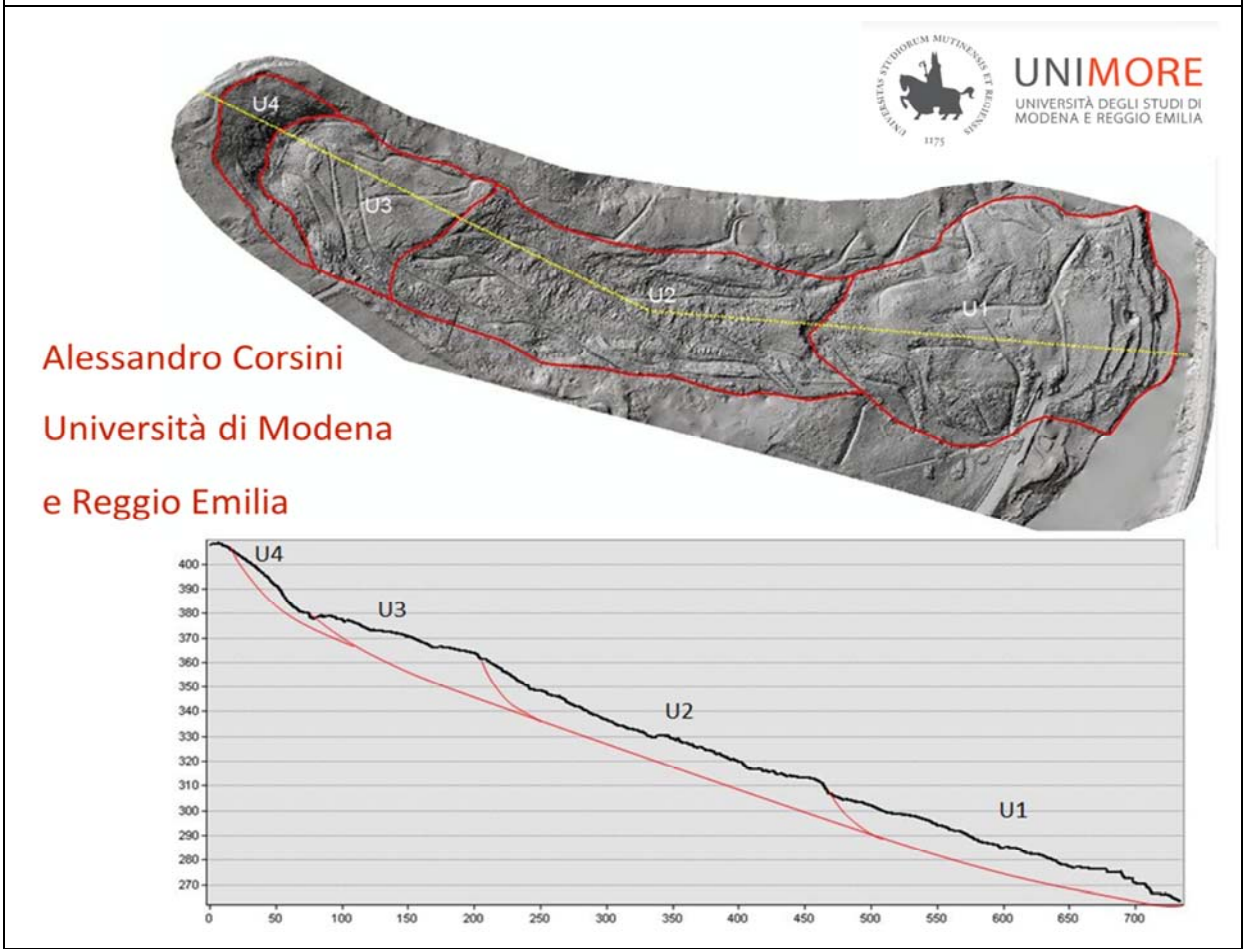
UNIMORE
UNIVERSITÀ DEGLI STUDI DI MODENA E REGGIO EMILIA
U4
U3
U2
U1
Alessandro Corsini
Università di Modena
e Reggio Emilia
U4
U3
U2
U1
400
390
380
370
360
350
340
330
320
310
300
290
280
270
0
50
100
150
200
250
300
350
400
450
500
550
600
650
700

IPL project 198: Multi-scale rainfall triggering models for Early Warning of Landslides (MUSE)

Veronica Tofani[(1)], Filippo Catani[(1)], Nicola Casagli[(1)], Guglielmo Rossi[(1)]

1) University of Florence, Department of Earth Sciences
50121, Via La Pira 4, Florence , Italy
e-mail: veronica.tofani@unifi.it

Abstract

In this work, we apply a physically-based model, namely the HIRESSS (High REsolution Stability Simulator) model, to forecast the occurrence of shallow landslides at regional scale. HIRESSS is a physically based distributed slope stability simulator for analysing shallow landslide triggering conditions during a rainfall event. The software is made of two parts: hydrological and geotechnical. The hydrological model is based on an analytical solution of an approximated form of the Richards equation while the geotechnical stability model is based on an infinite slope model that takes into account the unsaturated soil condition. In particular, the objectives of the work are: i) to properly characterise the geotechnical and hydrological parameters of the soil to feed the HIRESSS model and to spatialize this punctual information in order to have spatially-continuous maps of the model input data ii) to test the HIRESSS code for elected rainfall events that have triggered several shallow landslides and to validate the model results. The model has bee applied in two selected test sites in Italy.

Objectives

- To reconstruct the geotechnical characteristics of the soil cover in the study areas by means of shear strength and permeability in *situ* measurements integrated by laboratory measurements.
- To define the contribution of vegetation to the stability of slopes in terms of root cohesion.
- To use the measured data as input for distributed slope stability analysis.
- To assess the the relationships existing among the different parameters and the bedrock lithology in order to spatialize the geotechnical parameters.
- To test the capacity of a physical model, fed with measured parameters to predict shallow landslide occurrence in response of an intense meteoric precipitation.

HIRESSS model (Rossi et al., 2013)

HIgh REsolution Slope Stability Simulator

HIRESSS

- Physically based, high resolution model
- Large scale operativity
- Coded for real-time applications
- Fast parallel computational scheme

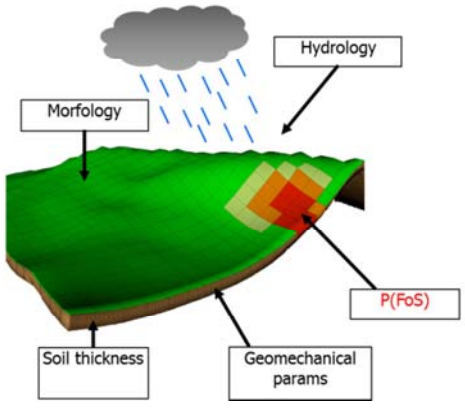

HIRESSS model (Rossi et al., 2013)

Model Structure and Governing Equations

Rainfall Intensity

Factor of Safety

Hydrological Model

$$\frac{\partial h}{\partial t}\frac{d\theta}{dh}=\frac{\partial}{\partial x}\left[K_x(h)\left(\frac{\partial h}{\partial x}-\sin\alpha\right)\right]+\frac{\partial}{\partial y}\left[K_y(h)\left(\frac{\partial h}{\partial y}\right)\right]+\frac{\partial}{\partial z}\left[K_z(h)\left(\frac{\partial h}{\partial z}-\cos\alpha\right)\right]$$

During rainfall

$$h(Z)=Z\beta\left(1-\frac{d}{Z}\right)+Z\frac{I}{K_z}\left[R\left(\frac{t}{Z^2/4D_0\cos^2\alpha}\right)\right]$$

After rainfall

$$h(Z)=Z\beta\left(1-\frac{d}{Z}\right)+Z\frac{I}{K_z}\left[R\left(\frac{t}{Z^2/4D_0\cos^2\alpha}\right)-R\left(\frac{t-T}{Z^2/4D_0\cos^2\alpha}\right)\right]$$

Pore Pressure

Slope Stability Model

Unsaturated conditions

$$FS=\frac{\tan\varphi}{\tan\alpha}+\frac{c'}{\gamma_{NS}z\sin\alpha}+\frac{(u_a-u_w)\tan\varphi^b}{\gamma_{NS}z\sin\alpha}$$

Saturated conditions

$$FS=\frac{\tan\varphi}{\tan\alpha}+\frac{c'}{(\gamma_{NS}(z-h)+\gamma_S h)\sin\alpha}-\frac{h(z,t)\gamma_w\tan\varphi}{(\gamma_{NS}(z-h)+\gamma_S h)\sin\alpha}$$

Hydrological model
- Parallel code solution of Richards equations
- Inclusion of hydraulic diffusivity in the model
- Real-time computational steps (during rainfall event)

Slope Stability Model
- Infinite slope with distributed cell
- Suction effects
- Variable soil density with saturation
- Variable depth analysis

HIRESSS model (Rossi et al., 2013)

The input data are:

Static data:
- effective cohesion (c')
- friction angle (ϕ')
- slope gradient,
- dry unit weight (γ_d)
- soil thickness
- hydraulic conductivity (k_s),
- initial soil saturation (S),
- pore size index (λ),
- bubbling pressure (h_s),
- effective porosity (n)
- residual water content (θ_r).

Dinamic data:
- rainfall

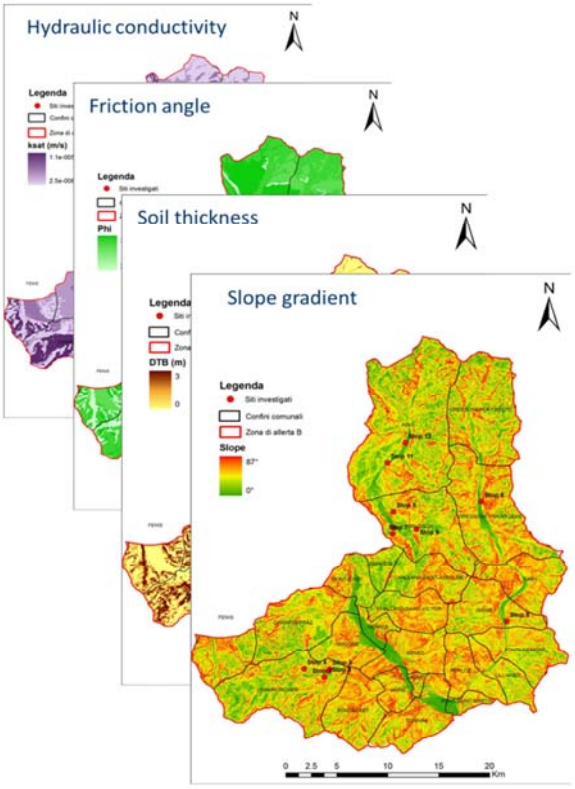

Test site– Northern Tuscany

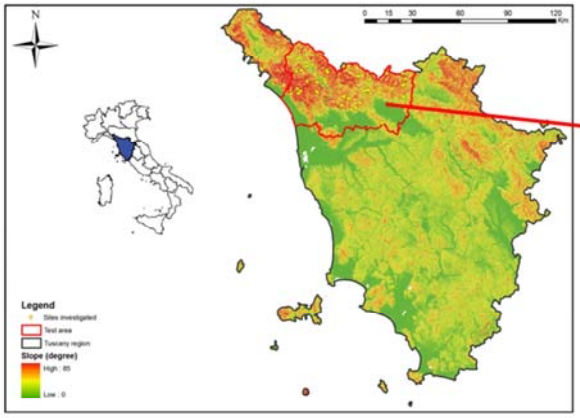

Area investigated:
Pistoia, Prato, Lucca Provinces.
(3103 Km^2)

The area is affected by landslides that mainly (up to 90%) involve their shallowest part (i.e. the first 2 m).

Test site– Valle d'Aosta region

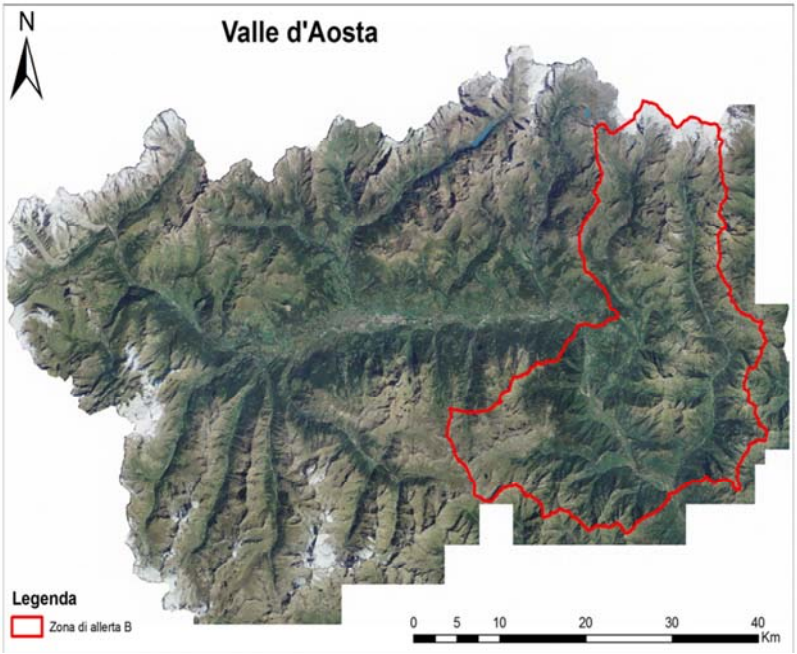

Alert Area B
(900 Km^2)

Shallow landslides (mainly soil slips) less than 1 m thick that evolve into flows

Field and laboratory geotechnical measurements

- Shear strength by using <u>in *situ*</u> Borehole Shear Test (BST) at **0.5-0.8 m** of depth.
- Matric suction measured <u>in *situ*</u> by tensiometer.
- Permeability measured using <u>in *situ*</u> Amoozmeter constant head permeameter.
- Grain size analysis
- Index properties and Atterberg limits

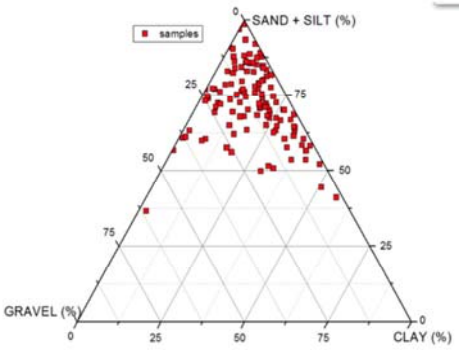

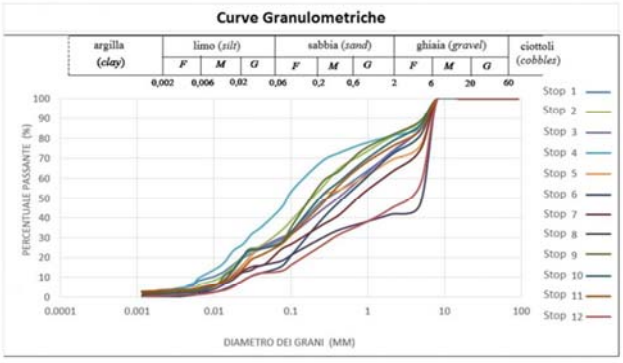

Methods and measurements

BST

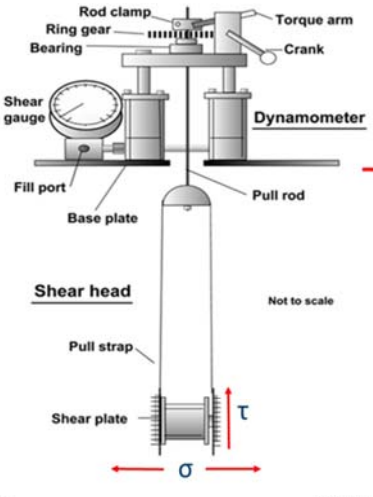

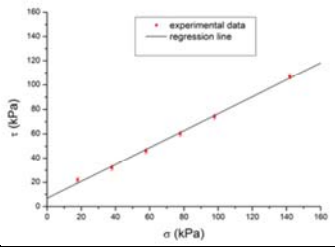

Tensiometer

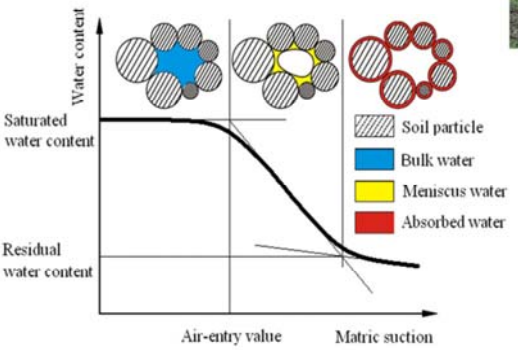

Amoozemeter

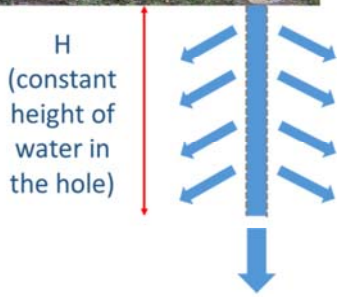

Tuscany - Survey points and lithological map of bedrock

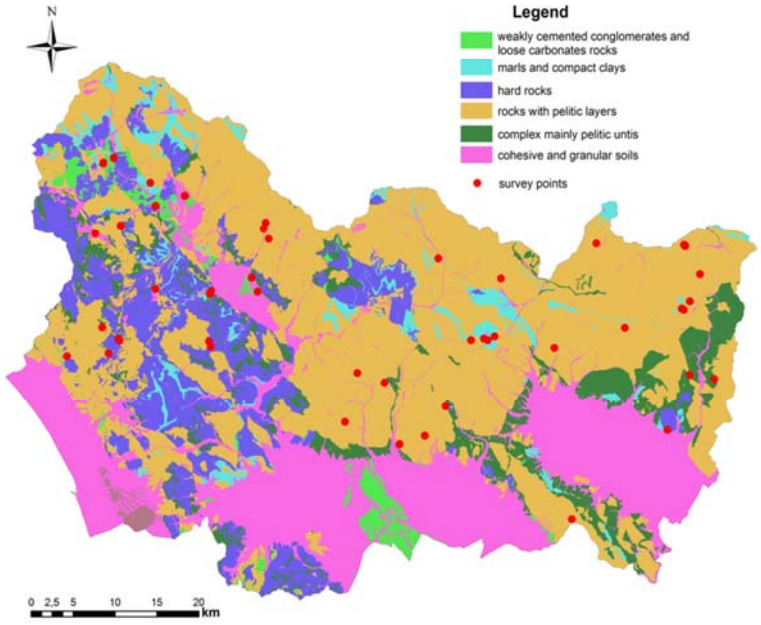

- **59 survey points**
- new lithological classification with Regional Geological Map at the scale of 1:10:000
- six lithological classes have been defined according to Catani et al. (2005)
- 68 geological maps have been used and 194 geological formations classified

Valle d'Aosta - Survey points and lithological map of bedrock

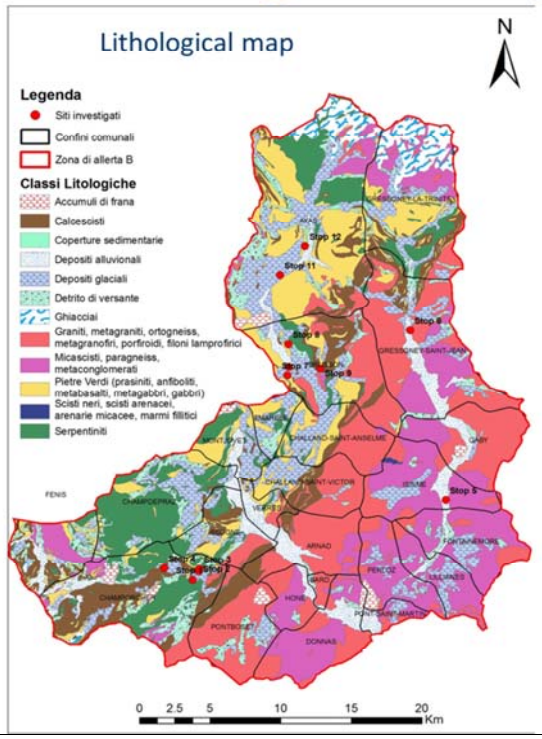

- **12 survey points**
- lithological map from Valle d'Aosta region with 12 classes
- 7 final lithological classes

Tuscany -Geotechnical parameters for lithology

bedrock lithological class	statistics	φ' (°)	c (kPa)	k_s ($m \cdot sec^{-1}$)	gravel (%)	sand (%)	silt (%)	clay (%)	w_n (%)	γ_d ($kN \cdot m^{-3}$)	W_L (%)	W_P (%)	IP (%)
conglomerates and poorly cemented carbonate rocks (5 sites)	mean	29	6	4,E-07	7,6	32,6	43,9	15,9	15,2	10,5	40	33	7
	median	28	5	3,E-07	6,8	31,9	42,4	14,5	15,0	10,5	41	34	7
	max	34	14	3,E-07	11,2	35,1	46,7	21,8	24,9	11,4	42	39	13
	min	23	2	1,E-07	4,8	29,7	41,1	12,6	4,1	9,7	36	23	2
marls and compact clays (5 sites)	mean	36	5	6,E-07	26,4	31,9	29,6	12,1	16,0	16,1	33	22	11
	median	37	4	6,E-07	23,3	34,6	27,9	9,1	16,2	15,0	35	23	10
	max	38	12	9,E-07	37,3	45,8	44,0	22,0	22,4	21,1	36	31	18
	min	32	0	3,E-07	15,9	18,0	19,0	7,5	9,6	12,3	26	16	5
hard rocks (4 sites)	mean	32	9	7,E-07	20,8	44,8	28,6	5,8	33,8	n.d.	47	29	18
	median	33	11	3,E-07	21,7	37,5	31,4	9,5	43,5	n.d.	53	29	19
	max	35	12	1,E-06	24,1	74,9	37,7	10,9	43,5	n.d.	57	37	29
	min	27	4	3,E-07	11,4	27,5	12,8	0,8	14,5	n.d.	26	20	6
hard rocks with pelitic layers (33 sites)	mean	33	5	3,E-06	15,7	42,5	34,7	7,1	21,7	13,1	34	24	10
	median	34	3	1,E-06	18,2	39,1	29,7	6,2	21,0	13,1	32	24	7
	max	39	19	3,E-05	50,9	85,4	56,7	25,7	43,5	16,5	57	37	33
	min	20	0	8,E-08	0,2	10,5	9,1	0,7	4,3	9,6	23	14	3
complex mainly pelitic units (2 sites)	mean	36	11	8,E-07	26,4	39,4	25,1	9,2	11,9	n.d.	n.d.	n.d.	n.d.
	median	36	11	8,E-07	26,7	38,4	26,0	9,0	11,9	n.d.	n.d.	n.d.	n.d.
	max	41	13	1,E-06	34,0	40,5	34,7	9,6	13,9	n.d.	n.d.	n.d.	n.d.
	min	31	9	5,E-07	19,4	36,3	17,2	8,3	9,9	n.d.	n.d.	n.d.	n.d.
cohesive and granular soils (10 sites)	mean	29	4	7,E-07	14,3	37,0	39,4	9,3	17,1	11,4	40	26	14
	median	29	3	4,E-07	11,4	32,9	31,5	4,3	16,2	11,4	36	30	14
	max	38	10	2,E-06	57,9	74,4	58,4	42,8	23,5	12,8	58	34	30
	min	23	0	8,E-07	0,4	3,7	12,5	0,7	13,4	10,2	25	11	2

Prevalent silty-clayey sand (SM, SC and SM-SC in USCS classification)

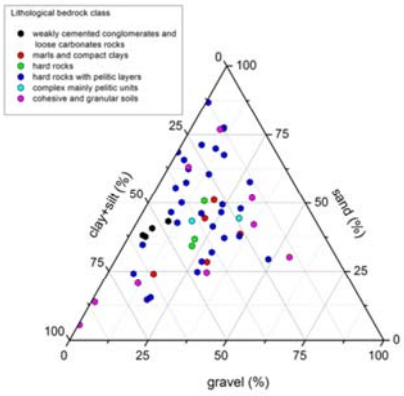

Tuscany - HIRESSS input data

bedrock lithological class	median grain size	φ' (°)	c' (kPa)	k_s ($m \cdot sec^{-1}$)	γ_d ($kN \cdot m^{-3}$)	effective porosity (% v/v)	bubbling pressure	grain size index	residual water content
weakly cemented conglomerates and loose carbonates rocks	sandy silt	29	0	3,E-07	10,5	41,2	14,66	0,322	0,041
marls and compact clays	silty gravelly sand	37	0	6,E-07	15,0	41,7	7,26	0,592	0,020
hard rocks with pelitic layers	silty gravelly sand	34	0	1,E-06	13,1	41,7	7,26	0,592	0,020
cohesive and granular soils	silty sand	29	0	4,E-07	11,4	40,1	8,69	0,474	0,035

Parameters directly measured in the field: the median values have been selected for each lithological class

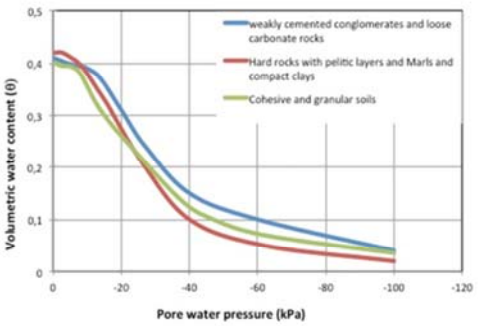

Parameters not measured in the field: derived from Rawls et al. (1982) by matching for each lithological class the corresponding (median) grain size derived from grain size distribution analyses

Valle d'Aosta - Geotechnical parameters for lithology

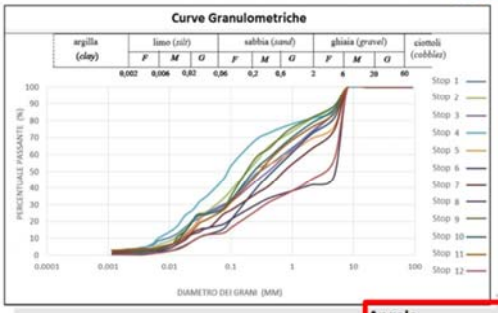

Prevalent silty sand (SM in USCS classification)

LITOLOGIA	Granulometria	Angolo d'attrito (°)	Coesione (Pa)	Peso di Volume secco (kN/m³)	Porosità (%)	Permeabilità satura (m/s)	Pressione di entrata dell'aria (m)	Contenuto d'acqua residuo	Indice dei pori
Calcescisti.	Sabbia con limo ghiaiosa	31	1000	16.5	39	1.1E-05	0.1466	0.041	0.322
Depositi alluvionali.	Sabbia con ghiaia e limo	26	1000	14	46	3.0E-06	0.1466	0.041	0.322
Depositi glaciali.	Sabbia con ghiaia limosa	31	1000	15.3	41	2.7E-06	0.1466	0.041	0.322
Detrito di versante.	Sabbia con ghiaia limosa	25	1000	13.7	47	2.5E-06	0.1466	0.041	0.322
Graniti, metagraniti, ortogneiss, metagranofiri, porfiroidi, filoni lamprofirici.	Ghiaia sabbiosa	30	1000	17.6	32	4.0E-06	0.1466	0.041	0.322
Micascisti, paragneiss, metaconglomerati.	Ghiaia sabbiosa limosa	30	1000	17.7	32	6.0E-06	0.1466	0.041	0.322
Pietre Verdi (prasiniti, anfiboliti, metabasalti, metagabbri, gabbri).	Ghiaia con sabbia limosa	32	1000	16.3	37	4.6E-06	0.1466	0.041	0.322

Vegetation

HYDROLOGICAL and MECHANICAL EFFECTS

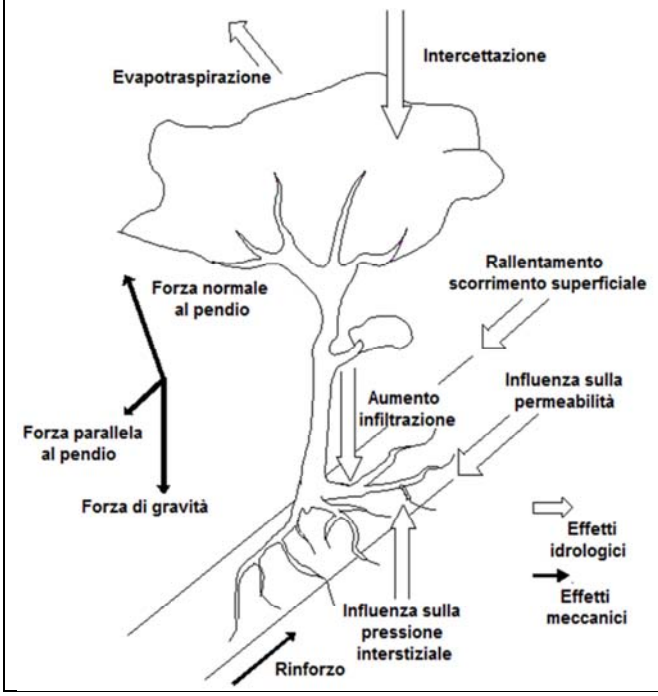

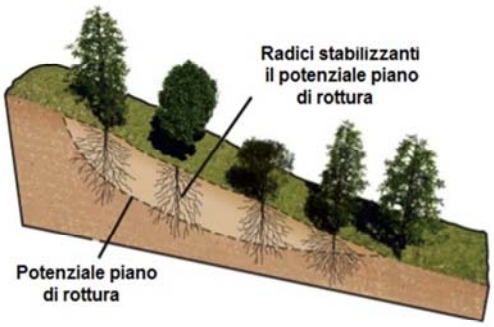

Root reinforcement

FBM (Fiber Bundle Model)
Pollen & Simon (2005).

Root reinforcement

$c_r = kT_r(A_r/A)$

Where T_r = tensile strenght of roots per unit of soil, A_r/A = Root Area Ratio (RAR, coefficient)

Tipologia forestale	c_r (kPa)
Abete bianco e rosso	4,94
Abete rosso	1,55
Boscaglia di fiume	2
Bosco a fago-abetine	1,84
Bosco misto a tiglio	8,86
Castagno	5,43
Larici	3
Pascolo	0
Pino Silvestre	4,94
Pino Uncinato	4,94
Querceta a roverella	0,01

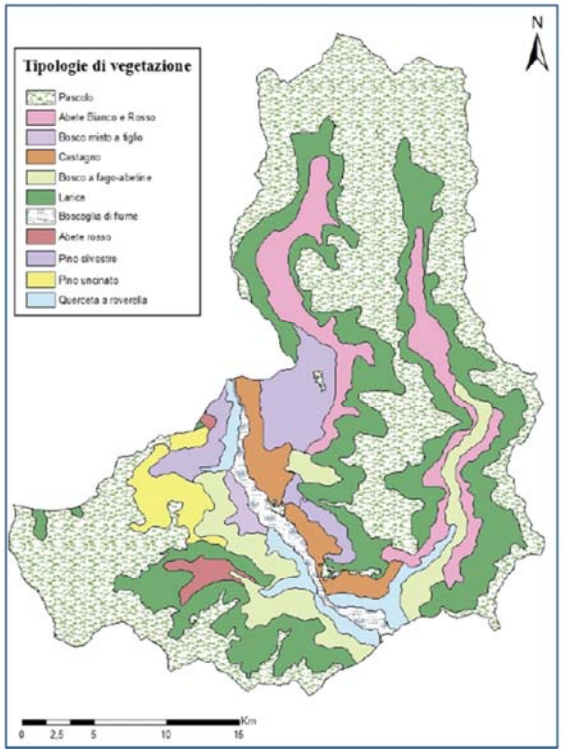

Tuscany - HIRESSS simulation

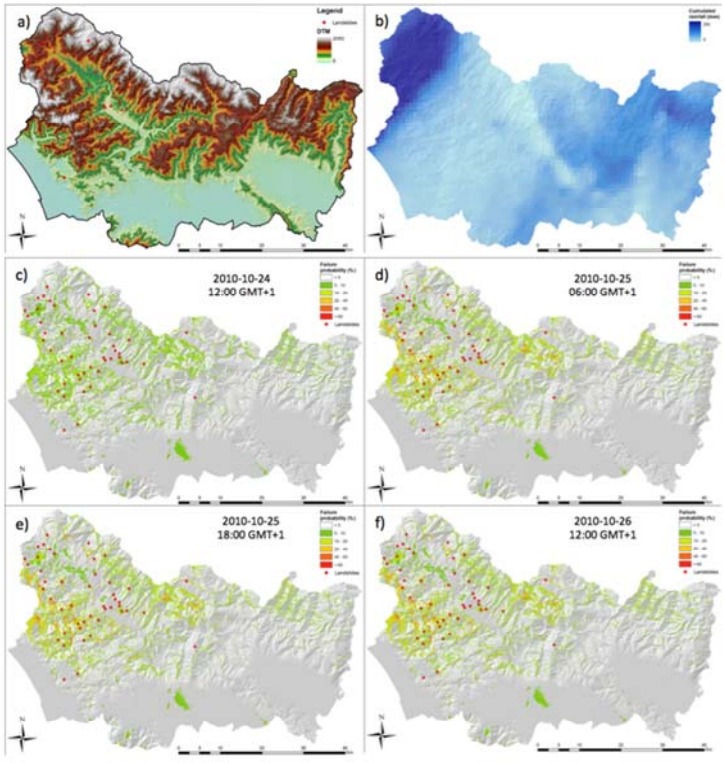

- simulation on a past event (24 October 2010 – 26 October 2010)
- total precipitation in three days of 250 mm (from national meteorological radar network)
- 50 reported shallow landslides
- spatial resolution of 10 m
- 1 hour time step

simulation results and the spatial distribution of landslides are partially in accordance

all the landslides are located in areas with >50% probability of failure

Valle d'Aosta - HIRESSS simulation

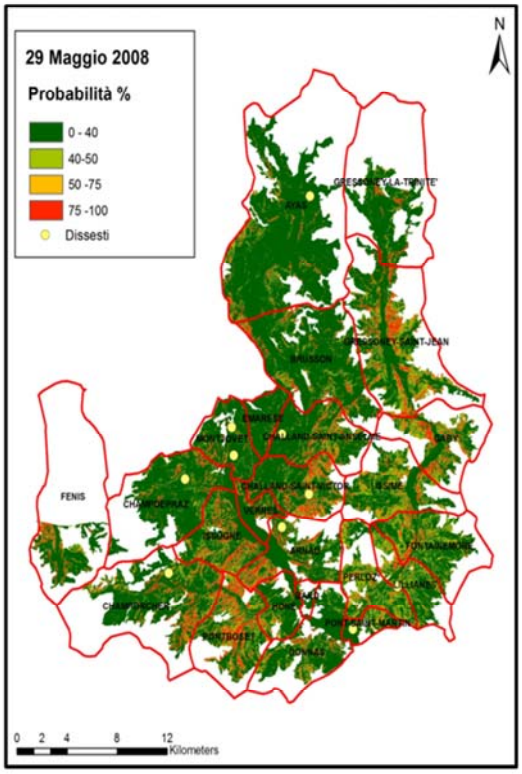

- spatial resolution of 10 m
- 1 hour time step
- two events simulated:
  - ✓ 24 - 31 May 2008
  - ✓ 25 - 28 April 2009

24 - 31 May 2008

- 250 mm of precipitation
- 9 landslides reported

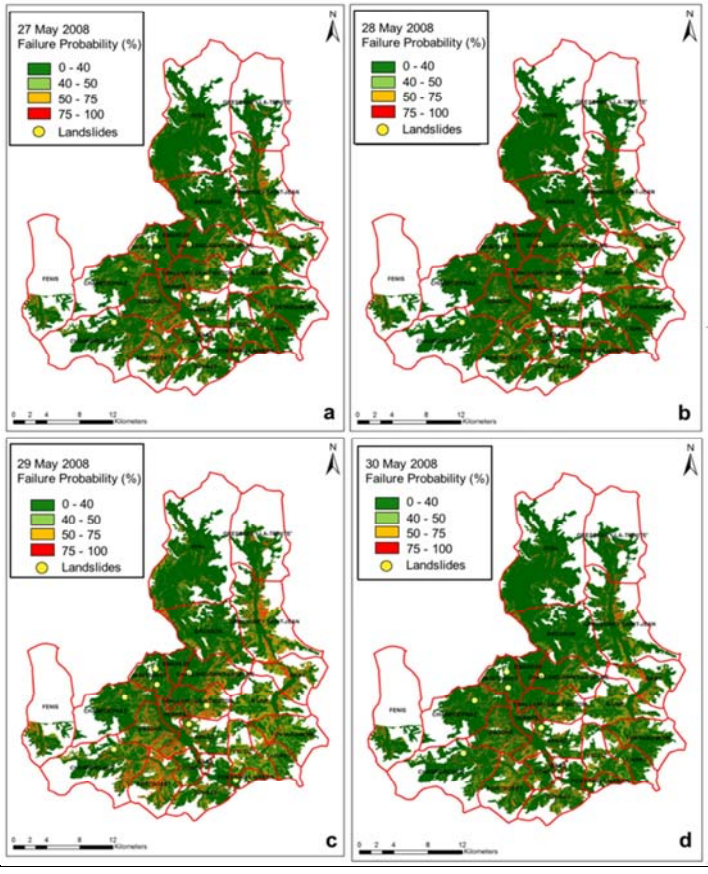

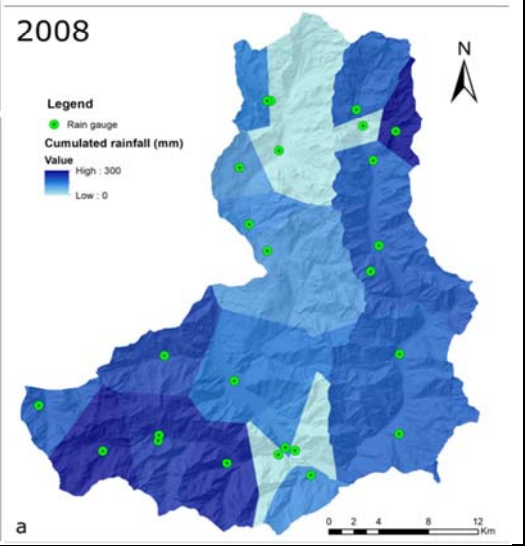

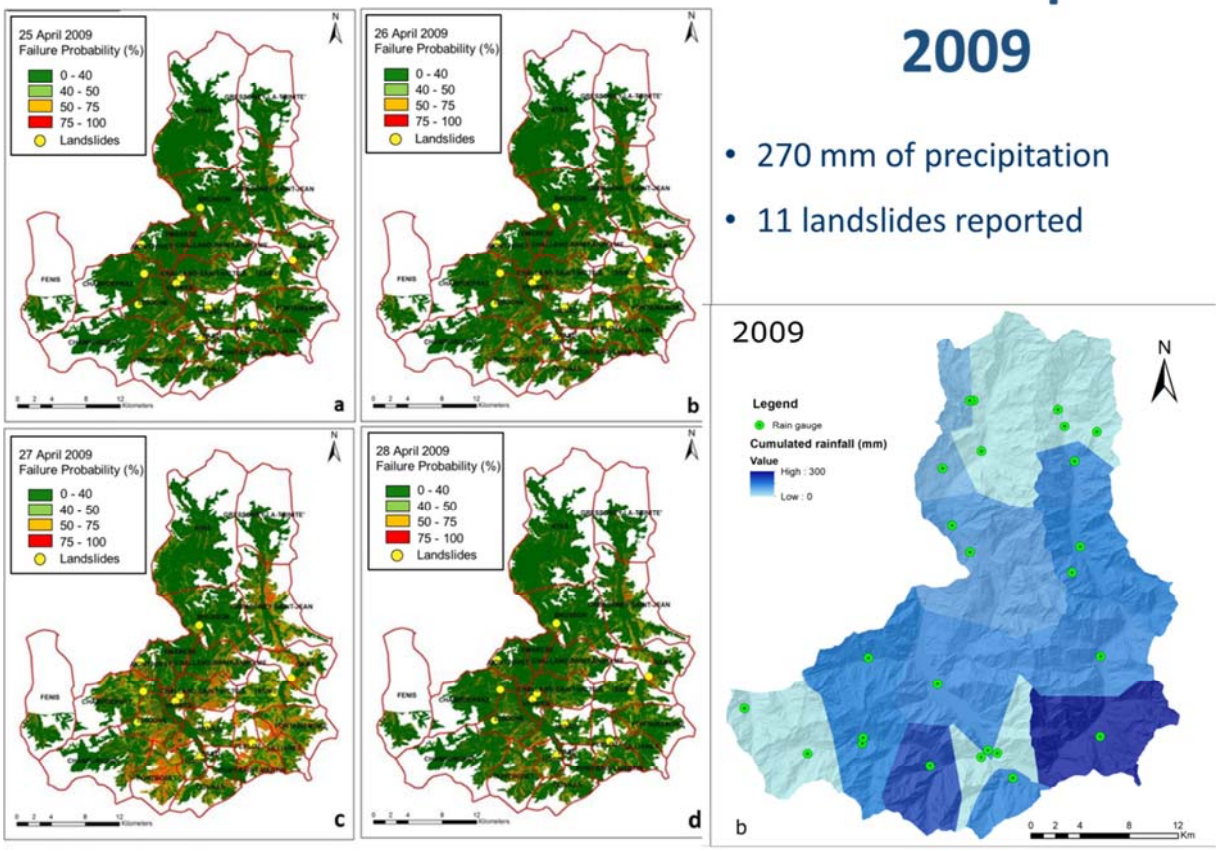

veronica.tofani@unifi.it

Tofani V., Bicocchi G., Rossi G., D'ambrosio M., Segoni S., Casagli N., Catani F. (2016) Soil characterization for shallow landslides modeling: a case study in the Northern Apennines (Central Italy), Landslides

Rossi G., Catani F., Leoni L., Segoni S., Tofani V. (2013), HIRESSS: a physically based slope stability simulator for HPC applications. NHESS

Landslide risk analysis and mitigation for the Monastery of Vardzia - 2018

Abstract

The rock-cut city of Vardzia is a cave monastery site in south-western Georgia, excavated inside the volcanic and pyroclastic rock layers of the Erusheti mountain on the left bank of the Mtkvari river. The site has been affected by frequent instability phenomena along the entire cliff. These pose serious constrains to future conservation, as well as to the safety of tourists. In order to improve knowledge about slope stability issues in the Vardzia site and to develop a proper site specific approach, the National Agency for Cultural Heritage Preservation of Georgia (NACHPG) promoted, with the support of Istituto Superiore per la Protezione e la Ricerca Ambientale (ISPRA), Geological survey of Italy, a landslide hazard assessment and monitoring for the entire area. The main goal of the ongoing project is to study the complex structure of Vardzia, to assess reliable mechanical parameters of outcropping rocks and to monitor slope and monument deformation in order to identify critical areas prone to collapse. All these information are allowing the elaboration of a sustainable approach for retrofitting and conservation of rock cut monuments.

Landslide risk analysis and mitigation for the Monastery of Vardzia

PROMOTED AN SUPPORTED BY
National Agency for Cultural Heritage Preservation of Georgia
Dr. Nikoloz Antidze - Director General

ISPRA Project Scientific Coordinator
Claudio MARGOTTINI & Daniele SPIZZICHINO

DICAM-UNIBO
Daniela Boldini

UNIMIB
Giovanni CROSTA,
Paolo Frattini,
Riccardo Castellanza

UNIFI
Nicola Casagli,
Giovanni Gigli,
William frodella

ILIA STATE UNIVERSITY
Dr. Mikheil Elashvili

VARDZIA: PERT ANALYSIS

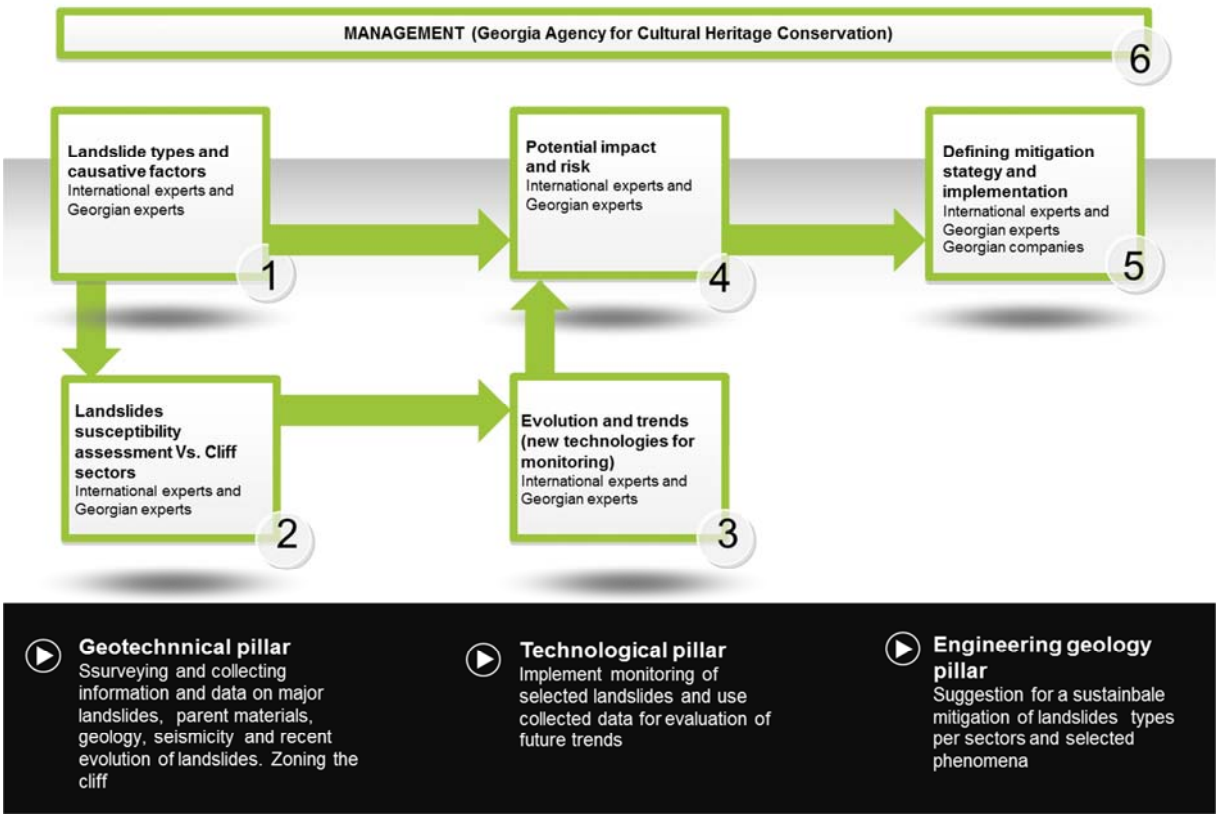

Geotechnnical pillar
Ssurveying and collecting information and data on major landslides, parent materials, geology, seismicity and recent evolution of landslides. Zoning the cliff

Technological pillar
Implement monitoring of selected landslides and use collected data for evaluation of future trends

Engineering geology pillar
Suggestion for a sustainbale mitigation of landslides types per sectors and selected phenomena

ISPRA

Landslide types and causative factors

THREATS RELEVANT PHENOMENA

Fall of blocks from volcanic breccia
Wedge and planar failure from volcanic breccia
Surface run off
Fall of small blocks from the edge

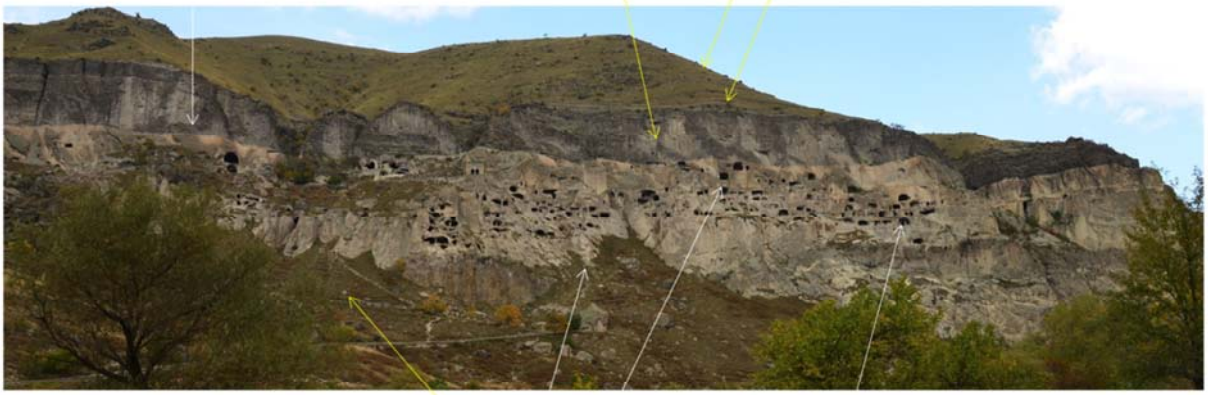

Fall of block from past rock fall/slide
Large potential sliding
Wedge, planar failure and fall from upper tuff
Wedge and planar failure from lower tuff and minor fall

Relevant for tourists
Relevant for Cultural Heritage conservation

ISPRA

Technological pillar Implement monitoring of selected landslides and use collected data for evaluation of future trends

TLS FIELD SURVEY - 2014 – 2015 - 2018

IN ORDER TO CARRY OUT A SITE-SCALE SPECIFIC ANALYSIS AND TO SUPPORT 2D and 3D ROCKFALLS MODEL, A DETAILED GEODETIC 3D LASER SCANNING SURVEY HAS BEEN PERFORMED AND IMPLEMENTED DURING THE LAST FIELD MISSION.

TERRESTRIAL LASER SCANNER (TLS) SURVEYS WERE PERFORMED BY A RIEGL **VZ1000** SENSOR FROM TWELVE DIFFERENT SCAN POSITIONS (FIGURE 8), IN ORDER TO REDUCE THE SHADOW ZONE.

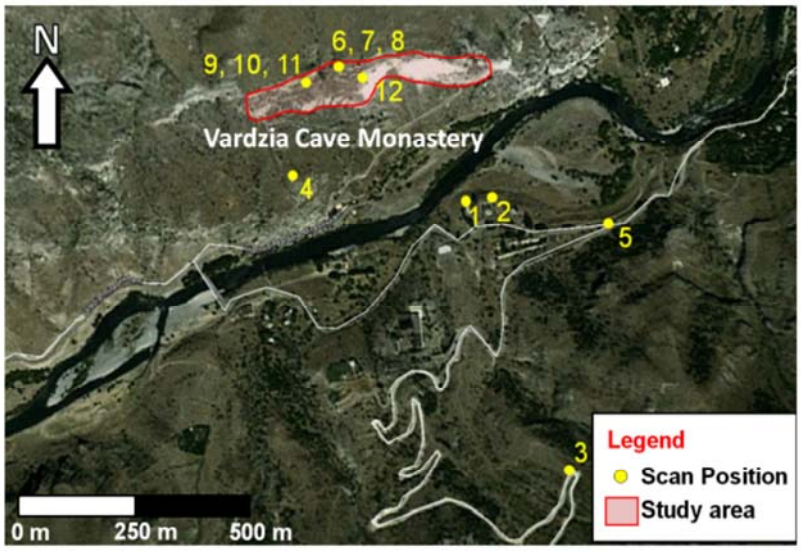

ISPRA

KINEMATIC ANALYSIS FOR THE WHOLE CLIFF - UNIFI

- THE EXPOSED ROCK FACES OF VARDZIA CLIFF AND DETECTED SLOPE ASPECT AND SLOPE ANGLE, ALSO ON A SCHMIDT-LAMBERT STEREONET.
- AREAS WITH KINEMATIC CONDITIONS SUITABLE TO GENERATE WEDGE AND/OR PLANAR SLIDING (RED).
- ANALYSIS WITH THE USE OF DIANA CODE (UNIVERSITY OF FLORENCE)

Set orientation
1: 65°/169°
2: 88°/253°
3: 70°/047°
4: 70°/003°

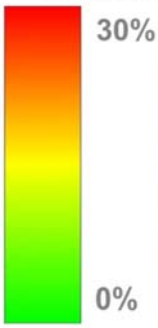

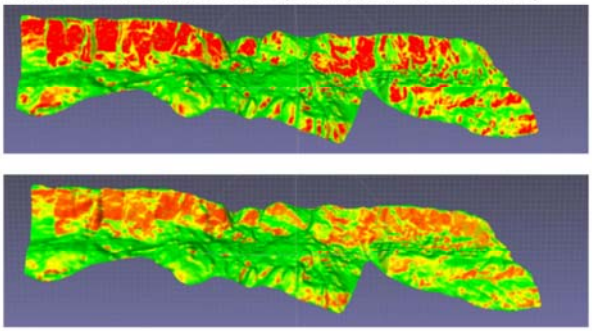

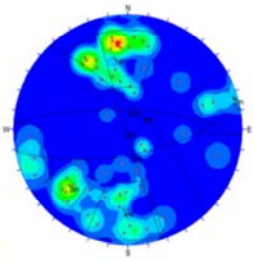

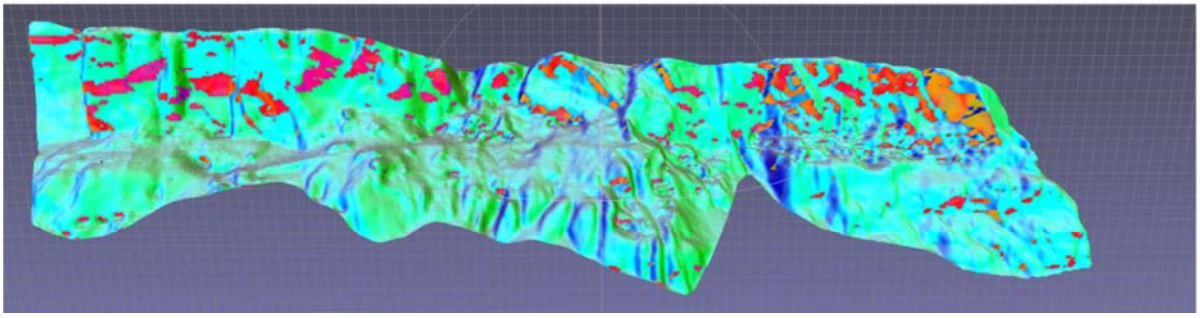

ISPRA

ROCK SLOPE CHARACTERISATION (archaeological strata) – University of Bologna and Milano jointly with ISPRA

Lithology	Unit weight g (KN/m³)	porosity (%)	σ_c dry MPa	σ_c sat MPa
Grey tuff (upper)	16.3	37.2	10.3	3.6
White tuff (lower)	15.9	38.8	8.7	2.8
	Basic friction angle (φ°)	GSI	σ_t dry Mpa	σ_t sat MPa
Grey tuff (upper)	22°-32°	70	0.8	0.3
White tuff (lower)	22°-32°	65	0.9	0.3

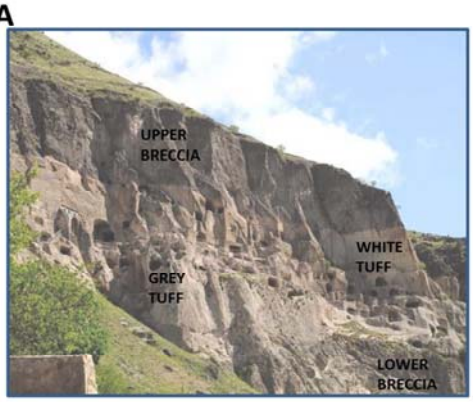

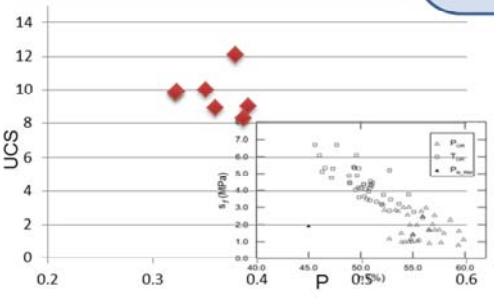

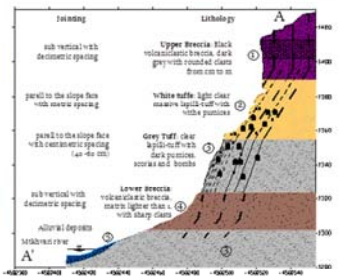

THE VOLCANIC ROCK (MEDIUM AND LOWER PART) OF THE SITE IS QUITE WEAK, AS USUAL IN AREAS WHERE HUMAN BEING REALISED IMPORTANT SETTLEMENT.
UNIAXIAL COMPRESSIVE STRENGTH IS RANGING BETWEEN 6-14 MPA, WITH DENSITY FROM 1,5 TIL 1,9, ACCORDING TO THE DIFFERENT LAYERS.
A BIG REDUCTION OF UCS AND TENSILE STRENGHT PASSING FROM DRY TO SATURATED CONDITION (such drop can reach up to 70% of original values, then suggesting an important role in rainy period);

3D simulation of rockfall propagation – University of MILANO BICOCCA

3D simulation of free fall, impact and rolling of non-interacting blocks on a DEM-derived topography

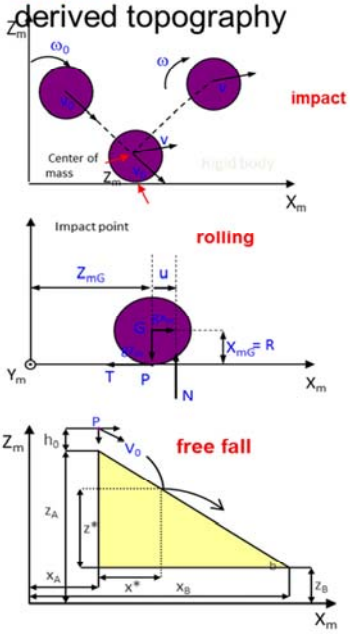

HY-STONE software

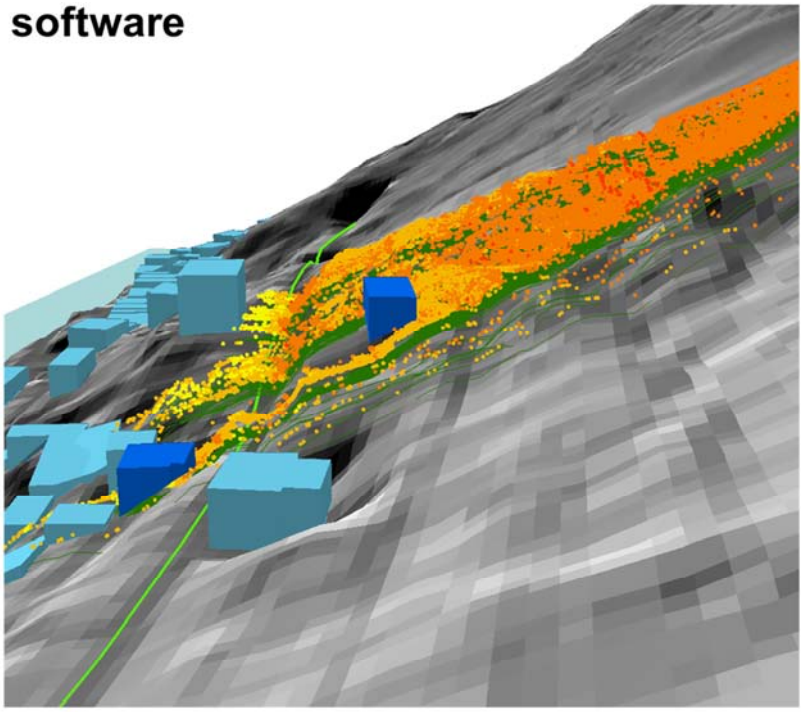

MOST UNSTABLE AREAS FROM FIELD SURVEY

Unstables block/areas

Joints, cracks, open fractures

ISPRA

MASTER PLAN AND MITIGATION MEASURES

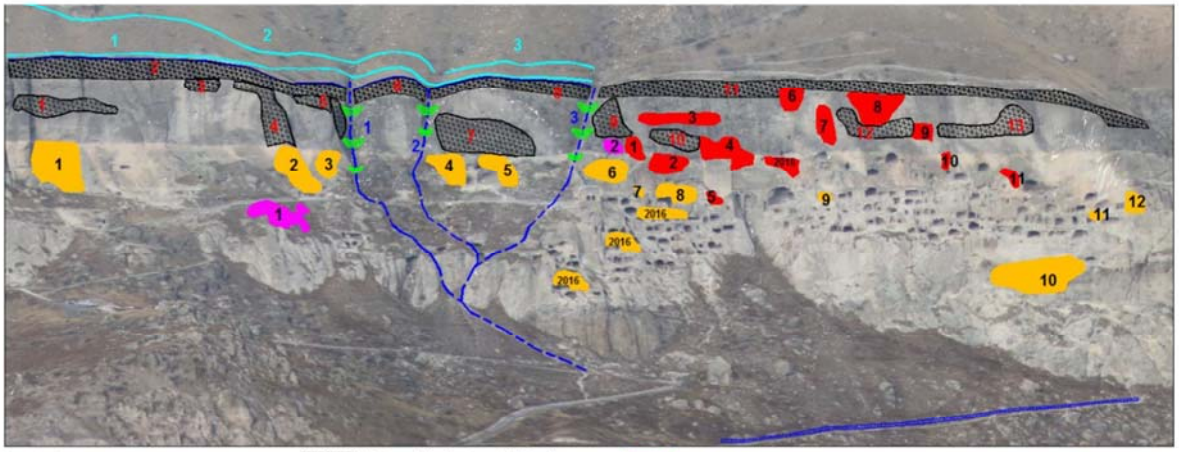

MONITORING GROUND-BASED RADAR INTERFEROMETRY (ABOUT 50.000 POINTS)

The system adopted for the monitoring of the entire cliff is based on a ground based interferometric radar which allows the monitoring of displacement in the line of sight with a resolution of mm.

Fields of Application:

High distance (≈ 1000 m) safety condition, thousands of measured points every five minutes. Velocity and displacement maps is the main output

Main Parameter	Unit of measure	Range of value
Distance from the slope	(m)	350 - 500
Antenna beam width	(deg)	> 70
Number of points	-	50.000
Range resolution	(m)	0.5
Cross range resolution	(mrad)	4.3
Scanning time	(min)	5

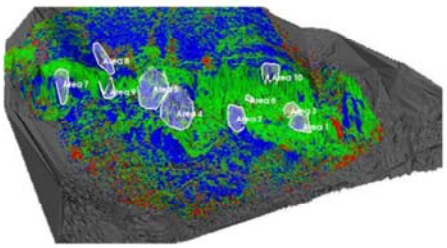

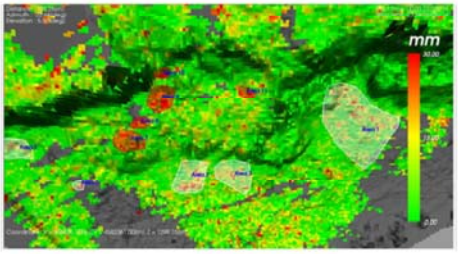

ISPRA
Istituto Superiore per la Protezione e la Ricerca Ambientale

Past event to calibrate the GBR system

ISPRA
Istituto Superiore per la Protezione e la Ricerca Ambientale

NATIONAL AGENCY FOR CULTURAL HERITAGE PRESERVATION OF GEORGIA

GBR calibration by back analysis on past event

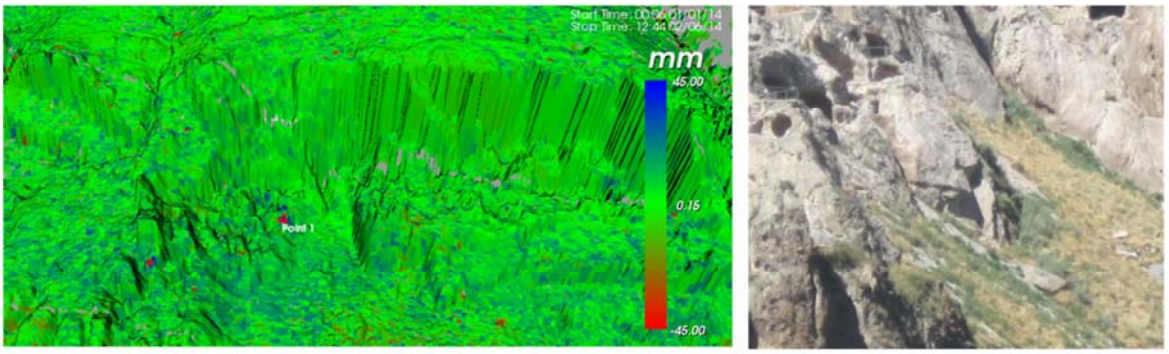

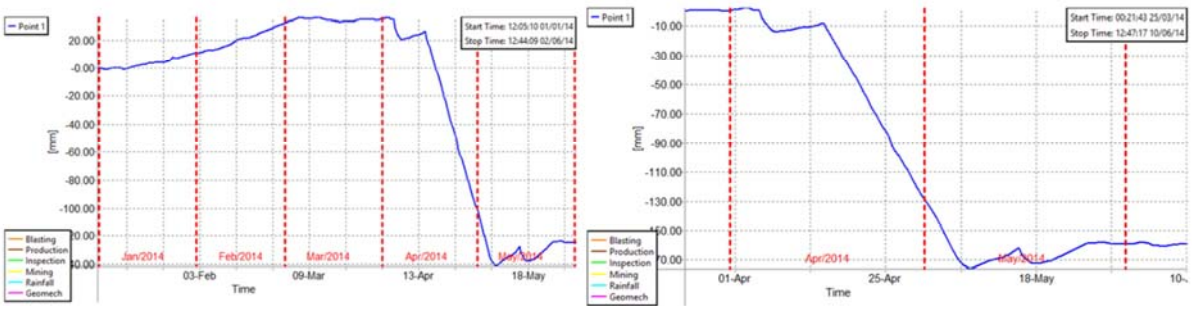

Rockfall 15-05-2014

ISPRA

NATIONAL AGENCY FOR CULTURAL HERITAGE PRESERVATION OF GEORGIA

GBR calibration by back analysis on past event

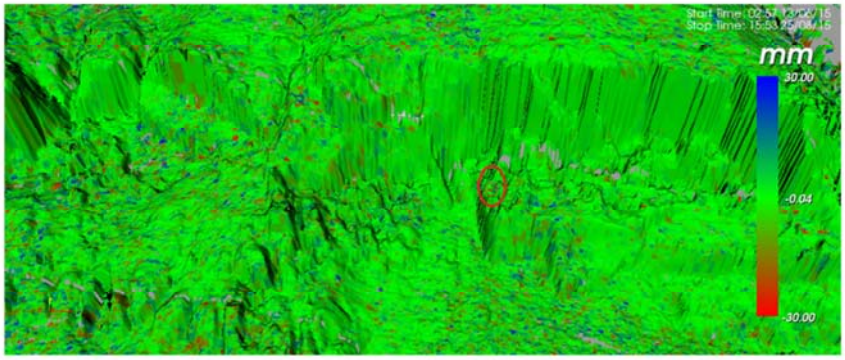

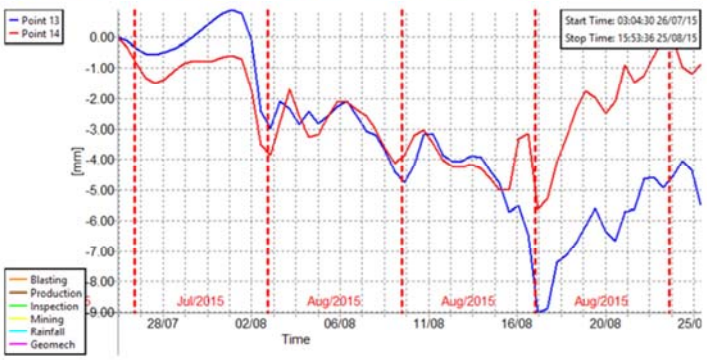

Rockslide 17-08-2015

ISPRA

Mitigation measures master plan is constantly updated with monitoring results

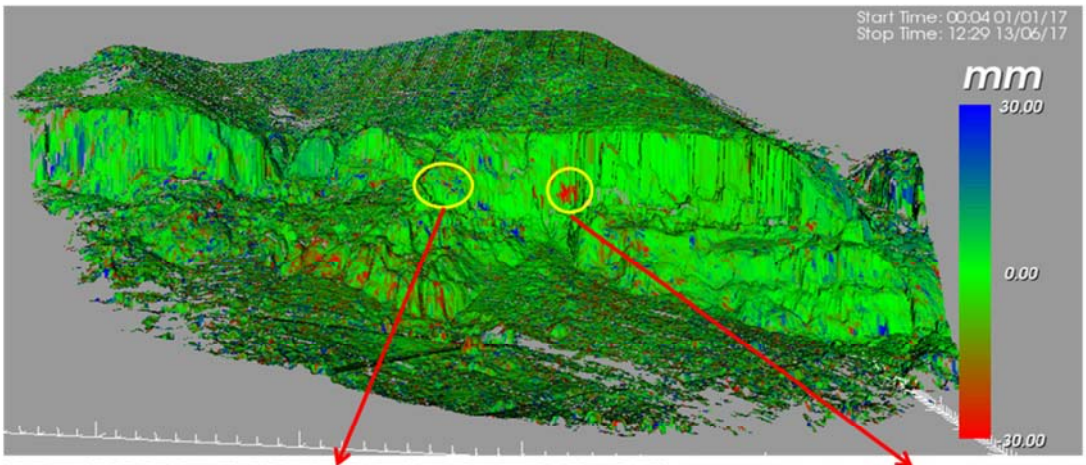

New critical area to mitigate 2018 - 2019

N.B.
For the block named Under the bridge the dowels should be realized using scaffolding or climbers.

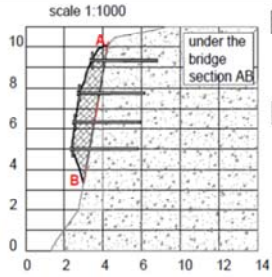

In this area the stabilization must be implemented with 4 dowels

In this area the stabilization must be implemented with small nails

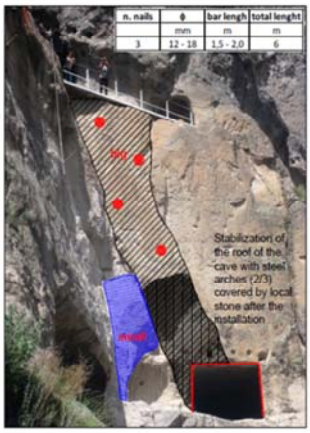

n. nails	ϕ	bar lengh	total lenght
	mm	m	m
3	12 - 18	1.5 - 2.0	6

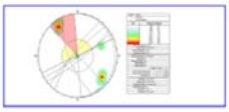

Area	Volume	n. bars	ϕ	bar lengh	total lenght	drill inclination
			mm	m	m	(°)
big	V1	4	28	4	16	5
small	V2	1	28	4	4	5

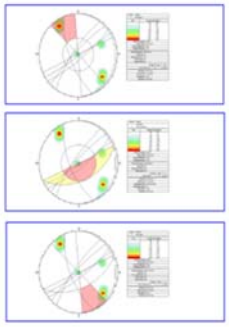

In this area the stabilization must be implemented with 4 dowels

In this area the stabilization must be implemented with small nails

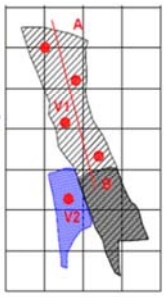

direct survey in the field 25-06-2017

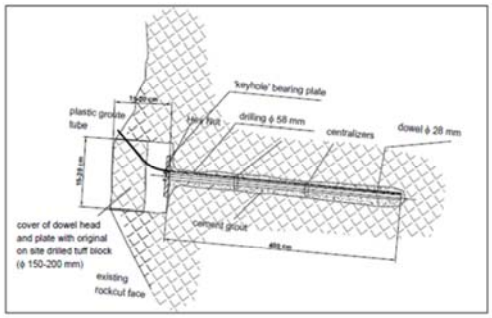

New critical area to mitigate 2018-2019

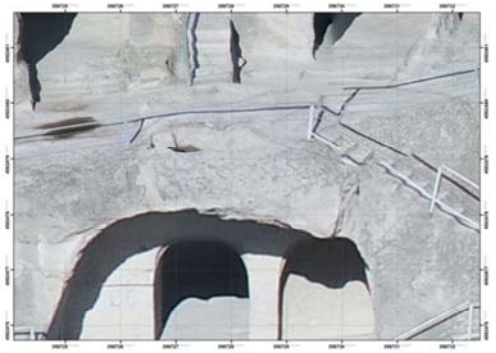

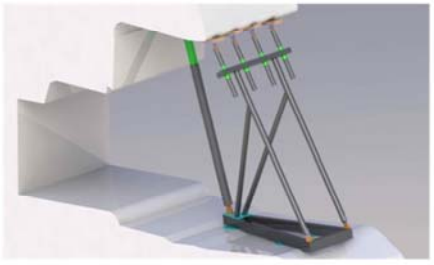

Temporary scaffolding to support unstable block before the final consolidation (anchors and passive bars – spring 2019)

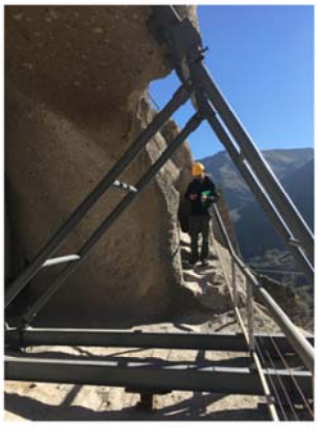

ISPRA

Network implementation 2018 Sept.-Nov.

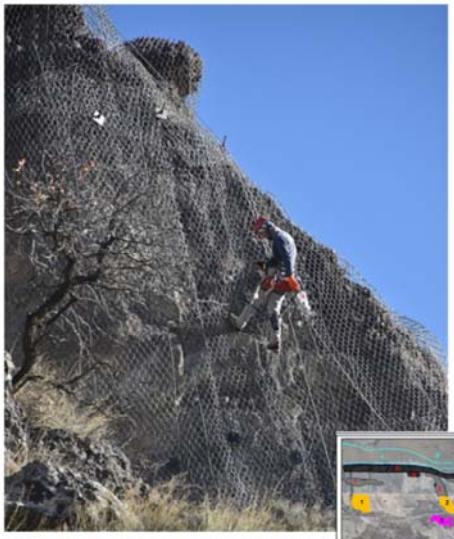

Network installation is constantly implemented every year with new portion of the cliff.

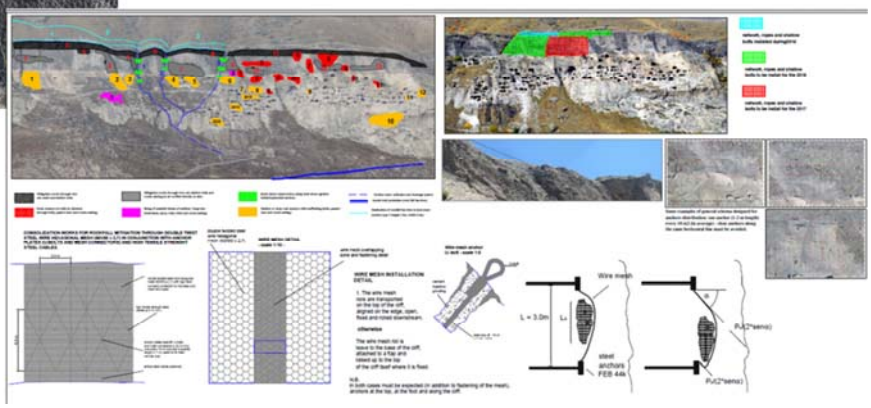

ISPRA

New 3D Rockfall modelling for the upper part

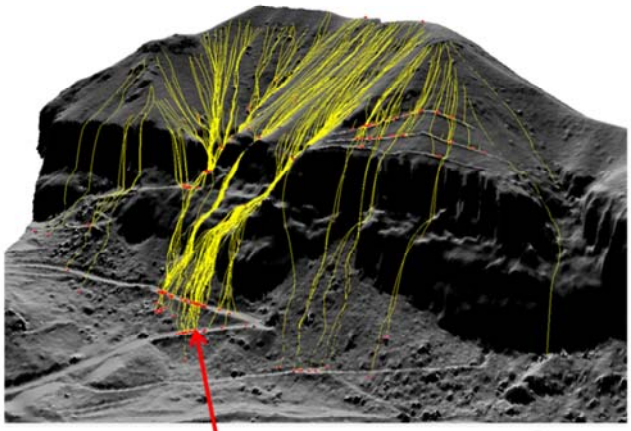

Dams and barriers were designed to control erosion and rock fall from upper part

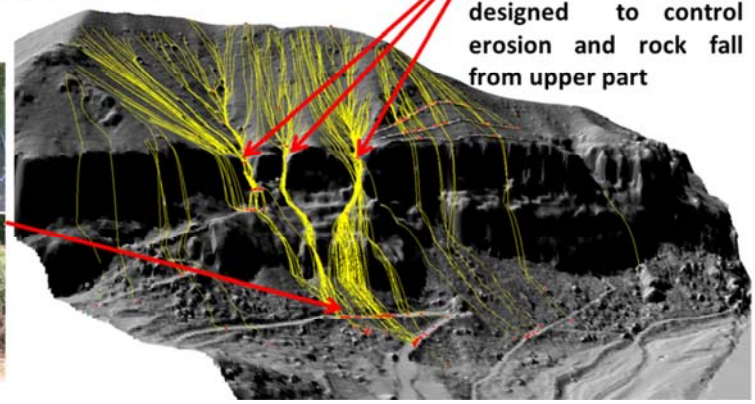

ISPRA

New 3D stability model to implement for the whole monastery

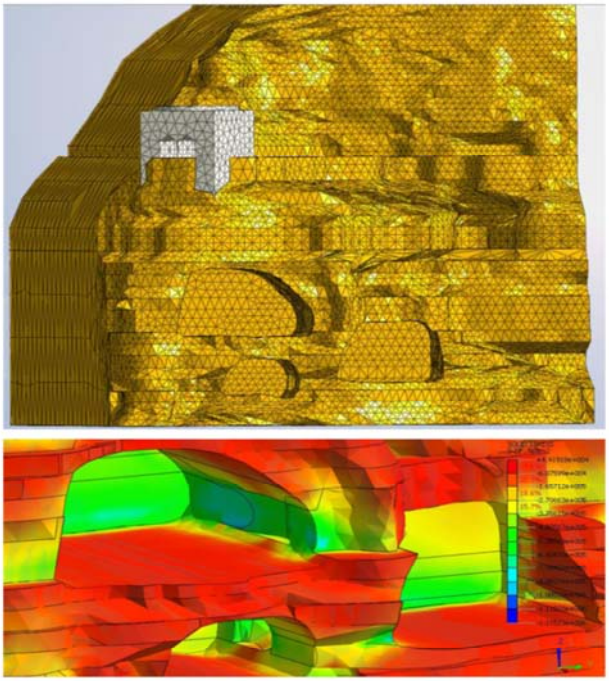

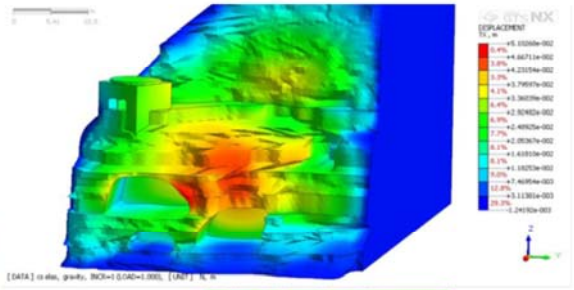

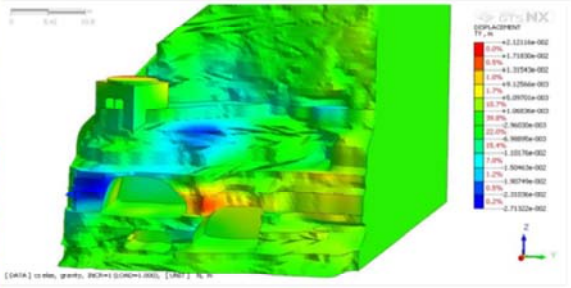

To verify stress condition inside the whole monastery and promote consolidation work for the caves and churches

UNIVERSITÀ DEGLI STUDI DI MILANO BICOCCA

ISPRA

NATIONAL AGENCY FOR CULTURAL HERITAGE PRESERVATION OF GEORGIA

Multi parametric in situ monitoring was installed by ILIA university the complex is under control H24

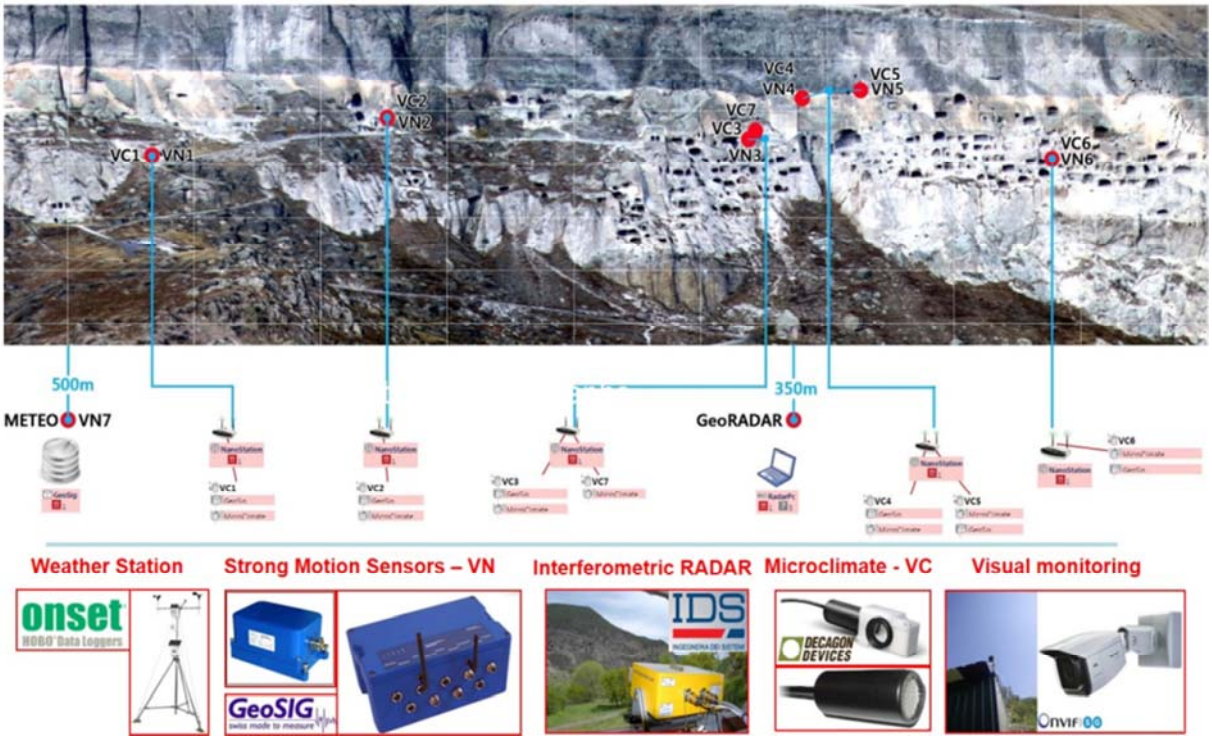

ISPRA

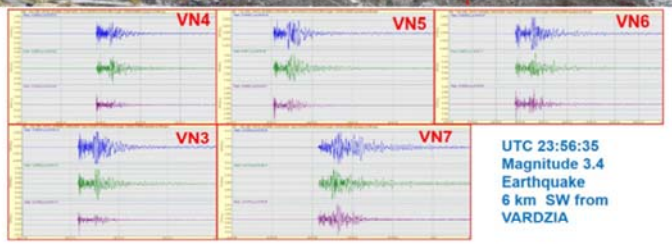

UTC 23:56:35
Magnitude 3.4
Earthquake
6 km SW from
VARDZIA

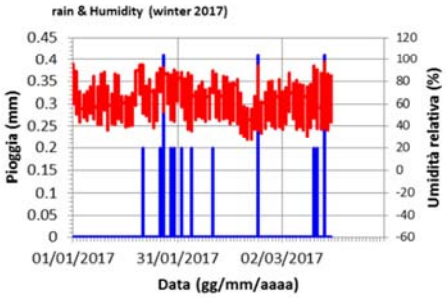

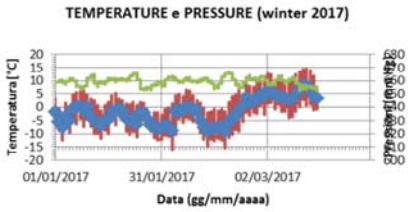

ISPRA

New monitoring system implementation 2018 - 2019

We are supporting Ilia University and the Agency for the implementation of the in situ monitoring. New sensor and new installation were adopted

ISPRA

Future prospective and challenges

Local Authority and University asked to adopt "The Vardzia integrated approach" in other Georgian CH sites affected and threaten by geo hazards

Vanis Kabebi Monastery

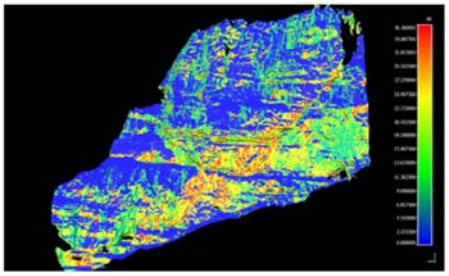
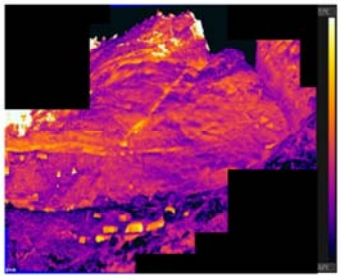

Uplistsikhe complex

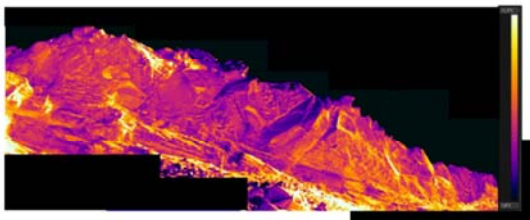
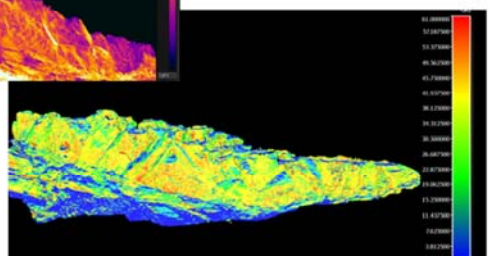

CONCLUSION

VARDZIA
A site at risk, for many kind of phenomena, with the combination of different predisposing factors such as: lithology, presence, frequency and orientation of discontinuities vs. slope orientation, physical and mechanical characteristics of materials, morphological and hydrological boundary conditions, seismic hazard

UNDERSTANDING PROCESSES
A large national and international effort, managed by the Georgian Agency for Cultural Heritage Conservation

MONITORING
The coupling of different survey techniques (e.g. 3D laser scanner, engineering geological and geomechanical field surveys, Ground based radar Interferometry); an international flagship in advanced technologies.

MITIGATION STRATEGIES AND IMPLEMENTATIONS
Establishing priorities, based on scientific processes and monitoring results. High attention will be paied to local knowledge and traditional expertise (UNESCO, 2014).

EO4GEO - Towards an innovative strategy for skills development and capacity building in the space geo-information sector supporting Copernicus User Uptake

Daniele Spizzichino(1), Luca Guerrieri (1), Gabriele Leoni, Valerio Comerci(1)

1) ISPRA - The Italian National Institute for Environmental Protection and Research
Via V. Brancati, 48 - 00144 ROMA; daniele.spizzichino@isprambiente.it

WHO WE ARE

EO4GEO is an Erasmus+ Sector Skills Alliance gathering 26 partners from 12 countries from academia, private and public sector active in the education/training and space/geospatial sectors.

EO4GEO Consortium

- GISIG (IT) (EO4GEO coordinator)
- KU Leuven (BE)
- PLUS (AT)
- UJI (ES)
- GEOF (HR)
- UPAT (GR)
- FSU-EO (DE)
- UT-ITC (NL)
- UNIBAS (IT)
- IGiK (PL)
- Planetek (IT)
- IGEA (SI)
- EPSIT (IT)
- NOVOGIT (SE)
- GIB (SE)
- Spatial Services (AT)
- CLIMATE-KIC (NL)
- EARSC (BE)
- ROSA (RO)
- UNEP-GRID (PL)
- NEREUS (BE)
- VITO (BE)
- CNR-IREA (IT)
- VRI IES (LV)
- ISPRA (IT)
- ALFA (IT)

EO4GEO Project
Towards an innovative strategy for skills development and capacity building in the space geo-information sector supporting Copernicus User Uptake

Duration: 4 years from January the 1st, 2018
Budget: 3,85 M€

Partnership: (from 16 EU Countries),
26 organisations + 22 (initially) Associated Partners from Academia, Companies and networks, many of them Members of the Copernicus Academy Network

Addressed Copernicus Areas:
Integrated Applications, Smart Cities, Climate Change

WHY EO4GEO

The space/geospatial sector is of strategic importance since it already provides support to many worldwide, European, national and sub-national policy domains. However, **data and services are still used in a sub-optimal way**.

Especially the uptake of existing data and services and their integration in added value services for government, business and citizens could be improved a lot.

Several studies have revealed that the **lack of specialized technical and scientific skills** impedes this uptake by private companies and other actors. Moreover there is also a **gap between the offerings** of academic and of vocational education and training at both universities and private companies, **and what is needed** to make this uptake happen fluently.

ISPRA
Istituto Superiore per la Protezione e la Ricerca Ambientale
Sistema Nazionale per la Protezione dell'Ambiente
eo4geo
IPL
ICL

OBJECTIVES

EO4GEO aims to help bridging the skills gap between supply and demand of education and training in the **space/geospatial sector** by reinforcing the existing ecosystem and fostering the uptake and integration of space/geospatial data and services in end-user applications.

STRATEGY

EO4GEO will work in an multi- and interdisciplinary way and apply innovative solutions for its education and training actions including: **case based and collaborative learning scenarios**; learning-while-doing in a living lab environment; on-the-job training; the co-creation of knowledge, skills and competencies; etc.

EO4GEO will define a **long-term and sustainable strategy** to fill the gap between supply of and demand for space/geospatial education and training taking into account the current and expected technological and non-technological developments in the space/geospatial and related sectors (e.g. ICT).

OUTCOMES

- Creation and maintenance of an ontology-based **Body of Knowledge for the space/geospatial sector** based on previous efforts;
- Design and development of a series of **curricula and a rich portfolio of training modules** directly usable in the context of Copernicus and other relevant programme;
- Development of a dynamic **collaborative platform** with associated **open tools**;
- Conduct a series of **training actions** for a selected set of scenario's in three sub-sectors – integrated applications, smart cities and climate change to test and validate the approach.

PROJECT WORKPLAN

Scientific and Technical (WP1-2-3) ;
Education and Training (WP4-5)
Exploitation (WP6)
Dissemination (WP7)
Management, Quality, Evaluation (WP8-9-10)

ISPRA will be involved especially in the WP5

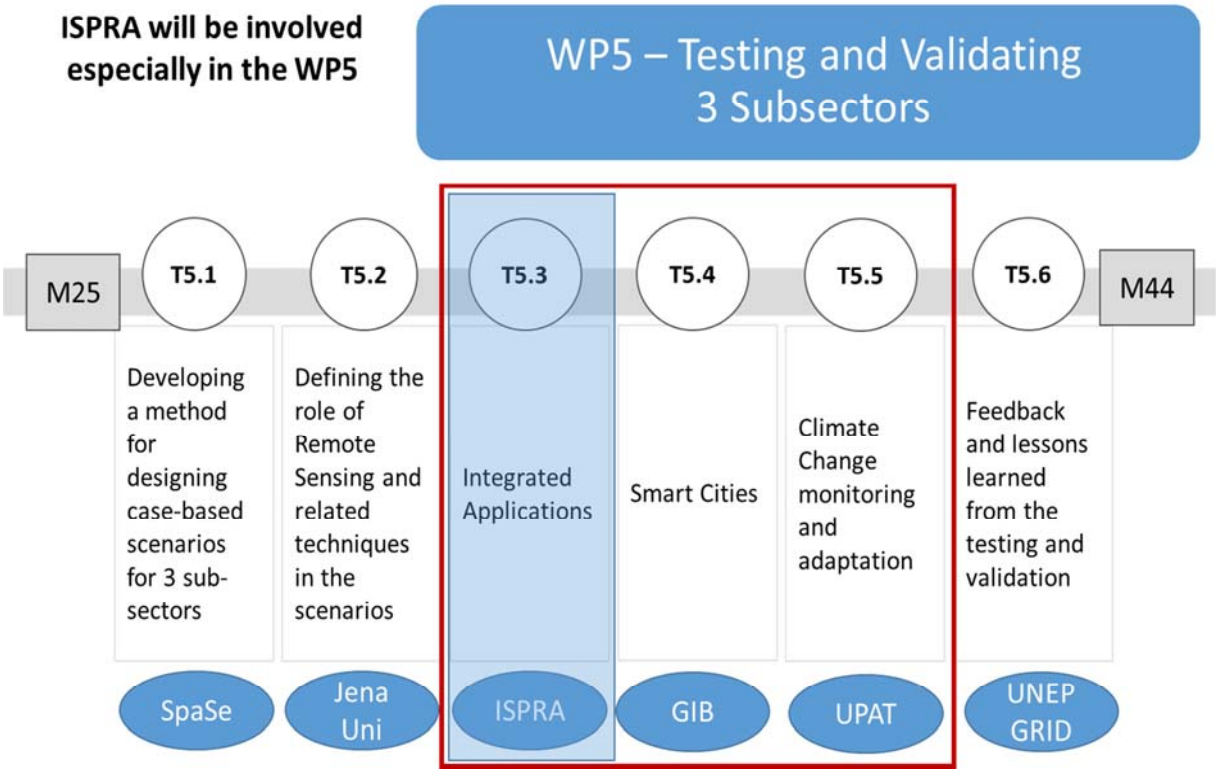

More in detail ISPRA research team will:

prepare and circulate among partners a list of potential integrated applications of satellite monitoring (at least 10) using open platforms (e.g. Copernicus) in the field of geo-hazard monitoring.

Among them, we preliminary propose a PS monitoring focused on (list not exhaustive):

- Landslides affecting linear infrastructures;
- Landslides affecting cultural heritage sites;
- Landslide and subsidence phenomena in urban areas ;

We propose to select 2-3 tutorials of integrated applications.

Successively, we will identify:

- the communities of users towards we will address the training;
- the proper training tool (e.g. workshop, internships, exchange programs among experts).

Landslides & Linear Infrastructures
EO-Geohazard

Topic

Application of satellite PSInSAR techniques to monitor landslide hazard affecting linear infrastructures

Spatial context (local, regional, national)

Local

Actors

- *data providers (ESA, ASI);*
- *data processing (private companies, SMEs, academic and research institutes);*
- *data interpretation (public bodies and local authorities)*

Political/socio-economic impact

Public safety, land planning, infrastructures management

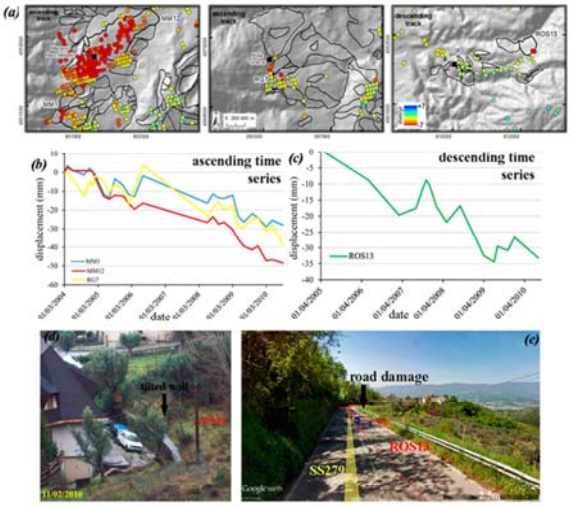

References: Giuseppe Cianflone , Cristiano Tolomei , Carlo Alberto Brunori, Stephen Monna and Rocco Dominici , 2018. Landslides and Subsidence Assessment in the Crati Valley (Southern Italy) Using InSAR Data. Geosciences

Ground Motion & Cultural Heritage
EO-Geohazard

Topic

Application of satellite PSInSAR techniques to monitor ground deformation affecting Cultural Heritage

Spatial context (local, regional, national)

Local to regional (High and low res data)

Actors

- *data providers (ESA, ASI);*
- *data processing (private companies, SMEs, academic and research institutes);*
- *data interpretation (academic and research institutes, public bodies and local authorities)*
- *Site manager and policy makers*

Political/socio-economic impact

Conservation, protection and exploitation of CH

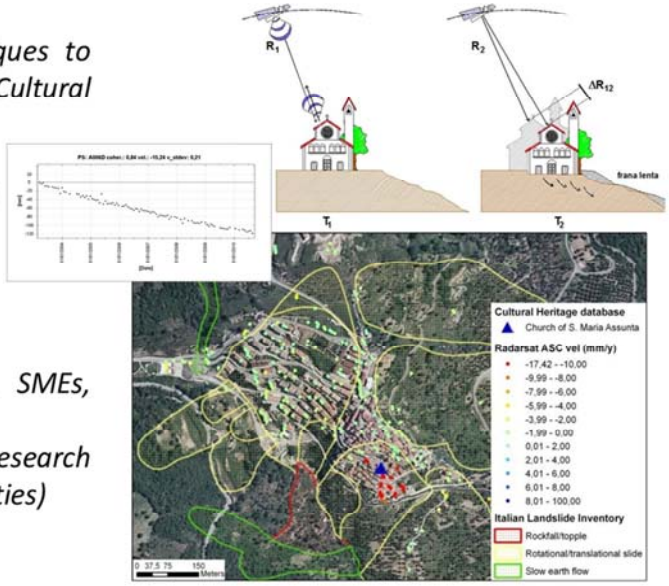

References: Iadanza C., Cacace C., Del Conte S., Spizzichino D., Cespa S., Trigila A. (2013) Cultural Heritage, Landslide Risk and Remote Sensing in Italy. In: C. Margottini et al. (eds.), Landslide Science and Practice, Vol. 6, Springer

Landslide and Subsidence Hazard
EO-Geohazard

Topic

Application of PSInSAR techniques to monitor land subsidence hazard affecting a city/town. Production of hazard maps indicating the city/town zones affected by subsidence. Map of subsidence rates. Vulnerability map of infrastructures and building stock

Spatial context (local, regional, national)

Local. City/town's zones affected by land subsidence

Actors

- *data providers: ESA (Sentinel data), ASI (CSK data);*
- *data processing (private companies, SMEs, academic and research institutes);*
- *data interpretation (academic and research institutes, Local Authorities,*
- *data end users: Local Authorities, Insurance companies, engineering firms, citizens, etc.*

Political/socio-economic impact

Public safety, land planning, infrastructures management, insurance policies

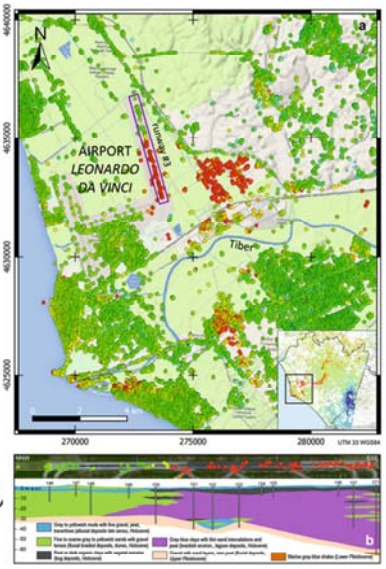

References: Comerci V., Vittori E., Cipolloni C., Di Manna P., Guerrieri L., Nisio S., Succhiarelli C., Ciuffreda M., Bertoletti E., 2015. *Geohazards Monitoring in Roma from InSAR and In Situ Data: Outcomes of the PanGeo Project.* Pure Appl. Geophys. 2015 Springer Basel

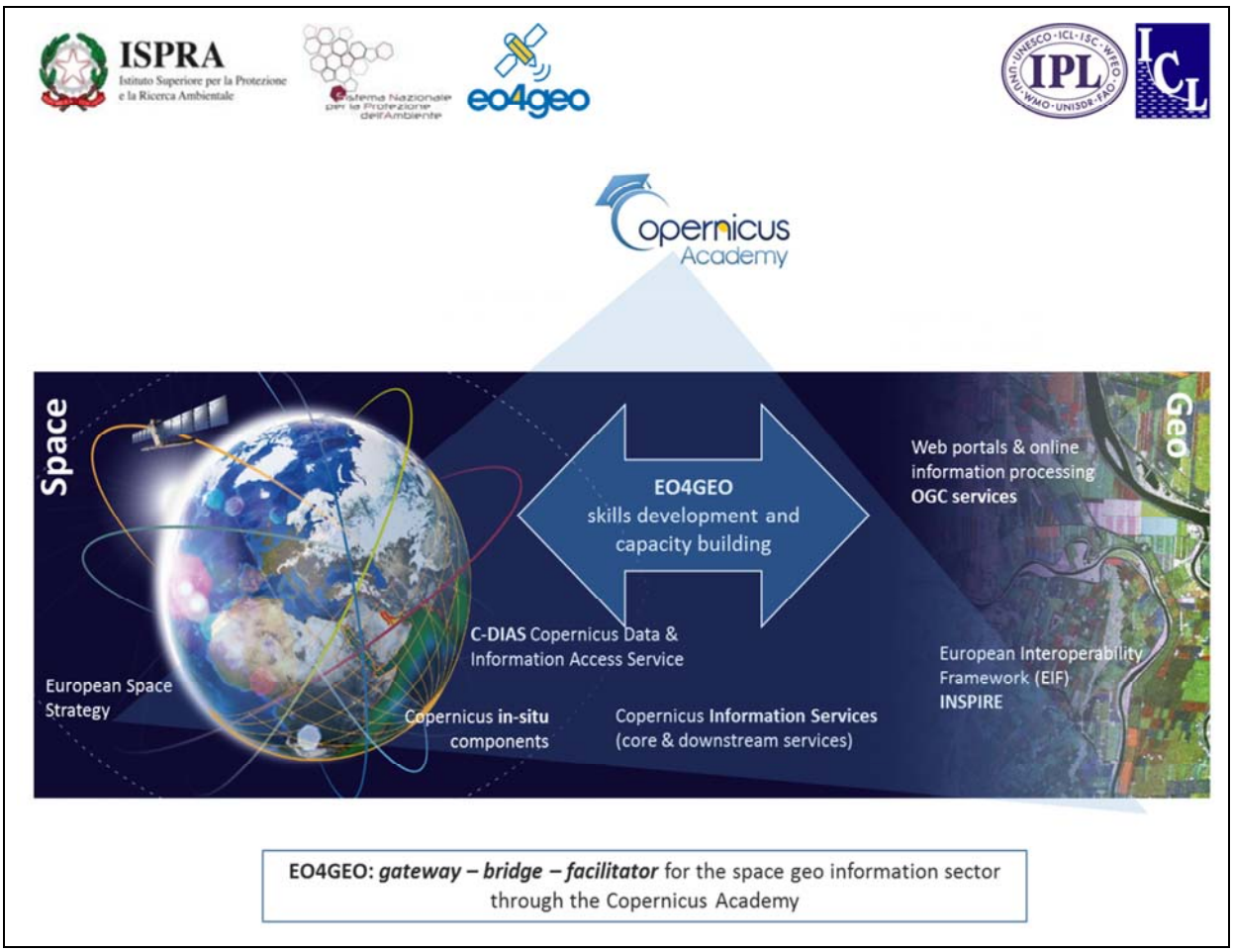
ISPRA
Istituto Superiore per la Protezione e la Ricerca Ambientale
Sistema Nazionale per la Protezione dell'Ambiente
eo4geo
IPL
Copernicus Academy
Space
Geo
EO4GEO
skills development and capacity building
Web portals & online information processing
OGC services
C-DIAS Copernicus Data & Information Access Service
European Space Strategy
Copernicus in-situ components
Copernicus Information Services (core & downstream services)
European Interoperability Framework (EIF)
INSPIRE
EO4GEO: gateway – bridge – facilitator for the space geo information sector through the Copernicus Academy

2018 ICL - IPL Conference
1-4 December 2018, Kyoto, Japan

CHALLENGES FOR OPERATIONAL FORECASTING AND EARLY WARNING OF RAINFALL INDUCED LANDSLIDES

Fausto Guzzetti
Istituto di Ricerca per la Protezione Idrogeologica
Consiglio Nazionale delle Ricerche

Abstract

In many areas, timely forecast of rainfall-induced landslides is of scientific interest and social relevance. Despite their relevance, only a few systems have been designed, and are operated. Inspection of the literature reveals that common criteria and standards for the design, the implementation, the operation, and the evaluation of the performances of the systems, are lacking. This limits the possibility to compare and to evaluate the systems critically, to identify their strengths and weaknesses and to improve their performance. The presentation focuses on regional to national-scale landslide forecasting systems, and specifically on operational systems based on rainfall thresholds. Building on the experience gained operating landslide forecasting systems in Italy, the contribution discusses concepts, limitations and challenges inherent to the design of reliable forecasting and early warning systems for rainfall-induced landslides, the evaluation of the performances of the systems, and on problems related to the use of the forecasts and the issuing of landslide warnings.

EARLY WARNING SYSTEM

Set of **capacities** needed to **generate** and **disseminate** timely and meaningful **warning information** to enable **individuals**, **communities** and **organizations** threatened by a hazard to **act appropriately** and in sufficient time to **reduce** the possibility of **harm** or **loss**.

UNISDR
United Nations Office for Disaster Risk Reduction

United Nations International Strategy for Disaster Reduction, 2009

ONE OR MANY LANDSLIDES

source: M. Reed, USGS

rainfall induced, Oso landslide, Washington, USA

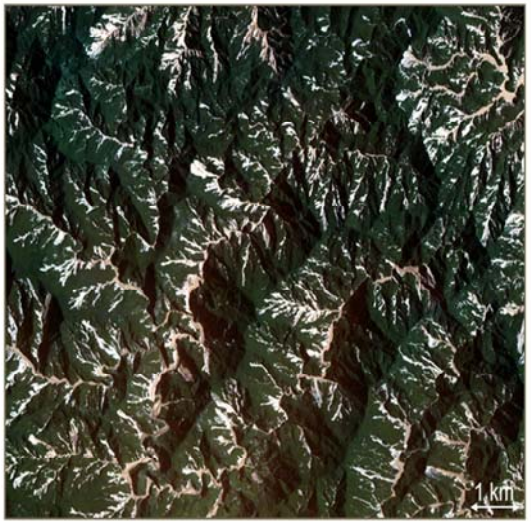

landslides caused by Typhoon Morakot, Taiwan

source: A.C. Mondini, CNR IRPI

OPERATIONAL LANDSLIDE EARLY WARNING

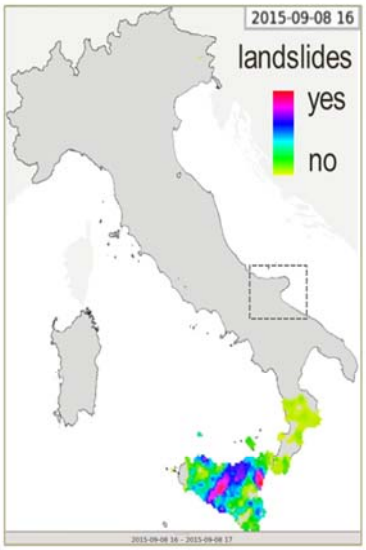

Italy, 8 Sep – 16 Oct, 2015

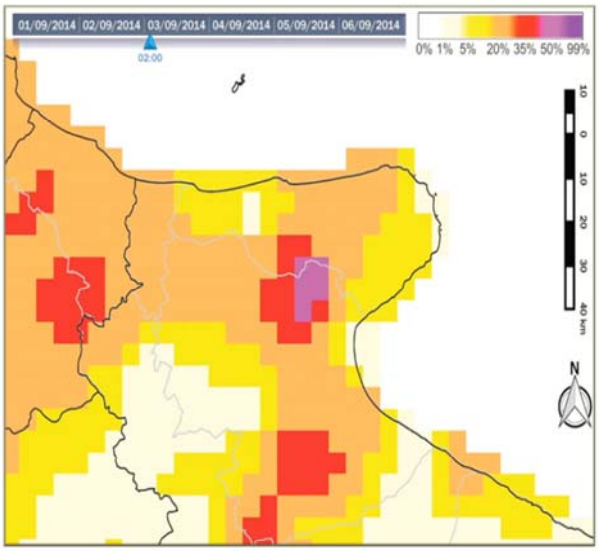

Gargano, Southern Italy, 2 – 6 Sep, 2014

OPEN ISSUES

- Quality of landslide and rainfall data
- Use of historical records
- Rainfall threshold modelling
- Integration of landslide susceptibility
- From forecasts to warnings
- Performance evaluation

LANDSLIDE & RAINFALL DATA

- How good is the **rainfall** and the **landslide** information?
- How can we check the **quality** of the information?

IS THE PAST A KEY TO THE FUTURE?

"Present-day measures and observations [...] may **add uncertainty** in the **prediction** of future trends"

Earth-Science Reviews

Is the present the key to the future?

Furlani & Ninfo (2015)

RAINFALL THRESHOLDS

- How **many** thresholds do we need?
- How do we **verify** the thresholds?
- How frequently should we **update** the thresholds?
- Is a threshold-based model **adequate**?

HOW MANY THRESHOLDS?

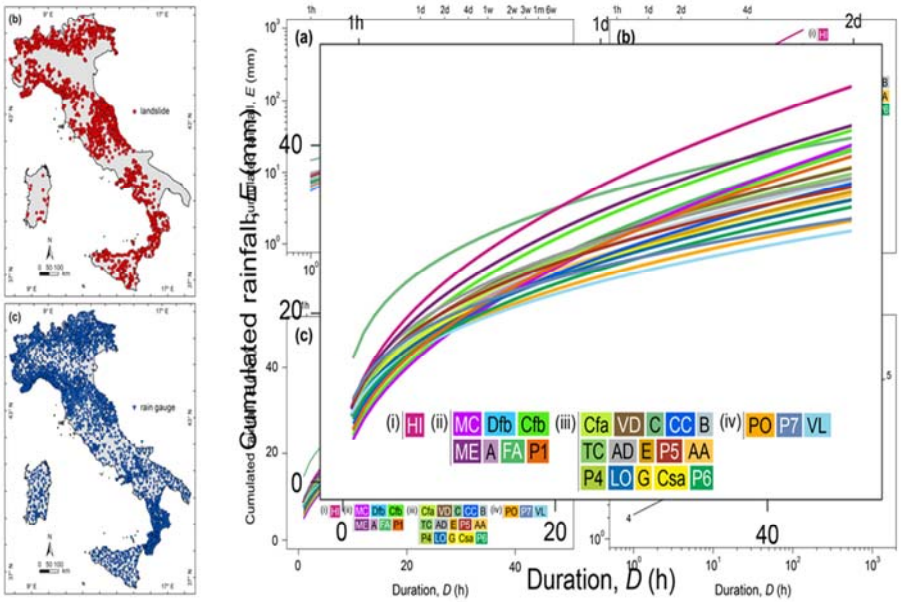

Peruccacci et al (2017)

SUSCEPTIBILITY

- How do we ascertain **susceptibility** for landslide forecasting and early warning?
- What is the **type** and **size** of an optimal **mapping unit**?
- How large is the area covered by the **susceptibility** zonation?

Reichenbach et al. (2018)

FROM FORECASTS TO WARNINGS

- How do we go from **forecasts** to **warnings**?
- How many **levels of warning** do we need?

FROM FORECASTS TO WARNINGS

Protocol to **define** and
issue warnings
in a threshold-based
regional landslide
early warning system

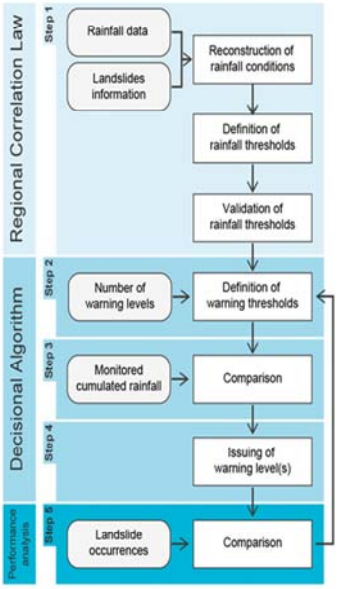

Piciullo et al (2016)

FORECAST EVALUATION

Lack of inform **dslides**
does not imply **curred.**

PREDICTED AND REPORTED ✓	PREDICTED BUT NOT REPORTED ?
NOT PREDICTED BUT REPORTED ✓	NOT PREDICTED AND NOT ?

Gariano et al (2015)

PERFORMANCE METRICS

Standard metrics used for forecast evaluation are **problematic** for the evaluation of **landslide forecasts**.

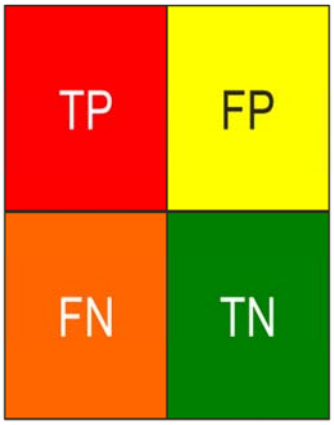

Gariano et al (2015)

FORECAST EVALUATION

all **52 fatal** rainfall-induced **landslides** in Italy from 1996 to 2014 were **hindcasted**

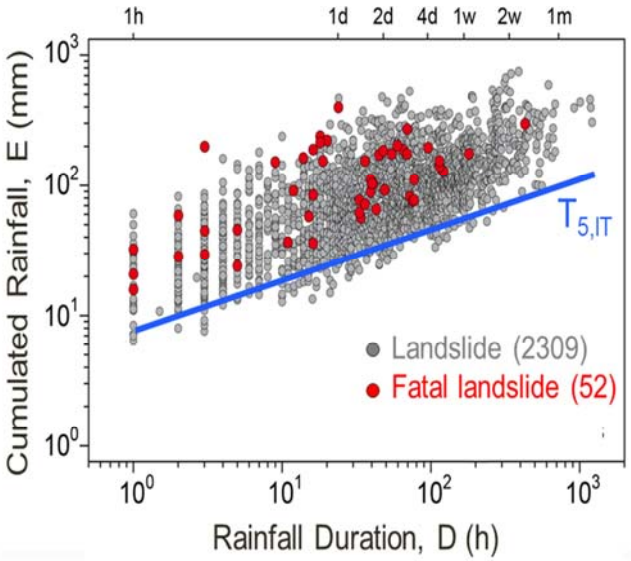

Peruccacci et al (2017)

PERFORMANCE

- How do we **measure** the system performance?
- What is an **acceptable** performance?
- Who **decides** on the performance?

TRANSPARENCY

- Should the system be **transparent** to the user?

LESSONS LEARNT

Operational forecasting of rainfall induced landslides:

- **is possible** and can **contribute** to **mitigate landslide risk**
- it remains a **difficult** and **uncertain** task

SCIENTISTS OR FORTUNE TELLERS?

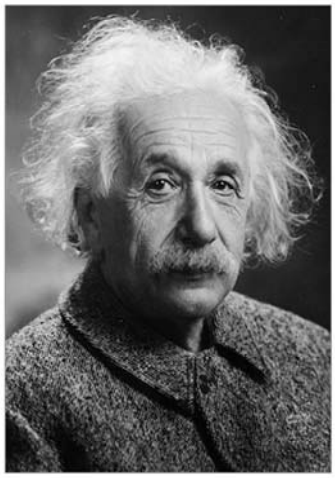

Albert **Einstein**
Physicist and Nobel laureate, 1922

Tiresia
Greek fortune teller

WORDS OF WISDOM

"Trying to predict the future is like trying to drive down a country road at night with no lights while looking out the back window"

Peter F. Drucker
Economist and writer

... THANK YOU!

Fausto.Guzzetti@irpi.cnr.it

2018 ICL - IPL Conference
1-4 December 2018, Kyoto, Japan

LANDSLIDES AND CLIMATE AND ENVIRONMENTAL CHANGES ADVANCES & PERSPECTIVES

Stefano Luigi Gariano & Fausto Guzzetti
Istituto di Ricerca per la Protezione Idrogeologica
Consiglio Nazionale delle Ricerche

Abstract

Landslides represent a serious threat to the population, causing fatalities and economic damages. Among different phenomena causing landslides, rainfall and temperature are influenced by climate and its variations. Consequently, climate changes influence slope stability at different temporal and geographical scales. In addition, environmental changes (e.g. land use) affect landslide predisposing conditions.

The presentation analyses the different approaches (retrospective and prospective) proposed by many scientists in the last years to analyse the effects of climate and environmental changes on landslides. Despite the influence of these changes on slope failures is quite undisputable, the evaluation of the type, extent, and directions of variations in landslide occurrence, frequency, hazard, and risk (to the population) are still debated.

The modelling results of landslide-climate studies depend more on the emission scenarios, the general circulation models, and the methods to downscale the climate variables, than on the description of the variables controlling slope processes. However, the adoption of sufficiently long data series and of ensembles of projections based on a range of emissions scenarios are becoming common in retrospective and prospective approaches, respectively. As best practice, the identification of the uncertainties in the projections must be quantified and communicated to decision makers and the public.

GLOBAL DISASTERS

7255 disasters occurred globally from 1998 to 2017

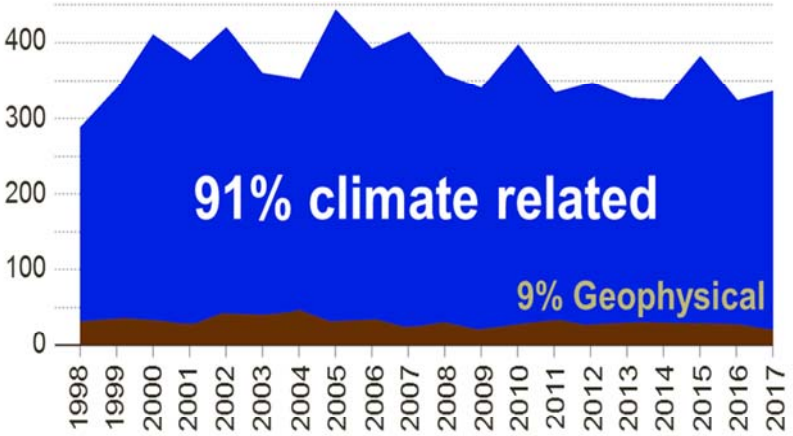

Landslides 5.4%

5 million persons affected

UNISDR | Wallemacq & House (2018)

CLIMATE

Global warming is **unequivocal**.

2007 2012 2014 2018

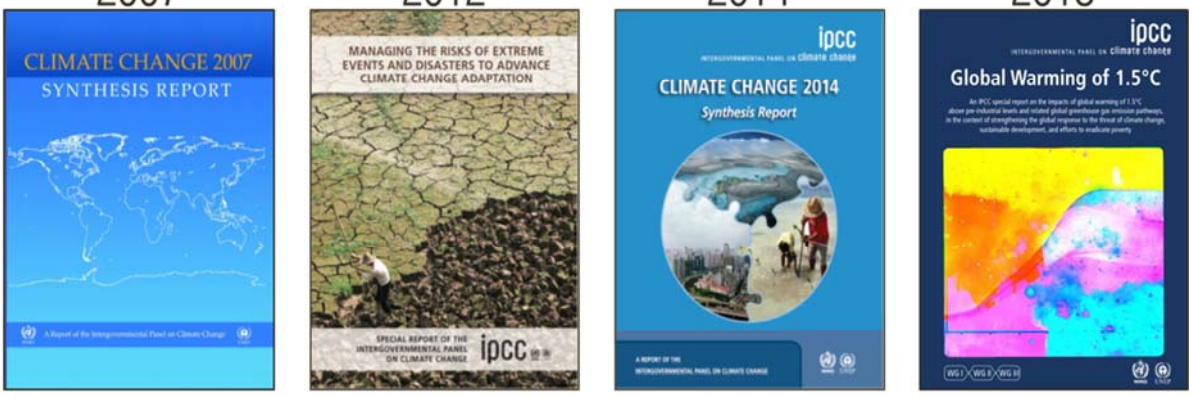

IPCC 2007, IPCC 2012, IPCC 2014, IPCC 2018

CLIMATE & GEO-HYDROLOGICAL HAZARDS

Global warming is unequivocal,

… but the effects on geo-hydrological hazards remain difficult to determine and to predict.

Gariano & Guzzetti (2016)

CLIMATE & GEO-HYDROLOGICAL HAZARDS

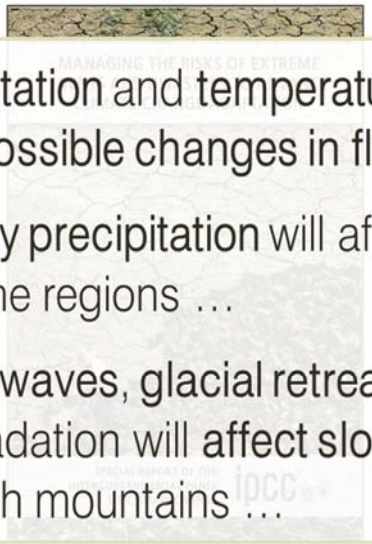

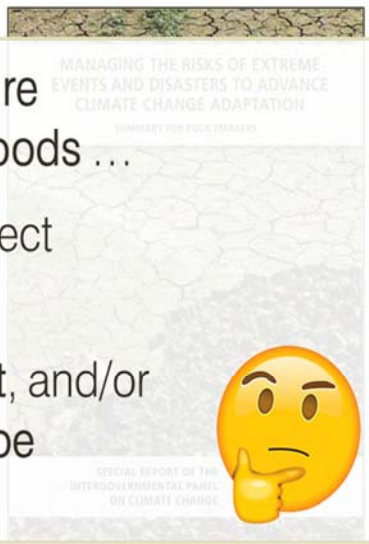

- Projected **precipitation** and **temperature changes** imply **possible changes in floods** …
- Changes in **heavy precipitation** will affect **landslides** in some regions …
- Changes in **heat waves**, **glacial retreat**, and/or **permafrost** degradation will **affect slope instabilities** in high mountains …

IPCC (2012)

IPCC (2012)

GLOBAL LANDSLIDE FATALITIES

55,997 fatalities caused by **4862 landslides** in the **13-year** period **2004 - 2016**.

map shows
non seismically triggered landslides

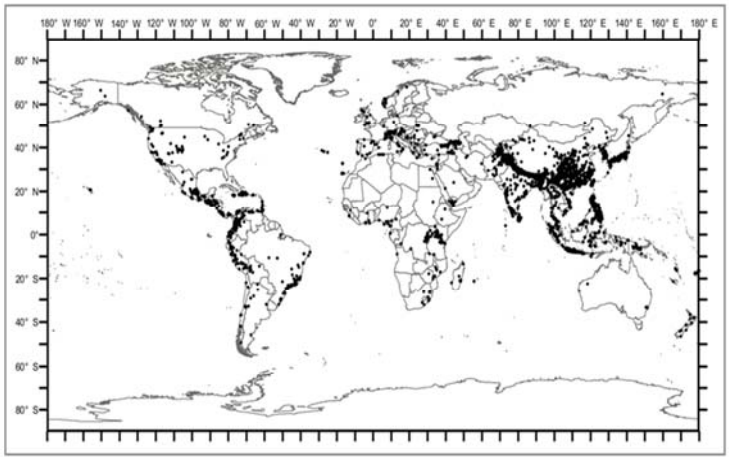

Froude & Petley (2018)

CHANGES IN LANDSLIDE RISK

To what extent **landslide risk** to the population **will change** in response to the expected **climate** and **environmental changes**?

LANDSLIDE VARIABILITY

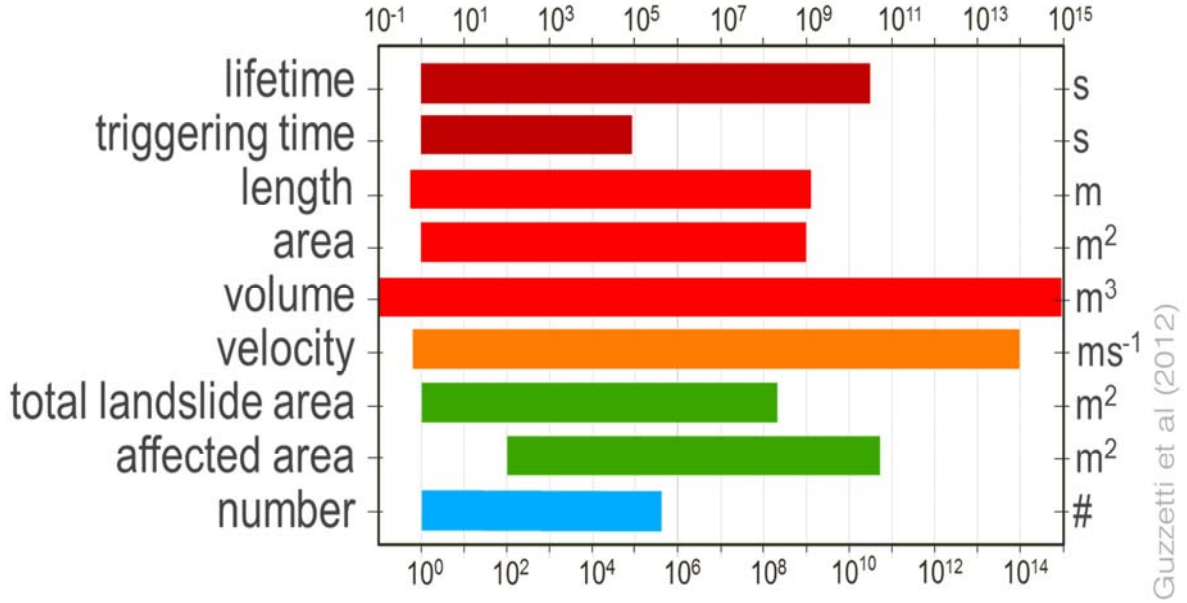

LANDSLIDE & CLIMATE VARIABILITY

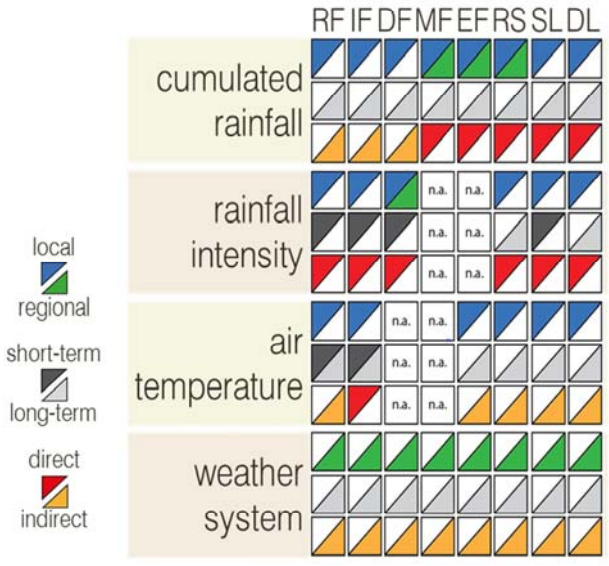

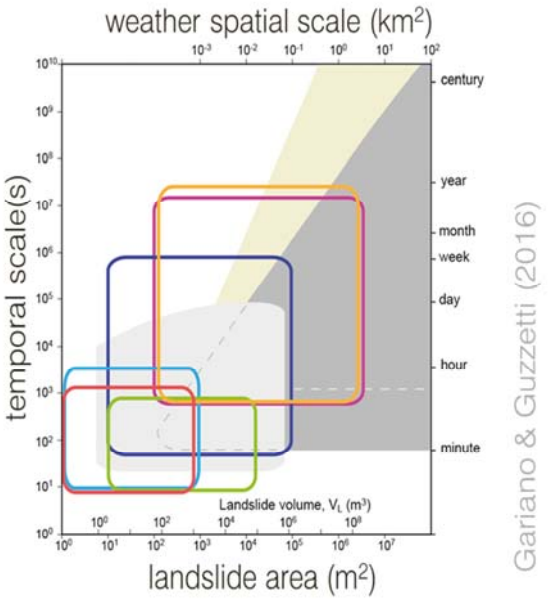

LANDSLIDES & CLIMATE STUDIES

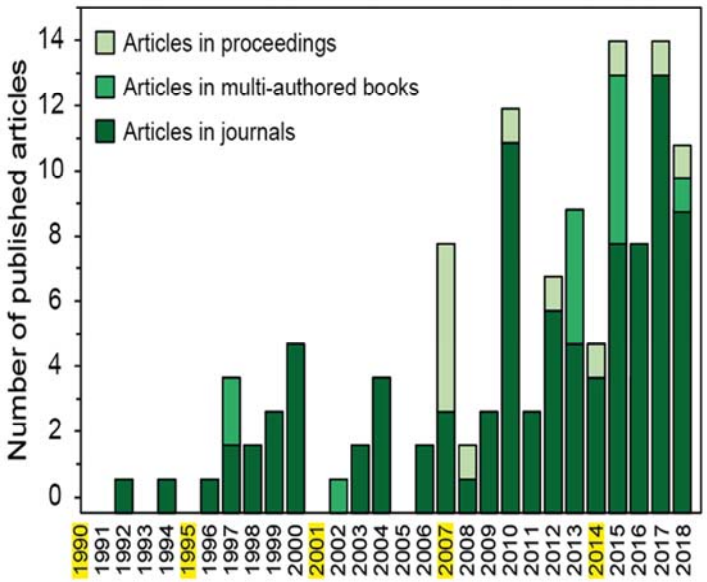

modified after: Gariano & Guzzetti (2016)

LANDSLIDES & CLIMATE STUDIES

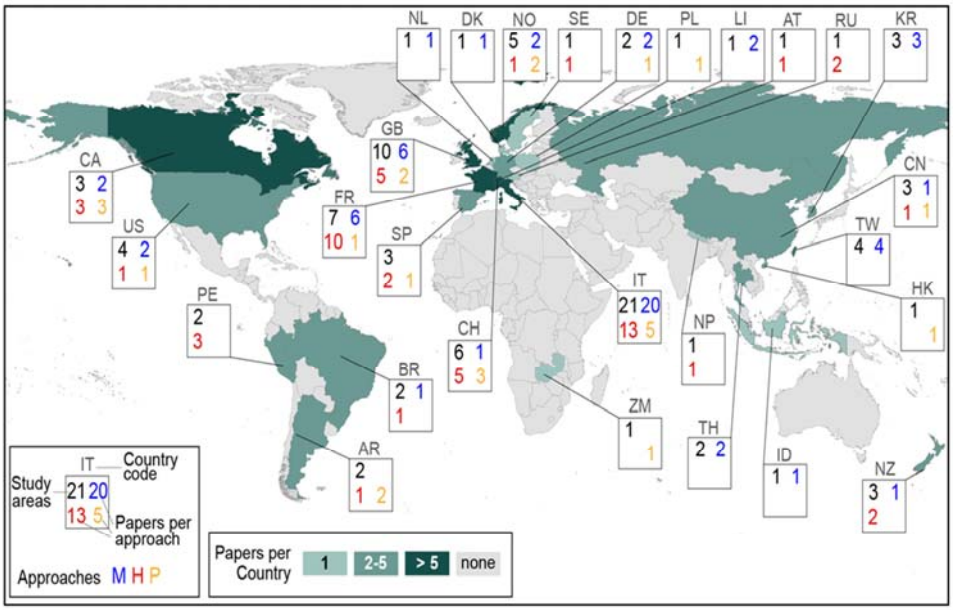

modified after: Gariano & Guzzetti (2016)

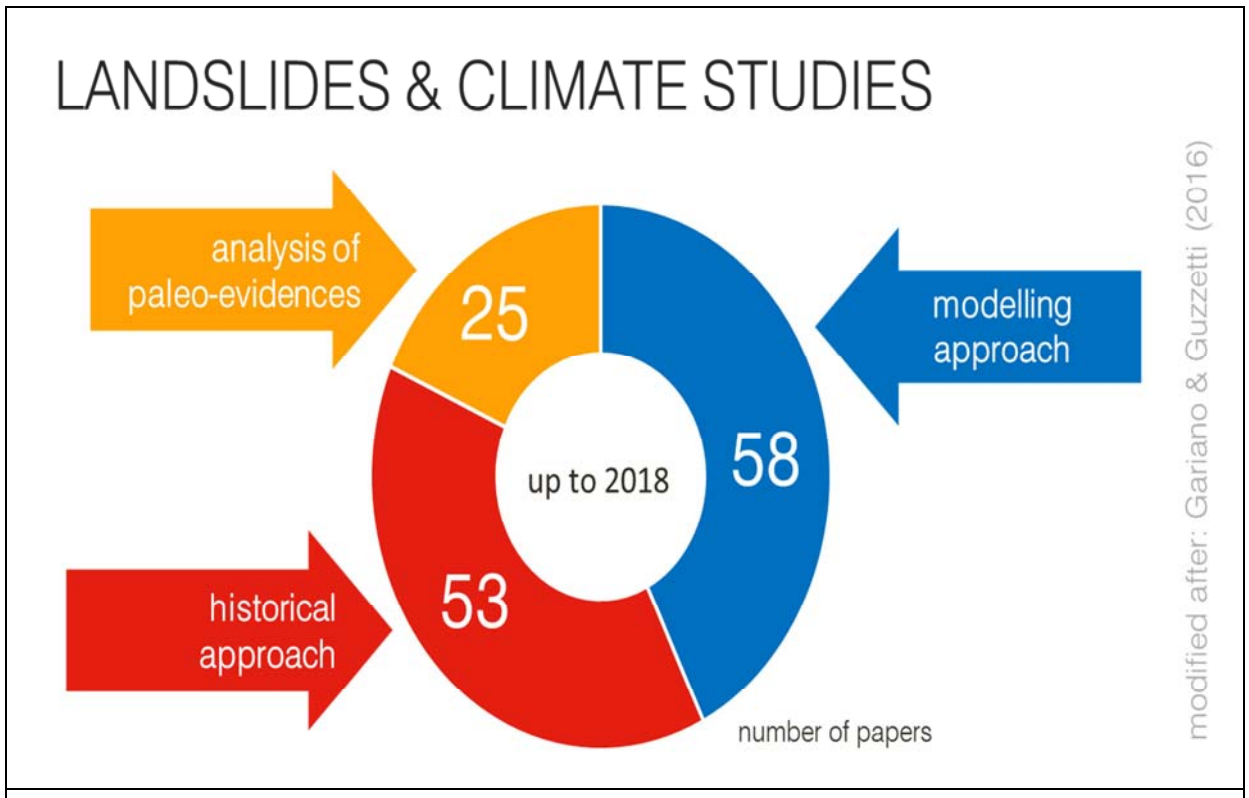
LANDSLIDES & CLIMATE STUDIES
analysis of paleo-evidences
25
modelling approach
58
up to 2018
historical approach
53
number of papers
modified after: Gariano & Guzzetti (2016)

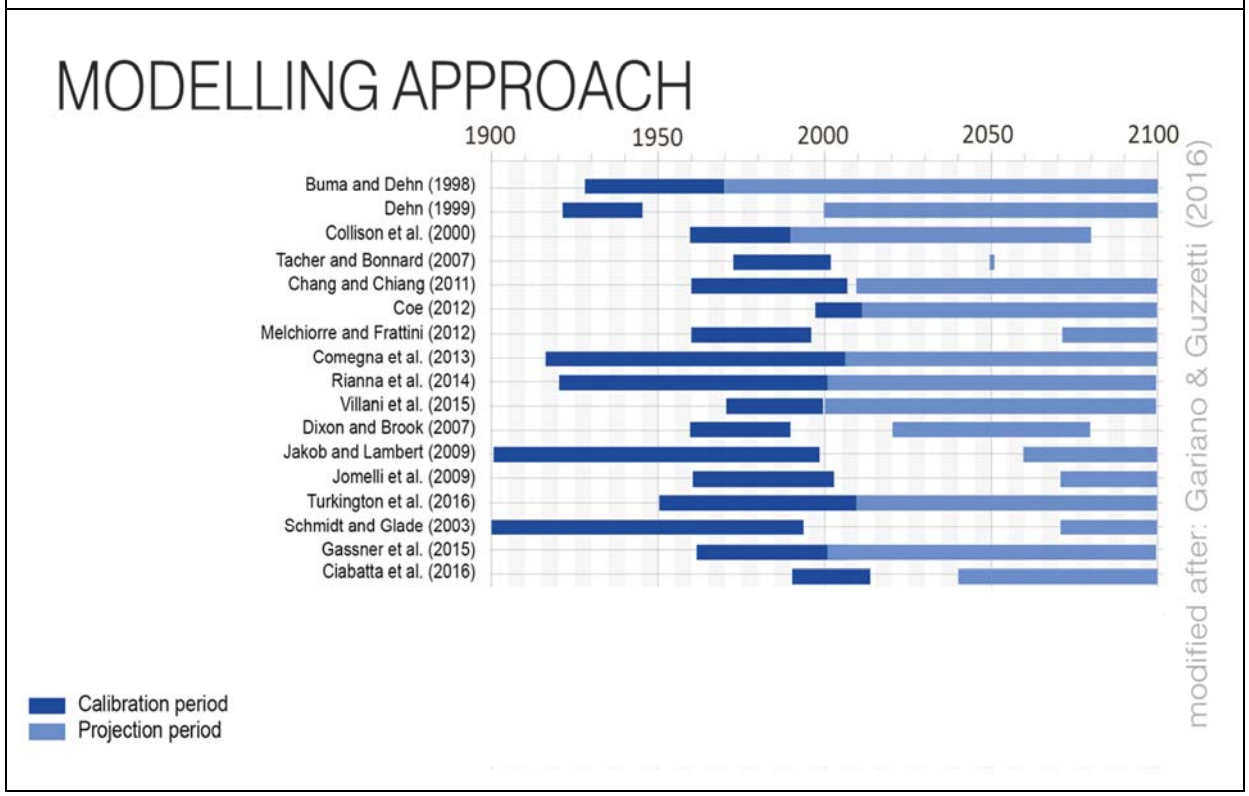
MODELLING APPROACH
1900
1950
2000
2050
2100
Buma and Dehn (1998)
Dehn (1999)
Collison et al. (2000)
Tacher and Bonnard (2007)
Chang and Chiang (2011)
Coe (2012)
Melchiorre and Frattini (2012)
Comegna et al. (2013)
Rianna et al. (2014)
Villani et al. (2015)
Dixon and Brook (2007)
Jakob and Lambert (2009)
Jomelli et al. (2009)
Turkington et al. (2016)
Schmidt and Glade (2003)
Gassner et al. (2015)
Ciabatta et al. (2016)
Calibration period
Projection period
modified after: Gariano & Guzzetti (2016)

MODELLING FRAMEWORK

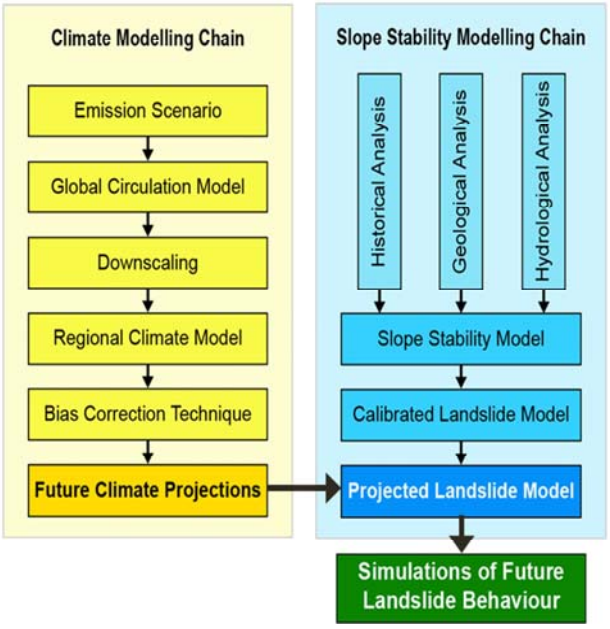

Gariano & Guzzetti (2016)

EMPIRICAL APPROACH

Catalogue of 603 rainfall-induced landslides from 1981 to 2010

2 Climate Variables:
- Mean Annual Rainfall
- Seasonal Cumulative Rainfall

Climate projections (2036–2065) RCP4.5 and RCP8.5 IPCC scenarios

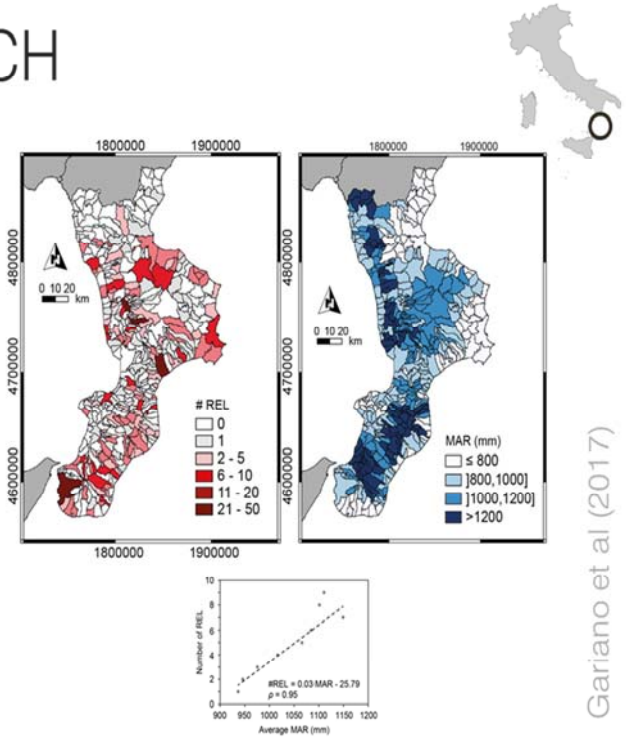

Gariano et al (2017)

EMPIRICAL APPROACH

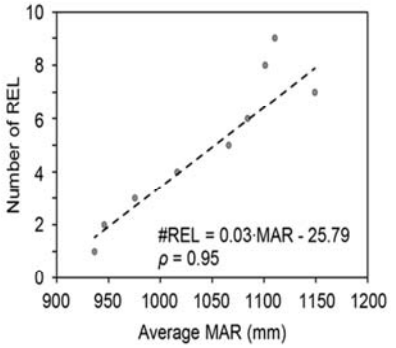

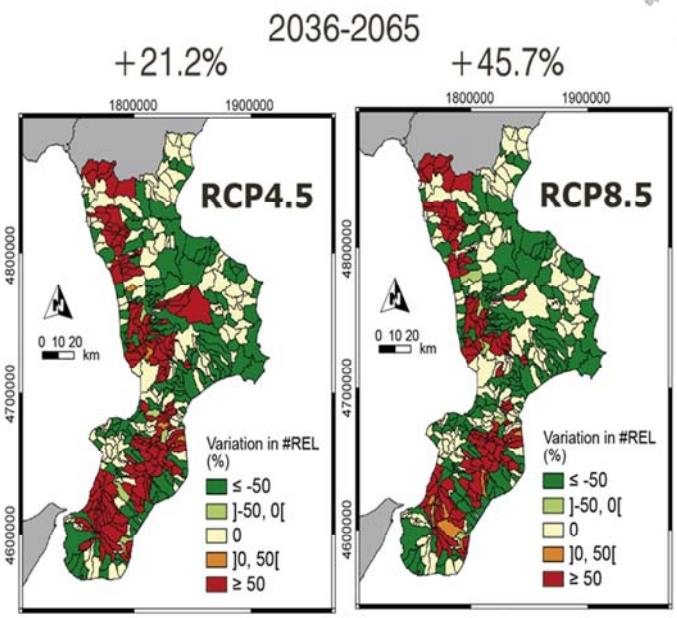

Gariano et al (2017)

PHYSICALLY-BASED APPROACH

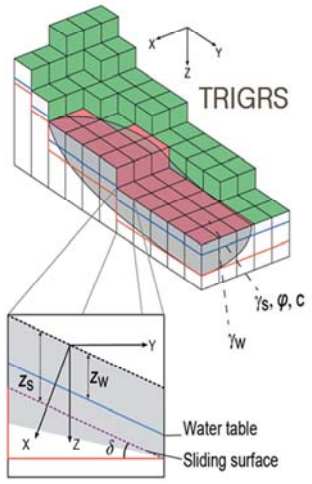

$$FS = \frac{R}{D} = \frac{tan(\varphi)}{tan(\delta)} + \frac{c - \psi \cdot \gamma_w \cdot tan(\varphi)}{\gamma_s \cdot z_s \cdot sin(\delta) \cdot cos(\delta)}$$

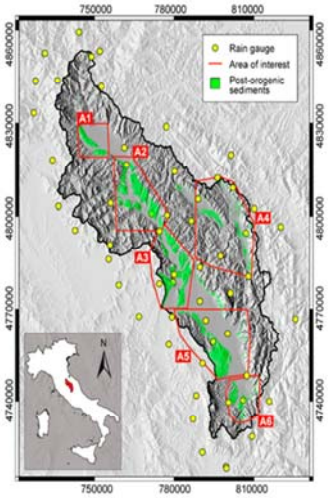

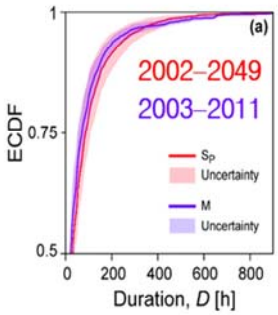

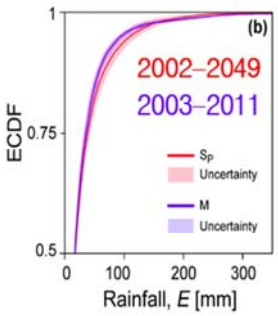

Alvioli et al (2018)

PHYSICALLY-BASED APPROACH

the distribution of landslide **areas** will **not change**

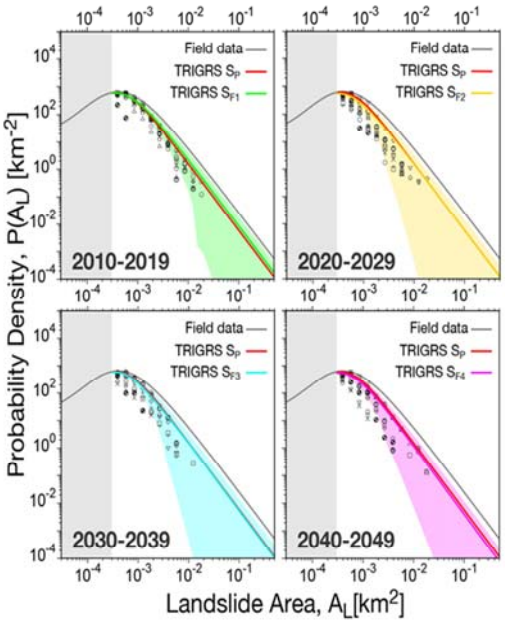

Alvioli et al (2018)

PHYSICALLY-BASED APPROACH

rainfall **thresholds** for landslide initiation will **change**

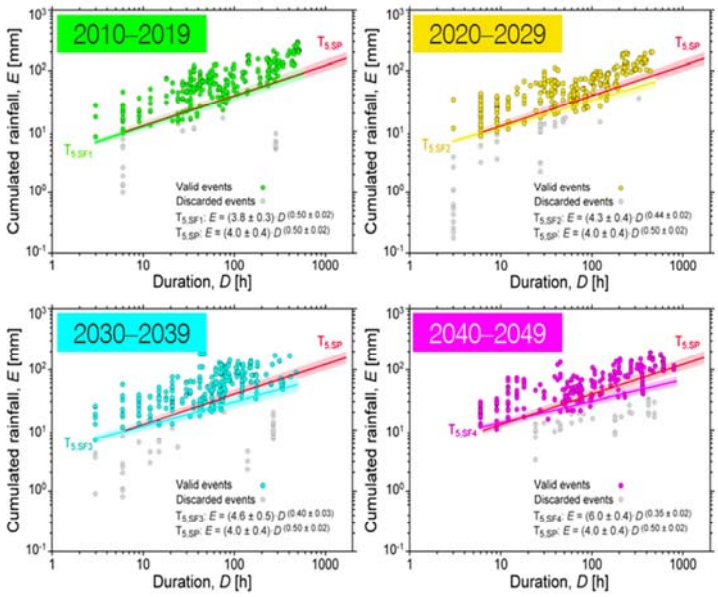

Alvioli et al (2018)

CLIMATE & GEO-HYDRO HAZARDS

Global warming is **unequivocal**, but the effects […] on **geo-hydrological hazards** remain difficult to determine and to predict.

Gariano & Guzzetti (2016)

CLIMATE & GEO-HYDRO HAZARDS

Global warming is **unequivocal**, but the effects […] on **geo-hydrological hazards** remain difficult to determine and to predict.

There is a need to **understand** and **measure** how climate-related variables and their variability affect **landslides**.

WHAT SHOULD WE DO?

Enhance the **modelling** capabilities

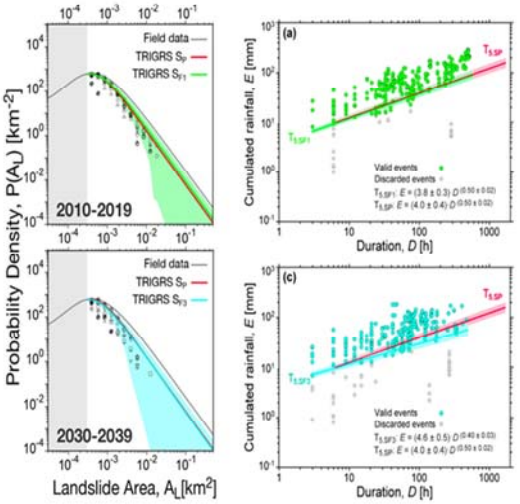

Alvioli et al (2018)

WHAT SHOULD WE DO?

More **regional** to global studies to assess the effects of the projected **climate and environmental changes** on **landslides**

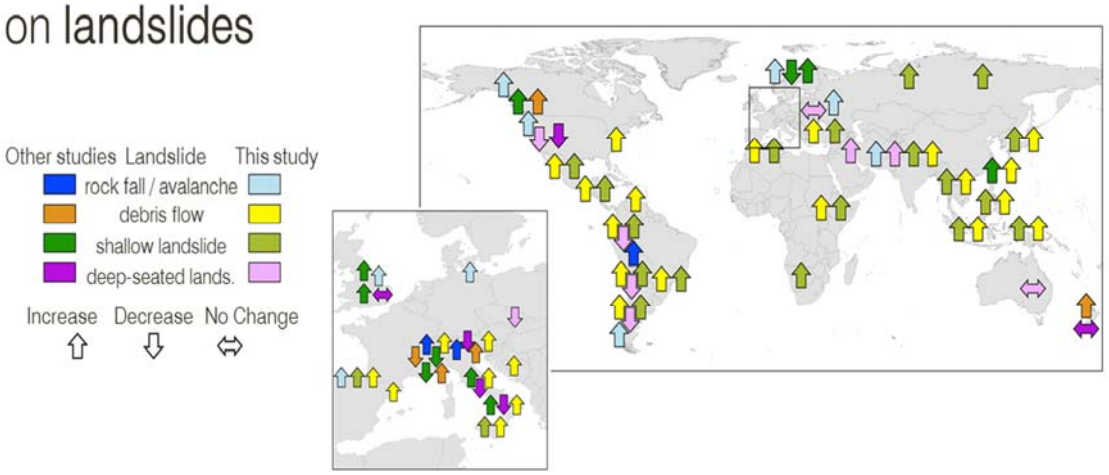

Gariano & Guzzetti (2016)

THANK YOU!

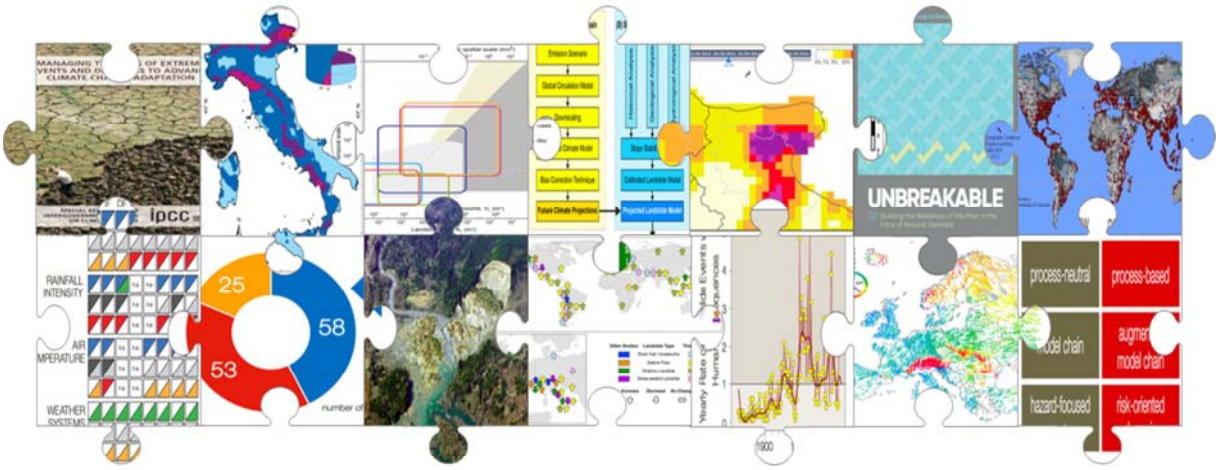

Fausto.Guzzetti@irpi.cnr.it
Stefano.Gariano@irpi.cnr.it

A multi-parametric field laboratory for the investigation on the relationship between material behavior and morphodynamic of landslides

Andrea Segalini[1*], Emma Petrella[2], Fulvio Celico[2], Alessandro Chelli[2], Roberto Francese[2], Andrea Carri[1], Alessandro Valletta[1]

1) Dept. of Engineering and Architecture, University of Parma, Italy
*Email address: andrea.segalini@unipr.it
2) Dept. of Chemistry, Life Sciences and Environmental Sustainability, University of Parma, Italy

1

Introduction

- A large complex landslide in the Northern Apennines will be equipped with an **integrated multi-parametric monitoring system** aimed to gain, with an integrated approach, data on the movement, groundwater circulation and the changes of physical properties of the landslide mass.

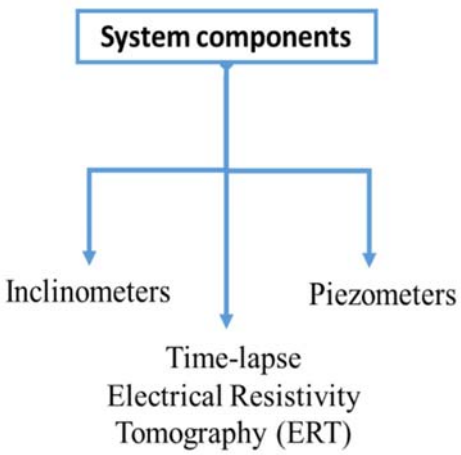

2

Project objectives

- ✓ Explore the relationship existing among **groundwater circulation** (landslide hydrology) and the **movements of the landslide**
- ✓ Investigate the **changes in the physical properties of the landslide** masses through the monitoring of electrical resistivity properties of the material involved because of the variation in water content and movement
- ✓ Improve the knowledge on the relationship and the roles played by the **triggering and predisposing causes** on the landslide masses
- ✓ Monitor the **in-depth propagation of the rainfalls** through the landslide deposit and how they induce the **modification of the electrical and physical properties** of the landslide materials leading to potential reactivation

PHASE 1	PHASE 2	PHASE 3
Geological, geotechnical and hydrogeological investigation, geomorphological mapping, and ERTs tests	Project, realization, and launch of the landslide monitoring system	Data acquisition by the monitoring system performed at full speed following a time-lapse modality

3

Scheme of the integrated monitoring system

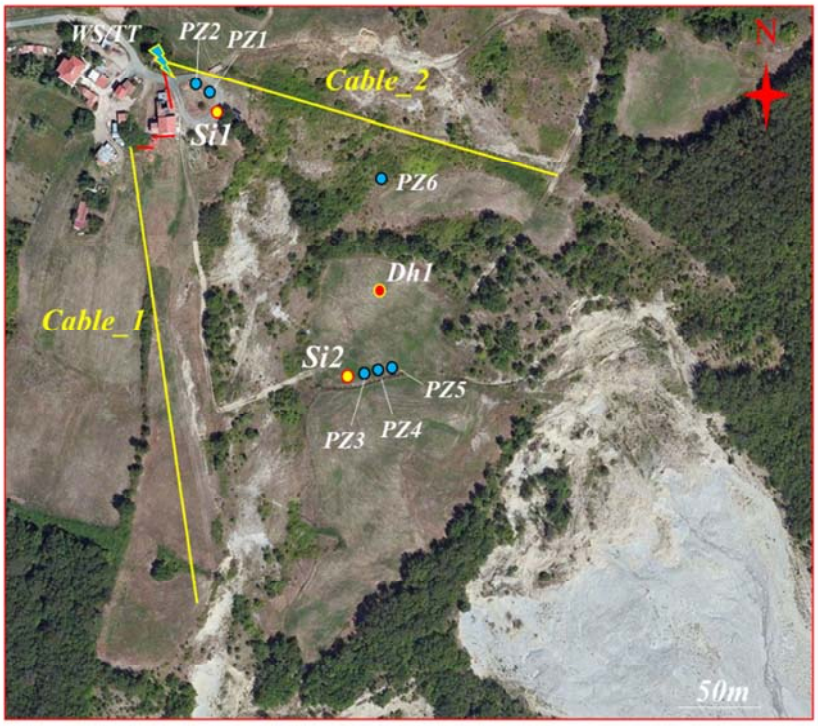

Earth Resistivity Tomography (ERT) acquisition system:
- ❑ Cable_1
- ❑ Cable_2
- ❑ Dh1

Boreholes/Inclinometers:
- ❑ SI1 (-35m g.s.)
- ❑ SI2 (-30,5m g.s.)

Piezometers:
- ❑ Pz1 (30-35m g.s.)
- ❑ Pz2 (1-25m g.s.)
- ❑ Pz3 (25-30m g.s.)
- ❑ Pz4 (20-23m g.s.)
- ❑ Pz5 (3-15m g.s.)
- ❑ Pz6 (3-20m g.s.)

Weather/gauge station:
- ❑ WS

Temperature probe
- ❑ TT

4

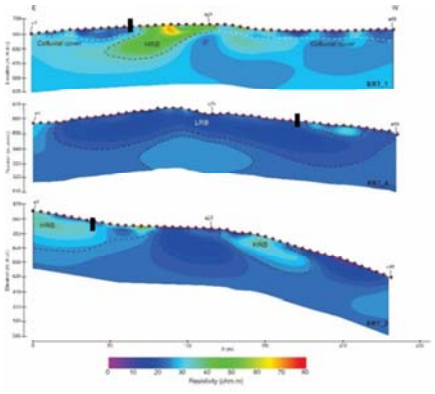

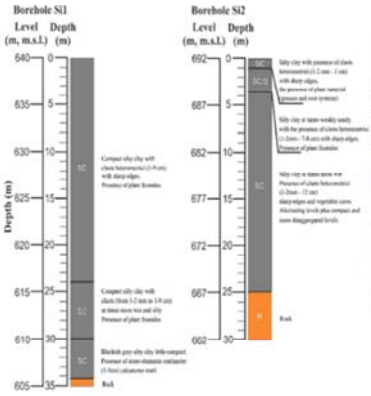

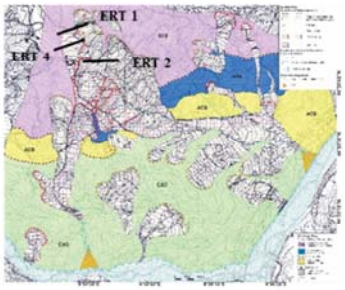

Geology, Geomorphology and Geophysics

AIM:
Perform the geological and geomorphological landslide model.

HOW:
1. Geological and geomorphological field work and borehole data acquisition on stratigraphy, geotechnics and hydrogeological rock properties. Geophysical data to test the response of rocks involved and evaluate the geometry of landslide in depth.

5

Geophysics
Time-lapse resistivity monitoring

AIM:
Gain a detailed insight in the subsurface fluid dynamics in both the landslide body and the underlying bedrock

HOW:
1. Monitoring short-term changes of electrical resistivity using surface and borehole electrode arrays.

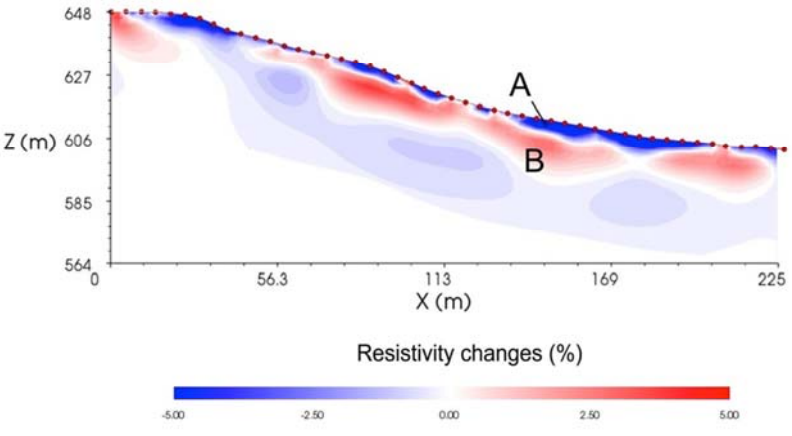

Test of electrode deployment showing negative (A) and positive (B) changes in subsurface resistivity just after a rainfall event.

6

Hydrogeology

AIM:
Characterize the groundwater circulation in an heterogeneous media of landslide

HOW:
1. Monitoring groundwater level fluctuation in relation with precipitation.
The monitoring should be performed in multilevel groundwater monitoring systems (cluster type PZ1-2 and Pz3,4,5) in order to take into account different piezometric head within the heterogeneous media.
The timing should be suitable for fast variations (1h at least) using a pressure transducer.

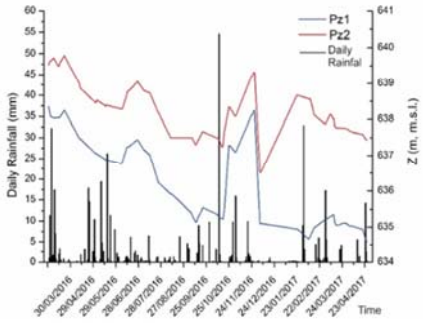

Comparison between Pz1-Pz2 and rainfall first readings during test site phase between March 2016 and May 2017.

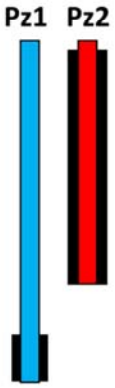

7

Hydrogeology

AIM:
Characterize the groundwater circulation in an heterogeneous media of landslide

HOW:
2. Monitoring of Electrical Conductivity variation vs depth in piezometers cluster type.
The timing should be with high frequencies during the recharge periods and with low frequencies during the recession periods.

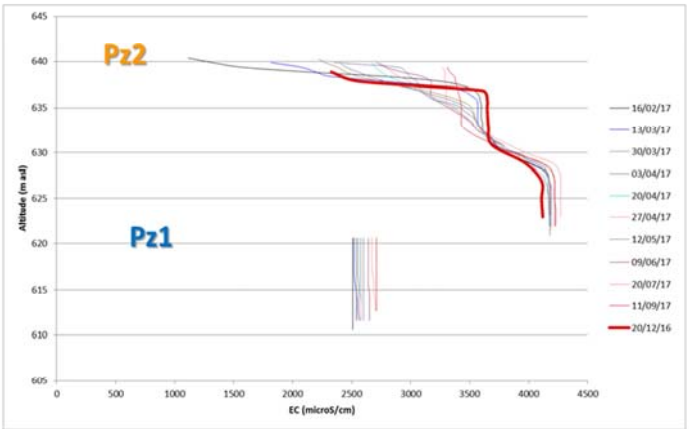

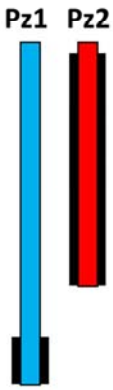

8

Geotechnics

AIM:
Detect the movements (horizontal displacements) of the landslide

HOW:
1. Installation of two inclinometer casings. The first one (SI1) with a total length of 35 m, near the cluster A of piezometers, monitors the crown of the investigated landslide. The reading step is of 0.5 m.

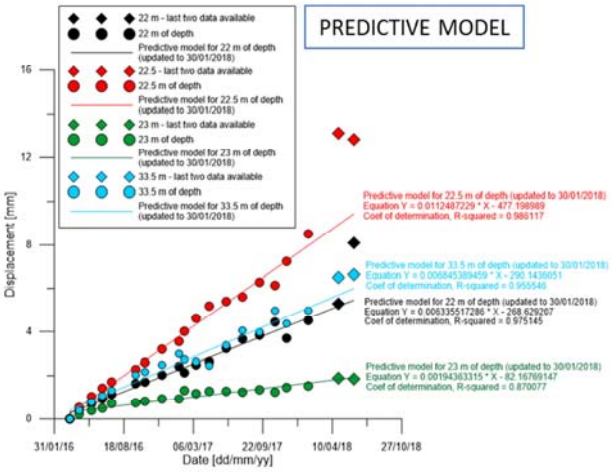

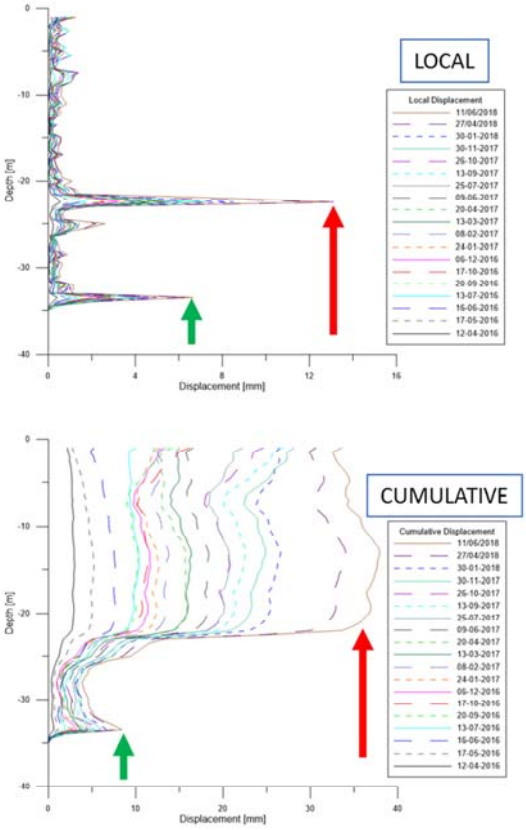

9

Geotechnics

AIM:
Detect the movements (horizontal displacements) of the landslide

HOW:
2. The second (SI2) is placed near the cluster B, in correspondence of the head of landslide and it has a total length of 30.5 m. The reading step is of 0.5 m.

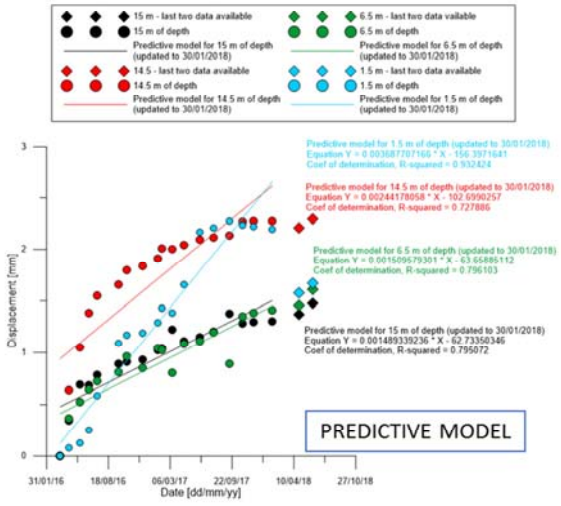

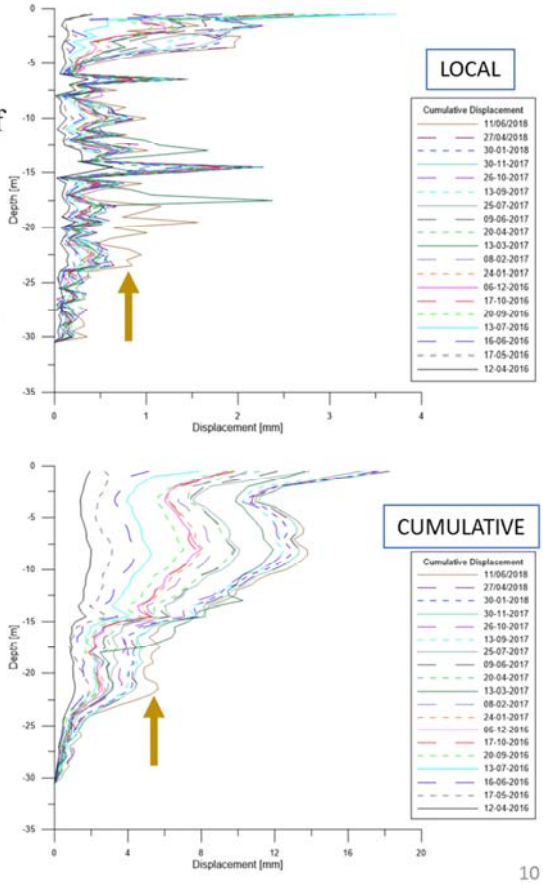

10

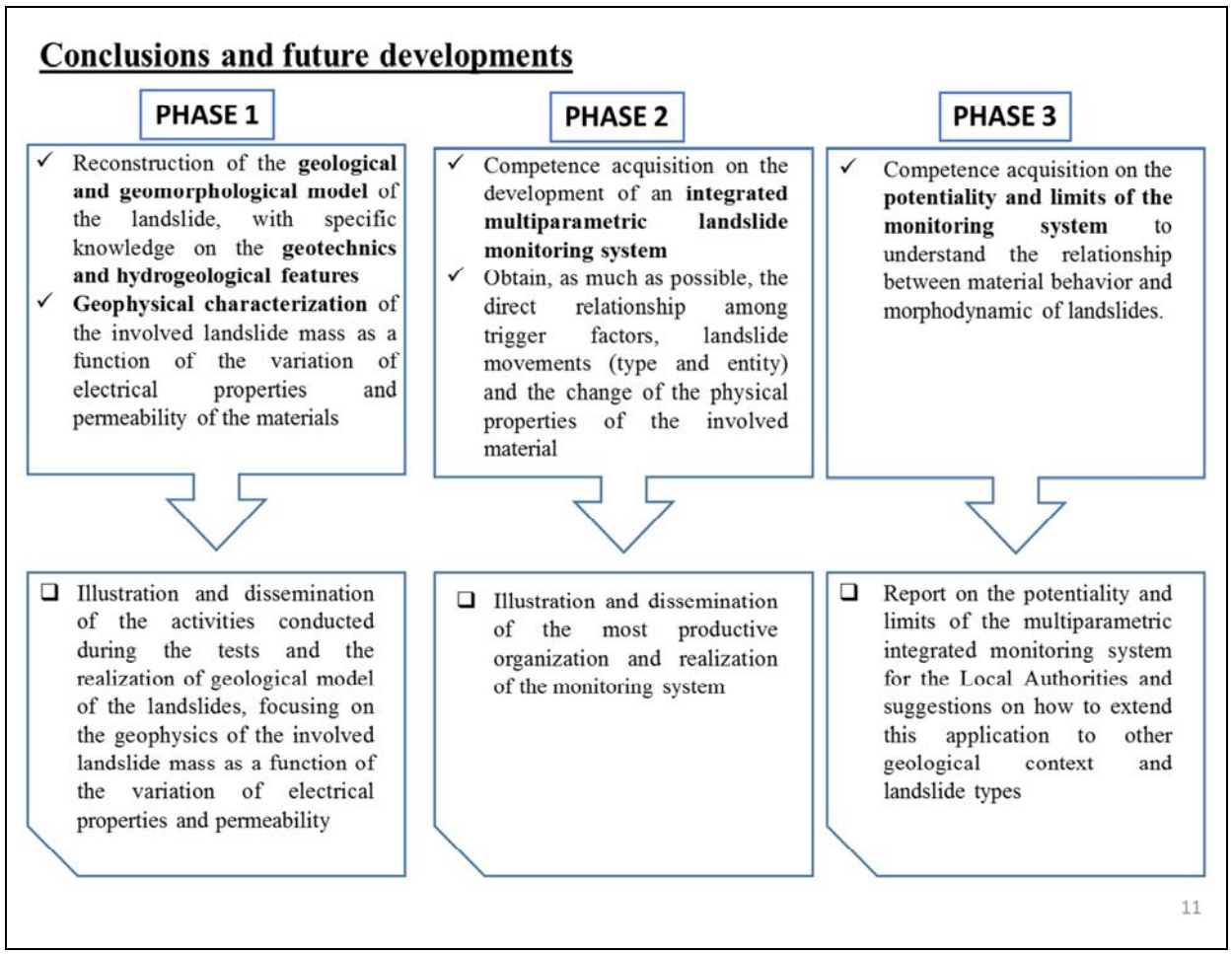
Conclusions and future developments
PHASE 1
✓ Reconstruction of the geological and geomorphological model of the landslide, with specific knowledge on the geotechnics and hydrogeological features
✓ Geophysical characterization of the involved landslide mass as a function of the variation of electrical properties and permeability of the materials
PHASE 2
✓ Competence acquisition on the development of an integrated multiparametric landslide monitoring system
✓ Obtain, as much as possible, the direct relationship among trigger factors, landslide movements (type and entity) and the change of the physical properties of the involved material
PHASE 3
✓ Competence acquisition on the potentiality and limits of the monitoring system to understand the relationship between material behavior and morphodynamic of landslides.
❑ Illustration and dissemination of the activities conducted during the tests and the realization of geological model of the landslides, focusing on the geophysics of the involved landslide mass as a function of the variation of electrical properties and permeability
❑ Illustration and dissemination of the most productive organization and realization of the monitoring system
❑ Report on the potentiality and limits of the multiparametric integrated monitoring system for the Local Authorities and suggestions on how to extend this application to other geological context and landslide types
11

A new methodology for assessing earthquake-induced landslide scenarios

Carlo Esposito[(1)], Salvatore Martino[(1)],Francesca Bozzano[(1)], Gabriele Scarascia Mugnozza[(1)]

1) CERI Research Centre – Sapienza University of Rome, Rome (Italy), P.le A. Moro 5
e-mail: carlo.esposito@uniroma1.it

Abstract

In the frame of co-seismic effects, landslides triggered by earthquakes represent a relevant and challenging issue, as they can potentially cause damages even comparable with the direct effects of seismic shaking. Thus, the assessment of earthquake-triggered landslide scenarios plays a key role for risk prevention and mitigation as well as for spatial planning, as clearly recalled by some national regulations. At the same such an assessment is a quite complex issue. Based on these premises, we conceived and implemented a comprehensive methodology called PARSIFAL (Probabilistic Approach to Provide Scenarios of Earthquake-Induced Slope Failures).

The most innovative aspects consist in: dealing with both first-time slope failures (rock slope failures and shallow landslides) and re-activations of already existing landslides; taking into account the combination of different seismic and hydraulic scenarios. The methodology is articulated in 3 sequential steps: 1) assessment of landslide susceptibility for different failure mechanisms, 2) calculation of the stability conditions and the related co-seismic displacements of landslide prone areas under different combinations of seismic and hydraulic loading, 3) synthetic mapping of the expected scenarios. The methodology has been applied to the seismic microzonation of a pilot area affected by the 2016 seismic sequence of central Apennines (Italy).

The Research Centre CERI

SAPIENZA
UNIVERSITÀ DI ROMA

CERI CENTRO DI RICERCA
PREVISIONE, PREVENZIONE E CONTROLLO
DEI RISCHI GEOLOGICI

Engineering
- Seismic engineering
- Hydraulic/Civil engineering

Earth Sciences
- Engineering Geology
- Hydrogeology
- Fluid chemestry

Chemestry
- Remediation of polluted sites

Relevant topics
- Slope stability
- Seismic local response and co-seismic effects
- Ground deformations (subsidence)

Tools
- Numerical modelling
- Geomatics
- Contact and Remote sensing

Introduction

- PARSIFAL (**P**robabilistic **A**pproach for **R**ating **S**eismically **I**nduced slope **FA**i**L**ures) is a comprehensive method to perform large-scale assessments of earthquake-induced landslide scenarios.

Esposito C., Martini G., Martino S., Pallone F., Romeo R.W. (2016). *A methodology for a comprehensive assessment of earthquake-induced landslide hazard, with an application to pilot sites in Central Italy*. Proceedings. In: Landslides and Engineered Slopes. Experience, Theory and Practice, 2, pp. 869-877. 12th International Symposium on Landslides, 2016; Napoli; Italy; 12 – 19 June 2016.

Martino, S., Battaglia, S., Delgado, J., Esposito, C., Martini, G., Missori, C. (2018). *Probabilistic approach to provide scenarios of earthquake-induced slope failures (PARSIFAL) applied to the Alcoy basin (South Spain)*. Geosciences (Switzerland), DOI: 10.3390/geosciences80200

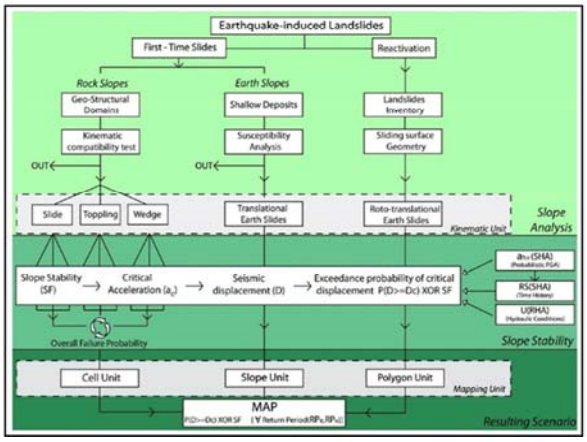

Introduction

PARSIFAL has the following features:

- is conceived to assess the hazard related to **seismically-induced landslides of both first-time failures** (i.e., proper co-seismic landslide) **and second generation** (i.e. already existing landslides with a potential of re-activation under seismic loading);
- performs differentiated analyzes according to the considered landslide mechanism (e.g. **rock toppling, rock wedge/planar sliding; shallow soil/debris slides; roto-translational earth/rock slides**);
- the results are expressed in terms of: i) **exceedance probability with respect to assumed critical thresholds of co-seismic displacements** (if any), or ii) **safety factor in seismic conditions** (in case not appreciable displacements are assessed or for purely rotational kinematics, such as toppling);
- for each territorial unit (i.e., elementary zones in which the study area is partitioned for analysis purposes) **a weighted probabilistic analysis is performed to account for the presence of different failure mechanisms and/or unstable volumes**;
- **different hydraulic conditions of the slope are also considered** in terms of pore water pressure ratio (ru) for soil slopes and percentage of water saturation (Hw) in the joints for the rock masses.

Method description

- The analyses follow three sequential steps, namely
  - Slope analysis
  - Slope stability
  - Resulting scenario (mapping)

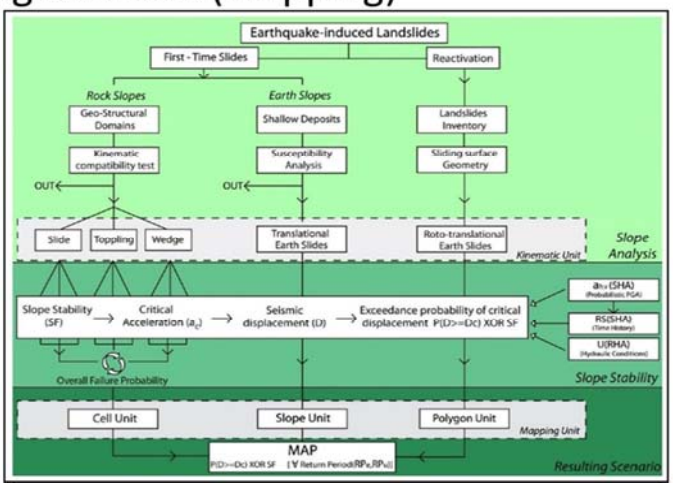

Step 1

- Slope analysis: identifying landslide-prone areas (first-time failures) and already existing landslides that can be reactivated under seismic loading

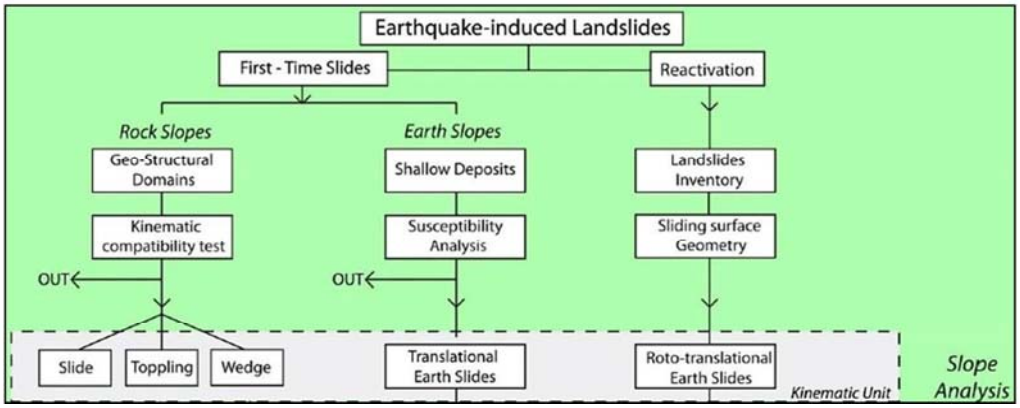

Procedure for rock slopes

1. Identification of homogeneous geo-structural zones

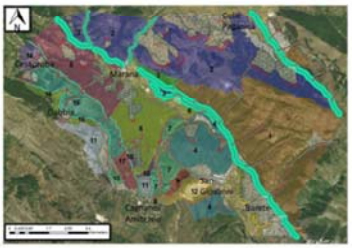

2. Attribution of a synthetic stereoplot to each hgsz

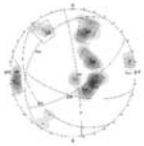

3. GIS-based kinematic compatibility analysis (comparison of joint attitude with slope and aspect of each mapping unit) and computation of rock block volumes

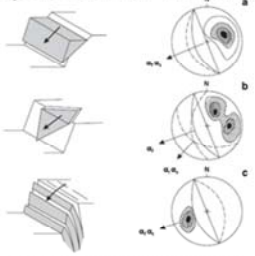

4. Identification of kinematically compatible mapping units (square grid cells) and related mechanism

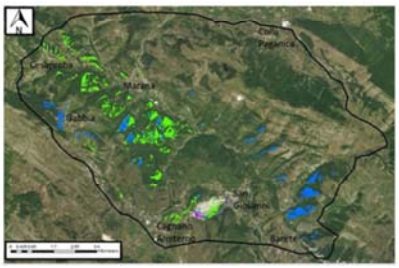

Procedure for shallow landslides and existing landslides

FIRST TIME SHALLOW LANDSLIDES

1. Mapping of soil/debris covers

2. Landslide susceptibility assessment (choice of the technique [qualitative vs quantitative] according to data availability)

3. Identification of areas prone to shallow soil/debris slides

EXISTING LANDSLIDES

1. Inventory of existing landslides (surveys, catalogues and archives)

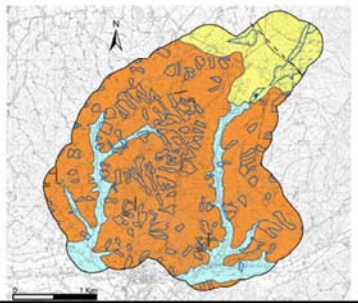

2. Kinematic model for each recognized roto/translational landslide

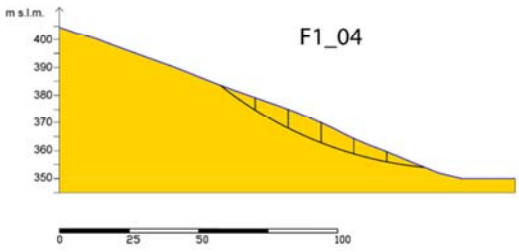

Step 2

- Slope Stability: for landslide-prone areas and already existing landslides, the slope stability under seismic condition is evaluated by computing a probability of exceedance of an assumed displacement threshold (P [D≥Dc | a (t), a_y]), i.e. 10 cm for earth-slides and 5 cm for rock failures according to Romeo (2000), through a pseudo-dynamic Newmark's (1965) approach.

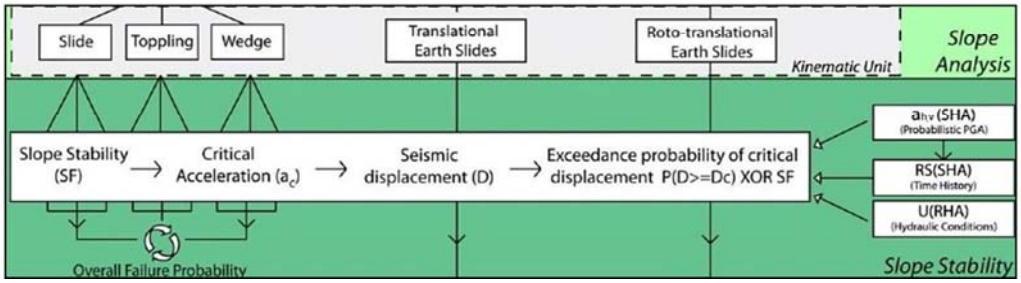

Approaches for slope stability analyses

- Bishop/Janbu method for re-activations

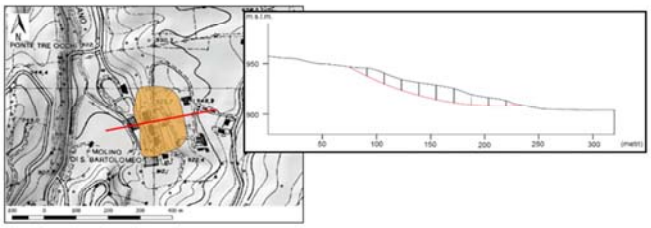

- Infinite slope for shallow landslides

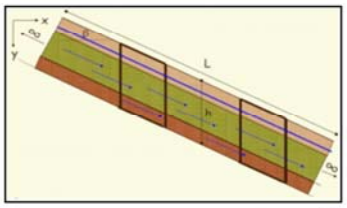

- Hoek and Bray approach for rock slopes

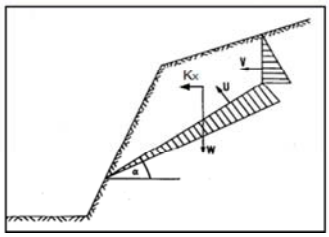

Approaches for slope stability analyses

- A critical pseudostatic threshold (a_y) is derived by a sensitivity analysis on horizontal pseudostatic acceleration (a_x) at different saturation conditions. For each considered scenario (which couples seismic loading and saturation conditions), the results of slope stability are referred to already existing landslides and first time failures in terms of P [D≥Dc], if any, or safety factor (SF) if no displacement is computed.

Analysis of sensitivity to pseudostatic acceleration and pore water pressure

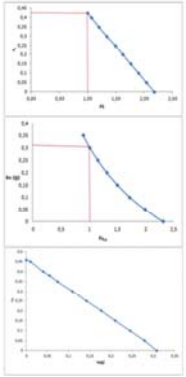

Seismic input selection and processing

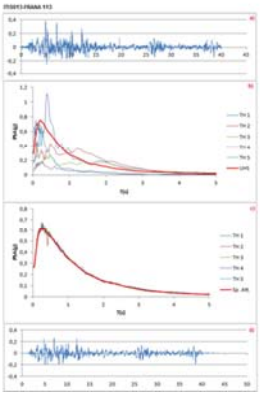

Pseudo-dynamic analysis: computation of co-seismic displacements

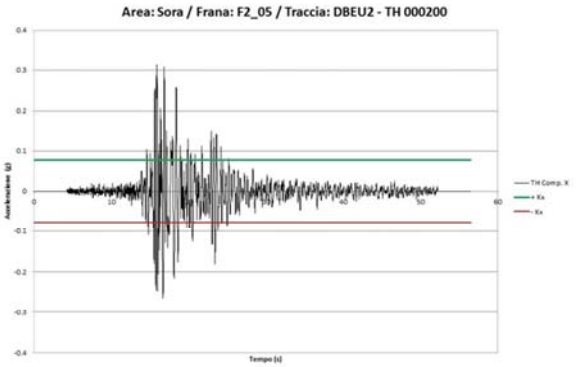

The peculiarity of rock slope instabilities

- For rock slope failures, more than 1 mechanism and/or potentially unstable block can be present in the same mapping unit

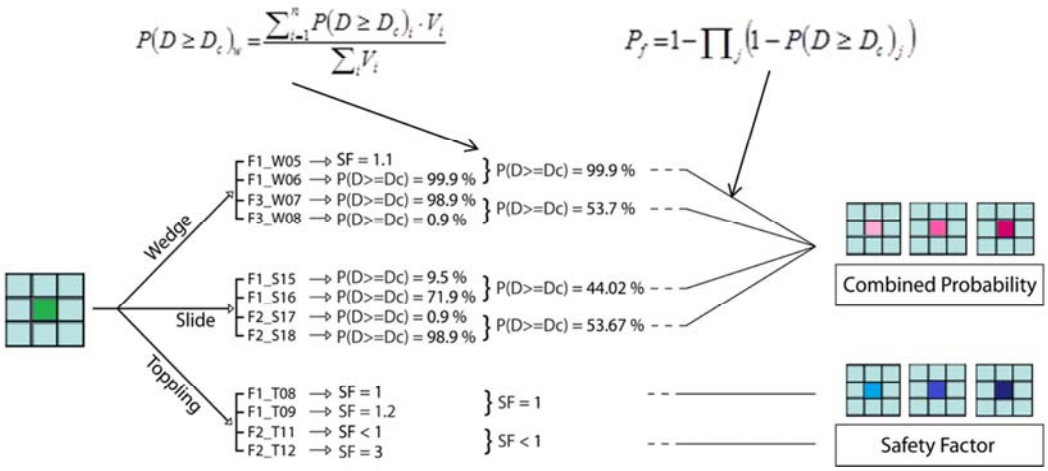

Step 3

- Mapping: the results for each considered scenario (seismic input + hydraulic conditions) are reported on a synthetic map

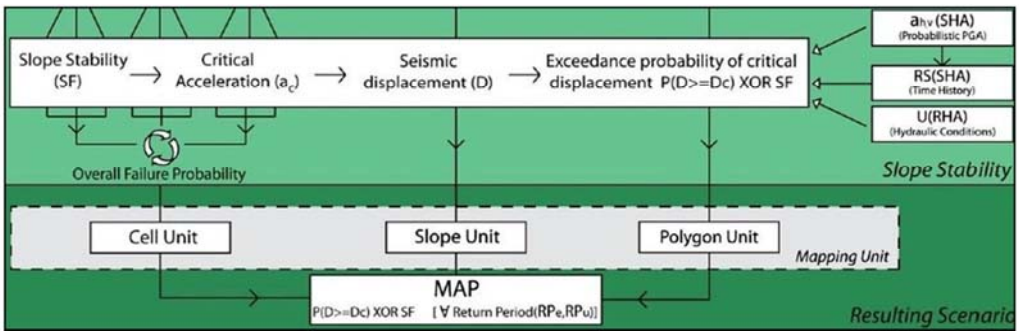

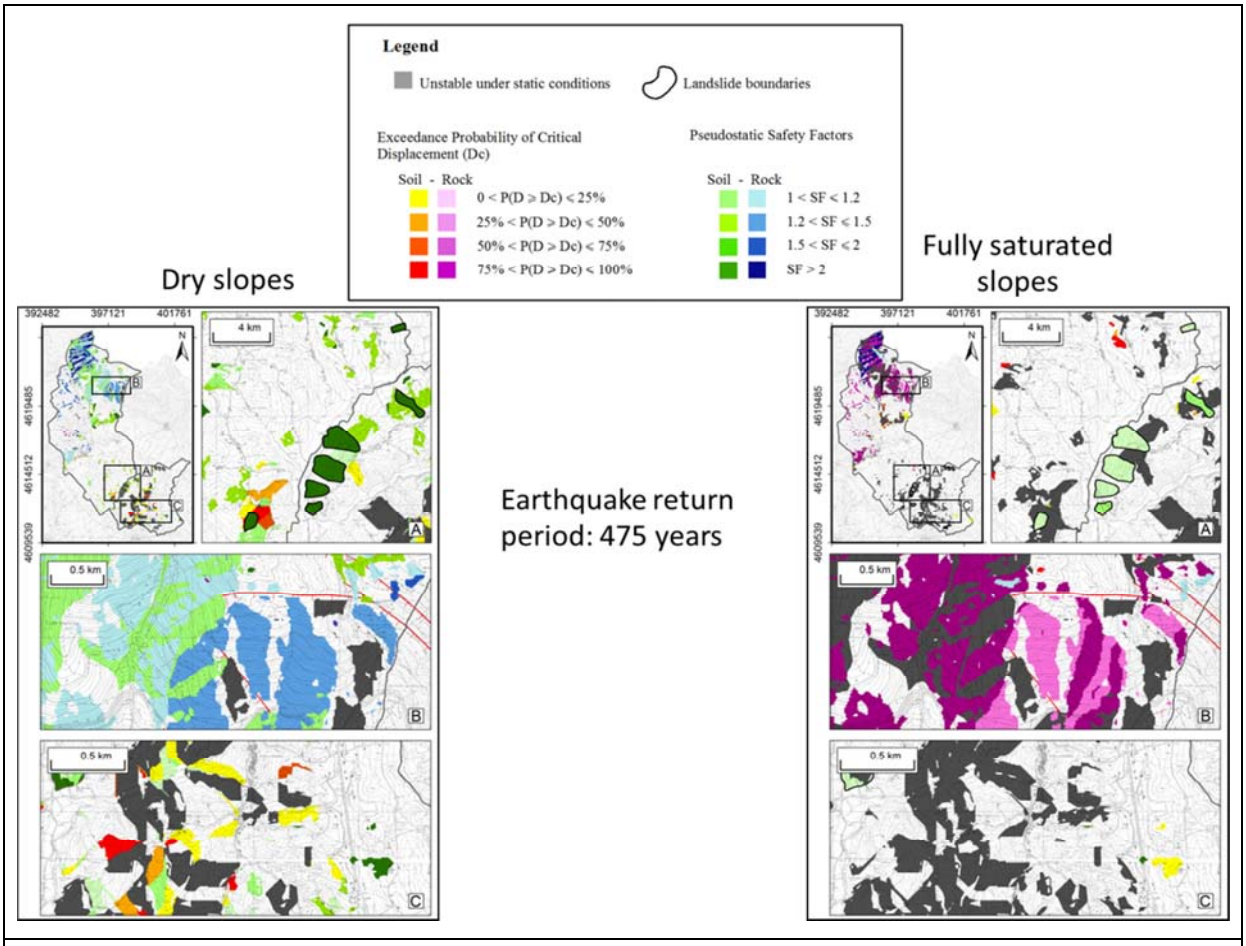

An application for regulatory purposes

- Seismic microzonation of a municipality struck by the 2016-2017 central Apennines seismic sequence
- Necessity to identify potential sites of earthquake-triggered landslides, according to national regulations and guidelines

An application for regulatory purposes

- Slope analysis: identification of existing landslides and landslide-prone areas

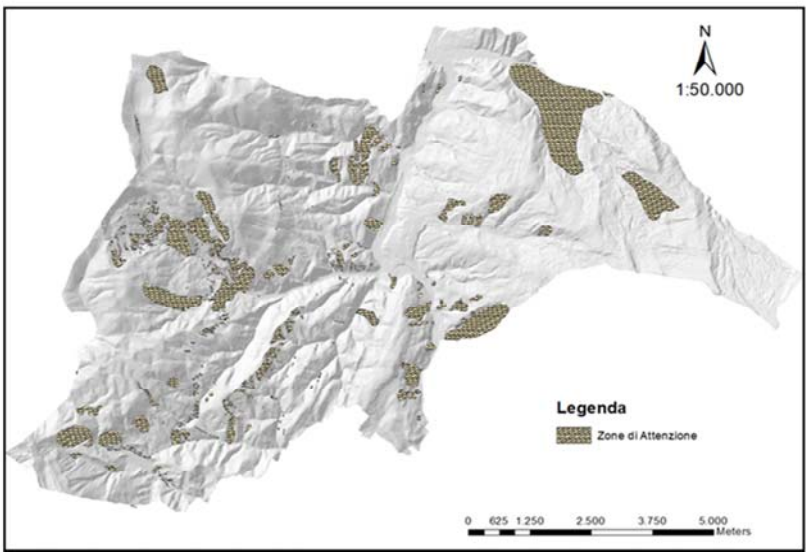

An application for regulatory purposes

- Slope stability and mapping: identification of existing landslides and landslide-prone areas actually sensitive to seismic trigger; computation of displacements or safety factors; mapping of combined scenarios

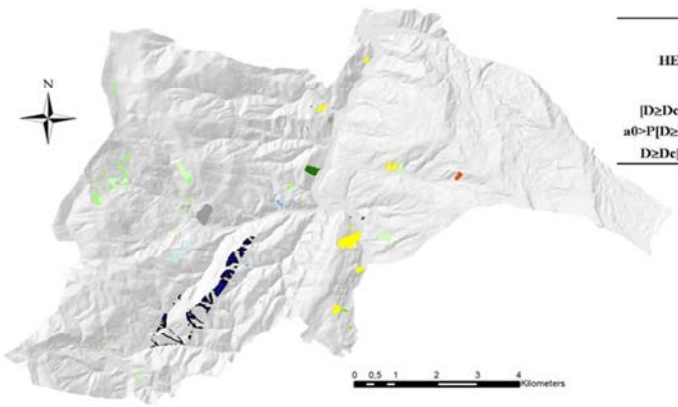

DRY SCENARIO RT=475 YEARS			
HEADER	Already existing landslides (%)	First-time earth slides (%)	First-time rock mass (%)
$[D \geq Dc \mid a(t), a_y]=0$	46	99	83
$a0>P[D \geq Dc \mid a(t), a_y]>1$	46	1	0
$D \geq Dc \mid a(t), ay]=1$	8	0	17

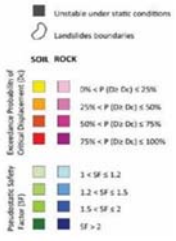

Conclusions

- The PARSIFAL approach was experienced in the Municipality of Accumoli (central Italy) in the framework of microzonation studies. It proved to be a reliable tool for screening landslide-prone areas (ZA_{FR}) and selecting those actually sensitive to the seismic trigger (ZS_{FR}) for microzonation maps, according to the current guidelines of the Italian Civil Protection.
- The results and related maps are currently part of the official technical documents annexed to the microzonation studies and available for reconstruction plans.

Characteristics of recent landslides triggered by two moderate-strong earthquakes in Japan

Fawu Wang(1), Shuai Zhang(2), Ran Li(2), Akinori Iio(2)

1) Shimane University, Matsue, 1060 Nishikawatsu, 690-8504, Japan
e-mail: wangfw@riko.shimane-u.ac.jp
2) Graduate School of Shimane University, Department of Earth Sciences, Japan

CONTENTS

1 Methodology for landslide motion simulation

2 Landslides triggered by 2016 Kumamoto Earthquake

3 Landslides triggered by 2018 Western Shimane Prefecture Earthquake

4 Conclusions

1 Methodology for landslide motion simulation

Sassa's geotechnical model for landslide motion (1988)

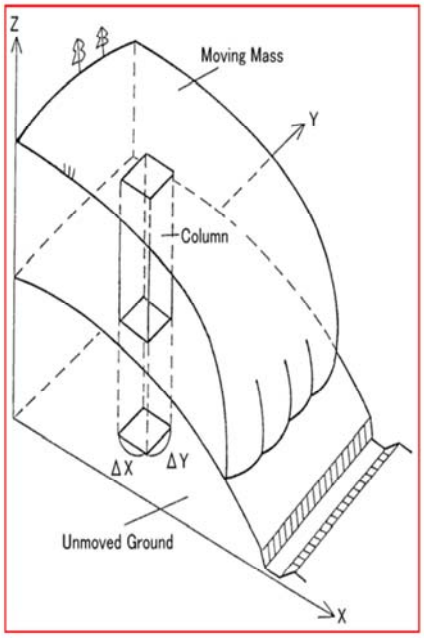

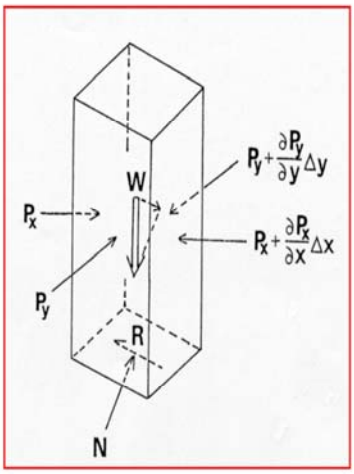

Forces acting on a sliding mass column

a = F/m

1 Methodology for landslide motion simulation

Equations of motion and continuity (Sassa, 1988)

$$\frac{\partial M}{\partial t}+\frac{\partial}{\partial x}(u_0 M)+\frac{\partial}{\partial y}(v_0 M)=$$

$$gh\frac{\tan\alpha}{q+1}-Kgh\frac{\partial h}{\partial x}-\frac{g}{(q+1)^{1/2}}\cdot\frac{u_0}{(u_0^2+v_0^2+w_0^2)^{1/2}}\{h_c(q+1)+h\tan\phi_a\}$$

$$\frac{\partial N}{\partial t}+\frac{\partial}{\partial x}(u_0 N)+\frac{\partial}{\partial y}(v_0 N)=$$

$$gh\frac{\tan\beta}{q+1}-Kgh\frac{\partial h}{\partial y}-\frac{g}{(q+1)^{1/2}}\cdot\frac{v_0}{(u_0^2+v_0^2+w_0^2)^{1/2}}\{h_c(q+1)+h\tan\phi_a\}$$

$$\frac{\partial h}{\partial t}+\frac{\partial M}{\partial x}+\frac{\partial N}{\partial y}=0$$

Shear resistance of sandy soils in steady state

The void ratios after consolidation were adjusted as e = 0.70.

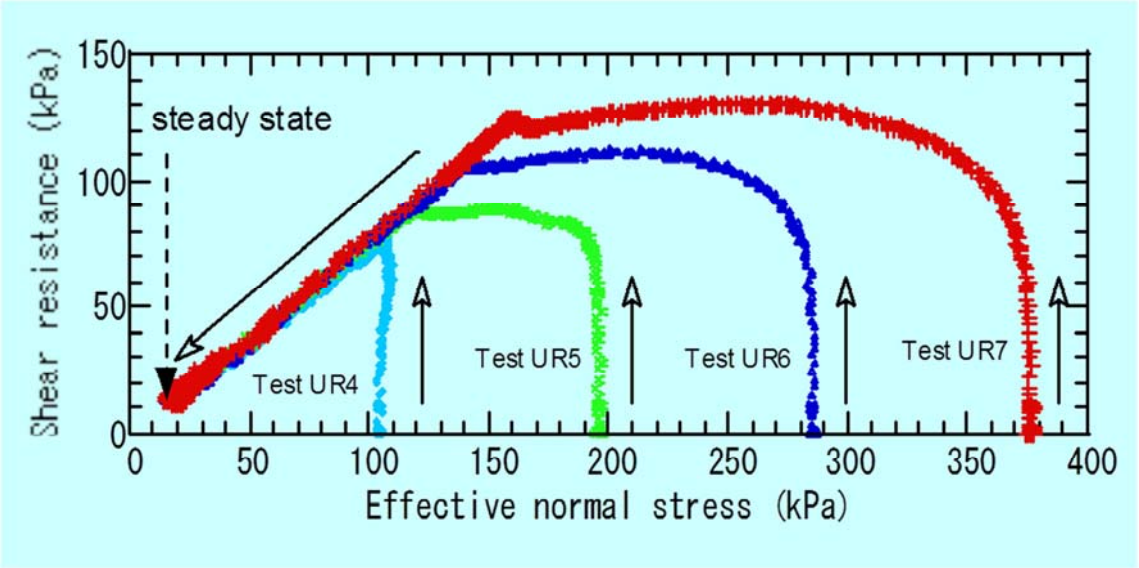

(Okada et al. 2002)

1 Methodology for landslide motion simulation

Apparent Friction Model (Wang & Sassa, 2002)

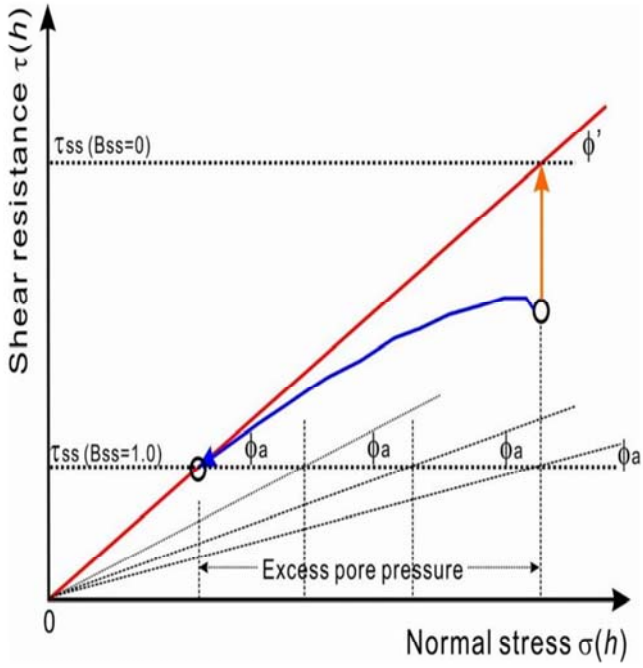

Bss: Pore pressure parameter at steady state

http://mini.eastday.com/a/170730224931018.html

2017-07-30 22:49:31 word国际

2 2016 Kumamoto Earthquake

United Nations Educational, Scientific and Cultural Organization · UNESCO Chair on Geoenvironmental Disaster Reduction, Shimane University, Matsue, Japan

The Kumamoto earthquake occurred in Kyushu Prefecture, Japan. The epicenter was located at 32.782°N, 130.726°E (Global Positioning System (GPS) coordinates), with a focal depth of about 10.0 km. A mainshock of Ms 7.3 occurred at 01:25 JST on April 16, 2016, just 28 h after the Ms 6.5 foreshock (Asano and Iwata, 2016).

This earthquake sequence occurred along the Futagawa fault zone and the northern part of the Hinagu fault zone in central Kyushu. The Futagawa-Hinagu fault system is one of the major active fault systems on Kyushu Island.

Asano K, Iwata T. Source rupture processes of the foreshock and mainshock in the 2016 Kumamoto earthquake sequence estimated from the kinematic waveform inversion of strong motion data. Earth, Planets and Space, 2016, 68(1): 147.

2 Kumamoto Earthquake-triggered landslides

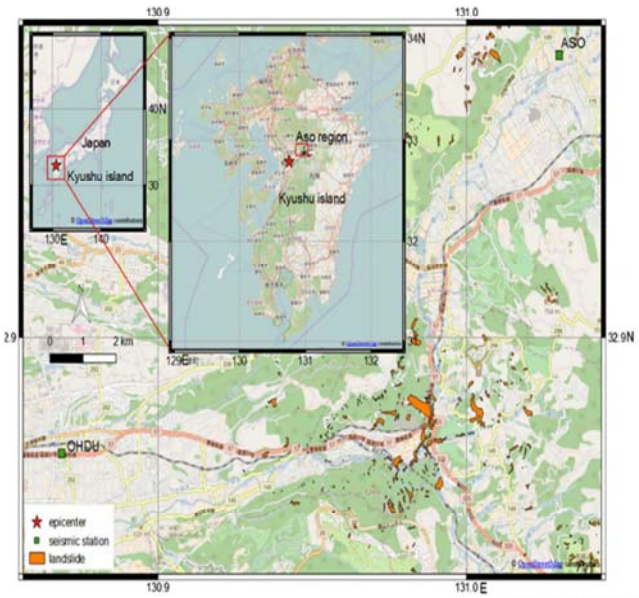

Distribution map of the landslides triggered by the earthquake (Hung et al. 2017)

The foreshock and mainshock generated very strong ground motions in the near-source region. According to Japanese government, at least 97 landslides were confirmed in the Aso area (Hung et al. 2017).

Hung C, Lin G W, Syu H S, et al. Analysis of the Aso-Bridge landslide during the 2016 Kumamoto earthquakes in Japan[J]. Bulletin of engineering geology and the environment, 2017: 1-11.

2 Kumamoto Earthquake-triggered landslides

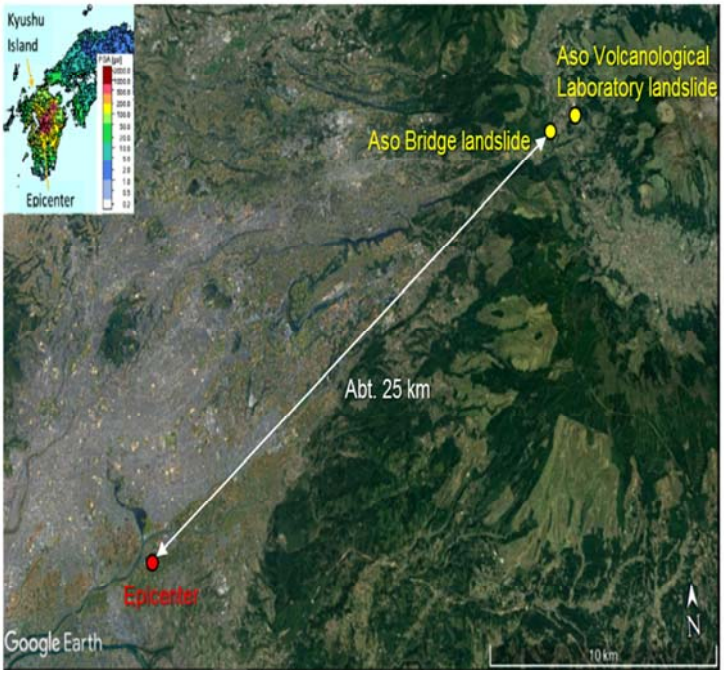

Among these earthquake-triggered landslides, the largest ones were two very substantial slope failures. One was located on the National Road 57 and destroyed an important bridge. The other one occurred near the Aso volcanological laboratory of Kyoto University and destroyed several houses.

2 Kumamoto Earthquake-triggered landslides

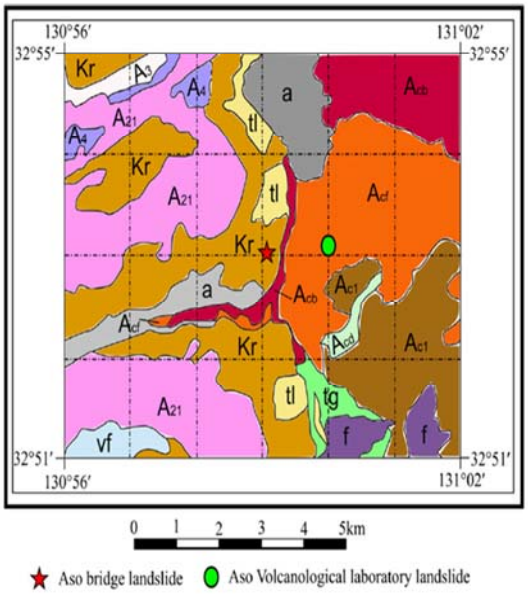

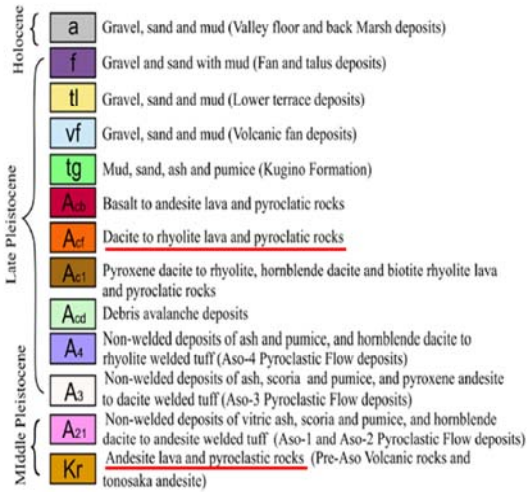

Geological map of Aso volcano (according to the Geological map display system of Geological Survey of Japan, AIST 2016)

2-1 Aso Bridge landslide

Aerial view of the Aso Bridge Landslide

The Aso Bridge Landslide is located at the western tip of the caldera of Mount Aso. It was triggered by the magnitude 7.3 mainshock on April 16.

This landslide was named after a 200-m long Aso Bridge that formerly spanned the 80-m deep gorge of the Kurokawa River before it was destroyed by the landslide during the earthquake.

The hillslope of the landslide area is overlain with lava and pyroclastic rocks from eruptions about 90,000 years ago. The pyroclastic rocks contain a lot of voids among composed particles, which has led to their aptness to adsorb water and be infiltrated by it. Their mechanical properties are likely to be prone to weakening after rainfall.

2-1 Aso Bridge landslide

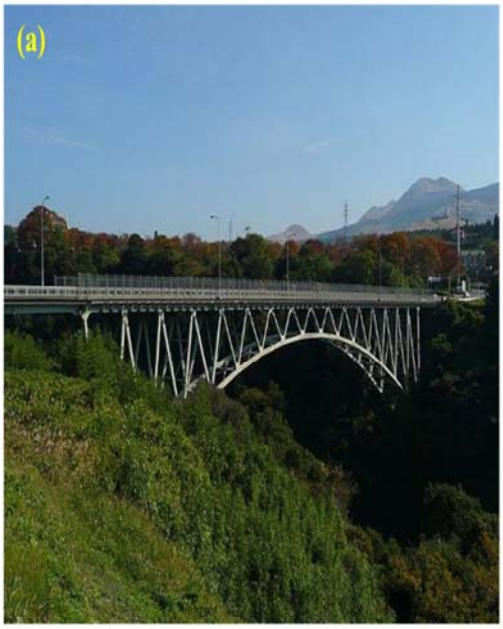

Aso bridge before landslide

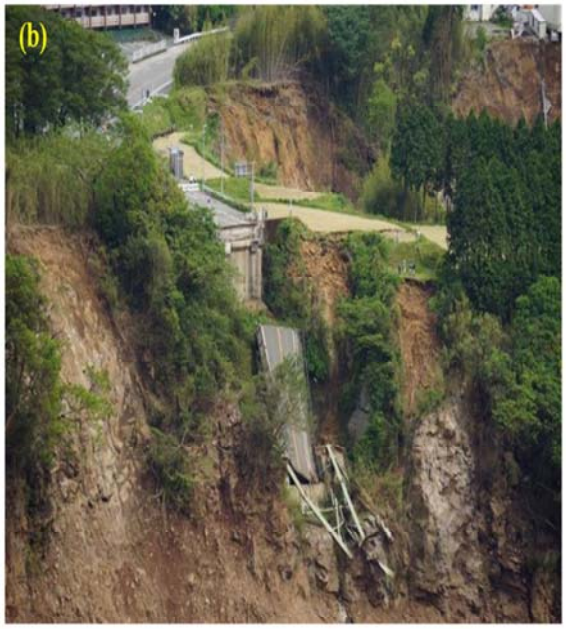

Aso bridge after landslide

2-1 Aso Bridge landslide

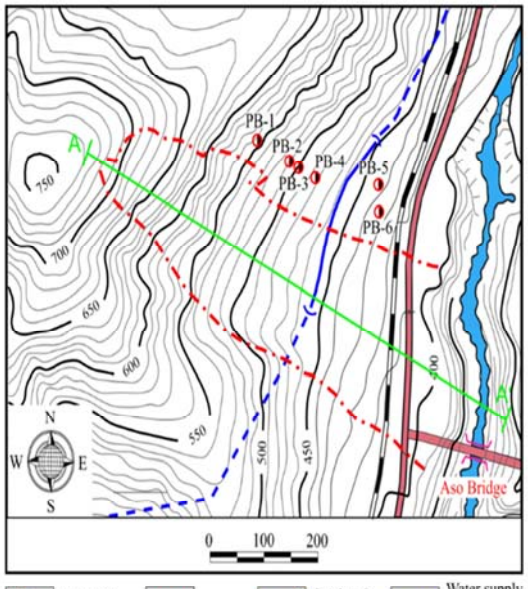

Topographic map of the Aso Bridge landslide

The shape of this landslide is like a tongue, and at the front of the landslide is Kurokawa River, an a 80 m deep gorge. The landslide lies in a slope with an average gradient of 23°, between elevations 385 m and 725 m, with a length of about 700 m, and an average width of approximately 200 m.

The thickness of the sliding mass is about 15 m on average, estimated after our geotechnical investigation. The sliding surface is nearly circular in shape and located in the shallow soil of the slope. The plane area is about 132,000 m^2 and the total estimated volume is about 1,980,000 m^3. The sliding direction was S61°E.

Besides the Aso Bridge, some other constructions were destroyed by the sliding, such as the Hohi railway, National Road 57, and a water supply channel.

From topography, the lower part of the slope may have high degree of saturation.

2-1 Aso Bridge landslide

This area is characterized by soft ground composed of weathered volcanic cohesive soil. The main body of the landslide is composed of cohesive soil with lapilli and block.

A vertical profile exists beyond the left flank of the landslide. It was created by soil collapse during the Kumamoto earthquake.

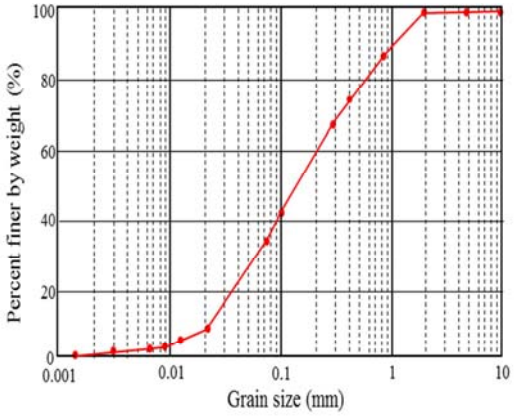

2-1 Aso Bridge landslide

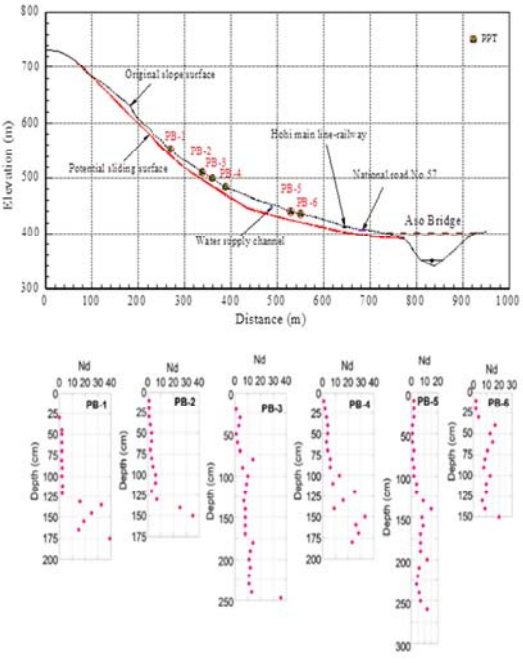

Portable dynamic cone penetration test (PDCP) in soil near left flank of the landslide

2-1 Aso Bridge landslide

Parameters used in the simulation

For sliding zone	
Initial apparent friction coefficient	0.40
Accumulation possibility of excess pore pressure	0.80
Lateral earth pressure coefficient (*K*)	0.70
Effective friction coefficient at sliding zone	0.70
Shear resistance of sliding zone at steady state	50 kPa
For sliding mass	
Unit weight of sliding mass	20 kN/m^3
Effective friction coefficient of the sliding mass	0.70

2-1 Aso Bridge landslide

United Nations Educational, Scientific and Cultural Organization · UNESCO Chair on Geoenvironmental Disaster Reduction, Shimane University, Matsue, Japan

Motion simulation result

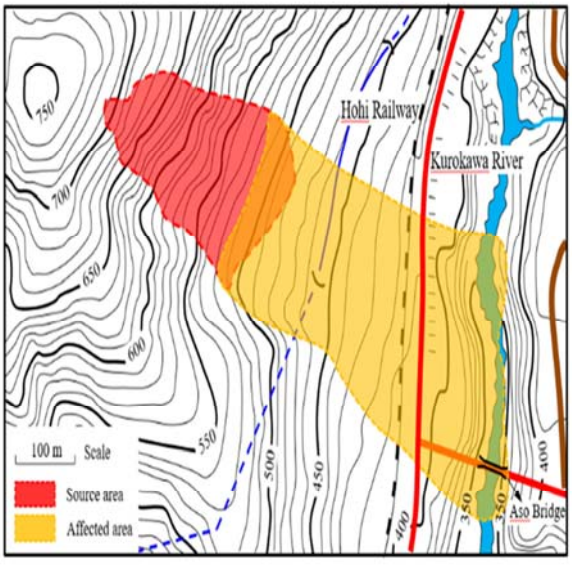

2-2 Aso Volcanological Laboratory landslide

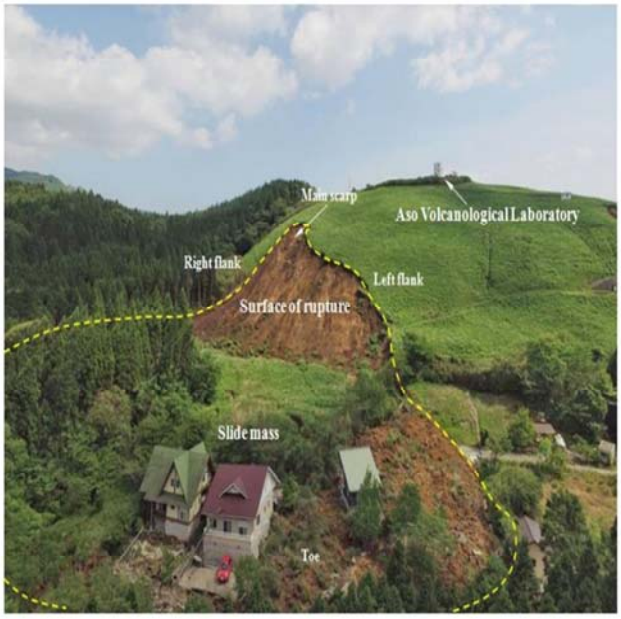

Oblique aerial view from the toe of the landslide towards the source area

The Aso Volcanological Laboratory landslide is located to the east of the Aso Bridge landslide, with a distance of about 2 km. It was also triggered by the mainshock.

The Aso Volcanological Laboratory of Kyoto University is located on the top of the slope, about 220 m to the SW.

The total volume is about 81,000 m^3, about 18,000 m^2 in area, with an average thickness of 4.5m.

2-2 Aso Volcanological Laboratory landslide

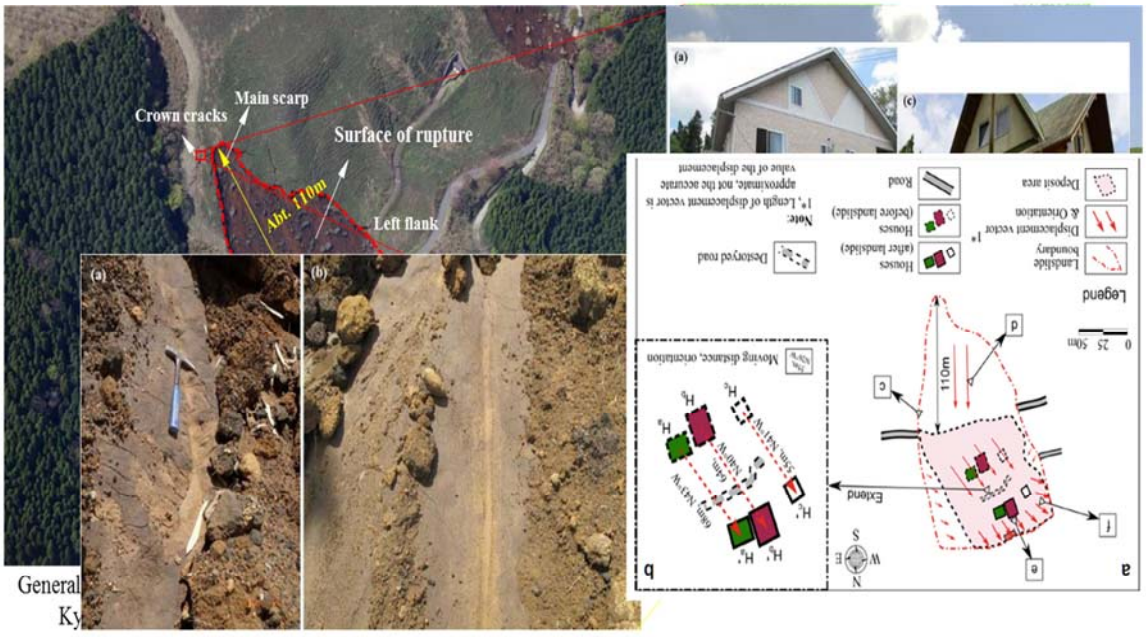

Close up view of the smooth surface of rupture

Kokusai Kogyo Co., Ltd 2016. Disasters Investigation for 2016 Kumamoto Earthquake (26 April 2016 update). http://www.kkc.co.jp/service/bousai/csr/disaster/201604_kumamoto/index.html

2-2 Aso Volcanological Laboratory landslide

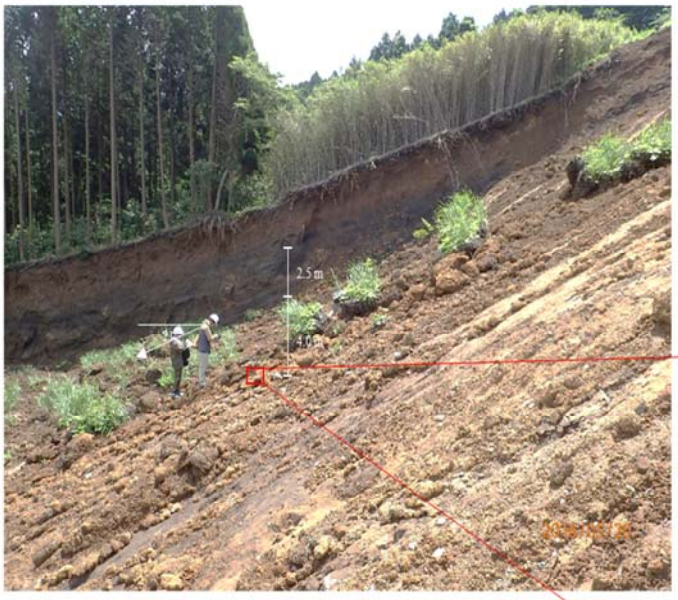

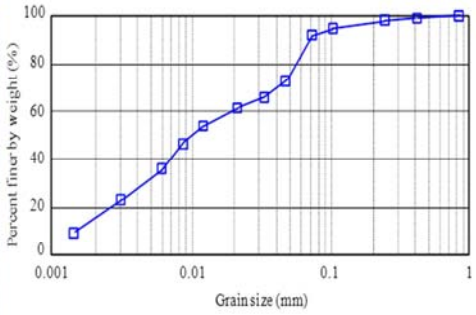

Layer-1 is medium brown cohesive soil with an average thickness of 2.5 m, and the plant root system is developed at 20 cm depth under the surface. Layer-2 is black cohesive soil.

2-2 Aso Volcanological Laboratory landslide

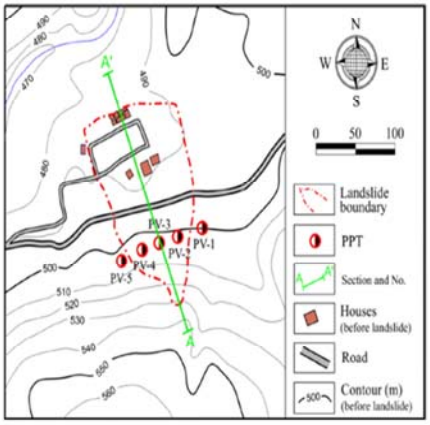

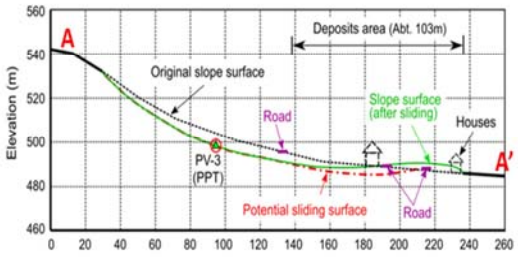

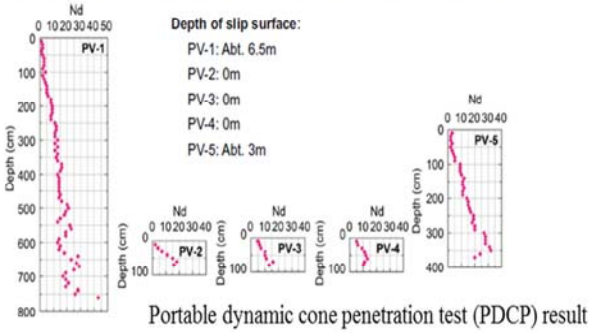

Portable dynamic cone penetration test (PDCP) result

2-2 Aso Volcanological Laboratory landslide

Parameters used in the simulation

For sliding zone	
Initial apparent friction coefficient	0.40
Accumulation possibility of excess pore pressure	0.9
Lateral earth pressure coefficient (*K*)	0.70
Effective friction coefficient at sliding zone	0.70
Shear resistance of sliding zone at steady state	10 kPa
For sliding mass	
Unit weight of sliding mass	18 kN/m^3
Effective friction coefficient of the sliding mass	0.70

2-2 Aso Volcanological Laboratory landslide

United Nations Educational, Scientific and Cultural Organization · UNESCO Chair on Geoenvironmental Disaster Reduction, Shimane University, Matsue, Japan

Simulation result

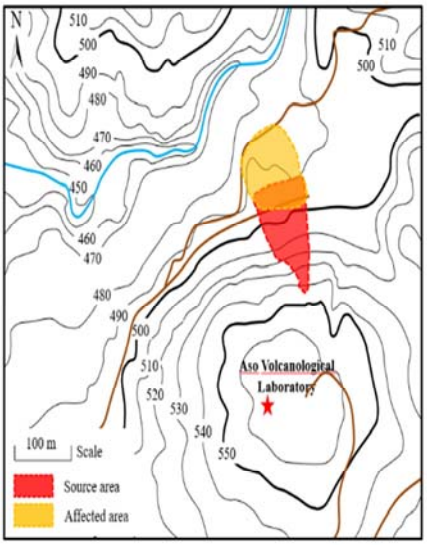

3 Western Shimane Prefecture Earthquake

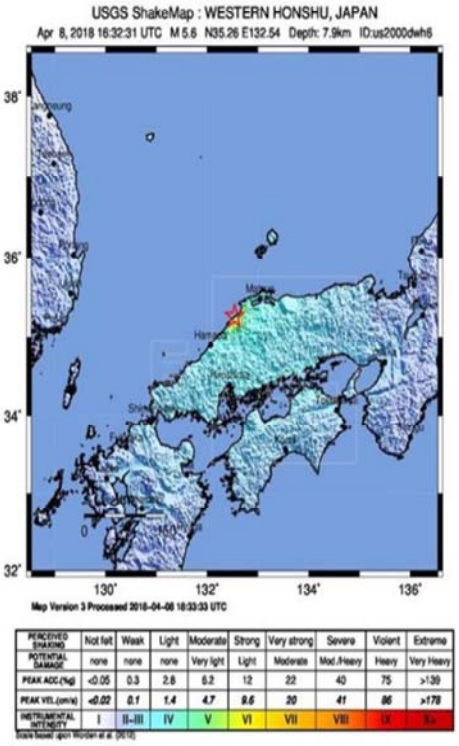

The M6.1 Western Shimane Prefecture Earthquake occurred on 9 April 2018 and made four people lightly injured, at least 1,000 buildings collapsed.

According to the Japan Meteorological Agency, the location of the hypocenter was 35.170°N 132.604°E, with the depth of 12 kilometers.

3 Western Shimane Prefecture Earthquake

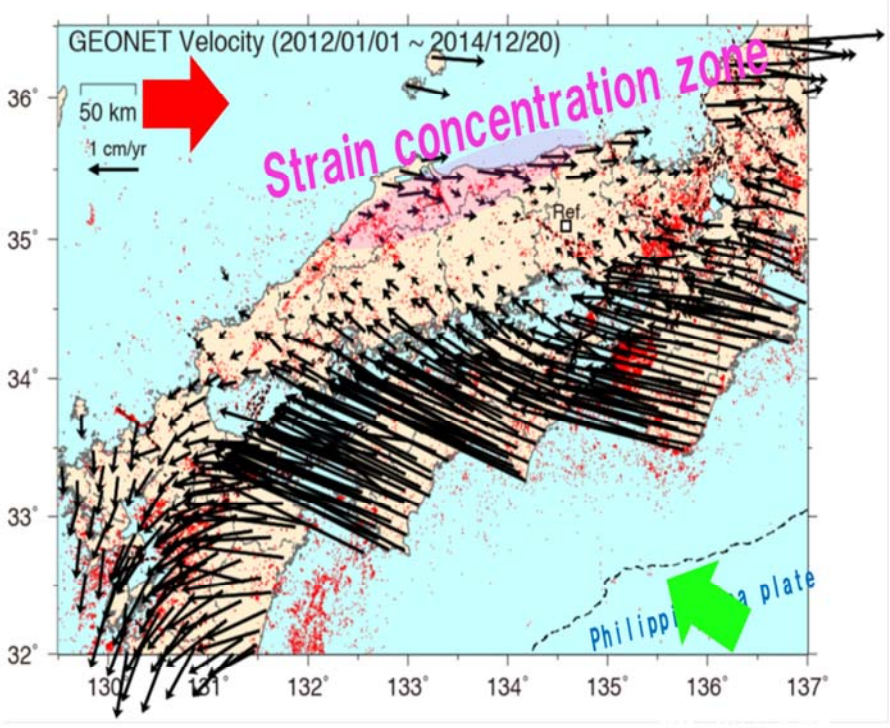

Liquefaction at harbor areas

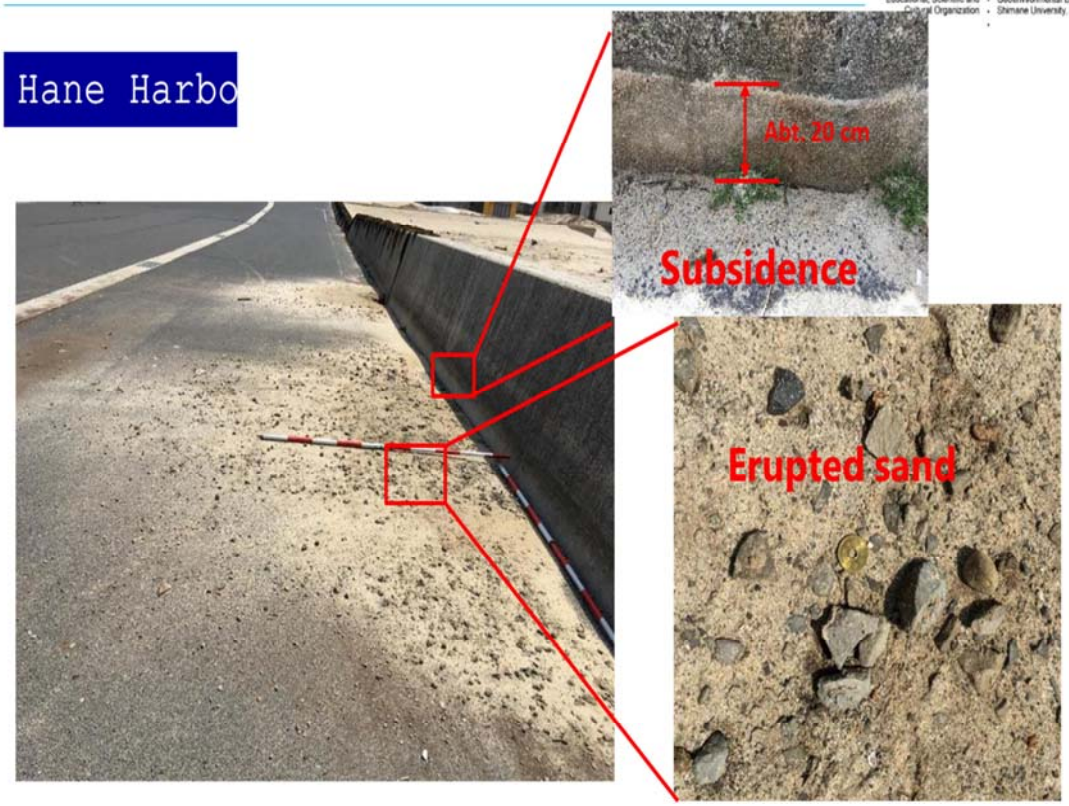

Rotation of the tombstone

3-1 Kamihashinami landslide

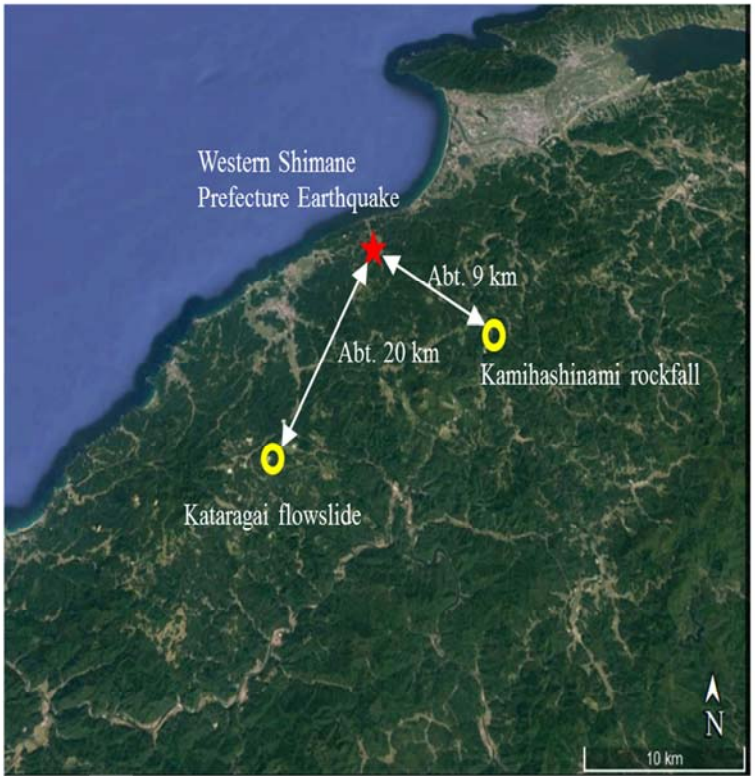

3-1 Kamihashinami rockfall

3-1 Kamihashinami rockfall

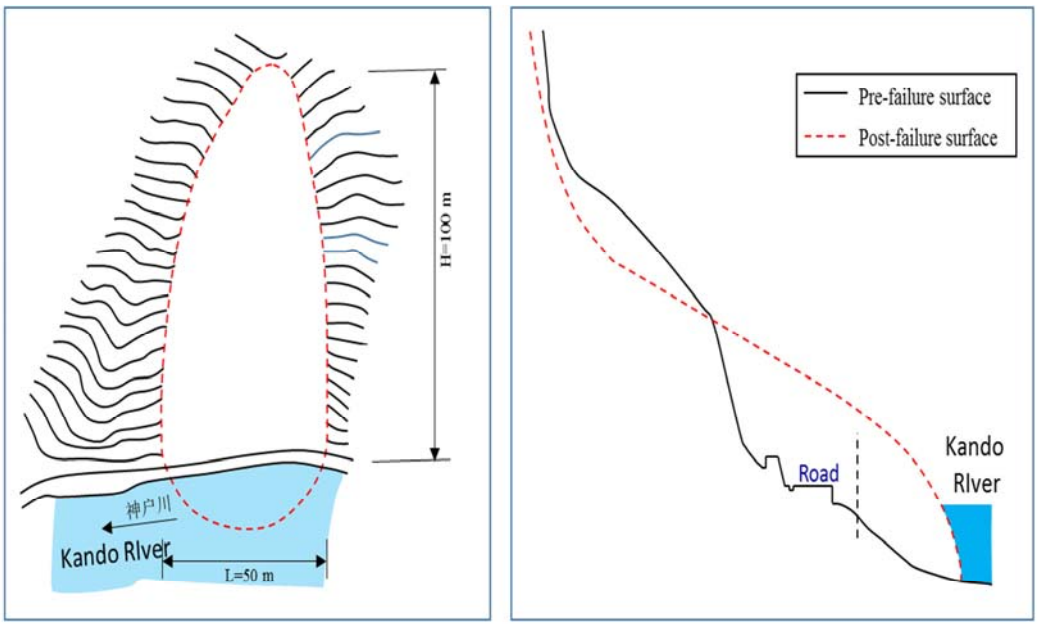

Sliding mass: Weathered rhyolite

3-1 Kamihashinami rockfall

Parameters used in the simulation

For sliding zone	
Initial apparent friction coefficient	0.50
Accumulation possibility of excess pore pressure	0.0
Lateral earth pressure coefficient (*K*)	0.70
Effective friction coefficient at sliding zone	0.70
Shear resistance of sliding zone at steady state	500 kPa
For sliding mass	
Unit weight of sliding mass	20 kN/m^3
Effective friction coefficient of the sliding mass	0.70

3-1 Kamihashinami rockfall

Simulation result

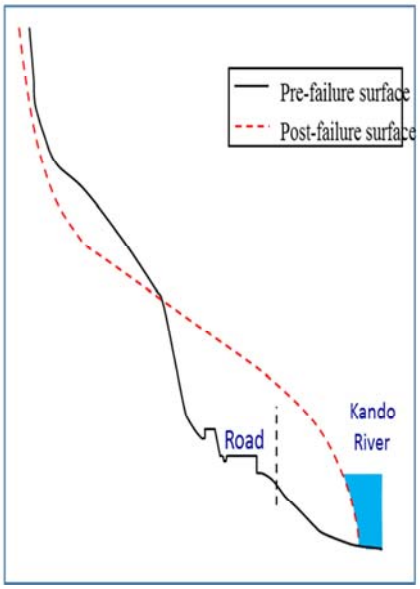

3-2 Kataragai flowslide

United Nations Educational, Scientific and Cultural Organization

UNESCO Chair on Geoenvironmental Disaster Reduction, Shimane University, Matsue, Japan

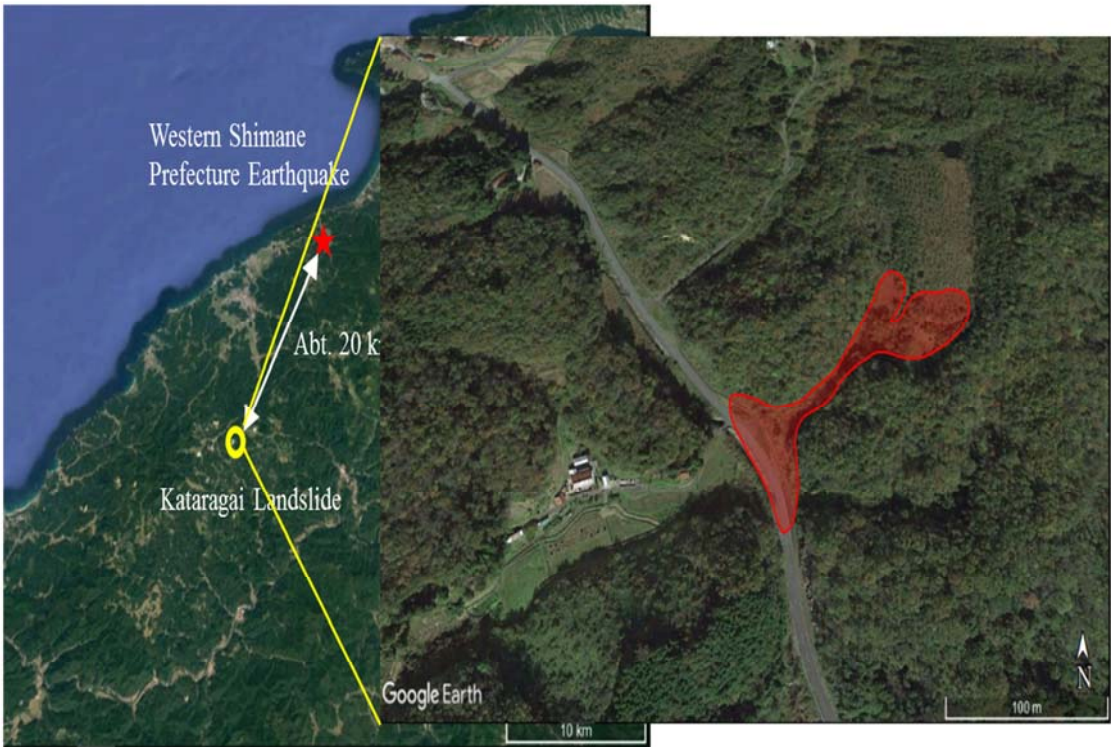

3-2 Kataragai flowslide

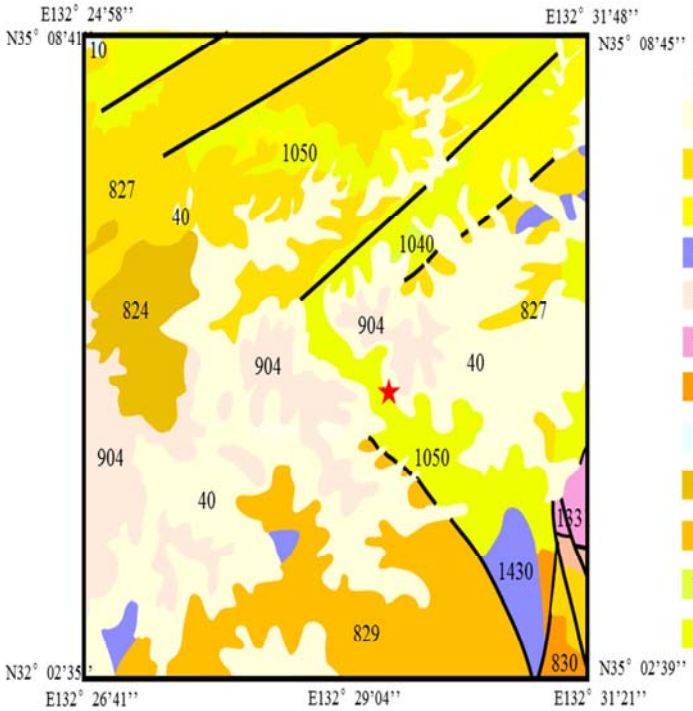

3-2 Kataragai flowslide

Source area

3-2 Kataragai flowslide

Source area

Portable dynamic cone penetration test (PDCP)

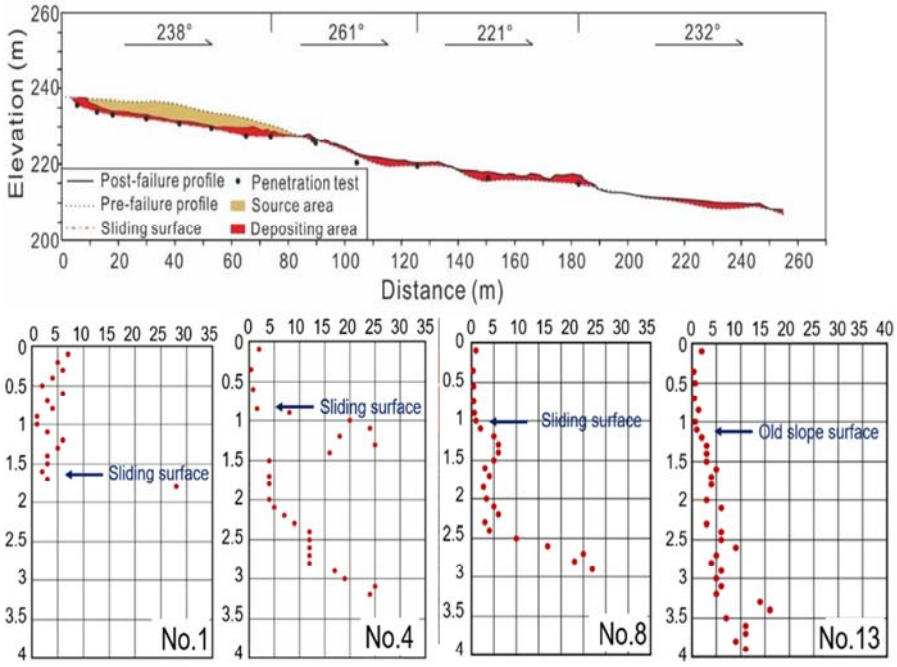

Portable dynamic cone penetration test (PDCP) results at points No. 1, 4, 13

3-2 Kataragai flowslide

Depositing area

3-2 Kataragai flowslide

Parameters used in the simulation

For sliding zone	
Initial apparent friction coefficient	0.10
Accumulation possibility of excess pore pressure	1.0
Lateral earth pressure coefficient (*K*)	0.85
Effective friction coefficient at sliding zone	0.577
Shear resistance of sliding zone at steady state	2 kPa
For sliding mass	
Unit weight of sliding mass	18 kN/m^3
Effective friction coefficient of the sliding mass	0.577

3-2 Kataragai flowslide

Simulation result

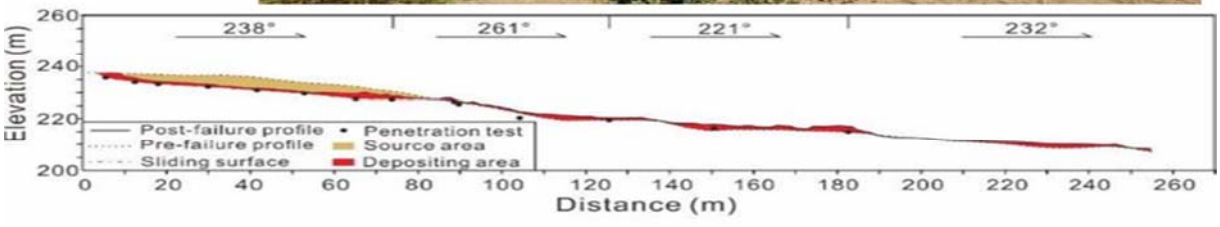

4 Comparison and conclusions

United Nations Educational, Scientific and Cultural Organization · UNESCO Chair on Geoenvironmental Disaster Reduction, Shimane University, Matsue, Japan

Features		Aso Bridge Landslide	Aso Volcanological Laboratory Landslide
Topography	Elevation difference	340 m	99 m
	Slope angle of the source area	30°	22°
	Free space conditions in front of the landslide	a 80-m gorge at the front	a hill in the NE corner and a platform at the front
Material compositions		cohesive soil with lapilli and block	strongly weathered lava
Deposit features		Most of the sliding mass ran into the Gorge and left loose residual deposits	The deposits were undivided, with some original soil structure and cracks remaining
Motion features	Sliding distance	Long, more than 700 m	About 110 m
	Sliding direction	S61° E, almost unchanged during propagation	Changes from N-direction of the scarp to NW-direction of the toe
	Speed	Rapid	Slow
Damage		Destroyed a bridge, national road, railway, and supply water channel, and killed one person	Three houses on the slope moved with the sliding mass, but did not collapse. The concrete road was damaged

4 Comparison and conclusions

United Nations Educational, Scientific and Cultural Organization · UNESCO Chair on Geoenvironmental Disaster Reduction, Shimane University, Matsue, Japan

Features		Kamihashinami rockfall	Kataragai flowslide
Topography	Elevation difference	100 m	28 m
	Slope angle of the source area	70°	10°
	Free space conditions in front of the landslide	Road and river	Gentle valley
Material compositions		Weathered rhyolite rock mass	Refilled sandy soil
Deposit features		Deposited in repose angle	Flow-like, debris flow deposit
Motion features	Sliding distance	Short, 30 m from the slope toe	About 230 m
	Sliding direction	Along the slope dip direction	Along the valley
	Speed	Very rapid	rapid
Damage		Dammed the road and river partially	Damaged the forest and road fence, and covered the road for longer than 40 m

4 Comparison and conclusions

United Nations Educational, Scientific and Cultural Organization

UNESCO Chair on Geoenvironmental Disaster Reduction, Shimane University, Matsue, Japan

Landslide name	Landslide type	Material	Volume (4×10^3 m^3)	Saturation situation	Runout	ϕa (o)
Aso Bridge Landslide	Rotational landslide	Weathered volcanic ash	1,980	High in lower part	375	22.5
Aso Volcanological Laboratory Landslide	Translational landslide	Weathered volcanic ash	50	High in foot part	65	13
Kamihashinami rockfall	Rockfall	Weathered rhyolite	4	Dry	15	43
Kataragai flowslide	Earthflow	Refilled sandy soils	10	Fully saturated	230	7

The Landslides triggered by the Hokkaido Iburi-Tobu Earthquake on September 6th 2018

Hiromitsu Yamagishi(1), Fumiaki Yamazaki(2)

1) Hokkaido Research Center of Geology(HRCG)
e-mail: hiromitsuyamagishi88@gmail.com
2) PENTAX TI Asahi Co. Ltd.

Abstract

On September 6th, 2018, an intense earthquake struck Hokkaido Iburi-Tobu area. This earthquake, triggered many landslides which claimed 36 lives. The landslide numbers were estimated at 8,000 and mostly are shallow landslides moving down of the air-fall pumice layer from active volcano which erupted ca. 9,000 years ago. However, deep-seated landslides are also found.

Damages by the earthquake Sep 6th 2018

- Landslide area: 200km^2
- Victims 41 (36 were by the landslides)
- Power off for the whole Hokkaido (43 hours black out)
- Liquefaction disasters: Kiyota-ku , Kita-ku and Higashi-ku, Sapporo
- 1463 houses and building: 1420

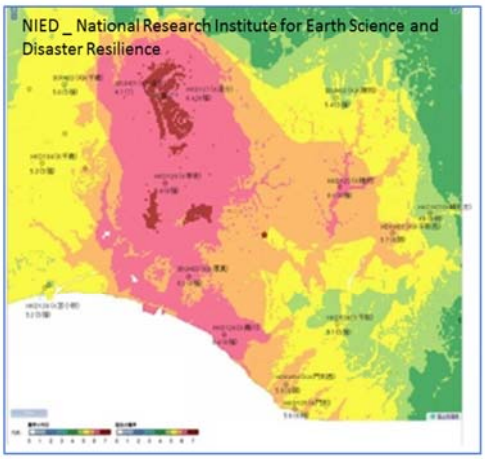

Seismic coefficient distribution

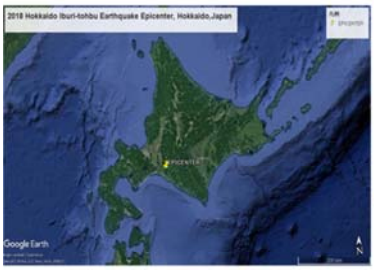

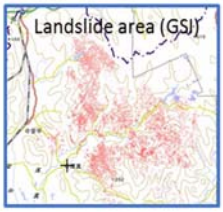

Open Access

JMA Magnitude was 6.7 and Maximum Intensity was 7 at Atsuma Town

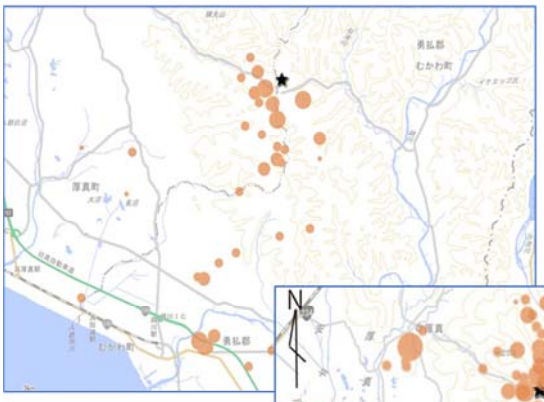

NIED(2018 Sep 11)

- These epicenter group was located in the southeast of Ishikari Lowland East Margin Fault zone and the depth was 37km

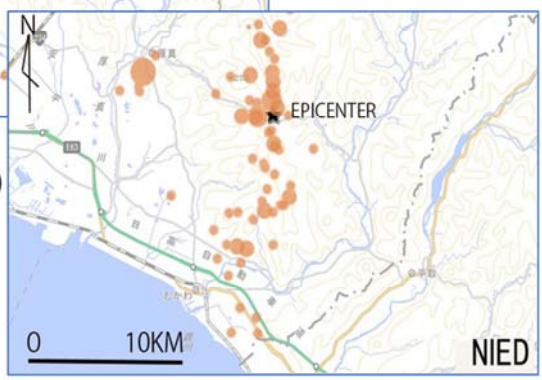

NIED （2018 Sep 17)

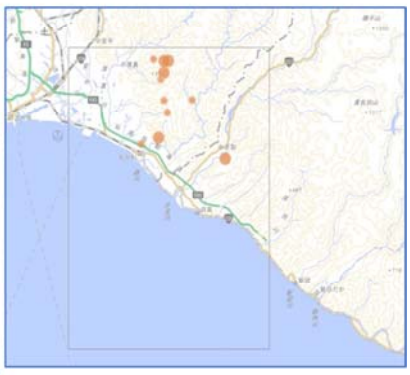

NIED （2018 Nov 17)

Climatic condition at the earthquake Typhoon Jebi (No 21 in Japan) was passing just before the earthquake

Total Precipitation from Sep 3 to 5

Maximum hourly precipitation from Sep 3 to 5

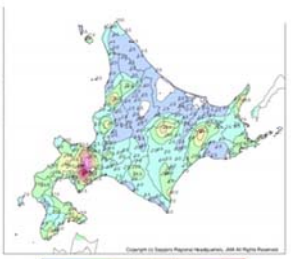

Warning issue of each town

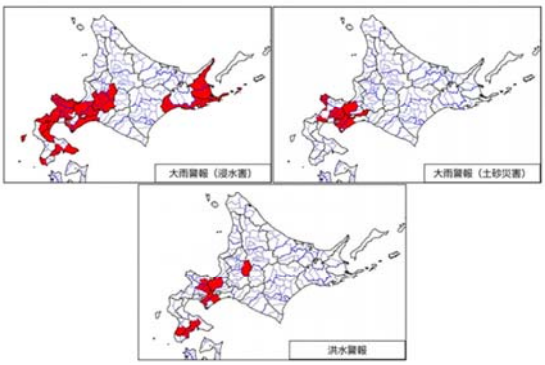

From Website of Meteorological Agency of Japan

6,000 to 8,000 landslides are identified by air photographs

Abandant shallow landslides. Taken by Asia Air Survey and Asahi Corporation

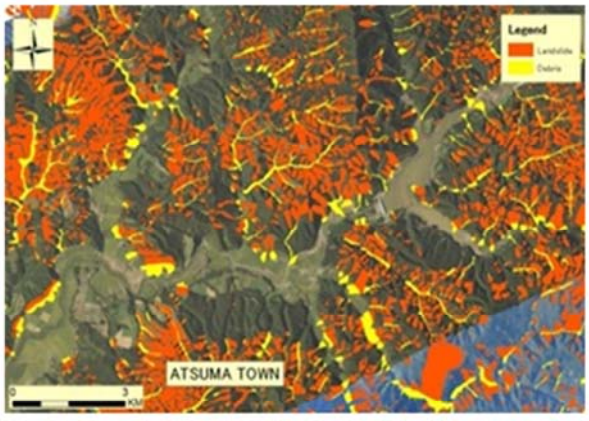

Total 6,000 landslides were inventoried by Kouichi Kita throughout the ortho photos of Geographical Survey of Institute, Japan (GSI)

Two types were recognized for shallow landslide (failure, hokai)1) Planar type, 2)Spoon type

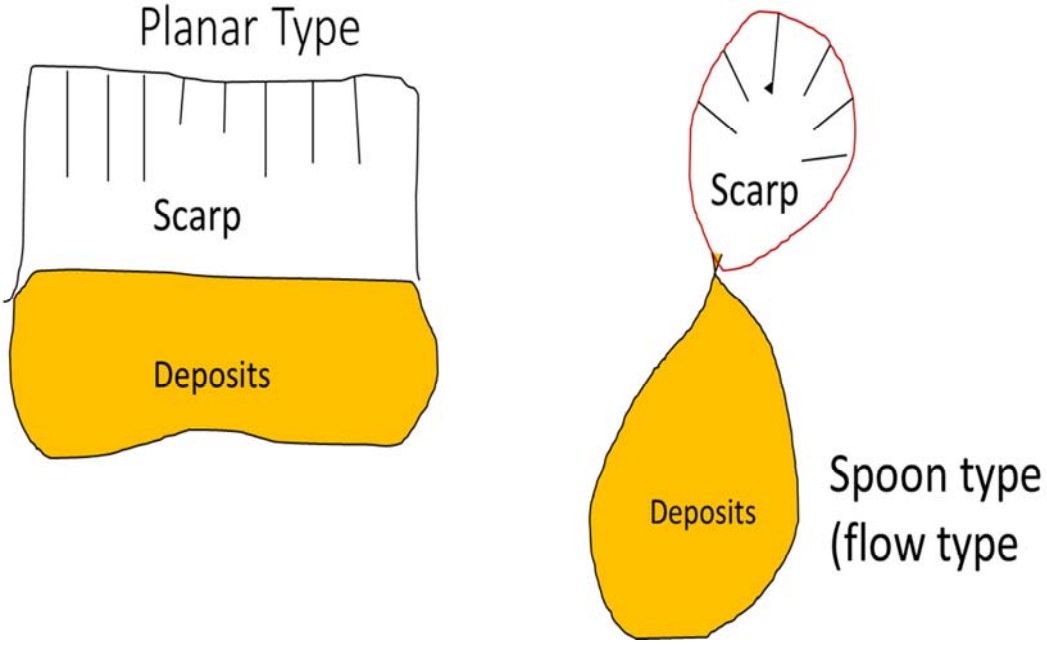

Interpretation of GSI: Chiriin Chizu

Shallow landslides (Failure, Hokai)

1) Planar Type 2) Spoon Type

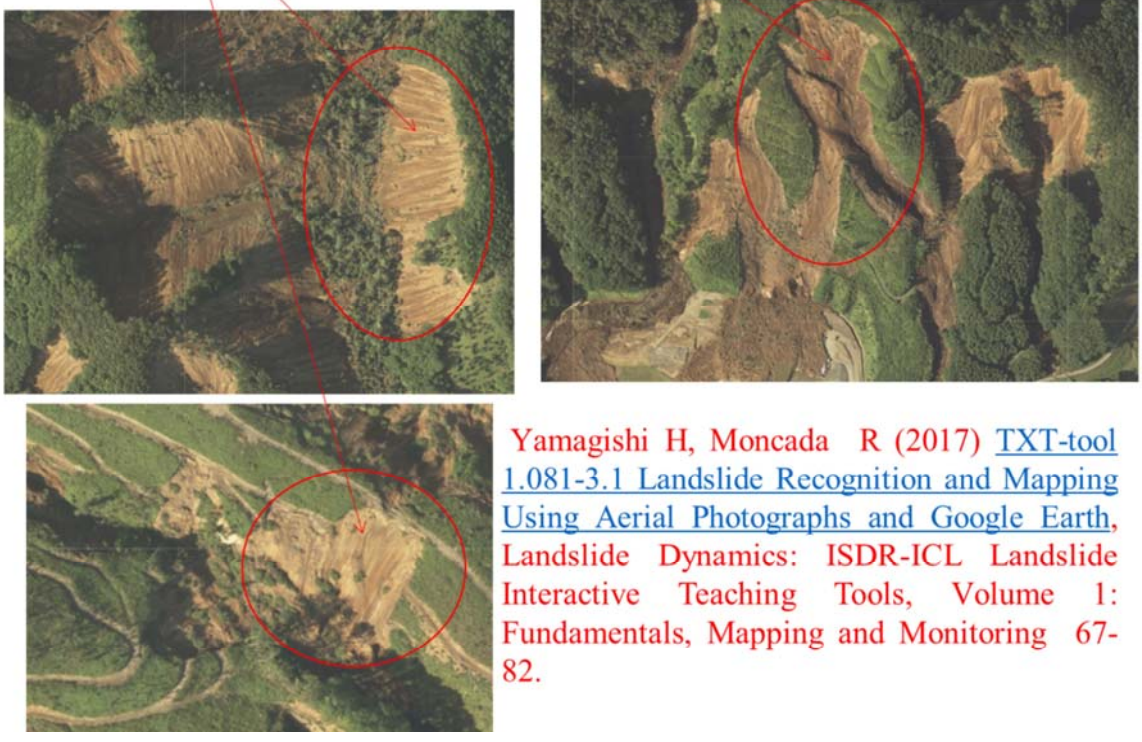

Yamagishi H, Moncada R (2017) TXT-tool 1.081-3.1 Landslide Recognition and Mapping Using Aerial Photographs and Google Earth, Landslide Dynamics: ISDR-ICL Landslide Interactive Teaching Tools, Volume 1: Fundamentals, Mapping and Monitoring 67-82.

Deep-seated landslides (Jisuberi) were also recognized

Deep-seated landslide types (Varnes , 1978, Highland and Bobrowsky, 2008)

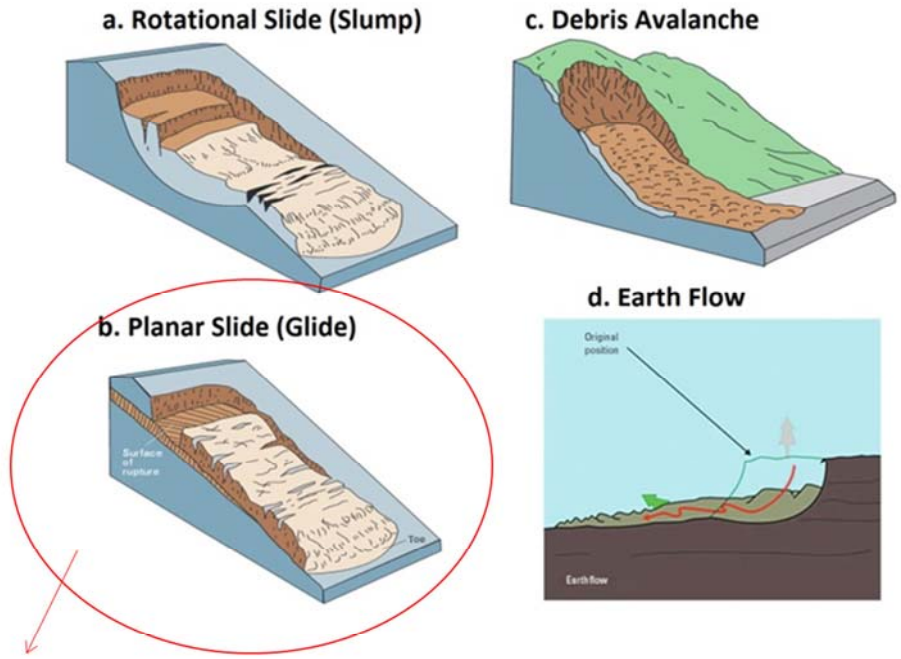

This type is many in the case of the earthquake-induced deep-seated landslides

3D image by Airphoto-SFM(by Shin Engineering CO. Ltd)

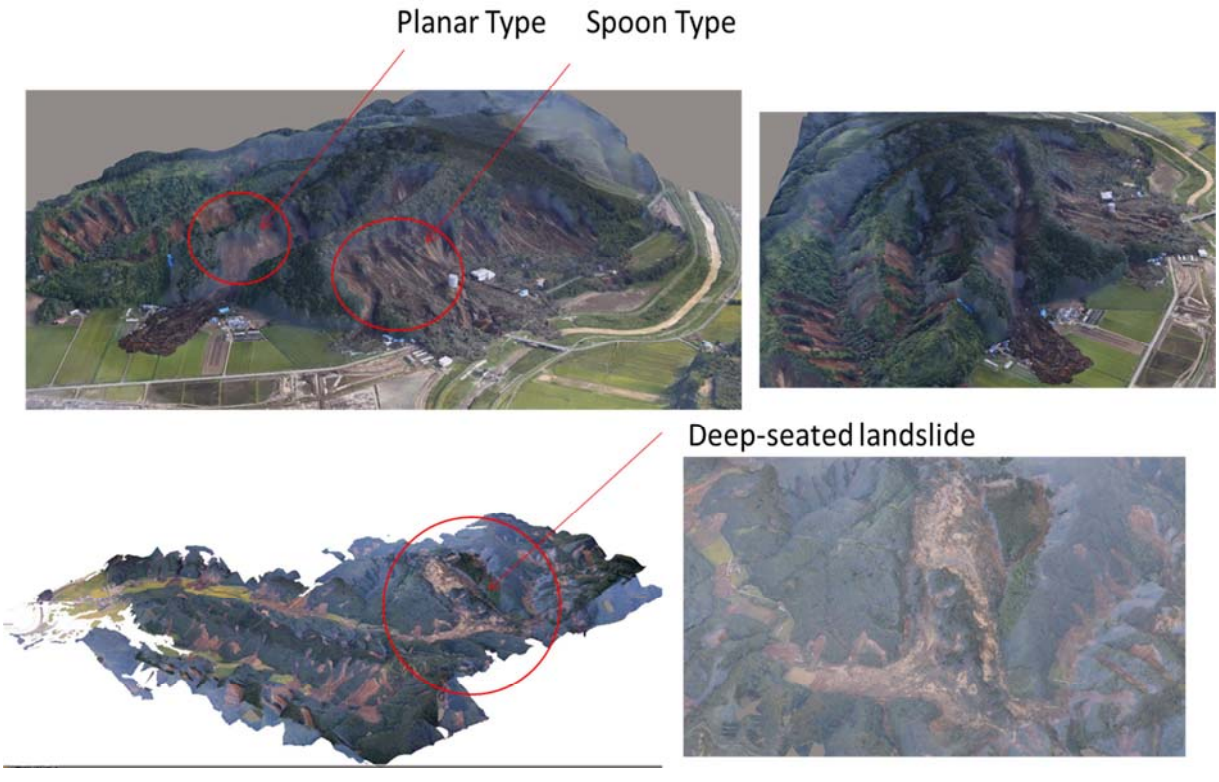

Deep-seated landslide occurred between the two old landslides by Yamagishi Landslide Map)

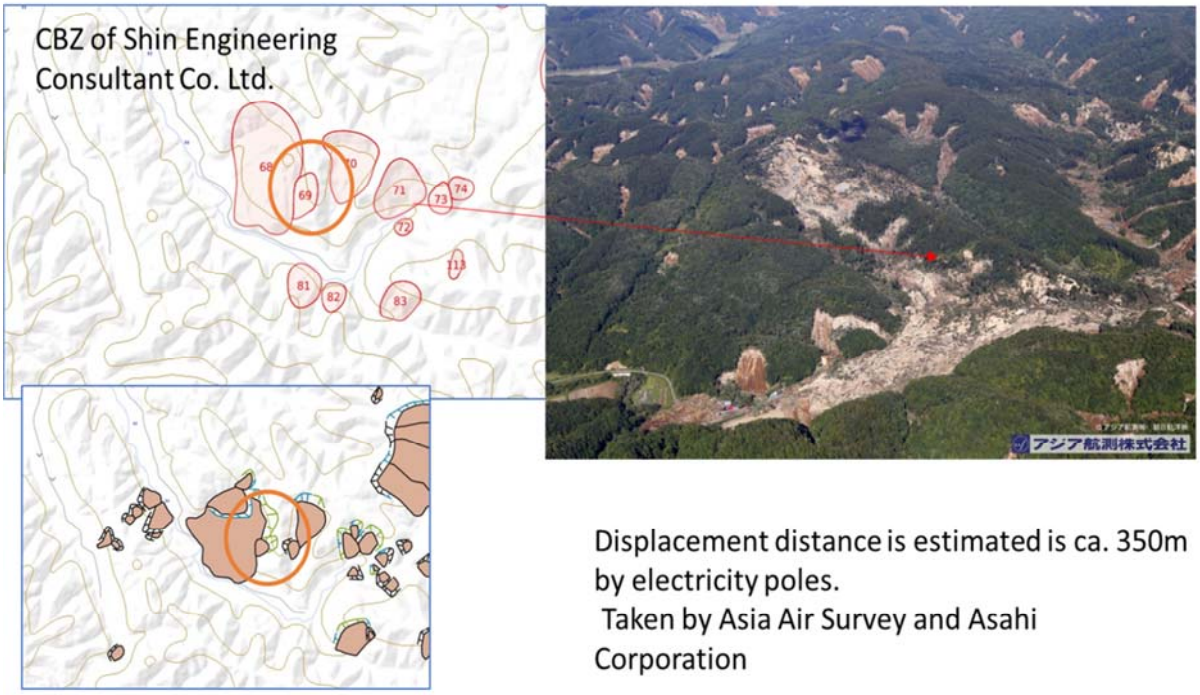

Displacement distance is estimated is ca. 350m by electricity poles.
Taken by Asia Air Survey and Asahi Corporation

Dip-slipping landslide caused by gentle dipping of sedimentary rocks

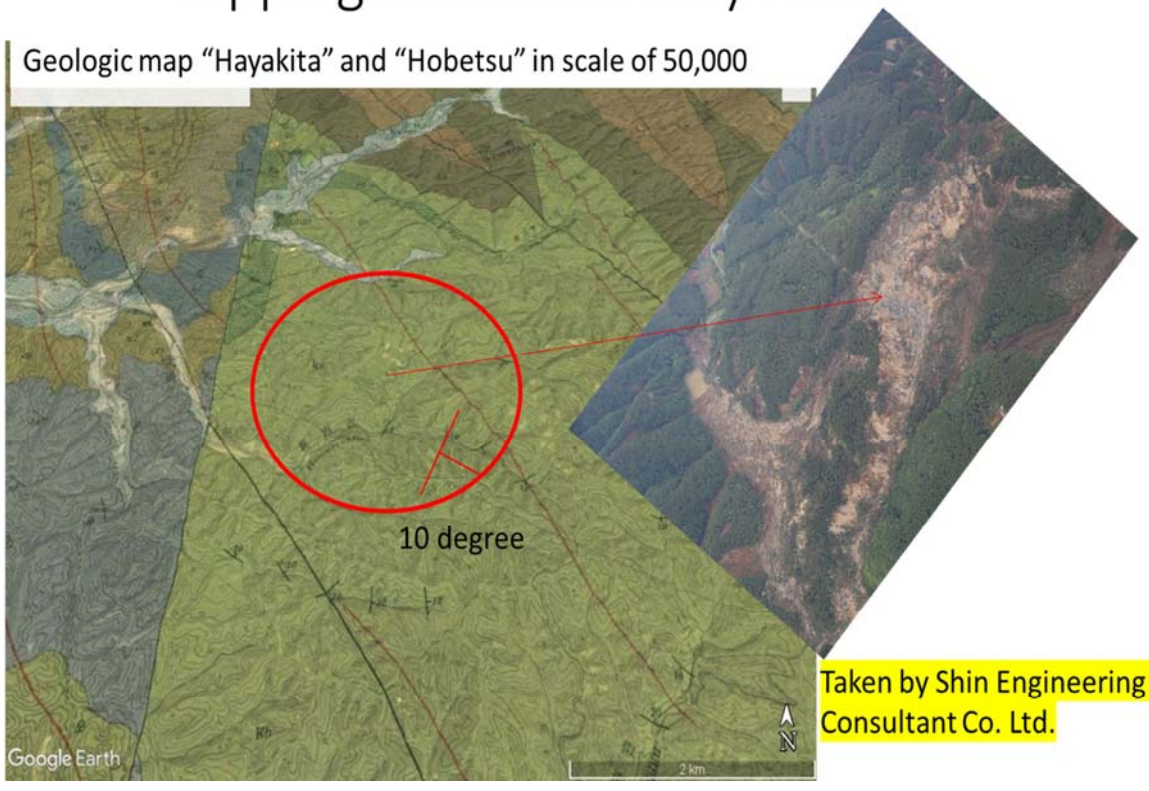

Taken by Shin Engineering Consultant Co. Ltd.

Deep-seated landslide (Jisuberi, glide type) are also identified in the orthophoto(Geographical Survey Institute, Japan)

Ongoing Project 1:
GIS Analyses of the landslide distribution

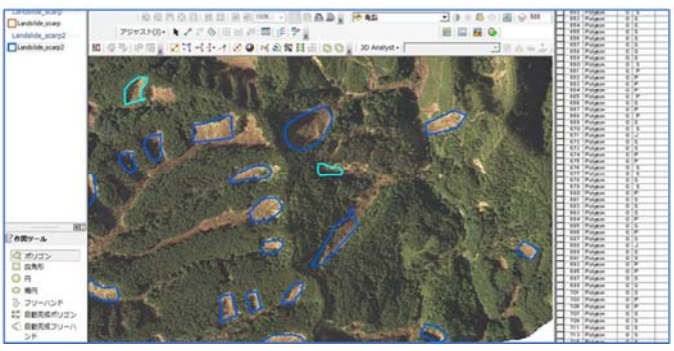

In order to reveal the relationship to the elevations, slopes, curvatures , geology and vegetations etc., we are statistical analyzing using ArcGIS 10.2. In this case, we are classifying into Planar type(P), Spoon type(S) and Deep-seated landslides(J)

GIS Analyses using DEM from GSI, Japan (ArcGIS10.2)

Landslide polygon
5M DEM Using

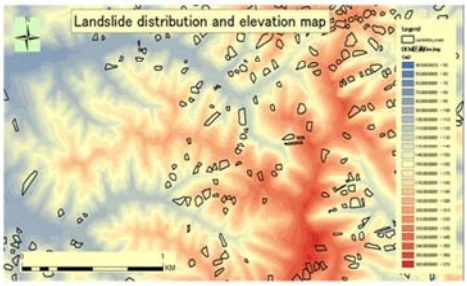

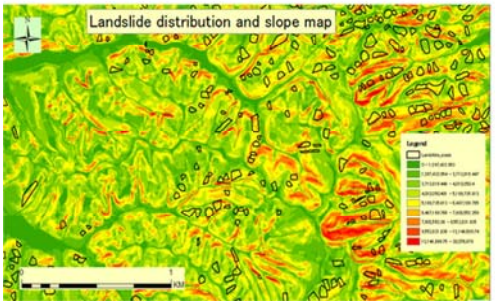

Landslide point
10m DEM Using

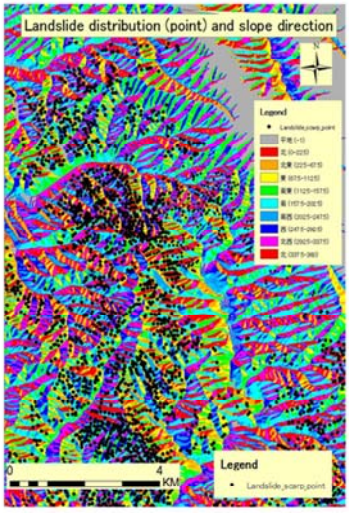

Landslide distribution
Related to slope direction

Landslide distribution
Related to slope curvature

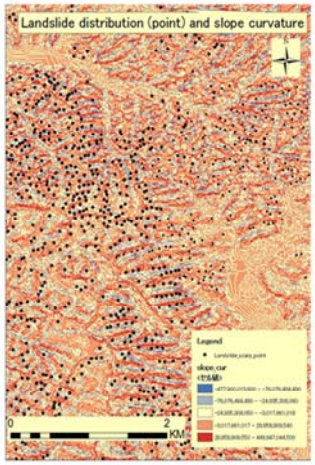

Ongoing Project 2:
3D-Point Cloud Analyses and Simulation for the sliding and flows

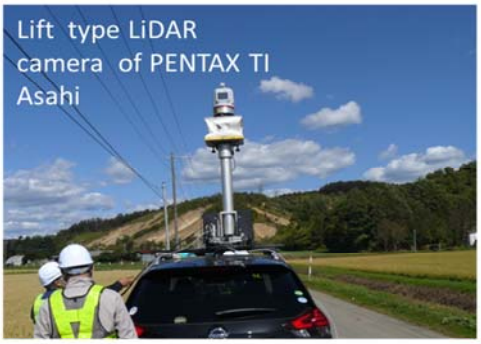

Bottom is fine grained pumice, and top is trees

Point cloud of 5M DEM from GSI and investigation site of long (2km) distance LiDAR (PENTAX TI-Asahi Co.Ltd)

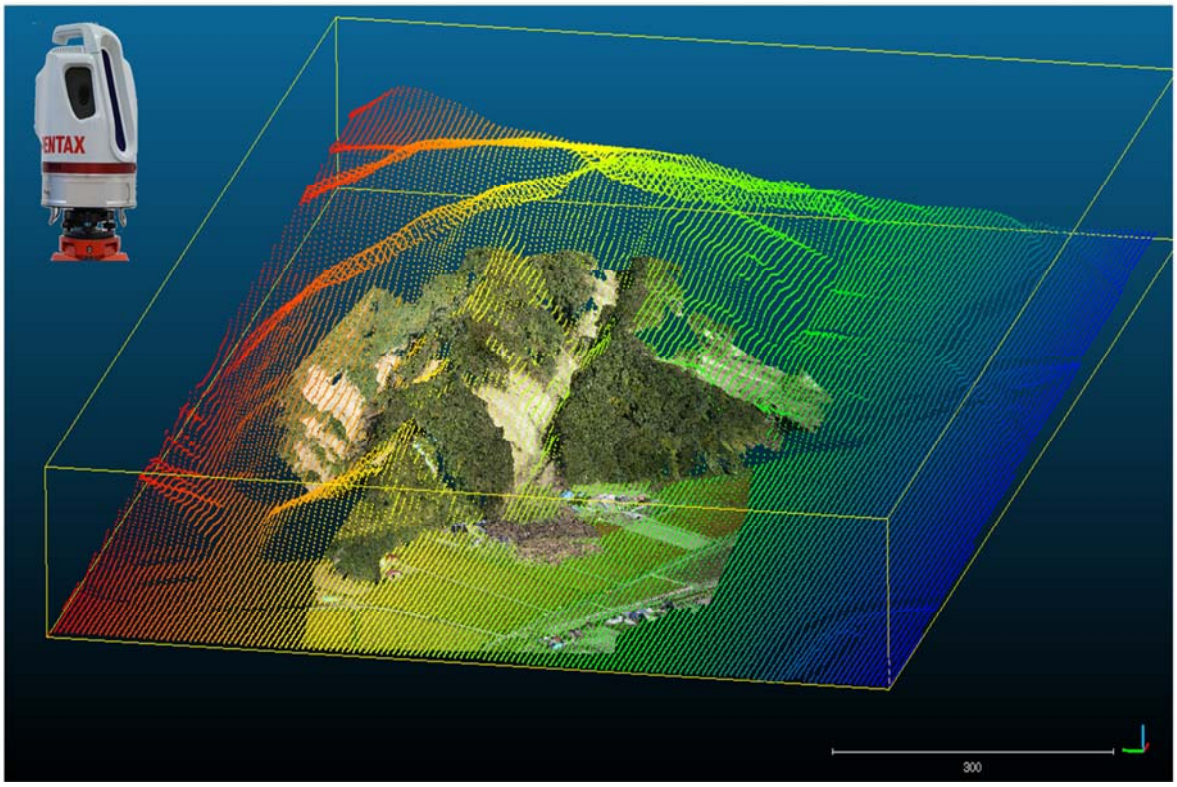

1． 3D SFM Model of 150 million points

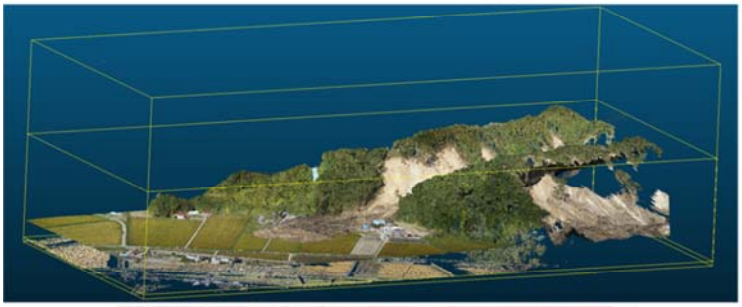

Image of profile of the surface layers

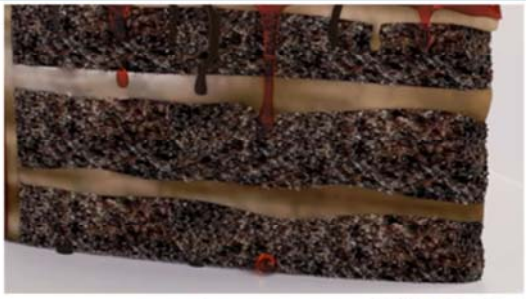

Similation model of pumice fragment on the slope and valley

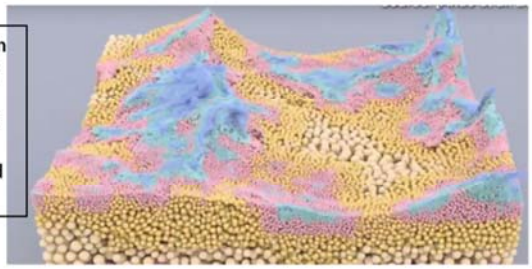

Dynamic Rigid Body Fragmentation

After the earthquake

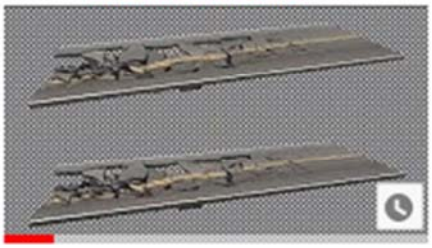

Agitation of pumice fall

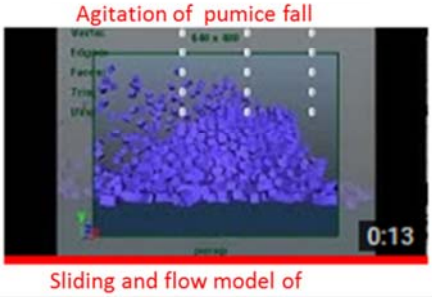

Sliding and flow model of slope and V-shaped valley

Expected Results of the simulation

3D Dynamics of mass movement (sliding and flow)

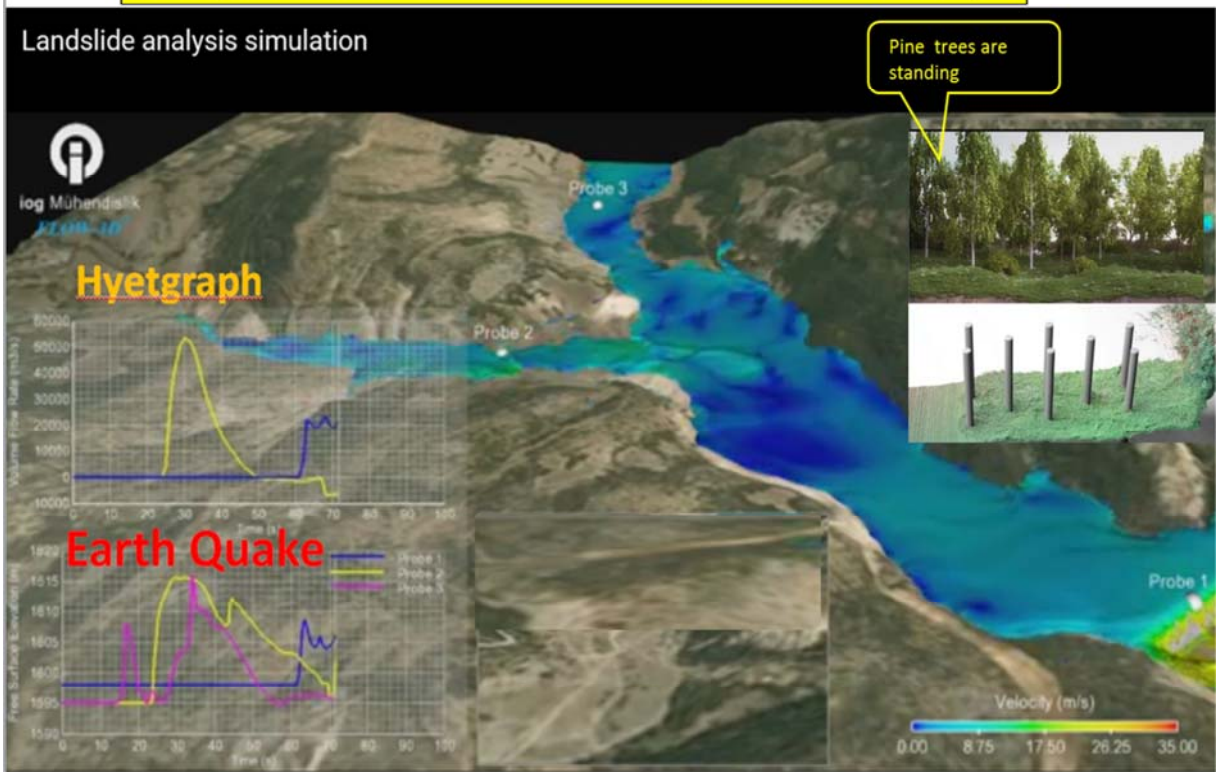

Preliminary Conclusion

- This earthquake is very similar to Chuetsu Earthquake on October 23, 2004 at Mid Niigata, Japan. The earthquake occurred struck the mountains and hills of the Neogene sedimentary rocks and M6.8 and 13 km depth, max intensity 7. The number of landslides was estimated at 3700.
- This earthquake was M6.7 and 37km depth, max intensity was 7. However, the geology is the pumice and ash from the active volcanoes to the west. Therefore, most of the sliding materials are pumice and soils with trees. These landslides are classified to 1) Planar type and 2) Spoon type, and 3)Deep-seated landslides. The number of the landslides is estimated at 6,000 to 8,000.

We are now doing the two projects:

1) GIS analyses for revealing how to related to the topographic and geologic factors.

2)3D point cloud analyses and simulation of sliding and flowing

Thank you for your attention!

Recognition of potentially hazardous torrential fans using geomorphometric methods and simulating fan formation (IPL-225 Project)

Matjaž Mikoš[(1)], Nejc Bezak[(1)], Matej Maček[(1)], Tomaž Podobnikar[(1)], Jošt Sodnik[(1,2)], Sandi Kaltak[(1)]

1) University of Ljubljana, Jamova c. 2, 1000 Ljubljana, Slovenia
e-mail: matjaz.mikos@fgg.uni-lj.si
2) TEMPOS Ltd., Ljubljana, Slovenia

Abstract

The preliminary results of the IPL-225 project will be presented. The project structure will be discussed, and the first project findings presented. The computer simulation program RAMMS was tested (sensitivity analysis performed) and then applied to the 2000 Stože debris flow, Slovenia. The computer software eCognition was applied to develop different algorithms to be used with digital elevation models (DEMs) in order to semi-automatically recognize torrential fans in the mountainous and hilly terrain. The SPH (Single Particle Hydrodynamics) method was tried to numerically simulate non-Newtonian rheological flows such as debris flows in laboratory controlled conditions. The 3-year research project will end in May 2020 – it will be fully financed by the Slovenian Research Agency (ARRS Project J7-8273).

I. Overview of the IPL-225 Project

- **WP I Project Management**
- **WP II Spatial Data Acquisition and Preprocessing**
  - Task (1) DTM and DSM acquisition, quality control, gross and systematic error removal, improving quality.
  - Task (2) Obtaining other information about the fans (based on fieldwork, geological maps, etc.).
  - Task (3) Data homogenization.
- **WP III Geomorphometric analysis for fan determination**
  - Task (1) Classic geomorphological fan mapping in selected areas, and field sedimentological inventory to define the fan's genesis; selection of key geomorphological characteristics of certain fan types.
  - Task (2) Processing variables (factors) for geomorphometric analysis.
  - Task (3) Analysis/modelling with spatial data, rheological information, and other relevant descriptive information.
  - Task (4) Comparison of the classical and developed methodology results.

I. Overview of the IPL-225 Project

- **WP IV Applying the Mathematical Model to Stimulate Triggering and Movement of Debris Flows**
  - Task (1) Application of 2D debris-flow models (RAMMS, triggering phase: LS-RAPID).
  - Task (2) Soil samples rheological analysis using large rheometer ConTec Viscometer 5.
  - Task (3) A comparison of both groups of analysis and a sensitivity analysis.
  - Task (4) Comparison of geomorphometric analysis and numerical simulations of the formation of torrential fans.
- **WP V Dissemination of Project Results**
  - Task (1) At international conferences (IPL, WLF, EGU).
  - Task (2) In international journals (Landslides, MDPI Geosciences).

II. Processing of selected (relevant) torrential fan variables (indicators)

WP III Geomorphometric analysis for fan determination – we focused on:

Task (2) Processing variables (indicators) for geomorphometric analysis.

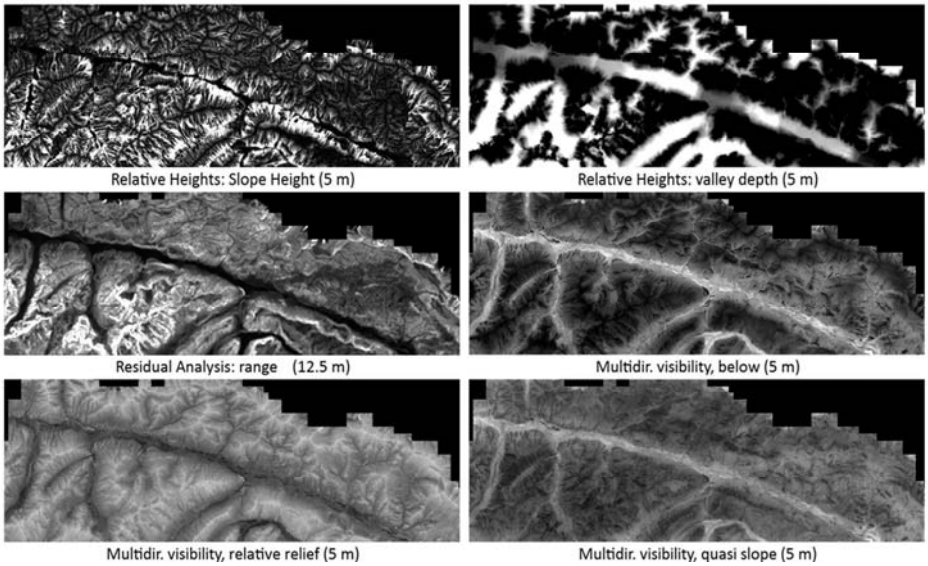

The Upper Sava River valley in NW Slovenia.

Potential multi-scale variables for fan prediction

II. Morphometric analysis of torrential fans – Revised principles, concrete solutions

Focus on more robust and automated solutions.

Multi-resolution (spatial scales defined):

- DTM (1), 5, 12.5, 25, 100

Testing and selecting the potential of software and algorithms for fan recognition:

- ~ 20 different software
  - ✓ArcGIS (+Terrain tools + Jenness), QGIS, SAGA GIS, GRASS GIS, GDAL, MICRODEM, GAT, eCognition…
- ~ 200 algorithms
  - ✓getting more relevant and robust variables
  - ✓providing higher level of automation, towards fully automated approach

II. Morphometric analysis of torrential fans – Revised principles, concrete solutions

- **Developing new algorithms for indicators processing**
  - focus on MVI (Multidirectional Visibility Index) principles (Podobnikar 2012) for geomorphological features recognition
  - → developing a number of enhanced solutions
  - → developing supportive enhanced visual methods
- **Optimizing algorithms for better processing**
  - important to process higher spatial resolution and large datasets, results:
    - ✓processing speed increased (with factor ~100)
    - ✓larger datasets processed (with factor >10)

II. Morphometric analysis of torrential fans – Supporting revised principles, concrete solutions

- **Orientation to two predicting principles**
  - empiric
    - ✓rule based, progressive approach (according to taxonomy)
  - statistic
    - ✓machine learning approaches
- **Developing taxonomy**
  - primary: for the torrential fan area determination
  - secondary: according to already determined fan area

Rheology – funnels and rheometer

Limestone flour was tested in different funnels and rheometer at different water contents in order to observe consistency between different measurement methods *and between measurements and numerical prediction (not yet performed).*

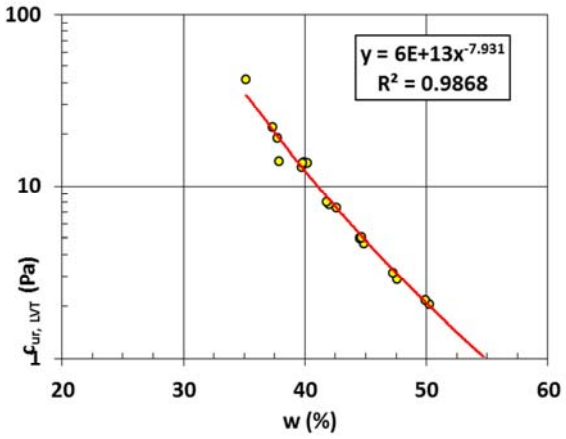

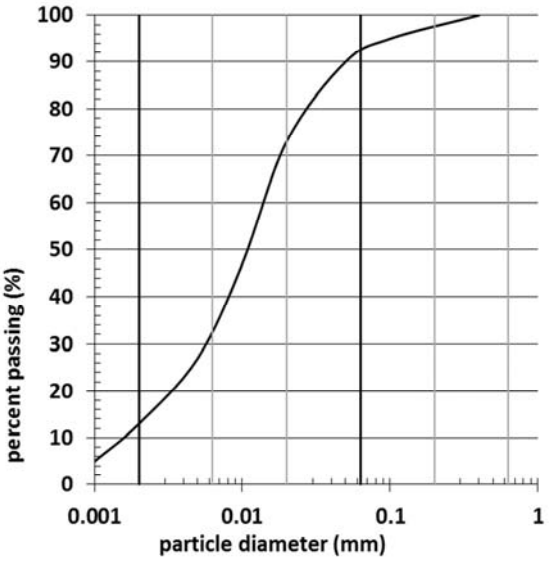

Remoulded undrained shear strength from laboratory vane test (LVT)

Rheology – Marsh Funnel, cone funnels

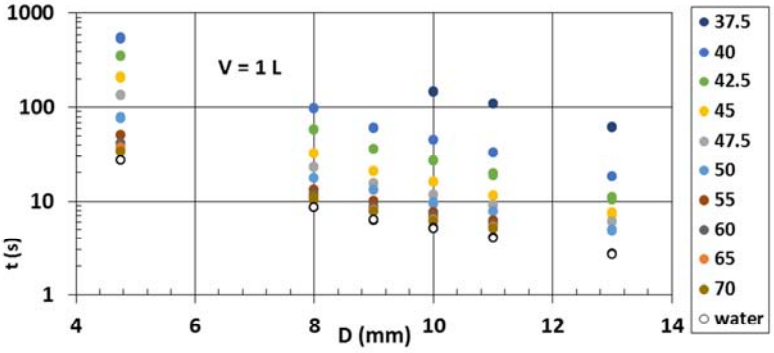

influence of water content and funnel orifice diameter

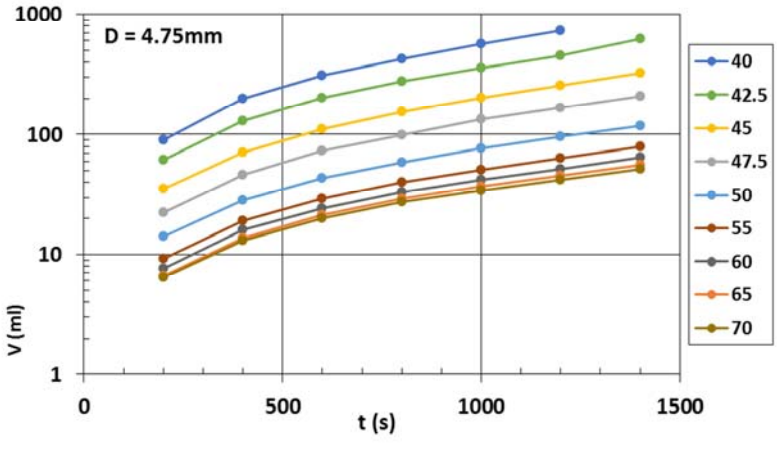

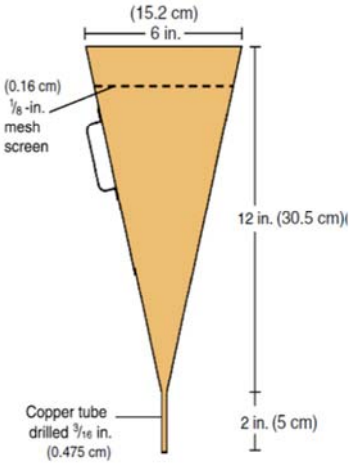

Rheology – Bingham model

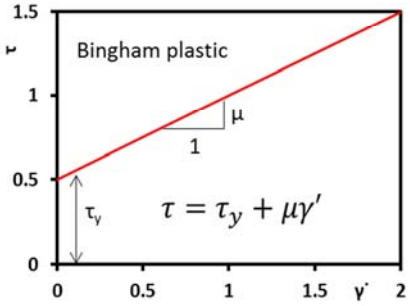

prediction based from flow in funnel based on τ_y estimation from LVT or by predicting both parameters (τ_y, μ)

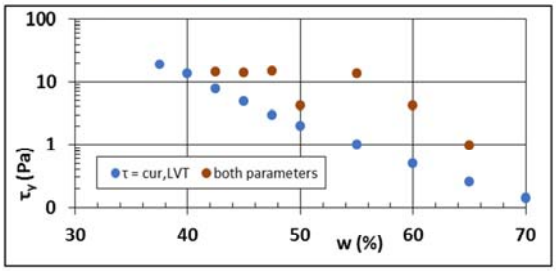

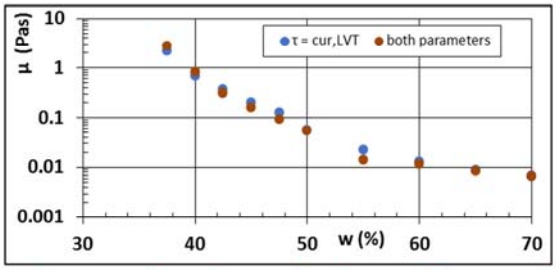

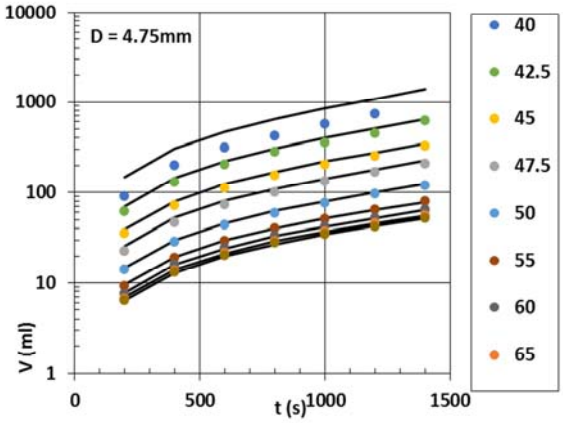

Determination of τ_y is problematic!

Nguyen et al. (2006) Flow of Herschel–Bulkley fluids through the Marsh cone. *J. Non-Newtonian Fluid Mechanics* 139

Rheology – V-funnel, Funnel groove

V-funnel

– only for specific water content

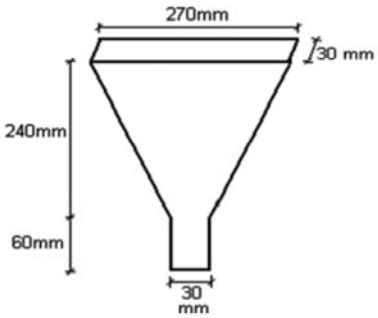

Funnel groove

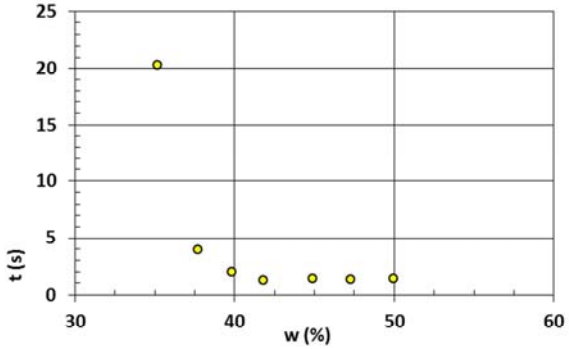

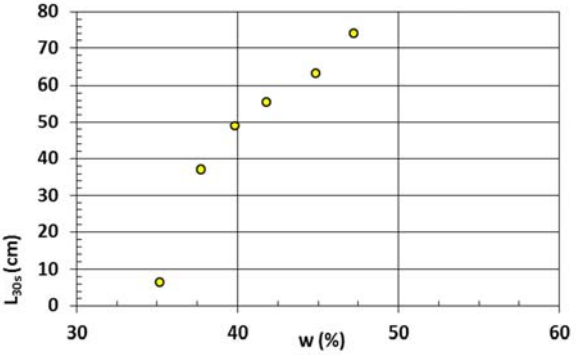

Rheology – rheometer

Brookfield DV3T rheometer with laboratory vanes was used:

– always plug flow regime!

– smaller τ_y than LVT (Bingham model)!

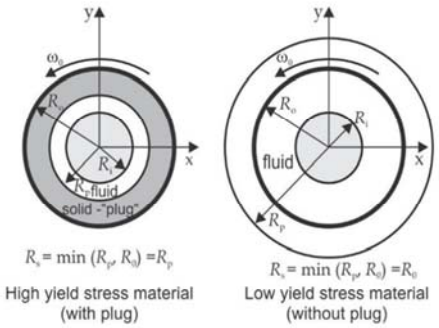

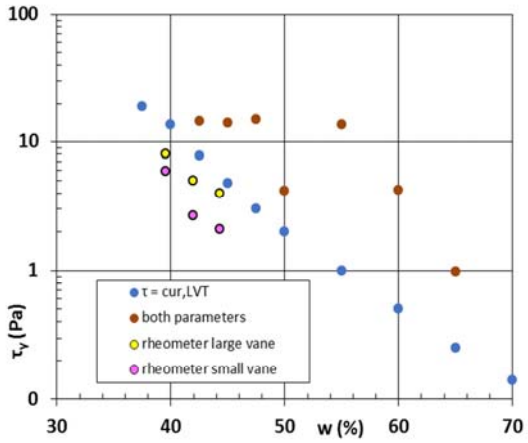

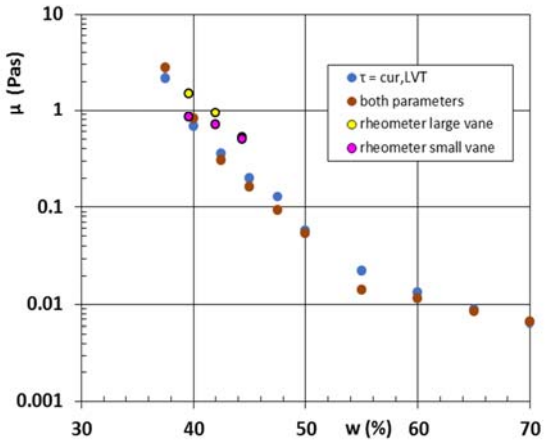

The RAMMS model (debris-flow module) used for the investigation of torrential fans' formation

- **RAMMS (Rapid Mass Movement Simulation) – a 2D dynamics modeling of rapid mass movements in 3D alpine terrain – developed at SLF, Davos, Switzerland – different modules for debris flows, rock falls, and avalanches (http://ramms.slf.ch/ramms/).**
- **Sensitivity analyses were carried out using artificial fan with constant slope (5°).**
- **Several RAMMS model parameters were investigated. Normalized sensitivity index (NSI) was calculated.**
- **RAMMS model was used for the 2000 Stože debris-flow case study modelling.**
- **RAMMS model was calibrated using field observations after the 2000 Stože debris-flow event.**
- **We also investigated impact of a coincidental sequence of debris flows on the debris-flow fan formation (using the Suhelj fan and artificial terrain).**

Sensitivity analyses using the RAMMS model with its debris-flow module

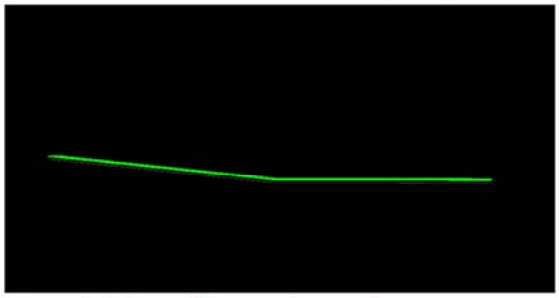

Sensitivity analyses were carried out using artificial fan with constant slope (5°). Deposition area was used as an output parameter.

$$NSI = \frac{|O - Om|}{|P - Pm|} \cdot \frac{|Pm|}{|Om|}$$

Sensitivity of investigated parameters using Normalized Sensitivity Index (NSI)

Note: higher NSI values indicate higher sensitivity of the investigated parameter. P_1,...P_5 are parameters variations related to the initial parameter value.

Parameter	P_1	P_2	P_3	P_4	P_5
Voelmy μ	0,859	1,171	0,665	0,514	0,351
Voelmy ξ	0,184	0,138	0,116	0,082	0,053
%Moving Mass	1,313	0,766	0,087	0,072	0,065
H_{cutoff}	0,243	0,021	0,014	0,009	0,008
Cell size	0,183	0,526	1,000	0,758	0,521

The 2000 Stože debris-flow case study

This event was (in the past) already modelled using several numerical models: Flo-2D & PCFLOW2D.

Graphical presentation of the modelled area of 2000 Stože debris flow event.

Areal photo of the devasted area in Log pod Mangartom.

The 2000 Log pod Mangartom case study

Graphical presentation of the input hydrograph location in the RAMMS model.

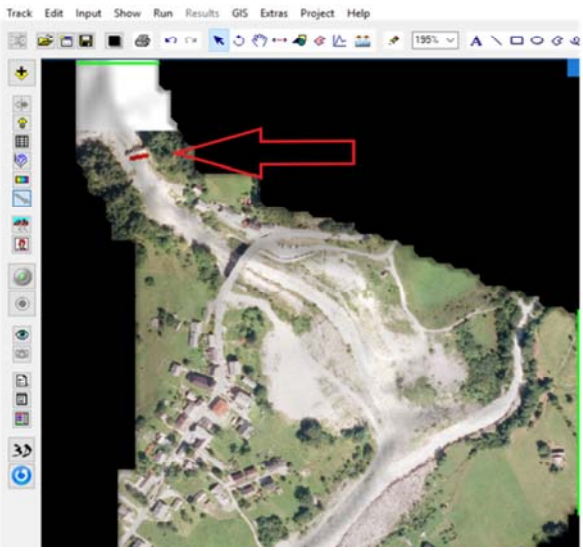

Input hydrograph of the 2000 Stože debris flow event.

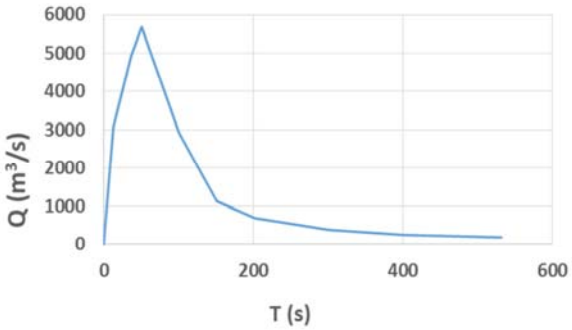

The 2000 Log pod Mangartom case study

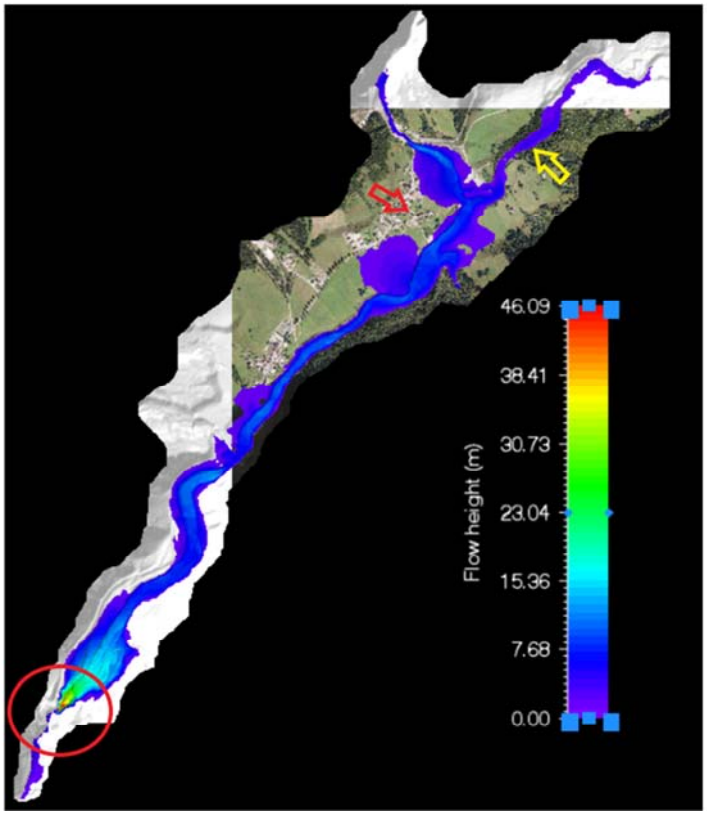

Presentation of modelled debris-flow depths using the calibrated model.

The optimal calibration results were obtained using Voelmy parameters: μ = 0.075 and ξ = 300.

These parameters values are relatively low according to values that can be found in the literature (μ is usually above 0.1, in some cases lower values can be found).

Relatively good agreement was obtained with other model results (e.g., Flo-2D and PCFLOW2D).

The coincidental sequence of debris flows and the debris-flow fan formation

We have tested the hypothesis that the order of debris flows in a sequence of debris flows has an impact of the final fan formation.
The hypothesis has not been confirmed (so far). Further testing is needed on real terrain surfaces.
Details follow on the next two slides.

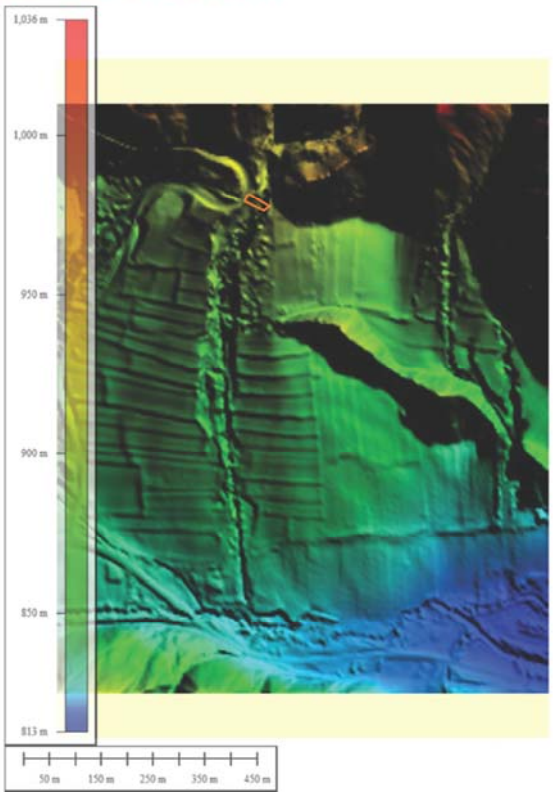

The Suhelj fan with indication of hydrograph input location (orange polygon).

The coincidental sequence of debris flows and the debris-flow fan formation

Magnitude-frequency relationship (from Stoffel (2010)) was used. 62 events (~150 years) were defined. The permutation was used to define the coincidental sequence of debris flow events.

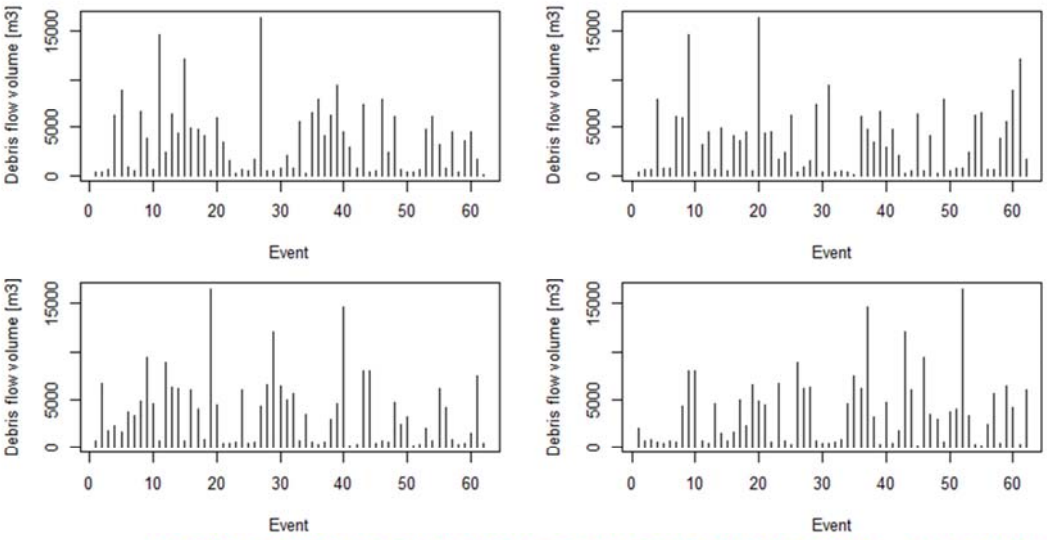

Stoffel, M. 2010. Magnitude-frequency relationship of debris flows – A case study based on field surveys and tree-ring records. Geomorphology, 116: 67-76.

The coincidental sequence of debris flows and the debris-flow fan formation

Sequence-of-events impact on fan characteristics (e.g., shape, area) was investigated. 62 events were used for this purpose.

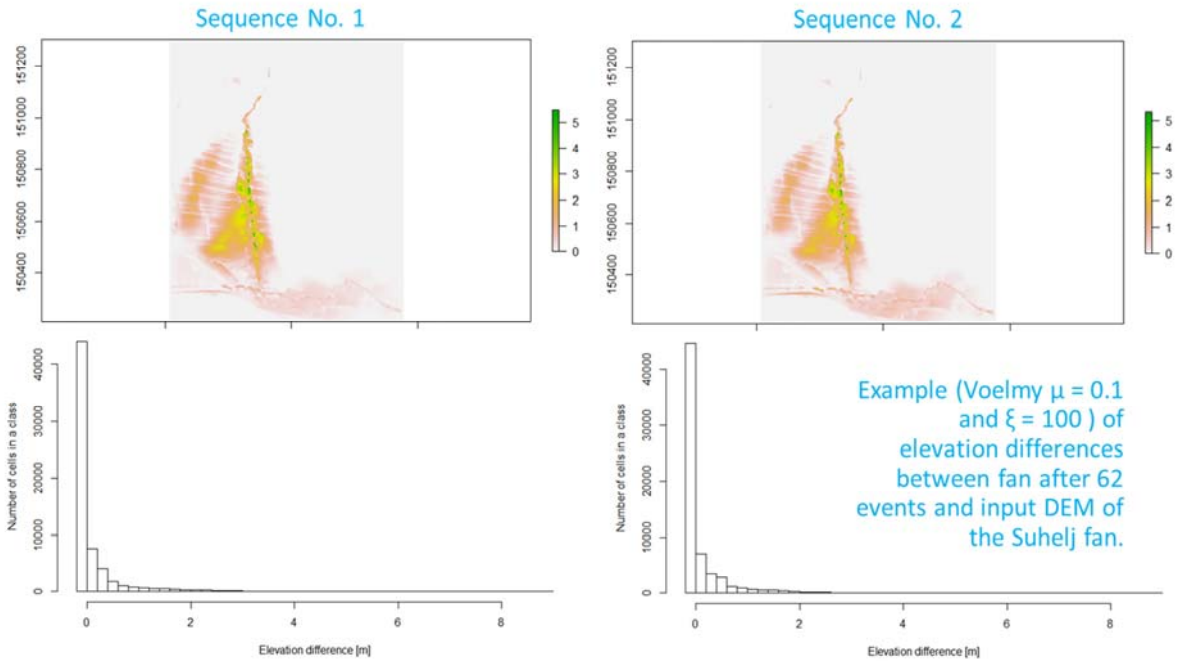

The coincidental sequence of debris flows and the debris-flow fan formation

- **t-test was used to compare impact of sequence on fan elevation distributions.**
- **Based on the DEM of difference map (DoD) we compared the distribution of differences (elevation) for two cases (shown in previous slide).**
- **t-test was used on log values to test if the null hypothesis can be rejected with the selected significance level or the null hypothesis cannot be rejected with the selected significance level of 0.05.**
- **In all cases (different Voelmy parameters; the Suhelj fan and an artificial terrain) the t-test null hypothesis could not be rejected with the selected significance level of 0.05, which indicates that sequence of debris flows does not have significant impact on the fan formation.**
- **Although, maximum and average elevetation differences (based on DoD maps) were up to cca. 10% for different debris-flow sequences.**

Further research aims of the IPL-225 project to be followed in 2019-20

- ❑ Further development and testing of variables in selected areas for fans prediction, and selection of significant ones for various scenarios.
- ❑ Further tests in laboratory using fine-grained debris material in L-Box (for mortars) and large V-funnel (for mortars).
- ❑ Comparison of laboratory rheological tests with numerical modelling using Smoothed Particle Hydrodynamics (SPH) models.
- ❑ Comparison of the 2000 Log pod Mangartom debris-flow simulation results using PCFLOW2D, Flo-2D Pro and RAMMS-DF with real field data.
- ❑ Further modelling of fan formation using real terrains from the Upper Sava River valley.

University of Ljubljana
Faculty of Natural Sciences and Engineering
Faculty of Civic and Geodetic Engineering

IPL-216 Project Annual Report for 2018

Diversity and hydrogeology of mass movements in the Vipava Valley, SW Slovenia

Timotej Verbovšek*, *Tomislav Popit, Jernej Jež, Ana Petkovšek, Matej Maček*

*Department of Geology, University of Ljubljana, Faculty of Natural Science and Engineering, Privoz 11, 1000 Ljubljana, timotej.verbovsek@ntf.uni-lj.si

ICL meeting, Kyoto, 1-4 December 2018

Abstract

Project is running according to the proposed plan. Most importantly, we have published a paper in the Landslides journal, entitled "GIS-assisted classification of litho-geomorphological units using Maximum Likelihood Classification, Vipava Valley, SW Slovenia". Geological and geomorphological investigations (mapping and GIS analyses) are in progress, a detailed engineering-geological map in GIS environment has been constructed for the northern region of the Vipava valley. We are performing the inclinometer measurements in all the boreholes in the Stogovce landslide and measuring the water tables in the boreholes to have an insight of the connection between the movements and groundwater levels. In three boreholes, we have installed the water divers, which measure the levels continuously (30-minute interval over few month period). Rheological investigations have not been active in last year, as most of the focus has been giver to beforementioned investigations. We have again performed two field trips in cooperation between two ICL ABN network members (Ljubljana and Zagreb Universities) to the Vipava valley with the students. Future activities in this year will include photogrammetric analyses of the Stogovce landslide, based on UAV scanning, and hopefully also InSAR measurements of the broader Vipava valley region, both being performed for the monitoring of mass movements.

Study Area

- SW Slovenia, the upper Vipava Valley
- Mesozoic carbonates overthrusted on the Eocene flysch

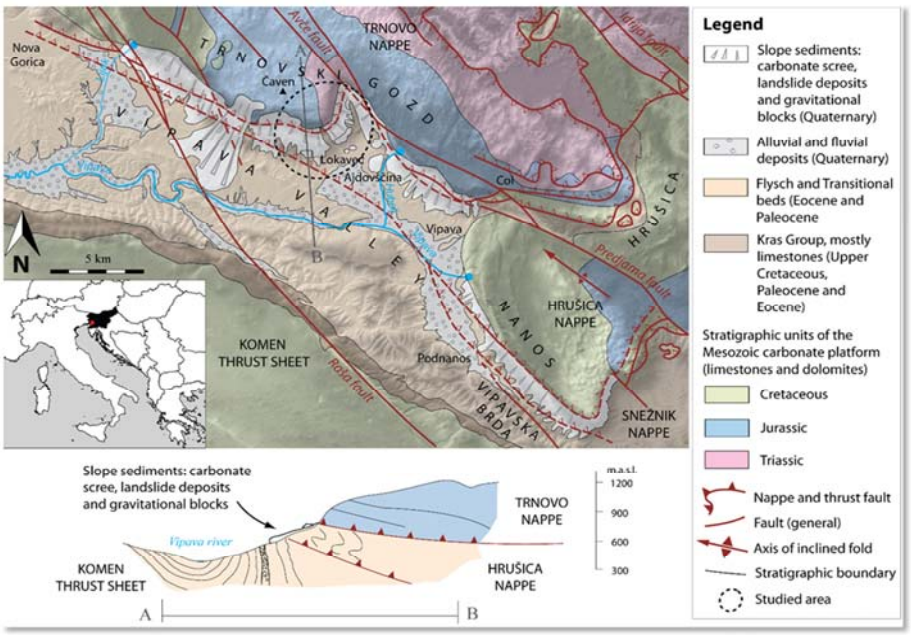

Project duration and objectives (from 2016 application)

- Project Duration: 3 years:
  - Year 1 (2017): Data collection and literature review of the mass movements in the Vipava Valley. Engineering-geological mapping of the area, creation of a GIS geodatabase.
  - Year 2 (2018): Continuation of previous year activities, plus hydrogeological measurements.
  - Year 3 (2019): Continuation of previous year activities, plus monitoring and geotechnical investigations.

- Objectives:
  - *To* create a landslide inventory (database) of the Vipava Valley in GIS environment.
  - Use of Cruden and Varnes classification, plus the use of updated Varnes classification (Hungr et al., 2014)
  - *To* perform a hydrogeological analysis of selected springs in this area, which are related to landslides.
  - *To* monitor the movement of some of the selected landslides, according to available budget.

2017 Activities – Papers

- published papers in 2018 for Vipava Valley:
  - **Landslides** - Verbovšek, Timotej, Popit, Tomislav. GIS-assisted classification of litho-geomorphological units using Maximum Likelihood Classification, Vipava Valley, SW Slovenia. Landslides : Journal of the international consortium on landslides, ISSN 1612-510X. [Print ed.], 2018, vol. 15, iss. 7, str. 1415-1424, doi: 10.1007/s10346-018-1004-2
  - Acta Geographica Slovenica – Kocjančič M, Popit T, Verbovšek T, Gravitational sliding of the carbonate megablocks in the Vipava Valley, SW Slovenia, doi: 10.3986/AGS.4851
  - 5th Slovenian Geological Congress - Jemec Auflič, Mateja, Mikoš, Matjaž, Verbovšek, Timotej, Bavec, Miloš. Recent developments in landslide research in Slovenia. V: Jemec Auflič, Mateja (ur.), Mikoš, Matjaž (ur.), Verbovšek, Timotej (ur.). Advances in landslide research : proceedings of the 3rd Regional Symposium on Landslides in the Adriatic Balkan Region, 11-13 October 2017, Ljubljana, Slovenia. Ljubljana: Geological Survey of Slovenia. 2018, str. 119-124.
  - 5th Slovenian Geological Congress - Verbovšek, Timotej, Mihevc, Nejc, Kočevar, Marko, Vrabec, Marko. Meritve premikov in podzemne vode na plazu Stogovce pri Ajdovščini = displacement and groundwater monitoring of the landslide Stogovce near Ajdovščina, SE Slovenia. V: Novak, Matevž (ur.), Rman, Nina (ur.). Zbornik povzetkov = Book of abstracts, 5. slovenski geološki kongres, Velenje, 3.-5. 10. 2018. Ljubljana: Geološki zavod Slovenije. 2018, str. 87-88.

2018 Activities – Mapping

- Production of GIS map of landslides in the project area, compilation of all known mass movements (in progress)

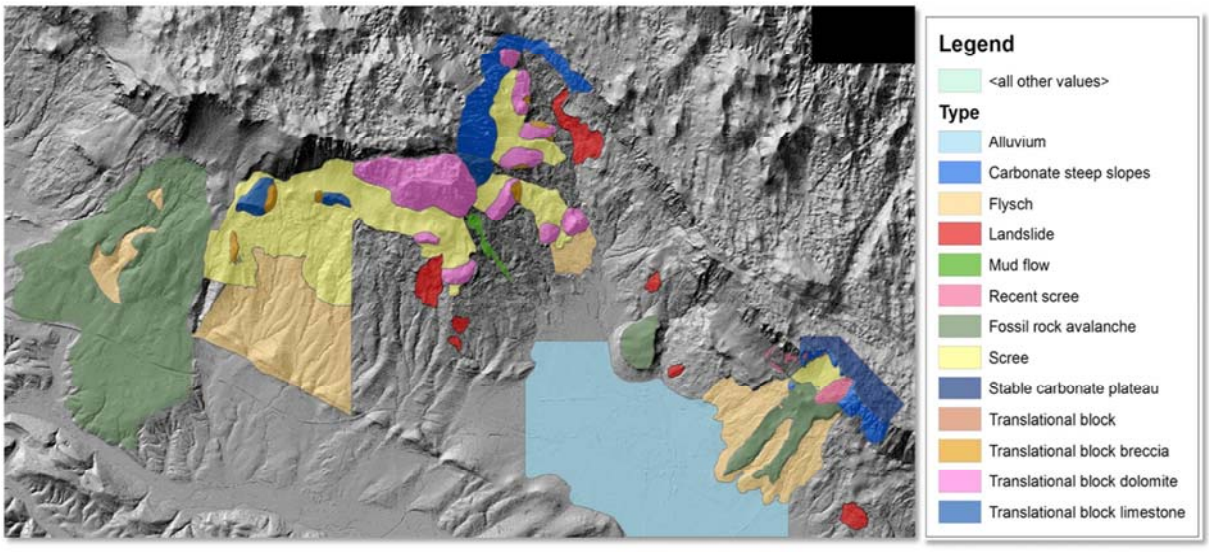

2018 Activities – Groundwater

- Monitoring of groundwater in Stogovce landslide
  - temperature, electroconduvity, water level (CTD diver)

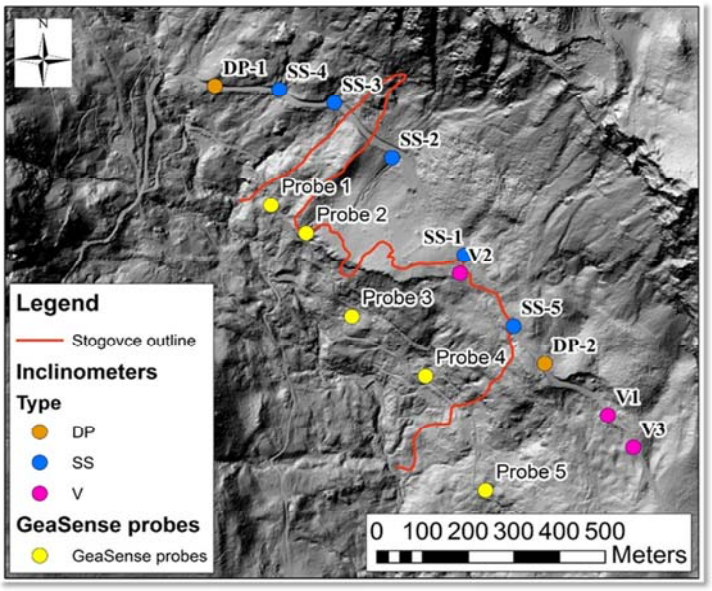

2018 Activities – Groundwater

- Monitoring of groundwater in Stogovce landslide

Level	SS-1	SS-2	SS-3	SS-4	SS-5	DP-2	V1	V2	V3
Depth (m)	*15.00*	*28.00*	*6.00*	*19.00*	*6.00*	*7.30*	*17.00*	*18.00*	*15.00*
Min (m)	12.50	25.11	3.13	*	1.43	7.24	12.71	12.02	10.44
Max (m)	14.18	26.40	4.91	*	3.02	7.40	12.82	16.61	12.53
Range (m)	1.68	1.29	1.78	*	1.59	0.16	0.11	4.59	2.09
H_water max (m)	2.50	2.89	2.87	*	4.57	0.06	4.29	5.98	4.56
H_water min (m)	0.82	1.60	1.09	*	2.98	-0.10	4.18	1.39	2.47

6 July 2018	SS-1	SS-2	SS-3	SS-4	SS-5	DP-2	V1	V2	V3
T (C)	11.5	11.9	11.9	*	11.3	*	8.4	10.9	10.9
EC (uS/cm)	547	451	152	*	795	*	845	539	421

2018 Activities – Groundwater

- V-2, V-3 and SS-2, **6.7.-27.9.2018**

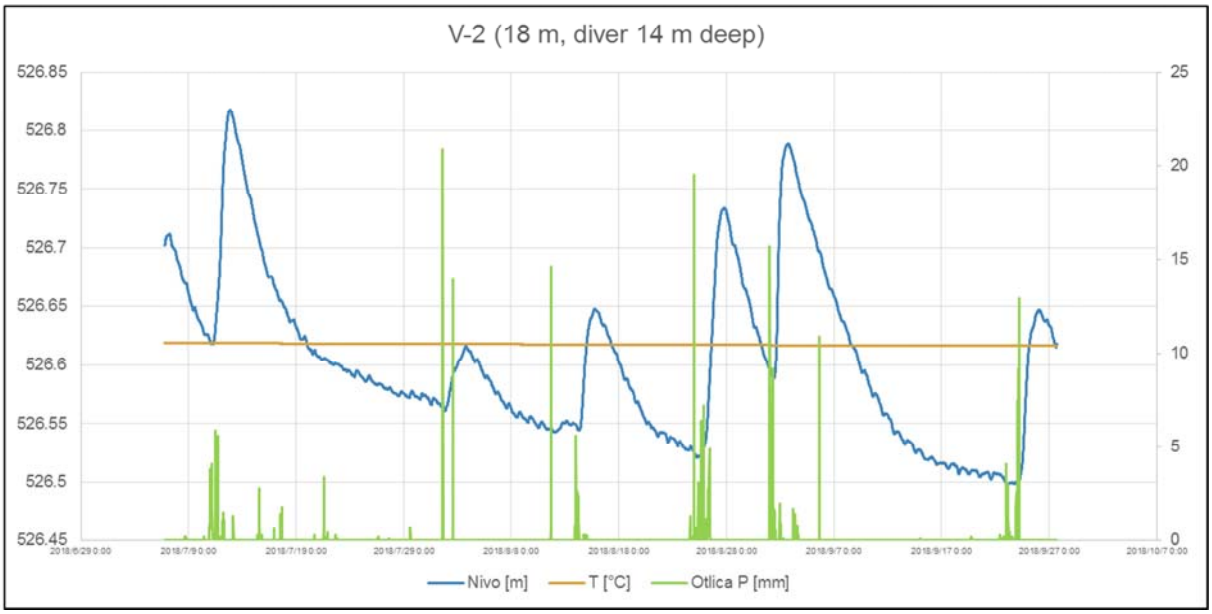

2018 Activities – Groundwater

- V-2, V-3 and SS-2, **6.7.-27.9.2018**

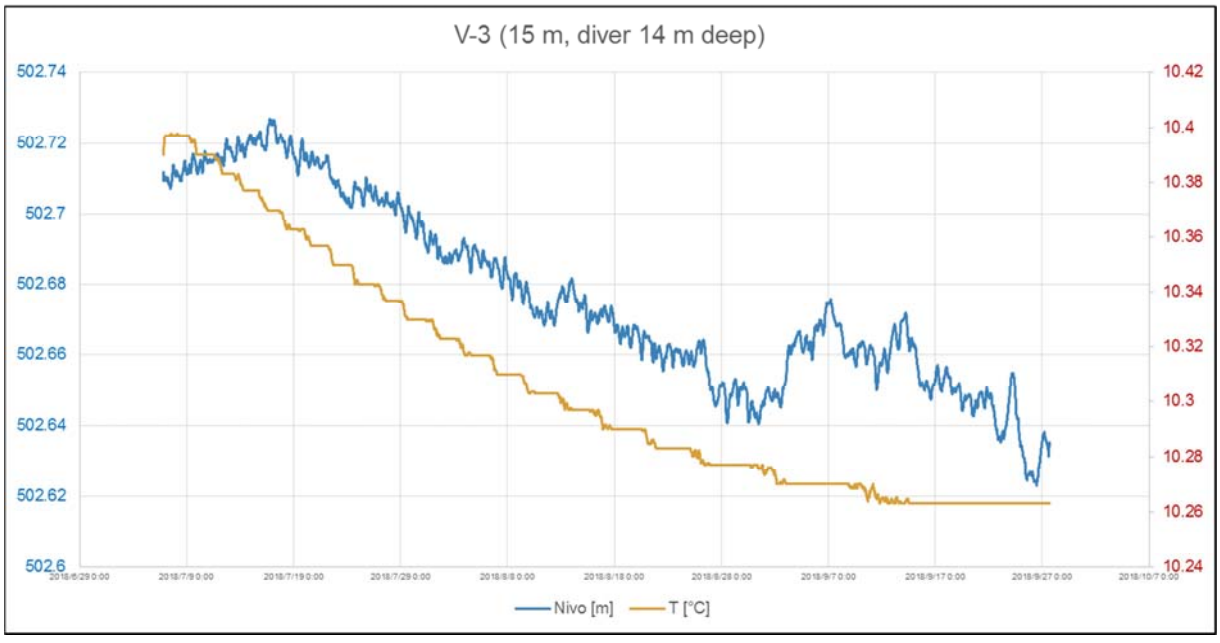

2018 Activities – Groundwater

- V-2, V-3 and SS-2, **6.7.-27.9.2018**

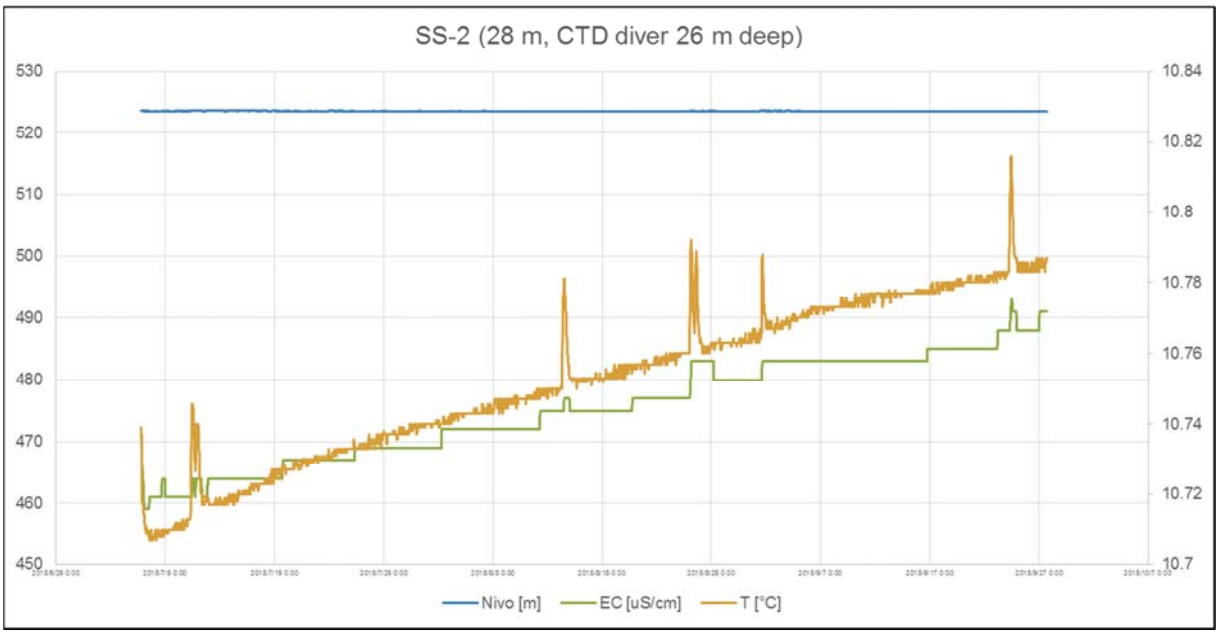

2018 Activities – Groundwater

- V-2, V-3 and SS-2, **6.7.-27.9.2018**

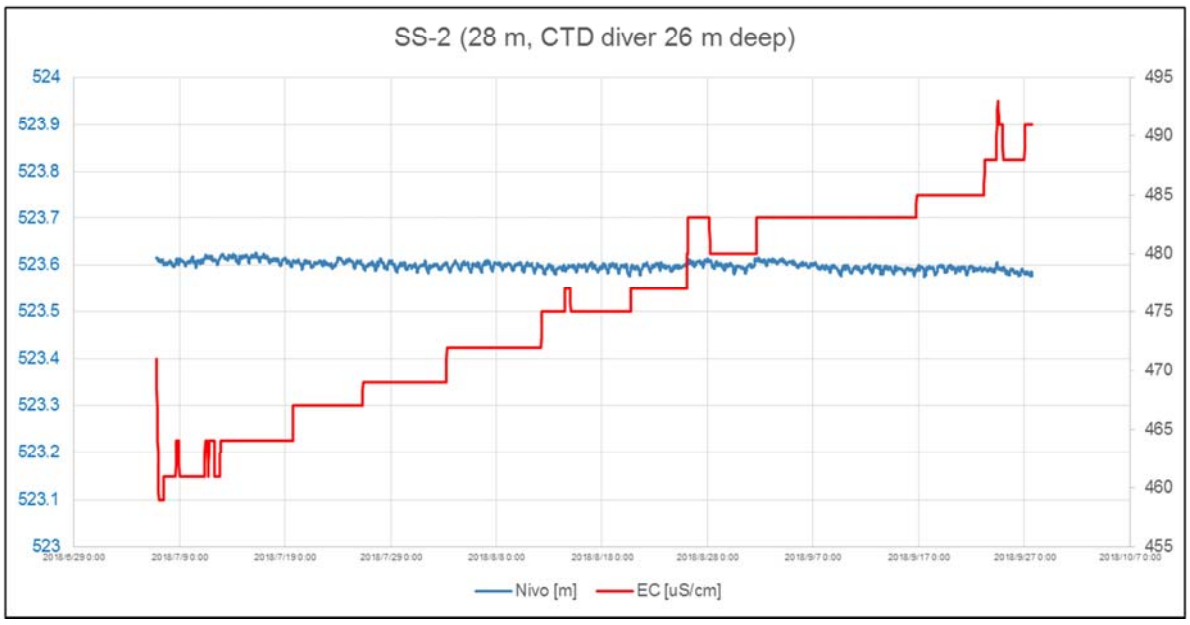

2018 Activities – Inclinometers

- **SS-1:**
- year 2011

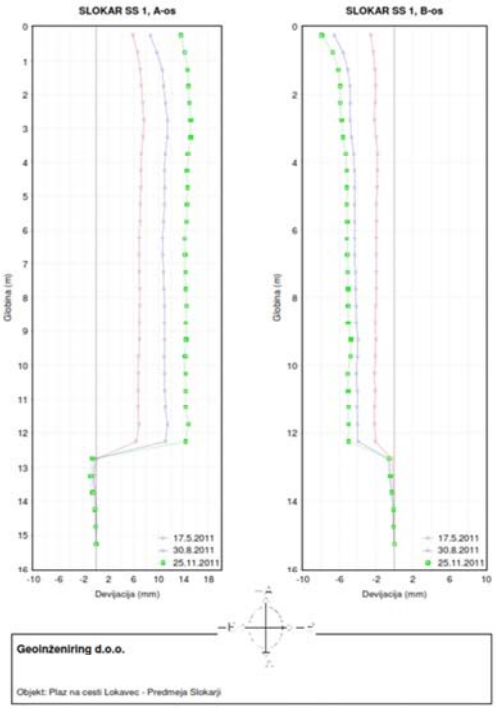

2018 Activities – Inclinometers

- **SS-2:**
- **0:** 22.11.2014
- **1:** 04.09.2015
- **2:** 09.08.2016
- **3:** 06.07.2018

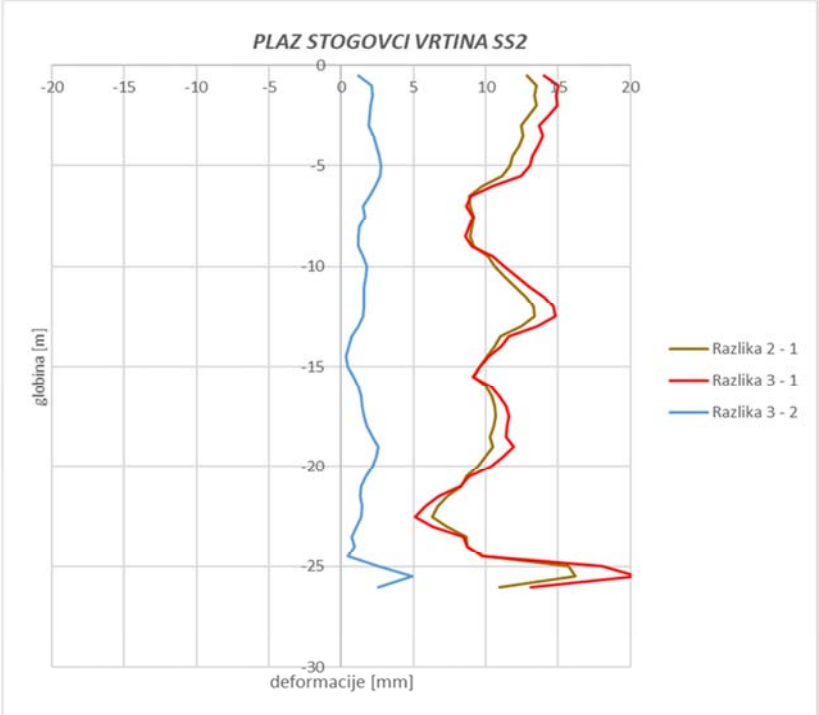

2018 Activities – Inclinometers

- **SS-4:**
- **0:** ?
- **1:** 06.07.2018
- no movement, in the error range

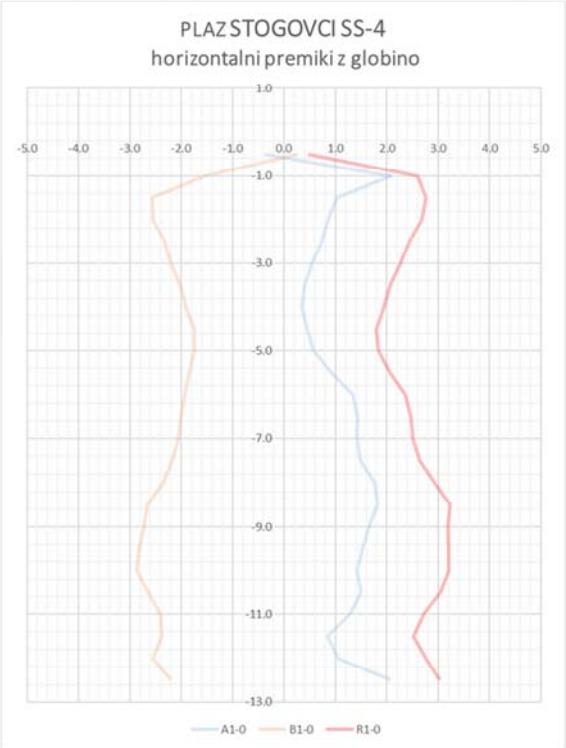

Precipitation

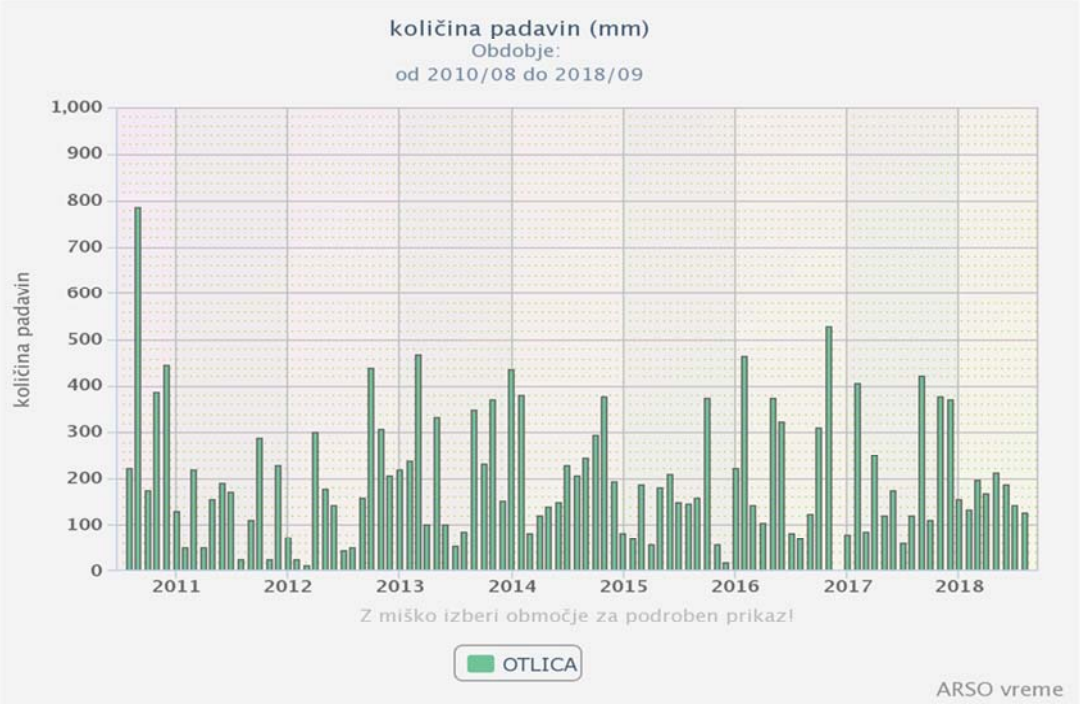

3D model and volume calculations

- UAV, August 2018
- 5 cm horizontal accuracy

3D model and volume calculations

- Google Earth

2018 Activities – Other

- Adriatic-Balkan network ICL ABN activities – second year of cooperation: field work with students of University of Ljubljana + University of Zagreb, Faculty of Mining, Geology and Petroleum Engineering to Stogovce, Slano blato and Podboršt landslides, June 2018

- Promotion of ICL during the Engineering geology lectures, University of Ljubljana, NTF and project KamPlaz (awareness at municipality level) (https://sites.google.com/view/kamplaz)

Contribution of Landslide group in National Central University to IPL

Ray-Shyan Wu [1], Chih-Chung Chung [2]

1) National Central University, Taoyuan, Taiwan. e-mail: raywux@gmail.com
2) National Central University, Taoyuan, Taiwan

Abstract

Landslide group in National Central University has a broad spectrum of expertise and research interest in the landslide areas of atmospheric, hydrogeology, groundwater hydrology, active fault and earthquake hazard, landslide hazard, engineering geology, geomechanics, geotechnical engineering, and environmental geochemistry. These not only provide students with excellent opportunities in acquiring hands-on experiences in conducting laboratory as well as field works, but also extend the collaborations between NCU and international society or universities. Further attendance to related conferences have been proceeded to share the latest academic and practical findings as one of priority actions of Kyoto 2020 Commitment for Global Promotion of Understanding and Reducing Landslide Disaster Risk.

NCU Campus Location

國立中央大學
National Central University

Department of Civil Engineering

國立中央大學土木工程系
Department of Civil Engineering

Faculty

- Professors：26
- Joint professors：19
- Administrative Staff ：9
- Research staff: 30+

Academic Divisions

Mechanics and Structural Engineering
Geotechnical Engineering
Civil Materials Engineering
Transportation Engineering
Water Resources Engineering
Geo-Information Engineering
Disaster Mitigation and Information Technology Engineering

Professor
Yong-Ming Tien
Rock Mechanics

Professor
Ray-Shyan Wu
Supply and Demand in Water Resources

Professor
Jin-Hung Hwang
Soil Dynamic and Pile Foundations

Professor
Hsien-Ter Chou
Debris Flows

Assoc. Professor
Wen-Chao Huang
Numerical analysis
Geotechnical reliability
Soft ground engineering

Professor
Ming-Hsu Li
Hydrology Simulation

Professor
Chung-Pai Chang
Geological Data Processing
Geologic Remote Sensing

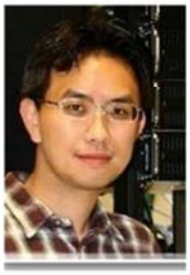

Assoc. Professor
Tso-Ren Wu
Tsunami Simulation

Assoc. Professor
Wen-Yi Hung(洪汶宜)
Centrifuge physical modeling

Assist. Professor
Chih-Chung Chung
Disaster Prevention and Monitoring

Graduate Institute of Applied Geology

應用地質研究所
Graduate Institute of Applied Geology

Earthquake and active fault
Landslides and dammed lakes
Landslide subsidence
Engineering related hazards
…

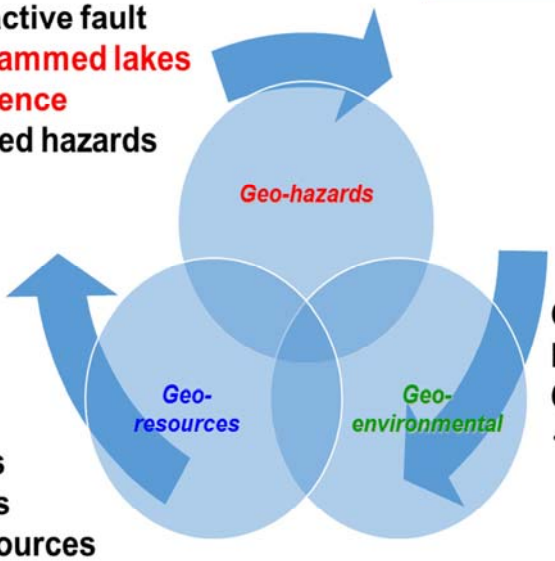

Ground water pollution
Nuclear waste disposal
CO_2 sequestration
…

Water resources
Fossil resources
Geo-thermo resources
Land resources
…

應用地質研究所
Graduate Institute of Applied Geology

Jia-Jyun Dong
Director and Professor
Engineering Geology

Chyi-Tyi Lee
Professor
Engineering Geology

Chuen-Fa Ni
Professor
Groundwater Hydrology

國立中央大學 環境研究中心
Center for Environmental Studies

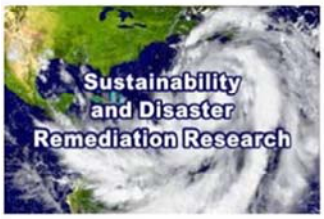

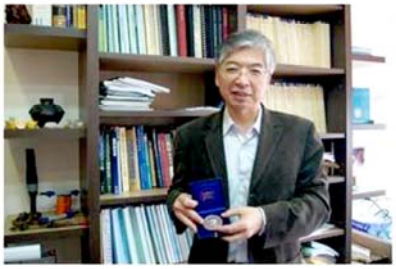

Professor
Shu-Kun Hsu
Geophysics, Oceanography

Catastrophic Tsaolin Landslide

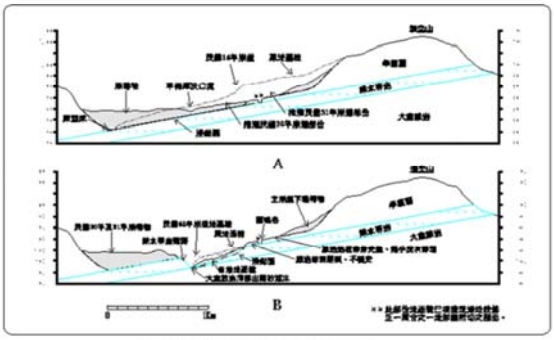

圖2 草嶺大崩山區地質剖面圖(圖1剖面A-A)
(A) 民國30年及31年第二次草嶺大崩山區環境地質剖面
(B) 民國88年第三次草嶺大崩山區環境地質剖面

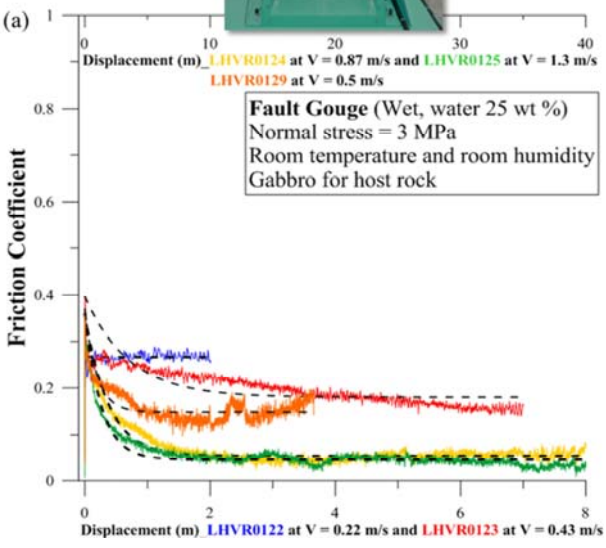

National landslide hazard map

Landslide inventory

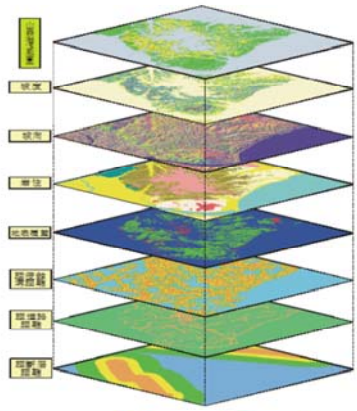

Causative Factors

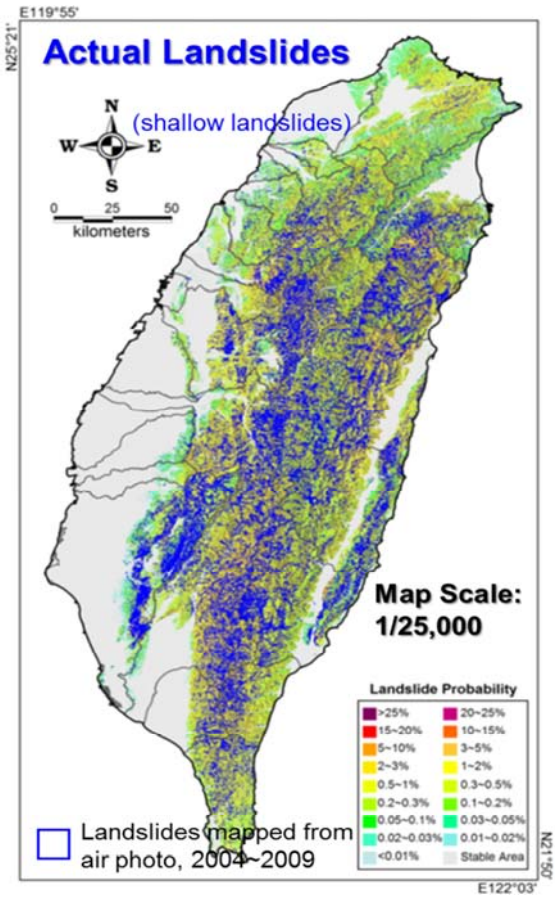

Triggering Factors

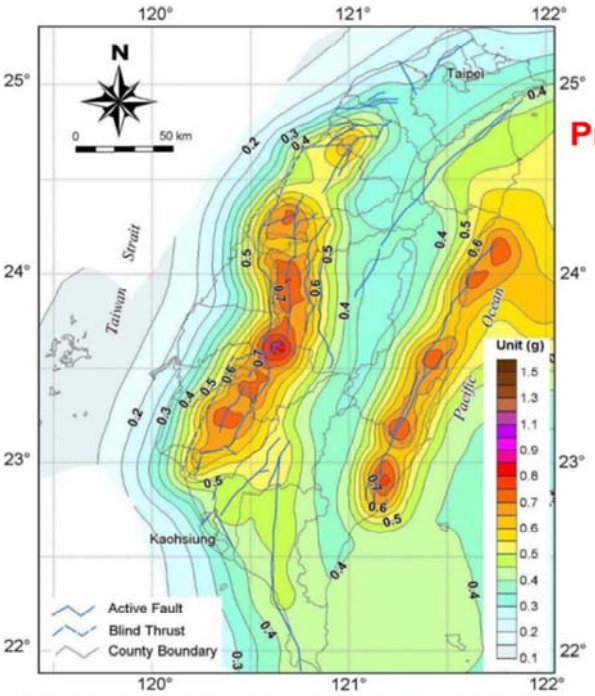

10% Exceedence in 50-year PGA Hazard Map for Soft Site

Probabilistic Seismic Hazard Analysis

Spectral Attenuation Relationships for Subduction Zone Earthquakes in Northeastern Taiwan

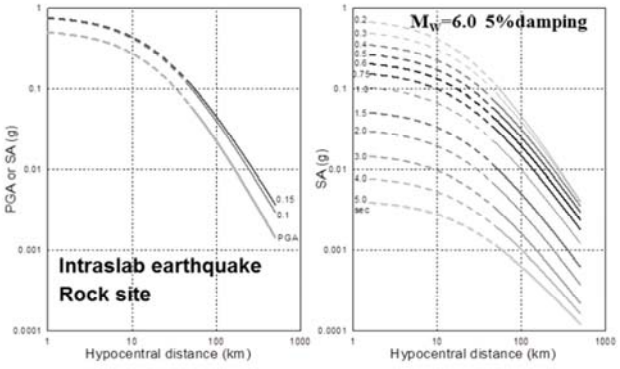

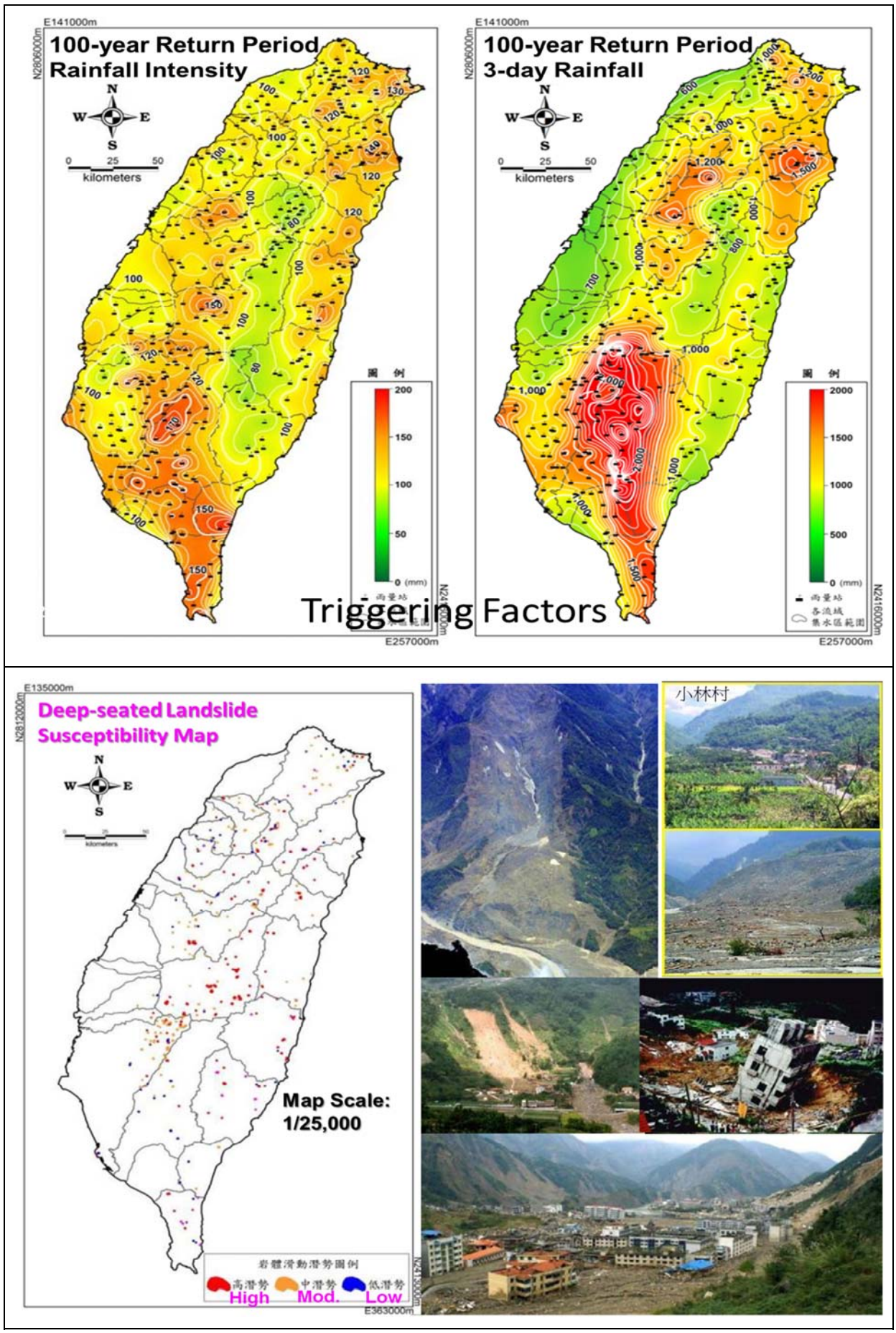
E141000m
N2806000m
100-year Return Period
Rainfall Intensity
N
W
E
S
0 25 50
kilometers
圖 例
200
150
100
50
0 (mm)
雨量站
各流域
集水區範圍
N2416000m
E257000m
100-year Return Period
3-day Rainfall
2000
1500
1000
500
Triggering Factors
E135000m
N2812000m
Deep-seated Landslide
Susceptibility Map
Map Scale:
1/25,000
岩體滑動潛勢圖例
高潛勢 中潛勢 低潛勢
High Mod. Low
E363000m
小林村

NCU Centrifuge Mechanical Assembly

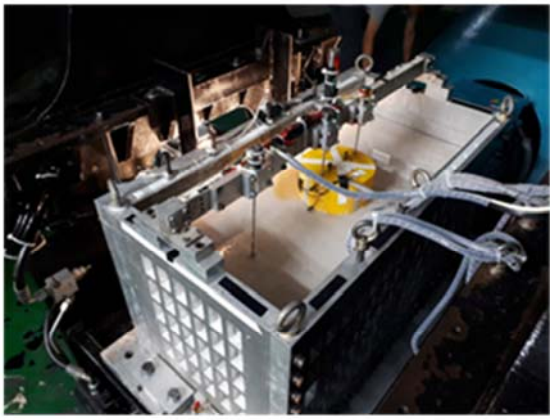

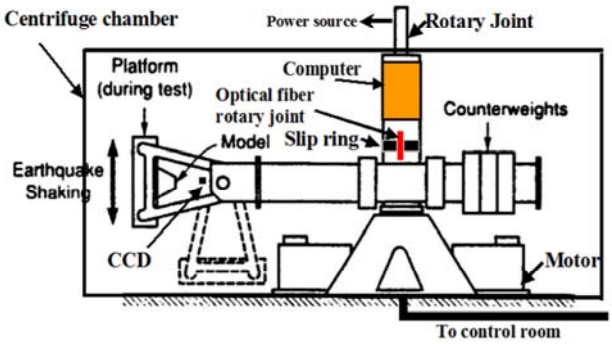

Time Domain Reflectometry for landslide monitoring

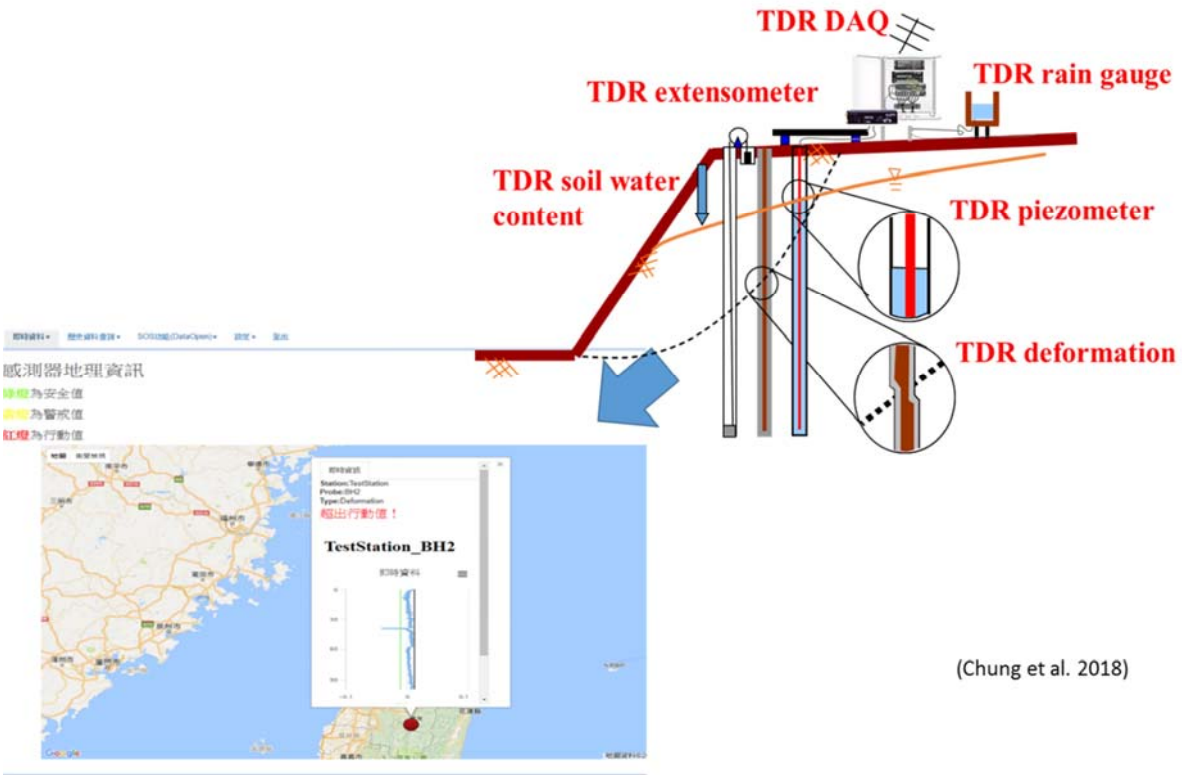

(Chung et al. 2018)

Multi-nodes for landslide monitoring

Arduino Fio / Pro Mini

U-blox GPS

RF / LoRaWAN

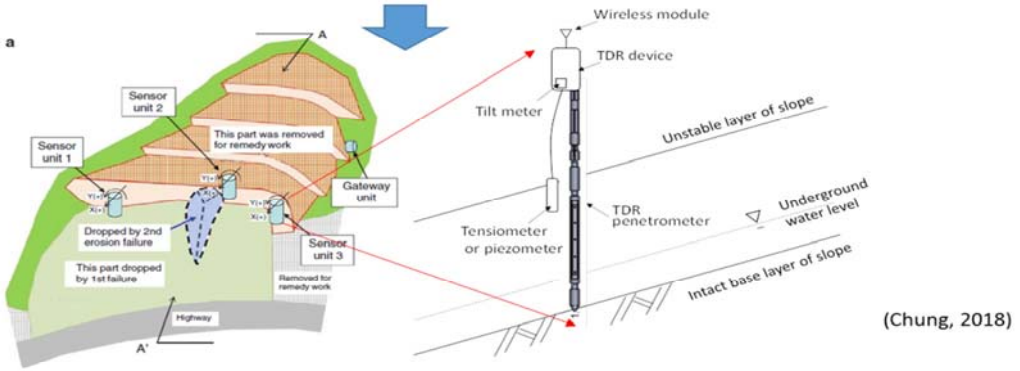

(Chung, 2018)

(Chung, 2018)

16

Landslide Issue Session Proposal

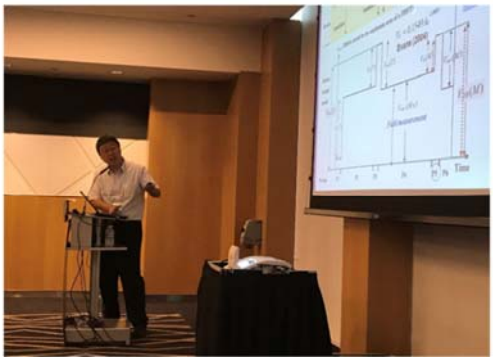

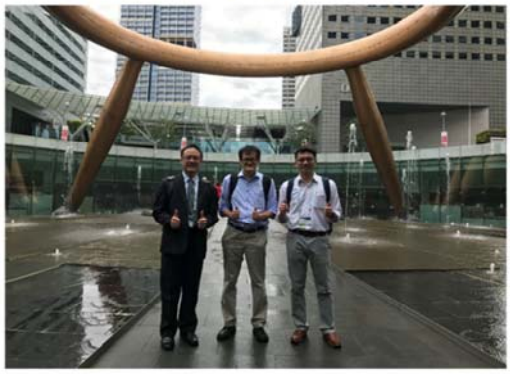

Landslide Short Training Courses

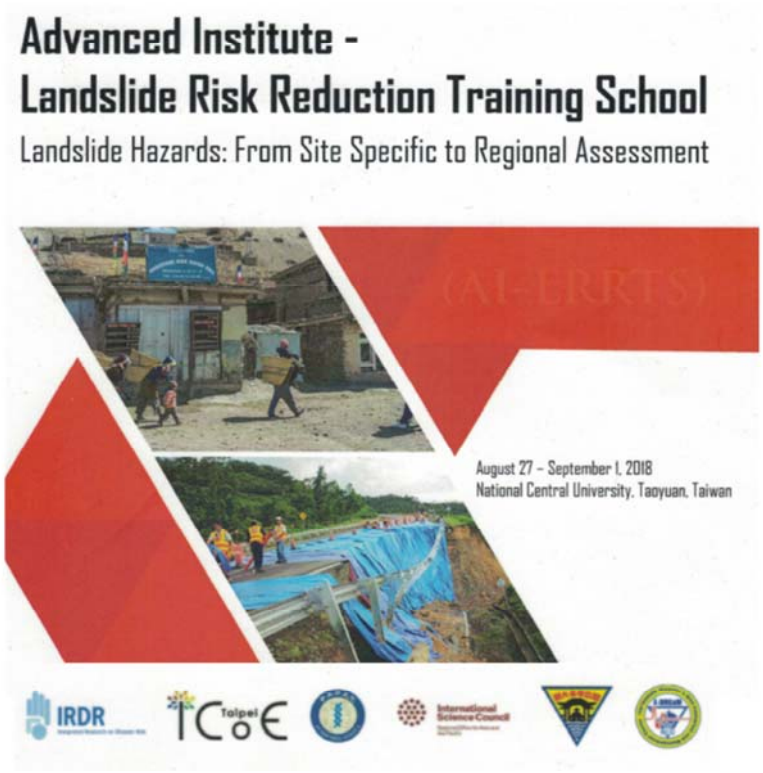

Landslide Short Training Courses

Introduction of Landslides hazards

Slope stability analysis – Infinite slopes and finite slopes

Determining strength parameters for slope stability analysis

- Drain/Undrain conditions
- Laboratory tests and back analysis

Incorporating environmental factors into slope stability analysis

- Rainfall and pore pressure
- Earthquake and seismic forces

Testing, Modeling and Monitoring of site specific landslides

- Landslide monitoring
- Landslide Modeling with Discrete Element Method (DEM)
- Centrifuge modeling on failure behavior of slope

Landslide hazard analysis and regional landslide mapping

- Overview of landslide hazard analysis and regional
- Landslide hazard model for rain- and earthquake- induced landslides

Post field trip

Landslide Short Training Courses
sk Reduction Training School (AI-LRRTS)
sk Reduction Training School (AI-LRRTS)
Specific to Regional Assessment

Global Promotion Committee
The International Programme on Landslides

A Programme of the ICL for Landslide Disaster Risk Reduction

Chair: Qunli Han (Integrated Research on Disaster Risk (IRDR), Executive Director)
Deputy Chairs:
Taikan Oki (United Nations University, Senior Vice-Rector/United Nations Assistant Secretary General)
Giuseppe Arduino (UNESCO, Chief, Section on Ecohydrology, Water Quality and Water Education)
Shoko Arakaki (UNISDR, Chief of Branch. Partnerships, Inter-governmental process and Inter-agency cooperation)
Peter Bobrowsky (ICL, President, Geological Survey of Canada)
Secretary: Kyoji Sassa (IPL World Centre, Director)

Members of IPL Global Promotion Committee (GPC/IPL)

ICL Full members:

Korea Institute of Geoscience and Mineral Resources (KIGAM), University of Ljubljana, Faculty of Civil and Geodetic Engineering (ULFGG), Slovenia, and all other full members of ICL are members of GPC/IPL with voting rights. Participation of governmental organizations for IPL is important for landslide disaster risk reduction.

Governmental members of ICL

Natural Resources Canada, Geological Survey of Canada, Government of Canada
City of Zagreb, Emergency management office, Republic of Croatia
Ministry of Home Affairs, National Institute of Disaster Management, Government of India
Agency for Meteorology, Climatology, and Geophysics of the Republic of Indonesia
Public Works Department of Malaysia, Slope Engineering Branch, Federal Government of Malaysia
Ministry of Disaster Management, National Building Research Organization, Government of Sri Lanka
Ministry of Agriculture and Cooperatives, Land Development Department, Royal Thai Government

ICL Supporting Organizations:

Members of ICL Supporting organizations are members of GPC/IPL with voting rights.

United Nations Educational, Scientific and Cultural Organization (UNESCO), World Meteorological Organization (WMO), Food and Agriculture Organization of the United Nations (FAO), United Nations Office for Disaster Risk Reduction (UNISDR), United Nations University (UNU), International Science Council (ISC), World Federation of Engineering Organizations (WFEO), International Union of Geological Sciences (IUGS), International Union of Geodesy and Geophysics (IUGG), the Government of Japan (Cabinet office, Ministry of Education, Sports, Science and Technology, Ministry of Agriculture, Forestry and Fisheries, Ministry of Land, Infrastructure and Tourism), and Kyoto University.

IPL World Centre:

IPL World Centre (IWC) was established in 2006 by the Tokyo Action Plan to serve as the secretariat of IPL and GPC/IPL. IWC is a part of the legal body (NPO-ICL registered in Kyoto, Japan) of ICL. The Council of the IWC consists of advisors from Kyoto University, Cabinet office, Ministry of Education, Sports, Science and Technology, Ministry of Agriculture, Forestry and Fisheries, Ministry of Land, Infrastructure and Tourism of the Government of Japan, and members from ICL Headquarters, ICL full members in Japan and Chair of IPL-GPC, President, Vice presidents for Europe and Americas and former Presidents of ICL as well as IPL and ICL Advisors.

GPC/IPL Secretariat:

Secretary: Kyoji Sassa
International Consortium on Landslides
138-1 Tanaka-Asukai cho, Sakyo-ku,
Kyoto 606-8226, Japan
Tel: +81 (75) 723 0640, Fax: +81(75) 950 0910
e-mail: secretariat@iclhq.org

International Consortium on Landslides
UNITWIN Headquarters Building
Kyoto University Uji Campus
Uji, Kyoto 611-0011, Japan, Tel: +81(774) 38 4834
URL: http://www.iplhq.org/ , http://icl.iplhq.org/

International Consortium on Landslides

An international non-government and non-profit scientific organization promoting landslide research and capacity building for the benefit of society and the environment

President: Peter Bobrowsky (Geological Survey of Canada)
Vice Presidents: Matjaz Mikos (University of Ljubljana), Slovenia, Dwikorita Karnawati (Agency for Meteorology, Climatology, and Geophysics), Indonesia, Nicola Casagli (University of Florence), Italy, Binod Tiwari (California State University), USA, Zeljko Arbanas (University of Rijeka), Croatia
Executive Director: Kaoru Takara (Kyoto University, Japan), Treasurer: Kyoji Sassa (Prof. Emeritus, Kyoto University, Japan)

ICL Full Members:

Korea Institute of Geoscience and Mineral Resources (KIGAM)
University of Ljubljana, Faculty of Civil and Geodetic Engineering (ULFGG), Slovenia

Albania Geological Survey / The Geotechnical Society of Bosnia and Herzegovina / Center for Scientific Support in Disasters – Federal University of Parana, Brazil/ Geological Survey of Canada / University of Alberta, Canada / Northeast Forestry University, Institute of Cold Regions Science and Engineering, China / China University of Geosciences / Huazhong University of Science and Technology / China Geological Survey / Chinese Academy of Sciences, Institute of Mountain Hazards and Environment / Tongji University, College of Surveying and Geo-Informatics, China / Universidad Nacional de Colombia / Croatian Landslide Group (Faculty of Civil Engineering, University of Rijeka and Faculty of Mining, Geology and Petroleum Engineering, University of Zagreb) / City of Zagreb, Emergency Management Office, Croatia / Charles University, Faculty of Science, Czech Republic / Institute of Rock Structure and Mechanics, Department of Engineering Geology, Czech Republic / Cairo University, Egypt / Technische Universitat Darmstadt, Institute and Laboratory of Geotechnics, Germany / National Environmental Agency, Department of Geology, Georgia / Universidad Nacional Autonoma de Honduras (UNAH), Honduras / Amrita Vishwa Vidyapeetham, Amrita University / Vellore Institute of Technology, India / National Institute of Disaster Management, India / Agency for Meteorology, Climatology, and Geophysics of the Republic of Indonesia (BMKG Indonesia) / University of Gadjah Mada, Center for Disaster Mitigation and Technological Innovation (GAMA-InaTEK), Indonesia / Parahyangan Catholic University, Indonesia / Research Center for Geotechnology, Indonesian Institute of Sciences, Indonesia / Building & Housing Research Center, Iran / University of Firenze, Earth Sciences Department, Italy / Italian Institute for Environmental Protection and Research (ISPRA) - Dept. Geological Survey, Italy / University of Calabria, DIMES, CAMILAB, Italy / Istituto de Ricerca per la Protezione Idrogeologica (IRPI), CNR, Italy / DIA–Universita degli Studi di Parma, Italy / University of Torino, Dept of Earth Science , Italy / Centro di Ricerca CERI - Sapienza Università di Roma, Italy / Kyoto University, Disaster Prevention Research Institute, Japan / Japan Landslide Society / Korean Society of Forest Engineering / National Institute of Forest Science, Korea / Korea Infrastructure Safety & Technology Corporation / Korea Institute of Civil Engineering and Building Technology / Slope Engineering Branch, Public Works Department of Malaysia / Institute of Geography, National Autonomous University of Mexico (UNAM) / International Centre for Integrated Mountain Development (ICIMOD), Nepal / University of Nigeria, Department of Geology, Nigeria / Norwegian Geotechnical Institute (NGI) / Grudec Ayar, Peru / Moscow State University, Department of Engineering and Ecological Geology, Russia / JSC "Hydroproject Institute", Russia / Russian State Geological Prospecting University n.a. Sergo Ordzhonikidze (MGRI-RSGPU) / University of Belgrade, Faculty of Mining and Geology, Serbia / Comenius University, Faculty of Natural Sciences, Department of Engineering Geology, Slovakia / Geological Survey of Slovenia / University of Ljubljana, Faculty of Natural Sciences and Engineering (ULNTF), Slovenia / Central Engineering Consultancy Bureau (CECB), Sri Lanka / National Building Research Organization, Sri Lanka / Landslide group in National Central University from Graduate Institute of Applied Geology, Department of Civil Engineering, Center for Environmental Studies, Chinese Taipei / Asian Disaster Preparedness Center, Thailand / Ministry of Agriculture and Cooperative, Land Development Department, Thailand / Institute of Telecommunication and Global Information Space, Ukraine / California State University, Fullerton & Tribhuvan University, Institute of Engineering, USA & Nepal / Institute of Transport Science and Technology, Vietnam / Vietnam Institute of Geosciences and Mineral Resources (VIGMR).

ICL Supporters:

Marui & Co., Ltd., Osaka, Japan / Okuyama Boring Co., Ltd., Yokote, Japan

Central Japan Railway Company, Nagoya, Japan / IDS GeoRadar s.r.l.,Pisa, Italy GODAI Development Corp., Kanazawa, Japan / Japan Conservation Engineers & Co., Ltd, Tokyo / Kokusai Kogyo Co., Ltd., Tokyo, Japan / NIPPON KOEI CO., Ltd., Tokyo, Japan / Ohta Geo-Research Co., Ltd., Nishinomiya, Japan / OSASI Technos Inc., Kochi, Japan / OYO Corporation, Tokyo, Japan / Sabo Technical Center, Tokyo, Japan / Sakata Denki Co., Ltd., Tokyo, Japan / Sinotech Engineering Consultants, Inc, Chinese Taipei

ICL Secretariat:

Secretary General: Kyoji Sassa

International Consortium on Landslides, 138-1 Tanaka Asukai-cho, Sakyo-ku, Kyoto 606-8226, Japan
Web: http://icl.iplhq.org/, E-mail: secretariat@iclhq.org
Tel: +81-75-723-0640, Fax: +81-75-950-0910